O **ITEGAM-JETIA: Journal of Engineering and Technology for Industrial Applications** is a publication of the Galileo Institute of Technology and Education of the Amazon (ITEGAM), located in the city of Manaus since 2008. JETIA publishes original scientific articles covering all aspects of engineering. Our goal is the dissemination of research original, useful and relevant presenting new knowledge on theoretical or practical aspects of methodologies and methods used in engineering or leading to improvements in professional practice. All the conclusions presented in the articles It should be state-of-the-art and supported by current rigorous analysis and balanced assessment. Public magazine scientific and technological research articles, review articles and case studies.

JETIA will address topics from the following areas of knowledge: Mechanical Engineering, Civil Engineering, Materials and Mineralogy, Geosciences, Environment, Information and Decision Systems, Processes and Energy, Electrical and Automation, Mechatronics, Biotechnology and other Engineering related areas.

SUMMARY

ITEGAM - JETIA

Journal of Engineering and Technology for Industrial Applicaons (JETIA)

INSTITUTO DE TECNOLOGIA
ITEGAM®

RESEARCH ARTICLE   **OPEN ACCESS**

A PHILOSOPHICAL ANALYSIS OF AISI 316/AISI 410 STAINLESS STEEL JOINT BY MEANS OF MECHANICAL AND METALLURGICAL PROPERTIES USING TIG WELDING METHOD

Kathiresan G[1], Prabakaran M P[2], Govindarasan D[3] and Vairavel. M*[4]

[1] Professor, Excel Engineering College, Namakkal, Tamil Nadu, India.
[2] Associate Professor, Erode Sengunthar Engineering College - Erode, Tamil Nadu, India.
[3] Assistant Professor, AVS Engineering College - Salem, Tamil Nadu, India.
[4] Professor, Annapoorna Engineering College, Salem, Tamil Nadu, India.

[1] http://orcid.org/0000-0002-6428-4482 ,[2] http://orcid.org/0009-0001-5234-6156 , [3] http://orcid.org/0009-0005-3062-728X
[4] http://orcid.org/0000-0002-8687-7887

Email: [1] kathirmechengg1980@gmail.com, [2] prabakaranmp89@gmail.com, [3] grajmech87@gmail.com, [4] phdannauniv2020@gmail.com

ARTICLE INFO	ABSTRACT
	This study employed Taguchi's Grey Relational Analysis (GRA) to assess the optimization of process boundaries. Improved metallurgical and mechanical qualities of Martensite (AISI 410) and Austenitic (AISI 316) stainless steel joints were the aim of the investigation. In order to do this, TIG welding experiments were carried out with different current flows, welding speeds, and shielding gas flow rates. Responses like tensile strength and microhardness were taken into consideration to determine the ideal procedure settings. Analysis of variance had been used to determine their impacts. The best set of parameters was found to be 10 lit/min shielding gas flow, 2 m/min welding speed, and 120-amp welding current based on the GRA. The distribution of alloys, the microhardness of different weld zones, and the characterisation of microstructural and mechanical properties were also investigated.

I. INTRODUCTION

Thermal power plants (TPPs) of today are made up of a lot of welded joints, either to meet design requirements or to save money. In those factories, a variety of welded joints were employed, such as those made of austenitic stainless steel (ASS) and martensitic stainless steel (MSS) [1]. ASS and MSS materials can be welded with TIG, SMAW, SAW, LBM, and EBM, among other welding techniques [2], [3]. Nevertheless, TIG welding is the most widely used welding process for connecting tubes and pipes in TPP because of its superior productivity, consistency, minimal skill need, and virtue-sounding nature [4]. Austenitic and martensite stainless steels are utilised in super-heaters and re-heaters due to their resilience to deterioration, creep strength, and temperature stability [5].

MSSs, on the other hand, are a type of alloy composed of Fe and C-Cr, which has a BCT crystal structure. These materials are ferro-magnetic, hard, brittle, and heat-tolerant, making them a cost-effective option for water-evaporator and steam headers [6]-[8] Ferritic stainless steel, nickel-based super-alloy, and creep strength increased austenitic/martensitic steel are the materials most frequently utilized in power plants that operate at over temperatures and pressures [9],[10]. As a result, combining dissimilar metals via welding is typically more difficult than joining identical metals. The microstructural changes and chemical gradients that result in notable variations in the structural, chemical, and physical properties of heterogeneous metal weldments.

II. THEORETICAL REFERENCE

The use of filler metal, which is frequently used in heterogeneous metal welding, adds even more complication [11]. The dissimilar metals that are commonly utilised for welded connections in the nuclear and chemical sectors were examined by [12], [13] examined the microstructural growth and corrosion behaviour of several 304/430 stainless steel welded joints. Sun et al. looked at the weldability and properties of austenitic or martensitic stainless-steel junctions. [14].

Gaurav Dak and Chandan Pandey conducted experimental investigation on the microstructure, mechanical characteristics, and stress residuals of a dissimilar welded junction composed of austenitic AISI 304L and martensitic P92 stainless steel [15]. When [16] Incoloy 800 and Inconel 600 Interlayer can somewhat minimize carbon migration.

In order to attain the desired qualities, welding must be done using optimal settings in every given procedure. Utilizing the scientific method yields the ideal process parameters. The process parameters have been optimized in the current study using the Taguchi-based grey relational analysis approach. The application of optimization approaches for fusion and non-fusion welding, including the TIG welding process of dissimilar metals, has been demonstrated by several researchers. [17].

GRA was used to analyze the study's outcomes. Using the Taguchi Based GRA Method, Prabhakaran et al.'s study from [18] looked at how different laser welding parameters affected the hardness and tensile strength of different laser welding techniques. An optimization algorithm to maximize the Taguchi-based GRA's TIG welding capability for the Incoloy 8800HT. [19] study from 20 centered on utilizing Taguchi-based GRA by [20]. The results of the study have been reported by all authors, demonstrating not only the effectiveness of optimization techniques for the optimization of TIG welding processes for different metals, but also demonstrating the scientific advantage of reducing the number of attempts to reach a desired weld property.

II.1 RESEARCH GAP

It has been observed in the literature that the mechanical and metallurgical characteristics of a joint are affected by welding parameters, including arc-gap measurement, weld bead measurement, torch speed measurement, welding current measurement, electrode apex measurement, welding voltage measurement, shielding gas measurement, etc. The quality and production of the industrial sectors will be significantly impacted by these welding parameters. For the manufacturer, controlling the process input parameters has proven to be a challenging issue because, in order to achieve a suitable joint with the desired weld quality, parameters must be optimized before welding begins. When parameters are not optimized, distortion, flaws, and faults may be found.

In the current work, the Taguchi L9 orthogonal array in conjunction with GRA was used to improve the TIG welding procedure settings for the AISI 316-ASS to AISI 410-MSS connection. The tests were carried out by varying the shielding gas flow rate, welding speed, and current using a Taguchi L9 orthogonal array. For analytical purposes, the mean of the replies was determined. The best parameters were then determined by doing an ANOVA. The analysis yielded the ideal parameters, which were then empirically confirmed. The findings were then presented and debated. To investigate the tensile strength, microhardness, HAZ, its WZ, and chemical composition, transverse cuts were made in the welds.

III. MATERIALS AND METHODS

The base metals in this investigation were AISI 410-MSS and AISI 316-ASS. Table 1 provided a list of the basic metals' chemical compositions. Table 2 lists the basic metals' mechanical characteristics. The dimensions of the machined welding work parts were 100 mm × 70 mm × 3 mm. Each work component was butt joined using TIG welding after being cleaned with acetone. The base metals microstructure is depicted in figure 1.a and 1.b; AISI 410-MSS stainless steel has austenitic and twin crystal structures, whereas AISI 316-ASS stainless steel has martensite and ferrite structures. Different process settings (current 100, 120, and 140 amps; welding speed 1, 1.5, and 2 m/min; shielding gas flow rate 8, 10, and 12) were employed to alter the welds' mixing ratio.

Figure 1.a: ASS-316 base metals' microstructure.
Source: Authors, (2024).

Table 1: The weight percentages of the filler and base metals' chemical compositions.

Materials	AISI 316	AISI 410	ER316
C	0.024	0.15	0.04 -.08
Si	0.28	1.0	0.30-0.65
Mn	1.44	1.0	1.0-2.5
P	0.041	0.04	0.03
S	0.017	0.03	0.03
Cr	16.95	11.5-3.5	18-20
Mo	2.06	-	2-3

Materials	AISI 316	AISI 410	ER316
Ni	10.09	0.75	11-14
Fe	Balance	Balance	Balance

Source: Authors, (2024).
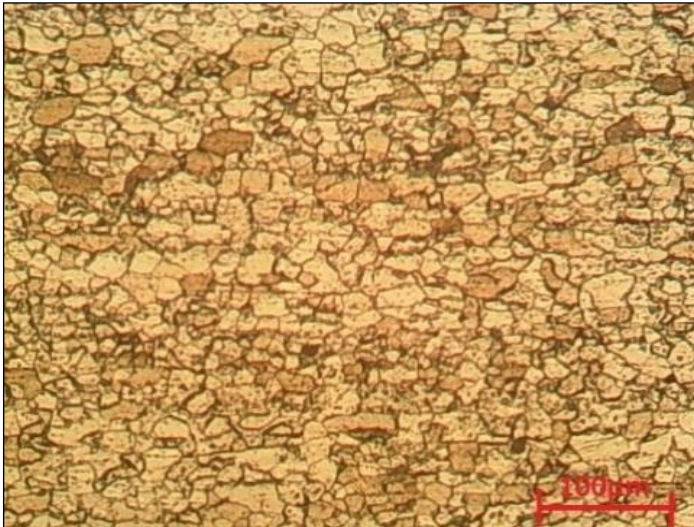
Figure 1.b: The MSS-410 basic metals' microstructure.
Source: Authors, (2024).

The shielding gas (lit/min) for each unique connection was argon. A range of significant process variables were determined through feasibility research. The maximum, middle, and lower levels of the TIG welding process parameters were found by a number of test runs; Table 2 shows these levels.

Table 2: Parameters of the TIG welding process and their values.

S.No		1	2	3
Process parameters		Current	Welding Speed	Shielding Gas Flow Rate
Units		amps	m/min	lit/min
Notation		A	S	G
Levels	-1	100	1	8
	0	120	1.5	10
	+1	140	2	12

Source: Authors, (2024).

The OA was chosen, and the tests were conducted in line with that choice. Micro hardness and Ultimate Tensile Strength (UTS) were selected as the goal functions. The ASTM E-08 standard was adhered to in the preparation of the tensile test specimen depicted in figure 2. Wire-cut EDM was used to cut test specimens for tensile strength. The TUE-CN-400 universal testing machine has been used to do tensile testing. The dissimilar welded joint's microstructure was made visible using aqua regia etchant. An etchant consisting of HCl: HNO3 = 3:1 was used. Using an OM Microscopy and SEM; Bruker outfitted with an EDS, the microstructures of the different welded samples were examined. EDS study was used to identify the weldment's chemical compositions.
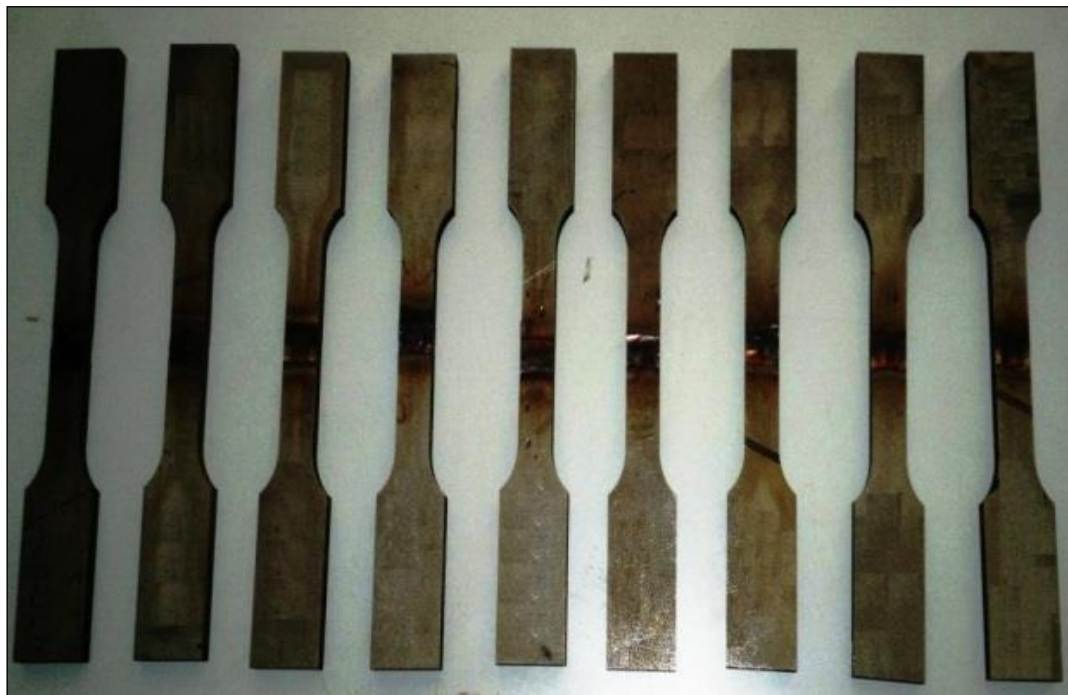
Figure 2: specimens tensile in accordance with ASTM E-08 standards.
Source: Authors, (2024).

IV. RESULTS AND DISCUSSION

Among the statistical performance metrics included in the Taguchi approach is the SNR. It is employed to gauge how well control elements that reduce product or process variation are detected. NB, LB, or HB are the three standard SNRs. SNR can be calculated independently for each quality characteristic and a high SNR indicates the best quality characteristics. The transition from the initial response values to the SNR is the pioneer step of the grey relationship analysis. Equation (1) of "Larger-the-Better"

was applied in this case. These SNR data served as the basis for further investigation. Table 3 displays the results for microhardness, computed SNR and (UTS) ultimate tensile strength. Better strength performance is shown in the present experiment by higher ultimate tensile strength and microhardness

values. Therefore, for microhardness and tensile strength, the "higher-the-better" criterion was used.

$$S/N = -10\log_{10} [\sum (1/y)^2/n] \qquad (1)$$

Table 3: Responses and SNR.

Run order	A amps	S m/min	G lit/min	UTS Mpa	HR HV1	SNR TS	SNR HR
1	100	1	8	483.617	197	53.69	45.89
2	100	1.5	10	492.298	198	53.84	45.93
3	100	2	12	495.152	201	53.89	46.06
4	120	1	10	491.593	207	53.83	46.32
5	120	1.5	12	497.512	199	53.94	45.98
6	120	2	8	494.356	200	53.88	46.02
7	140	1	12	486.984	202	53.75	46.11
8	140	1.5	8	493.467	206	53.87	46.28
9	140	2	10	491.873	221	53.84	46.89

Source: Authors, (2024).

$$x_i = (y_i (k) - \min y_i (k))/ (\max y_i (k) - \min y_i (k)) \qquad (2)$$

Equation (2) states that in GRG, the higher-the-better criterion is the outcome of the normalized tensile strength and microhardness. 4 presents the normalized investigational data in the range of 0-1 in GRA. The Grey Relational Coefficient (GRC) was assessed using this normalized data. Following the average of the GRC values associated with certain experimental outcomes, the Grey Relational Grade (GRG) was determined.

Equation (2) specifies the sequence after which the data are pre-processed and the corresponding comparability sequence is determined. (table 4) For WS, the corresponding sequence is k = 1; for experiments 1 to 9, the corresponding sequential sequence is k = 2. For microhardness, the corresponding sequences are i=1, 2=3=9. The remaining calculations were then

performed and all sequences after the pre-processing are consumed, as outlined in equation (3).

$$\Delta_{0i} (k) = |x_0 (k) - x_i (k)| \qquad (3)$$

Consequently, 0.5 and 0.5 are the weights that are used for microhardness and ultimate tensile strength, respectively. The grey relationship coefficient was computed using the weightage that was assigned. The GRG will be derived using table 5, which shows the GRC (ξ) that was calculated using equation (4), equation (5), as tabulated in table 6.

The variable n in this calculation denotes the total number of process answers.

Table 4: Grey relational generations of each performance characteristics and deviation sequences.

Run order	Sequences of Performance		Deviation Sequences	
	UTS Larger-the-better	HR Larger-the-better	UTS $\Delta_{0i}(1)$	HR $\Delta_{0i}(2)$
1	0.0000	0.0000	1.0000	1.0000
2	0.6248	0.0417	0.3752	0.9583
3	0.8302	0.1667	0.1698	0.8333
4	0.5740	0.4167	0.4260	0.5833
5	1.0000	0.0833	0.0000	0.9167
6	0.7729	0.1250	0.2271	0.8750
7	0.2423	0.2083	0.7577	0.7917
8	0.7089	0.3750	0.2911	0.6250
9	0.5942	1.0000	0.4058	0.0000

Source: Authors, (2024).

$$\xi_i(k) = \frac{\Delta_{min} + \psi \Delta_{max}}{\Delta_{0i}(k) + \psi \Delta_{max}} \qquad (4)$$

$$\gamma_i = \frac{1}{n} \sum_{k=1}^{n} \xi_i(k) \qquad (5)$$

Table 5: Relational coefficients in grey.

Run order	Grey Relational Coefficient	
	UTS $\xi_i (1)$	H $\xi_i (2)$
1	0.3333	0.3333
2	0.5713	0.3429
3	0.7465	0.3750
4	0.5400	0.4616

Run order	Grey Relational Coefficient	
	UTS ξ_i (1)	H ξ_i (2)
5	1.0000	0.3529
6	0.6877	0.3636
7	0.3976	0.3871
8	0.6320	0.4444
9	0.5520	1.0000

Source: Authors, (2024).

Table 6: Grey relational grades.

Run Order	GRG $\gamma_i = 1/2 \ (\xi_i \ (1) + \xi_i \ (2))$	Rank
1	0.3333	9
2	0.4571	7
3	0.5608	3
4	0.5008	6
5	0.6765	2
6	0.5257	5
7	0.3924	8
8	0.5382	4
9	0.7760	1

Source: Authors, (2024).

Table 6 displays the GRG value to be used for the calculation of SNR; Table 7 displays SNR relation based on the higher the better the overall GRG criterion; and figure 3 displays the SNR curve which is a graphical representation to identify the optimal set of parameters. The SNR is a ratio between the signal and the noise, so if a high ratio is present, the desired result is achieved with very low noise. Figure 3 shows the current, welding speed, and shielding gas flow.

Table 7: SNR for GRG.

Run order	SNR for GRG
1	-9.54329
2	-6.79978
3	-5.02384
4	-6.00671
5	-3.39464
6	-5.58524
7	-8.12542
8	-5.38113
9	-2.20277

Source: Authors, (2024).
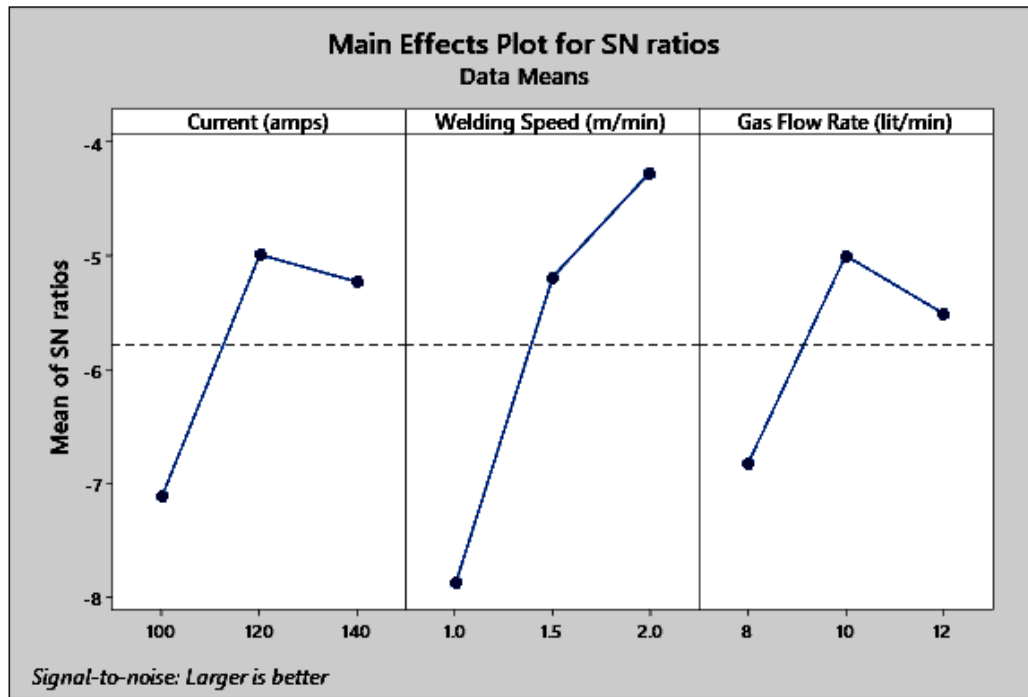
Figure 3: Main effects plot for SNR.
Source: Authors, (2024).

Table 8: Table of responses for GRG.

S. No	Process parameters	Levels			Range	Rank
		-1	0	+1		
1	A (amps)	0.4504	0.5676	0.5688	0.1368	2
2	S (m/min)	0.4088	0.5572	0.6208	0.2121	1
3	G (lit/min)	0.5952	0.4584	0.5332	0.1184	3

Source: Authors, (2024).

The welding speed has the most influence on responses, as can be observed from accordance table 8, where the welding speed range is maximum, this is consistent with data that other researchers have found previously [17, 19] about various welding procedures and other materials. The research indicates that the ideal set of variables is 120 amps of current, 2 m/min of welding velocity, and 10 lit/min of shielding gas flow rate. Verification testing must be done using TIG welding and the ideal process

parameters found from the analysis since the optimal set of TIG welding process parameters determined by GRG is not in the L_9 orthogonal array implemented to conduct the trials.

IV.1 ANALYSIS OF VARIANCE

To determine which parameter has the greatest desired influence on the mechanical characteristics, an ANOVA was conducted. All of the process parameters are crucial since they all have substantial F values. (Table 9) Accordingly, the welding speed also had the biggest influence on the results in this examination, which is in line with the findings of earlier studies for a variety of other materials.

Table 9: ANOVA.

Source	DOF	Adj. SS	Adj. MS	F-Value	P-Value	Contri bution
A (amps)	2	0.4744	0.2372	2.40	0.294	21.65
S (m/min)	2	1.2224	0.6112	6.19	0.139	55.78
G (lit/min)	2	0.2972	0.1485	1.51	0.399	13.56
Error	2	0.1974	0.0986			
Total	8	2.1914				

Source: Authors, (2024).

IV.2 MICROSTRUCTURAL STUDIES OF DISSIMILAR WELD ZONE

Investigations were conducted into the ideal heterogeneous welded joint of microstructure, alloying element distribution, and mechanical characteristics. The morphological characteristics of the dissimilar welded joints made using ER316 filler metal and AISI 410-MSS to AISI 316-ASS, respectively, are displayed in figure 4. To develop mirror-polished samples, dissimilar welded samples were cut from the cross-welds, ground, and polished. Aqua regia etchant was utilised to disclose the microstructure of the dissimilar welded junction. While the base metals of AISI 316-ASS stainless steel were composed of twin crystal and austenitic structures, those of AISI 410-MSS stainless steel were composed of martensite and ferrite structures.

Figure 4.a shows the optical architecture of the AISI 410-HAZ. Grain size in AISI 410-MSS increased progressively from the HAZ edge to the fusion boundary. As the distance from the weld contact decreased, the HAZ peak temperature actually rose, and grain development also depended on temperature. The HAZs of the two BMs were not the same. Figure 4.b illustrates the discovery of untreated ferrite δ stringers within the austenitic matrix in the AISI 316 HAZ during the welding process, as documented in reference [21].

Ferrite can have an impact on the attributes of AISI 316, leading to low fatigue resistance and great corrosion resistance because of the high chromium concentration. Furthermore, the grains' expansion may be slowed by the ferrite. Moreover, the existence of δ ferrite may limit the formation of AISI 316-HAZ grains [22].

Figures 4.c and 5 show the architecture of the dissimilar weld zone (WZ), which is based on the content of the filler metal. The optical microscope observation in WZ showed a skeletal ferrite microstructure inside a major austenitic matrix.
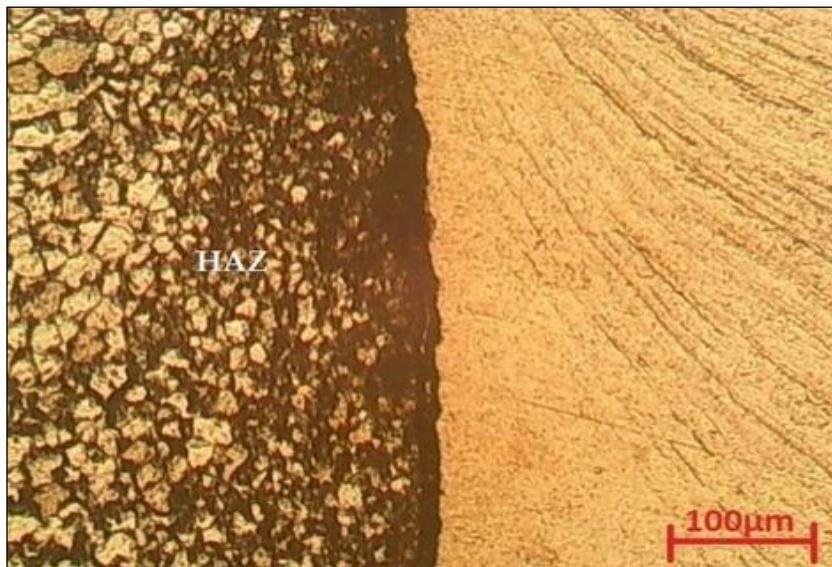
Figure 4.a: Microstructure of AISI 410-HAZ
Source: Authors, (2024).
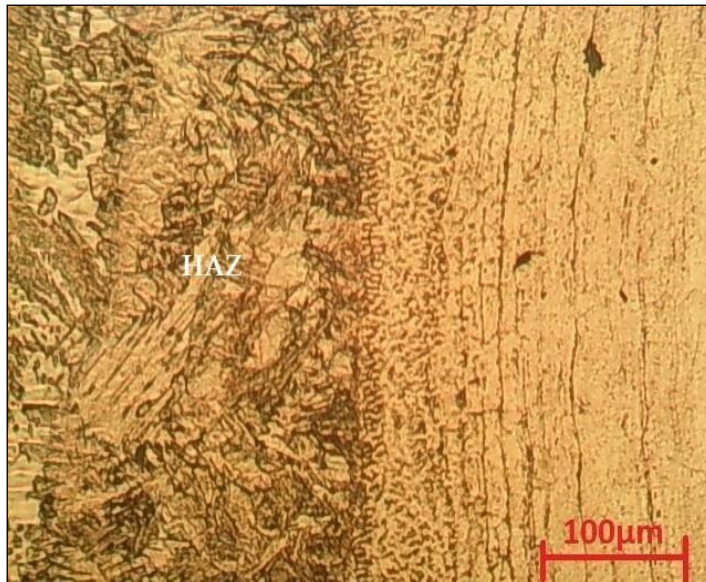
Figure 4.b: Microstructure of AISI 316-HAZ.
Source: Authors, (2024).
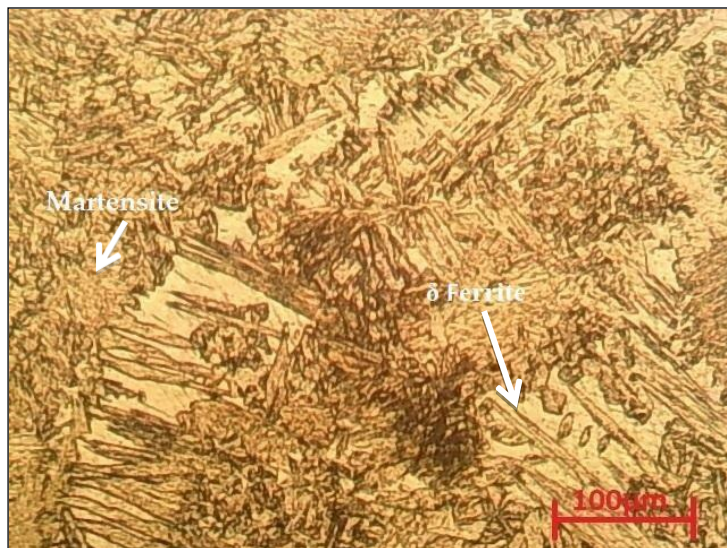
Figure 4.c: Microstructure of Dissimilar weld zone.
Source: Authors, (2024).
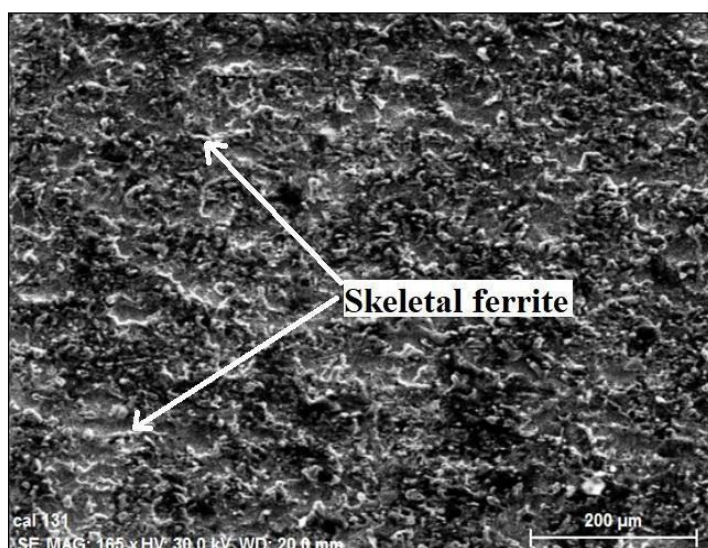
Figure 5: SEM image of a different weld zone.
Source: Authors, (2024).

IV.3 DISTRIBUTION OF ALLOYING COMPONENTS IN WELD ZONE

The distribution of alloying elements in the dissimilar joint was investigated using the EDS mapping technique. The AISI 316/AISI 410 stainless steel filler metal's composition was different from the base materials in the dissimilar welding junction. This alternative filler material can avoid weld cracking and generate the necessary weld metal feature, but it also has the potential to impair the weld quality by causing macro-segregation at the fusion boundary. Bulk welding is created when molten base alloy comes into contact with droplets of the dissimilar filler material during the welding process. According to the line mapping study, no appreciable variations were seen at the weld zone. The elemental mapping investigation showed that Fe, Cr, Ni, Mn, Zn, and Cu were found in similar amounts to figure 6. Figure 7 shows the site where the EDS analysis showed that the fusion zone and the matrix contained nearly similar percentages of elements.
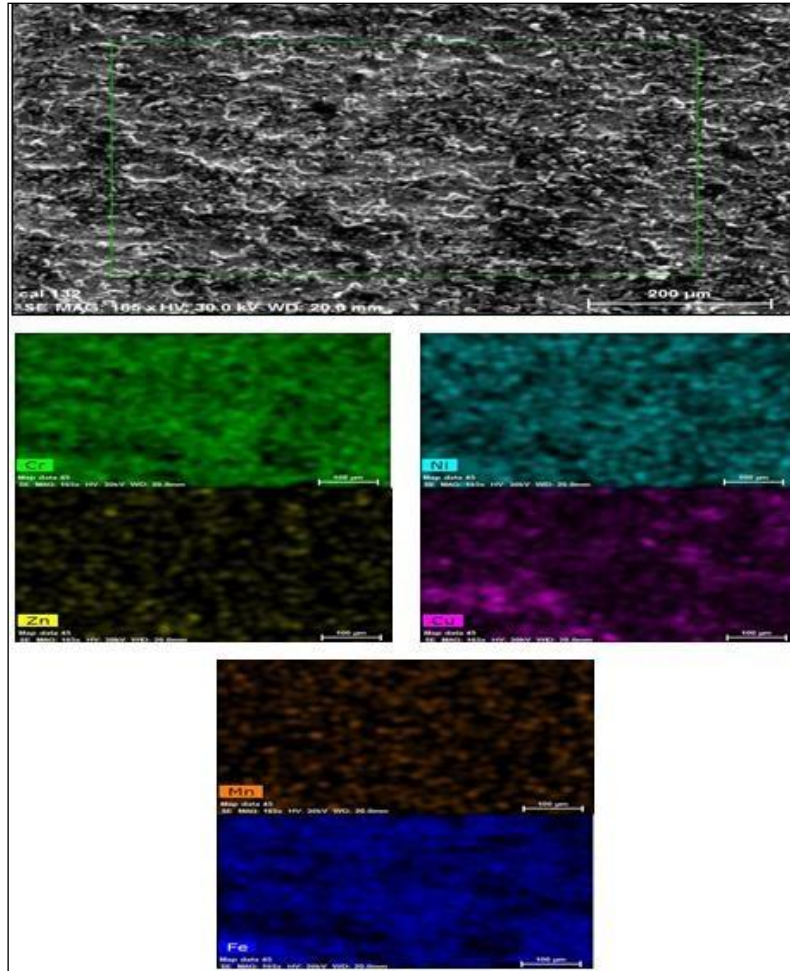
Figure 6: Distribution of alloying elements in Dissimilar weld zone.
Source: Authors, (2024).
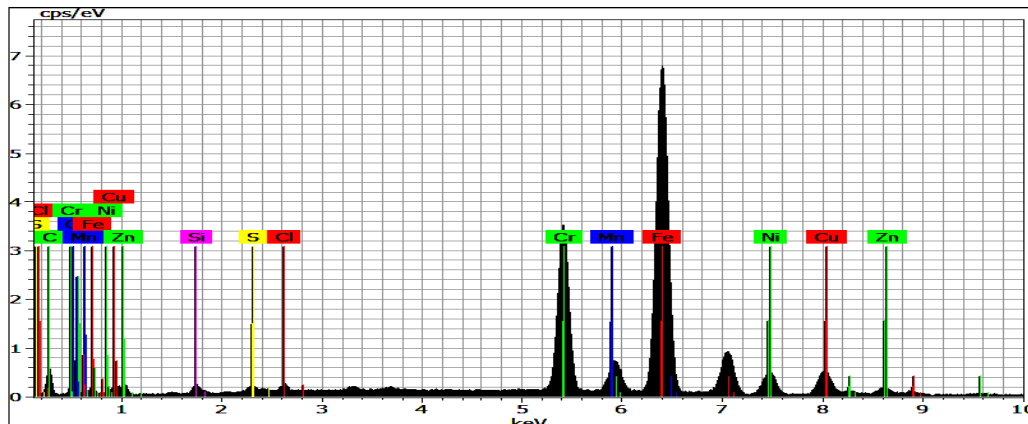
Figure 7: EDS Point Analysis in the weld zone.
Source: Authors, (2024).
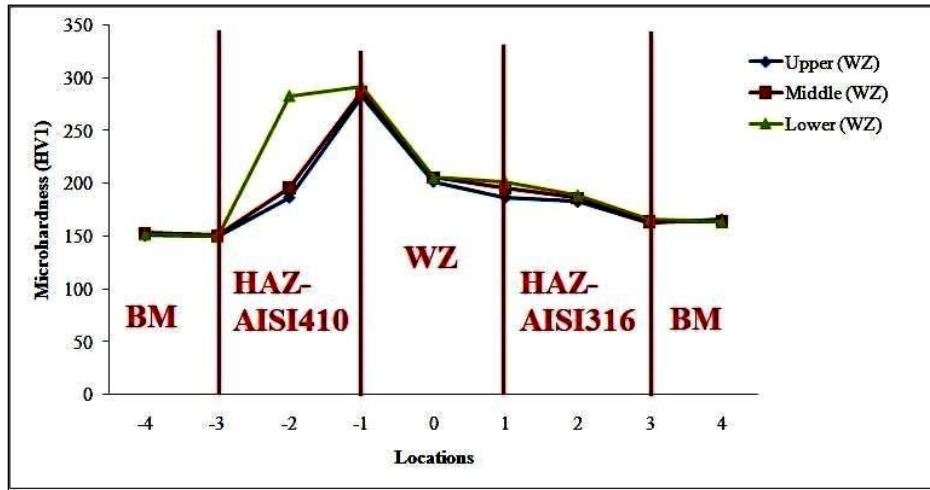
Figure 8: Microhardness Profile.
Source: Authors, (2024).

IV.4 MECHANICAL PROPERTIES OF DISSIMILAR WELD JOINT

Welding was used to create an efficient and faultless dissimilar metal connection between AISI 316 and AISI 410. In the dissimilar weld zone, the mechanical characteristics of tensile and hardness were discovered. The martensite-Heat Affected Zone's tensile strength failure cannot deform as much or as soon as the base metal and weld due to the high martensite content. Thus, martensite formation and grain growth are the main factors influencing tensile strength in HAZ on the AISI 410 side.

The microhardness profile at the top, middle, and bottom of the weld's cross section is shown in Figure 8. The presence of the martensitic microstructure increased the hardness of the weld zone. Every joint exhibited the highest level of microhardness and the same pattern.

V. CONCLUSIONS

Based on the successful and flawless heterogeneous welding of 410-Martensite and 316-Austenitic stainless steel in this investigation, the following conclusions might be drawn:

- It was determined that the optimal combination of three GRG test parameters for quality weld joints is 120 amps for welding current; 2 m/min for welding speed; and 10 lit/min for shielding gas flow rate.
- The welding velocity contributed the most (55.78%) among the experimental parameters, followed by the shielding gas flow rate (13.56%) and current (21.65%), according to ANOVA.
- The different WZ's morphology showed an integrated structure made up entirely of fragile ferrite and a mostly austenitic matrix with no flaws. Heat affected zone in AISI 316 was typically composed of an austenite matrix with low δ ferrite content. The ferrite grain boundaries in the Martensite 410-heat affected zone included a continuous coating of martensite that had developed at a high temperature.
- In dissimilar weld joint, the alloying elements were uniformly distributed in the WZ confirmed through EDS mapping analysis.
- A rise in microhardness upto a median measurement of around 205 HV further demonstrated the predominant

austenitic matrix and skeletal ferrite nature of the WZ microstructure.

VI. AUTHOR'S CONTRIBUTION

Conceptualization: Kathiresan G, Vairavel M and Prabakaran M P.
Methodology: Kathiresan G and Prabakaran M P.
Investigation: Prabakaran M P and Govindarasan D
Discussion of results: Kathiresan G, Govindarasan D and Prabakaran M P.
Writing – Original Draft: Kathiresan G.
Writing – Review and Editing: Prabakaran M P.
Resources: Govindarasan D.
Supervision: Dr. Vairavel.M
Approval of the final text: Kathiresan G, Vairavel.M and Prabakaran M P

VII. REFERENCES

[1] J. CaoJ, Y. Gong, Z. Yang, X. Luo, F. Gu and Z. Hu, "Creep fracture behavior of dissimilar weld joints between T92 martensitic and HR3C austenitic steels", International Journal of Pressure Vessels and Piping, vol. 88, no. 2-3, pp. 94-98, Feb – Mar.2011.

[2] B. Shanmugarajan, P. Sathiya and G. Buvanashekaran, "Mechanical and metallurgical properties of autogenous laser welded P92 material", Journal of Manufacturing Process, vol. 24, pp. 11– 18, Oct.2016.

[3] J. Ni, X. Wang, J. Gong and M. Abdel, "Thermal, metallurgical and mechanical analysis of circumferentially multi-pass welded P92 steel pipes", International Journal of Pressure Vessels and Piping, vol. 165, pp. 164–175, Aug. 2018.

[4] G. Dak, J. Joshi, A. Yadav, A. Chakraborty, N. Khanna, "Autogenous welding of copper pipe using orbital TIG welding technique for application as high vacuum boundary parts of nuclear fusion devices", International Journal of Pressure Vessels and Piping, vol. 188, no. 104225, Dec. 2020.

[5] C.R. Das, A.K. Bhaduri, G. Srinivasan, V. Shankar and S. Mathew, "Selection of filler wire for and effect of auto tempering on the mechanical properties of dissimilar metal joint between 403 and 304L(N) stainless steels", Journal of Material Processing Technology, vol. 209, no. 3, pp. 1428-1435, Feb. 2009.

[6] A.N. Isfahany, H. Saghafian and G. Borhani, "The effect of heat treatment on mechanical properties and corrosion behavior of AISI 420 martensitic stainless steel", Journal of Alloys Compounds, vol. 509, no. 9, pp. 3931-3936, Mar. 2011.

[7] P. Cisquini, S.V. Ramos, P.R.P Viana, V.F. Cunha Lins, A.R. Franco Jr and E.A. Vieira, "Effect of roughness produced by plasma nitro carburizing on

corrosion resistance of AISI 304 austenitic stainless steel", Journal of Materials Research and Technology, vol. 8, no. 2, pp. 1897-1906, Feb. 2019.

[8] R. Kacar and O. Baylan, "An investigation of microstructure/property relationships in dissimilar welds between martensitic and austenitic stainless steels", Materials & Design, vol. 25, no. 4, pp. 317-329, Jun. 2004.

[9] J. Bin Wen, C.Y. Zhou, X. Li, X. M. Pan, L. Chang, G.D. Zhang et al, "Effect of temperature range on thermal-mechanical fatigue properties of P92 steel and fatigue life prediction with a new cyclic softening model", International Journal of Fatigue, vol. 129, no. 1, Aug. 2019.

[10] W.G. Seo, J.Y. Suh, J.H. Shim, H. Lee, K. Yoo, S.H. Choi SH, "Effect of post-weld heat treatment on the microstructure and hardness of P92 steel in IN740H/P92 dissimilar weld joints", Material Characterization, vol. 160, no. 110083, Feb. 2020.

[11] M.P. Prabakaran, G.R. Kannan, "Effect of post weld heat treatment on dissimilar laser welded joints of austenitic stainless steel to low carbon steel", International Journal of Pressure Vessels and Piping, vol. 191, no. 104322, Jun. 2021.

[12] Abishek Ghosh and Pradip Kumar Pal, "Corrosion behaviour of dissimilar TIG welded austenitic stainless steel AISI 304 and martensitic stainless steel AISI 420", Indian Journal of Engineering & Materials Sciences, vol. 27, no.3, pp. 665-669, Jun. 2020.

[13] Caimei Wang, Yang Yu, Jianxing Yu, Zhang Yu, Yan Zhao, Qiwei Yuan, "Microstructure evolution and corrosion behavior of dissimilar 304/430 stainless steel welded joints", Journal of Manufacturing Processes, vol. 50, pp. 183–191, Feb. 2020.

[14] Z. Sun and H.Y. Han, "Weldability and properties of martensitic/ austenitic stainless steel joints", Materials Science and Technology, 1994; vol. 10, no. 9, pp. 823-829, Jul. 1994.

[15] Gaurav Dak and Chandan Pandey, "Experimental investigation on microstructure, mechanical properties, and residual stresses of dissimilar welded joint of martensitic P92 and AISI 304L austenitic stainless steel", International Journal of Pressure Vessels and Piping, vol. 194, no. 104536, Dec. 2021.

[16] A. Kulkarni, D.K. Dwivedi, M. Vasudevan, "Dissimilar metal welding of P91 steel- AISI 316L SS with Incoloy 800 and Inconel 600 interlayers by using activated TIG welding process and its effect on the microstructure and mechanical properties", Journal of Material Processing Technology, vol. 274, no. 116280, Dec. 2019.

[17] N.P. Chandresh, S. Chaudhary, "Parametric optimization of weld strength of metal inert gas welding and tungsten inert gas welding by using analysis of variance and grey relational analysis", International Journal of Research in Modern Engineering and Emerging Technology, vol. 1, no. 3, pp. 48–56, Apr. 2013.

[18] M.P. Prabakaran and G.R. Kannan, "Optimization of laser welding process parameters in dissimilar joint of stainless steel AISI316 / AISI1018 low carbon steel to attain the maximum level of mechanical properties through PWHT", Optics and Laser Technology, vol. 112. pp. 314–322, Apr. 2019.

[19] B. Shanmugarajan, Rishabh Shrivastava, P. Sathiya, G. Buvanashekaran G, "Optimization of laser welding parameters for welding of P92 material using Taguchi based grey relational analysis", Defence Technology, vol. 12, pp. 343–350, Aug. 2016.

[20] Arun Kumar Srirangan, Sathiya Paulraj, "Multi-response optimization of process parameters for TIG welding of Incoloy 800HT by Taguchi grey relational analysis", Engineering Science and Technology: An International Journal, vol. 19, pp. 811–817, Jun. 2016.

[21] Giuseppe Casalino, Andrea Angelastro, Patrizia Perulli, Caterina Casavola, Vincenzo Moramarco, "Study on the fiber laser/TIG weldability of AISI 304 and AISI 410 dissimilar weld", Journal of Manufacturing Processes, 2018; vol. 35, pp. 216-225, Oct. 2018.

[22] G.Casalino and F. Panella. "Microstructural analysis of AISI 304 bars welded with high speed pulsed discharges", Journal of Material Processing Technology, vol. 191, pp. 149–152, Aug. 2007.

Journal of Engineering and Technology for Industrial Applications

RESEARCH ARTICLE   **OPEN ACCESS**

INVESTIGATION OF LEACHATE MIGRATION USING ELECTRICAL RESISTIVITY IMAGING: A CASE STUDY FROM AN ACTIVE DUMPSITE, ILOKUN, ADO-EKITI, SOUTHWEST NIGERIA

Akintunde Akinola Oyedele*[1], Taofeek O. Ewumi[2] and Funmilola Olusola Ogunlana[3]

[1,2]Department of Physics, Ekiti State University, Ado – Ekiti, Nigeria
[3]Department of Physics, Bamidele Olumilua University of Education, Science and Technology, Ikere - Ekiti, Nigeria

[1] http://orcid.org/0000-0003-0428-7566 , [2] http://orcid.org/0009-0009-1724-155X ,
[3] http://orcid.org/0000-0001-9024-273X

Email: *[1]akintunde.oyedele@eksu.edu.ng, [2]taofik.ewumi@eksu.edu.ng, [3]ogunlana.funmilola@bouesti.edu.ng

ARTICLE INFO

ABSTRACT

Geophysical study involving electrical resistivity imaging was conducted at Ilokun municipal solid waste disposal site in Ado-Ekiti, Southwest Nigeria. The study was designed to map the leachate accumulation and extent of migration of leachate plumes in the subsurface. Leachate generated from dumpsite has been recognized as a major concern to public health. Three 2D resistivity profiles were established, one within and two outside the dumpsite. A traverse length of 140 m was kept for the survey. The apparent electrical resistivity data were subsequently inverted into the true electrical resistivity distributions using RES2DINV software to obtain the subsurface image. Electrical Resistivity Imaging (ERI) revealed leachate accumulation (low resistivity zones of 4.98 – 13.30 Ωm) within the shallow subsurface of the dumpsite up to a depth of 10 m. A fractured zone was delineated within the subsurface. This zone of enhanced porosity and permeability spanning a distance of about 20 m offers the main conduit / seepage path for the leachate to percolate through the subsurface formation. Landfill leachates are potentially harmful to the environment and to human health. Proper mitigation measures are necessary to protect the shallow groundwater system, soil and the environment.

I. INTRODUCTION

Municipal solid waste (MSW) is continuously produced by human being all over the world. Dumping of solid waste in the non-engineered landfills is very common in the developing countries. Land disposal facilities are increasingly becoming hazardous to human health and the environment [1-3]. Among the disadvantages of open dumping, leachate, the aqueous effluent generated from solid waste owing to physical, chemical, and biological alterations, has been identified as the major concern to public health. Leachate is a wastewater formed due to precipitation, deposited waste moisture, and water formed within the body of the dumpsite. The generation of landfill gasses and secretion of leachate constitute health concerns for the population on-site and vicinity of the dumpsites [1],[4],[5].

Leachate is a toxic by-product generated from the landfills. It remains one of the key anthropogenic heavy metal sources in environment and a major concern to human health [1],[6],[7]. The heavy metals leach out from the soil and enter the underlying aquifer, which affects the livelihood of the surrounding community. It has been a source of groundwater contamination worldwide [6]. Leachate can percolate to the groundwater and consequently migrate in surface water [4],[8],[9].

The leachate composition can vary widely depending on the age of the landfill and the type of waste it contains. It usually contains both dissolved and suspended materials. Precipitation is acknowledged as the principal contributor to generation of leachate [1],[5]. Detailed investigation revealing the leachate curtailment capacity (LCC) of the dumpsite and the adjoining areas is essential [2],[3],[7].

The Ilokun MSW dumpsite, is a piece of land located off Ado - Iworoko Road on the outskirts of Ado Ekiti, Southwest Nigeria (Figure 1). It is an open waste dumpsite designated for disposal of varied categories of waste materials. It accommodates household, industrial and commercial waste. Urban sprawl occasioned in part

by the rapid growth in the urban population is fast becoming evident within the axis.

The study area is underlain by the Precambrian Basement Complex, which comprises of the migmatite gneiss quartzite complex; the slightly migmatised to unmigmatised metasedimentary schists and metaigneous rocks; the charnockitic, gabbroic and dioritic rocks; and the members of the older granite suite. Migmatite constitutes the main rock unit at the location. The area is associated with two distinct seasons (wet and dry seasons) typical of the tropical climate with annual rainfall of about 1300 mm and mean annual temperature of 27°C [2],[10].
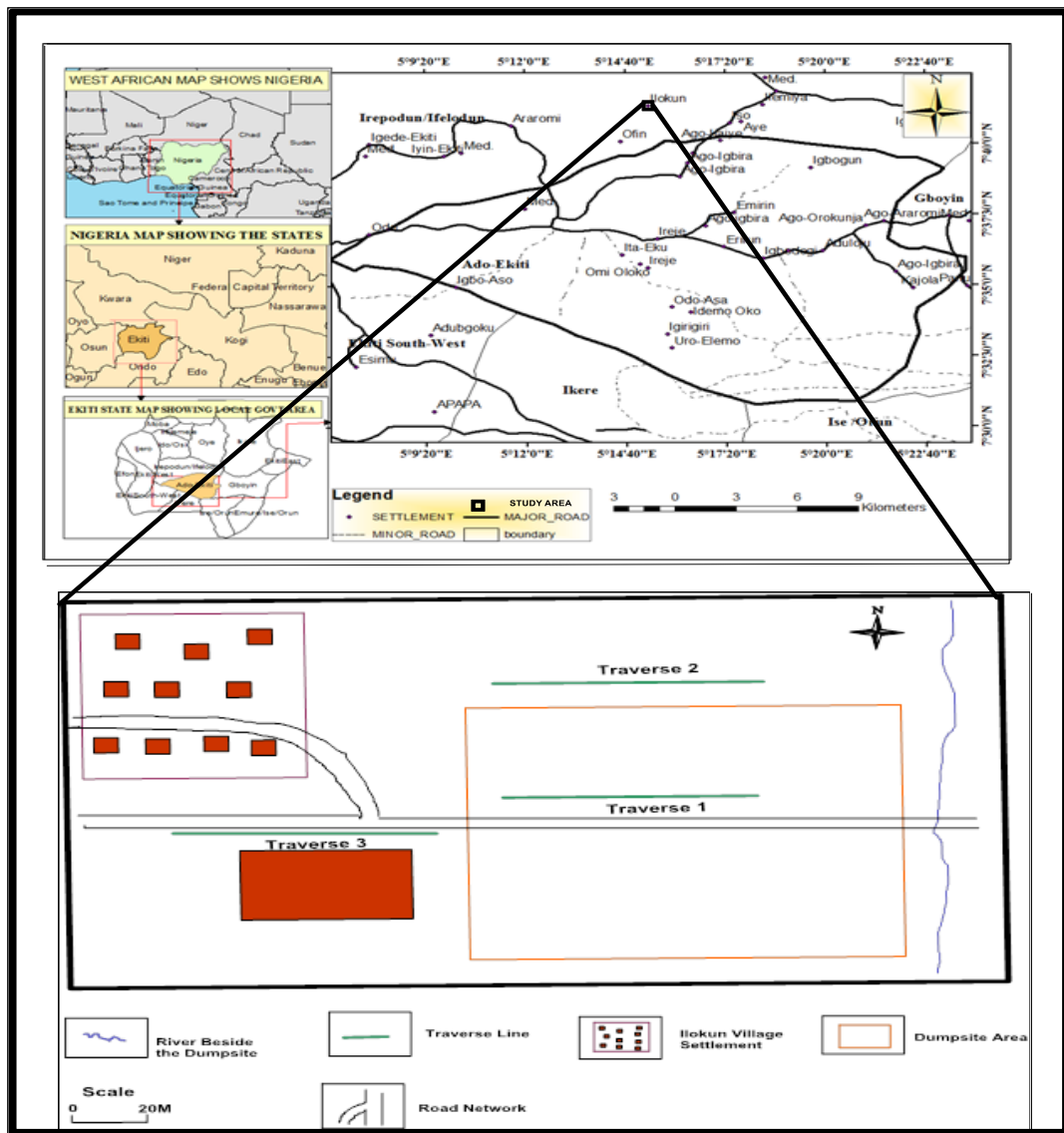
Figure 1: Location map showing the study area.
Source: Authors, (2024).

II. THEORETICAL REFERENCE

Electrical Resistivity Imaging (ERI) is a non-invasive geophysical technique developed to interpret the nature of the subsurface without altering the dynamic status of the soil mass [10-12]. ERI measures the resistivity changes both in the vertical direction, as well as in the horizontal direction along a common survey line simultaneously. The technique provides the electrical image of subsurface soil. It is well suited to investigate areas with moderately complex geology such as the crystalline basement complex of southwestern Nigeria [7],[11],[13].

Electrical resistivity tomography is increasingly becoming an essential tool in subsoil characterization including environmental studies as it provides high-resolution electrical images of the subsurface geomaterials and structural disposition. Geophysical methods have been applied to characterize the subsurface with huge success [7],[11],[14],[15]. Leachate accumulation/plume is characterized by typically low resistivity spectrum [13],[16],[15].

This paper examines the phenomenon of leachate migration in the soil at the Ilokun dumpsite, Ado-Ekiti. The use of electrical resistivity imaging, a noninvasive geophysical technique will

enable visualization of the leachate migration in the soils and in waste containment application systems in the absence of sanitary landfill liners.

III. MATERIALS AND METHODS

The field investigations utilized Electrical Resistivity Imaging (ERI) technique. It is a geophysical technique for imaging subsurface structures from electrical resistivity measurements made at the surface [11],[14].

Measurements were conducted along three 2-D ERI traverses using dipole-dipole array; a traverse of length 140m located within the dumpsite and two resistivity profiles established outside the dump basically to serve as controls. The field work was run with a unit of OMEGA CAMPUS SAS 1000 RESISTIVITY METER and its accessories. Point coordinates and elevations were recorded using a hand-held Garmin GPS device.

A controlled current (I) was injected into the ground by two steel current electrodes and the potential drop (V) was acquired by two others, the potential electrodes. The terrameter gave the apparent resistivity values digitally as computed from Ohm's law. The apparent electrical resistivity data were subsequently inverted into the true electrical resistivity distributions by the RES2DINV software to obtain the subsurface image. The software employs an optimization algorithm that adjusts the 2-D electrical resistivity model by iteratively reducing the difference between the calculated and measured apparent electrical resistivity values until good fit. Leachate plumes are often more electrically conductive than the host formation. Characteristically low resistivity values are thus diagnostic of the leachate accumulation within the local geological setting [10],[16],[17].

IV. RESULTS AND DISCUSSIONS

The 2-D resistivity image along traverse one located within the dumpsite (Figure 2) delineated leachate accumulation (characterized by typically low resistivity values ranging from 4.98 – 13.3 Ωm) with bluish coloration spanning a distance of about 85 m along the traverse and depth of 10m. [10], reported resistivity value less than 10 Ωm, as an evidence of leachate plume accumulation in the study of Lapite Dumpsite in Ibadan, Southwestern Nigeria. Dumont et al. [16] reported resistivity values of only a few Ωm inside the investigated waste dump. The characteristic value of as low as 5 Ωm was observed within the deposit area while the host formation outside of the landfill was characterized by higher values of resistivity. Similarly, the study of [13] showed the leachate plume as low resistivity zones (4.06 – 48.5 Ωm) in the investigation of leachate migration from Banwuya refuse dumpsite, Bida, Niger State, Nigeria. Higher resistivity values were obtained for areas outside the dump.

Significantly, a structural feature diagnostic of a fracture was observed within distances 90m to 110m along the traverse. Fractures are produced by weathering and tectonic processes. These features are associated with enhanced secondary porosity and permeability [17]. The fractured zone characterized by resistivity values ranging from 13.3 to 22.7 Ωm occurring within the zone suggests a preferred conduit or seepage path for the migration of the leachate into the subsurface formation [15],[18].
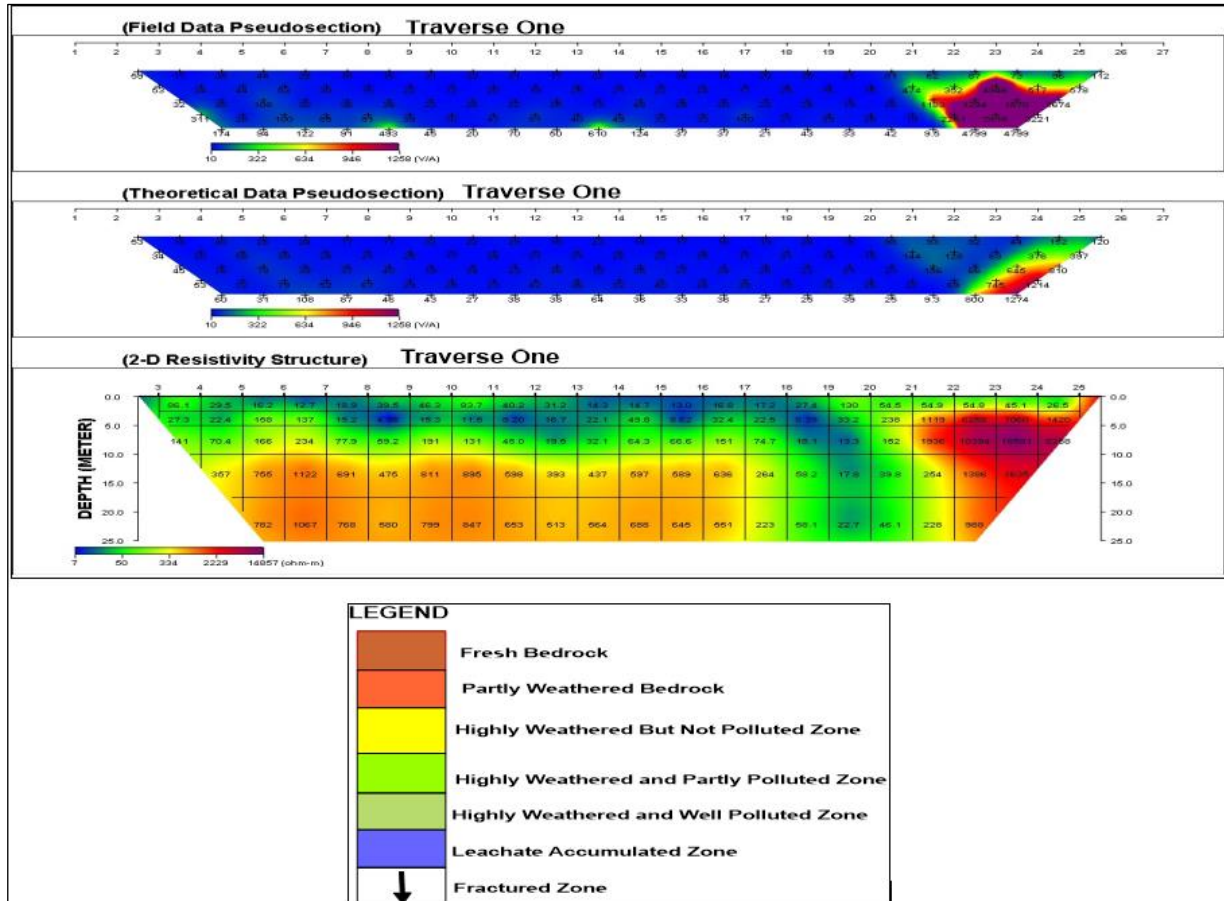
Figure 2: Resistivity 2-D image along traverse one.
Source: Authors, (2024).

The groundwater formations around this area are largely susceptible to the dumpsite leachate pollution as a result of the wide fracture extending to the bedrock. This can pose a great threat to the groundwater quality. [1],[4],[5] and similar works decried the release of pollutants from landfills into the soil, surface water, and groundwater of the surrounding environment as one of the most critical environmental problems of the present age.

Figure 3 shows the 2-D electrical resistivity image of traverse two located beside the dumpsite. This traverse was established to monitor the migration of the leachate into the formations around the dumpsite. The 2-D resistivity image indicated largely weathered and fractured bedrock. The fractures lying along North-south direction of the study area are characterized by resistivity values generally less than 100 Ωm. The graphic depth sections of the thickness and resistivity of the subsurface revealed leachate accumulation within distances 55 to 60m and 75 to 85m at a depth range of 3 to 10m.
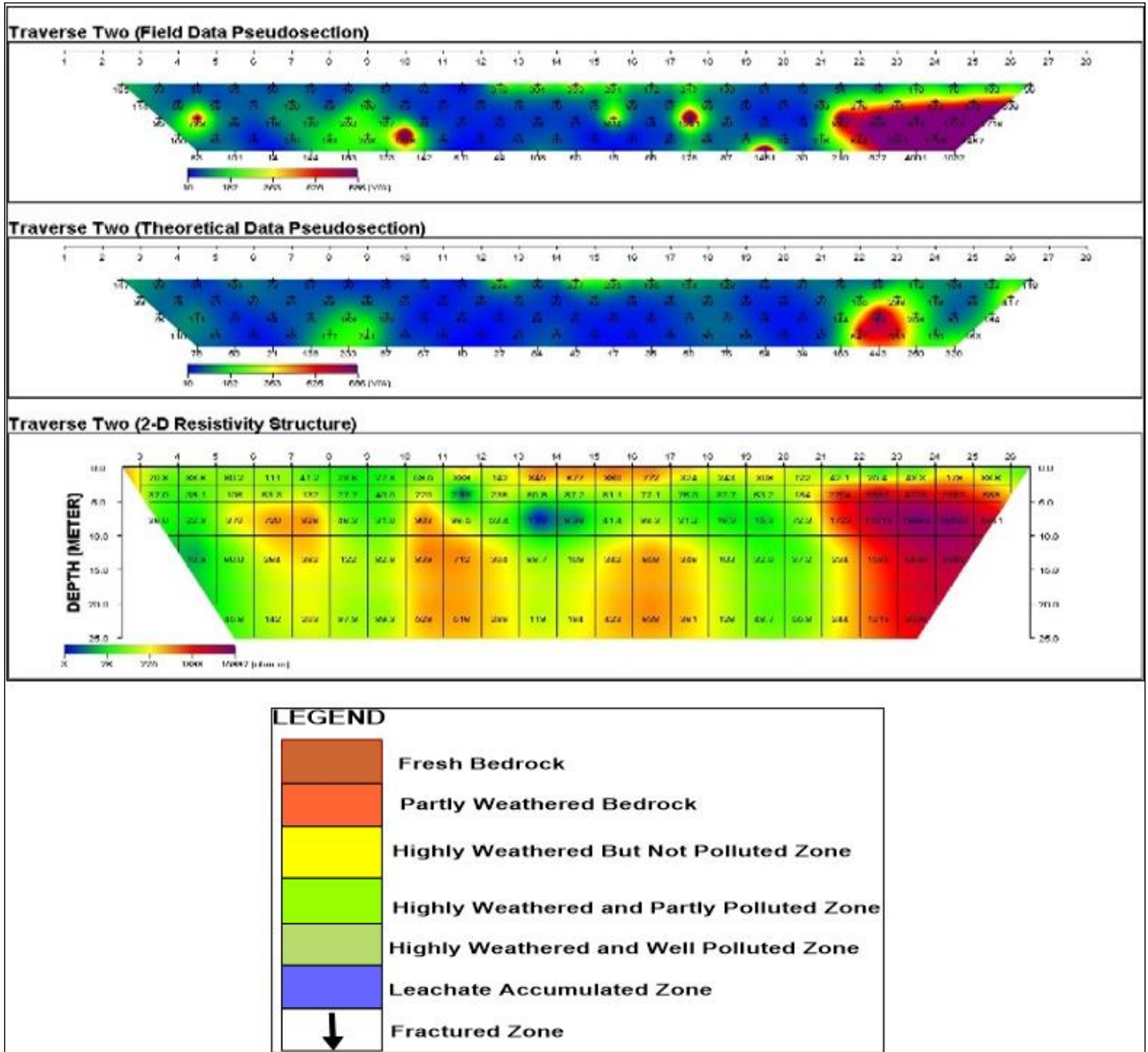
Figure 3: Resistivity 2-D image along traverse two.
Source: Authors, (2024).

The 2-D resistivity image along traverse three is presented in Figure 4. The traverse was established outside the dumpsite to observe the migration of the leachate along east-west direction. The section captured the leachate migration along east-west direction as indicated within distances 140/90m in the east-west direction. Relatively very low resistivity values ranging from 2.54 to 4.94 Ωm were observed across the accumulation of the migrated leachate occurring between distances 60 and 85m at depths ranging between 10m and 25 m. The potential of leachate accumulation is relatively higher along the east-western axis.
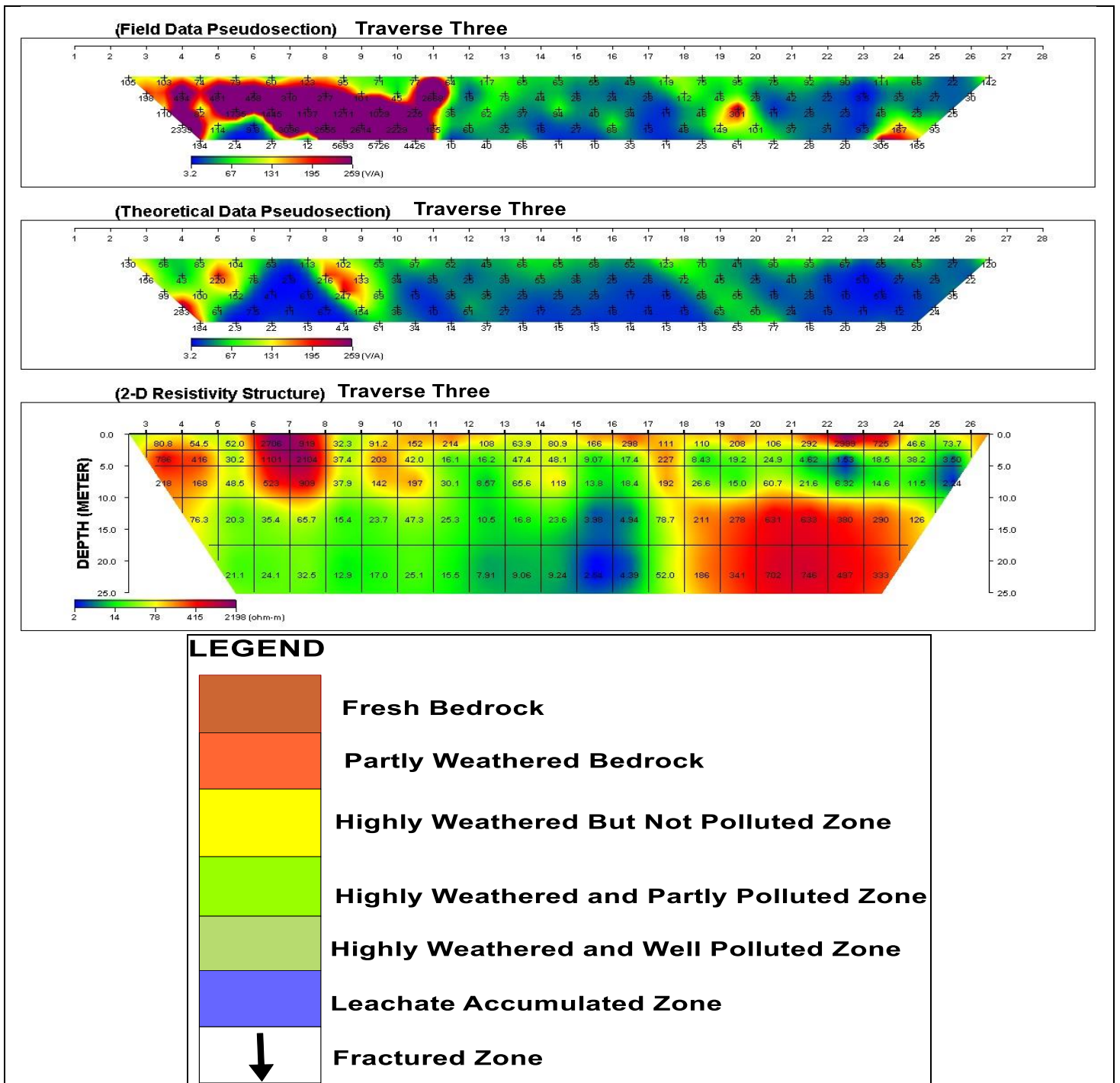
Figure 4: Resistivity 2-D image along traverse three.
Source: Authors, (2024).

The stacked inverse resistivity models of the subsurface, Figures 5 & 6 revealed the fractured zone, leachate accumulation, extent of leachate plumes, bedrock and seepage path from the dumpsite. Remarked that the plume would extend towards the main fracturing direction of the crystalline bedrock [15]. The leachate has virtually permeated the weathered portion of the study area with prevalence along the east-west axis (Figure 6). The horizontal and vertical extent of leachate plumes were delineated by the geo-electrical imaging as a response to the varying electrical resistivity in the contaminated area [10],[17].
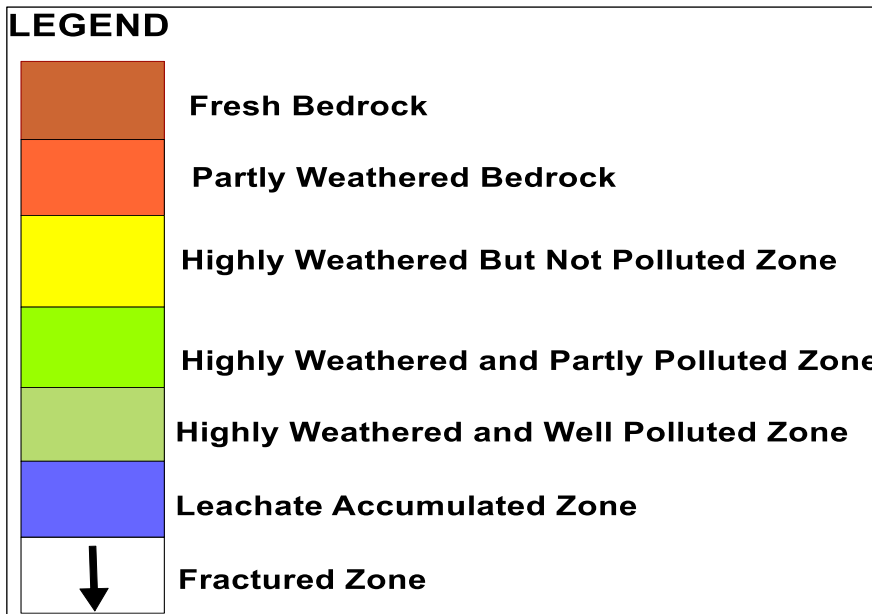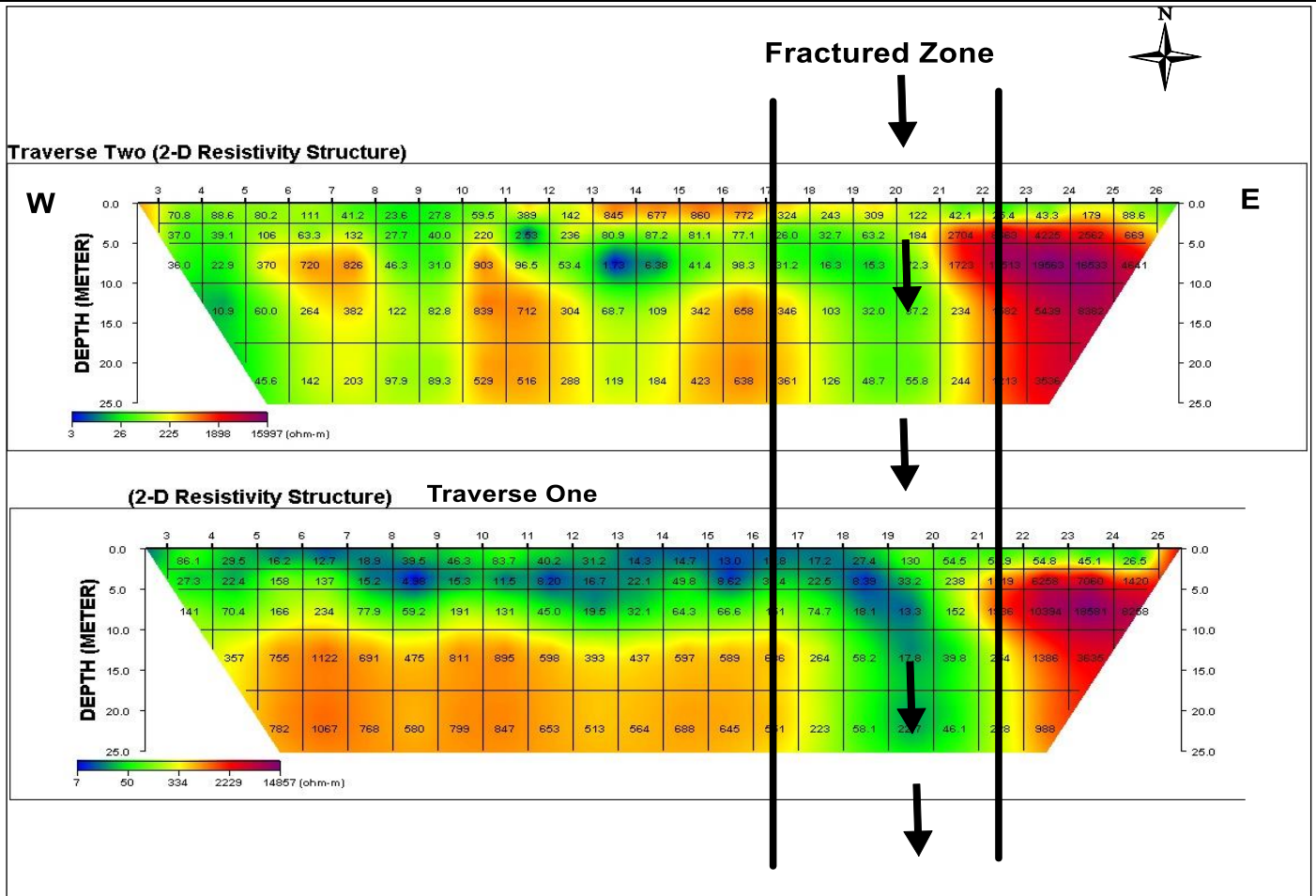
Figure 5: Stacked 2-D Resistivity image along traverse one and traverse two.
Source: Authors, (2024).

Solid waste disposal in a landfill causes leachate production whose discharge to soil layers carries soil and leachate contaminants to the groundwater. Observed that the rate of migration of leachate decreased when the fines content in the subsurface formation increased [6]. With the fines, associated porosity and permeability are reduced in contrast with enhanced porosity and permeability in weathered and fractured formations.
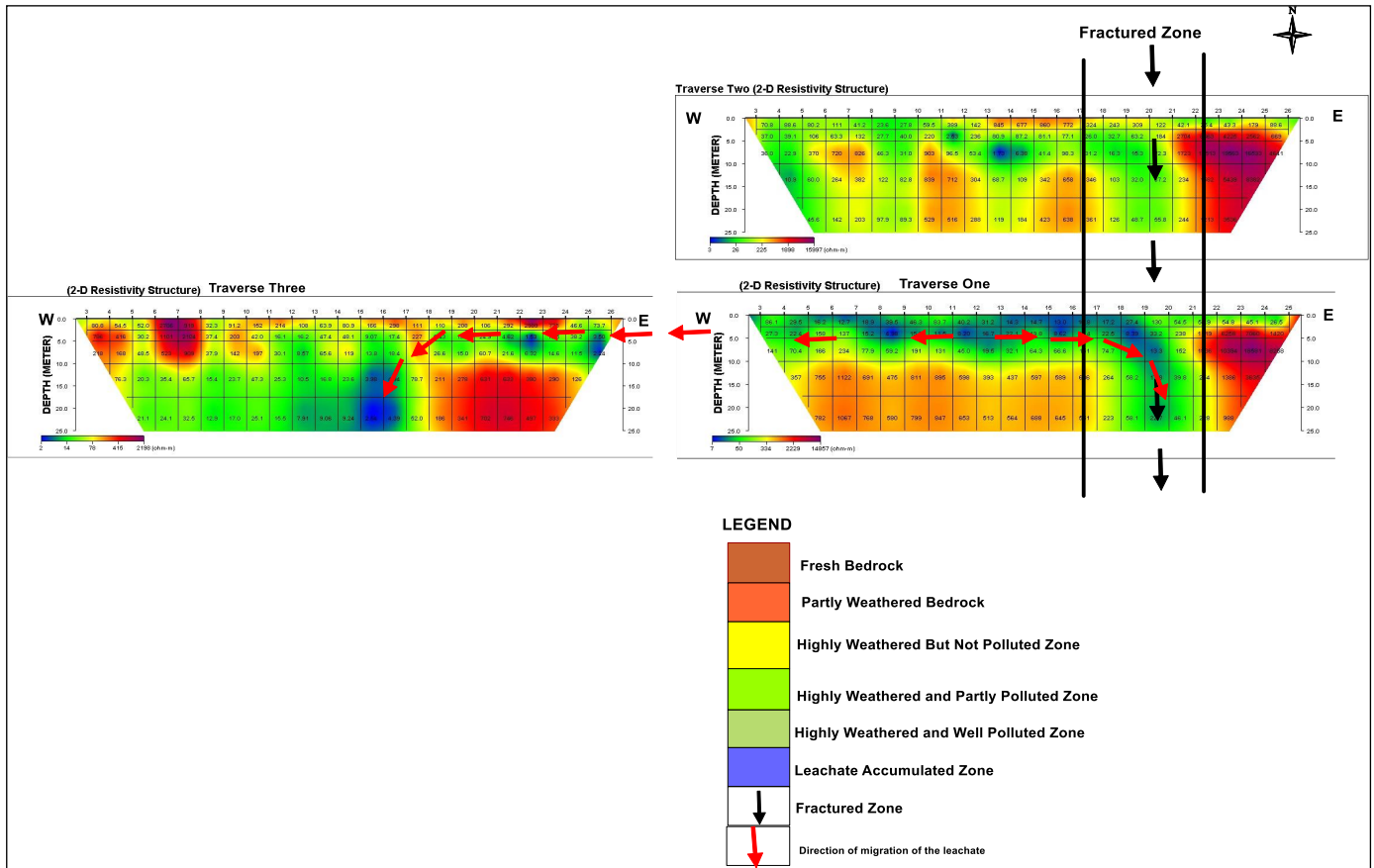
Figure 6: Stacked 2-D Resistivity image along the traverses.
Source: Authors, (2024).

Occurrence of tectonic activities such as fracturing, faulting and intense weathering promotes high porosity and permeability with increase in the rate of migration of leachate. A candidate landfill site should be sufficiently thick and of low permeability (clay material). The geological setting occurring at the Ilokun dumpsite as delineated by the electrical resistivity imaging does not offer requisite minimum leachate curtailment capacity (LCC). A clay overburden thickness of about 15 m which acts as leachate filter is a standard for determining the LCC of a dumpsite. Investigation of the subsurface is thus a compulsion before waste disposal site is developed [2],[7].

Poor management of municipal solid waste leads to potentially devastating environmental and health hazards. The dumpsite leachate inherently results in contamination of the soil, groundwater and surface water in the absence of containment systems with free leachate migration from the dumpsite into surrounding environment [17]. The need to protect groundwater resources cannot be overemphasized in any area where the majority of the population derive potable water from the shallow aquifers. Protection of domestic and public water supplies is sacrosanct basically to avoid unpleasant consequences. In developing countries, it is a general remark that high proportions of diseases are directly related to poor drinking water quality and unhygienic conditions [1],[2],[15]. Proper mitigation measures are necessary to protect the shallow groundwater system.

V. CONCLUSIONS

Leachate generated from dumpsite is a major concern to public health. ERI provides a noninvasive geophysical tool to map the leachate migration. The 2D-ERI method revealed features of the subsurface as topsoil, weathered, fractured and fresh basement. The study delineated the preferential leachate migration pathways within weathered/fractured overburden. This methodology has the added merits of saving cost and time compared to the drilling-sampling-analyses approach. The production of dumpsite leachate and its migration portend huge risk to the environment and public health. The dumpsite of such myriads of solid wastes would contain large numbers of pathogenic and opportunistic bacteria. Waste management should embrace engineered landfill sites in place of unregulated open dumping. Groundwater quality should be monitored with the use of observation wells. Remote sensing, rapid noninvasive field survey and screening should be encouraged for necessary response.

VI. AUTHOR'S CONTRIBUTION

Conceptualization: Oyedele
Methodology: Oyedele, Ewumi and Ogunlana
Investigation: Oyedele, Ewumi and Ogunlana
Discussion of results: Oyedele, Ewumi and Ogunlana
Writing – Original Draft: Oyedele
Writing– Review and Editing: Ewumi and Ogunlana
Resources: Oyedele, Ewumi and Ogunlana
Supervision: Ewumi and Ogunlana
Approval of the final text: Oyedele, Ewumi and Ogunlana

VII. ACKNOWLEDGMENTS

VIII. REFERENCES

[1] Daniel AN, Ekeleme IK, Onuigbo CM, Ikpeazu VO, Obiekezie SO, (2021) Review on effect of dumpsite leachate to the environmental and public health

implication. GSC Advanced Research and Reviews, 2021, 7(2), 051–060, DOI: https://doi.org/10.30574/gscarr.2021.7.2.0097

[2] Oyedele AA, Omosekeji AE, Ayeni OO, Ewumi TO, Ogunlana FO, (2022). Delineation of Landfill Sites for Municipal Solid Waste Management using GIS. Journal of Human, Earth, and Future, 3(3), 321 - 332. doi.org/10. 28991/HEF-2022-03-03-05

[3] Akhtar S, Hollaender H, Yuan Q, (2023) Impact of heat and contaminants transfer from landfills to permafrost subgrade in arctic climate: A review. Cold Regions Science and Technology, 206, 103737, https://doi.org/10.1016/j.coldregions.2022.103737.

[4] Naveen BP, Sumalatha J, Malik RK, (2018) A study on contamination of ground and surface water bodies by leachate leakage from a landfill in Bangalore, India. Geo-Engineering, 9(27), https://doi.org/10.1186/s40703-018-0095-x

[5] Dixit A, Singh D, Shukla SK, (2023) Assessment of human health risk due to leachate contaminated soil at solid waste dumpsite, Kanpur (India). International Journal of Environmental Science and Technology, https://doi.org/10.1007/s13762-023-04868-y

[6] Yamusa YB, Sa'ari R, Ahmad K, Alias N, Mustaffar M, Foong LK, (2019) Monitoring Leachate Migration in Compacted Soil Using Digital Image Technique, Engineering, Technology & Applied Science Research, 9(1), 3685-3691.

[7] Adenuga OA, Popoola OI, (2020) Subsurface characterization using electrical resistivity and MASW techniques for suitable municipal solid waste disposal site. SN Applied Sciences, 2(9), 1-16. doi:10.1007/s42452-020-03320-x.

[8] Isinkaye MO, Oyedele EA, (2014) Assessment of Radionuclides and Trace Metals in Soil of an Active Designated Municipal Waste-Dumpsite in Ado-Ekiti, Nigeria. Journal of International Environmental Application & Science, 9(3), 402-410.

[9] Parvin F, Tareq SM, (2021) Impact of landfill leachate contamination on surface and groundwater of Bangladesh: a systematic review and possible public health risks assessment. Applied Water Science, 11, 100 https://doi.org/10.1007/s13201-021-01431-3

[10] Ganiyu SA, Badmus BS, Oladunjoye MA., Aizebeokhai AP, Olurin OT, (2015) Delineation of Leachate Plume Migration Using

Electrical Resistivity Imaging on Lapite Dumpsite in Ibadan, Southwestern Nigeria. Geosciences, 5(2), 70-80 DOI: 10.5923/j.geo.20150502.03

[11] Loke MH, Chambers JE, Rucker DF, Kuras O, Wilkinson PB, (2013) Recent developments in the direct-current geoelectrical imaging method. Journal of Applied Geophysics, 95,135–156, http://doi.org/10.1016/j.jappgeo.2013.02.017.

[16] Dumont G, Robert T, Marck N, Nguyen F, (2017) Assessment of multiple techniques for characterization of municipal waste Deposit sites. Journal of Applied Geophysics, 145, 74–83.

[14] Sibula I, Plado J, Jõeleht A, (2017). Ground-penetrating radar and electrical resistivity tomography for mapping bedrock topography and fracture zones: a case study in Viru-Nigula, NE Estonia. Estonian Journal of Earth Sciences, 66(3), 142-151.

[17] Mosuro GO, Omosanya KO, Bayewu OO, Oloruntola MO, Laniyan TA, Atobi O, Okubena M, Popoola E, Adekoya F, (2016) Assessment of groundwater vulnerability to leachate infiltration using electrical resistivity method. Applied Water Science, 7, 2195–2207, https://doi.org/10. 1007/s/3201-016-0393-4

[15] Barry AA, Yameogo S, Ayach M, Jabrane M, Tiouiouine A, Nakolendousse S, Lazar H, Filki A, Touzani M, Mohsine I (2021) Mapping Contaminant Plume at a Landfill in a Crystalline Basement Terrain in Ouagadougou, Burkina Faso, Using Self-Potential Geophysical Technique. Water, 13, 1212, https://doi.org/ 10.3390/w13091212

[12] Metwaly M, AlFouzan F, (2013) Application of 2-D Geoelectrical Resistivity Tomography for Subsurface Cavity Detection in the Eastern Part of Saudi Arabia. Geoscience Frontiers, 4, 469-476. https://doi.org/10.1016/j.gsf.2012.12.005

[13] Rafiu AA, Abu MA, (2017) Investigation of Leachate Migration from Banwuya Public Refuse Dump Site, Bida, Niger State, Nigeria. Journal of disaster risk management, 2(1), 82-92.

[18] Oyedele AA, (2019) Use of remote sensing and GIS techniques for groundwater exploration in the basement complex terrain of Ado-Ekiti, SW Nigeria. Springer Applied Water Science, 9, 51 - 63.
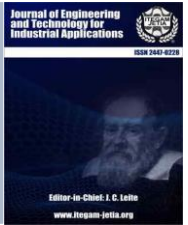
RESEARCH ARTICLE   **OPEN ACCESS**

WEAPON DETECTION AND CLASSIFICATION USING DEEP LEARNING

Sunil B. Mane[1]

[1]Dept. of Computer Science and Engineering COEP Technological University (COEP Tech) Pune, Maharashtra, India.

[1]http://orcid.org/0000-0002-7111-4908

Email: sunilbmane.comp@coeptech.ac.in

ABSTRACT

High gun-related crime rate poses a great threat to society in the present world. There is a serious need for systems to deal with such gun-related crimes. As CCTVs are installed in almost every part of the city, using the CCTV footage to detect the weapon is the simplest and efficient way to deal with such crimes. Unconcealed weapon detection, in images and videos, can help reduce the number of homicides due to the gun-related violence. In this work, we focus on developing a robust and automatic weapon detection system with ability to classify the detected weapon into different categories. This work provides and extensive survey on already existing weapon detection systems, weapon detection datasets, challenges in weapon detection and deep learning-based object detection technologies. We have developed a new image dataset for weapon detection and classification task. The experimental analysis shows the superiority of the Faster-RCNN models over SSD models for weapon detection systems. The detection results show how the final developed system deals with different challenges related to weapon detection and classification in real world scenarios.

I. INTRODUCTION

The crime rates due to the use of weapons have increased drastically in recent years. The survey [1] shows an average of 32.23% of total homicides by guns and a total of 128k homicides due to guns combined for all the countries. Gun violence is a very concerning issue in every nation, especially in countries where owning a gun is legal. According to a survey [1] average of 10.42 guns are owned per 100 people by the entire world. Despite the efforts taken to control gun violence, the crime rates have not fallen even a bit in the past few years. Crimes involving weapons like knife, hand-held guns, assault rifles, etc includes robbery and are primarily carries out in public places and banks where CCTVs are installed. Computer vision is a prominent domain in Artificial Intelligence as it deals with analysis and extraction of information from images or sequence images. The visual data present is vast, and it is ready to be used for dealing with real world issues. The image or video data generated and upload to the internet today is mind blowing. Forbes 2018 survey [2] tells that every minute 300 hrs of the video is uploaded just on YouTube, which is a very high amount of data for a single video sharing platform. Also, 300 million photos get uploaded on Facebook every day. CCTV and cameras are present everywhere and the data generated from them can be used for solving social issues. Object Detection is Computer Vision technology to detect instances of a real-world object in an image or a video. The problem definition of object detection is to spatially locate the object in the image, known as Object Localization and to predict the class of the object, known as Object Classification. The use of object detection for solving real-world problems has increased tremendously. Object detection has proved tremendous use in the field of Artificial Intelligence where image and video analysis are prominent. Object detection forms the basis for solving more complex problems such as autonomous vehicles, image segmentation, intelligent video surveillance, robotic vision, and many more. Due to the advancements in deep learning, there has been a drastic increase in accuracy as well as the performance of the deep learning models. Application of deep learning models

in computer vision has created a pathway for solving many problems related to object detection. With the introduction of Region based Convolutional Neural Network (R-CNN) [3] for feature extraction, the accuracy of the object detection systems has been significantly increased. Convolutional Neural Networks (CNN) are comparatively deeper than traditional feature extraction techniques and can learn multiple and more complex descriptors automatically. Deep convolutional neural networks (DCNN) used in deep learning models have proved way more accurate than hand-made technique in extracting features from images. The feature maps generated by CNNs are more useful for detection of the spatial location of the image while the features generated by the previous generation technique lacked the capability to spatially locate the detected image. The region-based deep CNN models are capable of detecting the object even if a part of the object is visible provided that the visible part is more than some threshold.

In this research work, the focus is on building a weapon detection system which would have capabilities to classify the detected weapon based on the predefined weapon categories. The task of classification is only possible if labels are provided with the bounding box annotations in the dataset used for training. We found that the dataset required for developing a weapon detection and classification dataset was not freely available. Hence, we also focus on developing an image dataset for weapon detection and classification dataset, with bounding box annotations as well as the weapon class labels. In Section 2, we have provided survey of the existing state of weapon detection systems along with its advantages and disadvantages and weapon detection datasets and their limitations. In Section 3, we provide the steps taken while preparing our own weapon detection and classification dataset and the details of the final dataset. In Section 6 we describe the implementation framework used in this work and evaluation results of all the models used in this experimental analysis. In Section 8 we show the detection results of the final system developed in this work and see how well the system addresses the different challenges in weapon detection systems. Finally, we conclude our work in Section 8.5 and provide some directions for future work related to the domain of weapon detection and classification using deep learning.

II. PREVIOUS WORK

Several weapon detection systems have been implemented in the last decade using various methods and algorithms. In current section will be discussing their assets and liabilities with respect to various aspects which includes the nature of the problem statement, approach and algorithm used to train and deploy the model, the dataset used for training and testing, the accuracy and efficiency of the system in terms of multiple metrics [4]. Used state-of-the-art Faster R-CNN [5] model on Internet Movie Firearm Database (IMFDB) using VGGNet-16 [6] architecture without the use of GPUs. The model was pre-trained on ImageNet [7] dataset and they used Stochastic Gradient Descent (SGD) for fitting the model and updating the weights. They talked about challenges in Firearm detection in terms of occlusion, inter-class variation, and noises in the images of the gun. The model used for detection achieved 93% accuracy with Boosted Tree classification which outperformed KNN with 91.5% accuracy and SVM classification with 92.6% accuracy. The trained model was only capable of detecting a weapon but not classifying a weapon into different weapon category. Talked about challenges such as occlusion and dataset creation, especially for gun detection. They compared two detection algorithms: Sliding window approach and region-based approach [8]. The dataset used contained 3000

images of handheld guns in varying context. Similar to [4], they used Faster R-CNN [5] model based on VGGNet16 [6] architecture which was pre-trained on ImageNet dataset. The model achieved 100% recall and 84.21% precision. Also, the system uses SVM classifier to fire the alarm based on the input from the detection algorithm which gave five successive True Positives within a 0.2s interval in 27 out of 30 different scenes. The dataset used for training purpose was not benchmarked and hence the comparative study of used models to the state-of-the-art models is not possible. Akcay et al. [9] compared different frameworks including Sliding Window based CNN (SW-CNN) [10], R-CNN [3], Fast R-CNN [11], R-FCN [12] and YOLOv2 [13] using architectures: AlexNet [14], VGGNet-16 [6] and ResNet [15] with different pipelining, for detection of guns, laptops and other items in X-ray images. The results they obtained while experimenting clearly shows the superiority of Faster R-CNN based ResNets in object detection with 98.6% accuracy. CNN feature extraction proved to be superior then Bag of VisualWords (BoVW) with entire network achieving 99.6% True positive, 99.4 Accuracy and 0.011 False positives. The trained model was only capable of detecting weapons in X-ray images that have only one channel (greyscale) and hence cannot be used for detection of weapons in normal images.

For [16] compared VGGNet-16 [6] and GoogleNetOverFeat [17] for detecting handguns in an input image or video file. The dataset used for training and evaluation purpose was IMFDB. OverFeat was used with three different sets of hyper-parameters. OverFeat with 30% confidence threshold and 0.0003 learning rate outperform other mentioned models and achieved an excellent training accuracy of 93% and test accuracy of 89%. The experimentation showed how hyper-parameter tuning can improve the accuracy and performance of the deep learning models. Despite achieving high accuracy rates, the model lacked the capability classify the detected gun to be introduced in real life system as the speed of the detection was very slow (1.3s per classification). Several weapon detection systems were developed using deep learning techniques, but these weapon detection systems lack some of the required features such as classifying the weapons detected into various categories based on the type of the gun, such as handguns, knives, assault rifles, etc.

III. DATASET PREPARATION

For training a deep learning model for detection of weapon, image dataset is required. Existing image datasets for weapon detection, cannot be used for classification of the weapon into various categories. For such classification, image dataset must have bounding box annotations with proper class labels. These labels are then used by the deep learning model to correctly predict the class of the weapon detected in the image. To overcome the accuracy-related issues, many image conditions were taken into consideration while preparing the dataset. The image conditions considered are: – Illumination conditions: day, night – Blur and Motion – Different viewpoints – Different colors – Different environments: war, city, movies, cartoons – Different conditional situation – firing, holding, – Various types of weapons in same category. (For e.g. in Handguns – automatic, folding, revolver, self-loading and in Assault-rifles – ak47, m4, g36) We have compiled an image dataset with images containing the instances of single or multiple weapons of various weapon categories. Figure 1 shows the working of the data collection and data preparation steps used for compiling the weapon dataset. The steps in the weapon dataset creation are as follows:
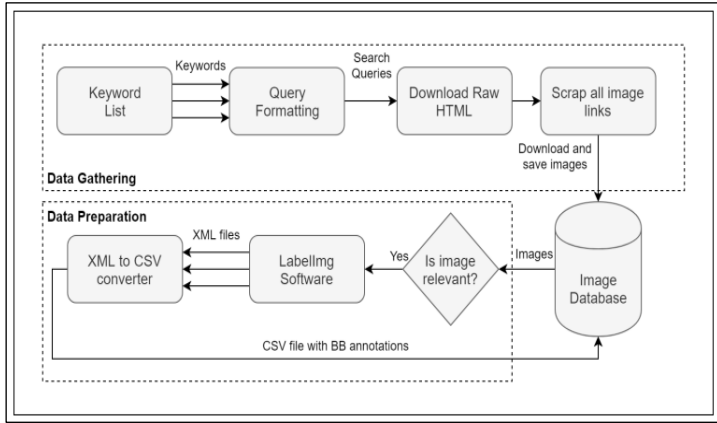
Figure 1: Workflow of weapon detection and classification.
dataset creation.
Source: Author, (2024).

IV. DATA COLLECTION USING WEB SCRAPING

We have used a pre-existing module to scrap the images from internet. The working of the script is as follows:

a. We input search keywords in the form of a list and specify the number of images to be downloaded per keyword.
b. A search query is created for 'Google Images' using the keyword specifies in the script and the search query is fired onto the internet. A raw HTML file is returned, which is downloaded on a temporary basis.
c. Image links are extracted from the raw HTML file and the links are used to download the images from the internet. The raw HTML is deleted.
d. These downloaded images are stored in their native shapes using the correct file extension.
e. Steps b to e are repeated for each keyword in the keyword list provided in the script.

V. MANUAL REMOVAL OF IRRELEVANT IMAGES

After scrapping the images, we found that there were a large number of irrelevant images in the dataset. We could have kept them in the dataset as the presence of images, with no instance of objects, does not affect the working or the accuracy of the deep learning models. But to make the dataset compact, we have removed the images with no instance any of the weapon categories. Before removal, the number of images in the dataset was 15,473, which reduced to 8,843 after pruning the irrelevant images from the dataset.

V.1 BOUNDING BOX ANNOTATIONS

For detection of the weapon in the image, deep learning models need to the have the bounding box highlighting the presence of weapon instance in the image. Deep learning models use the region of an image inside the bounding box to learn the features of the object. For annotating the images in our dataset, we have used 'Labelling' [18]. Labelling is image annotation tool written in Python and has an easy graphical interface for bounding box annotations. The output of the annotations is saved as an XML files which are in PASCAL VOC format. The weapon categories for class labels taken into consideration are Assault-rifle, Handgun, Knife, Shotgun, Sniper-rifle.

V.2 FINAL DATASET DESCRIPTION

The final image dataset compiled is now ready to be used for weapon detection and classification task. The image dataset can be used for detecting and classifying five different kinds of weapon categories: Assault rifles, Handguns, Knives, Shotguns and Sniper-rifles. The image dataset contains around 8.8k image files with 11.5k instances of weapons. Table 1 describes the actual number of images and weapon instances present in our dataset.

Figure 2: Some examples of the weapon detection and classification dataset.
Source: Author, (2024)

Table 1: Image Dataset description for weapon detection and classification.

Category	No. Of Images	No. Of Instances
Assault-rifle	1649	1826
Handgun	2866	3591
Knife	1640	2201
Shortgun	976	1610
Sniper-rifle	1712	2224
Total	8843	11452

Source: Author, (2024).

The Image dataset is uploaded on Google drive and is made open-source. The annotations are also uploaded along with the images. The dataset and the annotations are made freely available to anyone who wants to work in the field of weapon detection and classification.

VI. RESULTS AND DISCUSSIONS

We have used four different deep learning models for weapon detection and classification task trained and evaluated on our own dataset. The models used for experimental analysis of deep learning techniques are as follows: (1) Faster RCNN with Inceptionv2 (2) Faster RCNN with Resnet50 (3) SSD with Inceptionv2 (4) SSD with Resnet50 the image dataset was divided in two parts - 80% was used for training and 20% was used for evaluation. The training was performed for exactly 300k steps for each model inorder to compare them on equal grounds. Data Augmentation was used to boost the performance of each deep learning model used in this study. The technique of data augmentation was Horizontal Flip with Random 50% probability. Learning rate was kept constant with initial value at 0.0002 and the IoU threshold was set to 0.6. Training was performed on GPU - NVIDIA Quadro K620 with 2 GB of memory. The batch size was kept constant at 1 due to the low memory of the GPU.

VI.1 COMPARISON OF DEEP LEARNING MODELS

There are three types of losses calculated while training deep learning models:

1. Localization loss is the loss while localizing the object in the given images. The localization loss signifies how good the model detects the spatial location of the relevant objects in the image. Figure 3 shows the localization loss while training all four models used in this work. The graph clearly shows the superiority of Faster RCNN models over SSD models for localization task. The RPN used in Faster RCNN are very powerful for detection the spatial location of the object in the image.
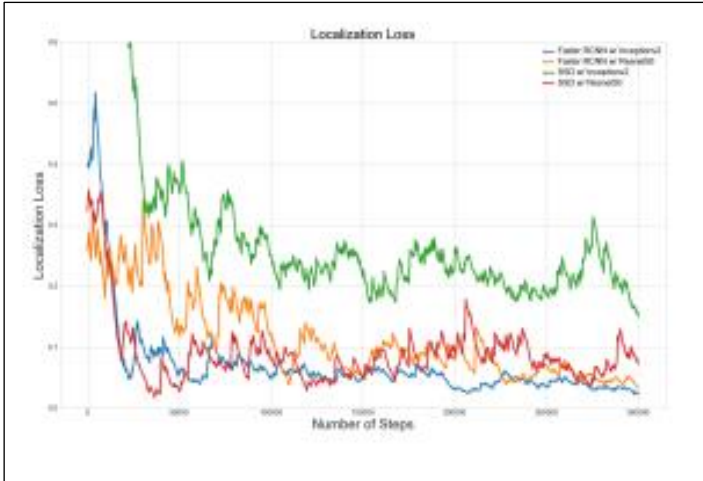
Figure 3: Localization Loss of the models while training.
Source: Author, (2024).
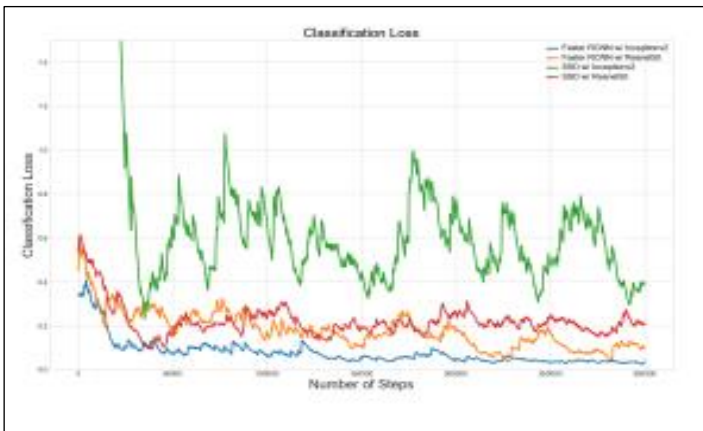
Figure 4: Classification Loss of the models while training.
Source: Author, (2024).
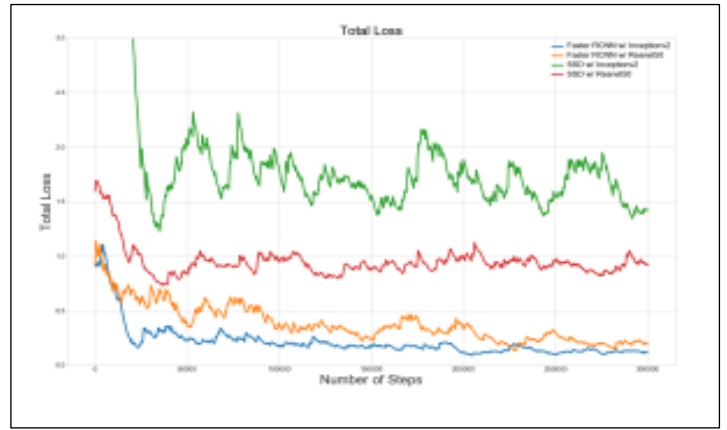
Figure 5: Total Loss of the models while training.
Source: Author, (2024).

2. Classification loss is the loss while classifying the detected object into correct category. The classification loss signifies how accurately the model classifies the object detected in the image. Figure 3 exhibits the classification loss while training all four models used in this work. Faster RCNN w/Inceptionv2 outperforms all other models in the classification task while SSD w/Inceptionv2 shows poor performance.

3. Total loss is the combined loss for localization and classification of objects in the input images. The total loss gives the overall performance of the model for detection and classification task. Figure 3 presents the total loss while training all four models used in this work. We see significant performance difference between Faster RCNN and SSD models. The loss for Faster RCNN models model stabilizes after 250k steps and remains constant afterwards but SSD models fail to do so.

For measuring how good the model works, we need to evaluate the model. The models were evaluated using the evaluation metrics of mAP used by COCO competition. The models were evaluated at 200k and 300k steps to compare the performance of the models. Table 2 shows the COCO metrics obtained by all four models used in this experimental analysis.

The results clearly states substantial accuracy difference between Faster RCNN and SSD models. Faster RCNN w/Inceptionv2 achieves highest mean Average Precision with a score of 0.662, followed by Faster RCNN w/Inceptionv2 with a mAP score of 0.573. SSD w/Inceptionv2 has worst performance of all with overall mAP of 0.238. Figure 6 shows the comparison between the mAP scores of all the four models used in this experimental analysis.

Table 2: Evaluation metrics obtained by all four models after training for 300k steps.

Evaluation Metrices	Faster RCNN w/Inception V2	Faster RCNN w/Resnet50	SSD w/Inception V2	SSD w/Resnet50
mAP	0.662	0.573	0.238	0.333
mAP@.50 IOU	0.837	0.720	0.454	0.484
mAP@.75 IOU	0.742	0.652	0.221	0.379
mAP (small)	0.151	0.000	0.000	0.101
mAP (medium)	0.293	0.189	0.012	0.093
mAP (large)	0.689	0.601	0.266	0.352
AR@1	0.605	0.557	0.286	0.465
AR@10	0.780	0.640	0.405	0.632
AR@100	0.790	0.000	0.444	0.656
AR@1 (small)	0.420	0.000	0.000	0.360
AR@10 (medium)	0.564	0.191	0.045	0.292
AR@100 (large)	0.806	0.671	0.485	0.680

Source: Author, (2024).

VI.2 DISCUSSIONS

Our inferences from the training and evaluation results are as follows:

– Faster RCNN models are better than SSD at detecting weapons in small regions.

– Training time for Faster RCNN and SSD models vary significantly even with the use of same backbone DCNNs.

– SSD models shows significant speed up on Faster RCNN models while detection.

– Faster RCNN w/Inceptionv2 outperforms every other model in our study, with high margin for weapon detection and classification task.
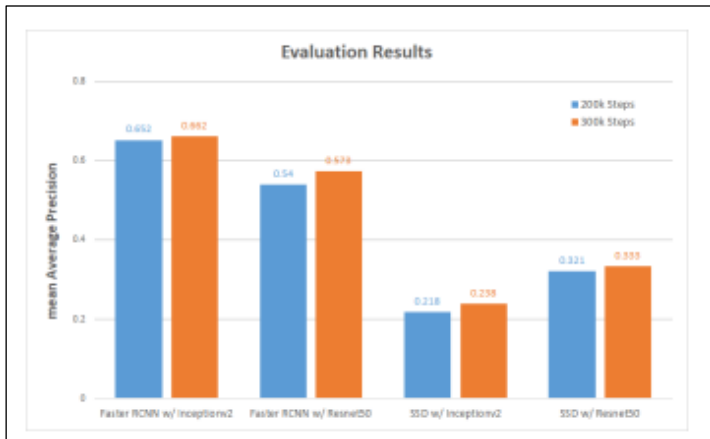
Figure 6: Comparison of mean Average Precision secured by four models.
Source: Author, (2024).

VI.3 DETECTION RESULTS

In this section, we have shown the results of detection and classification of the weapons using some real-life images. The Faster RCNN w/Inceptionv2 was used for the detection as it showed highest accuracy in the model comparison phase. The model was trained for 1 million steps with same configuration. The images chosen for the detection results contain various environments and various contextual situations. The detection results show how well our model tackles different challenges while detecting and classifying weapons.

Positive and Negative detection:

Some of the positive and negative results are shown in this section. Figure 7 shows the correct classification of gun with perfect bounding box prediction. Figure 8 shows that our trained model fails at certain situations to detect the weapon

X-ray images:

The trained model detects the weapon using the features of the weapon and not the color. Hence our model is able to detect weapons and classify them even in the X-ray images. This provides an extra use-case for our model. Figure 9 shows the weapon detection in the X-ray images.

Occlusion:

The major issue with weapon detection is occlusion of the weapon with the holder's hand or body. This issue is easily handled by our model. The model is able to detect the weapon in the image, even with as low as 30-40 percent visibility of the weapon in the image or video frame.

Illumination

The model is also capable of detecting weapon in lowlight or at night. The illumination is not a problem for the model until and unless the border edges are somewhat visible in the image. Figure 11 shows the detection of weapon in low-light situations.

View-point and Angles

The weapon should be detected from any angle and view-point if it appears in the image. Our model is capable of detecting gun in any view-point. This is only possible because the images of weapons with different angles and view-points are present in the image dataset we prepared in the earlier stage. Figure 12 shows the weapon detection in different angles and viewpoints.

Figure 7: Positive examples of the weapon detection.
Source: Author, (2024).

Figure 8: Some Positive examples of the weapon detection.
Source: Authors, (2024).
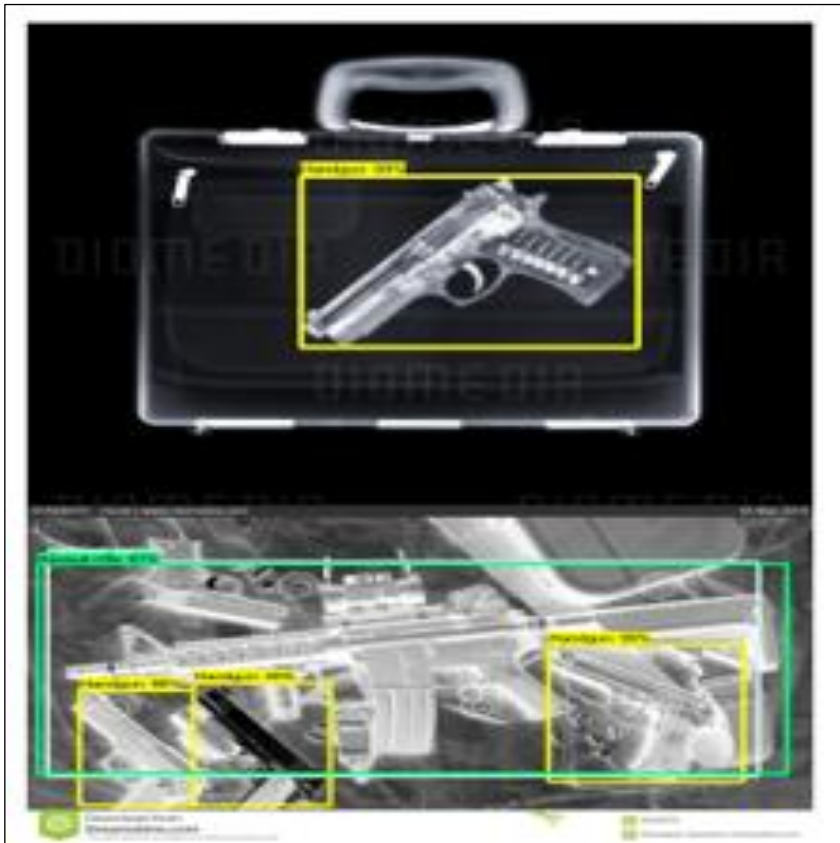
Figure 9: Weapon detection in X-ray images.
Source: Author, (2024).

Figure 10: Solving the issue of occlusion and scale.
Source: Author, (2024).

Figure 11: Low illumination condition.
Source: Author, (2024).

Figure 12: Handling different viewpoints.
Source: Author, (2024).

VII. CONCLUSIONS

The proposed work was mainly focused on creation of a new image dataset for weapon detection and classification and implementation of weapon detection system with ability to classify the weapon based on the weapon type, using Deep learning techniques. We have created an image dataset with more than 11.5k instances of weapon. The weapons in the images have bounding box annotations with five different categories of weapons. The dataset was then used for training the state-of-the-art deep learning models used for salient object detection problems. We have used four different models for training and evaluated them on the test set using different evaluation metrics. Our experimental results shows that Faster R-CNN w/Inceptionv2 outperformed all the other models used in this work and achieved mean Average Precision of 0.69 and mean Average Recall of 0.62. The detection speed of Faster-RCNN is not quick, but this can be fastened by using high performance GPUs. Even though SSD models are incredibly fast at detection task, lack the real-life use as the accuracy of the detection boxes and classification is not acceptable. Due to the lack

of computing power, we were not able to perform comparison of modern DCNNs such as Inception-ResNets or SE-ResNets.

The deep learning models trained on our image dataset overcomes many challenges in the field of weapon detection such as illumination, blur, motion, and occlusion. The models are also capable of detecting weapons in X-ray images; hence the system can be used for detecting concealed weapons in baggage at airports, railway stations, malls, etc. SSD w/ Resnet50 can be used for real-time weapon detection in CCTV cameras as the detection speed of this model is high. The research work done in this thesis can be extended in many different ways:

1. More complex models such as Faster R-CNN w/ Inception-Resnetv2 can be trained for more accurate detection and classification of weapons.

2. The dataset can be used to train small and light deep learning models, which can be used for detecting weapons on mobile or embedded systems

3. Our image dataset can be extended by adding new categories of weapons for detection of new types of weapons such as missiles, grenades, etc.

VIII. AUTHOR'S CONTRIBUTION

Conceptualization: Sunil B. Mane.
Methodology: Sunil B. Mane.
Investigation: Sunil B. Mane.
Discussion of results: Sunil B. Mane.
Writing – Original Draft: Sunil B. Mane.
Writing – Review and Editing: Sunil B. Mane.
Resources, Supervision: Sunil B. Mane.
Approval of the final text: Sunil B. Mane.

IX. REFERENCES

[1] "Estimated number of civilian guns per capita by country," Wikipedia, 29-Apr-2019. [Online]. Available: https://en.wikipedia.org/wiki/Estimated number of civilian guns per capita by country. [Accessed: 03-May-2019].

[2] B. Marr, "How Much Data Do We Create Every Day? The Mind-Blowing Stats Everyone Should Read," Forbes, 11-Mar-2019. [Online]. Available: https://www.forbes.com/sites/bernardmarr/2018/05/21/howmuch-data-do-we-create-every-day-the-mind-blowingstats-everyone-should-read/#2ecf668960ba. [Accessed: 03-May-2019].

[3] R. Girshick, J. Donahue, T. Darrell, and J. Malik, "Rich Feature Hierarchies for Accurate Object Detection and Semantic Segmentation," 2014 IEEE Conference on Computer Vision and Pattern Recognition, 2014.

[4] G. K. Verma and A. Dhillon, "A Handheld Gun Detection using Faster R-CNN Deep Learning," Proceedings of the 7th International Conference on Computer and Communication Technology - ICCCT-2017, 2017.

[5] S. Ren, K. He, R. Girshick, and J. Sun, "Faster R-CNN: Towards Real-Time Object Detection with Region Proposal Networks," IEEE Transactions on Pattern Analysis and Machine Intelligence, vol. 39, no. 6, pp. 1137–1149, 2017.

[6] Simonyan K., Zisserman A., "Very deep convolutional networks for large scale image recognition," ICLR, 2015.

[7] J. Deng, W. Dong, R. Socher, L.-J. Li, K. Li, and L. Fei-Fei, "ImageNet: A large-scale hierarchical image database," 2009 IEEE Conference on Computer Vision and Pattern Recognition, 2009.

[8] R. Olmos, S. Tabik, and F. Herrera, "Automatic handgun detection alarm in videos using deep learning," Neurocomputing, vol. 275, pp. 66–72, 2018.

[9] S. Akcay, M. E. Kundegorski, C. G. Willcocks, and T. P. Breckon, "Using Deep Convolutional Neural Network Architectures for Object Classification and Detection Within X-Ray Baggage Security Imagery," IEEE Transactions on Information Forensics and Security, vol. 13, no. 9, pp. 2203–2215, 2018.

[10] H. Nakahara, H. Yonekawa and S. Sato, "An object detector based on multiscale sliding window search using a fully pipelined binarized CNN on an FPGA," 2017 International Conference on Field Programmable Technology (ICFPT), Melbourne, VIC, 2017, pp. 168-175.

[11] R. Girshick, "Fast R-CNN," 2015 IEEE International Conference on Computer Vision (ICCV), 2015.

[12] Dai, J.; Li, Y.; He, K. & Sun, J. Lee, D. D.; Sugiyama, M.; Luxburg, U. V.; Guyon, I. & Garnett, R. (Eds.), "R-FCN: Object Detection via Region-based Fully Convolutional Networks Advances", Neural Information Processing Systems (NIPS) 29, 2016, 379-387.

[13] J. Redmon and A. Farhadi, "YOLO9000: Better, Faster, Stronger," 2017 IEEE Conference on Computer Vision and Pattern Recognition (CVPR), 2017.

[14] He, Kaiming, et al. "Deep residual learning for image recognition." Proceedings of the IEEE conference on computer vision and pattern recognition. 2016.

[15] K. He, X. Zhang, S. Ren, and J. Sun, "Deep Residual Learning for Image Recognition," 2016 IEEE Conference on Computer Vision and Pattern Recognition (CVPR), 2016.

[16] J. Lai, "Developing a Real-Time Gun Detection Classifier," 2017.

[17] Sermanet, Pierre, David Eigen, Xiang Zhang, MichaÂ l Mathieu, Rob Fergus and Yann LeCun. "OverFeat: Integrated Recognition, Localization and Detection using Convolutional Networks," CoRR, 2014, abs/1312.6229.

[18] Tzutalin "LabelImg". Git code (2015). https://github.com/tzutalin/labelImg

Journal of Engineering and Technology for Industrial Applications

RESEARCH ARTICLE   **OPEN ACCESS**

RELEVANCE AND RELIABILITY OF NO₂ AND NO MONITORING IN LOW-INCOME COUNTRIES USING LOW-COST SENSORS

*Olivier Schalm[1], Rosa Amalia González-Rivero[2], Erik Hernández-Rodríguez[3], Mayra C. Morales-Pérez[4], Daniellys Alejo-Sánchez[5], Alain Martinez[6], Werner Jacobs[7] and Luis Hernández[8].

[1,7]Antwerp Maritime Academy, Noordkasteel Oost 6, 2030 Antwerpen, Belgium.
[2,3,4,5,6,8]Universidad Central "Marta Abreu" de Las Villas", Faculty of Chemistry, Road to Camajuaní Km 5.5, Santa Clara 54830, Villa Clara, Cuba.

[1] http://orcid.org/0000-0001-8705-7293 , [2] http://orcid.org/0000-0002-6905-4379 , [3]http://orcid.org/0000-0003-3947-5487 ,
[4]http://orcid.org/0000-0001-7506-0145 , [5]http://orcid.org/0000-0001-9107-7190 , [6]http://orcid.org/0000-0002-6873-126X
[7]http://orcid.org/0000-0002-2205-9711 , [8]http://orcid.org/0000-0003-0558-3690

Email: Olivier.schalm@hzs.be[1], roagrivero@gmail.com[2], ehrodriguez@uclv.edu.cu3, mmora-lesp@uclv.edu.cu4, daniellysas@uclv.edu.cu5, amguardia@uclv.edu.cu6, werner.jacobs@hzs.be7, luishs@uclv.edu.cu8.

ARTICLE INFO

ABSTRACT

Assessing air quality's impact on human health involves monitoring pollutant concentrations such as NO_2, O_3, CO, SO_2, and particulate matter. While high-income countries rely on expensive reference instruments, low-income nations face technological limitations. This study explores the potential of low-cost scientific devices as a viable solution for these regions. The research focuses on evaluating the reliability of low-cost NO_2 sensors and consistency across five identical sensors. Calibration tests in controlled settings reveal a linear model with high coefficients of determination, contrasting with lower coefficients observed during field tests. Variability in intercepts and slopes is evident across time and campaign contexts. Time series analysis using low-cost NO_2 sensors showed that many of the tall peaks atop a fluctuating baseline correlates with peaks identified by reference instruments. Additionally, NO gas sensors are also able to identify pollution peaks in monitoring campaigns. Therefore, such affordable sensors provide valuable insights into pollutant concentration trends, offering indicative magnitude information. However, improving calibration and reliability of these sensors necessitates further research.

I. INTRODUCTION

Nitrogen dioxide (NO_2) typically ranges in average concentrations from 1 to 20 ppb in Belgian outdoor air, while nitric oxide (NO) averages between 1 and 2 ppb [1],[2]. These gases are released into the atmosphere through the high-temperature combustion of fossil fuels in a range of human activities, including mobility (cars, ships), power plants, industrial processes, residential heating, and cooking [3-7]. There are also several natural processes that contribute to their formation (e.g., lightning, volcanic activity, or forest fires). The sum of NO and NO_2 is usually expressed as NO_x (i.e., x is a variable) where the total concentration is expressed in NO_2 equivalents.

The air used to burn fuel contains around 21 vol% oxygen (O_2), 78 vol% nitrogen (N_2), traces of other gases such as carbon dioxide (CO_2) or argon (Ar), and varying amounts of moisture (H_2O). When the fuel reacts with the oxygen in the air, the main products formed are carbon dioxide (CO_2) and water vapor (H_2O), though small quantities of carbon monoxide (CO), volatile organic compounds (VOC) and black carbon (i.e., soot) are also produced. When the air is burned with the fuel, a fraction of the nitrogen (N_2) is transformed into nitrogen oxides [7]. According to the extended Zeldovich reaction mechanism, NO (nitric oxide) is produced when free radicals (e.g., O-atoms, N-atoms, H-atoms, and OH) attack N_2 in the flame region. The generation of NO is influenced by the air-fuel ratio, with higher levels observed when the oxygen content surpasses the ideal stoichiometric ratio for fuel combustion [8],[9].

This formation occurs until all available oxygen is consumed, particularly at temperatures exceeding 1300°C. At temperatures below 760°C, the production of NO is significantly reduced or sometimes nonexistent. In cooler areas (around 400-500°C) near the flame front, smaller quantities of NO might transform into NO_2 [10]. When NO is emitted in the atmosphere it converts through a reaction with O_3: $NO + O_3 \rightarrow NO_2 + O_2$.

NO_2 is a reactive gas involved in the formation of ozone and particulate matter. It is known to be irritating to the human respiratory system. Children and people with respiratory disease are the groups most at risk when exposed to NO_2 concentrations higher than 40-200 µg/m^3 [11],[12]. Moreover, there is a short-term and long-term effect of NO_2 on hospital admissions for cardiovascular diseases [13],[14].

To understand the impact of air on human health, monitoring NO_x concentrations is crucial. NO_x reference gas analyzers utilize chemiluminescence detection technology to measure ultra-low concentrations of NO_x in air. However, the cost of purchasing, operating and maintaining such devices can be prohibitive. An alternative method to analyze these pollutants at lower cost is to use gas sensors paired with an in-house developed data logger [15-20]. An important advantage of such devices is that they are affordable by low-income countries. As a result, such measuring devices contribute to the inclusivity of research. However, the reliability of low-cost measuring devices is often questioned in scientific literature, especially when such devices are compared to the gold standard. Therefore, it is not clear to what extent one can trust the collected data gathered. This contribution will explore the feasibility of using low-cost NO_2 and NO monitoring. The study will be illustrated with measuring campaigns conducted in Belgium and in Cuba.

II. MATERIALS AND METHODS

II.1. DESIGN OF THE LOW-COST DATA LOGGER

A first low-cost, in-house-developed data logger utilizes an Arduino Mega 2560 as a microcontroller board as its central component. In order to transform this microcontroller board into a versatile data logger that can be tailored to the user's specific requirements, we have designed a compact, custom-made expansion shield. This design has been previously published and no changes have been made on the hardware during this work [21-23]. This shield serves the purpose of connecting sensors to the data logger and converting sensor signals into a format that the microcontroller board can interpret. For air quality monitoring campaigns, sensors that measure temperature, relative humidity, inorganic gaseous pollutants, and particulate matter are connected to the expansion shield. In this setup, NO was not measured while NO_2 has been measured with an A-series Alphasense gas sensors. The gas sensors are inserted into an analog conditioning board (Analog Front End no. 810-0023-00 from Alphasense), and that board is connected to the expansion shield using a flat cable and suitable connectors. The advantage of this data logger is that the user can insert or remove sensors and configure the data logger according to his needs.

A second data logger design uses a Raspberry Pi 3B+ as its central processing unit that is connected to a larger PCB sensor shield. The sensors are directly interfaced to the sensor shield without external wiring. Since the array of sensors fixed to the sensor shield is extensive, this single-purpose data logger can be used across a diverse range of applications. Among the various sensors, it features six Alphasense B-type gas sensors that targets CO, NO_2, OX ($NO_2 + O_3$), NO, H_2S, and SO_2. Each gas sensor is connected to an Alphasense Individual Sensor Board, which in turn is seamlessly incorporated into the architecture of the sensor shield. This design has been described in earlier publications [24],[25].

II.2. SENSOR CALIBRATION

The Alphasense gas sensors generate a concentration dependent signal at the working electrode WE and an internal signal that is supposed to be concentration independent at the auxiliary electrode AE. For both electrodes, the signal at zero pollution is denoted by WE_0 and AE_0 respectively. The sensor signal is calculated as $(WE - WE_0) - (AE - AE_0)$ [26]. For the sake of simplicity, it is assumed that the temperature has no effect on the signal. Since WE_0 and AE_0 are only constant for shorter periods, the values are either measured during the calibration experiments, or determined as the minimum value of WE and AE of the time series. Although Alphasense furnishes calibrations for each individual gas sensor, these calibrations must be subject to scrutiny and necessitate periodic verification [27]. Therefore, the reliability of these sensors must be evaluated by calibration experiments. For this reason, the NO_2-sensors have been submitted to 4 different calibration methods [28-32]. The collected data have been processed by linear regression:

- **Low-cost laboratory-based calibration:** In addition to the low-cost data logger, cost-effective calibration methods have been devised to ensure the inclusivity of air quality research in lower-income countries. The calibration setup uses a closed plastic box containing the NO_2 gas sensor. Within the calibration box, the air is initially purified by passing it through a $Ca (OH)_2$-saturated solution. The cleaned air is used to determine WE_0 and AE_0 (i.e., zero calibration). Subsequently, controlled amounts of NO_2 are generated within a closed setup constructed from medical disposables [33],[34]. The generated NO_2 gas, held within a syringe, is then introduced into a second plastic box for dilution. After approximately 20 minutes, a sequence of gas volumes (0.6, 1, 1.6, 1.6, 2, and 2.6 mL) is introduced into the calibration box. The corresponding concentrations inside the calibration box can be calculated from the ideal gas law. Each injection results in a calibration point where sensor signal $(WE - WE_0) - (AE - AE_0)$ and corresponding pollutant concentration is known (i.e., span calibration). The calibration is determined by a linear regression through these points;

- **Calibration in a high-end climate chamber:** The two data logger configurations have been subjected to calibration within a climate chamber at the laboratories of VITO, Belgium, enabling precise regulation of temperature and relative humidity. Certified calibration gas cylinders holding specific concentrations of the target gas in nitrogen are blended with pure nitrogen to achieve the desired concentration level. The gas mixture is then introduced into the calibration chamber. Through modulation of the calibration gas dilution, a step-like function is generated over a defined time span. Furthermore, the concentration of the target gas within the calibration chamber is continuously tracked with the Airpointer, which consists of several reference instruments [24]. At every step in the staircase function, the average reference concentration is calculated and the corresponding sensor signal $(WE - WE_0) - (AE - AE_0)$ is determined as well where WE_0 and AE_0 are the measurements in zero air. As a result, every step results in a calibration point

through which calibration can be determined by linear regression;

- **Field calibration in outdoor air:** One NO_2 sensor underwent field calibration by installing a data logger device in the proximity of a reference measurement station whose data is publicly available [35]. Both devices measure the same ambient pollutant concentrations in outdoor air under realistic conditions. This calibration procedure took place at station 42R801 in Antwerp, Belgium, that is operated by the Flemish Environment Society (Vlaamse Milieu Maatschappij VMM). The natural variations in pollutant levels present in the outdoor air assures for a calibration over a specific concentration range. That range is usually smaller than the one used in the laboratory calibration methods. WE_0 and AE_0 can be determined as the minimum value of WE and AE within the time series when it does not contain low sensor values due to instrumental errors. The time series of the reference instruments and of the low-cost data logger are 1 hour and 2 minutes respectively. With the function VLookUp in Microsoft Excel, the sensor signals WE and AE could be resampled so that values for WE and AE are obtained at the same timestamps as the measurements in the reference time series. The resampling allows the integration of the sensor signal $(WE - WE_0) - (AE - AE_0)$ and the corresponding reference concentration in a single database. The calibration is determined by the linear regression through the large set of data points;
- **In situ calibration:** The quick-and-dirty in situ calibration method assumes that the minimum and average pollutant concentration in the region where the measuring campaign takes place are known. In Antwerp, the minimum sensor signal $(WE - WE_0) - (AE - AE_0)$ of NO_2 in a time series is associated to 0 ppb, while the average value of $(WE - WE_0) - (AE - AE_0)$ is associated to 16.22 ppb. The average concentration has been determined by measurements at other VMM reference stations in the neighborhood, or from literature information. These two calibration points define the linear calibration curve. In principle, this method can be improved by actual in situ measurements of the minimum and average concentration but low-cost methods to perform such field measurements are not yet part of our possibilities.

II.3. COLLECTED DATA

Several experiments and measurement campaigns have been conducted to calibrate the gas sensors and evaluate the reliability of the collected data. The description of these tests are previously published [25],[34]. In this contribution, only the results for NO_2 will be emphasized.

A measurement campaign was carried out on board a 36-year-old ship that is dedicated to near shore operations at the Belgian coast. During the measuring campaign at March 15-18, 2021, the Raspberry Pi-based data logger has been installed in the engine room. In parallel, a measurement campaign is performed with the Air pointer, which was used as a reference-grade instrument [24]. They both measure NO_2 and NO.

In Cuba, a field measuring campaign has been performed in Cienfuegos, from March 14 to April 22, 2022 with a sampling time of 2 minutes using the Arduino-based data logger.

III. RESULTS AND DISCUSSIONS
III.1. SENSOR CALIBRATION

To comprehend the influence of the situational context in which a measurement campaign is conducted, calibration of the A-type NO_2 gas sensor in combination with the Arduino-based data logger has been undertaken using four distinct methods. When looking at the peaks in Figure 1a, almost all NO_2 peaks observed in the field campaign, resulted in a peak in the sensor's signal except when the peak is below the detection limit of the sensor. This suggests that the NO_2 low-cost sensor is able to generate reliable information about the dynamic pattern that can be observed in Figure 1a. However, some tall peaks in the reference measurements resulted in smaller sensor peaks and vice versa. The high scattering in Figure 2a and the low coefficient of determination (i.e., 0.1976) confirm this complicated relationship. In addition, the calibrations performed in laboratory conditions (VITO and low-cost calibration) have a slope that is substantial higher when compared to the linear regression of the field data. There is a factor 5 difference between the VITO and field calibration. However, the VITO-calibration is characterized by a coefficient of determination that is close to 1 (i.e., 0.9997). The in-situ calibration, which is considered as quick and dirty, seems to approach the field calibration the best. It should be remarked that micro-conditions can substantially deviate from the average pollution concentration that is used in the in-situ calibration. The differences between calibration methods suggest that the context of laboratory and real-life outdoor conditions has a substantial effect. The well-controlled conditions in laboratory conditions do not seem to be representative for outdoor conditions.
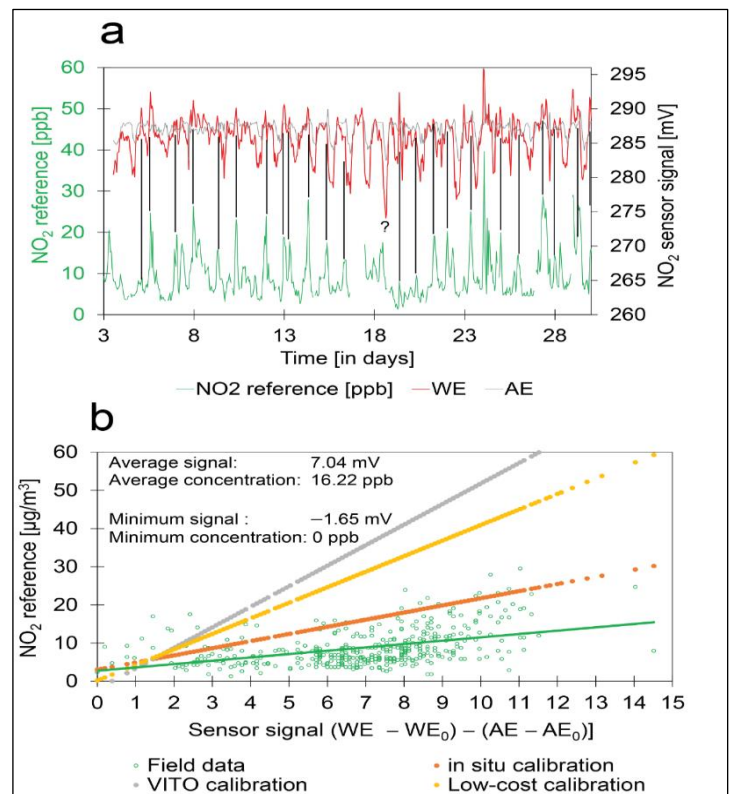

Figure 1: Different calibration methods applied on the same NO_2 sensor. a) NO_2 time series obtained at a VMM air quality monitoring station where the environmental conditions fluctuate in an uncontrolled way; b) Calibration of the low-cost NO_2 sensors using the field data and a superposition of the calibration curves obtained with the other methods.
Source: Authors, (2024).

To understand the impact of the selection of a random sensor from a pool of identical gas sensors and the sensor's history, five distinct B-type NO_2 sensors coupled to the Raspberry Pi-based data logger have been calibrated by VITO. For 3 of them, the calibration has been done twice. Figure 2a shows that the signal of WE at zero air does not restore to the same value. It is also noticed that after exposure to an elevated pollutant concentration, the sensor needs time to regain its equilibrium. This suggest that the sensor's history has an impact on current calibration. Figure 2a shows that each calibration results in a calibration with a high coefficient of determination. However, there is a factor 2 difference between the lowest and highest sensor signal generated by the same NO_2 concentration. In addition, the repeated calibration experiments also resulted in different slopes. Apparently, the sensors do not (always) generate the same response under identical conditions. This suggests that regular in situ calibrations are required to enhance the reliability of quantitative measurements.
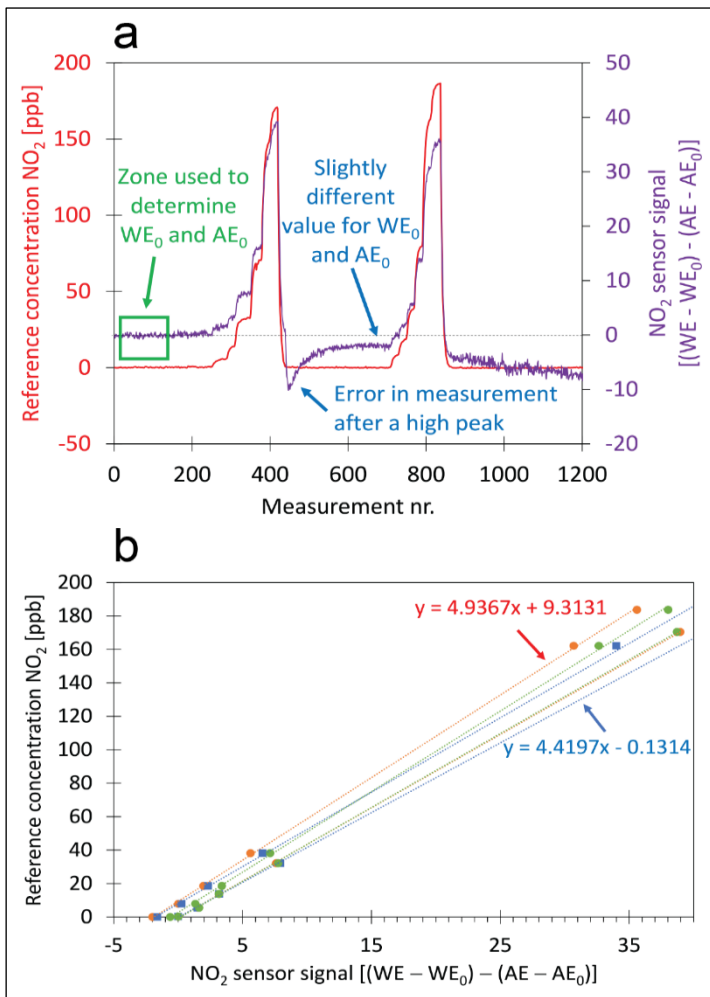
Figure 2: Calibration of 5 NO_2 gas sensors; a) Raw signal of a NO_2 sensor during 2 consecutive calibration experiments; b) Calibration curves for a pool of 5 sensors where the calibration of 3 sensors have been repeated.
Source: Authors, (2024).

III.2. MEASURING CAMPAIGN IN BELGIUM

Figure 3 presents the outcomes of a measuring campaign conducted in the engine room of a ship. More comprehensive details of this campaign are available elsewhere [24],[25]. The time series depicted in Figure 3 reveals that the structure within these series has arisen from a dynamic process. This can be observed in the NO and NO_2 series, where narrow peaks at elevated concentrations are superposed over a slowly fluctuating baseline. From the dynamics and absolute values of Figure 3, the following can be learned:

- **Precision and accuracy of sensor measurements:** Regarding NO_2, both peaks and background concentrations as measured by the sensor consistently remained above the detection limit. In contrast, the background concentrations of NO frequently approach or even fall below the detection limit, but detectable peaks occur regularly at elevated concentrations. The most obvious difference with the reference measurements is that the NO and NO_2 sensors severely underestimate the peak maxima. This is in contrast with the field calibration in Figure 2b where the in-situ calibration overestimates the concentrations. This is another indication that the calibration in laboratory conditions cannot be extrapolated to other situational contexts in a simple way. The underestimation introduces an uncertainty when the measurements are compared with health-related thresholds. This uncertainty can be reduced by improving the calibration of the gas sensors;

- **Reliability of the dynamic pattern:** The field campaign (see Figure 1a) has shown that peaks superposed on a slowly fluctuating baseline can be identified and that these peaks are observed by the low-cost NO_2 gas sensor. Also, in the measurement campaign on board the ship, a dynamic pattern consisting of tall peaks superposed on a baseline is observed. The position of the peaks as measured with the low-cost NO and NO_2 gas sensors are in register with the ones observed in the reference measurements. Moments where such peaks occur are characterized by a poorer indoor air quality. The dynamics in the structure of the time series contain valuable information and for that reason it is worthwhile to perform monitoring campaigns with a high temporal resolution;

- **Occurrence of events:** The peaks in the time series can be interpreted as events corresponding to instances when the ship's exhaust emissions or the exhaust gas from a passing ship enter the engine room via the ventilation inlet. In most cases, NO and NO_2 peaks occur concurrently. However, events where only one of the NO or NO_2 peaks occur have been observed as well. For the periods that both peaks occur simultaneously, the NO_2/NO ratio varies from 0.16 to 1.5 and in the majority of cases, the peak maximum of NO surpasses that of the corresponding NO_2 peak. While the synchronicity of most NO and NO_2 peaks implies a common pollution source, the variable ratio suggests that this source generates a diverse mixture of pollutants. This brief study suggests that the distribution of valuable information in the time series is not homogeneous. Events contain valuable information about the pollution source and moments of poorer air quality. Therefore, it seems worthwhile to develop mathematical methods that can extract and analyze events in time series.

III.3. MEASURING CAMPAIGN IN CUBA

The measurement campaign conducted in Cienfuegos, as depicted in Figure 4, has been calibrated using a combination of low-cost methods and VITO calibrations. The structure of the temperature and relative humidity exhibit peaks and valleys in counterphase. Obvious differences with campaigns in Belgium are the elevated levels of O_3 and SO_2. The high concentrations of SO_2 are attributed to the combustion of sulfur-containing fuels, a type

of fuel that is not used in the Western world (except for seagoing ships). In the case of NO_2, a prominent peak reaching up to 200 ppb is evident at the onset of the campaign, which suppresses the minor fluctuations in the remainder of the time series. The NO_2 peaks coincide with the ones of relative humidity. It is unknown if this is due to an environmental cause or an instrumental artifact. The average concentration of NO_2 (47 ± 16 ppb) is higher than the average value of the Belgian field campaign (19 ± 11 ppb).
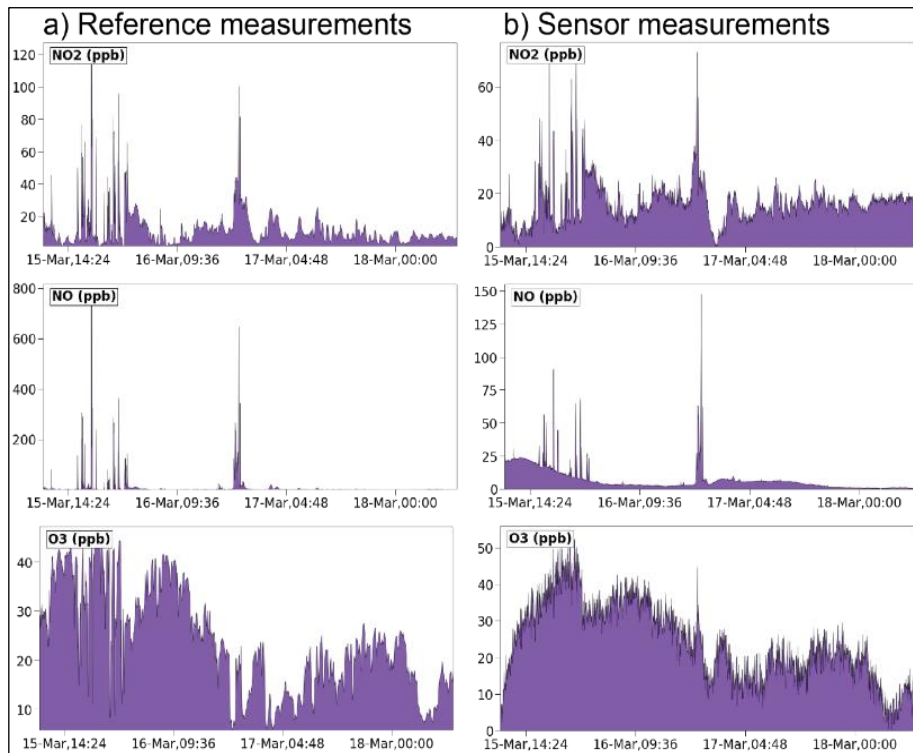
Figure 3: Measurement campaigns of NO_2, NO and O_3 at the same location in the engine room. The measuring campaign covers the period March 15, 2021 – March 18, 2021; (a) 1-minute data collected by the Airpointer containing reference instruments; (b) 3-minute data collected by the Raspberry Pi based data logger.
Source: Authors, (2024).
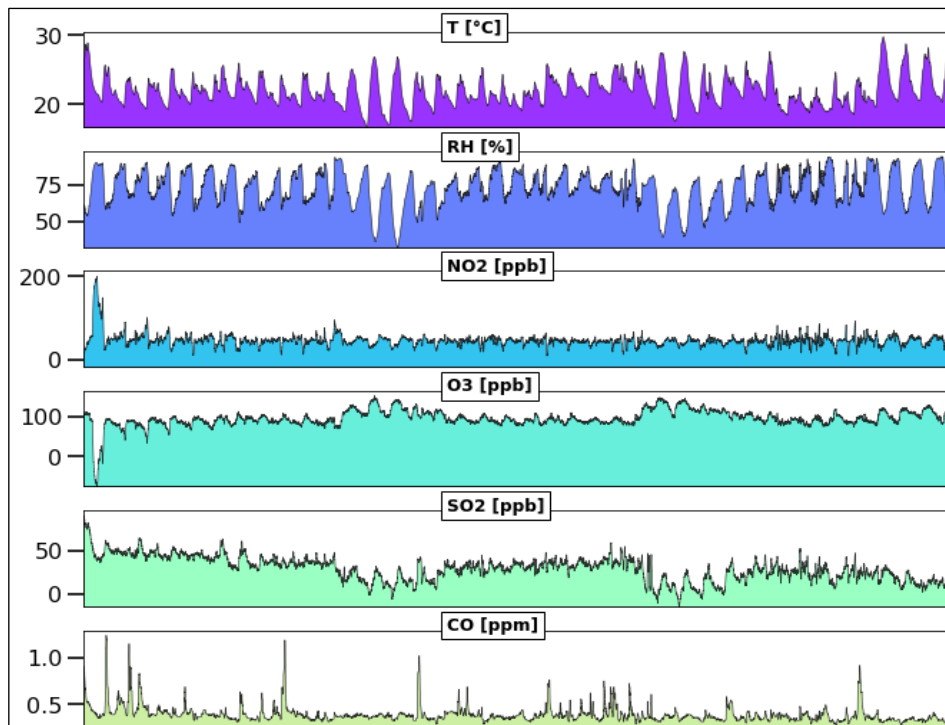
Figure 4: Measurement campaign performed at Cienfuegos, Cuba with the low-cost monitoring system from March 14 to April 22, 2022.
Source: Authors, (2024).

V. CONCLUSIONS

The coefficient of determination of the linear calibration in the field campaign is lower due to variable climatic conditions. This study has shown that the calibration of low-cost gas sensors in laboratory conditions result in linear calibration curves with a coefficient of determination close to 1. Despite this good correlation, intercept and slope appears to vary over time, with the situational context, the sensor's history, and from sensor to sensor. The situational sensitivity introduces an additional uncertainty in the measurement of pollutant concentration.

The dynamic patterns observed in time series measured by low-cost gas sensors appear to be sufficiently reliable to extract meaningful information. Specifically, the NO gas sensor appears to provide valuable insights by detecting peaks that surpass the detection limit. The peaks in time series contain elevated amounts of information regarding both pollution source and instances of poorer air quality.

Future research is necessary to enhance our understanding of gas sensor behavior in zero air under varying conditions of temperature, relative humidity, and pressure. This will lead to an improved accuracy of zero calibration (i.e., intercept of the calibration curve). In addition, also the effect of environmental parameters on the slope of the calibration curve should be studied. Such calibration experiments might be hampered by an equilibrium reaction of NO_2, NO and SO_2 with moisture, resulting in the formation of acids that might not be detectable by the respective sensor. Considering the relatively low reactivity of CO under ambient conditions, it is advisable to assess the span calibration for this gas first. Additionally, it is important to evaluate the replicability of zero and span calibrations by conducting a series of repeated experiments using zero air and a constant target gas concentration. The scientific literature contains numerous publications on the calibration of low-cost gas sensors, illustrating the importance of this topic.

VI. AUTHOR'S CONTRIBUTION

Conceptualization: Olivier Schalm.
Methodology: Rosa Amalia González-Rivero, Erik Hernández-Rodríguez, Mayra C. Morales-Pérez, Daniellys Alejo-Sánchez, Alain Martinez
Investigation: Olivier Schalm, Rosa Amalia González-Rivero, Erik Hernández-Rodríguez
Discussion of results: Olivier Schalm
Writing – Original Draft: Olivier Schalm.
Writing – Review and Editing: Olivier Schalm, Werner Jacobs, Luis Hernández
Supervision: Olivier Schalm
Approval of the final text: Olivier Schalm

VII. ACKNOWLEDGMENTS

VIII. REFERENCES

[1] B. Krupińska *et al.*, "Assessment of the air quality (NO2, SO2, O3 and particulate matter) in the Plantin-Moretus Museum/Print Room in Antwerp, Belgium, in different seasons of the year," *Microchemical Journal*, vol. 102, pp. 49–53, May 2012, doi: 10.1016/j.microc.2011.11.008.

[2] G. Carro, O. Schalm, W. Jacobs, and S. Demeyer, "Exploring actionable visualizations for environmental data: Air quality assessment of two Belgian locations," *Environ. Modell. Softw.*, vol. 147, p. 105230, Jan. 2022, doi: 10.1016/j.envsoft.2021.105230.

[3] S. Paraschiv, N. Barbuta-Misu, and S. L. Paraschiv, "Influence of NO2, NO and meteorological conditions on the tropospheric O3 concentration at an industrial station," *Energy Reports*, vol. 6, pp. 231–236, Dec. 2020, doi: 10.1016/j.egyr.2020.11.263.

[4] J. A. Miller and C. T. Bowman, "Mechanism and modeling of nitrogen chemistry in combustion," *Progress in Energy and Combustion Science*, vol. 15, no. 4, pp. 287–338, Jan. 1989, doi: 10.1016/0360-1285(89)90017-8.

[5] H. H. Schrenk and L. B. Berger, "Composition of Diesel Engine Exhaust Gas," *Am J Public Health Nations Health*, vol. 31, no. 7, pp. 669–681, Jul. 1941, doi: 10.2105/AJPH.31.7.669.

[6] B. Degraeuwe *et al.*, "Impact of passenger car NOx emissions and NO2 fractions on urban NO2 pollution – Scenario analysis for the city of Antwerp, Belgium," *Atmospheric Environment*, vol. 126, pp. 218–224, Feb. 2016, doi: 10.1016/j.atmosenv.2015.11.042.

[7] M. A. Elliott, G. J. Nebel, and F. G. Rounds, "The Composition of Exhaust Gases from Diesel, Gasoline and Propane Powered Motor Coaches," *Journal of the Air Pollution Control Association*, vol. 5, no. 2, pp. 103–108, Aug. 1955, doi: 10.1080/00966665.1955.10467686.

[8] Clean Air Technology Center, "Nitrogen Oxides (NOx), Why and How They are Controlled," Environmental Protection Agency, EPA-456/F-99-006a, 1999.

[9] C. E. Baukal Jr., Ed., *Oxygen-Enhanced Combustion, Second Edition*. in Industrial combustion series. New York: CRC Press, 2013.

[10] J. C. Hilliard and R. W. Wheeler, "Nitrogen Dioxide in Engine Exhaust," presented at the Passenger Car Meeting & Exposition, Feb. 1979, p. 790691. doi: 10.4271/790691.

[11] Environmental Protection Agency, "Air Quality Index Reporting; Final rule," *Federal Register*, vol. 64, no. 149, pp. 42530–42549, 1999.

[12] U. Latza, S. Gerdes, and X. Baur, "Effects of nitrogen dioxide on human health: Systematic review of experimental and epidemiological studies conducted between 2002 and 2006," *International Journal of Hygiene and Environmental Health*, vol. 212, no. 3, pp. 271–287, May 2009, doi: 10.1016/j.ijheh.2008.06.003.

[13] P. Collart, D. Dubourg, A. Levêque, N. B. Sierra, and Y. Coppieters, "Short-term effects of nitrogen dioxide on hospital admissions for cardiovascular disease in Wallonia, Belgium," *International Journal of Cardiology*, vol. 255, pp. 231–236, Mar. 2018, doi: 10.1016/j.ijcard.2017.12.058.

[14] A. Faustini, R. Rapp, and F. Forastiere, "Nitrogen dioxide and mortality: review and meta-analysis of long-term studies," *European Respiratory Journal*, vol. 44, no. 3, pp. 744–753, Sep. 2014, doi: 10.1183/09031936.00114713.

[15] F. Karagulian *et al.*, "Review of the Performance of Low-Cost Sensors for Air Quality Monitoring," *Atmosphere*, vol. 10, no. 9, p. 506, Aug. 2019, doi: 10.3390/atmos10090506.

[16] M. Ródenas García *et al.*, "Review of low-cost sensors for indoor air quality: Features and applications," *Applied Spectroscopy Reviews*, pp. 1–33, Jun. 2022, doi: 10.1080/05704928.2022.2085734.

[17] E. G. Snyder *et al.*, "The Changing Paradigm of Air Pollution Monitoring," *Environ. Sci. Technol.*, vol. 47, no. 20, pp. 11369–11377, Oct. 2013, doi: 10.1021/es4022602.

[18] L. Morawska *et al.*, "Applications of low-cost sensing technologies for air quality monitoring and exposure assessment: How far have they gone?," *Environ. Int.*, vol. 116, pp. 286–299, Jul. 2018, doi: 10.1016/j.envint.2018.04.018.

[19] G. Fanti *et al.*, "Features and Practicability of the Next-Generation Sensors and Monitors for Exposure Assessment to Airborne Pollutants: A Systematic Review," *Sensors*, vol. 21, no. 13, p. 4513, Jun. 2021, doi: 10.3390/s21134513.

[20] G. Fanti *et al.*, "Evolution and Applications of Recent Sensing Technology for Occupational Risk Assessment: A Rapid Review of the Literature," *Sensors*, vol. 22, no. 13, p. 4841, Jun. 2022, doi: 10.3390/s22134841.

[21] E. Hernandez-Rodriguez, D. Kairuz-Cabrera, A. Martinez, R. A. Gonzalez-Rivero, and O. Schalm, "Low-cost portable system for the estimation of air quality," presented at the 19th Latin American Control Congress (LACC 2022), La Habana, Cuba, 2022.

[22] E. Hernández-Rodríguez *et al.*, "Reliability Testing of a Low-Cost, Multi-Purpose Arduino-Based Data Logger Deployed in Several Applications Such as Outdoor Air Quality, Human Activity, Motion, and Exhaust Gas Monitoring," *Sensors*, vol. 23, no. 17, p. 7412, Aug. 2023, doi: 10.3390/s23177412.

[23] A. Martinez, E. Hernandez-Rodriguez, L. Hernandez, O. Schalm, R. A. Gonzalez-Rivero, and D. Alejo-Sanchez, "Design of a low-cost system for the measurement of variables associated with air quality," *IEEE Embedded Syst. Lett.*, pp. 1–1, 2022, doi: 10.1109/LES.2022.3196543.

[24] O. Schalm, G. Carro, B. Lazarov, W. Jacobs, and M. Stranger, "Reliability of Lower-Cost Sensors in the Analysis of Indoor Air Quality on Board Ships," *Atmosphere*, vol. 13, no. 10, p. 1579, Sep. 2022, doi: 10.3390/atmos13101579.

[25] O. Schalm, G. Carro, W. Jacobs, B. Lazarov, and M. Stranger, "The Inherent Instability of Environmental Parameters Governing Indoor Air Quality on Board Ships and the Use of Temporal Trends to Identify Pollution Sources," *Indoor Air*, vol. 2023, pp. 1–19, Apr. 2023, doi: 10.1155/2023/7940661.

[26] R. A. Gonzalez-Rivero, A. Álvarez-Cruz, D. Alejo-Sanchez, M. C. Morales-Perez, A. Martinez, and O. Schalm, "Calibration of a low-cost sensor for SO2 monitoring in a rural area of Cienfuegos," presented at the VIII Simposio Internacional de Química (SIQ 2022), Cayo Santa Maria, Cuba, 2022.

[27] B. Mijling, Q. Jiang, D. de Jonge, and S. Bocconi, "Field calibration of electrochemical NO2 sensors in a citizen science context," *Atmos. Meas. Tech.*, vol. 11, no. 3, pp. 1297–1312, Mar. 2018, doi: 10.5194/amt-11-1297-2018.

[28] N. Karaoghlanian, B. Noureddine, N. Saliba, A. Shihadeh, and I. Lakkis, "Low cost air quality sensors 'PurpleAir' calibration and inter-calibration dataset in the context of Beirut, Lebanon," *Data Br.*, vol. 41, p. 108008, Apr. 2022, doi: 10.1016/j.dib.2022.108008.

[29] P. Wei *et al.*, "Impact Analysis of Temperature and Humidity Conditions on Electrochemical Sensor Response in Ambient Air Quality Monitoring," *Sensors*, vol. 18, no. 2, p. 59, Jan. 2018, doi: 10.3390/s18020059.

[30] D. Wahlborg, M. Björling, and M. Mattsson, "Evaluation of field calibration methods and performance of AQMesh, a low-cost air quality monitor," *Environ Monit Assess*, vol. 193, no. 5, p. 251, May 2021, doi: 10.1007/s10661-021-09033-x.

[31] A. Bigi, M. Mueller, S. K. Grange, G. Ghermandi, and C. Hueglin, "Performance of NO, NO2 low cost sensors and three calibration approaches within a real world application," *Atmos. Meas. Tech.*, vol. 11, no. 6, pp. 3717–3735, Jun. 2018, doi: 10.5194/amt-11-3717-2018.

[32] T. Sayahi *et al.*, "Development of a calibration chamber to evaluate the performance of low-cost particulate matter sensors," *Environmental Pollution*, vol. 255, p. 113131, Dec. 2019, doi: 10.1016/j.envpol.2019.113131.

[33] R. A. González Rivero *et al.*, "A Low-Cost Calibration Method for Temperature, Relative Humidity, and Carbon Dioxide Sensors Used in Air Quality Monitoring Systems," *Atmosphere*, vol. 14, no. 2, p. 191, Jan. 2023, doi: 10.3390/atmos14020191.

[34] R. A. González Rivero *et al.*, "Relevance and Reliability of Outdoor SO2 Monitoring in Low-Income Countries Using Low-Cost Sensors," *Atmosphere*, vol. 14, no. 6, p. 912, May 2023, doi: 10.3390/atmos14060912.

[35] "Belgian Interregional Environment Agency (IRCEL - CELINE) — English." Accessed: May 18, 2022. [Online]. Available: https://www.irceline.be/en/front-page?set_language=en
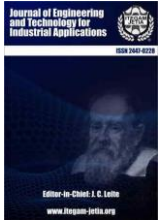
RESEARCH ARTICLE   **OPEN ACCESS**

A SYSTEMATIC REVIEW OF MOVIE RECOMMENDER SYSTEMS

Yuri Ariyanto[1] and *Triyanna Widiyaningtyas[2]

1,2 Department of Electrical Engineering and Informatics, Universitas Negeri Malang, Malang, Indonesia
1 Department Information Technology, State Polytechnic of Malang, Soekarno Hatta 9, Malang, 65142, Indonesia.

[1] http://orcid.org/0000-0001-8678-5184 , [2] http://orcid.org/0000-0001-6104-6692

Email:[1] yuri.ariyanto.2305349@students.um.ac.id, [2]*triyannaw.ft@um.ac.id.

ARTICLE INFO

ABSTRACT

Recommender systems are vital to everyone's information selection. Managing massive amounts of data is common with recommendation system technology. Annual film releases are rising, and currently films are released within months. With movie releases, apps like Netflix, Viu, Amazon Prime Video, Disney+, etc. have emerged. Thus, Movie Recommender Systems (MRS) are essential to simplify and improve user experience. This research gives a systematic literature review (SLR) of MRS's current condition. Our comprehensive review addresses recommendation algorithms, data processing, and evaluation approaches. In SLR MRS, content-based filtering, collaborative filtering, knowledge-based recommender systems, and hybrid approaches are employed. To achieve this, 66 high-quality studies were selected from 27,187 2019-2023 studies using strict quality criteria. The study found that most MRSs use content-based filtering and machine learning to deliver non-personalized movie suggestions in various domains. The review helps researchers choose MRS development strategies. This study can assist MRS development catch up to other recommendation systems by improving efficiency. The MRS investigation found accuracy, sparsity, scalability, cold start, and operating time issues. Future study will examine how temporal and demographic data affect movie recommendation system relevancy and customization.

I. INTRODUCTION

With the current abundance of information, accessing essential information quickly is becoming more challenging [1]. In order to address this issue, Recommendation Systems (RS) have been developed and implemented [2]. RS, short for Recommender System, is a software solution that uses data filtering techniques to provide users with personalized recommendations for the most suitable items and services [3]. Recommendation systems are gaining popularity and are utilized in several domains, including music, movies, news, comedy, health, and article recommendations.

Consumers are presented with many options as the Netflix movie supplier service gives a diverse range of things tailored to their individual tastes [4]. Optimizing the alignment between customers and the most suitable items is crucial for enhancing

customer happiness and fostering loyalty [5]. As a result, recommendation systems (RS) are gaining popularity on e-commerce platforms due to their ability to analyze user interest patterns and provide personalized suggestions based on user preferences [6]. Companies at the forefront of e-commerce, such as Netflix, Amazon, Flipkart, and YouTube, have effectively incorporated RS (Recommendation Systems) into their online platforms to improve the customer experience [7]. Content-based filtering (CB) and collaborative filtering (CF) are two elements of the recommendation system (RS) approach. Nevertheless, CB techniques necessitate the involvement of multiple experts to gather knowledge that is not accessible through external sources [8]. Conversely, collaborative filtering approaches depend on users' previous actions without a distinct profile. CF uncovers novel connections by analyzing user interactions and interdependencies across items [9]. The primary benefit of the CF

strategy is its domain independence, making it more precise than the CB approach [10].

System recommender tasks can be broadly classified into two basic categories: item recommendation and ranking prediction [11]. Item recommendation predicts the collection of products that users are likely to utilize [12]. Rating prediction is a method used to estimate ratings for products that users have not provided, typically employed on movie-sharing platforms [13]. Collaborative filtering (CF) is widely recognized as a prominent method for implementing recommendation systems [14]. The underlying principle is that consumers with comparable tastes have a tendency to select the same products. The often-employed CF model is matrix factorization (MF) [15]. In order to express the ranking matrix and complete the missing values in the matrix [16], Matrix Factorization (MF) employs the multiplication of two feature matrices with low ranks [17]. Nevertheless, most collaborative filtering (CF) techniques suffer from a shared limitation: the precision of the anticipated outcomes may diminish when ranking data is scarce [18]. Recommendation systems [19] manage three entities: users, things, and explicit item ratings.

Movie Recommendation Systems are autonomous machine learning algorithms that utilize big movie libraries like Netflix and Amazon to filter movies according to customer preferences [20]. The primary objective of this study piece is to enhance the user and movie environment factors by adjusting the number of row and column clusters in co-clustering [21].

Recommendation systems are highly effective solutions for addressing the challenges of the modern digital environment, and movie recommendation systems, in particular, have reached a high level of sophistication [22]. Regression-based methods are primarily employed to forecast rating values as preference scores for user-movie pairs. Movies can be presented in numerous modalities, including text, video, and audio. To assess the efficiency of multimodal models, researchers have employed different combinations of display modalities. Consequently, numerous experiments have been conducted to create real-time systems specifically for this objective [23].

Several recommendation systems employ hybrid filtering techniques that integrate characteristics from both content-based filtering (CBF) and collaborative filtering (CF) methodologies [24]. Collaborative filtering (CF) addresses certain drawbacks of content-based filtering (CBF) by generating suggestions based on the comparison of user-item similarities [25]. The system leverages information about past user preferences and the preferences of comparable users to provide recommendations.

A knowledge graph representing human emotions in movies can enhance the movie recommendation process by considering the user's emotional state and decision-making influenced by this element [13]. Emotions extracted from prior movie reviews are utilized in a knowledge graph [26].

Contemporary collaborative recommendation models prioritize user preferences in the context of multimodal information while disregarding user aversions. Nevertheless, integrating user dislikes into user modeling is crucial for a comprehensive understanding of user profiles. Therefore, while constructing collaborative recommendation models, it is essential to incorporate user dislikes [27].

The recommender system comprises a content-based system, a collaborative filtering system employing the SVD algorithm [28], and a fuzzy expert system [29]. The recommender algorithm utilizes the user's preferred and less preferred genres to generate a conclusive compilation of suggested movies. The fuzzy expert system evaluates the significance of movies by considering

multiple characteristics [30], including the average rating, number of ratings, and degree of similarity [31].

SLR and a detailed study of all the latest MRS domains contribute to this paper. Several crucial elements must be considered during system development to achieve this. This review covers movie recommendation methods, data and preprocessing, assessment and metrics, and pros and cons. The availability of data sets and codebases also affects research replication. To gather data on these components, 66 high-quality research from 27187 were selected using strict quality standards. Table 1 shows 66 MRS use in this work. These five research questions summarized MRS now.

This paper follows this structure. Section 2 describes movie recommender system research materials and methodology. Section 3 presents the results, explains the movie recommender system, and suggests future research. Section 4 outlines this study's result.

Table 1: Research Question.

No		Research Question
1	RQ1	What methods do movie recommendation systems use?
2	RQ2	What data and preprocessing methods do Movie Recommendation Systems use?
3	RQ3	Movie recommendation systems: how are they assessed?
4	RQ4	How current is movie recommendation system research?
5	RQ5	What are the pros and cons of movie recommendation systems?

Source: Authors, (2024).

II. MATERIALS AND METHODS

II.1 MOVIE RECOMMENDER SYSTEM (MRS)

The exponential growth of the film industry and its establishment in multiple nations has elevated movie-watching to a prominent leisure pursuit for the general populace [32]. Nevertheless, the ongoing advancement of films, coupled with the swift evolution of technology, is progressively shifting the paradigm of movie consumption. It is transitioning from the conventional practice of seeing movies in theaters to the convenience of online streaming platforms, enabling consumers to enjoy films from the comfort of their own homes. Online media streaming platforms have enhanced and implemented numerous features by integrating new technologies and prioritizing the trends of the substantial data era [33]. These functionalities enable users to evaluate films and exchange their experiences with peers. Furthermore, this platform utilizes user score data to establish a recommendation engine capable of forecasting the choices made by each user [34]. The assessment of MRS recommendations involves using objective or subjective ground truth values. This is done by gathering data and comparing it with the item database. The diagram in Figure 1 below illustrates the overall framework and methodology for conducting a comprehensive investigation of the MRS literature in order to address a specific research question (RQ).

Is an e-learning platform designed to provide educators, students, and administrators with one integrated system [23]. E-learning is the principle of direct learning, and in its application, it promotes independent learning, namely web-based distance learning that can be accessed via the Internet network [24]. Moodle provides digital classrooms to access material or anything related

to learning that is freely accessible to anyone, anytime, anywhere [25]. The advantage of using Moodle is that it is open source, so someone with programming skills can adjust and develop existing features according to their needs and desires [26].
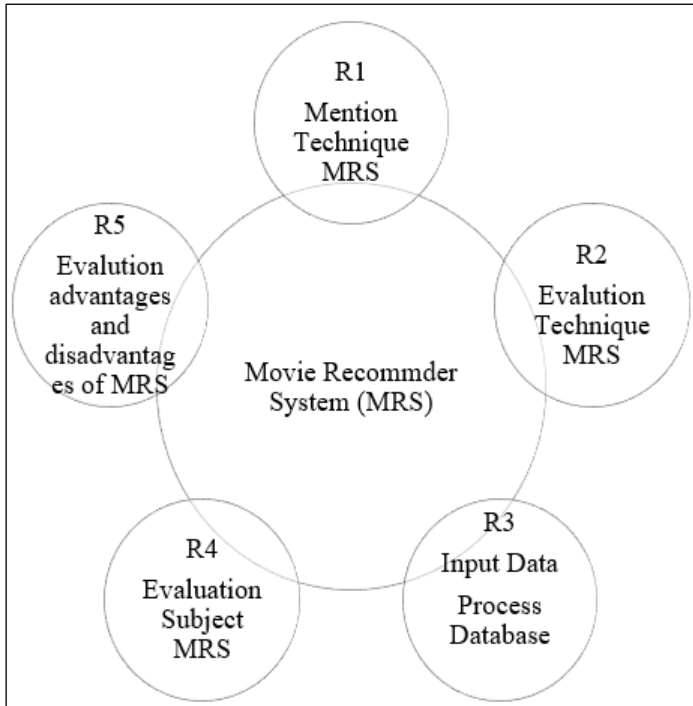

Figure 1: The general architecture used in MRS and RQ relates to the system's relevant aspects.
Source: Authors, (2024).

II.2 RECOMMENDATION METHODS

The MRS recommendation approach elucidates the rationales and characteristics employed in generating movie selection suggestions. The classification of these methods is based on the components utilized for making suggestions. The designs are categorized into four distinct groups: content-based filtering, collaborative filtering, knowledge-based recommender systems, and hybrid approaches recommender systems [35].

1) Content-Based Filtering (CBF)

Content-based filtering (CBF) systems primarily depend on two types of data: a) the description and structure of data attributes and b) user profiles derived from their feedback on different items [36]. An advantage of this system is its capability to address cold start issues related to new users [37]. The system operates at a somewhat basic level since it generates recommendations by considering users' ratings of goods [38]. The primary determinant of the system's quality and accuracy is its capacity to extract and analyze the content of things in order to measure their resemblance to other items [39].

2) Collaborative Filtering

Collaborative filtering (CF) is one of the most suggested and successful algorithms [40]. CF approaches can be classified into model-based and memory-based [41]. A learning approach based on a ranking pattern model acquires a model and generates predictions [42]. Memory-based collaborative filtering (CF) algorithms determine the similarity between users or products [43] by analyzing their current ranks. This allows them to identify neighbors who share similar tastes [44]. User-based or item similarity is the foundation for creating suitable surroundings,

anticipating evaluations of unfamiliar items, and producing suggestions for specific users [33].

3) Knowledge-Based Recommender Systems

This system employs user profiles to ascertain the correlation between user preferences and various forms of content, such as products, information, services, and others [45]. Unlike content-based or collaborative recommendation systems, these systems utilize information about movies and user interests to offer suitable recommendations [46]. It provides personalized recommendations by directly correlating movie attributes with user preferences. The primary constraints include the challenge of accurately recording user preferences and the reliance on data quality [47].

4) Hybrid Methods Recommender Systems

As implied by its name, this strategy can amalgamate multiple methodologies to leverage their respective capabilities [24]. Hybrid methods enable the combination of multiple approaches to address the limitations of each other, resulting in enhanced recommendation accuracy and performance. Nevertheless, the enhancement of performance relies on how the approaches are integrated [48], as these methods can offer thorough and precise recommendations to users [49].

The systematic literature review (SLR) approach categorizes published research and its findings in an organized manner by thoroughly examining the primary material, methodology, and results. This process aims to minimize bias and draw conclusions based on statistical meta-analysis, which is supported by empirical data [50]. We employed a methodical methodology to gather, categorize, and scrutinize the most up-to-date data on MRS [51], given the limited number of thorough studies that have endeavored to assess MRS research [52]. Therefore, we relied on recognized methodologies for conducting Systematic Literature Reviews (SLR) in this investigation.

The SLR review process has multiple steps: 1. Determining research goals and questions; 2. Choose a database and gather data for the initial investigation; 3, define extraction and extraction points; 4, analyze, synthesize, and report results.

The purpose of this SLR is to investigate and evaluate the present condition of MRS [37]. To accomplish this objective, we employed the review process outlined in Table 2. This study examines five primary facets of Magnetic Resonance Spectroscopy (MRS). The initial part examines the methodologies employed in MRS, encompassing diverse potential amalgamations of recommendation systems and algorithms while leveraging individual traits. The second component of MRS pertains to the data employed for generating movie suggestions. The data encompasses several attributes such as source, format, size, characteristics, pre-processing, and representation. The third aspect of this research pertains to MRS evaluation, encompassing the assessment techniques and metrics that are employed and computed.

The fourth aspect pertains to the study conducted on movie recommendation systems. Subsequently, it is employed for conducting essential experiments aimed at reproducing the experiments and achieving desired learning outcomes; the feasibility of this component relies on the presence of relevant data. Lastly, the scope encompasses the advantages and disadvantages of MRS. In order to guarantee that this systematic literature review (SLR) includes only recent articles, we establish restrictions based on publication dates. Hence, the data utilized for conducting this research comprised literature studies on movie recommendation systems that were published between 2019 and 2023.

III. RESULTS AND DISCUSSIONS

In order to accomplish the objectives of this Systematic Literature Review (SLR), we employed the summary review standards presented in Table 2 to investigate and evaluate the present condition of the MRS. This study examines five primary facets of Magnetic Resonance Spectroscopy (MRS). The initial part examines the methodologies employed in MRS, encompassing many potential amalgamations of recommendation systems and algorithms while also leveraging human qualities. Another crucial element of MRS is the data utilized for movie suggestions. The data includes information on its source, format, size, features, pre-processing, and representation. The third aspect of this study pertains to the assessment of MRS, encompassing both evaluation techniques and the quantifiable metrics obtained through measurement and calculation. The fourth component pertains to the regression of research in the domain of movie suggestions. The replication of the experiment and the achievement of learning results rely on the availability of the code used in the experiment. The benefits and drawbacks of MRS are the ultimate element of the scope. In order to ensure that recent studies are included in this systematic literature review (SLR), we have established certain criteria for the publication date. Hence, we exclusively examined studies that were published between 2019 and 2023.

Table 2: Summary Review Guidelines (SRG).

No		Research Question
1	Research Question	RQ1 What methods do movie recommendation systems use?
		RQ2 What Movie Recommendation Systems employ what data and pre-processing methods?
		RQ3 How do you evaluate movie recommendation systems?
2	Search string	RQ4 How recent is movie recommendation system research?
		RQ5 What are the pros and cons of movie recommendation systems?
		Existing movie suggestions
		Movie recommendation system
		Movie collaboration filtering
3	Search strategy	Database search: ScienceDirect, LinkSpringer, IEEExplore, Tandfonline
4	Paper inclusion standards	SRG1 Full text.
		SRG2 Paper is English.
		SRG3 Paper describes a movie recommendation system.

Source: Authors, (2024).

The research question serves as the primary driver for the comprehensive systematic review, guiding the search for publications that pertain to the fundamental elements of each systematic review. This is because the entire research methodology is founded upon this inquiry. Determining research questions follows establishing the research's goal and scope, a suggested starting step to mitigate bias throughout the research process. To ensure the dependability of this approach, the research question must be stated in a manner that encompasses the entirety of the study issue.

We created precise and detailed research questions by following criteria and drawing from prior SLRs. Interventions are different suggestion methods in MRS investigations. The advantages and downsides of MRS emerge from this approach. These findings enable this research to uncover significant MRS information. Table 1 shows key research question topics. Figure 1 shows the research question and the MRS architecture relationship. We searched all four journal databases using search strings. Vary database standards make search strings vary. Searches change the paper's title, abstract, and keywords. The research objectives are usually brief to identify just relevant studies to the search phrase. Data from 27,187 papers from various databases in December 2023 is displayed in Table 3.

Table 3: The Total Number of Literature That Was Obtained from The Various Databases.

No	Literature Database	Result
1	ScienceDirect	6825
2	LinkSpringer	6389
3	IEEExplore	68
4	Tandfonline	13.905
	Total	**27187**

Source: Authors, (2024).

We filter articles from four journal databases using MRS. Direct study selection yielded 66 high-quality MRS-compatible primary publications. Table 4 summarizes each source's main research.

Table 4: The Latest Collection of Primary Research Conducted.

No	Literature Database	Result	Percentage of Studies
1	ScienceDirect	22	33
2	LinkSpringer	27	41
3	IEEExplore	3	5
4	Tandfonline	24	21
	Total	**66**	**100**

Source: Authors, (2024).

Metadata collection follows primary study collection and evaluation. After determining the extraction point, Table 5 shows the extraction form based on Table 2's research questions.

Table 5: Data Extraction.

No	Research Field	Input type	Research Question
1	Filename	Free text	**-**
2	Paper title	Free text	**-**
3	Authors	Free text	-
4	Publication year	Numeric year	-
5	Publication venue	Category Search	-
6	Paper type	Category Search	-
7	Aim	Free text	-
8	Recommendation method	Category Search	RQ1
9	Recommendation algorithm	Category Search	RQ1
10	Dataset used	Category Search	RQ2
11	Evaluation method	Category Search	RQ3
12	Repository	Free text	RQ4
13	Advantages	Free text	RQ5
14	Limitations research	Free text	RQ5

Source: Authors, (2024).

After collecting the main study data, analysis began. Data includes category frequencies and percentages. A qualitative study is needed to determine MRS pros and cons. Summaries and categories of pros and cons. Each category is reported beyond its primary study.

As shown in Figure 2, there is a steady growth in the number of paper publications on movie recommendation systems (MRS) from 2019 to 2023. However, it is more probable that this rise is attributable to the date of collecting of these sea level records.
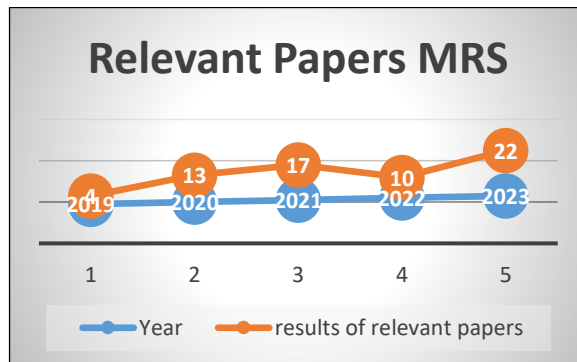
Figure 2: Relevant MRS Papers from 2019 to 2023.
Source: Authors, (2024).

Many movie recommendation algorithms have major issues. The sparsity problem [53] occurs when large data sets have numerous empty items. This makes pattern recognition and recommendation accuracy harder. Scalability is the ability to handle more users and items without sacrificing performance. A cold start occurs when the system lacks historical data to provide relevant offers for new customers or products. Complex systems take longer to create recommendations, which might hurt user experience. MRS experiments are used to test recommendation system algorithms to calculate data accuracy, as shown in Figure 3.
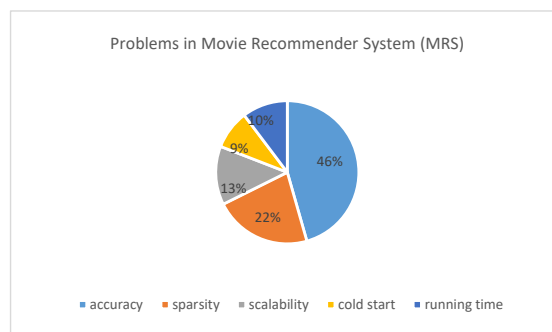
Figure 3: Problems in MRS.
Source: Authors, (2024).

Commonly utilized datasets in film recommendation research include MovieLens, IMDb, Netflix, and TMDB Movie Dataset [54]. The MovieLens dataset, offered by GroupLens Research, encompasses a range of movie ratings, user data, and movie metadata that is accessible in different dimensions [55]. The IMDb dataset provides comprehensive data on movies, including their title, genre, rating, and description. This dataset is well-suited for content analysis and developing content-based recommendation systems [56]. The Netflix Dataset contains more than 100 million reviews provided by Netflix users [57] and plays a crucial role in the development of recommendation systems. Concurrently, the TMDB film dataset offers comprehensive information regarding movies, including a summary, genre, and popularity [36]. This dataset is valuable for conducting research on audience preferences and analyzing the sentiment of films. The MRS literature study included a total of 66 works that focused on film recommendations using public datasets in the field of data, as shown in Figure 4.
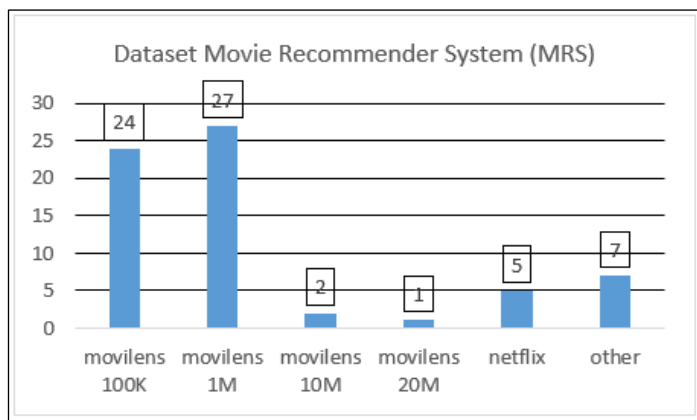
Figure 4: Dataset MRS.
Source: Authors, (2024).

Literature studies on MRS show that MRS can recommend movie-viewing items to users using various methods, algorithms, data sets, pre-processing techniques, and data representation [58]. MRS can also handle information overload by filtering out irrelevant items. This is useful considering the increasing number of film service provider sites [59]. Expanding the e-commerce sector of film service providers is expected to make these systems increasingly important [60]. In addition, MRS has drawbacks, and several limiting factors have been found for various applications. The review shows that content-based filtering and machine learning techniques are used to create most MRSs, which can result in non-personalized recommendations [61]. Non-personalized recommendations are recommendations given without considering a person's characteristics. These recommendations are based on general data or trends rather than personal data, so they are more available to everyone and do not raise privacy issues. This shows that MRS personalization can still be improved. Because movie selection is so diverse and has no common technique, comparing and assessing systems is difficult.

MRS research has become active in the previous five years, as shown by the number of publications. Most research have not examined movie recommendation systems' demographic and timing effects [62]. Demographic and time-based movie recommendation systems will be studied for relevance and customisation [63].

In future research, MRS should use this data to counteract dynamic preference changes with time data, such as watching trends or seasonal popularity. Using demographic data like age, gender, and region, the algorithm can determine group preferences and make more targeted suggestions. Analyzing who and when consumers watch can improve user happiness and suggestion accuracy.

IV. CONCLUSIONS

Movie Recommendation Systems (MRS) use algorithms, datasets, preprocessing methods, and data representations to recommend movies. Multiple evaluation methodologies and indicators are employed to assess recommendation and system quality. This system reduces data overload by filtering unimportant objects. This system becomes increasingly important as more sites provide movie viewing. This system is beneficial, but various limitations can limit its application. This systematic literature evaluation covers several film recommendation topics. The quality of MRS is fully shown here.

Content-based filtering has become the most common movie recommendation approach during the previous five years. As previously said, this greatly diminishes the level of personalization in MRS. Machine learning algorithms are commonly employed to obtain recommendations. The predominant pairing of movie recommendations involves non-personalized content-based machine learning, followed by near-personalized graph-based machine learning. This appears to be the most advanced method. Most of the UCI public film dataset systems are utilized as data sources in MRS.

V. AUTHOR'S CONTRIBUTION

Conceptualization: Yuri Ariyanto and Triyanna Widiyaningtyas.
Methodology: Yuri Ariyanto and Triyanna Widiyaningtyas.
Investigation: Yuri Ariyanto and Triyanna Widiyaningtyas.
Discussion of results: Yuri Ariyanto and Triyanna Widiyaningtyas.
Writing – Original Draft: Yuri Ariyanto and Triyanna Widiyaningtyas.
Writing – Review and Editing: Yuri Ariyanto and Triyanna Widiyaningtyas.
Resources: Yuri Ariyanto and Triyanna Widiyaningtyas.
Supervision: Yuri Ariyanto and Triyanna Widiyaningtyas.
Approval of the final text: Yuri Ariyanto and Triyanna Widiyaningtyas.

VI. ACKNOWLEDGMENTS

VII. REFERENCES

[1] P. Mondal, P. Kapoor, S. Singh, S. Saha, J. P. Singh, and N. Onoe, "Task-Specific and Graph Convolutional Network based Multi-modal Movie Recommendation System in Indian Setting," Procedia Comput. Sci., vol. 222, pp. 591–600, 2023, doi: 10.1016/j.procs.2023.08.197.

[2] Z. Hu, S. M. Cai, J. Wang, and T. Zhou, "Collaborative recommendation model based on multi-modal multi-view attention network: Movie and literature cases," Appl. Soft Comput., vol. 144, p. 110518, 2023, doi: 10.1016/j.asoc.2023.110518.

[3] F. García-Sánchez, R. Colomo-Palacios, and R. Valencia-García, "A social-semantic recommender system for advertisements," Inf. Process. Manag., vol. 57, no. 2, p. 102153, 2020, doi: 10.1016/j.ipm.2019.102153.

[4] Y. Hu, F. Xiong, D. Lu, X. Wang, X. Xiong, and H. Chen, "Movie collaborative filtering with multiplex implicit feedbacks," Neurocomputing, vol. 398, pp. 485–494, 2020, doi: 10.1016/j.neucom.2019.03.098.

[5] Y. Gu, Z. Ding, S. Wang, and D. Yin, "Hierarchical user profiling for e-commerce recommender systems," WSDM 2020 - Proc. 13th Int. Conf. Web Search Data Min., pp. 223–231, 2020, doi: 10.1145/3336191.3371827.

[6] D. P. D. Rajendran and R. P. Sundarraj, "Using topic models with browsing history in hybrid collaborative filtering recommender system: Experiments with user ratings," Int. J. Inf. Manag. Data Insights, vol. 1, no. 2, p. 100027, 2021, doi: 10.1016/j.jjimei.2021.100027.

[7] G. Behera and N. Nain, "Collaborative Filtering with Temporal Features for Movie Recommendation System," Procedia Comput. Sci., vol. 218, pp. 1366–1373, 2022, doi: 10.1016/j.procs.2023.01.115.

[8] V. Jain and K. Bansal, "Novel Approach using user-based Similarity for Recommendation Systems," Proc. 4th Int. Conf. Inven. Syst. Control. ICISC 2020, no. Icisc, pp. 522–526, 2020, doi: 10.1109/ICISC47916.2020.9171214.

[9] B. Walek and V. Fojtik, "A hybrid recommender system for recommending relevant movies using an expert system," Expert Syst. Appl., vol. 158, 2020, doi: 10.1016/j.eswa.2020.113452.

[10] S. Putta and O. Kulkarni, Analytical Study of Content-Based and Collaborative Filtering Methods for Recommender Systems, vol. 936. Springer Nature Singapore, 2022.

[11] B. Dai, X. Shen, J. Wang, and A. Qu, "Scalable Collaborative Ranking for Personalized Prediction," J. Am. Stat. Assoc., vol. 116, no. 535, pp. 1215–1223, 2021, doi: 10.1080/01621459.2019.1691562.

[12] M. S. Kim, B. Y. Lim, H. S. Shin, and H. Y. Kwon, "Historical credibility for movie reviews and its application to weakly supervised classification," Inf. Sci. (Ny)., vol. 630, no. February, pp. 325–340, 2023, doi: 10.1016/j.ins.2023.01.138.

[13] A. Breitfuss, K. Errou, A. Kurteva, and A. Fensel, "Representing emotions with knowledge graphs for movie recommendations," Futur. Gener. Comput. Syst., vol. 125, pp. 715–725, 2021, doi: 10.1016/j.future.2021.06.001.

[14] Y. J. Leng, Z. Y. Wu, Q. Lu, and S. Zhao, "Collaborative filtering based on multiple attribute decision making," J. Exp. Theor. Artif. Intell., vol. 34, no. 3, pp. 387–397, 2022, doi: 10.1080/0952813X.2021.1882000.

[15] P. M. T. Do and T. T. S. Nguyen, "Semantic-enhanced neural collaborative filtering models in recommender systems," Knowledge-Based Syst., vol. 257, p. 109934, 2022, doi: 10.1016/j.knosys.2022.109934.

[16] H. Lei, J. Liu, and Y. Yu, "Exemplar-based large-scale low-rank matrix decomposition for collaborative prediction," Int. J. Comput. Math., vol. 100, no. 3, pp. 615–640, 2023, doi: 10.1080/00207160.2022.2141571.

[17] I. Fernández-Tobías, I. Cantador, P. Tomeo, V. W. Anelli, and T. Di Noia, "Addressing the user cold start with cross-domain collaborative filtering: exploiting item metadata in matrix factorization," User Model. User-adapt. Interact., vol. 29, no. 2, pp. 443–486, 2019, doi: 10.1007/s11257-018-9217-6.

[18] V. P, V. G, and K. S. Joseph, "A Combined Approach For Collaborative Filtering Based Recommender Systems with Matrix Factorisation and Outlier Detection," J. Bus. Anal., vol. 4, no. 2, pp. 111–124, 2021, doi: 10.1080/2573234X.2021.1947752.

[19] P. Zhang, Z. Zhang, T. Tian, and Y. Wang, "Collaborative filtering recommendation algorithm integrating time windows and rating predictions," Appl. Intell., vol. 49, no. 8, pp. 3146–3157, 2019, doi: 10.1007/s10489-019-01443-2.

[20] R. Nesmaoui, M. Louhichi, and M. Lazaar, "A Collaborative Filtering Movies Recommendation System based on Graph Neural Network," Procedia Comput. Sci., vol. 220, no. 2019, pp. 456–461, 2023, doi: 10.1016/j.procs.2023.03.058.

[21] S. Airen and J. Agrawal, "Movie Recommender System Using Parameter Tuning of User and Movie Neighbourhood via Co-Clustering," Procedia Comput. Sci., vol. 218, pp. 1176–1183, 2022, doi: 10.1016/j.procs.2023.01.096.

[22] Y. L. Chen, Y. H. Yeh, and M. R. Ma, "A movie recommendation method based on users' positive and negative profiles," Inf. Process. Manag., vol. 58, no. 3, p. 102531, 2021, doi: 10.1016/j.ipm.2021.102531.

[23] J. Bobadilla, A. Gutiérrez, R. Yera, and L. Martínez, "Creating Synthetic Datasets for Collaborative Filtering Recommender Systems using Generative Adversarial Networks," vol. 280, no. September, 2023, doi: 10.1016/j.knosys.2023.111016.

[24] Z. Movafegh and A. Rezapour, "Improving collaborative recommender system using hybrid clustering and optimized singular value decomposition," Eng. Appl. Artif. Intell., vol. 126, no. PD, p. 107109, 2023, doi: 10.1016/j.engappai.2023.107109.

[25] T. Mohammadpour, A. M. Bidgoli, R. Enayatifar, and H. H. S. Javadi, "Efficient clustering in collaborative filtering recommender system: Hybrid method based on genetic algorithm and gravitational emulation local search algorithm," Genomics, vol. 111, no. 6, pp. 1902–1912, 2019, doi: 10.1016/j.ygeno.2019.01.001.

[26] R. Sun, A. Akella, R. Kong, M. Zhou, and J. A. Konstan, "Interactive Content Diversity and User Exploration in Online Movie Recommenders: A Field Experiment," Int. J. Hum. Comput. Interact., vol. 0, no. 0, pp. 1–15, 2023, doi: 10.1080/10447318.2023.2262796.

[27] S. Natarajan, S. Vairavasundaram, S. Natarajan, and A. H. Gandomi, "Resolving data sparsity and cold start problem in collaborative filtering recommender system using Linked Open Data," Expert Syst. Appl., vol. 149, 2020, doi: 10.1016/j.eswa.2020.113248.

[28] M. Jallouli, S. Lajmi, and I. Amous, "When contextual information meets recommender systems: extended SVD++ models," Int. J. Comput. Appl., vol. 44, no. 4, pp. 349–356, 2022, doi: 10.1080/1206212X.2020.1752971.

[29] Y. W. • Y. Zh. • S. Wei, "Collaborative filtering recommendation algorithm based on interval-valued fuzzy numbers," Appl. Intell., vol. 4, no. 1, pp. 31–44, 2020, doi: 10.1108/IJCS-10-2019-0030.

[30] S. Lee, "Fuzzy clustering with optimization for collaborative filtering-based recommender systems," J. Ambient Intell. Humaniz. Comput., vol. 13, no. 9, pp. 4189–4206, 2022, doi: 10.1007/s12652-021-03552-8.

[31] K. Kim, "A new similarity measure to increase coverage of rating predictions for collaborative filtering," Appl. Intell., no. 123, 2023, doi: 10.1007/s10489-023-05041-1.

[32] S. Kumar, K. De, and P. P. Roy, "Movie Recommendation System Using Sentiment Analysis from Microblogging Data," IEEE Trans. Comput. Soc. Syst., vol. 7, no. 4, pp. 915–923, 2020, doi: 10.1109/TCSS.2020.2993585.

[33] J. Parthasarathy and R. B. Kalivaradhan, "An effective content boosted collaborative filtering for movie recommendation systems using density based clustering with artificial flora optimization algorithm," Int. J. Syst. Assur. Eng. Manag., 2021, doi: 10.1007/s13198-021-01101-2.

[34] K. K. Jena et al., "Neural model based collaborative filtering for movie recommendation system," Int. J. Inf. Technol., vol. 14, no. 4, pp. 2067–2077, 2022, doi: 10.1007/s41870-022-00858-4.

[35] G. Behera and N. Nain, "The State-of-the-Art and Challenges on Recommendation System's: Principle, Techniques and Evaluation Strategy," SN Comput. Sci., vol. 4, no. 5, 2023, doi: 10.1007/s42979-023-02207-z.

[36] K. Iliopoulou, A. Kanavos, A. Ilias, C. Makris, and G. Vonitsanos, Improving Movie Recommendation Systems Filtering by Exploiting User-Based Reviews and Movie Synopses, vol. 585 IFIP. Springer International Publishing, 2020.

[37] A. Jha, N. Agarwal, D. K. Tayal, and V. A. B, Movie Recommendation Using Content-Based and Collaborative Filtering Approach, vol. 1. Springer Nature Switzerland.

[38] A. Torkashvand, S. M. Jameii, and A. Reza, Deep learning-based collaborative filtering recommender systems: a comprehensive and systematic review, vol. 3. Springer London, 2023.

[39] F. Berisha and E. Bytyçi, "Addressing cold start in recommender systems with neural networks: a literature survey," Int. J. Comput. Appl., vol. 45, no. 7–8, pp.

485–496, 2023, doi: 10.1080/1206212X.2023.2237766.

[40] Y. Koren, S. Rendle, and R. Bell, Advances in Collaborative Filtering. 2022.

[41] M. R. Zarei and M. R. Moosavi, "A Memory-Based Collaborative Filtering Recommender System Using Social Ties," 4th Int. Conf. Pattern Recognit. Image Anal. IPRIA 2019, pp. 263–267, 2019, doi: 10.1109/PRIA.2019.8786023.

[42] T. Anwar and V. Uma, "Comparative study of recommender system approaches and movie recommendation using collaborative filtering," Int. J. Syst. Assur. Eng. Manag., vol. 12, no. 3, pp. 426–436, 2021, doi: 10.1007/s13198-021-01087-x.

[43] A. Gupta and P. Srinath, "A recommender system based on collaborative filtering, graph theory using HMM based similarity measures," Int. J. Syst. Assur. Eng. Manag., vol. 13, no. s1, pp. 533–545, 2022, doi: 10.1007/s13198-021-01537-6.

[44] X. Peng, H. Zhang, X. Zhou, S. Wang, X. Sun, and Q. Wang, Chestnut: Improve serendipity in movie recommendation by an information theory-based collaborative filtering approach, vol. 12185 LNCS. Springer International Publishing, 2020.

[45] Z. Zhang, Y. Zhang, and Y. Ren, "Employing neighborhood reduction for alleviating sparsity and cold start problems in user-based collaborative filtering," Inf. Retr. J., vol. 23, no. 4, pp. 449–472, 2020, doi: 10.1007/s10791-020-09378-w.

[46] N. Pavitha et al., "Movie recommendation and sentiment analysis using machine learning," Glob. Transitions Proc., vol. 3, no. 1, pp. 279–284, 2022, doi: 10.1016/j.gltp.2022.03.012.

[47] S. Raza and C. Ding, News recommender system: a review of recent progress, challenges, and opportunities, vol. 55, no. 1. Springer Netherlands, 2022.

[48] S. R. Mandalapu, B. Narayanan, and S. Putheti, "A hybrid collaborative filtering mechanism for product recommendation system," Multimed. Tools Appl., no. 0123456789, 2023, doi: 10.1007/s11042-023-16056-8.

[49] G. Parthasarathy and S. Sathiya Devi, "Hybrid Recommendation System Based on Collaborative and Content-Based Filtering," Cybern. Syst., vol. 54, no. 4, pp. 432–453, 2023, doi: 10.1080/01969722.2022.2062544.

[50] F. E. Zaizi, S. Qassimi, and S. Rakrak, "Multi-objective optimization with recommender systems: A systematic review," Inf. Syst., vol. 117, p. 102233, 2023, doi: 10.1016/j.is.2023.102233.

[51] M. Nasir and C. I. Ezeife, A Survey and Taxonomy of Sequential Recommender Systems for E-commerce Product Recommendation, vol. 4, no. 6. Springer Nature Singapore, 2023.

[52] A. Ghannadrad, M. Arezoumandan, L. Candela, and D. Castelli, "Recommender Systems for Science: A Basic Taxonomy," CEUR Workshop Proc., vol. 3160, 2022.

[53] H. Koohi and K. Kiani, "Two new collaborative filtering approaches to solve the sparsity problem," Cluster Comput., vol. 24, no. 2, pp. 753–765, 2021, doi: 10.1007/s10586-020-03155-6.

[54] L. Wang, Z. Huang, Q. Pei, and S. Wang, "Federated CF: Privacy-Preserving Collaborative Filtering Cross Multiple Datasets," IEEE Int. Conf. Commun., vol. 2020-June, 2020, doi: 10.1109/ICC40277.2020.9148791.

[55] A. Abdolmaleki and M. H. Rezvani, "An optimal context-aware content-based movie recommender system using genetic algorithm: a case study on MovieLens dataset," J. Exp. Theor. Artif. Intell., vol. 00, no. 00, pp. 1–27, 2022, doi: 10.1080/0952813X.2022.2153279.

[56] and S. S. R. Prajna Paramita Parida, Mahendra Kumar Gourisaria Manjusha Pandey, Hybrid Movie Recommender System - A Proposed Model. Springer Singapore, 2022.

[57] R. Kirubahari and S. M. J. Amali, "An improved restricted Boltzmann Machine using Bayesian Optimization for Recommender Systems," Evol. Syst., no. 0123456789, 2023, doi: 10.1007/s12530-023-09520-1.

[58] R. Abolghasemi, P. Engelstad, E. Herrera-Viedma, and A. Yazidi, "A personality-aware group recommendation system based on pairwise preferences," Inf. Sci. (Ny)., vol. 595, pp. 1–17, 2022, doi: 10.1016/j.ins.2022.02.033.

[59] Y. Lee, S. H. Kim, and K. C. Cha, "Impact of online information on the diffusion of movies: Focusing on cultural differences," J. Bus. Res., vol. 130, no. September 2019, pp. 603–609, 2021, doi: 10.1016/j.jbusres.2019.08.044.

[60] L. S. Al-Abbas, A. S. Haider, and B. Saideen, "A quantitative analysis of the reactions of viewers with hearing impairment to the intralingual subtitling of Egyptian movies," Heliyon, vol. 8, no. 1, p. e08728, 2022, doi: 10.1016/j.heliyon.2022.e08728.

[61] Y. Li, C. Chen, X. Zheng, J. Liu, and J. Wang, "Making recommender systems forget: Learning and unlearning for erasable recommendation," Knowledge-Based Syst., vol. 283, no. August 2023, p. 111124, 2024, doi: 10.1016/j.knosys.2023.111124.

[62] G. Jain, T. Mahara, and S. C. Sharma, "Performance Evaluation of Time-based Recommendation System in Collaborative Filtering Technique," Procedia Comput. Sci., vol. 218, no. 2022, pp. 1834–1844, 2023, doi: 10.1016/j.procs.2023.01.161.

[63] N. R. Kermany, W. Zhao, T. Batsuuri, J. Yang, and J. Wu, "Incorporating user rating credibility in recommender systems," Futur. Gener. Comput. Syst., vol. 147, pp. 30–43, 2023, doi: 10.1016/j.future.2023.04.029.
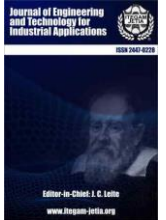
RESEARCH ARTICLE   **OPEN ACCESS**

CSA IMPLEMENTATION STRATEGIES: UNRAVELING SUCCESS AND CHALLENGES

Alliy Adewale Bello

Northeastern University, Roux Institute, USA, College of Professional Studies Project Management Department.

http://orcid.org/0009-0005-6617-8578,

Email: alliybello2@gmail.com

ABSTRACT

This study investigated Corporate Sociopolitical Activism (CSA) and its multilayered dimensions within organizational contexts. The study aimed at examining the likelihood of organizations employing a comprehensive set of CSA strategies to achieve positive outcomes, the impact of CSA strategies on stakeholder engagement and the association between successfully navigating challenges in CSA implementation and adaptive organizational approaches. By employing a quantitative survey research design, data were gathered through a meticulously designed structured questionnaire administered to a sample of 120 respondents. The study revealed that organizations adopting a comprehensive set of CSA strategies indeed have the potential to achieve positive outcomes, challenging the notion that such endeavours might not be fruitful. Additionally, the effectiveness of CSA strategies displayed a significant impact on stakeholder engagement, emphasizing the pivotal role of sociopolitical initiatives in fostering robust relationships with stakeholders. The implications of these findings underscore the importance of proactive engagement with sociopolitical issues, not only for organizational success but also for building and maintaining stakeholder support. Recommendations arising from the study encourage organizations to carefully plan and implement CSA strategies to harness their positive impacts fully.

I. INTRODUCTION

Corporate Sociopolitical Activism (CSA) has become a pivotal aspect of corporate behavior, reflecting a shift in the role of businesses within society [1]. This paradigm shift signifies the recognition by organizations of the need to actively participate in sociopolitical issues extending beyond their immediate economic concerns. Stakeholders, including customers, employees and investors, are increasingly expecting corporations to take a stance on social and political matters, indicating a change in the dynamics of corporate behavior [2].

The implementation of CSA strategies involves corporations deliberately and proactively influencing or shaping sociopolitical issues beyond their traditional business interests [3].

These issues encompass a wide range of concerns, such as environmental sustainability, human rights, diversity and inclusion and political engagement. The proactive nature of CSA distinguishes it from conventional corporate social responsibility, involving a more direct and intentional effort to drive change in societal issues [4].

One key strategy in CSA implementation is the alignment of corporate values with sociopolitical causes [5], argue that organizations strategically align themselves with causes that resonate with their core values and business objectives. This alignment serves as a foundation for authentic and credible sociopolitical engagement, fostering a connection between the organization and its stakeholders. Such alignment is evident in the case of Nike and Colin Kaepernick, where Nike's engagement with

the sociopolitical issue of racial justice was in harmony with the brand's history of endorsing athletes with strong social stands [6]. The multidimensionality of CSA also encompasses the internal dynamics within organizations. Bhattacharya and Elsbach, [7] delve into the concept of organizational identification and disidentification, highlighting how employees' alignment with or detachment from their organization's sociopolitical initiatives can impact the success of such endeavors. An exploration of internal dynamics is crucial for understanding the effectiveness of CSA strategies, as it elucidates the role of organizational culture and leadership in driving sociopolitical engagement [8]. This internal dimension adds a layer of complexity to the scope of CSA, demonstrating that successful implementation goes beyond external communications to encompass internal cohesion and support.

One crucial dimension of assessing the effectiveness of CSA strategies is the impact on organizational reputation [9]. Corporate reputation is a valuable intangible asset that influences stakeholder perceptions and behaviors [10]. Organizations engaging in sociopolitical issues need to evaluate how their actions contribute to building a positive reputation. For instance, the study by del Mar García-De los Salmones and Perez, [11] delves into the effectiveness of CSR advertising in shaping reputation, consumer attributions and emotions. The impact of CSA strategies on brand image is a key consideration. Organizations recognize that their sociopolitical engagements can significantly shape how their brand is perceived by consumers [6]. Successful implementation of CSA strategies should result in a positive association between the organization's brand and the sociopolitical causes it supports [5]. explore the link between corporate sociopolitical activism and firm value, shedding light on how these engagements contribute to overall brand equity.

Effectiveness also extends to the influence of CSA strategies on consumer behaviour. Organizations need to understand whether their sociopolitical initiatives resonate with consumers and drive their choices. Studies, such as [12], focus on understanding consumer responses to CSR activities, emphasizing the mediating role of brand image and brand attitude in shaping consumer behaviour.

Moreover, the integration of sociopolitical considerations into corporate policies and practices is a crucial strategy. Organizations often go beyond symbolic gestures and incorporate sociopolitical values into their operations. This includes adopting environmentally sustainable practices, ensuring diversity and inclusion in the workplace and supporting human rights [5], [13]. The implementation of such policies reflects a commitment to sociopolitical issues that go beyond public relations, fostering a systemic and sustained impact on the organization's practices and its stakeholders.

Furthermore, proactive engagement with stakeholders is a pivotal strategy in CSA implementation. Organizations recognize the importance of involving diverse stakeholders, including customers, employees and investors, in shaping their sociopolitical initiatives [14],[15]. This participatory approach not only enhances the effectiveness of the initiatives but also ensures that they are aligned with the expectations and values of key stakeholders. The study by [16], delves into the reflection of preferences in corporate sociopolitical involvement, shedding light on the intricate dynamics between organizations and stakeholders.

Organizations often leverage partnerships and collaborations as part of their CSA implementation strategies. Collaborations with NGOs, governmental bodies, or other corporations allow organizations to pool resources, share expertise and amplify the impact of their sociopolitical initiatives [6],[17]. Such partnerships can enhance the credibility and reach of an organization's sociopolitical endeavors, enabling them to address complex challenges more effectively.

One of the prominent challenges in CSA implementation relates to the potential backlash from various stakeholders. As highlighted by [12], consumers may respond differently to CSR activities and organizations must anticipate and manage potential negative reactions. The study emphasizes the need to recognize the diverse perspectives and values held by stakeholders, highlighting the challenge of striking a balance that aligns with societal expectations. Understanding and categorizing these varying stakeholder responses provides insights into potential pitfalls and aids organizations in devising strategies to mitigate backlash.

Navigating the complex landscape of sociopolitical issues poses another significant challenge. The study by [18], on sociopolitical activist brands emphasizes the intricacies involved in taking a stance on societal issues. Organizations must carefully navigate diverse perspectives, cultural variations and the ever-evolving nature of sociopolitical concerns [19]. Identifying and categorizing the challenges associated with understanding and responding to the multifaceted nature of sociopolitical issues enables organizations to develop subtlety and context-specific strategies.

Moreover, regulatory challenges and legal considerations represent a substantial hurdle in CSA implementation. As identified by [19], corporations engaging in sociopolitical activism may encounter legal constraints and regulatory scrutiny. Identifying and categorizing these legal challenges provides organizations with a comprehensive understanding of the constraints within which they must operate. This insight is vital for ensuring compliance while still effectively contributing to sociopolitical causes.

While there is a growing acknowledgment of the importance of CSA, existing literature reveals several gaps and challenges that necessitate further exploration. One notable gap pertains to the lack of a comprehensive understanding of the specific strategies employed by organizations in implementing CSA activities. The current literature provides limited insights into the approaches that companies adopt to navigate the complex landscape of sociopolitical issues [5]. Without a detailed exploration of these strategies, there is a dearth of knowledge on the best practices and potential pitfalls in CSA implementation. Addressing this gap is crucial for both academics and practitioners seeking to enhance the effectiveness of sociopolitical engagement. Another critical gap lies in the assessment of the effectiveness of CSA strategies employed by organizations. While there is a growing body of research highlighting the potential positive outcomes of CSA, there is a need for an understanding of the differential impacts observed across various contexts [20].

The study's significance is underscored by the current organizational state, where corporations are increasingly expected to play a proactive role in addressing sociopolitical issues. As societal expectations evolve, businesses are compelled to reassess their roles and responsibilities. This research responds to the pressing need for insights into how corporations can effectively navigate this landscape, contributing not only to academic scholarship but also to guiding corporate entities in aligning their strategies with contemporary societal demands.

The specific objectives of this study were to:
- Explore the strategies employed by organizations in implementing Corporate Sociopolitical Activism (CSA) activities.

- Assess the effectiveness of these strategies in achieving positive outcomes.
- Investigate cases where organizations have successfully navigated challenges in CSA implementation and achieved positive impacts.

To guide the research, the following questions were posed:
- What strategies do organizations employ in implementing Corporate Sociopolitical Activism (CSA) activities?
- How effective are these strategies in achieving positive outcomes?
- Can successful cases be identified where organizations have navigated challenges in CSA implementation and achieved positive impacts?

II. THEORETICAL REFERENCE

II.I INSTITUTIONAL THEORY

In understanding Corporate Sociopolitical Activism (CSA) initiatives, Institutional Theory offers a valuable lens to examine how organizations conform to or diverge from institutional norms. Institutional Theory posits that organizations are influenced by external societal structures, norms and expectations, shaping their behaviour and strategies. Research by [21] provides insights into how organizations conform to or diverge from institutional norms in their pursuit of corporate social change activities. The study explores the role of ideologically motivated activism, emphasizing how activist groups can influence corporate social change within the broader institutional context. This perspective aligns with Institutional Theory, as it recognizes the impact of external actors on shaping organizational responses to sociopolitical issues.

Additionally, the study by [22] on the activist company, using an institutional theoretical lens, delves into how companies pursue societal change through corporate activism. The research examines how organizations strategically adopt societal change initiatives, aligning with or challenging prevailing institutional norms. This approach provides an understanding of how organizations navigate institutional pressures when implementing CSA strategies.

II.2 STAKEHOLDER THEORY

Stakeholder Theory is a pivotal framework for analyzing the role of stakeholders in influencing and shaping Corporate Sociopolitical Activism (CSA) activities undertaken by organizations. This theory posits that organizations are beholden to various stakeholders and their actions and decisions are influenced by the interests and expectations of these key groups. Examining the role of stakeholders provides an understanding of how organizations navigate sociopolitical issues with consideration for the diverse perspectives of those invested in or impacted by their actions.

Mishra and Modi, [23] explores the relationship between Corporate Social Responsibility (CSR) and shareholder wealth, emphasizing the role of stakeholders. This research delves into how stakeholders, particularly shareholders, perceive and respond to CSR activities. The findings contribute to Stakeholder Theory by illustrating the interconnectedness between organizational actions related to sociopolitical issues and stakeholder perceptions, which can impact shareholder wealth.

III. MATERIALS AND METHODS

For this study, a quantitative survey research design has been chosen due to its appropriateness in exploring the relationships and patterns associated with Corporate Sociopolitical Activism (CSA). This design ensures a systematic and structured approach to data collection, ensuring consistency in gathering information from a large sample of respondents. This structure is vital for maintaining uniformity in data collection processes and instruments, enhancing the reliability and validity of the study.

The target population for this study encompasses professionals and stakeholders actively engaged in organizational decision-making processes, particularly those possessing valuable insights into the implementation of Corporate Sociopolitical Activism (CSA) strategies. The rationale behind selecting the target population is rooted in methodological considerations and aligns with recommendations from [24]. The justification for the chosen target population size revolves around the imperative to ensure adequate representation and diversity within the sample.

Simple Random Sampling technique was utilized to select respondents for this study, this technique is grounded in its ability to provide an equal chance of selection for each member of the target population. This approach aligns with the principles of fairness and impartiality in participant selection, as advocated by [25]. The Taro Yamane formula, recommended by [26] for estimating sample sizes within finite populations, was utilized to determine the appropriate sample size from a total population of 171 respondents. Using this formula, the sample size (n) is calculated as: $n = N/(1+Ne^2)$

where n represents the sample size, N is the population size and e is the margin of error.

Applying the values to the formula, with a population size (N) of 171 and an error margin (e) of 0.05:

$$n = N/(1+171 \times 0.05^2)$$
$$n = 171/(1+171 \times 0.0025)$$
$$n = 171/1+0.4275$$
$$n \approx 119.69$$

Rounded to the nearest whole number, the calculated sample size using the Taro Yamane formula is approximately 120. Therefore, a sample size of 120 respondents was adopted for this study.

This study employed the use of structured questionnaires as primary sources of data collection, this strategically aligns with the quantitative approach adopted in this study. The structured nature of questionnaires offers a standardized format for data collection, ensuring consistency and facilitating efficient responses from a diverse range of participants.

The statistical software adopted for this study analysis is Statistical Package for Social Sciences (SPSS), version 27. The questionnaires were serially numbered for recall purposes and coded. This was followed by entering the data into SPPSS, frequency counts were carried out to check for missing variables. Descriptive and inferential statistics was carried out to analyse and present the outcomes of the study data.

IV. RESULTS

Table 1: Sociodemographic Characteristics.

		F (%)
1	**Distribution of questionnaire**	
	Returned/Completed	101(84.2)
	Not Returned/Not Completed	19(15.8)
	Total	120(100)
2	**Gender of respondents**	
	Male	69(68.3)
	Female	32(31.7)
	Total	101(100)
3	**Age group**	
	18-24	4(4)
	25-34	43(42.6)
	35-44	42(41.6)
	45-54	8(7.9)
	55 and above	4(4)
	Total	101(100)
4	**Years of Professional Experience**	
	1-5 years	8(7.9)
	6-10 years	25(24.8)
	More than 10 years	68(67.3)
	Total	101(100)
5	**Occupation**	
	Corporate Executive/Management	28(27.7)
	Middle Management	1(1)
	Entry level Employee	50(49.5)
	Entrepreneur/Business owner	22(21.8)
	Total	101(100)
6	**Industry Sector**	
	Technology/IT	52(51.5)
	Healthcare	24(23.8)
	Finance	14(13.9)
	Manufacturing	11(10.9)
	Total	101(100)

Source: Author, (2024).

The distribution of the questionnaires, as presented in Table1, reflects valuable insights into the respondents' engagement and willingness to participate in the study. Out of the total 120 distributed questionnaires, 101 were returned and completed, resulting in a response rate of 84.2%. The high response rate indicates a significant level of interest and cooperation from the targeted participants.

Further, the data indicates that the majority of the respondents are male, constituting 68.3% of the total sample, while females represent 31.7%. The majority of respondents fall within the age range of 25-34, constituting 42.6% of the total sample, followed closely by the 35-44 age group at 41.6%. The majority of respondents, constituting 67.3%, reported having more than 10 years of professional experience. This substantial proportion indicates a significant representation of seasoned professionals who have witnessed and likely contributed to the evolution of CSA over an extended period. The group with 6-10 years of professional experience comprises 24.8% of the respondents, indicating a sizable contingent of mid-career professionals. This segment represents individuals who have accumulated substantial experience but may still be influenced by evolving trends and shifting paradigms within the organizational landscape. Respondents with 1-5 years of professional experience constitute a smaller, yet noteworthy, group at 7.9%.

The largest group, constituting 49.5% of the respondents, comprises entry-level employees. This segment represents the operational workforce, individuals actively engaged in the day-to-day activities of organizations. Corporate executives and management professionals make up 27.7% of the respondents. This group includes individuals in leadership positions who play a pivotal role in shaping organizational policies and strategies. Their perspectives provide a strategic viewpoint on the motivations and decision-making processes behind CSA initiatives. Entrepreneurs and business owners, constituting 21.8% of the respondents, as individuals responsible for the overall direction of their enterprises, their viewpoints offer insights into how CSA aligns with the strategic vision and values of small and medium-sized businesses. Middle management is represented by 1% of the respondents.

Furthermore, the data reveals a notable concentration in the Technology/IT sector, with 51.5% of respondents belonging to this industry. This dominance suggests a significant interest in CSA within the technology-driven business landscape. The prevalence of respondents from the Technology/IT sector implies a keen awareness and engagement with sociopolitical issues in industries characterized by rapid innovation and societal impact. Healthcare constitutes the second-largest sector, representing 23.8% of respondents. The prominence of the healthcare industry aligns with its inherent societal responsibilities, as organizations within this sector often deal with issues related to public health, ethics and

social welfare. The Finance sector, comprising 13.9% of respondents, reflects the involvement of financial institutions and organizations in discussions surrounding sociopolitical issues.

Manufacturing, with 10.9% representation, signifies the engagement of traditional industries in sociopolitical activism.

Table 2: Effectiveness of CSA implementation strategies.

	Strongly Agree F (%)	Agree F (%)	Uncertain F (%)	Disagree F (%)	Strongly Disagree F (%)
Organizations engage in proactive efforts to shape sociopolitical issues beyond immediate economic interests	18(17.8)	53(52.5)	10(9.9)	9(8.9)	11(10.9)
Companies actively participate in initiatives related to environmental sustainability, human rights, diversity and inclusion and political engagement	18(17.8)	56(55.4)	7(6.9)	9(8.9)	11(10.9)
Organization strategically align their business practices with sociopolitical values and causes	18(17.8)	56(55.4)	7(6.9)	9(8.9)	11(10.9)
Corporations invest resources in fostering positive sociopolitical changes beyond legal or regulatory requirements.	18(17.8)	56(55.4)	7(6.9)	9(8.9)	11(10.9)
Implemented CSA strategies lead to tangible positive outcomes for the organization	14(13.9)	52(51.5)	15(14.9)	9(8.9)	11(10.9)
Organizations witness increased stakeholder support due to their sociopolitical activism efforts	13(12.9)	52(51.5)	16(15.9)	9(8.9)	11(10.9)
Successful cases of organizations effectively navigating challenges in CSA implementation can be identified	18(17.8)	52(51.5)	16(15.8)	4(4)	11(10.9)
Companies that actively address challenges in CSA implementation tend to achieve positive impacts	18(17.8)	52(51.5)	16(15.8)	4(4)	11(10.9)
Recognizing and overcoming challenges is essential for organizations to achieve success in CSA initiatives	18(17.8)	45(44.6)	18(17.8)	9(8.9)	11(10.9)
Organizations that learn from past challenges in CSA implementation are more likely to achieve positive impacts in the future.	18(17.8)	43(42.6)	20(19.8)	9(8.9)	11(10.9)

Source: Author, (2024).

Regarding organizations engaging in proactive efforts to shape sociopolitical issues beyond immediate economic interests, as shown in Table 2 a majority of respondents, 70.3%, either strongly agreed or agreed with the statement, indicating a prevailing positive outlook toward corporations taking an active role in societal and political matters. When asked about companies actively participating in initiatives related to environmental sustainability, human rights, diversity and inclusion and political engagement, the "Agree" category, with 55.4% of respondents, represents the largest segment, indicating a widespread acknowledgement and acceptance of companies actively participating in initiatives related to societal and political issues.

This finding suggests that a significant portion of the sample perceives companies as actively contributing to causes such as environmental sustainability, human rights, diversity and inclusion and political engagement.

Further, when questioned on whether organizations strategically align their business practices with sociopolitical values and causes. The results reveal a predominant positive sentiment among the respondents, with 73.2% either strongly agreeing or agreeing with the statement. This finding suggests that many respondents perceive a conscious effort by organizations to integrate sociopolitical considerations into their business strategies. Responses concerning whether corporations invest resources in fostering positive sociopolitical changes beyond legal or regulatory requirements indicates a prevalent positive inclination among the respondents, with the largest segment, "Agree," representing 55.4% of respondents. This indicates a significant majority acknowledging that corporations invest resources in fostering positive sociopolitical changes beyond legal or regulatory requirements. This finding suggests a widespread perception among respondents that corporations are actively committing resources to drive positive sociopolitical impacts. For

the distribution of responses regarding whether implemented Corporate Sociopolitical Activism (CSA) strategies lead to tangible positive outcomes for organizations. The majority of respondents fall into the "Agree" category, representing 51.5%. This substantial portion of respondents indicates a prevailing belief that CSA strategies contribute positively to tangible outcomes for organizations. It suggests a consensus among a significant segment of participants that engaging in sociopolitical issues leads to positive results, aligning with the overarching objectives of organizational endeavours.

The respondents responses on whether organizations learn from past challenges in CSA implementation are more likely to achieve positive impacts in the future yielded a 42.6% "Agree" response, which suggests a substantial consensus among participants affirming the belief that organizations learning from past challenges in CSA implementation are more likely to achieve positive impacts in the future. This majority agreement indicates a shared conviction that drawing insights from past experiences is a valuable approach for enhancing the effectiveness of future sociopolitical activism.

Table 3: One-Sample Statistics.

	N	Mean	Std. Deviation	Std. Error Mean
The strategies employed by organizations in implementing Corporate Sociopolitical Activism (CSA) activities.	4	85.0000	7.74597	3.87298
The effectiveness of these strategies in achieving positive outcomes.	4	85.5000	7.32575	3.66288
Cases where organizations have successfully navigated challenges in CSA implementation and achieved positive impacts.	4	81.7500	9.87843	4.93921

Source: Author, (2024).

Table 3 presents the One-Sample Statistics for the three dimensions of Corporate Sociopolitical Activism (CSA) activities, providing a glimpse into the central tendency and variability of responses on a Likert scale.

Strategies Employed by Organizations in CSA:

The mean score of 85.00 suggests a relatively high average agreement among respondents regarding the strategies employed by organizations in implementing CSA activities. The narrow standard deviation of 7.75 indicates a relatively low level of variability in responses, implying a degree of consensus among participants. However, the wide standard error of the mean (3.87) points to potential variability in the population and suggests caution in generalizing these findings.

Effectiveness of CSA Strategies:

The mean score of 85.50 indicates a high average agreement among respondents regarding the effectiveness of CSA strategies in achieving positive outcomes. The standard deviation of 7.33 suggests a moderate level of variability in responses, indicating that while there is general agreement, there are variations in opinions among participants. The standard error of the mean (3.66) again highlights potential variability in the broader population.

Success in Navigating Challenges in CSA Implementation:

The mean score of 81.75 suggests a relatively high average agreement among respondents regarding the successful navigation of challenges in CSA implementation leading to positive impacts. The higher standard deviation of 9.88 indicates a

greater degree of variability in responses compared to the other dimensions. The wider standard error of the mean (4.94) suggests potential variability in the population.

IV.I DISCUSSIONS

The study delved into the multifaceted realm of Corporate Sociopolitical Activism (CSA), aiming to unravel the strategies employed, their effectiveness and the overarching impact on organizational outcomes. A comprehensive exploration was undertaken, involving an in-depth analysis of the perspectives of professionals and stakeholders engaged in organizational decision-making processes.

Summarily, the data obtained collectively portray a positive perception among respondents regarding organizations' involvement in sociopolitical activism. The high percentages of agreement across these dimensions suggest that organizations are not only seen as actively engaging in shaping sociopolitical issues but are also strategically aligning their business practices with sociopolitical values. Moreover, the willingness to invest resources in fostering positive changes beyond legal obligations highlights a proactive approach among organizations in addressing broader societal concerns. These findings underscore the growing importance of sociopolitical considerations in shaping organizational strategies and activities, reflecting a broader shift towards socially responsible and conscientious business practices.

The majority of respondents also believe that engaging in sociopolitical activism contributes to improved reputation, enhanced societal influence, positive outcomes and increased stakeholder support. These findings suggest a recognition among respondents of the multifaceted benefits associated with CSA, reinforcing the idea that organizations are increasingly

acknowledging the importance of sociopolitical considerations in shaping their overall image and impact.

Strategies Employed in CSA Implementation:

The findings revealed that a significant majority of respondents acknowledged organizations' proactive efforts in shaping sociopolitical issues beyond immediate economic interests (Table 2). This underscores a prevailing sentiment that companies are strategically aligning their business practices with sociopolitical values and causes. Moreover, the results indicated that corporations are actively participating in initiatives related to environmental sustainability, human rights, diversity and inclusion and political engagement (Table 2). The consensus among respondents suggests a widespread acknowledgement of organizations' commitment to a holistic approach in addressing sociopolitical issues.

Effectiveness of CSA Strategies:

The study further explored the perceived effectiveness of CSA strategies, revealing a positive inclination among respondents. A majority agreed that these strategies contribute positively to the reputation and brand image of organizations (Table 2). This aligns with the overarching narrative that organizations strategically investing resources in fostering positive sociopolitical changes beyond legal or regulatory requirements are viewed favourably. The positive mean scores in Table 3 further support the notion that respondents generally perceive CSA strategies as impactful and effective.

Challenges and Adaptive Approaches:

The findings highlighted a prevalent belief that recognizing and overcoming challenges is crucial for organizations to achieve success in CSA initiatives (Table 2). Respondents also acknowledged that organizations learning from past challenges are more likely to achieve positive impacts in the future (Table 2). The identification of successful cases where organizations effectively navigated challenges in CSA implementation received substantial agreement. These findings collectively underscore the significance of adaptive and proactive organizational approaches in the face of challenges associated with sociopolitical activism.

Stakeholder Engagement and Societal Influence:

Examining stakeholder engagement, the results indicate that organizations witness increased stakeholder support due to their sociopolitical activism efforts (Table 2). Respondents also recognized the societal influence and standing of organizations that engage in sociopolitical activism, further emphasizing the interconnectedness of organizational actions with broader societal perceptions.

V. CONCLUSIONS

The investigation into Corporate Sociopolitical Activism (CSA) and its implications on organizational outcomes has yielded significant findings, shedding light on the effectiveness of strategies employed and their impact on stakeholder engagement. The findings suggested a positive association between the breadth of strategies and favourable organizational outcomes. This highlights the importance of a holistic approach to sociopolitical activism, encompassing diverse initiatives related to environmental sustainability, human rights, diversity and inclusion and political engagement. Organizations embracing a multifaceted strategy

appear to reap benefits in terms of enhanced reputation, stakeholder support and societal influence.

The results also asserted that stakeholders, including employees, customers and investors, are influenced by the perceived effectiveness of sociopolitical activism initiatives. The positive correlation between the effectiveness of CSA strategies and increased stakeholder support underscores the importance of strategic and impactful sociopolitical engagement in fostering positive relationships and garnering support from key stakeholders. Further, as evidenced by the results, organizations that effectively address challenges in CSA implementation tend to achieve positive impacts, emphasizing the role of adaptability and proactivity in the face of sociopolitical complexities. Learning from past challenges emerges as a key factor in shaping future success, aligning with the adaptive nature required for effective sociopolitical activism.

The results of this study has provided compelling evidence that organizations adopting a comprehensive set of strategies, ensuring their effectiveness and navigating challenges with adaptability tend to realize positive outcomes. These insights are instrumental for organizations seeking to enhance their sociopolitical engagement, build positive reputations and foster stakeholder support. As organizations continue to navigate the dynamic sociopolitical landscape, the study's findings offer actionable insights and strategic considerations for effective and impactful CSA implementation. Recommendations arising from the study results is the encouragement of organizations to carefully plan and implement CSA strategies to harness their positive impacts fully.

VI. AUTHOR'S CONTRIBUTION

Conceptualization: Alliy Adewale Bello
Methodology: Alliy Adewale Bello
Investigation: Alliy Adewale Bello
Discussion of results: Alliy Adewale Bello
Writing – Original Draft: Alliy Adewale Bello
Writing – Review and Editing: Alliy Adewale Bello
**Supervision:** Alliy Adewale Bello
Approval of the final text: Alliy Adewale Bello

VII. REFERENCES

[1] M. A. L. Latapí Agudelo et al., "A literature review of the history and evolution of corporate social responsibility," *Int. J. Corp. Soc. Respons.*, vol. 4, no. 1, pp. 1-24, 2019. doi:10.1186/s40991-018-0039-y.

[2] E. Sjöström, "Shareholder activism for corporate social responsibility: What do we know?" *Sustain. Dev.*, vol. 16, no. 3, pp. 141-154, 2008. doi:10.1002/sd.361.

[3] L. Blenninger et al., "Under pressure: An analysis of the perceived positioning pressure on sociopolitical issues and its influence on the external communication of German companies," vol. 81780, pp. 15-42, 2022.

[4] B. Graham, "CSA-Practice-Leads-Programme-CGL-evaluation," Centre of expertise on child sexual abuse, Sep. 2020. https://www.csacentre.org.uk/ (accessed Feb. 01, 2024).

[5] Y. Bhagwat et al., "Corporate sociopolitical activism and firm value," *J. Mark.*, vol. 84, no. 5, pp. 1-21, 2020. doi:10.1177/0022242920937000.

[6] J. Avery and K. Pauwels, "Brand activism: Nike and C. Kaepernick," *Harv. Bus. Rev.*, 2019.

[7] C. B. Bhattacharya and K. D. Elsbach, "Us versus Them: The roles of organizational identification and disidentification in social marketing initiatives," *J. Public Policy Mark.*, vol. 21, no. 1, pp. 26-36, 2002. doi:10.1509/jppm.21.1.26.17608.

[8] R. Hay and E. Gray, "Social responsibilities of business managers," *Acad. Manag. J.*, vol. 17, no. 1, pp. 135-143, 1974. doi:10.2307/254777.

[9] Y. Ji and C. Wan, "Working too much in China's tech industry: Corporate social advocacy as a crisis response strategy to issue-based opinion polarization," *Internet Res.*, 2023.

[10] G. Davies et al., "A corporate character scale to assess employee and customer views of the organization's reputation," *Corp. Reputation Rev.*, vol. 7, no. 2, pp. 125-146, 2022.

[11] M. del Mar García-De los Salmones and A. Perez, "Effectiveness of CSR advertising: The role of reputation, consumer attributions and emotions," *Corp. Soc. Respons. Environ. Manag.*, vol. 25, no. 2, pp. 194-208, 2018. doi:10.1002/csr.1453.

[12] K. Ramesh et al., "Consumer's response to CSR activities: Mediating role of brand image and brand attitude," *Corp. Soc. Respons. Environ. Manag.*, vol. 26, no. 2, pp. 377-387, 2018.

[13] E. C. Chaffee, "The origins of corporate social responsibility," *Univ. Cinci. Law Rev.*, vol. 85, pp. 347-373, 2017.

[14] A. B. Carroll, "Corporate social responsibility: Evolution of a definitional construct," *Bus. Soc.*, vol. 38, no. 3, pp. 268-295, 1999. doi:10.1177/000765039903800303.

[15] C.-S. Lai et al., "The effects of corporate social responsibility on brand performance: The mediating effect of industrial brand equity and corporate reputation," *J. Bus. Ethics*, vol. 95, no. 3, pp. 457-469, 2010. doi:10.1007/s10551-010-0433-1.

[16] M. Nalick et al., "Corporate sociopolitical involvement: A reflection of whose preferences?," *Acad. Manag. Perspect.*, vol. 30, no. 4, pp. 384-403, 2016. doi:10.5465/amp.2015.0033.

[17] M. Porter and M. Kramer, "Strategy and society: The link between competitive advantage and corporate social responsibility," *Harv. Bus. Rev.*, vol. 84, no. 12, pp. 78-92, 2022.

[18] H. J. Schmidt et al., "Sociopolitical activist brands," *J. Prod. Brand Manag.*, 2021.

[19] S. Staudt et al., "Corporate social responsibility, perceived customer value and customer-based brand equity: A cross-national comparison," *J. Strateg. Innov. Sustain.*, vol. 10, no. 1, pp. 65-87, 2022.

[20] W. M. Hur et al., "How CSR leads to corporate brand equity: Mediating mechanisms of corporate brand credibility and reputation," *J. Bus. Ethics*, vol. 125, no. 1, pp. 75-86, 2014. doi:10.1007/s10551-013-1910-0.

[21] F. Den Hond and F. G. A. De Bakker, "Ideologically motivated activism: How activist groups influence corporate social change activities," *Acad. Manag. Rev.*, vol. 32, no. 3, pp. 901-924, 2007. doi:10.5465/amr.2007.25275682.

[22] M. Eilert and A. N. Nappier Cherup, "The activist company: Examining & Company's pursuit of societal change through corporate activism using an institutional theoretical lens," *J. Public Policy Mark.*, vol. 39, no. 4, pp. 461-476, 2020. doi:10.1177/0743915620947408.

[23] S. Mishra and S. B. Modi, "Corporate social responsibility and shareholder wealth: The role of marketing capability," *J. Mark.*, vol. 80, no. 1, pp. 26-46, 2016. doi:10.1509/jm.15.0013.

[24] M. Saunders et al.. Chapter 5, "Formulating research design" in *Research Methods for Business Students*, 8th ed. Harlow: Pearson Education, 2019.

[25] D. MacKay and K. W. Saylor, "Four faces of fair subject selection," *Am. J. Bioeth.*, vol. 20, no. 2, pp. 5-19, 2020. doi:10.1080/15265161.2019.1701731.

[26] T. Yamane, *Statistics: An Introductory Analysis*, 1973.
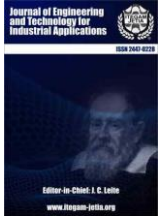
RESEARCH ARTICLE | **OPEN ACCESS**

AWARENESS AND ADOPTION READINESS OF MACHINE LEARNING TECHNOLOGY IN THE CONSTRUCTION INDUSTRY OF A DEVELOPING COUNTRY: A CASE OF NIGERIA

*Samuel Osusha Loya[1], Emmanuel Chidiebere Eze[2], Imoleayo Abraham Awodele[3], Onyinye Sofolahan[4], Olayinka Omoboye[5]

[1]Quantity Surveying Department, Federal Polytechnic Kaltungo, Nigeria.
[2]Department of Architecture and Built Environment, Northumbria University Newcastle, UK.
[3]Construction Management and Quantity Surveying Department, Durban University of Technology, Durban, 4001, South Africa.
[4]Quantity Surveying Department, Lagos State University of Science and Technology, Ikorodu Nigeria.
[5]School of Applied Management, Westminster Business School, University of Westminster, London, UK.

[1] http://orcid.org/0009-0008-9146-8181 , [2] http://orcid.org/0000-0001-7919-6322 , [3] http://orcid.org/0000-0003-1602-7294 , [4] http://orcid.org/0009-0008-1023-4843 , [5] http://orcid.org/0000-0002-3565-7745

Email: *loya.osu@gmail.com, emmanueleze001@gmail.com, a.imole@yahoo.com, onyxnwoko@gmail.com, o.omoboye@westminster.ac.uk.

ARTICLE INFO

ABSTRACT

This study investigated the awareness of the Nigerian construction organisations on some identified ML application areas, and the readiness of the organisations to adopt ML learning in the identified application areas. A comprehensive Literature review was undertaken to identify the application areas of ML, then, a well-structured questionnaire was developed and used to gather relevant data from construction professionals using the snowball sampling method via electronic means. 143 valid responses were obtained, and the gathered data were analysed using arrays of descriptive and inferential analytical tools. The study revealed that the critical applications areas of ML with higher awareness level and adoption readiness in Nigeria are (1) Health and Safety prediction and management, (2) Waste management, (3) Prediction of and management of construction costs, (4) Risk Management, (5) Structural Health Monitoring and Prediction, and (6) Building Life-Cycle assessment and management. Further, a significant statistical difference was observed between the opinions of the participants regarding the awareness and adoption readiness of the various ML application areas. This study identified critical application areas of ML where the awareness and adoption readiness are very high, thus, signalling the preparedness of the Nigerian construction industry (NCI) to embrace ML to drive sustainable construction.

I. INTRODUCTION

The construction industry is considered a significant sector on a worldwide scale since it plays a key role in promoting growth and development in countries by driving infrastructure development and creating employment opportunities [1]. Despite its significant economic contributions, the industry is recognised for its poor productivity, low cost, quality concerns, and time-consuming performances, among other challenges [2]. The slow acceptance of new and innovative technology and methods, along with the fragmented and traditional nature of the construction industry, exacerbates this predicament [3].

The necessity for sophisticated technologies in order to fulfil the industry's productivity and growing requirements for technological advancements arises from the inadequacy of conventional construction methods to achieve anticipated

competitive outcomes [4]. The conventional practices in the construction business are no longer effective in promoting the global aim of sustainability in all human activities [5]. Sustainability is essential and acts as the bridge between environmental and developmental issues, and it influences the responses of governments, professionals, and environmental groups. The traditional approach does not make any meaningful impact on sustainability, and it has also been cited as one of the major causes of construction projects falling behind expected performance outcomes [6].

Artificial intelligence (AI) holds tremendous opportunities and potential opportunities to revolutionise the construction industry by enhancing productivity and addressing some of the performance challenges of the industry [7]. AI has the potential to kickstart a new industrial revolution during the transition to digitalization. AI is a comprehensive entity that includes all other digital technologies, with Machine learning being a component of it. Machine learning artificial intelligence (AI) assists construction experts and organisations in comprehending intricate issues, organising large amounts of data, accelerating learning processes, and producing answers to problems more rapidly [8]. By employing iterative machine learning techniques and analysing historical and real-time data to forecast and learn from it, AI and machine learning provide cost-saving advantages, aid in uncovering concealed patterns, enhancing quality, and improving responsiveness [9]. Machine learning (ML) plays a significant role in sustainable computing and has been identified as an emerging technology that effectively facilitates the adoption of sustainable practices [10]. Specific machine learning algorithms possess significant ramifications for sustainable innovation objectives and are important for tackling construction industry problems [11]. Machine learning, a branch of Artificial Intelligence (AI), focuses on creating and implementing computer programmes that can learn from previous data to model, control, or forecast using statistical methods without direct programming [12]. Machine learning is used in a wide range of fields and scenarios. Examples include our daily lives, healthcare, security, and agriculture [11]. It has been observed that machine learning algorithms aid in predicting unpredictable performance difficulties, monitoring them in real time, and detecting vulnerabilities in the system [13]. Data mining is the most prominent use of machine learning, among several others [14]. Machine learning can be utilised to build relationships between different features, increasing the design and efficiency of the system. The dataset consists of features that can be categorised as binary, continuous, or categorical.

Even though studies that touched on AI abound, there is limited research in academic literature on the use of Machine Learning technology in the construction industry from the viewpoint of developing economies. Prior studies primarily focus on technical or application-specific elements. For instance, [15] examined how AI can be used to address supply chain issues. [16] studied the use of Machine Learning AI in vehicle manufacturing, whereas [17] examined how AI is being applied in the retailing business. [14] suggested a technical framework for digital platforms using machine learning. [13] conducted a cutting-edge review of Machine Learning Algorithms (MLA) to forecast the efficiency of biological wastewater treatment processes. [11] Investigated the use of supervised and unsupervised machine learning methods in sustainable engineering. An examination of the literature from the perspective of advanced nations suggests a steady increase in the implementation of innovative tools and digital technologies. But the story is different when considering developing economies like Nigeria. This is due to many reasons

and challenges. [18] assert that efforts at digitalization of the industry have been hampered by low levels of digital and smart technologies, cost factors, absence of qualified personnel and lack of capacity, and absence of standard references among other factors. [19] attributed the low level of adoption of innovative technologies to its infancy state in Nigeria.

With the growing interest in AI and machine learning in different economic sectors (construction inclusive), the extent of awareness and use of machine learning technologies in the field of construction management in Nigeria is uncertain, despite its widespread acceptance and significant advantages in other industries. This study aims to address this significant gap by evaluating the level of awareness and readiness for adopting machine learning technology in the construction industry of Nigeria. The specific objectives are (1) to assess the awareness of the Nigerian construction organisations on some identified ML application areas, and (2) to determine their readiness to adopt ML learning in the identified application areas. ML can be applied in different areas of applications in construction and comprehending the awareness as well as the adoption readiness of the construction stakeholders will aid in decision-making that triggers and brings the needed changes, particularly in the adoption and implementation of ML technologies in the construction industry. This study will also contribute to the sustainability discourse and targets of the sector as AI and ML are critical contributors to the digitalization and sustainability of the construction sector.

II. THEORETICAL REFERENCE.

II.1 MACHINE LEARNING AWARENESS AND ADOPTION IN CONSTRUCTION.

The idea of developing machines exhibiting intelligence like humans (otherwise known as Artificial Intelligence) can be traced back to fields of computer science, fiction, philosophy, and engineering [20]. Sixty years after Alan Turing's test for machine intelligence [21], intelligent machines are now outperforming humans in domains such as learning [22]. A major capability of machine learning is the utilization of a trained dataset in identifying a trend or pattern to predict an outcome [23]. Unlike other computational approaches, ML does not require outright programming before identifying or predicting such outcomes. Such ability gives ML an edge over other analytical tools. ML has the capability of predicting outcomes based on historical observations, image recognition and group objects. The required algorithms to carry out this task are provided by existing libraries of programmes. Such libraries include Numpy, MatPlotLib, Pandas and Scikit [23].

There are mainly two categories of Machine learning (ML) and these are Shallow learning and Deep learning.

Shallow Learning - This is the traditional machine learning where data transformation and learning occur in a single layer. In this, data description occurs using pre-defined features [24]. Shallow Learning is further categorized into three; supervised learning, unsupervised learning, and Reinforcement learning data sets [25]. Over the years, the most used shallow algorithms in construction are K-nearest Neighbors (KNN), Support Vector Machines (SVM), Logistic Regression, Linear Regression, and Decision Trees (DT) [26].

Deep Learning - A most recent approach in ML that has proven to give more reliable predictions than conventional ML techniques (known as shallow learning) is the Deep Learning approach [12], [27]. Deep learning is an advanced development of Artificial

Neural Networks (ANNs). Typical deep learning architecture network structures that have gained prominent attention in construction are Convolutional Neural Networks (CNNs), Recurrent Neural Networks (RNNs) and transfer learning [26].

The role of innovative technologies in improving time and cost performance, productivity improvement, learning and safety performance is widely acknowledged in the literature. Within the non-construction sectors, [28] reported that the awareness level of AI usage in the libraries of tertiary education institutions is high, but their adoption is low. The awareness of machine learning is very low among financial institutions, and their adoption of credit risk prediction is not in place in developing countries [29]. In the media sector, [30] reported a high awareness level of the role of ML in new production, while [31] found a low awareness of the usefulness of AI in the media. In the energy sector, the awareness level is however high [32].

In the construction industry, via interviews with construction experts, [33] reported a low level of awareness and acceptability of AI. Low awareness and acceptance are among the major barriers to the widespread adoption of AI and other emerging digital technologies in the NCI. The knowledge, awareness and usage of automation techniques are limited in the NCI [34]. Found a moderate level of awareness of construction 4.0 technologies, and their adoption readiness in the construction industry is at the initial level [35]. Notwithstanding the low awareness and adoption of some industry 4.0 technologies, there is an absence of studies that have focused on some specific applications of ML in the construction industry. Within the construction industry, there is a dearth of studies on the awareness and adoption readiness of construction organisations to adopt ML in specific activities in construction.

II.2 APPLICATION AREAS OF MACHINE LEARNING IN THE CONSTRUCTION INDSUTRY.

ML technology is essential and makes a significant impact in the construction industry, evident in its growing popularity in the sector. According to [36], ML is making a significant impact in the construction industry, making it a powerful tool for automating processes in the construction industry [36]. For [37] and [38] believe it has the potential and capacity to manage tacit and explicit knowledge in the management of construction projects. In their study, [39] identified Robotics/Automation, and Big Data Analytics as two machine learning technologies that are currently being adopted in the construction industry worldwide.
Machine Learning has a wide range of applications in the construction industry highlighted as follows:

Site Works: The use of robotics for construction activities such as loading, brick/block laying and painting is becoming more apparent [39]. Such adoption of robotics is highly beneficial to construction sites by helping significantly reduce time spent on repetitive tasks as well as improve efficiency. The major robotics applied for construction according to [39] are interior wall painting robots, KIST floor robotics, ASRERRISK robot and WASEDA robot.

Health and Safety in Construction Sites: The construction business is regarded as one of the most hazardous businesses globally, and this has made health and safety in construction a topmost priority for stakeholders in the sector [40]. Due to the inefficiency of the traditional approach involving the use of questionnaires to collect data [41], machine learning is found to offer high-tech solutions to safety problems that include temporary and permanent injuries in construction sites.
Decision Tree (DT), and Neural network techniques have been adopted in developing models that assess unsafe acts while working on scaffolds [42]. In their assessment of Big Data and Data Analytics utilization in construction, [39] found that new technologies capable of predicting site incidents and issuing prompt warnings have been adopted to improve risk detection and assessment during construction. Technology such as smart wearables capable of collecting relevant data and machine learning algorithms that address possible site incidents as well as creating new strategies for increased efficiency were also adopted in construction [43]-[44]. Also, a computer vision-based approach has been used in addressing postural-based hazards [45]. [40] affirmed the adoption of ML to develop construction site safety indicators as well as injury prediction in construction sites [46]. [47] in his study used Random Forest (RF) and Stochastic Gradient Tree Boosting (SGTB) to develop safety models capable of predicting the type of injury and the body part accurately as well as providing a reliable probable forecast of likely outcomes should an accident occur. A study by [48] combined CNN with a physical fatigue model to detect the level of fatigue among workers on the construction site.

Assessment of Workforce and Activity Recognition: To assist construction project managers in ensuring project deliverables are met, models that can monitor the activities of construction workers on site were developed. [49] developed a model that can detect automatically if a worker on the site is working within a designated boundary. Similarly, [50], proposed a CNN-based model that monitors the activities carried out by workers during reinforcement work.

Cost prediction and Management: Machine learning techniques have been adopted in the prediction of cost of various projects such as highway projects [51],[52], railway projects [53], hydro-power projects [54], building projects [55-56], and tunnel projects [57]. Fuzzy mathematics has been used to develop cost-estimating models [55]. Artificial Neural Network has also been used in estimating the cost of structural projects [56]. For [57] developed a DBM (Deep Boltzmann Machines) based cost estimation model.

Risk identification and Management: An exceptional aspect of ML is its ability the predict danger before it occurs, which aids humans in determining preventive measures for such dangers before they occur [58]. According to [59], machine learning can assist in reducing risks in construction sites by identifying risks and measuring their impacts. Consequently, numerous research on the application of machine learning in the prediction and assessment of risks in construction sites have been carried out [60],[61]. An ML model was developed to assess the risks of delays in high-rise building projects in Nigeria [60]. An expanded cloud model was used to assess potential risks on construction sites [61].

Building Energy Management: The prediction of long to medium-term electricity consumption in buildings is made easier with the adoption of machine learning technology. RNN models were used by [62] for the prediction of long-period heat demand in commercial buildings. [63] in their study developed a neural network-based model that can forecast medium-term to long-term electricity consumption.

Structural Health Monitoring and Prediction: CNN, DBN and CNN are deep learning approaches that have been adopted in developing vibration-based and vision-based monitoring techniques for the purpose of investigating construction materials durability prior to and after construction [64], [65]. For pavement stress detection and classification, [66] developed a DCNN model. A deep learning-based model was developed to detect asphalt and pavement ruts [67],[68]. According to [69] used softmax regression to develop a CNN model for predicting the compressive strength of recycled concrete before construction, and [70] developed a DNN-based model for predicting foamed concrete strength which will assist engineers in optimizing mixture design.

Building Occupancy Modelling and Performance Simulation: The building occupancy model is developed to predict a building energy requirement using the potential number of occupants as the basis for the prediction. This enables construction firms to simulate the building requirements before construction. Simulation results enhance proper and efficient energy allocation to building facilities. According to [71] developed a GAN model for occupancy modelling which outperformed two conventional occupancy modelling approaches (Inhomogeneous Markov Chain and Agent-based Model). For [72] proposed a DNN model that outperformed the performance of a Building Performance Simulation (BPS) at a faster rate.

Building Life-Cycle: ML has also been adopted for building life-span prediction [73], the bankruptcy of construction business prediction [74], and building comfortability prediction [75].

Schedule Management: [76] developed a schedule-learning platform with the adoption of a support vector machine (SVM) and artificial neural network (ANN) ensemble. [77] in their study used a machine learning algorithm to identify the major causes of construction delay.

Based on the foregoing literature review and other related matters, 20 ML application areas were identified and summarized in Table 1.

Table 1: Areas of application of machine learning in construction.

Code	ML Application area in construction	Source(s)
ML01	Site works (e.g., wall painting, plastering, etc.)	[39]
ML02	3D models classification in BIM	[78-79]
ML03	Prediction of and management of construction costs	[51-52, 55-57]
ML04	prediction of the energy system behaviour of buildings	[63]
ML05	Prediction of short-term cooling loads of buildings	[80]
ML06	detection and classification of pavement stress	[66]
ML07	Rutting prediction of asphalt pavement	[67-68]
ML08	prediction of design energy of buildings	[63]
ML09	Prediction of recycled concrete compressive strength and failure	[69-70]
ML10	Waste management	[22]
ML11	construction Workforce Assessment and Activity Recognition	[49], [81]
ML12	Prediction of the long-term heating and electricity loading of buildings	[63]
ML13	Construction equipment assessment and activity recognition	[82]
ML14	prediction of heavy equipment parameters	[83]
ML15	Building Occupancy Modelling and Performance Simulation.	[71-72]
ML16	Health and Safety prediction and management	[39-40], [45-46], [48]
ML17	Schedule Management	[76], [78]
ML18	Risk Management	[58-61]
ML19	Structural Health Monitoring and Prediction	[64-70]
ML20	Building Life-Cycle assessment and management	[73-75]

Source: Authors, (2024).

III. MATERIALS AND METHODS.

III.1 RESEARCH DESIGN.

This research was guided by a post-positivism philosophical lens which allowed for the use of a quantitative research design approach. Quantitative research allows for the collection of numerical data that can be statistically analysed to provide a reliable and objective research outcome [84]. A close-ended questionnaire was utilised in the collection of primary data owing to its capacity to reach larger audiences separated by space and distance in a relatively shorter time. Data collected from close-ended questionnaires are measurable and quantitative [18]. An internet-mediated questionnaire was used since it enables data collection to take place remotely, economically and at a much faster rate [85]. The online survey is an eco-friendly means of data collection as it involves no use of papers made from trees/forests

[86]. Construction professionals in Nigeria were the respondents and units of analysis in the study.

III.2 QUESTIONNAIRE DESIGN, SAMPLING AND DATA COLLECTION.

The questionnaire was designed to have three sections. The first section garnered data on the background information of the respondents, and information obtained in this section served as a quality check to data obtained from the other two sections. The second section gathered data on the awareness level of the respondents regarding the selected application areas of machine learning in the construction industry. The participants were required to rate the variables based on their experiences and knowledge of the level of awareness of the application areas of machine learning in construction on a 5-point Likert scale where; 1= very low awareness, 2= low awareness, 3= moderate awareness, 4= high awareness, and 5= very high awareness. The third section

collected data on the adoption readiness of machine learning in the construction industry. The respondents were required to rate the variables based on their organisations' level of readiness to adopt machine learning in the identified applications areas in their construction projects, on a 5-point Liker scale, where (1= very low readiness level, 2= low readiness level, 3=moderate readiness level, 4=high readiness level, and 5 very high readiness level). The Likert scale offers a better reliability coefficient and improves the chances of getting adequate results that represent the true reality of the research interest [87]. Further, the Likert scale is not cumbersome and enables the respondents to choose from available options their level of agreement or disagreement on a statement with ease [88]. The content and face validity of the questionnaire were ascertained via a pilot study of a small proportion of the sample population (5 construction practitioners and 7 academics), to get the adequacy, suitability, correctness, and fluency of the contents (questions) of the questionnaire to meet the study objectives. Piloting a survey prior to the actual survey is in line with the recommendations of [89]. The inputs from these experts were incorporated into the questionnaire before launching the actual survey.

It was impractical to obtain a separate sampling frame of construction professionals (Engineers, architects, builders, and quantity surveyors) with knowledge and experience in Machine learning (ML), therefore, the study was not restricted to any state or region of Nigeria. Also, the need to obtain significant responses informed the choice of not limiting the study to an area. The survey participation criteria are (i)Experts experienced in construction project delivery, (ii) knowledge of machine learning as well as other emerging technologies applicable to construction, and (iii) involvement in project delivery in Nigerian cities/regions. These criteria are boldly written in the introductory section of the questionnaire to ensure that only qualified experts take part in the study [90]. The researchers have taken the highlighted measures to ensure that the questionnaire obtained reliable and acceptable data whose analyses would yield credible outcomes that represent the true status of affairs with regard to machine learning applications in Nigeria.

The snowball sampling was adopted in the administration of the questionnaire to the construction experts via electronic means (Google form). The snowball sampling technique has the capability to increase the response rate as it is reliant on an effective referral system [91], and thus, completely driven by the respondents. The initial set of respondents was identified via the preliminary survey and from the researcher's cycle [92]. The Google form is amenable to Microsoft Excel and the statistical package for social science (SPSS) used for data analysis. After a sampling period that lasted for 16 weeks, a total of 157 responses were received, out of which only 143 responses were usable. The responses of 14 participants who indicated 'No' to the question regarding knowledge of industry 4.0 technologies (including Machine learning), were discarded. The 143 responses obtained in this study are higher than previous, similar technology and sustainability-focused studies that utilised snowball sampling and electronic means. For example, 134 responses were obtained and used by [93], 105 were gathered by [1], and 133 were obtained by [94]. Thus, the 143 responses for this study are satisfactory for the arrays of analyses carried out and presented in the results and discussion section of this paper. Although considering that the study was not limited to any specific region of Nigeria, the 143 could be argued to be small, however, data collection from experts involving emerging technologies in construction via electronic means usually returns a low response rate [95].

III.3 DATA ANALYSIS METHODS UTILISED.

Descriptive and inferential statistical techniques were used to analyse the gathered data. Frequency and percentage were used to analyse the background information of the respondents. Mean score ($\bar{x}$) and standard deviation (SD) were utilised in ranking the assessed variables based on the relative weightings. The mean normalisation value (NV) was used to determine the most critical factors assessed. Variables with NV ≥ 0.50 were considered critical [96]. The relative importance index (RII) was further used to determine the importance of the ranking of the variables. For interpretation purposes the scale: 0 < RII ≤ 20% (not high); 20 < RII ≤ 40% (very little high); 40 < RII ≤ 60 (somewhat high); 60 < RII ≤ 80% (high); and 80 < RII ≤ 100% (very high) by [97] was adapted. The Kendall's coefficient of concordance or (Kendall's W) and Chi-square (X^2) value were used to determine the overall level of agreement in the ranking of the variables by the respondents. Analysis of variance (ANOVA) was used to determine if there is a statistically significant difference between the various respondents' groups regarding, the awareness level of the application areas of ML in construction, and the adoption readiness of the experts to use ML in the identified application areas. The use of ANOVA for comparison of different survey respondents' groups is common in construction literature [8], [97]. However, prior to all these tests, Cronbach's alpha coefficient was used to determine the reliability of the gathered data. The results showed that the data are highly reliable and of good quality, as the Cronbach's alpha coefficient of 0.944 and 0.909 were obtained for awareness level and adoption readiness of ML, which are closer to 1 [98]. The skewness and kurtosis values from the descriptive test were used to determine the normality of the data. It is advised that the skewness value should range from -2 to 2, and the kurtosis value fall within -7 to 7 [99], and based on the results obtained, the data were adjudged to be normally distributed.

IV. RESULTS AND DISCUSSIONS.
IV. 1 RESPONDENTS BACKGROUND INFORMATION.

Results in Table 2 showed that 32.87% of the respondents are in consulting business, 43.36% are in contracting, and 23.78% are clients. This is a fair representation of the three key stakeholders in the built environment. The profession of the participant's showed Engineers are more with 28.67%, followed by Quantity Surveyors (25.17%), then, project managers (25.17%), Builders (14.69%), Architects (12.59%), and other professions (1.40%). This is a good distribution of the experts who drive innovation penetration in the construction industry. Furthermore, 91.61% of these professionals are chartered members of their various professional bodies, and only a negligible number 8.39% are probationers. The years of experience of the professionals showed that those who have spent 11-15 are constitute 43.36% of the participants. This is followed by those with 16-20 years' experience (21.68%), then 6-10 years' experience (18.88%), 3- 5 years ' (10.49%) and lastly those with 20 years and above (5.59%). Overall, the average years of the experience of the participants was 13 years, and this is a considerable length of time to have acquired sufficient experience and knowledge to contribute meaningfully to the success of this study. Further, the respondents have the requisite education to understand the content of the questionnaire as the minimum level of education attained by the respondents is HND.

Table 2: Background information of the respondentes.

Variables	Classification	Frequency	%
Business of organisations	Consulting	47	32.87
	Contracting	62	43.36
	Clients	34	23.78
	TOTAL	**143**	**100.00**
Profession of respondents	Architect	18	12.59
	Builders	21	14.69
	Engineers	41	28.67
	Quantity Surveyors	36	25.17
	Project managers	25	17.48
	Other (Environmentalist=1, Town planner = 1)	2	1.40
	TOTAL	**143**	**100.00**
Years of experience	3-5years	15	10.49
	6-10 years	27	18.88
	11-15 years	62	43.36
	16-20 years	31	21.68
	20+ years	8	5.59
	TOTAL	**143**	**100.00**
Educational Qualification	Higher National Diploma (HND)	10	6.99
	Bachelor of Science/technology (B.Sc./Batch)	42	29.37
	Master's Degree (MSc./M.Tech.)	79	55.24
	Doctorate degree (PhD)	12	8.39
	TOTAL	**143**	**100.00**
Professional affiliation	Chartered members	131	91.61
	Probationer	12	8.39
	TOTAL	**143**	**100.00**

Source: Authors, (2024).

IV. 2 AWARENESS OF ML APPLICATION AREAS IN CONSTRUCTION

Table 3 shows the results obtained on the awareness of the application areas of machine learning in the construction industry by the respondents. Overall, the respondents showed that they have a high awareness level of ML application areas, and this is premised on the overall mean score of 3.86 (RII=77.14%). Further, RII values showed that 11(55%) of the variables fell within the 'high' category, and 9(45%) were within the 'very high' category. Further, the top ranked application areas with NV>0.50 are prediction of the energy system behaviour of buildings ($\bar{x}$=4.41; NV=1.00), Prediction of short-term cooling loads of buildings ($\bar{x}$=4.41; NV=0.99), Health and Safety prediction and management ($\bar{x}$=4.29; NV=0.89), Waste management ($\bar{x}$=4.28; NV=0.88), Prediction of and management of construction costs ($\bar{x}$=4.22; NV=0.83), Risk Management ($\bar{x}$=4.20; NV=0.81), Structural Health Monitoring and Prediction ($\bar{x}$=4.11; NV=0.73), Building Life-Cycle assessment and management ($\bar{x}$=4.11; NV=0.73), and 3D models classification in BIM ($\bar{x}$=4.04; NV=0.67).

The ANOVA results (Table 3, columns 7 & 8) showed that the views of the respondents' groups (consultants, contractors and clients), have a non-significant difference with a p-value≥0.05 in nine of the variables. Eleven of the variables, however, showed a divergent view among the respondents, as the p-value<0.05 was obtained. The differences in knowledge and experiences as well as different organisational technology cultures could have an impact on this result. Further, the overall ANOVA is significant with p-value =0.042 and F=3.248. Based on this, the study concluded that there is a significant statistical difference in the awareness level of the consultants, contractors and clients regarding the awareness level of ML application areas in construction.

From Kendall's test, the critical X^2 of 30.114 from the table is less than the calculated X^2 of 238.66. This implies closely related rankings with insignificant differences in the opinions of the participants. The use of the chi-square values of Kendall's test to interpret the relatedness of assessed variables ranking within participants is evident in the literature [90, 93].

Table 3: Awareness of ML applications areas in construction.

Code	ML Application area in construction	⊠	NV	RII	Remark	Rank	ANOVA F-stat	ANOVA Sig.
ML01	Site works (e.g., wall painting, plastering, etc.)	3.67	0.340	73.43%	H	14	2.483	0.087
ML02	3D models classification in BIM	4.05	0.68a	80.98%	VH	9	17.245	0.000*
ML03	Prediction of and management of construction costs	4.22	0.83a	84.34%	VH	5	10.324	0.000*
ML04	prediction of the energy system behaviour of buildings	4.41	1.00a	88.25%	VH	1	10.115	0.000*
ML05	Prediction of short-term cooling loads of buildings	4.41	0.99a	88.11%	VH	2	10.430	0.000*
ML06	detection and classification of pavement stress	3.29	0.00	65.73%	H	20	1.528	0.220
ML07	Rutting prediction of asphalt pavement	3.36	0.07	67.27%	H	17	3.155	0.046*
ML08	prediction of design energy of buildings	3.50	0.19	69.93%	H	16	0.407	0.666
ML09	Prediction of recycled concrete compressive strength and failure	3.35	0.06	66.99%	H	18	0.957	0.386
ML10	Waste management	4.28	0.88a	85.59%	VH	4	10.763	0.000*
ML11	construction Workforce Assessment and Activity Recognition	3.69	0.35	73.71%	H	12	0.132	0.876
ML12	Prediction of the long-term heating and electricity loading of buildings	3.32	0.03	66.43%	H	19	3.090	0.049*
ML13	Construction equipment assessment and activity recognition	3.61	0.29	72.17%	H	15	1.260	0.287
ML14	prediction of heavy equipment parameters	3.71	0.38	74.27%	H	11	1.894	0.154
ML15	Building Occupancy Modelling and Performance Simulation.	3.69	0.35	73.71%	H	12	1.046	0.354
ML16	Health and Safety prediction and management	4.29	0.89a	85.87%	VH	3	7.464	0.001*
ML17	Schedule Management	3.87	0.52a	77.48%	H	10	9.145	0.000*
ML18	Risk Management	4.20	0.81a	84.06%	VH	6	25.577	0.000*
ML19	Structural Health Monitoring and Prediction	4.11	0.73a	82.24%	VH	7	4.176	0.017*
ML20	Building Life-Cycle assessment and management	4.11	0.73a	82.24%	VH	7	2.833	0.062
ANOVA	N	143						
	Kendall's W^a	0.088						
	calculated Chi-Square (X^2) value	238.66						
	Critical Chi-Square (X^2) value from Table	30.114						
	df	19						
	Asymptotic level of significance	0.000						
		Between Groups	Within Groups	Total				
	Sum of Squares	5.054	108.97	114.028				
	df	2	140	142				
	Mean Square	2.527	0.778					
	F	3.248						
	Sig.	0.042						

*p-value≤0.05; ^{a}Normalisation value ≥0.50 indicate criticality of assessed variables

Source: Authors, (2024).

IV. 2 ADOPTION READINESS OF ML APPLICATION AREAS IN CONSTRCTION

Table 4 shows the results obtained on the adoption readiness of ML in assessed application areas in the construction industry. Overall, the participants indicate high adoption readiness of ML in the various areas of application in construction, and this is based on the overall mean of 3.83 (RII=76.75%). A further breakdown of each ranking of the adoption readiness on each application area showed that 14(70%) of the variables fell within the 'high' category, and 6(30%) were within the 'very high' category. Notwithstanding, the top six ranked application areas based on relative weights of the adoption readiness and whose NV>0.50 are Prediction of and management of construction costs ($\bar{x}$=4.34; NV=1.00), Health and Safety prediction and management ($\bar{x}$=4.32; NV=0.99), Risk Management ($\bar{x}$=4.32; NV=0.99), Building Life-Cycle assessment and management ($\bar{x}$=4.26; NV=0.93), Waste management ($\bar{x}$=4.16; NV=0.84), and structural Health Monitoring and Prediction ($\bar{x}$=4.11; NV=0.79).

The ANOVA result shows that the opinion of the participants differs significantly in 70% of the assessed ML application areas. The adoption readiness of the ML in the application areas had a p-value<0.05, and thus, was ranked differently by the consultants, contractors and clients. The result further revealed that 30% of the variables were ranked in a similar

way by the respondents, as their p-value >0.05. The significant differences observed in the adoption readiness of ML in construction could be based on the financial capabilities of the different organisations, and their technology innovation culture and policies. Furthermore, the overall ANOVA is significant with p-value =0.050 and F=3.061. This is confirmation that there is a significant statistical difference in the adoption readiness of the consultants, contractors and clients to adopt ML in some or all of the application areas in construction.

From Kendall's test, the critical X^2 of 30.114 from the table is less than the calculated X^2 of 251.29. This implies an insignificant difference and similar rankings of the variables within the participants' groups. The use of the chi-square values of Kendall's test to interpret the relatedness of assessed variables ranking within participants is evident in the literature [90], [93].

Table 4: Adoption readiness of ML in construction.

Code	ML Application area in construction	☐	NV	RII	Remark	Rank	ANOVA F-stat	ANOVA Sig.
ML01	Site works (e.g., wall painting, plastering, etc.)	3.97	0.66[a]	79.44%	H	8th	17.367	0.000*
ML02	3D models classification in BIM	3.80	0.50[a]	75.94%	H	11th	1.231	0.295
ML03	Prediction of and management of construction costs	4.34	1.00[a]	86.71%	VH	1st	3.785	0.025*
ML04	prediction of the energy system behaviour of buildings	3.83	0.54[a]	76.64%	H	10th	1.825	0.165
ML05	Prediction of short-term cooling loads of buildings	3.52	0.25	70.49%	H	15th	10.774	0.000*
ML06	detection and classification of pavement stress	3.25	0.00	65.03%	H	20th	6.231	0.003*
ML07	Rutting prediction of asphalt pavement	3.31	0.06	66.29%	H	18th	8.578	0.000*
ML08	prediction of design energy of buildings	3.45	0.18	68.95%	H	17th	5.236	0.006*
ML09	Prediction of recycled concrete compressive strength and failure	3.52	0.25	70.49%	H	15th	6.225	0.003*
ML10	Waste management	4.16	0.84[a]	83.22%	VH	5th	9.066	0.000*
ML11	construction Workforce Assessment and Activity Recognition	3.80	0.50[a]	75.94%	H	11th	1.231	0.295
ML12	Prediction of the long-term heating and electricity loading of buildings	3.31	0.05	66.15%	H	19th	5.291	0.006*
ML13	Construction equipment assessment and activity recognition	3.78	0.49	75.66%	H	13th	2.282	0.106
ML14	prediction of heavy equipment parameters	3.91	0.61[a]	78.18%	H	9th	4.726	0.010*
ML15	Building Occupancy Modelling and Performance Simulation.	3.99	0.68[a]	79.86%	H	7th	4.415	0.014*
ML16	Health and Safety prediction and management	4.32	0.99[a]	86.43%	VH	2nd	3.906	0.022*
ML17	Schedule Management	3.78	0.49	75.66%	H	13th	1.504	0.226
ML18	Risk Management	4.32	0.99[a]	86.43%	VH	2nd	5.374	0.006*
ML19	Structural Health Monitoring and Prediction	4.11	0.79[a]	82.24%	VH	6th	1.351	0.262
ML20	Building Life-Cycle assessment and management	4.26	0.93[a]	85.17%	VH	4th	4.605	0.012*
	N	143						
	Kendall's W[a]	0.092						
	calculated Chi-Square (X^2) value	251.29						
	Critical Chi-Square (X^2) value from Table	30.114						
	df	19						
	Asymptotic level of significance	0.000						
		Between Groups	**Within Groups**	**Total**				
	Sum of Squares	3.853	88.134	91.987				
	df	2	140	142				
ANOVA	Mean Square	1.927	0.630					
	F	3.061						
	Sig.	0.050						
	*p-value≤0.05; [a]Normalisation value ≥0.05 indicate criticality of assessed variables.							

Source; Authors, (2024).

IV. 3 DISCUSSION OF FINDINGS

The study revealed nine critical ML application areas with very high awareness levels. The corresponding readiness of the organisations to adopt ML in these application areas (Figure 1) is briefly discussed below.

The study revealed that ML is applied in the Prediction of the energy system behaviour of buildings (ML04) as well as the Prediction of short-term cooling loads of buildings (ML05). This function helps in the design and management of energy requirements and consumption in a building. The use for the

prediction of the heat demand of commercial buildings was demonstrated by [68] using the RNN model. While the awareness of these functions (ML04 and ML05) is 'very high', their adoption readiness is rated 'high'. This shows how important energy management is for buildings, and in recent times where the global energy cost is high, there is a need to adopt ML to guide the design and management of energy in building projects.

Another key application area according to this study is 'Health and Safety prediction and management (ML16)'. ML helps in the identification of possible sources of accidents and injuries on construction sites, and this enables proactive planning of mitigation strategies to avoid the occurrence of accidents on construction projects. The importance of ML in accident and injury prediction and prevention on-site is evident in studies such as [39], [46]. The 'Health and Safety prediction and management' function of ML has very high awareness and adoption readiness according to the participants. The waste management (ML10) function of ML is also important in the construction industry. Poor waste management in the construction industry has been a critical cause of cost and time overruns and the distortion of environmental aesthetics through the build-up of waste in landfills. ML algorithm in AI technologies offers quick and more effective ways of different waste identification, sorting and disposal from site [22]. The waste management function of ML also has a 'very high' awareness and adoption readiness.

ML's role in the prediction and management of construction costs is one that has been given adequate attention in construction management literature. It is an essential function of the ML in construction projects, be it building or civil engineering construction as evident in [52], [55]. The awareness and adoption readiness of ML's role in the prediction and management of construction costs (ML03) is very high.

Risk Management (ML18) goes beyond just the identification of hazards on construction sites. It includes every measure taken to prevent such risks from happening. Risks include those that could have important on the overall baselines of the projects which include time, cost and other events that can retard or even lead to stoppage of work on site. The role of ML in risk prediction and management is well-documented in the literature [60], [61]. While the awareness of ML's role in risk management is very high, the adoption readiness of the industry to apply ML in the management of risks is also very high.

ML plays a pivotal role in determining the structural health of a building or structure. The use of ML in Structural Health Monitoring and Prediction (ML19) can take place either before or after construction, and this is supported by literature [64], [69]. It is rated very high in both awareness level and adoption readiness by the participants.

Studies have shown that ML helps in Building Life-Cycle assessment and management (ML20). The life cycle prediction of ML goes beyond building projects but also the survival of or otherwise of a construction business [73], [74]. The application area has very high awareness and adoption readiness according to this study. Keeping and maintaining a 3D model library is difficult and expensive. The use of ML in the classification of 3D models from traditional CAD is the fastest and most efficient way to maintain a robust 3D model library for reuse on a project. the application of ML for 3D models classification (ML02) in BIM (ML02) is vital and has been identified as a novel way of BIM development in the built environment [78].
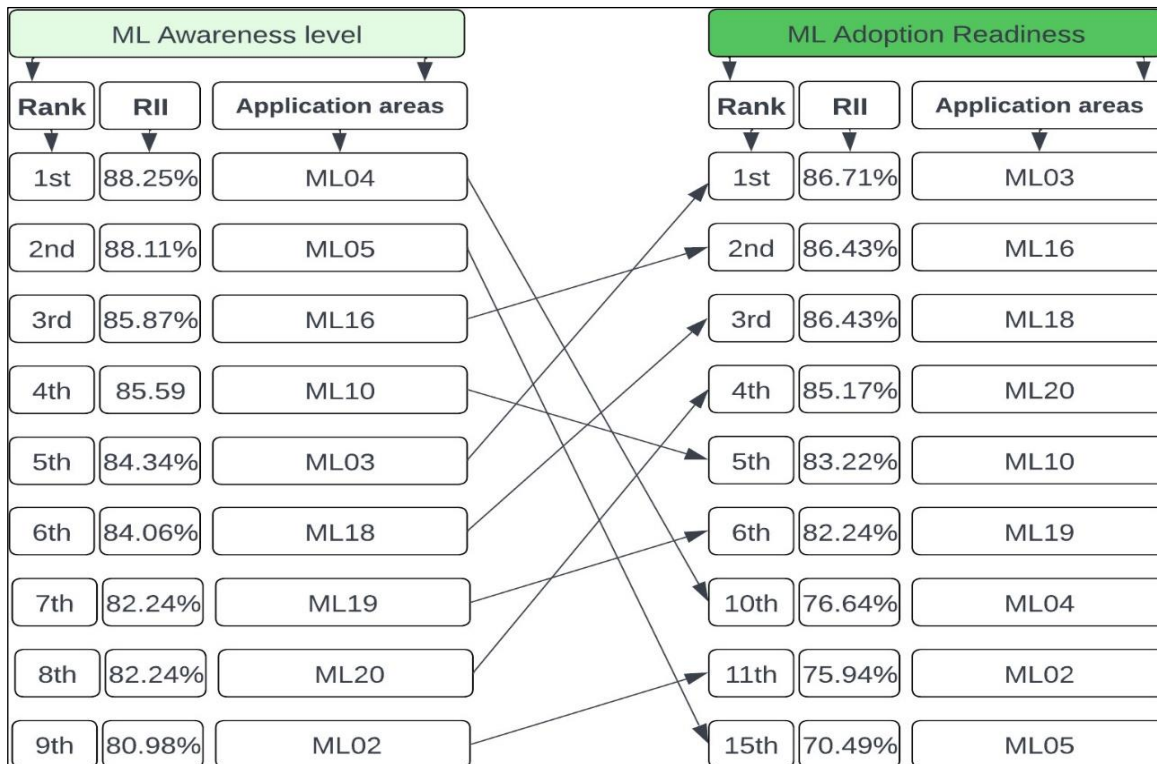
Figure 1: ML application areas with very high awareness and their corresponding adoption readiness.
Source: Authors, (2024).

V. CONCLUSIONS

This study investigated the awareness of the Nigerian construction organisations on some identified ML application areas, and the readiness of the organisations to adopt ML learning

in the identified application areas. The study utilised structured questionnaires to remotely gather relevant data from construction professionals within the sampled organisations using a snowball sampling technique. Arrays of descriptive and inferential statistical tools were used to analyse the gathered data, and meaningful results were obtained and discussed and conclusions drawn.

It was found that the awareness and adoption readiness of Nigerian construction organisations on the assessed ML application areas is high. Also, six of the nine application areas with very high awareness levels equally have a very high adoption readiness level. These critical ML application areas are (1) Health and Safety prediction and management, (2) Waste management, (3) Prediction of and management of construction costs, (4) Risk Management, (5) Structural Health Monitoring and Prediction, and (6) Building Life-Cycle assessment and management. Although, within the various organisations, there were agreements in the way they rated the variables according to Kendall's test, the overall ANOVA test revealed a significant statistical difference between the opinions of the participants regarding the awareness and adoption readiness of the various ML application areas.

This study offers some useful implications in the built environment. First, it provides an overall idea of the awareness and adoption readiness of construction organisations regarding the utilisation of ML to carry out various prediction functions in the life of construction projects. Soaring energy bills is a global problem, and the use of ML in predicting how the energy system of a building will behave will help construction experts and other stakeholders to produce energy-efficient buildings to drastically reduce energy losses in buildings. ML helps in the construction industry's drive towards a more sustainable built environment.

ML is based on Artificial intelligence, and it has the potential to offer construction organisations improved production efficiency and productivity. Construction organisations can gain from the knowledge presented in this study to explore ways of integrating ML in their operational functions to curb risks and waste, and in addition, improve cost prediction and management.

The application areas of ML cover the key activities that happen in construction. Thus, the adoption of ML in carrying out these functions will help in meeting the sustainability targets of the industry. Thus, could guide the government in making favourable policies and regulations to encourage their penetration in construction. While the awareness of ML is high among the participants, incorporating it into the tertiary education curriculum will further improve the awareness of the future built environment experts from the various engineering and environmental sciences faculties and departments.

This study contributed to the body of knowledge in the Nigerian context, despite this, the sample size, research approach and number of variables assessed could limit its generalisation. A similar study should be embarked upon using the mixed research approach to confirm or improve on what has been found in this study. A study that could focus on specific construction professionals, e.g., Quantity surveyors, Engineers, etc., could be carried out to comprehend the depth of ML diffusion and penetrate among the various professional groups in the country.

VI. AUTHOR'S CONTRIBUTION

Conceptualization: Samuel Osusha Loya, Emmanuel Chidiebere Eze, Imoleayo Abraham Awodele
Methodology: Emmanuel Chidiebere Eze, Onyinye Sofolahan, Olayinka Omoboye

Investigation: Samuel Osusha Loya, Emmanuel Chidiebere Eze, Imoleayo Abraham Awodele, Onyinye Sofolahan, Olayinka Omoboye
Discussion of results: Samuel Osusha Loya, Emmanuel Chidiebere Eze, Imoleayo Abraham Awodele, Onyinye Sofolahan, Olayinka Omoboye
Writing – Original Draft: Samuel Osusha Loya, Emmanuel Chidiebere Eze, Imoleayo Abraham Awodele.
Writing – Review and Editing: Samuel Osusha Loya, Emmanuel Chidiebere Eze, Imoleayo Abraham Awodele, Onyinye Sofolahan, Olayinka Omoboye.
Resources: Samuel Osusha Loya, Emmanuel Chidiebere Eze, Imoleayo Abraham Awodele, Onyinye Sofolahan, Olayinka Omoboye.
Supervision: Emmanuel Chidiebere Eze, Imoleayo Abraham Awodele, Olayinka Omoboye.
Approval of the final text: Samuel Osusha Loya, Emmanuel Chidiebere Eze, Imoleayo Abraham Awodele, Onyinye Sofolahan, Olayinka Omoboye.

VII. REFERENCES

[1] A.I. Awodele, M.C. Mewomo, and E.C. Eze, "Inhibitors to the Adoption of Building Information Modelling in Modular Construction: A Case Study of the Nigerian Construction Industry", Journal of Construction in Developing Countries, vol. 28 no. 2, pp.19-36, 2023.

[2] E.A. Sekou, "Promoting the use of ICT in the construction industry: Assessing the factors hindering usage by building contractors in Ghana", MSc dissertation, Kwame Nkrumah University of Science and Technology, 2012.

[3] R. Ruparathna, and K. Hewage, "Review of contemporary construction procurement practices", Journal of Management in Engineering, vol. 31, no. 3, pp.04014038, 2015. https://doi.org/10.1061/(asce)me.1943-5479.00002799.

[4] Y. Yang, M. Pan, and W. Pan, "Co-evolution through interaction of innovative building technologies: The case of modular integrated construction and robotics", Automation in Construction, vol. 107, no.4, pp. 1-10, 2019.

[5] W.E. Rees, "Achieving sustainability: reform or transformation? In The Earthscan reader in sustainable cities", Routledge, pp.22-52, 2021.

[6] E.C. Eze, O. Sofolahan, R.A. Ugulu, and E.E. Ameyaw, "Bolstering circular economy in construction through digitalization", Construction Innovation. DOI 10.1108/CI-10-2023-0245, 2024.

[7] O.J. Adebowale, and J.N. Agumba, "Artificial Intelligence technology applications in building construction productivity: a systematic literature review", Acta Structilia, vol. 30, no.2, pp.161-195, 2024.

[8] I.A. Awodele, M.C. Mewomo, A.M.G. Municio, A.P. Chan, A. Darko, R. Taiwo, N.A. Olatunde, E.C. Eze, and O.A. Awodele, "Awareness, adoption readiness and challenges of railway 4.0 technologies in a developing economy", Heliyon, p.e25934, 2024. https://doi.org/10.1016/j.heliyon.2024.e259344.

[9] S. Bag, G. Yadav, P. Dhamija, and K.K. Kataria, "Key resources for industry 4.0 adoption and its effect on sustainable production and circular economy: an empirical study", Journal of Cleaner Production, vol. 281, 2021.

[10] V.A. Wankhede, R. Agrawal, A. Kumar, S. Luthra, D. Pamucar, and Ž. Stević, "Artificial intelligence an enabler for sustainable engineering decision-making in uncertain environment: a review and future propositions", Journal of Global Operations and Strategic Sourcing, Vol. ahead-of-print No. ahead-of-print, 2023.

[11] V. Bhatnagar, S. Sharma, A. Bhatnagar, and L. Kumar, "Role of machine learning in sustainable engineering: a review", IOP Conference Series: Materials Science and Engineering, vol. 1099, no.1, pp.12036, 2021.

[12] S. Kotsiantis, I. Zaharakis, and P. Pintelas, "Supervised machine learning: A review of classification techniques", Emerging Artificial Intelligence Application in Computer Engineering, vol.160, pp.3-24, 2007.

[13] B. Sundui, O.A. Ramirez Calderon, O.M. Abdeldayem, J. Lˊazaro-Gil, E.R. Rene, and U. Sambuu, "Applications of machine learning algorithms for biological

wastewater treatment: updates and perspectives", Clean Technologies and Environmental Policy, vol. 23, no.1, Doi: 10.1007/s10098-020-01993-x, 2021.

[14] M. Ribeiro, K. Grolinger, and M.A. Capretz, "Mlaas: Machine learning as a service", In 2015 IEEE 14th international conference on machine learning and applications (ICMLA), pp.896-902, 2015.

[15] B. Hellingrath, and S. Lechtenberg, "Applications of artificial intelligence in supply chain management and logistics: focusing onto recognition for supply chain execution. The art of structuring: Bridging the gap between information systems research and practice", pp.283-296, 2019. DOI: 10.1007/978-3-030-06234-7_27

[16] Q. Demlehner, D. Schoemer, and S. Laumer, "How can artificial intelligence enhance car manufacturing? A Delphi study-based identification and assessment of general use cases", International Journal of Information Management, vol.58, pp.102317, 2021.

[17] F.D. Weber, and R. Schütte, "State-of-the-art and adoption of artificial intelligence in retailing", Digital Policy, Regulation and Governance, vol. 21, no.3, pp.264-279, 2019.

[18] J. Aliu, and A.E. Oke, "Construction in the digital age: exploring the benefits of digital technologies", Built Environment Project and Asset Management, vol. 13 No. 3, pp. 412-429, 2023. DOI: https://doi.org/10.1108/BEPAM-11-2022-01866.

[19] A. Ebekozien, and C. Aigbavboa, "COVID-19 recovery for the Nigerian construction sites: the role of the fourth industrial revolution technologies", Sustainable Cities and Society, vol.69, pp.102803, 2021.

[20] B. Buchanan, "A (very) brief history of artificial intelligence", AI Magazine, vol.26, no.4, pp.53, 2005.

[21] A. Turing, "Computing Machinery and Intelligence", Mind, vol.59, no.236, pp.433-460, 1950.

[22] S.O. Abioye, L.O. Oyedele, L. Akanbi, A. Ajayi, J.M.D. Delgado, M. Bilal, O.O. Akinade, and A. Ahmed, "Artificial intelligence in the construction industry: A review of present status, opportunities and future challenges", Journal of Building Engineering, vol.44, 2021. DOI: https://doi.org/10.1016/j.jobe.2021.1032999.

[23] G. Xie, Chen, Tiange, Y. Li, Chen, Tingyu, X. Li, and Z. Liu, "Artificial intelligence in nephrology: How can artificial intelligence augment nephrologists' intelligence?", KDD, vol.6, pp.1–6, 2020. DOI: https://doi.org/10.1159/0005046000.

[24] A. Mahmoud, "Introduction to Shallow Machine Learning", Available at: https://shorturl.at/bEI26 [accessed 7th March 2024].

[25] C. Egwim, H. Alaka, O. Toriola-Coker, H. Balogun, F. Sunmola, "Applied artificial intelligence for predicting construction projects delay", Machine Learning with Applications, vol.6, pp.1-15, 2021. DOI: https://doi.org/10.1016/j.mlwa.2021.1001666.

[26] Y. Xu, Y. Zhou, P. Sekula, and L. Ding, "Machine learning in construction: From shallow to deep learning", Developments in the Built Environment, vol.6, pp.1-13, 2021.

[27] Y. LeCun, Y. Bengio, and G. Hinton, "Deep Learning", Nature, vol.521, pp.7553, 2015.

[28] O.K. Abayomi, F.N. Adenekan, O.A. Adeleke, T.A. Ajayi, and A.O Aderonke, "Awareness and perception of the artificial intelligence in the management of University libraries in Nigeria", Journal of Interlibrary Loan, document Delivery & Electronic Reserve, vol. 29, no.1-2, pp.13-28, 2020.

[29] A.A. Iorkaa, M. Barma, and H. Muazu, "The assessment of financial institutions' awareness and application of machine learning techniques for credit risk prediction- the case of Nigeria", Annals. Computer Science Series, vo.19, no.1, pp.16-22, 2021.

[30] W.A. Udoh, I. Nsude, and A.S. Oyeleke, "Awareness of artificial Intelligence for news production among journalists in Ebonyi State Nigeria, International Journal of Network and Communication Research, vol.7, no.1, pp.33-45, 2022.

[31] J.S. Guanah, "Mainstream media and artificial intelligence awareness amongst residents of Asaba metropolis, Delta State, Nigeria", Journal of Contemporary Social Research, vol.5, no.1, pp.65-79, 2021.

[32] J.O. Mobayo, A.F. Aribisala, S.O. Yusuf, and U. Belgore, "Artificial intelligence: Awareness and adoption for effective facilities management in the energy sector", Journal of Digital Food, Energy & Water Systems, vol.2, no.2, pp.1-18, 2021.

[33] I.C. Osuizugbo, and A.S. Alabi, "Built environment professionals' perceptions of the application of artificial intelligence in construction industry", Covenant Journal of Research in the Built Environment (CJRBE), vol. 9, no.2, pp.48-66, 2021.

[34] A.E. Oke, J. Aliu, P.O. Fadamiro, P.O. Akanni, and S.S. Stephen, "Attaining digital transformation in construction: An appraisal of the awareness and usage of automation techniques", Journal of Building Engineering, vol.67, pp.1-13, 2023. DOI: https://doi.org/10.1016/j.jobe.2023.1059688.

[35] N.A. Olatunde, A.M. Gento, V.N. Okorie, O.W. Oyewo, M.C. Mewomo, and I.A. Awodele, "Construction 4.0 technologies in a developing economy: awareness, adoption readiness and challenges", Frontiers in Engineering and Built Environment, vol. 3 no. 2, pp. 108-121, 2023. DOI: https://doi.org/10.1108/FEBE-08-2022-0037.

[36] P.M. Teicholz, "Labor-productivity declines in the construction industry: Causes and Remedies", 2013. Available at: https://www.aecbytes.com/viewpoint/2004/issue_4.html (Accessed on: 11/01/2024).

[37] R. Sacks, G. Mark, and B. Ioannis, "Building information modelling, artificial intelligence and construction", Technology Developments in the Built Environment, vol.4, 2020. DOI: https://doi.org/10.1016/j.dibe.2020.1000111.

[38] D. Singer, M. Bügler, A. Borrmann, and L.O. Center, "Knowledge based bridge engineering-artificial intelligence meets building information modeling", Proceedings of the EG-ICE Workshop on Intelligent Computing in Engineering, 2016.

[39] M. Regona, T. Yigitcanlar, B. Xia, and R.Y.M. Li, "Opportunities and adoption challenges of AI in the construction industry: A prisma review", Journal of Open Innovation: Technology, Market, and Complexity, Vol.8, no.45, 2022. DOI: https://doi.org/10.3390/joitmc80100455.

[40] C.Q.X. Poh, C.U. Ubeynarayana, and Y.M. Goh, "Safety leading indicators for construction sites: A machine learning approach", Automation in Construction, vol.93, pp.375–386, 2018. DOI: https://doi.org/10.1016/j.autcon.2018.03.0222.

[41] L. Straker, A. Campbell, J. Coleman, M. Ciccarelli, and W. Dankaerts, "In vivo laboratory validation of the physiometer: a measurement system for long-term recording of posture and movements in the workplace", Ergonomics, vol.53, no.5, pp.672–684, 2010.

[42] Y.M. Goh, and D. Chua, "Neural network analysis of construction safety management systems: A case study in Singapore", Construction Management and Economics, vol.31, no.5, pp460-470, 2013.

[43] X. Yan, H. Li, A.R. Li, and H. Zhang, "Wearable imu-based real-time motion warning system for construction workers' musculoskeletal disorders prevention", Automation in Construction, vol.74, pp.2–11, 2017.

[44] L. Wonil, E. Seto, K.Y. Lin, and G.C. Migliaccio, "An evaluation of wearable sensors and their placements for analyzing construction worker's trunk posture in laboratory conditions", Applied Ergonomics, vol.65, pp. 424-436, 2017.

[45] J. Seo, S. Han, S. Lee, and H. Kim, "Computer vision techniques for construction safety and health monitoring", Advanced Engineering Informatics, vol.29, no.2, pp.239–251, 2015.

[46] E. Harirchian, V. Kumari, K. Jadhav, R.R. Das, S. Rasulzade, and T. Lahmer, "A machine learning framework for assessing seismic hazard safety of reinforced concrete buildings", Applied Sciences (Switzerland), vol.10, no.20, pp.1–18, 2020.

[47] A.J.-P. Tixier, M.R. Hallowell, B. Rajagopalan, and D. Bowman, "Application of machine learning to construction injury prediction", Automation in Construction, vol.69, pp.102–114, 2016. DOI: https://doi.org/10.1016/j.autcon.2016.05.016.

[48] Y. Yu, H. Li, X. Yang, L. Kong, X. Luo, and A.Y. Wong, "An automatic and non-invasive physical fatigue assessment method for construction workers", Automation in Construction, Vol. 103, pp.1–12, 2019. DOI: https://www.sciencedirect.com/science/article/pii/S0926580 518308422.

[49] Q. Fang, H. Li, X. Luo, L. Ding, T.M. Rose, W. An, and Y. Yu, (2018). Detecting non-hardhatuse by a deep learning method from far-field surveillance

videos. Automation in Construction, Vol.85, pp.1–9, 2018. http://www.sciencedirect.com/science/article/pii/S0 926580517304429.

[50] H. Luo, and C. Xiong, "Convolutional neural networks: vision-based workforce activity assessment in construction", Automation in Construction, vol.94, pp.282–289, 2018. https://doi.org/10.1016/j.autcon.2018.06.007.

[51] S. Kim, "Hybrid forecasting system based on case-based reasoning and analytic hierarchy process for cost estimation", Journal of Civil Engineering and Management, vol.19, no.1, pp.86-96, 2013.

[53] M. Gunduz, L.O. Ugur, and E. Ozturk, "Parametric cost estimation system for light rail transit and metro trackworks", Expert Systems with Applications, vol.38, no.3, pp.2873-2877, 2011.

[52] G. Mahalakshmi, and C. Rajasekaran, "Early cost estimation of highway projects in India using artificial neural network. In: Das, B., Neithalath, N. (eds) Sustainable Construction and Building Materials. Lecture notes in civil engineering", Springer, Singapore, 2019. https://doi.org/10.1007/978-981-13-3317-0_599.

[54] M. Gunduz, and H.B. Sahin, "An early cost estimation model for hydroelectric power plant projects using neural networks and multiple regression analysis", Journal of Civil Engineering and Management, vol.21, no.4, pp.470-477, 2015.

[55] X. Wang, "Application of fuzzy math in cost estimation of construction project", Journal of Discrete Mathematical Sciences and Cryptography, vol.20, no.4, pp.805-816, 2017.

[56] V. Chandanshive, and A.R. Kambekar, "Estimation of building construction cost using artificial neural networks", Journal of Soft Computing in Civil Engineering, vol.3, no.1, pp.91-107, 2019.

[56] N.I. El-Sawalhi, and O. Shehatto, "A neural network model for building construction projects cost estimating", Journal of Construction Engineering and Project Management, vol.4, no.4, pp.9-16, 2014.

[57] K. Petroutsatou, and S. Lambropoulos, "Road tunnels construction cost estimation: A structural equation model development and comparison", Operational Research, vol.10, no.2, pp.163-173, 2010.

[57] M. Rafiei, and H. Adeli, "Novel machine-learning model for estimating construction costs considering economic variables and indexes" Journal of Construction Engineering and Management, Vol.144, no.12, 2018. DOI: https://doi.org/10.1061/(ASCE)CO.1943-7862.0001570.

[58] N.V. Tam, and N.Q. Toan, "Reasearch trends on machine learning in construction management: A scientoetric analysis", Journal of Applied Science and Technology Trends, vol.2, no.3, pp.96-104, 2021.

[59] A. Gondia, A. Siam, W. El-Dakhakhni,and A.H. Nassar, "Machine learning algorithms for construction projects delay risk prediction", Journal of Construction Engineering and Management, vol.146, no.1, 2020. DOI: https://doi.org/10.1061/(ASCE)CO.1943-7862.0001736.

[60] M.O. Sanni-Anibire, R.M. Zin, and S.O. Olatunji, "Machine learning model for delay risk assessment in tall building projects", International Journal of Construction Management, vol.22, no.11, pp.2134-2143, 2020. DOI: https://doi.org/10.1080/15623599.2020.17683266.

[61] H. Liu, and G. Tian, "Building engineering safety risk assessment and early warning mechanism construction based on distributed machine learning algorithm", Safety Science, vol.120, pp.764-771, 2019.

[62] A. Rahman, and A. Smith, "Predicting heating demand and sizing a stratified thermal storage tank using deep learning algorithms", Applied Energy, vol.228, pp.108–121, 2018.

[63] A. Rahman, V. Srikumar, and A.D. Smith, "Predicting electricity consumption for commercial and residential buildings using deep recurrent neural networks", Applied Energy, vol.212, pp.372-385, 2018.

[64] Y. Zhong, and J. Xiang, "A two-dimensional plum-blossom sensor array-based multiple signal classification method for impact localization in composite structures", Computer- Aided Civil and Infrastructural Engineering, vol.31, no.8, pp.633–643, 2016.

[65] J. Shan, W. Shi, and X. Lu, "Model-reference health monitoring of hysteretic building structure using acceleration measurement with test validation", Computer-Aided Civil and Infrastructural Engineering, vol.31, no.6, pp.449–464, 2016.

[66] S. Khaitan, K. Gopalakrishnan, A. Choudhary, and A. Agrawal, "Deep convolutional neural networks with transfer learning for computer vision-based data-driven pavement distress detection", Construction and Building Matererials Vol.157, pp. 322–330, 2017.

[67] S. El-Badawy, and A. Awed, "Performance of mepdg dynamic modulus predictive models for asphalt concrete mixtures: local calibration for Idaho", Journal of Materials in Civil Engineering, vol.24, no.11, 2012. DOI: https://doi.org/10.1061/(ASCE)MT.1943-5533.0000518.

[68] Y. Tian, J. Lee, T. Nantung, and J. Haddock, "Calibrating the mechanistic empirical pavement design guide rutting models using accelerated pavement testing", Journal of the Transportation Research Board, vol.2672, no.40, pp.304–314, 2018.

[69] F. Deng, Y. He, S. Zhou, Y. Yu, H. Cheng, and X. Wu, "Compressive strength prediction of recycled concrete based on deep learning", Construction and Building Materials vol.175, 2018. DOI: https://doi.org/10.1016/j.conbuildmat.2018.04.169.

[70] T. Nguyen, A. Kashani, T. Ngo, and S. Bordas, "Deep neural network with high-order neuron for the prediction of foamed concrete strength", Computer-Aided Civil and Infrastructural Engineering, vol.34, no.4, pp.316–332, 2019.

[71] Z. Chen, and C. Jiang, "Building occupancy modelling using generative adversarial network", Energy Build. 174, 372–379, 2018.

[72] S. Singaravel, J. Suykens, P. Geyer, "Deep-learning neural-network architectures and methods: using component-based models in building-design energy prediction", Advanced Engineering Informatics, vol.38, pp.81-90, 2018. DOI: https://doi.org/10.1016/j.aei.2018.06.004.

[73] S. Ji, B. Lee, M.Y. Yi, "Building life-span prediction for life cycle assessment and life cycle cost using machine learning: A big data approach", Building and Environment, vol. 205, 2021. DOI: https://doi.org/10.1016/j.buildenv.2021.108267.

[74] H. Alaka, L. Oyedele, H. Owolabi, O. Akinade, M. Bilal, and S. Ajayi, "A big data analytics approach for construction firms failure prediction models", IEEE Transactions on Engineering Management, vol.66, pp.689–698, 2019. DOI: https://doi.org/10.1109/TEM.2018.2856376.

[75] H. Park, and D.Y. Park, "Comparative analysis on predictability of natural ventilation rate based on machine learning algorithms", Building and Environment, vol. 195, 2021. DOI: https://doi.org/10.1016/j.buildenv.2021.107744.

[76] Y. –R. Wang, C.Y. Yu, and H.H. Chan, "Predicting construction cost and schedule success using artificial neural networks ensemble and support vector machines classification models", International Journal of Project Management, vol.30, no.4, pp.470-478, 2012.

[77] H. Kim, L. Soibelman, and F. Grobler, "Factor selection for delay analysis using knowledge discovery in databases", Automation in Construction, vol.17, no.5, pp.550-560, 2008.

[78] L. Wang, Z. Zhao, and X. Wu, "A deep learning approach to the classification of 3D models under BIM environment', International Journal of Control, Automation and Systems, vol. 9, pp.179–188, 2016.

[79] L. Wang, Z.K. Zhao, and N. Xu, "Deep belief network based 3d models classification in building information modeling", International Journal of Online Engineering, vol.11, no.5, pp.57–63, 2015.
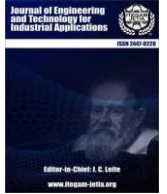
[80] C. Fan, F. Xiao, and Y. Zhao, "A short-term building cooling load prediction method using deep learning algorithms", Applied Energy, vol.195, pp.222–233, 2017.

[81] X. Luo, H. Li, D. Cao, F. Dai, J. Seo, and S. Lee, "Recognizing diverse construction activities in site images via relevance networks of construction-related objects detected by convolutional neural networks", Journal of Computing in Civil Engineering, vol.32, no.3, 2018. DOI: https://doi.org/10.1061/(ASCE)CP.1943-5487.0000756.

[82] K.M. Rashid, and J. Louis, "Times-series data augmentation and deep learning for construction equipment activity recognition", Advanced Engineering Informatics vol.42, 2019. DOI: http://www.sciencedirect.com/science/article/pii/S1474034619300886.

[83] C. Hernandez, T. Slaton, V. Balali, R. Akhavian, "A deep learning framework for construction equipment activity analysis", in: Computing in Civil Engineering 2019: Data, Sensing, and Analytics. American Society of Civil Engineers Reston, VA, pp.479–486. DOI: https://ascelibrary.org/doi/labs/10.1061/9780784482438.061.

[84] J. Aliu, C. Aigbavboa, and W. Thwala, "A 21st Century Employability Skills Improvement Framework for the Construction Industry", 2021. DOI: https://doi.org.10.1201/9781003137504.

[85] I.F. Mohamed, D.J. Edwards, M. Mateo-Garcia, G. Costin, and W.D.D. Thwala, "An investigation into the construction industry's view on fire prevention in high-rise buildings post Grenfell", International Journal of Building Pathology and Adaptation, vol. 38, no.3, pp. 451-471, 2020. DOI: https://doi.org/10.1108/IJBPA-05-2019-0048.

[86] W.N. Nwaki, and C.E. Eze, "Lean construction as a panacea for poor construction projects performance", Journal of Engineering and Technology for Industrial Applications (ITEGAM-JETIA), vol.6, no.26, pp.61-72, 2020. doi: https://doi.org/10.5935/jetia.v6i26.723.

[87] A. Joshi, S. Kale, S. Chandel, and D.K. Pal, "Likert scale: explored and explained", British Journal of Applied Science and Technology, vol.7, no.4, pp.396, 2015.

[88] H. Taherdoost, "What is the best response scale for survey and questionnaire design; review of different lengths of rating scale/attitude scale/Likert scale", International Journal of Academic Research in Management, vol.8, no.1, pp.1-10, 2019. Available at SSRN: https://ssrn.com/abstract53588604.

[89] K.L. Moores, G.L. Jones, and S.C. Radley, "Development of an instrument to measure face validity, feasibility and utility of patient questionnaire use during health care: the QQ-10", International Journal for Quality in Health Care, vol.24, no.5, pp.517-524, 2012.

[90] E.C. Eze, O. Sofolahan, and O.G. Omoboye, "Assessment of barriers to the adoption of sustainable building materials (SBM) in the construction industry of a developing country", Frontiers in Engineering and Built Environment, vol.3, no.3, pp.153-166, 2023. DOI: https://doi.org/10.1108/FEBE-07-2022-0029.

[91] D.D. Heckathorn, "Comment: snowball versus respondent-driven sampling", Sociological Methodology, vol.41, no.1, pp.355-366, 2011. doi: 10.1111/j.1467-9531.2011.01244.x.

[92] W. Nwaki, O. Sofolahan, and E. Eze, "Inhibitors to earth-based materials adoption in urban housing construction: The view of design experts", Civil and Sustainable Urban Engineering, vol.3, no.2, pp.123–137, 2023. DOI: https://doi.org/10.53623/csue.v3i2.329.

[93] D. Aghimien, M. Ikuabe, L.M. Aghimien, C. Aigbavboa, N. Ngcobo, and J. Yankah, "PLS-SEM assessment of the impediments of robotics and automation deployment for effective construction health and safety", Journal of Facilities Management, 2022. DOI: https://doi.org/10.1108/JFM-04-2022-0037.

[94] E.C Eze, D.O. Aghimien, C.O. Aigbavboa, and O. Sofolahan, "Building information modelling adoption for construction waste reduction in the construction industry of a developing country", Engineering, Construction and Architectural Management, Vol. ahead-of-print No. ahead-of-print, 2022 DOI: https://doi.org/10.1108/ECAM-03-2022-0241.

[95] E.A. Ameyaw, D.J. Edwards, B. Kumar, N. Thurairajah, D.G. Owusu-Manu, and G.D. Oppong, "Critical factors influencing adoption of blockchain-enabled smart contracts in construction projects", Journal of Construction Engineering and Management, vol.149, no.3, pp.1-16, 2023.

[96] R. Osei-Kyei, and A.P. Chan, "Developing a project success index for public–private partnership projects in developing countries", Journal of Infrastructure Systems, vol.23, no.4, 2017. 04017028.

[97] N. Al Azmi, G. Sweis, R. Sweis, and F. Sammour, (2023). Exploring Blockchain-enabled smart contracts technology implementation within ready-mixed concrete plants industry in Saudi Arabia", International Journal of Construction Management, vol.23, no.14, pp.2400-2408, 2023. DOI: 10.1080/15623599.2022.2059914.

[98] J. Pallant, "SPSS Survival Manual: A step-by-step guide to data analysis using SPSS for windows", (Version 12), 2nd ed., Allen & Unwin, Crows Nest NSW, 2005.

[99] J.F. Hair, W.C. Black, B.J. Babin, R.E. Anderson, "Multivariate data analysis: Pearson new international edition. Essex: Pearson Education Limited vol.1, no.2, 2010. Available at: https://shorturl.at/SYZ04.

RESEARCH ARTICLE   **OPEN ACCESS**

COLOUR BASED IDENTIFICATION AND SORTING OF INDUSTRIAL ITEMS USING LABVIEW

Badri Narayan Mohapatra[1]

[1] Assitant Professor, Department of Instrumentation AISSMS IOIT, Pune, INDIA.

[1] http://orcid.org/0000-0003-1906-9932

Email: badri1.mohapatra@gmail.com

ABSTRACT

This paper focuses on Colour based separation of Industry based products or raw materials using LabVIEW Software for creation of process accurate to Colour identification using Colour Spectrum tool (an add-on of LabVIEW 2023 QI software), various devices used in the project are real-time sensing and actuating devices. Colour Sensing and separation is a very useful application in Food processing, Plastic product based Industries, Marble Industry etc. In this model we use Arduino UNO, USB Webcam, Solenoid Pusher, 12V Electric motor and other Framework modules. This module works based on live action and response type of Industrial process where time is of the essence. LabVIEW software being an integral part of creation of the process and automation, has a number of tools to offer and be used to interface with external devices through wired connection.

I. INTRODUCTION

This paper is based on Colour Sensing and separation using LabVIEW as it is has a real time application it is a very useful in Food processing, Fiber and plastic product Industries, Marble Industry, Textile Industry etc. RGB Modeling is the base of this project for which weused Vision and Motion a special drive of LabVIEW 2023 QI used for Colour based operations

The RGB color model is an additive color model in which the red, green and blue primary colors of light are added together in various ways to reproduce a broad array of colors. The name of the model comes from the initials of the three additive primary colors, red, green, and blue. The main purpose of the RGB color model is for the sensing, representation, and display of images in electronic systems, such as televisions and computers, though it has also been used in conventional photography. Before the electronic age, the color model already had a solid theory behind it, based in human perception of colors. It is a device-dependent color model: different devices detect or reproduce a given RGB value differently, since the color elements (such as phosphors or dyes) and their response to the individual red, green, and blue levels vary from manufacturer to manufacturer, or even in the same device over time. Thus an RGB value does not define the same color across devices without some kind of color management.

II. THEORETICAL REFERENCE

The advancement of technology has led to the development of automated systems for industrial processes, including the identification and separation of products based on color [1]. This literature explores the implementation of color-based identification and separation systems using LabVIEW, a graphical programming platform widely used for automation and control applications [2]. The integration of LabVIEW with image processing techniques enables efficient color recognition and sorting of industrial products, enhancing productivity and quality control in manufacturing processes [3] and [4]. Various methodologies and algorithms are discussed, highlighting the effectiveness of LabVIEW in achieving accurate and reliable color-based identification and separation [5].

In modern industries, the need for efficient and reliable methods of product identification and separation is crucial for ensuring quality control and productivity. Traditional manual methods are often time-consuming and prone to errors, highlighting the importance of automated systems. Color-based identification and separation systems have emerged as a viable solution, utilizing the unique spectral characteristics of colors to differentiate and sort products [6]. Different Control Strategies can be possible through LabVIEW [7] and [8].

III. MATERIALS AND METHODS

The Software architecture of this system consists of a Desktop/Laptop and LabVIEW Software, in this the Digital webcam is joined to the Desktop/ Laptop which has a LabVIEW 2023 QI (32-bit) Software installed. We used the Webcam for sensing and the actuating par was left to Solenoid pusher which is controlled through LabVIEW via Arduino R3 SMD board when certain condition of Program created in LabVIEW is satisfied. The creation of program required the installation of particular drives from NI and VI Package Manager which are supporting software's for LabVIEW created by National Instruments. The basic block diagram is shown in Figure 1.
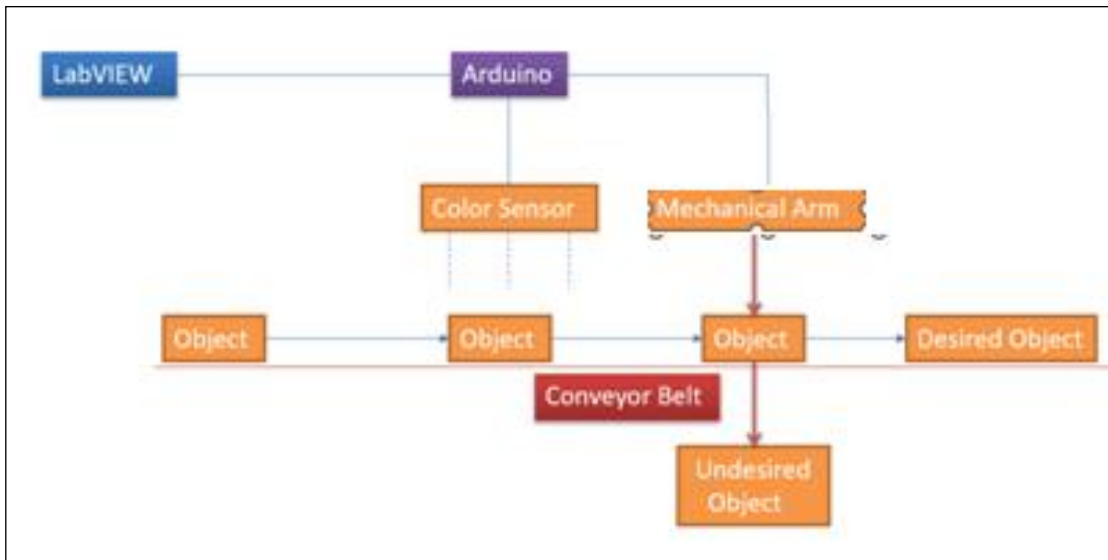
Figure 1: Basic Block Diagram.
Source: Authors, (2024).

ATmega328P controller has 14 digital input/output pins (of which 6 can be used as PWM outputs), 6 analog inputs, a 16 MHz ceramic resonator, a USB connection, a power jack, an ICSP header and a reset button. It contains everything needed to support the microcontroller; simply connect it to a computer with a USB cable or power it with a AC-to-DC adapter or battery to get started [9]. The" SMD" stands for surface-mount device, and the microcontroller (ATmega328p) is soldered directly to the board.

III.1 RELAY MODULE

Relay is one kind of electro-mechanical component that functions as a switch. The relay coil is energized by DC so that contact switches can be opened or closed. A single channel 5V relay module generally includes a coil, and two contacts like normally open (NO) and normally closed (NC).A 5v relay is an automatic switch that is commonly used in an automatic control circuit and to control a high-current using a low-current signal. The input voltage of the relay signal ranges from 0 to 5V.Pin1 (End 1): It is used to activate the relay; usually this pin one end is connected to 5Volts whereas another end is connected to the ground.

Pin2 (End 2): This pin is used to activate the Relay.

Pin3 (Common (COM)): This pin is connected to the main terminal of the Load to make it active.

Pin4 (Normally Closed (NC)): This second terminal of the load is connected to either NC/ NO pins. If this pin is connected to the load then it will be ON before the switch.

Pin5 (Normally Open (NO)): If the second terminal of the load is allied to the NO pin, then the load will be turned off before the switch.
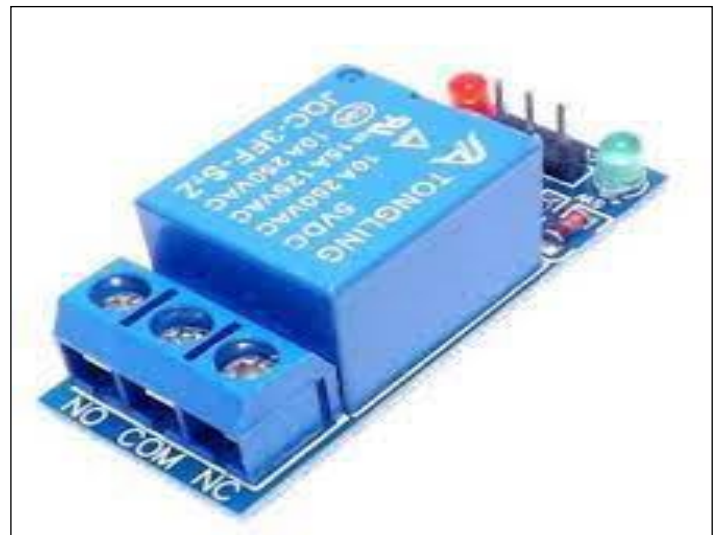
Figure 2: 5V Relay Module.
Source: Authors, (2024).

Full HD Video Calls with Stereo Audio: The Lenovo 300 FHD Webcam is powered by a Full HD 1080P 2.1 Megapixel CMOS camera that allows your friends, family, and colleagues to see you as clear as day, even when they are worlds

away. With full stereo dual-mics that are perfect for conferencing or long-distance video calls, they'll be able to hear you loud and clear, every time. High resolution FHD 1080P Webcam with dual mics: The innovative FHD 1080P camera delivers perfect high-resolution video and lets you set the scene with its ultra-wide 95° lens. Video alone is not enough, though, which is why two built-in

mics capture crisp stereo audio from all directions. Easy Plug-and-Play Setup: Simply unpack and unfold the camera when you want to do a call, and plug the USB 2.0 cable into any Windows or Mac device. Within seconds, you will be ready to go live on your favorite conferencing or streaming software, with no drivers necessary.
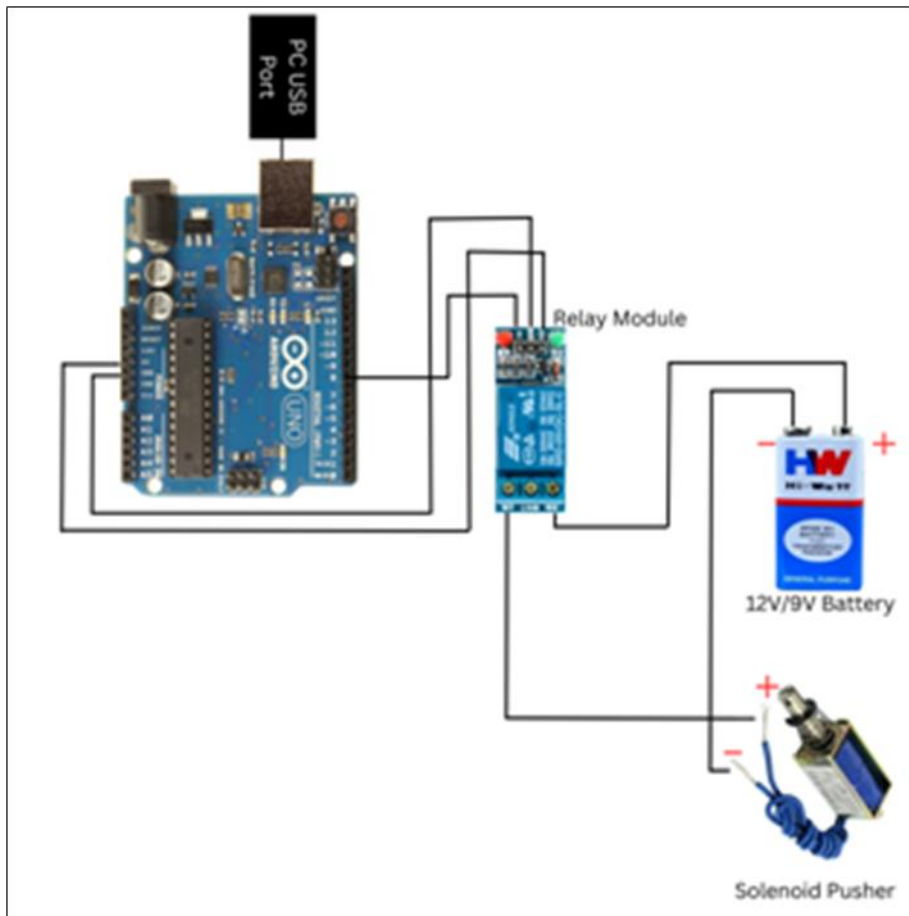
Figure 3: Circuit Connection.
Source: Authors, (2024).

III.2 ELECTROMAGNETIC SOLENOID

DC 12V rated voltage, 300mA rated current, 10mm stroke, 5GF force Pull push type, linear motion, plunger return, DC solenoid electromagnet DC Solenoid Electromagnet mainly used in vending machines, transport equipment, office facility household appliance, mechanical, etc Solenoids of this category work externally through pulling pushing in plunger When energized, doing work through pulling pushing in plunger joined object

DC Motor‐60RPM‐12Volts geared motors are generally a simple DC motor with a gearbox attached to it. This can be used in all-terrain robots and variety of robotic applications. These motors have a 3 mm threaded drill hole in the middle of the shaft thus making it simple to connect it to the wheels or any other mechanical assembly.

12V DC geared motors widely use for robotics applications. Very easy to use and available in standard size. Also, you don't have to spend a lot of money to control motors with an Arduino or compatible board. The most popular L298N H-bridge module with onboard voltage regulator motor driver can be used with this motor that has a voltage of between 5 and 35V DC or you can choose the

most precise motor diver module from the wide range available in our Motor divers category as per your specific requirements.

Jumper wires are simply wires that have connector pins at each end, allowing them to be used to connect two points to each other without soldering. Jumper wires are typically used with breadboards and other prototyping tools in order to make it easy to change a circuit as needed. Jumper wires typically come in three versions: male-to-male, male-to female and female-to-female. The difference between each is in the end point of the wire. Male ends have a pin protruding and can plug into things, while female ends do not and are used to plug things into another end.

The Sensing part is the first process to take place as it is the heart of operation for which we use Digital webcam which is connected to Desktop/Laptop through its USB port as primary sensing device, webcam is interfacd with LabVIEW where RGB(Red-Green-Blue) colours are pre-defined and placed under certain case where the output at the end enables the actuator to do its work later [10].

The processing part is dependent on LabVIEW program and Arduino R3 Board which is connected with Laptop through usb port where after the sensing phase the coulour of the object is detected, in this case the Red colour object will be eliminated by

the Mechanical arm which is powered by Solenoid Electromagnet as the Red Boolean turns Green when the colour is detected as red, the boolean function further is connected with Boolean to Binary Function because the Arduino write function which enables the actuator through its Digital Pin 8 only takes Input as Binary(0,1).

The Actuating part is based on the devices connected to Arduino and are interfaced to LabVIEW by '. VI' program instead of Arduino code the only need of Arduino software is to recognize and select the type of Arduino connected with the laptop or desktop. The Electromagnetic Solenoid is commanded to actuate when Red colour is sensed and its boolean is turned on, after a delay the Solenoid hits the sensed red object as accurately timed with Conveyor belt speed.

IV. SOFTWARE

Before moving to the programming part, you need to install drivers to the LabVIEW 2023 QI and Arduino IDE Software must be installed in the same Computer to help the LabVIEW software identify Arduino Board [11]. The following are the list of Drivers that are used in the Program below.

Vision and Motion compiler enables you to use various Camera and image processing functions which interfaces your Pc with Cam modules such as IMAQ-dx which includes Snap, Configure Grab, Grab, etc.

• Vision and Motion Runtime Driver:

The V an M Runtime driver allows you to run LabVIEW Program and normal pc operations side by side as interfacing with 3rd party devices may cause nobilities in routine operation of operating system.

• Vision Acquisition Driver:

This package contains an interactive designs and Boolean programs which act as Indicators, Controllers as well as constants, for digital display through Camera this is necessary drive. All compiler and drivers are downloaded through NIPM.

• PC interfacing with Arduino:

This is the most popular cross platform connecting drive for connecting any hardware to the LabVIEW Software directly, designing systems and control them, and managing your deployed products at scale. Figure 4 shows the circuit connection in Arduino platform.
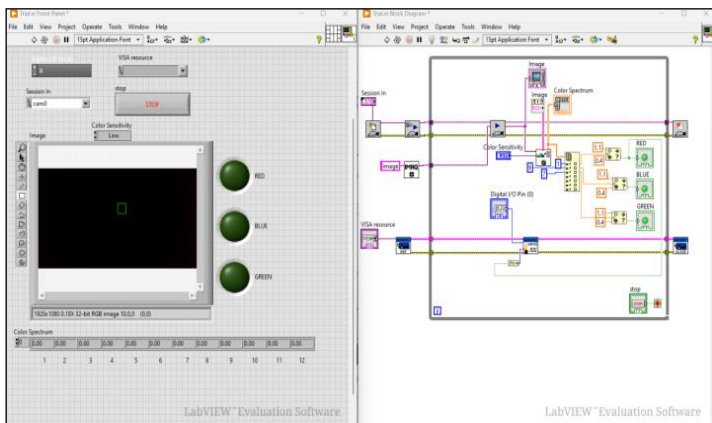
Figure 4: Circuit Connection.
Source: Authors, (2024).

IV. RESULTS AND DISCUSSIONS

Successful Detection of Colours categorized as Red, Green and Blue which is shown in figure 5.
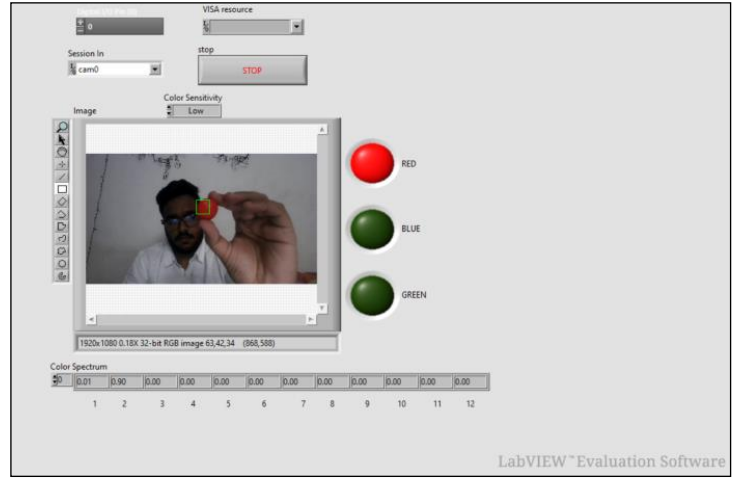
Figure 5: Detection of Red Colour.
Source: Authors, (2024).

• The conditions satisfying Detection were met without any errors to the program and hence are operational.

V. CONCLUSIONS

This System has wide range on Applications in Automation Industry for effective Colour Detection and Separation.

• Good scope in Food Processing industry as Fruits and Vegetables can be sorted automatically by their colour characteristics such as Green Apple from Red Apples, Grapes, Capsicum etc.

• The system is capable for variations and addition of excess parameters to be added so it is fit to be added to any real time processing industry.

• The system is a profitable solution for various small scale industries as well because of its flexibility and cost efficiency.

The objective was to produce a system that allows for colour sensing and separation of an object from other of different colour characteristic, Lab-VIEW and Webcam for colour detection will be used to detect the colour of the object in real-time as Red, Green and Blue in the detection node via the use of Colour Spectrum driver, it's only possible when the object passes through sensing box in same areas, distant detection can be made possible by calibrating the sensitivity of certain Function blocks and Scope of camera making the program significantly effective. With the use of IMAQ, Colour Write, Colour Spectrum organization tools, people can detect the colour pattern through operating station to take precise identification. The detection results in form on Boolean ON/OFF are transferred to" Write' function block via a" Bool to Num" to receive it in binary o,1 so that Arduino can recognize command ON/OFF. Thus, fulfilling the objective of creating the program to serve real time automation. There is a lot of scope improvisation and innovation on basis of colour with detection of fragmentation and mixing of colour. In order to increase the range of detection for conveying excessive parameters in the future, we mainly focus to use of a wide range of specialist ways. Also, we advise using LabVIEW for operation as addition of new drivers is constantly happening for creation and designing of various interactive functions and real-time processing rather than just the present. We truly want to move forward and continue to develop the framework in order to increase range of parameters that can be detected and operated like wisely. Also, we must include the possibility of remote control into main programming control interfacing.

VI. AUTHOR'S CONTRIBUTION

Conceptualization: Badri Narayan Mohapatra.
Methodology: Badri Narayan Mohapatra.
Investigation: Badri Narayan Mohapatra.
Discussion of results: Badri Narayan Mohapatra.
Writing – Original Draft: Badri Narayan Mohapatra.
**Writing – Review and Editing:** Badri Narayan Mohapatra.
Resources: Badri Narayan Mohapatra.
Supervision: Badri Narayan Mohapatra.
Approval of the final text: Badri Narayan Mohapatra.

VIII. REFERENCES

[1] S. K. Behera, A. K. Rath, A. Mahapatra, and P. K. Sethy, 'Identification, classification & grading of fruits using machine learning & computer intelligence: a review', Journal of Ambient Intelligence and Humanized Computing, pp. 1–11, 2020.

[2] J. A. Arat et al., 'A Novel Implementation of a Color-Based Detection and Tracking Algorithm for an Autonomous Hexacopter', International Journal of Automation and Smart Technology, vol. 11, no. 1, pp. 2143–2143, 2021.

[3] A. Papavasileiou, G. Michalos, and S. Makris, 'Quality control in manufacturing--review and challenges on robotic applications', International Journal of Computer Integrated Manufacturing, pp. 1–37, 2024.

[4] Y. Joba, M. Halahlah, and M. Herbawi, 'Smart Products Sorting Line Using Computer Vision', 2023.

[5] M. F. S. Titu, S. M. R. Haque, R. Islam, A. Hossain, M. A. Qayum, and R. Khan, 'Experiments with cooperative robots that can detect object's shape, color and size to perform tasks in industrial workplaces', International Journal of Intelligent Robotics and Applications, pp. 1–14, 2023.

[6] J. Dong, 'Design of smart operating table based on HCI and virtual visual tracking technology', International Journal on Interactive Design and Manufacturing (IJIDeM), vol. 18, no. 2, pp. 1019–1031, 2024.

[7] B. N. Mohapatra, A. Walse, D. Patil, and N. Barwade, 'Data Acquisition System with Different Control Application Strategies Using LabVIEW', SAR Journal (2619-9955), vol. 6, no. 2, 2023.

[8] B. N. Mohapatra, N. Barwade, A. Walse, and D. Patil, 'Data acquisition system of temperature measurement using LabVIEW application', Andalasian International Journal of Applied Science, Engineering and Technology, vol. 3, no. 1, pp. 26–31, 2023.

[9] A. Lakshmi, N. Mahidhar, M. Manoj, and K. Kalyan, 'Accident avoiding system using multisensors using labview', Sustainable development in engineering and technology, p. 225, 2022.

[10] L. J. Bradley and N. G. Wright, 'Electrical measurements and parameter extraction of commercial devices through an automated MATLAB-Arduino system', IEEE Transactions on Instrumentation and Measurement, vol. 70, pp. 1–9, 2021.

[11] R. Keesey et al., 'An open-source environmental chamber for materials-stability testing using an optical proxy', Digital Discovery, vol. 2, no. 2, pp. 422–440, 2023.
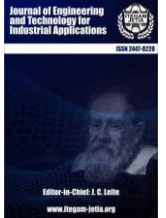
RESEARCH ARTICLE   **OPEN ACCESS**

DESIGN AND DEVELOPMENT OF A DOUBLE-EDGED TRENCHING MACHINE FOR REUSABLE WOOD COMPOSITE MATERIAL TILES

*Badri Narayan Mohapatra[1], Yash Lokhande[2] and Rajwardhan Patil[3]

[1] Assistant Profesor, Department of Instrumentation Engineering, AISSMS IOIT, Pune, INDIA .
[2, 3] Final Year Students Of of Instrumentation Engineering, AISSMS IOIT, Pune, INDIA .

[1] http://orcid.org/0000-0003-1906-9932 ⓘ, [2] http://orcid.org/0009-0009-5283-2179 ⓘ, [3] http://orcid.org/0009-0004-1216-7219 ⓘ

Email: [1] badri1.mohapatra@gmail.com*, [2] yashlokhande51@gmail.com, [3] rajwardhanpatil9090@gmail.com

ABSTRACT

The industrial sector has undergone significant advancements in recent years, adopting efficient and state-of-the-art technologies that have reduced waste production and improved product quality and production efficiency. The wood cutting industry is no exception, benefiting from technological evolution that has drastically reduced job completion times compared to two decades ago. However, this progress contrasts with the limitations of older machines, which are two to three decades old and suffer from outdated technology and methods. These machines exhibit reduced accuracy, lack precision, consume excessive power, and face challenges in finding spare parts for obsolete systems in case of breakdowns. Consequently, owners are often forced to discard these machines, leading to disposal challenges. The solution lies in upgrading these machines to address these issues effectively. This paper presents the design and development of a double-edged trenching machine tailored for the production of reusable wood composite material tiles. The machine is equipped with an embedded controller to facilitate the precise embedding of windows into the tiles. The system offers a sustainable solution for tile manufacturing, enhancing the efficiency and accuracy of window integration. The embedded controller ensures the tiles meet quality standards, contributing to the overall durability and aesthetics of the final product. This research bridges the gap between traditional tile manufacturing processes and modern sustainable practices, offering a promising approach for the future of construction materials.

I. INTRODUCTION

Reusable wood tiles, also known as bio-based composite tiles, are becoming increasingly popular in the construction and design industries due to their environmentally friendly nature and aesthetic appeal. These tiles are made from wood fibers bonded together with a calcium sulphate (Reusable Wood) binder, offering several advantages over traditional wood or ceramic tiles. They are sustainable, utilizing recycled wood fibers to minimize environmental impact, and are durable, being resistant to moisture, fire, and wear and tear. Additionally, they are versatile, available in various colors, textures, and sizes to cater to diverse design needs.

However, processing Reusable Wood tiles poses challenges due to their unique material properties. Conventional edge trimming methods often result in chipping or damage to the tile edges, necessitating the use of a specialized double-edged trenching machine.

In the past, CNC wood routers were equipped with DC servo motors and induction spindle motors, offering optimal accuracies and functionality but consuming considerable power and having lower power factors. Nowadays, the demand for 3D machining and complex work at high speeds with high accuracies has increased. This demand is met by new AC servo and high-speed spindle motors, along with modern Windows OS-based

control systems. These advancements in technology not only improve performance but also reduce power consumption.

By upgrading old machines with new motion control systems, low-frequency, and ultra-low backlash mechatronics equipment, it is possible to revive old woodworking machines. This revitalization enables these machines to deliver 3D patterns and other applications with better speed and accuracy, offering a cost-effective and sustainable solution for the woodworking industry.

II. THEORETICAL REFERENCE

The design and development of a double-edged trenching machine for reusable wood composite material tiles is a topic of growing interest in the construction and manufacturing industries [1]. This machine is specifically tailored to address the challenges associated with processing reusable wood composite material tiles, which are gaining popularity due to their eco-friendly nature and aesthetic appeal. Trenching machines, in general, are utilized across industries for tasks ranging from construction to agriculture. However, the specific requirements for processing wood composite materials, such as those used in reusable wood tiles, necessitate specialized considerations.

Conventional trenching machines are typically designed for soil excavation and may not be suitable for processing wood composite materials. These machines often lack the precision and control required for working with delicate materials like wood composites. Additionally, the cutting mechanisms and blade designs of traditional trenching machines may cause excessive chipping or damage to wood composite tiles, leading to suboptimal results. Several research studies have focused on different aspects of trenching machines and wood composite materials [2]. The use of trenching machines in the construction industry and highlighted the importance of precision and efficiency in trenching operations [3] and [4]. Their findings underscored the need for specialized machines to handle the unique properties of wood composite materials.

In another study, the mechanical properties of reusable wood composite materials and the challenges they pose in manufacturing processes [5] and [6]. They emphasized the importance of developing machines that can accurately and efficiently process these materials to ensure product quality and durability.

Additionally, recent advancements in CNC technology have led to the development of CNC wood routers that are capable of handling complex machining tasks with high precision [7]. These machines offer a promising solution for the efficient processing of reusable wood composite material tiles [8].

In contrast, modern CNC (Computer Numerical Control) machines offer a more promising solution for processing wood composite materials. CNC technology allows for precise control of cutting parameters, such as speed, depth, and tool orientation, enabling efficient and accurate machining of wood composite tiles [9]. CNC routers, in particular, are well-suited for cutting and shaping wood composites, offering versatility and high repeatability.

In the context of reusable wood composite material tiles, the design and development of a double-edged trenching machine present a novel approach to addressing the challenges of processing these materials. By incorporating features such as dual cutting edges, specialized blade designs, and precise control systems, this machine aims to improve the efficiency and quality of trenching operations for wood composite tiles.

III. MATERIALS AND METHODS

The necessary resources for the modifications include a Syntec controller WA60 with integrated four servo and built-in PLC system, featuring a Windows CE-based operating system and CNC control application. Additionally, a three-phase isolation step-down transformer for power supply, a high-frequency variable frequency drive with programmable V/F curve and up to 600 Hz output frequency type VFD for high-speed spindles, an M-to-M router for remote connectivity, and CAM software on an additional PC for converting 3D drawings and sketches into G-Code-based CNC programming are required [10]. Figure 1 represents the basic block diagram.

The new AC servo motor drives incorporate absolute encoder feedback with a 17-bit resolution, coupled with a Windows-based CNC control system and a customized GUI application. This setup allows for easy access to controls and the programmability of various functions, enhancing user convenience. Additionally, these drives offer higher bandwidth for servo control and utilize high-speed vector control for spindle motors, resulting in improved position accuracy and lower power consumption. Compared to older systems, the new drives provide an enhanced operator interface and diagnostic capabilities, making them easier to use and maintain. Furthermore, they offer better tool selection, offset, and wear compensation features, ensuring fast and accurate program execution.
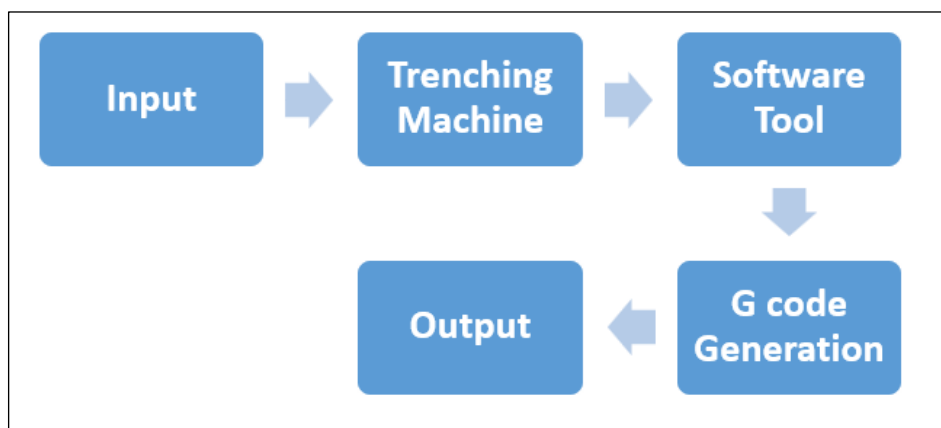
Figure 1: Functional block diagram of Trenching Machine.
Source: Authors, (2024).

We acquired an old Alberty dual pallet woodworking machine from a used scrap market, equipped with an outdated DOS-based CNC controller and DC drives. Despite its age, we opted to modify this machine to meet our specific needs for large-format sheet processing, accommodating the use of modern materials such as FMDF, HPLM, DERELIN, HYLAM, and reusable wood panels.
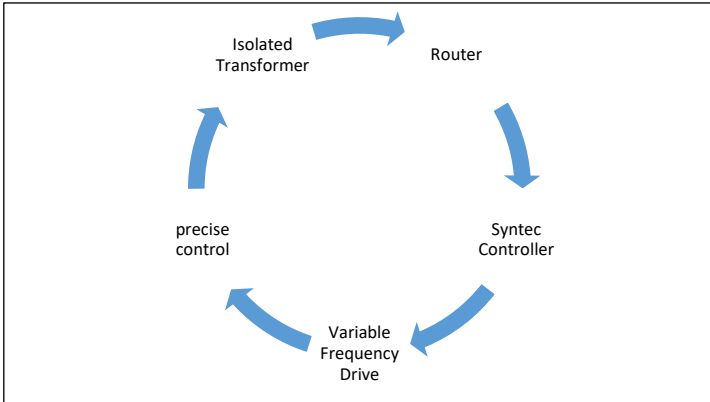

Figure 2: Precise control over the machining process.
Source: Authors, (2024).

The isolated transformer serves to step down voltage for the power supply, ensuring a safe and stable electrical environment for the machinery. Meanwhile, the router enables remote connectivity, facilitating remote monitoring and control of the machine. The Syntec controller acts as the central control unit for the CNC machine, overseeing the servo motors and PLC system. It features a Windows CE-based operating system and CNC control application. Lastly, the VFD (Variable Frequency Drive) controls the speed of the high-speed spindles. It offers a programmable V/F curve and supports up to 600 Hz output frequency, enabling precise control over the machining process, which is shown in figure 2. Figure 3 represent the outer look of trenching machine.

Figure 3: The machine was in a scrapyard state before being prepared for processing capabilities.
Source: Authors, (2024).

To enhance the precision and finishing of 3D operations, we have undertaken several modifications to the machine. Firstly, we replaced the machine slides with LM guide ways to ensure smooth and accurate movement. Next, we upgraded the lead screws to high-accuracy ball screws for improved precision. The DC motors were then replaced with high-resolution absolute AC servo motors to enhance control and accuracy. Additionally, we installed new high-speed AC spindles to replace the old ones. The outdated DOS system was upgraded to a Syntec CNC controller WA60, which features four axes integrated with absolute feedback and a user-friendly Windows-based GUI for part programming and CAM interface. The implementation of new-generation high-speed and high PWM has led to a reduction in peak currents and overall power consumption. The use of new-generation AC servo motors with 10 magnetic poles and rare earth magnets has further improved performance and current-to-torque ratio, resulting in lower power consumption. Furthermore, the presence of serial remote IO has reduced field wiring, streamlining the overall system.

Figure 4: Actual Double Edge Trenching machine.
Source: Authors, (2024).

The double-edge trenching machine (in figure 4) is equipped with several key features to enhance its performance. It features a cutting mechanism that includes a pair of high-precision, diamond-tipped saw blades specially designed for cutting Reusable Wood wood tiles. These blades ensure clean and precise cuts without chipping or damage. The machine is controlled by a Syntech controller, a renowned industrial automation platform that provides accurate control over the machine's operation, including blade speed, feed rate, and depth of cut. Additionally, the machine integrates a Windows embedded system, offering a user-friendly interface for setting cutting parameters, monitoring machine status, and troubleshooting any issues that may arise. Figure 5 shows the G code for designing of hexagonal shape.
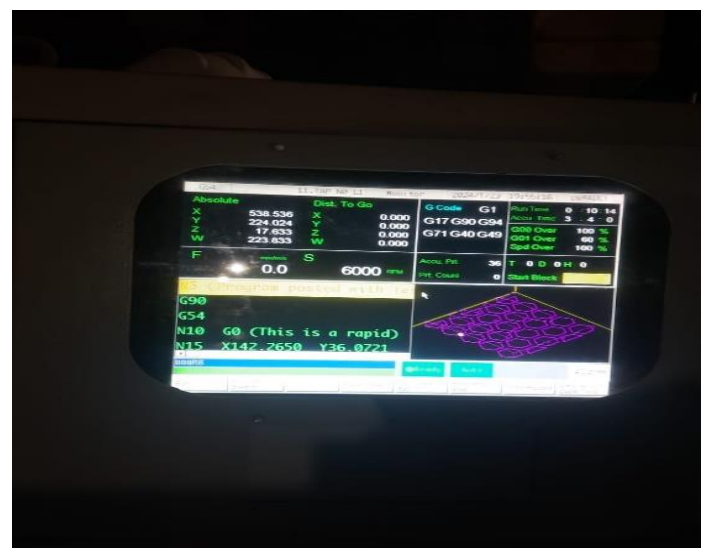
Figure 5: Generated G code for variable designing.
Source: Authors, (2024).

When Using Acronyms - UA, they must be explained the first time the term is mentioned. The same condition must be used to define the equation variables.

IV. RESULTS AND DISCUSSIONS

It is the logical presentation of the results that demonstrate the true contribution of the research and also justify the conclusion. The parts indicated above, Introduction, Material and Methods serve to explain how the results are obtained. Use tables and figures for your explanation. The results must be written in the past, in a brief and simple way. Avoid redundancy.

Table 1: Time consuming for design.

Design Style	Drilling for (one) design	Time consuming
Cylinderical	1	1.8 min
Hexagonal	1	2.0 min
Square	1	1.9 min
Total	3	5.7 min

Source: Authors, (2024).

Table 1 shows the time consuming of different shape of design but it may vary as per the size and length of the design. Equation 1 and 2 are the area calculation formula for hexagonal and cylindrical shape.

Area of hexagonal shape [11]:

$$A1 = \frac{3\sqrt{3}}{2} \; S^2 \qquad (1)$$

where A1 is the area and S is the side length.

Area of cyliderical shape:

$$A2 = 2\pi r^2 + \; h(2\pi r) \qquad (2)$$
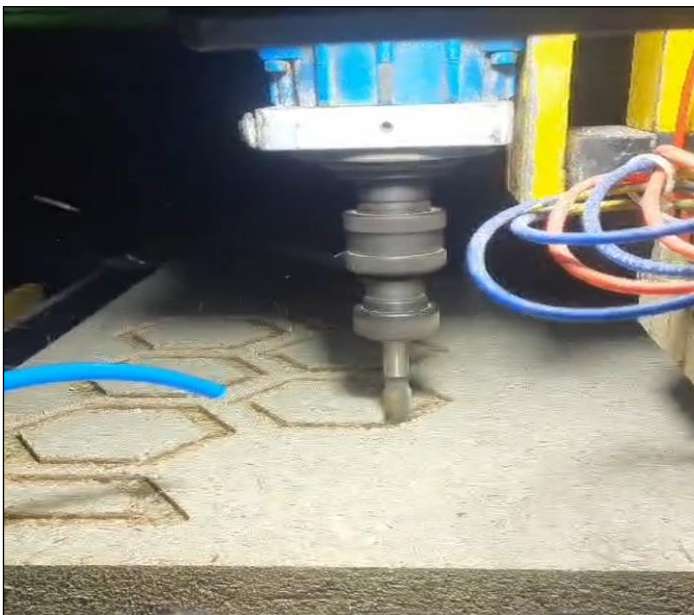
Figure 6: Hexagonal shape drilling.
Source: Authors, (2024).

Figure 6 represents illustrates the process of creating a hexagonal hole using a specialized drill bit or machining technique.

Figure 7 shows When arranged closely together, hexagonal shapes minimize wasted space, which can be beneficial in applications like honeycomb structures or bolt patterns.

Figure 7: Drilling in the wood.
Source: Authors, (2024).

Figure 8: Hexagonal shaped output.
Source: Authors, (2024).

Figure 9: Cylindrical shaped output.
Source: Authors, (2024).

Figure 8 and 9 drill press with a hexagonal and cylindrical bit bores a hole into a plank of wood. Wood dust accumulates around the drill bit.

V. CONCLUSIONS

This paper presented the design and development of a novel double edge trenching machine specifically tailored for processing reusable wood tiles. The machine leverages the Syntech controller and a Windows embedded system for operation. We explored the potential applications of this machine and analyzed the advantages and limitations of this approach. The findings suggest that the machine has the potential to significantly impact the processing of reusable wood tiles, making it a more efficient and viable solution. Further research and development efforts could explore the possibility of remote control, operation, and diagnostics of the machine via the internet. This would enhance user convenience and enable real-time monitoring and troubleshooting. Additionally, optimizing the machine's design, control system, and software interface could lead to even greater efficiency and user-friendliness. By addressing these aspects, this technology has the potential to revolutionize the processing of reusable wood tiles, paving the way for wider adoption and a more sustainable construction industry.

VI. AUTHOR'S CONTRIBUTION

Conceptualization: Yash and Rajwardhan.
Methodology: Badri Narayan Mohapatra.
Investigation: Yash and Rajwardhan.
Discussion of results: Badri, Yash and Rajwardhan.
Writing – Original Draft: Badri Narayan Mohapatra.
Writing – Review and Editing: Badri Narayan Mohapatra.
Resources: Yash.
Supervision: Badri Narayan Mohapatra.
Approval of the final text: Badri , Yash and Rajwardhan.

VII. ACKNOWLEDGMENTS

VIII. REFERENCES

[1] S. M. Elgizawy, 'A framework for sustainable slum development based on zero waste concept:" Learn to Earn Model"', 2019.

[2] B. Castanié et al., 'Wood and Plywood as eco-materials for sustainable mobility: a review', Composite Structures, p. 117790, 2023.

[3] M. Kassem, E. Mahamedi, K. Rogage, K. Duffy, and J. Huntingdon, 'Measuring and benchmarking the productivity of excavators in infrastructure projects: A deep neural network approach', Automation in Construction, vol. 124, p. 103532, 2021.

[4] S. Park, J. Kim, S. Lee, and J. Seo, 'A Comparative Analysis of Automated Machine Guidance and Control Systems for Trench Excavation', KSCE Journal of Civil Engineering, vol. 25, pp. 4065–4074, 2021.

[5] M. M. A. Nassar, K. I. Alzebdeh, T. Pervez, N. Al-Hinai, and A. Munam, 'Progress and challenges in sustainability, compatibility, and production of eco-composites: A state-of-art review', Journal of Applied Polymer Science, vol. 138, no. 43, p. 51284, 2021.

[6] M. Abdur Rahman, S. Haque, M. M. Athikesavan, and M. B. Kamaludeen, 'A review of environmental friendly green composites: production methods, current progresses, and challenges', Environmental Science and Pollution Research, vol. 30, no. 7, pp. 16905–16929, 2023.

[7] M. Ramos-Maldonado, C. Aguilera-Carrasco, and M. Gong, 'Trends and opportunities of Industry 4.0 in wood manufacturing processes', in Engineered Wood Products for Construction, IntechOpen London, UK, 2021.

[8] J. Butt, V. Mohaghegh, S. Sadeghi-Esfahlani, and H. Shirvani, 'Subtractive and additive manufacturing applied to drilling systems', Advances in Terrestrial Drilling: Ground, Ice, and Underwater, vol. 39, 2020.

[9] J. Gisip, Improvement of wood-based machining operations on a CNC router through extending tool life. North Carolina State University, 2015.

[10] K. Latif, A. Adam, Y. Yusof, and A. Z. A. Kadir, 'A review of G code, STEP, STEP-NC, and open architecture control technologies based embedded CNC systems', The International Journal of Advanced Manufacturing Technology, vol. 114, pp. 2549–2566, 2021.

[11] E. Denenberg, 'Surface area and volume-Learn it, live it, and apply it', Retrieved from, 2011.

Journal of Engineering and Technology for Industrial Applications
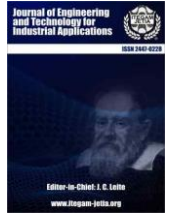
ENHANCING IOT NETWORK SECURITY THROUGH ADVANCED DATA PREPROCESSING AND HYBRID FIREFLY-SALP SWARM OPTIMIZED DEEP CNN-BASED INTRUSION DETECTION

*Bijili Jayan[1], Tamilarasi Ganesan[2] and Binu Bhaskara Kurup[3].

[1,2,3] Faculty in College of Computing and Information Sciences, University of Technology and Applied Sciences - Al Musanna, Oman.

[1]http://orcid.org/0009-0008-0526-4511, [2]http://orcid.org/0009-0000-3466-7549, [3]http://orcid.org/0009-0002-1220-3553.

Email: [1]bijilijayan861@gmail.com*, [2] prithvi678@gmail.com, [3]binubk@gmail.com

ABSTRACT

This concept addresses the imperative need for robust Intrusion Detection system (IDs) in Internet of Things (IoT) networks by presenting a comprehensive approach that integrates advanced data preprocessing techniques and Deep Convolutional Neural Network (DCNN) based IDS. The process commences with raw and inherently noisy data generated by IoT sensors. To fortify the detection capabilities, a sequence of preprocessing steps is applied, including data cleaning, one-hot encoding and normalization, ensuring the prepared data is resilient to outliers and irrelevant information while being conducive to Deep Learning (DL) models. The core of the proposed system is a DCNN, adept at capturing sequential patterns within diverse and dynamic IoT data. To further optimize the performance of the DCNN, a hybrid firefly-salp swarm optimization algorithm is employed. This hybrid approach leverages the strengths of both Firefly and salp swarm optimization techniques (FFA-SSA), enhancing the model's ability to identify potential security threats effectively. The synergy of advanced data preprocessing and nature-inspired optimization methods not only strengthens the security posture of IoT networks but also contributes to the resilience and adaptability of intrusion detection systems. The presented concept signifies a crucial step towards ensuring more secure and resilient IoT deployments, acknowledging the pivotal role played by innovative techniques in preparing data and optimizing deep learning models for enhanced cybersecurity.

I. INTRODUCTION

The most important indicators of the power quality provided to customers in electrical IoT is an emerging technology that has been rapidly developing and being used in recent years [1],[2]. It allows several devices to communicate and interact with each other through a network, which is driving the development of new business process technologies. Owing to nodes joining and leaving the network instantly, IoT networks have an open topology that is dynamic. Their absence of centralized network management solutions exposes them vulnerable to security issues. [3],[4]. The increasing risk to network security has made the use of intrusion detection technologies essential to protecting computer systems and network security [5]. Through the analysis of activity patterns and network traffic monitoring, IDs are intended to quickly detect and address security breaches. Through the detection of numerous attack types, they are essential to preserving the security and integrity of computer networks [6]. Traditional IDS frequently fail to detect new or sophisticated assaults because they rely on established rules as well as signatures to recognize existing attack patterns. Innovative techniques are therefore essential for prompt intrusion detection and assault prevention

strategies [7],[8]. DL and Machine Learning (ML) algorithms have been employed recently for intrusion detection and prevention as well as network abnormality detection [9]. The ML techniques include support vector machine (SVM) models [10], k-means [11], k-nearest neighbor (kNN) [12], and several more are employed to IoT-based IDs systems. There are difficulties with improving the existing system's performance and identifying subcategories of cyber-attacks [13]. Beyond the constraints of conventional IDS approaches, sophisticated methods like deep learning have been developed [14]. The

conventional DL techniques like CNN [15], RNN [16] and LSTM [17] have demonstrated incredible abilities to automatically extract complicated patterns and characteristics from complex data like network traffic. Although, it takes more computation time and has complexity [18]. Thus, the proposed work integrated with the DL based classifier DCNN technique, which minimize false positives by accurately differentiating between malicious activity and typical network behavior with high accuracy.
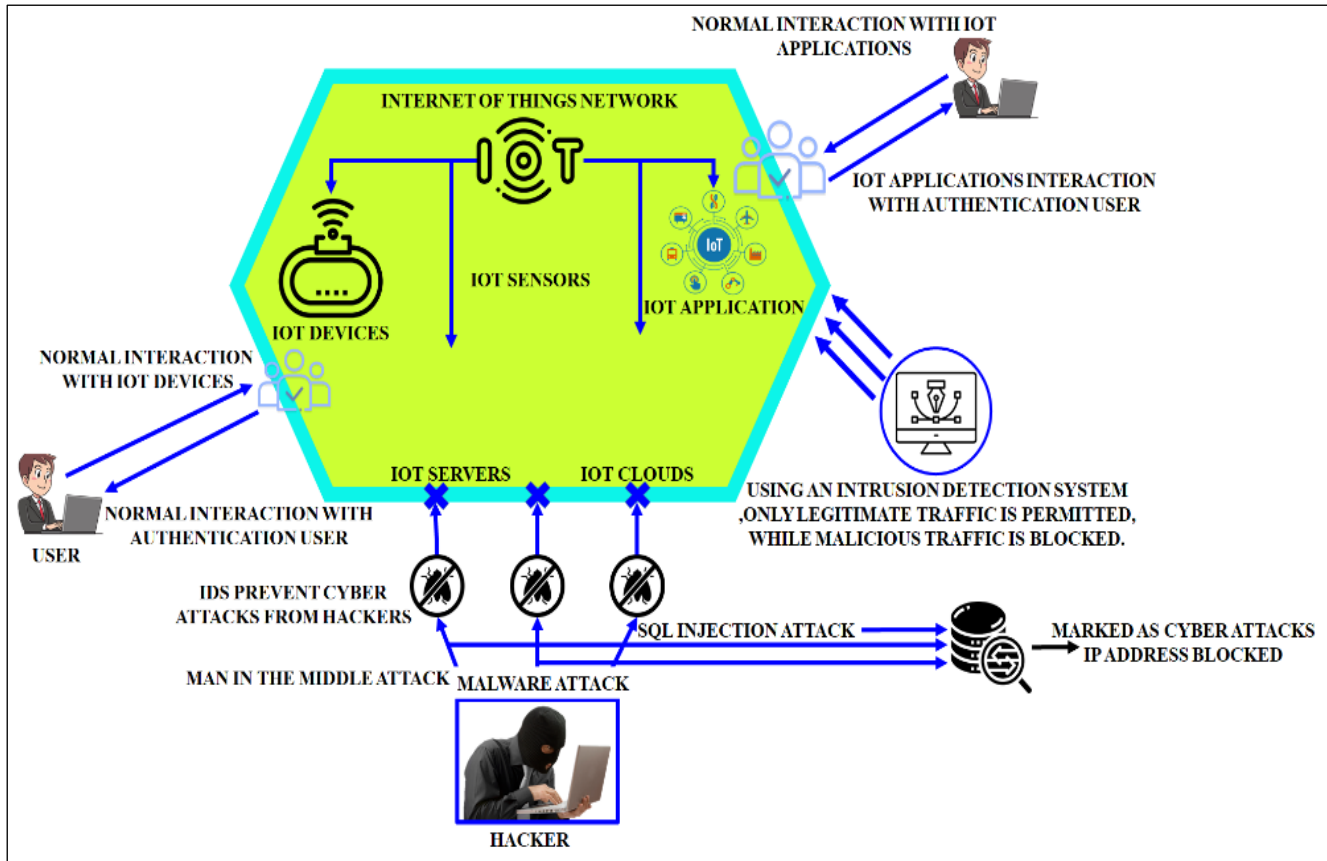
Figure 1**:** Protecting the IoT network with an IDs.
Source: Authors, (2024).

Additionally, the metaheuristic (MH) optimization technique is needed to tune the parameters for the DCNN classifier [19]. MH is primarily used for IDSs, including the genetic algorithm [20], Harris Hawk algorithm [21], and Crow Search Algorithm (CSA) [22] andParticle Swarm Optimization (PSO) algorithm [23]. Nevertheless, those conventional topologies has the limitations of low convergence rate, slow convergence speed and complexity [24]. Due to this, the proposed work implemented the hybrid FFA-SSA optimization approach for efficiently tuning the parameter of DCNN with rapid convergence speed with reduced complexity. The objectives:

- To effectively capture relevant patterns and discriminate between normal and anomalous network traffic in IoT devices.
- To boost the classification accuracy of intrusion detection system, the DCNN classifier is employed.

- To tune the parameters of DCNN effectively, a novel hybrid FFA-SSA optimization technique is utilized.

II. PROPOSED METHODOLOGY

The rapid propagation of IoT devices has brought about numerous benefits and opportunities for numerous industries. However, the growing number of interconnected devices also presents significant challenges in terms of network security.Protecting IoT networks from malicious activities and intrusions is crucial to ensure privacy, integrity as well as availability of data. To address this issue, the advanced data preprocessing techniques and hybrid optimization algorithms with deep Convolutional Neural Networks (CNNs) is employed to enhance IoT network security and enable effective ID and the block diagram of the developed work is illustrated in Figure 2.This approach can significantly bolster the security posture of IoT networks and protect them from a wide range of intrusions and cyber threats.
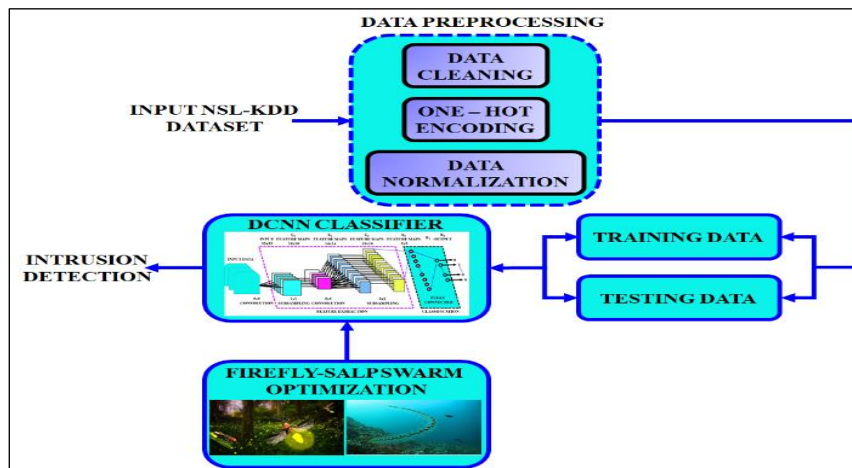
Figure 2: Block diagram for the proposed work.
Source: Authors, (2024).

The NSL-KDD dataset collected from IoT devices is taken as input and fed to the preprocessing stage. Data cleaning, one hot encoding and data normalization is done in preprocessing process, the collected data undergoes preprocessing steps, such as filtering, normalization and feature extraction. These steps ensure the data is clean, standardized, and ready for analysis. The preprocessed data is divided into two sets: the training set and the testing set. Training Set: A portion of the data is employed for training the DCNN model and optimizing its parameters. Testing Set: The remaining data is set aside for evaluating performance of the trained model. The processed training data is given to the DCNN classifier, which Extract high-level features and patterns from input data. Hyper parameters of the DCNN model is efficiently tuned by the novel hybrid FFA-SSA optimization algorithm with rapid convergence speed. Finally, by utilizing the optimized DCNN classifier, the intrusion detection is efficiently performed with high accuracy

II.1 PREPROCESSING MODEL

The original data collection needs to be treated appropriately before the network model is examined. One-hot coding, data normalization as well as data cleaning are the three components of data processing.

II.1.1 Data Cleaning

It is also known as replacing, modifyingand deleting the dirty data, which correct or clear the incorrect data from the data file. This includes processing invalid and missing values in the data as well as reasonableness detection. Data cleaning involves not only identifying missing values and content issues but also performing procedures like deleting duplicate values. Logical flaws and excessive data repetition will both have an impact on model's performance. No treatment steps are taken because there are no logical faulty data detected throughout the search and there is less data repetition.

II.1.2 One Hot Encoding

Numerous discrete data can be found in the data gathered by the IoT, The labels are deemed to be digitalized in string format because of its string data format. The above data cannot be incorporated straight into the model if labels are changed to numbers. This issue can be resolved using One-Hot Encoding. The first step is to encode the n states. A single number denotes a single state, and n digits are required to represent n states. When a state is reached, the associated digit is 1, and all other digits are 0. Moreover, it is clear that following One-Hot Encoding, every feature with m potential values will transform into m binary features. Furthermore, only one of these qualities can be active at once, which is mutually exclusive. Consequently, there will be less data. In addition to resolving the data attributes issue, One-Hot Encoding creates sparse label variables with matching dimensions from the numerous labels present in the experimental data set.

II.1.3 Data Normalization

Normalizing data has two primary benefits, one is to increase the model's rate of convergence, and the other is to increase the model's accuracy.Discrete or continuous values make up the features in the NSL-KDD dataset. It was impossible to compare values because of their disparate ranges. Using the mean and standard deviation of each feature from the train datasets, the test features were then normalized. This was done by subtracting the mean from each feature and dividing the result by its standard deviation. Data between (0, 1) are scaled employing the Min-Max normalization system, which is a linear transformation. To determine the new value, apply the following equation (1),

$$X_n = \frac{X - X_{min}}{X_{max} - X_{min}} \tag{1}$$

II.2 MODELLING OF DCNN FOR CLASSIFICATION

Convolution, pooling as well as fully connected layers constitute DL method, CNN is typically used for speech recognition and picture classification. In order to identify harmful behaviors in IoT networks, we employed a DCNN followed by a DNN in this study. As illustrated in Figure 3, the proposed approach consist the initial convolutional layer receives an input shape of (none, 62, 1). In this case, third-dimension value is "1," the number of input characteristics is "62," and the dynamic number of occurrences is "none." This layer, which yields output in a form of (none, 62, 62), uses a kernel with a size of three and sixty-two filters. The max-pooling layer takes as its input the output of the first convolutional layer. Pool size four was employed in this layer, with output of (none, 15 and 62). It consists of two 1D convolution layers, two max-pooling layers, flatten, and three dense layers. This is the location of the second convolutional layer, which uses thirty filters with a kernel size of three and generates an output in the form of (none, 15 and 30). The max-pooling layer receives the second convolutional layer's output as an input. Pool size two, which yields (none, 7, 30) output, has been used in this layer.

The convolutional layer lowers noise in addition to placing the most significant features closer together. Equations (2) and (3) show how the 1D convolutional layer works.

$$x_k = b_k + \sum_{i=1}^{N}(s_k, w_{ik}) \tag{2}$$

$$y_k = f(x_k) \tag{3}$$

Here, where x_k the 1D convolutional layer's is input, s_k specifies the preceding layer neuron's output, and w_{ik} represents the kernel from i to k. The bias value of neuron in convolutional layer is signified by bk. $f(x_k)$ specifies the ReLU activation function. This ReLU is expressed in equation (4). The 1D convolutional layer produces y_k. Equation (5) illustrates the pooling layer's input, which is the convolutional layer's output. The output values of convolutional layer are included in region $\Re$, from which we take the maximum value. The output of the max-pooling layer is s_k.

$$f_{(x_k)} = max(0, x_k) \tag{4}$$

$$s_k = \max_{i \in \Re} y_k \tag{5}$$

The last pooling layer's output shape is flattened into a single-dimensional array using this technique. The Input of the first dense layers is (None, 210) and the output of flatten is the same as that. The input for the second dense layer is (None, 50), which is the output of the first dense layer. The output (none, 25) from the second dense layer is transferred to the last dense layer. Applying the ReLU activation function in dense layers. The last dense layer's output outcomes employ the sigmoid function for binary classification and the softmax function for multi-class classification, correspondingly. Equations (6) and (7) illustrate sigmoid and softmax.

$$\sigma(x) = \frac{1}{1+e^{-x}} \tag{6}$$

$$softmax(x)_i = \frac{e^{xi}}{\sum_{j=1}^{k} e^{xj}} \tag{7}$$
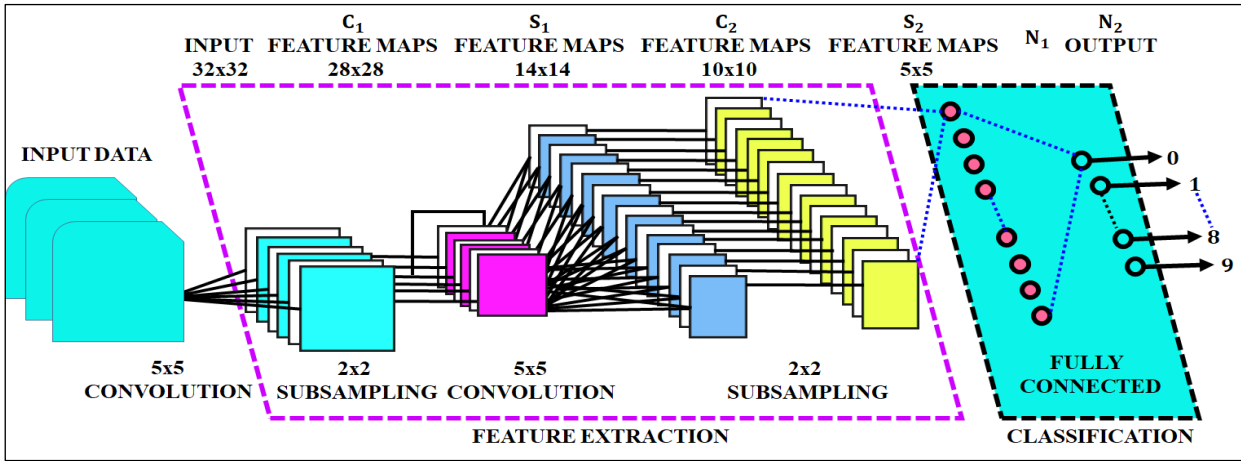
Figure 3: Structure of DCNN.
Source: Authors, (2024).

Table 1: DCNN model structure.

Layer	Output Volume	Description
Input	M, 1,80	
Conv1D-1	100,1,171	Number of filters: 100 Kernal size: 1 x 10, Activation: ReLu
Dropout	100,7,71	Gaussian dropout: 0.3
Pool	100,1,35	Maxpooling1D: 2 x 2
Conv1D-2	50,1,36	Number of filters: 50 Kernal size: 1 x 10, Activation: ReLu
Dropout	50,1,26	Gaussian dropout: 0.3
Pool	50,1,13	Maxpooling1D: 2 x 2
Dense_CNN	n	Fully connected n units, Activation: Softmax
MLP-1	100,1,80	Number of nodes: 100, Activation: ReLu
Dropout	100,1,80	Gaussian dropout: 0.3
MLP-1	50,1,80	Number of nodes: 50, Activation: ReLu
Dropout	50,1,80	Gaussian dropout: 0.3
Dense-DNN	n	Fully connected n units, Activation: Softmax
Softmax Average	n	Average: [Dense_CNN, Dense_CNN] Fully connected n units' activation: Softmax

Source: Authors, (2024).

II.3 MODELLING OF HYBRID SSA-FFA ALGORITHM

To present a improved optimization IDs than the recent one, the proposed approach uses the combination of the FF optimization algorithm with SS algorithm to build a hybrid FFA-SSA approach. In the part that follows, the HSSFF algorithm is briefly described.

II.3.1 Modelling of Ssa

Based on SS conduct, each population is split into two categories in this case: leaders and followers. In a slap chain, the salp in the front is referred to as the leader salp and the salp at the back is referred to as the follower salp. Follower salp receives the essential directives and instructions from the leader salp. The swarm intelligence algorithms and the SS optimization algorithm's processes and procedures are comparable. Here is a description of two steps of the SS optimization algorithm.

Stage 1: Leader phase

The updating procedure is used in the leader phase and is signified by the subsequent equation (8).

$$x_j^I = \begin{cases} x_J^{BEST} + C_1\{(UB^J - LB^J)C_2 + LB^J\}: & IF C_3 \geq 0.5 \\ x_J^{BEST} - C_1\{(UB^J - LB^J)C_2 + LB^J\}: & ELSE \end{cases} \quad (8)$$

The food source as well as the new leader position with the Jth dimension are signified by x_J^{BEST} and x_j^I in Equation 10. LB^J And UB^J stand for the upper and lower limits, respectively, with regard to the Jth dimension. Next, random numbers between the intervals of [0, 1] are created. The SS algorithm's significant factor is represented by the parameters C_1, C_2 and C_3. Equation 13 states that C_1 steadily decreases in relation to the number of repetitions.

$$C_1 = 2E^{-\left(\frac{4T}{t}\right)^2} \quad (9)$$

T and t specifies for the current iteration count and the maximum number of iterations, correspondingly.

Stage 2: Follower phase

According to Newton's law of motion, the solution is updated in the follower phase. In relation to Jth dimension, the expression for the follower phase is then shown as follows.

$$x_j^I = \frac{1}{2}GT^2 + \omega_0 T : I \geq 2 \quad (10)$$

The Jth dimension's follower salp is denoted by x_j^I. After that, the optimization's acceleration, time, and velocity are denoted by GT and ω_0, respectively. Next, the time change is indicated by $\Delta T = 1$, while the fixed starting speed is represented by $\omega_0 = 0$. As a result, the following equation represents the modified expression for the follower phase.

$$x_j^I = \frac{1}{2}\left(x_J^I + x_J^{I-1}\right) \quad (11)$$

The next part provides an algorithmic description of an SS optimization.

II.3.2 Modelling of ff Algorithm

The FF method's great exploration ability and flashing light demonstrating ability make it the greatest effective algorithm for solving engineering-related problems. The FF algorithm generally relies on three postulates. According to the first postulate, the FF moves to a different FF that is brighter than it is, and if it is brighter than all the other fireflies combined, it moves randomly. Next, the fitness function is used to assess the light's intensity. According to the third postulate, FFs are all fascinated by FFs, regardless of gender.28

Consider that nP and d are the firefly count and their respective dimensions. Accordingly, Equation 12 expresses the location of the FF in relation to space.

$$X_i = \left|X_I^1, X_I^2, \dots \dots X_I^d\right| \quad (12)$$

The subsequent section assesses the search space's random initialization.

$$X_i = l + RAND.(Upp - Low) \quad (13)$$

Equation 17 shows that the search agent's upper and lower bounds are indicated by the terms Upp and Low, respectively. Next, Equation 18 is used to compute the mathematical equation for the Euclidean distance.

$$R_U = \sqrt{\sum_{T=1}^{d}(X_{IT} - X_{JT})^2} \quad (14)$$

Consequently, the following is an explanation of the arithmetical derivation for light intensity.

$$i(R) = i_0 E^{-\beta R^2} \quad (15)$$

The initial light intensity i_0 and the light absorption coefficient is specified as β a correspondingly when $R = 0$. Similarly, Equation 20 provides arithmetic equation for FF with respect to attractiveness.

$$\alpha(R) = \alpha_0 E^{-\beta R^2} \quad (16)$$

The initial value of α0 represents the attractiveness of the FF at $R = 0$, as determined by Equation 18. X_I Moves in the direction of X_J if $X_J's$ light output is brighter than $X_I's$. Subsequently, the following is the position update formula.

$$X_I^{T+1} = X_I^T + a\left(X_J^T - X_I^T\right) + \gamma(Rand - 0.5) \quad (17)$$

II.3.3 Proposed Hssff Approach.

The HSSFF technique is enlightened in this section by combining two algorithms, like FF algorithm and SS optimization algorithm. By combining the advantages of the SS and FF algorithms, this HSSFF optimization algorithm offers a more rapid detection system with highly tuned DCNN parameters. The HSSFF approach flow diagram is shown in Figure 4, offers a Multiobjective framework that integrates the SS and FF algorithms.
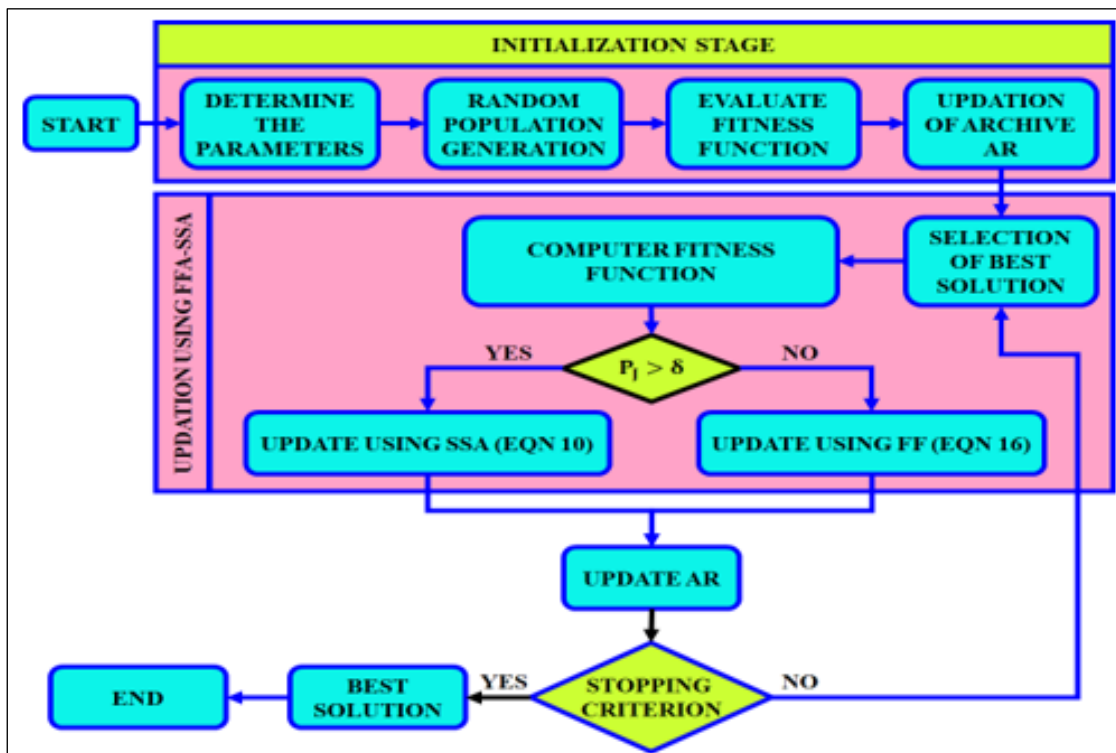
Figure 4: Flowchart of the proposed hybrid FFA-SSA algorithm.
Source: Authors, (2024).

Initially, the parameters are established and then a random population is created, Next, the fitness function is assessed, using Multiobjective fitness functions to assess the two primary goals, to develop the exploitation potential of the SS optimization method, archive AR is updated to identify the nondominated solution set. Subsequently, the nondominated and dominated solution sets are determined by an AR with a new population.

The delay is then calculated using the best solution that was found. If P_J is greater than δ, then SSA is used to update the solution; if not, FF is used. Afterwards, an optimal solution is obtained by checking the condition. An ideal solution is found if the criterion is met, if not, go back and choose the best option; this iterative process continues until the best value is found.

III. RESULTS AND DISCUSSION

To enhance IoT network security, the use of advanced data preprocessing and a hybrid Firefly-Salp swarm optimized DCNN-based IDsis proposed in this research. This approach aimed to enhance accuracy and efficiency of ID in IoT networks. Furthermore, the python software is used to foreshow the prominence of the proposed topology and the comparative analysis is made over the conventional methods, which is illustrates as below.
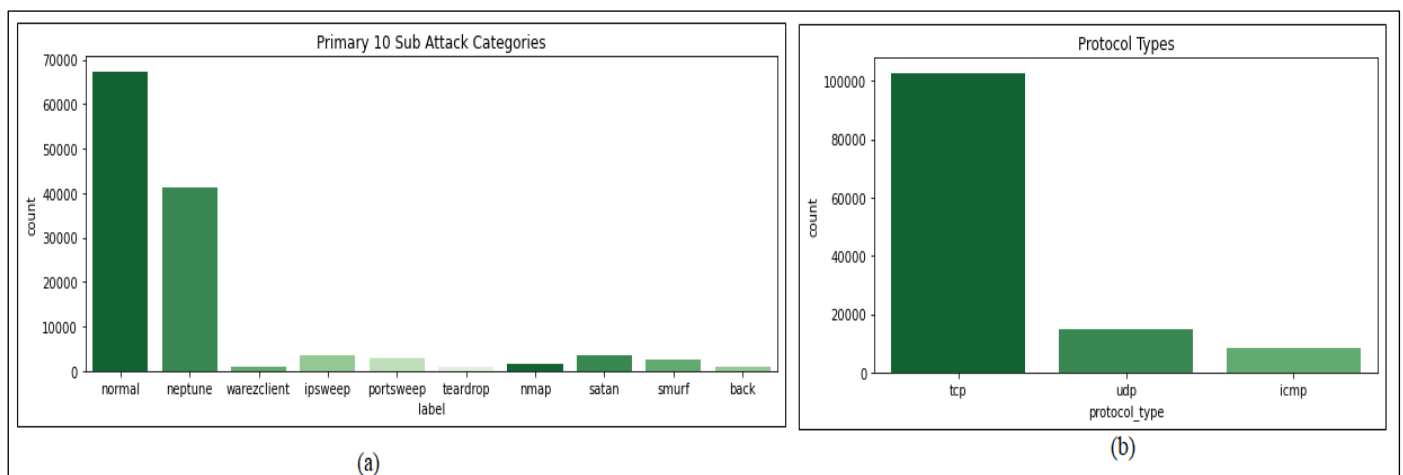
Figure 5: (a) 10 sub attack categories (b) Protocol types.
Source: Authors, (2024).

The primary 10 sub attack categories is displayed in Figure 5 (a), which includes normal, neptune, warez client, ipsweep, portsweep, teardrop, nmap, satan, smuff and back. The normal and Neptune has the high count rather than the others.

Likewise, Figure 5(b) illustrate the protocol types that contains tcp, udp and icmp, the high count is obtained in tcp protocol respectively.
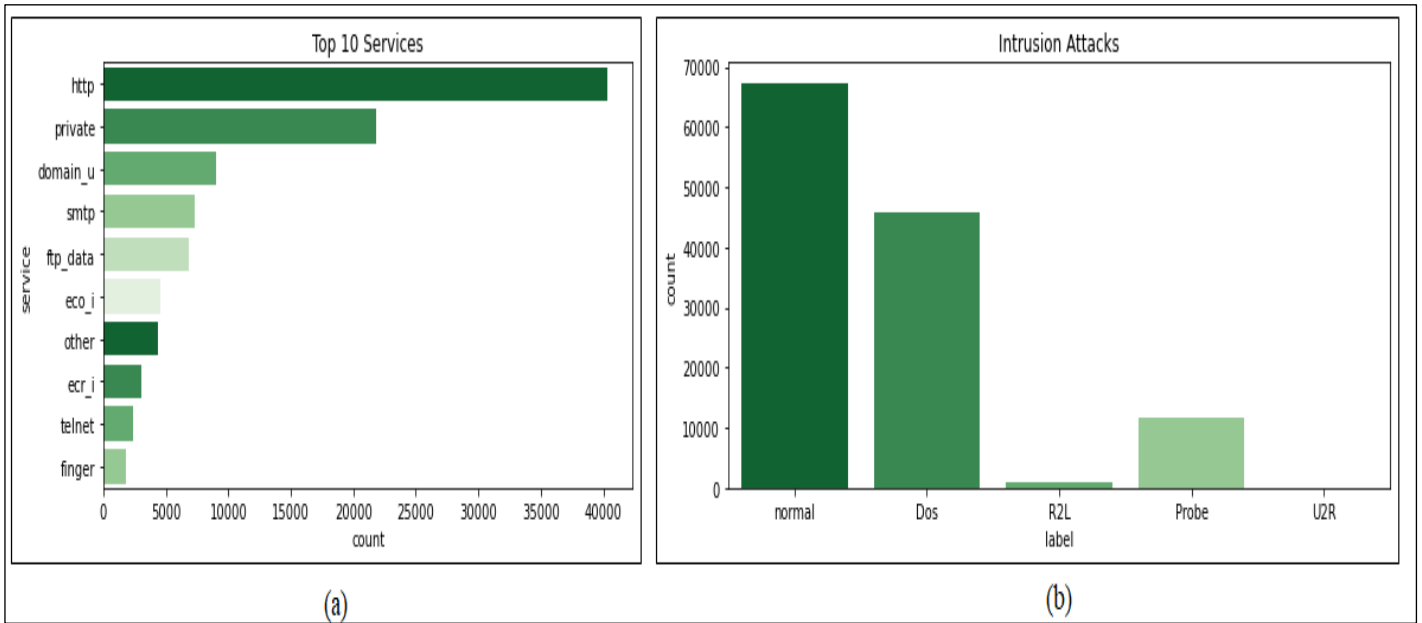
Figure 6: (a) Top 10 IoT services and (b) Intrusion attacks.
Source: Authors, (2024).

The top 10 IoT services are demonstrated in Figure 6(a), which specifies the services like http, private, domain_u, smtp, ftp_data, eco_i, other, ecr_i, telnet and finger along with the count. The http has the high count of 4000 than the others. Furthermore, the IDs attack is illustrated in Figure 6(b), the proposed work employ the NSL-KDD dataset, which contains normal, Dos, R2L, Probe and U2R respectively. In that, the normal has high intrusion attacks count of 65000.
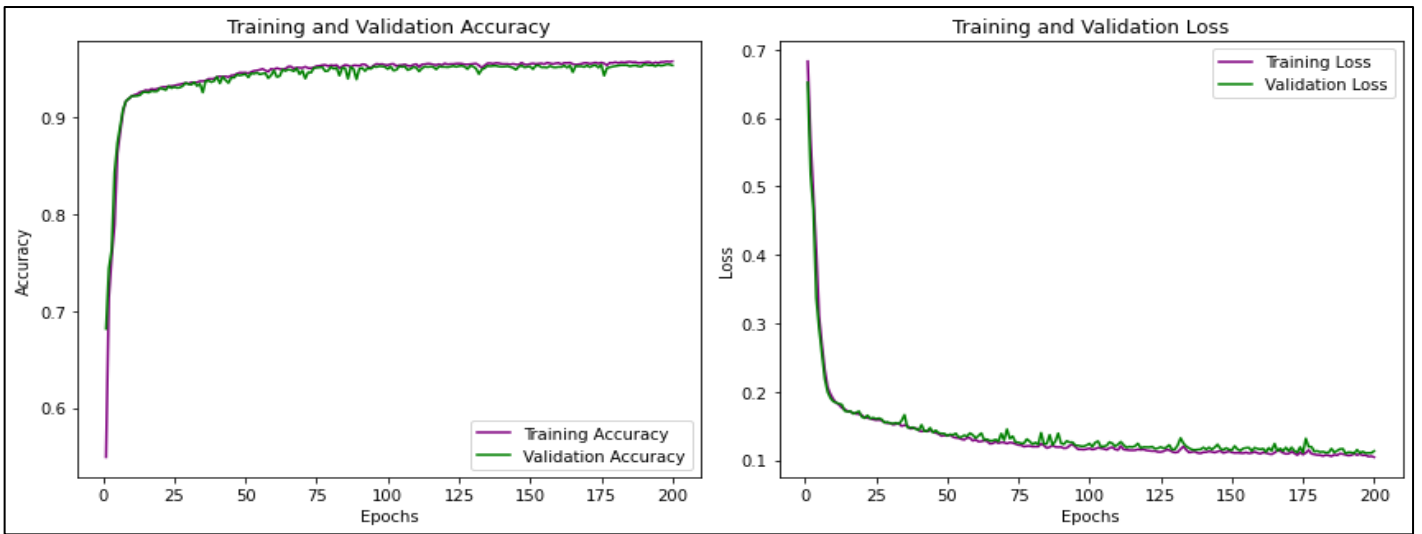
Figure 7: (a) training and validation accuracy (b) Training and validation loss.
Source: Authors, (2024).

Figure 7 shows the evaluation of the optimized DCNN approach's training loss ($Loss_{Tra}$) and validation loss ($Loss_{val}$) in terms of the effectiveness of intrusion detection performed in the IoT context. Figure 7 shows that the proposed approach performs better while using less $Loss_{Tra}$ and $Loss_{val}$. $Loss_{Tra}$'s decreasing sequence suggests that the developed model successfully reduces training loss during the learning process, which enhances convergence and facilitates efficient learning from the training set. Likewise, declining values of $Loss_{val}$ indicate that the model performs well in terms of generalizing to data that has not yet been encountered during the validation stage, which lowers the validation loss Finally, the developed optimized DCNN classifier attains the accuracy of 96.54% respectively as demonstrated in Figure 7(a).
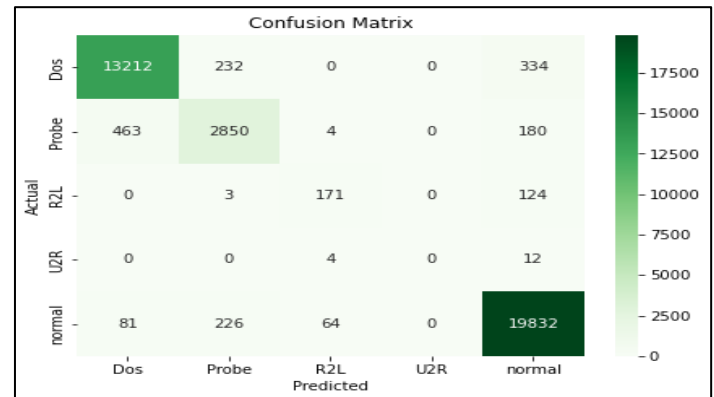
Figure 8: Confusion matrix for the proposed work.
Source: Authors, (2024).

Through the analysis of the intrusion detection data samples, it became evident that some identical property operations shared by the malicious network attack types like DOS, U2R, PROBE, R2L, and others cause the Src_byte and dst_byte byte values to decrease. Malicious interactions showed a high temporal link, and hot, num_failed_logins feature behaviour might be used to identify R2L and U2R-type attacks. As a result, it was possible to conduct an early investigation of the correlation between assault kinds, which led to the successful alteration of the DCNN selection results. This work conducted a large number of experiments for intrusion type detection. Based on these results, comparisons with the true type were done to create a suitable confusion matrix in Figure 8
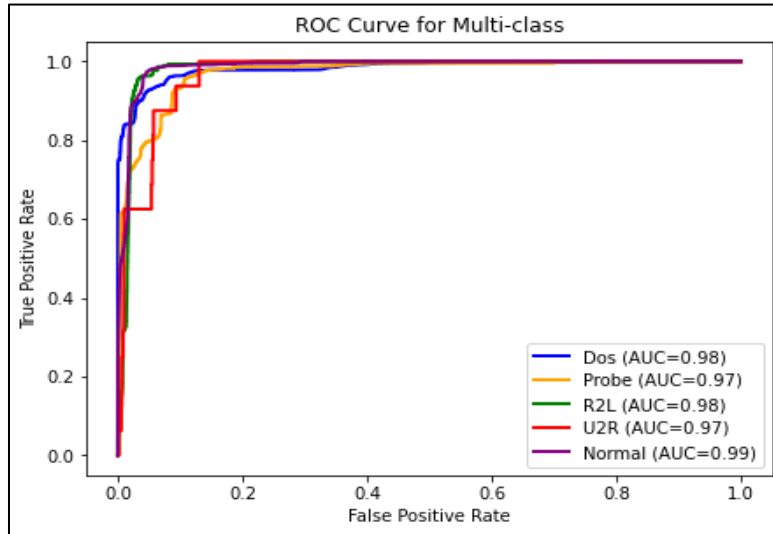
Figure 9: ROC curve for Multiclass.
Source: Authors, (2024).

Figure 9, the AUC value for the normal classes reaches 99%. This is because the prediction sequence sensibly predicts the subsequent behaviour sequence while capturing the abnormal behaviour characteristics of the current sequence, which aids in improving anomaly detection for the classification model.

The subsequent indices are significantly used for the evaluation metrics,

(a) Precision:

It is the percentage of the classifier's positive predictions which turn out true, as shown in the equation that follows.

$$precision = \frac{TP}{TP+FP} \qquad (18)$$

(b) F1-score:

It is the outcome of recall divided by precision

$$F1\ Score = 2 \times \frac{precision \times Recall}{Precision + Recall} \qquad (19)$$

(c) Accuracy:

$$Accuracy = \frac{TP+TN}{Total\ Number\ of\ samples} 100 \qquad (20)$$

(d) ROC curve:

$$AUC = \int_0^1 \frac{TP}{TP+FN} d \frac{FP}{TN+FP} \qquad (21)$$
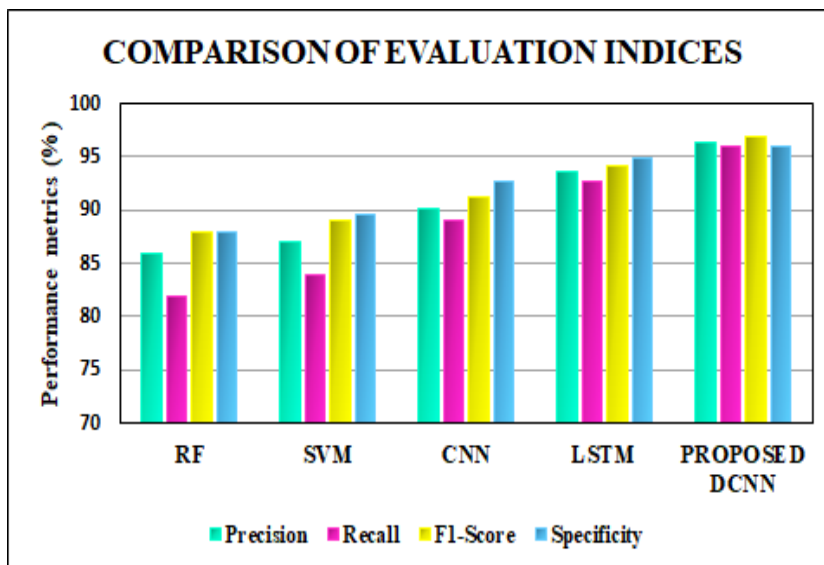
Figure 10: Comparison of evaluation indices with various classifier.
Source: Authors, (2024).

The proposed DCNN is contrasted with the other classifier approaches to determine the better precision, Recall, F1 score and specificity as illustrated in Figure 10, which is analyzed that the proposed classifier approach outperforms in evaluation metrics than the other existing techniques. Furthermore, Table 2 specifies the multiclass comparison for the original dataset with conventional classifiers.

Table 2: Multiclass comparison on the original dataset.

Classifiers	Dos	Normal	R2L	U2R	Probe
ERF [25]	75.58	87.78	56.62	25.15	75.66
LSTM [26]	74.58	97.1	27.54	20	74.21
SVM [27]	81.09	78.34	40.23	30.98	76.43
CNN [28]	85.26	96.73	17.78	8.95	73.97
Proposed DCNN	88.78	97.21	70.43	42.12	81.87

Source: Authors, (2024).
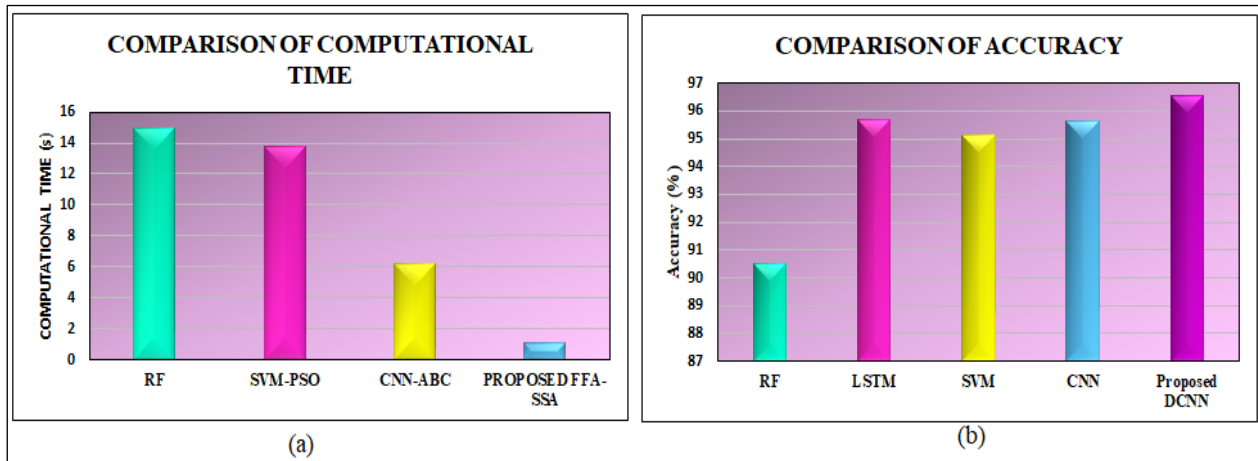
Figure 11: (a) Comparison of (a) Computational time and (b) Accuracy.
Source: Authors, (2024)

The proposed DCNN based hybrid FFA-SSA optimization algorithm is contrasted with the other existing approaches like RF, SVM-PSO and CNN-ABC as represented in Figure 11(a). From the graph it is prove that the developed optimized DCNN has less computational time than the others. Moreover, Figure 11(b) and Table 3 represents the comparison graph for determining the better accuracy using various conventional topologies, which stated that the implemented DCNN classifier has high accuracy of 96.54% than the other topologies correspondingly.

Table 3: Comparison of accuracy.

Classifier Techniques	Accuracy (%)
RF [29]	90.51
LSTM [30]	95.70
SVM [31]	95.14
CNN [32]	95.65
Proposed DCNN	96.54

Source: Authors, (2024)

IV. CONCLUSION

The integration of the hybrid Firefly-SALP swarm optimization algorithm with deep CNN-based intrusion detection further enhances the effectiveness of the system. The hybrid optimization algorithm intelligently adjusts the parameters of the deep CNN model, optimizing its performance and improving the detection accuracy of IoT network intrusions. This combination of advanced preprocessing and optimization techniques offers a robust and scalable solution for securing IoT networks against various types of intrusions and attacks. By leveraging advanced data preprocessing techniques, such as feature extraction and dimensionality reduction, the approach effectively reduces the complexity and noise in IoT data, enhancing the accuracy and efficiency of subsequent ID processes. Moreover, the deep CNN architecture enables the system to automatically learn and adapt to evolving intrusion patterns, enhancing its ability to detect previously unseen attacks. By continuously improving and advancing IoT network security solutions, it foster a safer and more secure IoT ecosystem, enabling the full potential of IoT technologies while mitigating the risks associated with them. The proposed system is executed in python software to show the prominence of the developed work and the comparative analysis is made with the other conventional topologies. From that it is prove that the developed DCNN classifier has better performance indices and accuracy by the value of 96.54%. Also, the proposed hybrid FFA-SSA optimization technique provides low computational with high convergence speed respectively.

V REFERENCES

[1] N. A. Hikal, and M. M. Elgayar, "Enhancing IoT botnets attack detection using machine learning-IDS and ensemble data preprocessing technique", In *Internet of Things—Applications and Future: Proceedings of ITAF 2019*, pp. 89-102, Singapore: Springer Singapore, 2020.

[2] X. Larriva-Novo, V. A. Villagrá, M. Vega-Barbas, D. Rivera, and M. S. Rodrigo, "An IoT-focused intrusion detection system approach based on

preprocessing characterization for cybersecurity datasets", Sensors, vol. 21, no. 2, pp. 656, 2021.

[3] K. M. Abuali, L. Nissirat, and A. Al-Samawi, "Advancing Network Security with AI: SVM-Based Deep Learning for Intrusion Detection", *Sensors,* vol. 23, no. 21, pp. 8959, 2023.

[4] S. Singh, A. S. M. Sanwar Hosen, and Byungun Yoon, "Blockchain security attacks, challenges, and solutions for the future distributed iot network", IEEE Access, vol. 9, pp. 13938-13959, 2021.

[5] M. A. Hossain, and M. S. Islam, "Ensuring network security with a robust intrusion detection system using ensemble-based machine learning", Array, vol. 19, pp. 100306, 2023.

[6] J. M. Kizza, "System intrusion detection and prevention", In Guide to computer network security, pp. 295-323, Cham: Springer international publishing, 2024.

[7] J. Díaz-Verdejo, J. Muñoz-Calle, A. E. Alonso, R. Estepa Alonso, and G. Madinabeitia, "On the detection capabilities of signature-based intrusion detection systems in the context of web attacks", Applied Sciences, vol. 12, no. 2 pp. 852, 2022

[8] R. Krishnan, R. Santhana Krishnan, Y. Harold Robinson, E. Golden Julie, H. V. Long, A. Sangeetha, M. Subramanian, and R. Kumar, "An intrusion detection and prevention protocol for internet of things based wireless sensor networks", Wireless Personal Communications, vol. 124, no. 4, pp. 3461-3483, 2022.

[9] J. F. C. Garcia, and G. E. Taborda Blandon, "A deep learning-based intrusion detection and preventation system for detecting and preventing denial-of-service attacks", IEEE Access, vol. 10, pp. 83043-83060, 2022.

[10] M. A. Rahman, A. TaufiqAsyhari, L. S. Leong, G. B. Satrya, M. Hai Tao, and M. F. Zolkipli, "Scalable machine learning-based intrusion detection system for IoT-enabled smart cities", Sustainable Cities and Society, vol. 61, pp. 102324, 2020.

[11] S. Dina, and D. Manivannan, "Intrusion detection based on machine learning techniques in computer networks", Internet of Things, vol. 16, pp. 100462, 2021.

[12] R. Gad, A. A. Nashat, and T. M. Barkat, "Intrusion detection system using machine learning for vehicular ad hoc networks based on ToN-IoT dataset", IEEE Access, vol. 9, pp. 142206-142217, 2021.

[13] K. H. Le, M. H. Nguyen, T. D. Tran, and N. D. Tran, "IMIDS: An intelligent intrusion detection system against cyber threats in IoT", Electronics, vol. 11, no. 4, pp. 524, 2022.

[14] Y. Otoum, D. Liu, and A. Nayak, "DL-IDS: a deep learning–based intrusion detection framework for securing IoT", Transactions on Emerging Telecommunications Technologies, vol. 33, no. 3, pp. e3803, 2022.

[15] D. Kalaivani, "An Intrusion Detection System Based on Data Analytics and Convolutional Neural Network in NSS-KDD dataset", Machine Learning Algorithms for Intelligent Data Analytics, pp. 93, 2022.

[16] B. Wang, Y. Su, M. Zhang, and J. Nie, "A deep hierarchical network for packet-level malicious traffic detection", IEEE Access, vol. 8, pp. 201728-201740, 2020.

[17] A. Abhale, and S. S. Manivannan, "Deep Learning Algorithmic Approach for Operational Anomaly Based Intrusion Detection System in Wireless Sensor Networks", 2021.

[18] M. A. Khan, "HCRNNIDS: Hybrid convolutional recurrent neural network-based network intrusion detection system", Processes, vol. 9, no. 5, pp. 834, 2021.

[19] A. El-Ghamry, A. Darwish, and A. E. Hassanien, "An optimized CNN-based intrusion detection system for reducing risks in smart farming", Internet of Things, vol. 22, pp. 100709, 2023.

[20] N. Kunhare, R. Tiwari, and JDhar, "Intrusion detection system using hybrid classifiers with meta-heuristic algorithms for the optimization and feature selection by genetic algorithm", Computers and Electrical Engineering, vol. 103, pp. 108383, 2022.

[21] L. Narengbam, and S. Dey, "Harris hawk optimization trained artificial neural network for anomaly-based intrusion detection system", Concurrency and Computation: Practice and Experience, vol. 35, no. 23, pp. e7771, 2023.

[22] A. Khanna, P. Rani, P. Garg, P. KSingh, and A. Khamparia, "An enhanced crow searches inspired feature selection technique for intrusion detection based wireless network system", Wireless Personal Communications, vol. 127, no. 3, pp. 2021-2038, 2022.

[23] W. Elmasry, A. Akbulut, and A. H. Zaim, "Evolving deep learning architectures for network intrusion detection using a double PSO metaheuristic", Computer Networks vol. 168, pp. 107042, 2020.

[24] M. Faris, M. Mahmud, M. F. MohdSalleh, and B. Alsharaa, "A differential evolution-based algorithm with maturity extension for feature selection in intrusion detection system", Alexandria Engineering Journal, vol. 81, pp. 178-192, 2023.

[25] T. Wu, H. Fan, H. Zhu, C. You, H. Zhou, and X. Huang, "Intrusion detection system combined enhanced random forest with SMOTE algorithm", EURASIP Journal on Advances in Signal Processing 2022, no. 1, pp. 1-20, 2022.

[26] C. M. Hsu, H. Yen, S. W. Prakosa, M. Z. Azhari, and J. ShiouLeu, "Using long-short-term memory based convolutional neural networks for network intrusion detection", In Wireless Internet: 11th EAI International Conference, WiCON 2018, Taipei, Taiwan, October 15-16, 2018, Proceedings, vol. 11, pp. 86-94, Springer International Publishing, 2019.

[27] K. Samunnisa, G. S. Vijaya Kumar, and K. Madhavi, "Intrusion detection system in distributed cloud computing: Hybrid clustering and classification methods", Measurement: Sensors, vol. 25, pp. 100612, 2023.

[28] Y. Ding, and Y. Zhai, "Intrusion detection system for NSL-KDD dataset using convolutional neural networks", on computer science and artificial intelligence, pp. 81-85, 2018.

[29] A. A. Awad, A. F. Ali, and T. Gaber, "An improved long short term memory network for intrusion detection", Plos one, vol. 18, no. 8, pp. e0284795, 2023.
[30] F. Laghrissi, S. Douzi, K. Douzi, and B. Hssina, "Intrusion detection systems using long short-term memory (LSTM)", Journal of Big Data, vol. 8, no. 1, pp. 65, 2021.

[31] A. Agarwal, P. Sharma, M. Alshehri, A. A. Mohamed, and O. Alfarraj, "Classification model for accuracy and intrusion detection using machine learning approach", PeerJ Computer Science, vol. 7, pp. e437, 2021.

[32] Z. Ahmad, A. S. Khan, C. W. Shiang, J. Abdullah, and F. Ahmad, "Network intrusion detection system: A systematic study of machine learning and deep learning approaches", Transactions on Emerging Telecommunications Technologies, vol. 32, no. 1, pp. e4150, 2021.
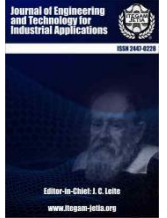
RESEARCH ARTICLE   **OPEN ACCESS**

DYNAMICS ASSESSMENT OF AN INVERTER FED INDUCTION MOTOR DRIVE BY AN IMPROVED PREDICTIVE CONTROLLER LEVERAGING FINITE CONTROL SET MECHANISM

Shaswat Chirantan*[1], Dr. Bibhuti Bhusan Pati[2]

[1]PhD. Scholar, Department of Electrical Engineering, Veer Surendra Sai University of Technology, Burla, Sambalpur, 768018, India.
[2]Department of Electrical Engineering, Veer Surendra Sai University of Technology, Burla, Sambalpur, 768018, India.

[1]http://orcid.org/0000-0001-9052-3582 , [2]http://orcid.org/0009-0009-3897-5712

Email: *shaswat.chirantan443@gmail.com, bbpati_ee@vssut.ac.in

ARTICLE INFO

ABSTRACT

Accenting the importance of Model Predictive Control (MPC) accross used optimization tools in current engineering applications, the proposed scheme establishes the predictive skills by well-defined mathematical model in terms of present state variables. This paper projected a predictive current control (PCC) approach scheduled by fininite control set(FCS) inverter switching mechanism executed by a current modulated objective function.. The anatomy of this controller deals with selecting the control signal from a finite set of signals which satisfies minimum value of the predefined objective function, which is formulated by calculating the square error, i.e. the reference current against the stator measured current of the designed induction motor (IM). The proposed work further enriched with an improved predictive aspect named as integral finite control set (IFCS) action synchronized with a cascade feedback structure with appropriate controller gain to obtain an optimal set of control variables. With the direction in minimization of principle, these methods provide the control of the switching states for inversion, to the inverter and inverter generates actuating voltage signals to the induction motor. IFCS-MPC has the inherent capabilities of compensating steady state errors and slewrates which potrayed this as the preferred forecasted controller as compared to FCS-MPC. This work is also advanced with a comparative demonstration of torque, load currents and speed characteristics of IM, obtained from each of the implemented control techniques to identify the most flexible and dynamic predictive strategy. All these control methods have been investigated using MATLAB/Simulink environment.

I. INTRODUCTION

In electrical field, MPC has been more effective to utilize and the control the switching of power converters, synchronous and induction machine drives and for various power system parameters control. Wide range of predictive control algorithms have been implemented by many researchers. MPC has received widespread attention due to its flexibility, robustness and fast dynamic responses. MPC topology can be categorized in to analogous mode, i.e. continuous control set (CCS) and discrete mode, i.e. finite control set(FCS), depending on their operation and control actions.

Predictive current control schemes for power converters and electrical drives have been proposed in [1], which demonstrates CCS-MPC algorithm, receding horizon control principle with forward Euler approximation and cost function for discrete time load model of PMSM (permanent magnet synchronous motor) for switching states of the inverter. The introduction of Integral FCS is to minimize the steady state error those cannot be significantly reduced by FCS. Implementation of IFCS in AC motor drive to analyze the steady state error in d & q axis currents has been presented in [2]. Earlier to the evolution of MPC techniques conventional controllers such as PI, PD, PID have been used widely.

In [3], the algorithms of FCS & IFCS MPC topologies to control various synchronous and asynchronous motor drives have been designed and compared with conventional controllers. A new FCS MPC technique to regulate the flux dynamics of an Induction Motor is proposed [4]. In this control approach, to minimize the problems associated with switching frequency PWM technique is implemented. A comparative study between FCS & CCS method has been highlighted in [5]. This work discussed the execution methodology of both FCS & CCS action such as modulation control and SVPWM control scheme respectively. Predictive control strategy of an inverter fed IM drive can be designed with current evaluation or with flux/torque evaluation [6]. This study provides the practical perception of MPC for converter fed drive systems. In order to diagnose the performance of IM various strategies have been incorporated, considering the field oriented control, with the direct torque control and the predictive controllers [7]. Basically optimization problems are assigned with specific cost functions depending on system parameters. To achieve fast dynamic behaviour of Induction machine an innovative control strategies with two different objective functions have been defined for both torque and flux respectively [8]. A MPC scheme has been proposed in [9] to direct flux control of multi-three phase structure induction motor for improvement of the fault tolerant behavior of the drives by independently controlling the three phases. IFCS MPC strategy for a single phase Z-source inverter has been implemented in [10] to compensate the steady state error caused by FCS method.

II. RELATED WORKS

FCS MPC is found to be a promising control method for converter fed IM drive. Two case studies of inverter fed induction machine with and without LC filter have been analyzed in [11]. A predictive control approach is proposed in [12] to determine the length of control horizon of an induction motor drive. As already discussed in the earlier literature, predictive control can be a fast-acting action for optimal control of inverter switching states [13]. Generally finite control set based controller provides fast dynamic response and overcomes the limitations of conventional PI controller. In [14], a deadbeat FCS predictive current control topology has been proposed for enhancing the IM dynamics. The adaptability, robustness and flexibility of FCS technique has been compared with classical controllers [15] and a sliding mode based MPC method has been introduced for torque and flux control of induction motor [16]-[17]. Field oriented control of a three-phase induction motor by constraints incorporated FCS-MPC method with direct current control strategy is demonstrated in [18]. Through this algorithm the deviations between desired currents and predicted currents can be minimized. Apart from single or three phase IM, predictive mechanism has also provided a genuine control algorithm for multi-phase machines such as five phase or six phase [19]-[21] to optimize the machine performances. To regulate the phase angles of stator phase currents a predictive phase angle controller has been assigned [22] and overall machine characteristics have been analyzed. The main aspects of controlling the induction machine dynamics are to monitor the flux and current behaviour. Accordingly, an observer based predictive flux control [23] and various current control [24]-[25] strategies have been implemented to observe and control the machine parameter variations. The development of MPC methods has been growing in much faster rate due to its reputation of quick response and simple system algorithm. Many advantages of this novel technique include current and torque harmonic distortion minimization [26], multiple

objectives optimization and fast fault tolerant approach [27]. In current scenario, predictive controllers are significantly used in high performance drives systems such as Induction machine, Synchronous machine, linear motors, reluctance motors and multi-phase machine drives [28]. A total disturbance observer-based PCC model of IM has been presented in [29], which takes the disturbance directly in the prediction mechanism and hence eliminates the need of a separate controller. The recent advancement of MPC action has the fast-acting control mechanism of multi-phase induction motor drives [30]-[33]. Application of model predictive control in power electronics enhances the flexibility, robustness and fastness of designed control architectures. For increasing dynamics, different predictive controllers are used such as deadbeat, hysteresis current controller (HCC) and trajectory-based controllers. Predictive controllers of machine drives are based on current or torque/flux control [34]-[35]. Although FCS-MPC method applied by researchers has mostly improved the dynamic response of the system, the technique has drawbacks in regard to the steady state error minimization. Hence this work is motivated to apply finite control set model predictive control (IFCS-MPC) with integral action to keep minimizing the steady state error and with fast dynamic response. Therefore, two integral gain constants K_d and K_q for direct & quadrature axis currents are introduced in the control structure respectively. Hence it is required to have a proper value of these two parameters to obtain the system with minimum steady state error and acceptable switching losses. Further, intelligent techniques also used for machine control [36].

The detailed case studies of the implemented techniques have been thoroughly analyzed. The remainder of the article is organized as follows. Section 2 demonstrates the inverter topology, dynamic model, control methodologies and algorithms involved to designed the proposed predictive controllers for a IM drive. Section 3 plots and discusses the responses of torque, currents and speeds with respect to step changes of various control action proposed. Section 4 sites the performance comparison of designed MPCs in terms of torque and current dynamic characteristics. And finally, Section 5 concludes the paper.

III. PROPOSED MODEL AND CONTROL METHODS

The working principle of the Model predictive control (MPC), where the variable of interest is control for the, predicted for finite horizon and compares with desired reference value to get the required command signal. This proposed work is based on simplification of inverter states optimization without any PWM technique. Here eight combinations of inverter states are formed as constraints to the control design. The load model is taken into action for the better prediction of the future behavior, the variables so the name model predictive control arises. The optimization technique works with receding horizon control principle. We can say that a constraint free FCS-MPC method is similar to the discrete time deadbeat feedback control system in which the controller gain is varies with time with the condition that closed loop poles are located at the origin of the complex plane. To improve the steady-state behavior of the normal FCSMPC method an integral action is added via a cascade control structure. The objective function for minimization in normal FCS-MPC method is just the square difference between predicted current and measured current in d-q reference fame. The main utility of the objective function in a I-FCS-MPC method, is explicitly related with the sampling time Δt.

III.1 MPC METHODOLGY

MPC works with a finite-horizon control principle. The controller or MPC block makes evaluation of control signals for a definite future time. As the time passes the finite predictive horizon get updates by including a future time span and leaving a past time span. Based on the predicted output of the plant, MPC generates a control sequence which is applicable only at the current time sampling. After one sampling interval, the control sequence get modified based on the new measured variables. (Figure 1).
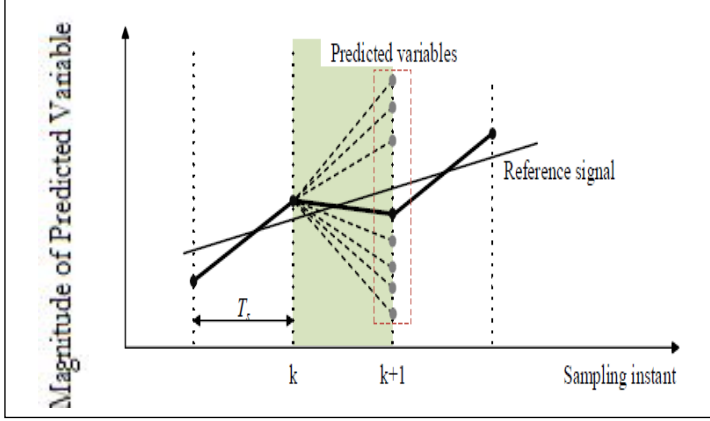
Figure 1: MPC Methodology.
Source: [3].

In Figure 1, the red trajectory is the reference signal which is to be followed. The green trajectory is the controlled signal obtained after due measurements and manipulation at the time instant k. The yellow curve is the past measured variable which is used for making the prediction for the future. At the current state k, the MPC evaluates the control sequence for the prediction horizon as indicated by the purple line. Similarly at the sampling instant k+1, k+2 etc., MPC generates different sets of controlled sequence for there respective prediction horizon.

This proposed work is based on simplification of inverter states optimization with out any PWM technique. Here eight combination of inverter states are formed as constraints to the control design. A load model is used to predict the future behaviour of the variables so the name model predictive control arise. The optimization technique works with receding horizon control principle. We can say that a constraints free FCS-MPC method is similar to the discrete time deadbeat feedback control system in which the controller gain is varies with time with the condition that closed loop poles are located at the origin of the complex plane. To improve the steady-state behaviour of the normal FCS-MPC method an integral action is added via a cascade control structure. The objective function for minimization in normal FCS-MPC method is just the square difference between predicted current and measured current with respect to the d-q referral fame, whereas explicitly related with the sampling time Δt, in the I-FCS-MPC method.

III.2 DYNAMIC MODEL OF INDUCTION MOTOR

For our experimental setup in a simulation environment, we have taken a case of a squirrel cage type, induction motor. The current and torque dynamics are represented in following mathematical equations with respect to the d-q referral frame [3].

$$\frac{di_{sd}}{dt} = -\frac{1}{\tau_\sigma}i_{sd} + \omega_s i_{sq} + \frac{k_r}{r_\sigma \tau_\sigma \tau_r}\varphi_{rd} + \frac{1}{r_\sigma \tau_\sigma} \quad (1)$$

$$\frac{di_{sq}}{dt} = -\omega_s i_{sd} - \frac{1}{\tau_\sigma}i_{sq} - \frac{k_r}{r_\sigma \tau_\sigma}\omega_e \varphi_{rd} + \frac{1}{r_\sigma \tau_\sigma} \quad (2)$$

$$\omega_s = \omega_e + \frac{L_h}{\tau_r} \quad (3)$$

$$\omega_s = \omega_e + \frac{1}{\tau_r}\frac{i_{sq}}{i_{sd}} \quad (4)$$

Where

i_{sd} & i_{sq} are the measured currents in d-axis, q-axis, expressed in Ampere (A)

v_{sd} & v_{sq} are the measured currents in d-axis, q-axis, expressed in Volt (V)

ω_s, ω_e are the angular speed of the stator and rotor, expressed in rad/sec

φ_{rd}= Rotor flux of d-axis (Wb)

All other parameters used in the dynamic equations of IM drive are defined below.

Leakage factor:

$$\sigma = 1 - \frac{L_h^2}{L_s L_r} \quad (5)$$

Stator time constant:

$$\tau_s = \frac{L_s}{R_s} \quad (6)$$

Rotor time constant:

$$\tau_r = \frac{L_r}{R_r} \quad (7)$$

Coefficients:

$$k_r = \frac{L_h}{L_r} \quad (8)$$

$$r_\sigma = R_s + R_r k_r^2 \quad (9)$$

$$\tau_\sigma = \frac{\sigma L_s}{r_\sigma} \quad (10)$$

The torque generated due to magnetic field, commonly known as electromagnetic troque, is proportional to, the $\varphi_{rd}i_{sq}$, which is expressed as

$$T_e = \frac{3}{2}Z_p \frac{L_h}{L_r}\varphi_{rd}i_{sq} \quad (11)$$

The mechanical parametric of the induction motor need to be consider and derived from the general motor equation for rotation, which is given as follows,

$$J_m \frac{d\omega_m}{dt} + f_d \omega_m = T_e - T_L \quad (12)$$

Where $\omega_m(t)$, the mechanical velocity of the rotor$(\omega_m = \frac{\omega_e}{Z_p})$, $J_{m,}$ inertia of the motor, f_d ,the friction coefficient, T_e & T_L are the torque in the electromagnetic Field and the load, respectively. With

consideration of the dynamics, the model and using the above in to the motion equation, representing in (12),

$$\frac{d\omega_m}{dt} = \frac{-f_d}{J_m}\omega_m + \frac{3}{2}\frac{Z_p L_h}{L_r J_m}\varphi_{rd}i_{sq} - \frac{T_L}{J_m} \qquad (13)$$

The velocity of the rotor in the electrical field can express as follow,

$$\frac{d\omega_e}{dt} = \frac{-f_d}{J_m}\omega_e + \frac{3}{2}\frac{Z_p^2 L_h}{L_r J_m}\varphi_{rd}i_{sq} - \frac{Z_p T_L}{J_m} \qquad (14)$$

The physical and technical parameters defined, and used earlier in the IM model have been consider and tabulated below for system performance evaluation.

Table 1: 3-Φ IM model parameters.

Parameters	Values
Winding resistance offer to Stator (R_s)	11.2 Ohms
Winding resistance offer to Rotor (R_r)	8.3 Ohms
Winding inductance offer by Stator (L_s)	0.6155 Henrys
Winding inductance offer by Rotor (L_r)	0.6380 Henrys
Mutual inductance of Machine (L_h)	0.57 Henrys
Moment of inertia (J_m)	0.00176 kg-meter square
Friction viscous gain (f_d)	0.00038818 newton meter per radian per second
Number of Pole pairs(Zp)	2nos

Source: [3].

III.3 THREE PHASE INVERTER MODEL

We consider a 3-φ invertor, which convert 520V to 3-φ AC, for a induction motor of squirrel cage type, whose physical parameter are mention in the Table 1. The operation of the invertor, in the mode of, a non-linear discrete time system and having 180° mode of operation, with 7 number of output & 8 number of configuration state. For simplicity and rounding off, in the modeling and mathematical calculation on simulation we ignore the IGBT saturation voltage, and diode forward voltage drop. The schematic power circuit as the voltage source, inverter to the 3-φ IM is given below in Figure 2.
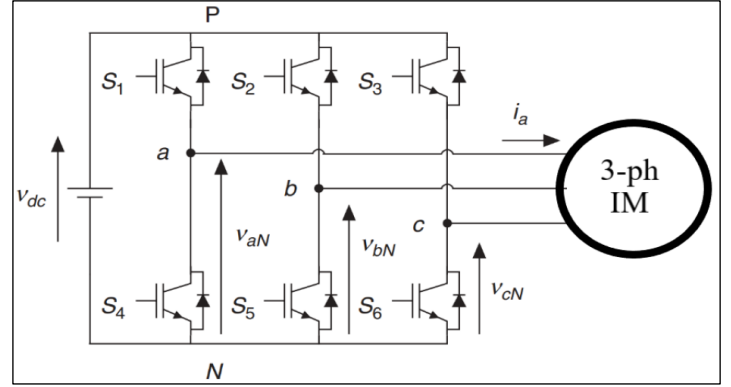
Figure 2: VSI fed 3-ph IM.
Source: Authors, (2024).

The switching state for conversions is carryout with the reference of the gating signals S_a, S_b and S_c , and represented as follows [1]:

$$S_a = \begin{cases} 1, \text{if } Switch_1 \text{ on and } Switch_4 \text{ off} \\ 0, \text{if } Switch_1 \text{ off and } Switch_4 \text{ on} \end{cases}$$

$$S_b = \begin{cases} 1, \text{if } Switch_2 \text{ on and } Switch_5 \text{ off} \\ 0, \text{if } Switch_2 \text{ off and } Switch_5 \text{ on} \end{cases}$$

$$S_c = \begin{cases} 1, \text{if } Switch_3 \text{ on and } Switch_6 \text{ off} \\ 0, \text{if } Switch_3 \text{ off and } Switch_6 \text{ on} \end{cases}$$

The concept of space vector modulation [33] has been adopted for voltage vector with respect to optimum switching states. The generation of switching states, give rise to eight voltage vectors provided in Table 2 which can be predicted by Equation (15) as follows:

$$v = \frac{2}{3}V_{dc}(S_a + aS_b + a^2 S_c) \qquad (15)$$

Where,

$a = e^{-j(2\pi/3)} = -\frac{1}{2} + j\frac{\sqrt{3}}{2}$, with a phase displacement of 120° between any two phases.

Table 2: Switching states with voltage vectors.

1	0	0	$\overrightarrow{v_0} = 0$
1	0	0	$\overrightarrow{v_1} = \frac{2}{3}v_{dc}$
0	1	0	$\overrightarrow{v_2} = \frac{1}{3}v_{dc} + j\frac{\sqrt{3}}{3}v_{dc}$
0	1	0	$\overrightarrow{v_3} = -\frac{1}{3}v_{dc} + j\frac{\sqrt{3}}{3}v_{dc}$
0	1	1	$\overrightarrow{v_4} = -\frac{2}{3}v_{dc}$
1	0	1	$\overrightarrow{v_5} = -\frac{1}{3}v_{dc} - j\frac{\sqrt{3}}{3}v_{dc}$
1	0	1	$\overrightarrow{v_6} = \frac{1}{3}v_{dc} - j\frac{\sqrt{3}}{3}v_{dc}$

Source: Authors, (2024).

The simple mathematical model of three phase inverter circuit which defines the generated output voltages (phase to neutral) by means of switching signal application has been depicted

in Figure 3. The optimum operational of predictive algorithms, gives arise the switching state listed as above.
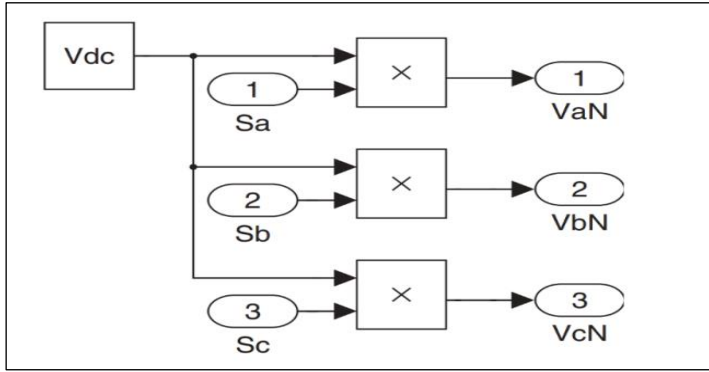
Figure 3: Ouput Voltage of VSI.
Source: Authors, (2024)

III.4 GENERALIZED PREDICTIVE CURRENT 9CONTROL ALGORITHM

Predictive current control algorithm can be states as:

1. The measurement of the reference current, **i***(t$_{i+1}$) is done from the outer control loop, whereas the load current **i**(t) measurement need to be carryout at every states with respect to sampling interval.

2. The evaluation and prediction of the load current value for each upcoming sampling interval **i**(t$_{i+1}$), with considering the different voltage vector in consideration.

3. The cost function **J** deploy for the error calculation, difference of the reference against predicted currents, with each upcoming sampling frame with corresponding voltage vector.

$$J=\{i_d{}^*(t_i)-i_d(t_{i+1})\}^2+\{i_q{}^*(t_i)-i_q(t_{i+1})\}^2 \qquad (16)$$

4. The switching state signals, are generated minimizes the current error, are need to listed and consider for utilization.

In this algorithm the previous value the load current and the next state of the current, leads to predict 7 different states and 8 configurations, for operation of the inverter switching. For each discrete state, we need to calculate, the predict current value and compare, with the reference current for minimal error and changes. We need to calculate for all 8 stated as table above and record the errors. The optimal operational states are feed to the inverter, which used as voltage source. The flow diagram of the above process is shown in the Figure 4.
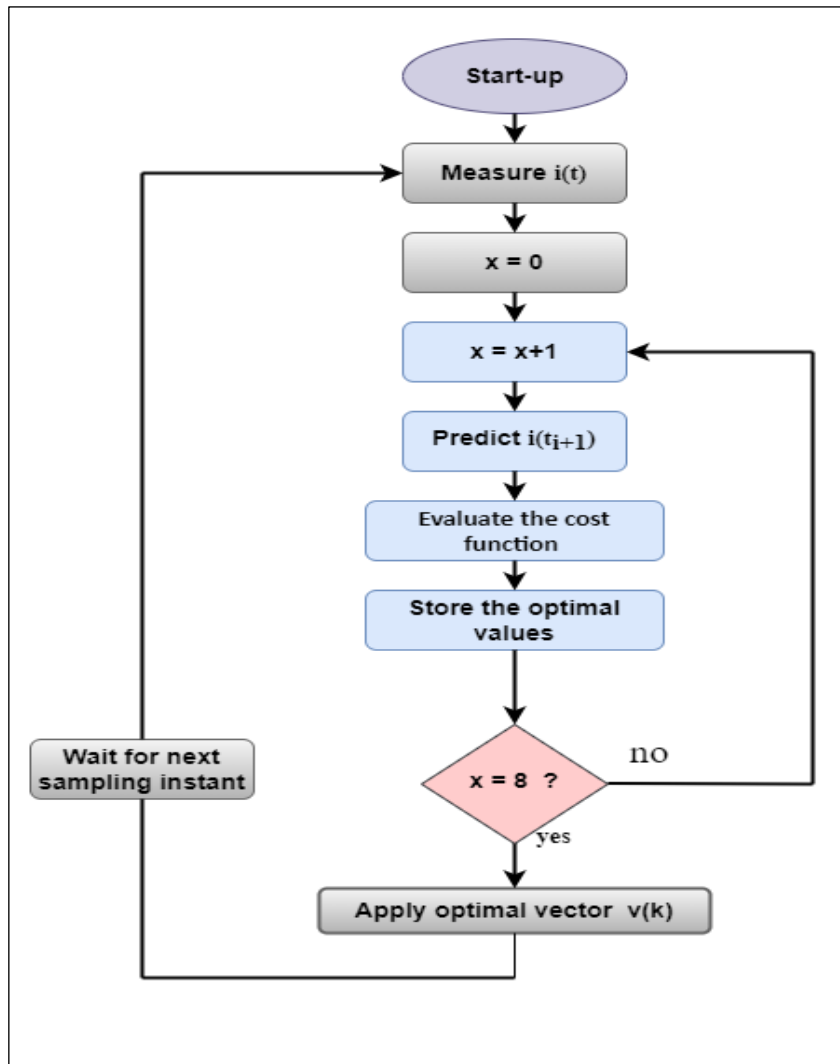
Figure 4: Flow Chart for PCC.
Source: Authors, (2024).

III.5 FCS-MPC SCHEME FOR IM

On generalization of equations, predicted load currents in d-q frame for sampling time **t$_i$** can be derived from forward Euler Approximations [1].

$$\frac{di_{sd}(t)}{dt} \approx \frac{i_{sd}(t_{i+1})-i_{sd}(t_i)}{\Delta t} \quad (17)$$

$i_d{}^*$ and $i_q{}^*$ are the desired values of current in d-q frame.

Now by using Equations (17) & (18) in Equations (1) & (2) respectively, The discrete differential equations become the difference equations and can be represented as follows:

$$i_{sd}(t_{i+1}) = i_{sd}(t_i) + \Delta t(-\frac{1}{\tau_\sigma}i_{sd}(t_i) + \omega_s i_{sq}(t_i) + \frac{k_r}{r_\sigma\tau_\sigma\tau_r}\varphi_{rd}(t_i) + \frac{1}{r_\sigma\tau_\sigma}u_{sd}(t_i)) \quad (19)$$

$$i_{sq}(t_{i+1}) = i_{sq}(t_i) + \Delta t(-\omega_s i_{sd}(t_i) - \frac{1}{\tau_\sigma}i_{sq}(t_i) - \frac{k_r}{r_\sigma\tau_\sigma}\omega_e(t_i)\varphi_{rd}(t_i) + \frac{1}{r_\sigma\tau_\sigma}u_{sq}(t_i)) \quad (20)$$

The discretized prediction equations corresponding to Equation (19) and (20) are also presented in matrix form.

$$\begin{bmatrix}i_{sd}(t_{i+1})\\i_{sq}(t_{i+1})\end{bmatrix} = (I + \Delta t A_m(t_i))\begin{bmatrix}i_{sd}(t_i)\\i_{sq}(t_i)\end{bmatrix} + \Delta t B_m\begin{bmatrix}u_{sd}(t_i)\\u_{sq}(t_i)\end{bmatrix} + \begin{bmatrix}\frac{k_r\Delta t}{r_\sigma\tau_\sigma\tau_r}\varphi_{rd}(t_i)\\-\frac{k_r\Delta t}{r_\sigma\tau_\sigma}\omega_e(t_i)\varphi_{rd}(t_i)\end{bmatrix} \quad (21)$$

Where,

I is a 2*2, identity matrix and

$$A_m(t_i) = \begin{bmatrix}-\frac{1}{\tau_\sigma} & \omega_s(t)\\-\omega_s(t) & -\frac{1}{\tau_\sigma}\end{bmatrix}: \qquad B_m = \begin{bmatrix}\frac{1}{r_\sigma\tau_\sigma} & 0\\0 & \frac{1}{r_\sigma\tau_{\sigma q}}\end{bmatrix}$$

The structure of FCS-MPC Model used for 3-ph induction motor is presented in Figure 5.
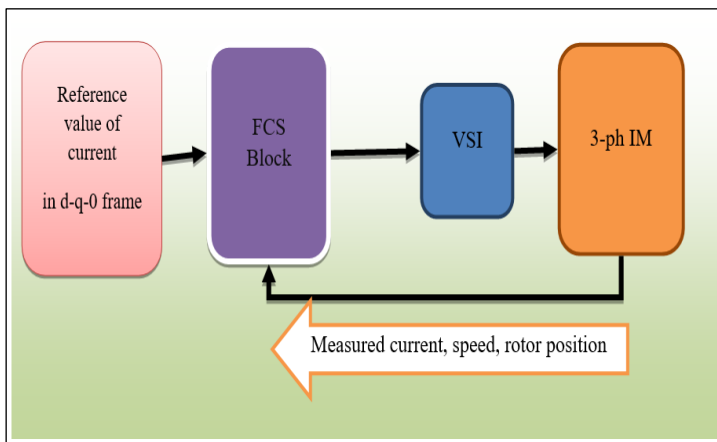
Figure 5: Structure of FCS-MPC for IM.
Source: Authors, (2024).

This method is processed in the following ways.

1) The reference value is presented in d-q frame(i$_{dref}$ and i$_{qref}$).
2) Measured currents in d-q frame, speed in radians per second, rotor angular position in radians are used as input to the FCS control block.
3) The output of the FCS block, are the switching states to the voltage source inverter.
4) The control output of the inverter, as a voltage sources, is fed to the IM model.

In this article a two level three phase VSI is considered for application of predictive schemes. As the overall modelling and computations are in d-q-0 reference frame the voltage vectors generated need to be transformed to d-q-0 coordinate from a-b-c coordinate by means of Park's Transformation.

$$\begin{bmatrix}u_{sd}\\u_{sq}\end{bmatrix} = \frac{2}{3}\begin{bmatrix}cos\theta & \cos(\theta-\frac{2\pi}{3}) & \cos(\theta+\frac{2\pi}{3})\\-sin\theta & -\sin(\theta-\frac{2\pi}{3}) & -\sin(\theta+\frac{2\pi}{3})\end{bmatrix}\begin{bmatrix}V_{an}\\V_{bn}\\V_{cn}\end{bmatrix} \quad (21)$$

Where,

u_{sd} = Voltage in d-axis,

u_{sq} = voltage in q-axis,

θ = Rotor position angle

V_{an}, V_{bn}, V_{cn} are the phase voltages of a-b-c with respect to neutral respectively,

V_{dc} = DC voltage supplied to VSI

In FCS-MPC approach, there are seven sets of u_{sd} and u_{sq} values are presented based on the rotor angular position and sampling time. In this control strategy, we deploy the objective function, which is defined as sum of the square of the errors difference, between the desired and predicted current values in d-q frame. The objective function **J,** considers the variables, measured with the sampling time t_i and the manipulated variables $u_{sd}(t_i)$ and $u_{sq}(t_i)$, Equation (16) can be expressed as below :

$$J_k = \left(i_{sd}^*(t_i) - i_{sd}(t_i) - \Delta t(-\frac{1}{\tau_\sigma}i_{sd}(t_i) + \omega_s i_{sq}(t_i) + \frac{k_r}{r_\sigma\tau_\sigma\tau_r}\varphi_{rd}(t_i) + \frac{1}{r_\sigma\tau_\sigma}u_{sd}(t_i))\right)^2 + \left(i_{sq}^*(t_i) - i_{sq}(t_i) - \Delta t(-\omega_s i_{sd}(t_i) - \frac{1}{\tau_\sigma}i_{sq}(t_i) - \frac{k_r}{r_\sigma\tau_\sigma}\omega_e(t_i)\varphi_{rd}(t_i) + \frac{1}{r_\sigma\tau_\sigma}u_{sq}(t_i))\right)^2 \quad (22)$$

Where

φ_{rd}= rotor flux linkage and k is an index from 0 to 7.

The receding horizon control principle is used here that predicts one step ahead value from the feedback parameters such as $i_{sd}(t_i)$, $i_{sq}(t_i)$, ω_e and θ_e from 3-ph IM model. The objective function is calculated based on the above feedback values, parameters of 3-ph IM model and the pair of $u_{sd} - u_{sq}$ values. Seven sets of objective function are calculated based on seven pairs of $u_{sd} - u_{sq}$ values. The index value is 0 or 7, will be determine with the Previous states of the inverter.

The switching combinations and corresponding voltage vectors imposed in FCS-MPC technique are shown in Table 3.

Table 3: Switching states with voltage vectors of FCS Scheme.

Sa	Sb	Sc	Voltage Vector(v)	V_{an}		V_{bn}	V_{cn}
0	0	0	$\overrightarrow{v_0}$	$-\dfrac{V_{dc}}{2}$		$-\dfrac{V_{dc}}{2}$	$-\dfrac{V_{dc}}{2}$
1	0	0	$\overrightarrow{v_1}$	$\dfrac{V_{dc}}{2}$		$-\dfrac{V_{dc}}{2}$	$-\dfrac{V_{dc}}{2}$
1	1	0	$\overrightarrow{v_2}$	$\dfrac{V_{dc}}{2}$		$\dfrac{V_{dc}}{2}$	$-\dfrac{V_{dc}}{2}$
0	1	0	$\overrightarrow{v_3}$	$-\dfrac{V_{dc}}{2}$		$\dfrac{V_{dc}}{2}$	$-\dfrac{V_{dc}}{2}$
0	1	1	$\overrightarrow{v_4}$	$-\dfrac{V_{dc}}{2}$		$\dfrac{V_{dc}}{2}$	$\dfrac{V_{dc}}{2}$
0	0	1	$\overrightarrow{v_5}$	$-\dfrac{V_{dc}}{2}$		$-\dfrac{V_{dc}}{2}$	$\dfrac{V_{dc}}{2}$
1	0	1	$\overrightarrow{v_6}$	$\dfrac{V_{dc}}{2}$		$-\dfrac{V_{dc}}{2}$	$\dfrac{V_{dc}}{2}$
1	1	1	$\overrightarrow{v_7}$	$\dfrac{V_{dc}}{2}$		$\dfrac{V_{dc}}{2}$	$\dfrac{V_{dc}}{2}$

Source: Authors, (2024).

The phase to neutral voltages of each phase can be defined w.r.t switching states and DC input voltage of inverter as below:

$$\begin{bmatrix} V_{an} \\ V_{bn} \\ V_{cn} \end{bmatrix} = \begin{bmatrix} S_a - \frac{1}{2} \\ S_b - \frac{1}{2} \\ S_c - \frac{1}{2} \end{bmatrix} V_{dc} \qquad (23)$$

III.6 PROPOSED IFCS-MPC SCHEME FOR IM

IFCS-MPC method employs the same concept as that of normal FCS-MPC method but the control action is differed such that in I-FCS-MPC method the objective function has variable in terms of voltage signals whereas in normal FCS-MPC method the same has been formed in terms of current signals. The optimal control signals obtained from the feedback control framework is given as

$$\begin{bmatrix} u_{sd}(t_i)^{opt} \\ u_{sq}(t_i)^{opt} \end{bmatrix} = K_{fcs} \left(\begin{bmatrix} i_{sd}{}^*(t_i) \\ i_{sq}{}^*(t_i) \end{bmatrix} - \begin{bmatrix} i_{sd}(t_i) \\ i_{sq}(t_i) \end{bmatrix} \right) \qquad (24)$$

Where,

K_{fcs} is the gain matrix of the controller and can be extracted from Equation (21) as:

$$K_{fcs}(t_i) = (\Delta t^2 B_m^T B_m)^{-1} B_m^T \Delta t (I + \Delta t A_m(t_i)) \qquad (25)$$

Further simplifying by putting the matrix form of A_m & B_m,

$$K_{fcs}(t_i) = \begin{bmatrix} \dfrac{r_\sigma \tau_\sigma}{\Delta t}(1 - \dfrac{\Delta t}{\tau_\sigma}) & \omega_s(t_i) r_\sigma \tau_\sigma \\ -\omega_s(t_i) r_\sigma \tau_\sigma & \dfrac{r_\sigma \tau_\sigma}{\Delta t}(1 - \dfrac{\Delta t}{\tau_\sigma}) \end{bmatrix} \qquad (26)$$

Using integral action in discrete time control system, Equation (24) can be modified as:

$$\begin{bmatrix} u_{sd}(t_i)^{opt} \\ u_{sq}(t_i)^{opt} \end{bmatrix} = K_{fcs}(t_i) \begin{bmatrix} \dfrac{K_d}{1-q^{-1}} (i_{sd}{}^*(t_i) - i_{sd}(t_i)) \\ \dfrac{K_q}{1-q^{-1}} (i_{sq}{}^*(t_i) - i_{sq}(t_i)) \end{bmatrix} - \begin{bmatrix} i_{sd}(t_i) \\ i_{sq}(t_i) \end{bmatrix} \qquad (27)$$

Where 'k$_d$' and 'k$_q$' are the value of integral block parameters used for current error at both d-axis and q-axis respectively, $0 < Kd \le 1$ and $0 < Kq \le 1$ and $\frac{1}{1-q^{-1}}$ represents functionality of an integrator.

Now at sampling time t$_i$ the optimum control signals are calculated as

$$\begin{bmatrix} u_{sd}(t_i)^{opt} \\ u_{sq}(t_i)^{opt} \end{bmatrix} = \begin{bmatrix} u_{sd}(t_{i-1})^{opt} \\ u_{sq}(t_{i-1})^{opt} \end{bmatrix} + K_{fcs}(t_i) \begin{bmatrix} K_d (i_{sd}{}^*(t_i) - i_{sd}(t_i)) \\ K_q (i_{sq}{}^*(t_i) - i_{sq}(t_i)) \end{bmatrix} - K_{fcs}(t_i) \begin{bmatrix} \Delta i_{sd}(t_i) \\ \Delta i_{sq}(t_i) \end{bmatrix} \qquad (28)$$

The modified objective function for I-FCS-MPC is given as:

$$J_K = \frac{\Delta t^2}{(r_\sigma \tau_\sigma)^2} (u_{sd}(t_i)^K - u_{sd}(t_i)^{opt})^2 + \frac{\Delta t^2}{(r_\sigma \tau_\sigma)^2} (u_{sq}(t_i)^K - u_{sq}(t_i)^{opt})^2 \qquad (29)$$

This is the objective function which is being calculated for each control with index K = 0, 1, 2, ……,6. The index value and corresponding control set for which the objective function is minimum is selected for the generation of respective switching pulse to the inverter. The schematic of IFCS-MPC for IM have been depicted in figure 6.
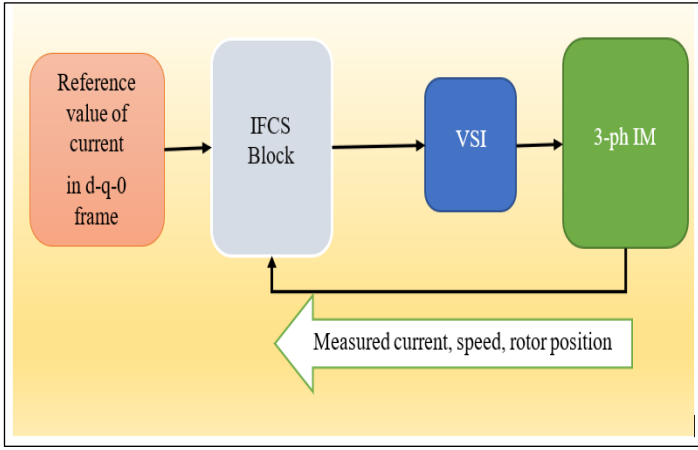
Figure 6: Structure of IFCS-MPC for IM.
Source: Authors, (2024).

The control architecture of I-FCS-MPC for designed three phase induction motor with integral gain parameters and optimal voltage vectors is sited in Figure 7. From the below depicted block diagram we can visualize the control structure of predictive current controller in d-q reference frame. Also it demonstrates the mathematical representation of Equation (27) defined earlier. Further modification with gain parameters, Equation (28) is extracted for optimal evaluation of integral FCS control mechanism. In the implemented control algorithm values of integral gain parameters k_d & k_q are set to be 0.1 [3]. Further analysis can also be done by taking different values of gain parameters between 0 to 1.
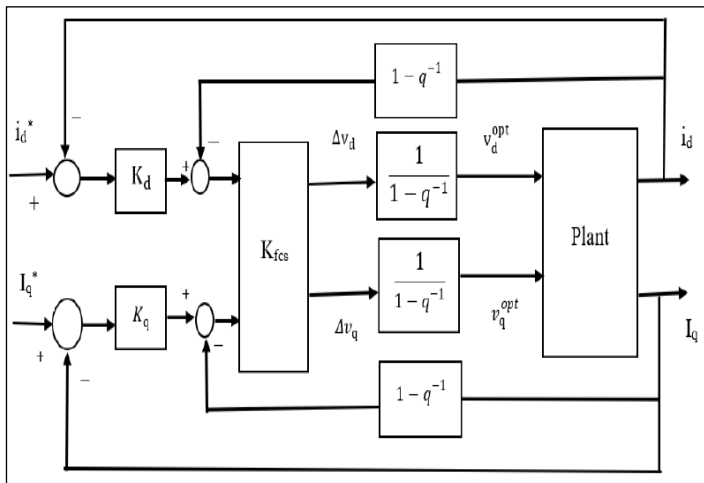
Figure 7: Architecture of Proposed IFCS-MPC.
Source: Authors, (2024).

IV. RESULTS AND DISCUSSIONS

The three phase induction motor with specified parameters mentioned earlier has been modeled and executed with FCS & I-FCS control algorithms applied to inverter circuit. The dynamic characteristics of currents, torque and angular speed of IM have been analyzed for different predictive schemes implemented here. Overall simulation & sampling time are set to be 0.2s and 10μs respectively.

IV.1 CURRENT DYNAMICS ANALYSIS

The reference input current in d-q axis is depicted in Figure 8. From the input current plots it can be seen that d-axis current is taken to be a constant value of i_{sd}=0.8A and q-axis current is

considered to be a step signal of amplitude i_{sq}=3A and changes to 1A at 0.1 sec.
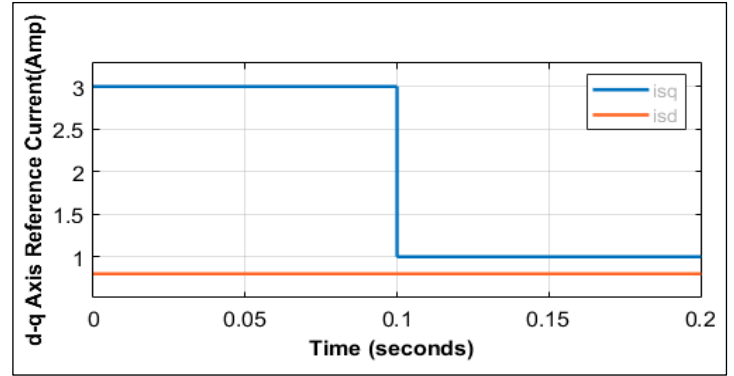
Figure 8: Reference Current in d-q frame
Source: Authors, (2024).

With reference to the d-q axis currents and change in rotor angle (θ), characteristics of desired currents in three phase quantities also change at a particular instant. These currents can be set as a reference to the currents at next execution cycle and it is assumed to be the benchmark for all the proposed approximations. The output currents in d-q and a-b-c forms obtained by FCS MPC techniques are presented in figure 9 and Figure 10 respectively.
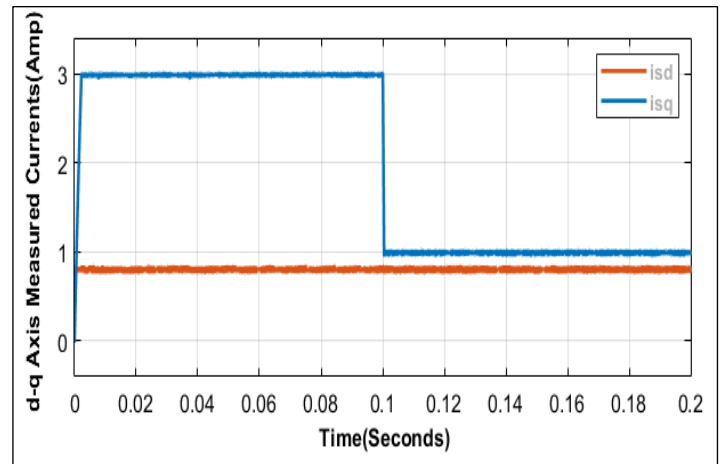
Figure 9: Output Currents of FCS-MPC in d-q frame.
Source: Authors, (2024).
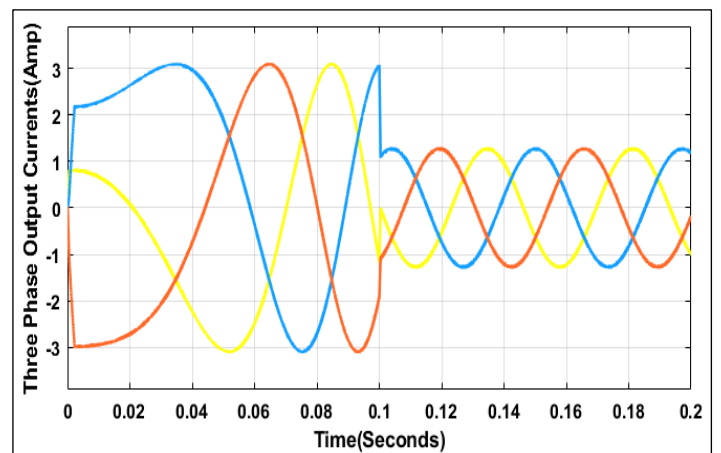
Figure 10: Output Currents of FCS-MPC in abc frame.
Source: Authors, (2024).

In I-FCS-MPC method an integral action is introduced as an outer closed loop for steady state performance enhancement [2],

[10]. The currents obtained by I-FCS action have been presented in both d-q (Figure 11) and a-b-c reference frame (Figure 12).
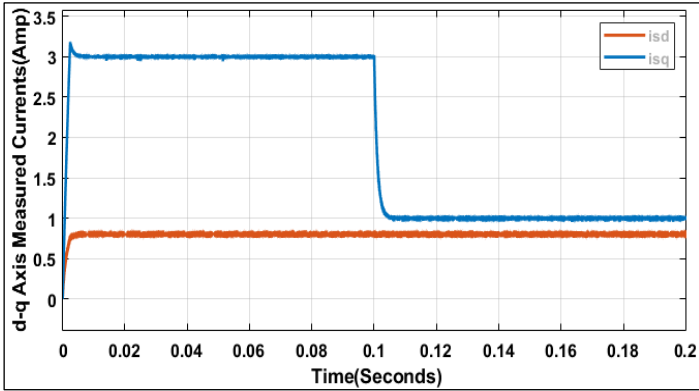
Figure 11: d-q axis currents of I-FCS-MPC Method.
Source: Authors, (2024).
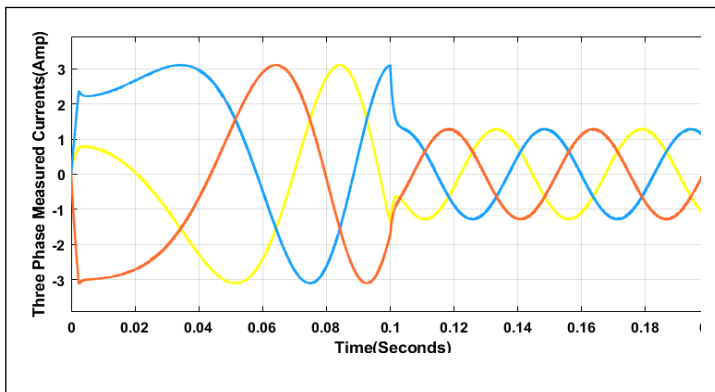
Figure 12: Output Currents of IFCS-MPC Method in abc frame.
Source: Authors, (2024).

IV.2 TORQUE DYNAMICS ANALYSIS

From Equation. (11) it can be clearly adopted that electrical torque output (T_e) is a function of quadrature axis current and rotor flux of an induction motor. As a result the behaviour of q-axis current controls the torque characteristics.

The plots of reference load torque (Figure 13) and output torque obtained from FCS and I-FCS predictive control schemes are depicted in Figure 14 & Figure 15 respectively. The applied load torque to the induction motor drive is a step signal of amplitude 2Nm and step change occurs to 1Nm at time 0.1second.
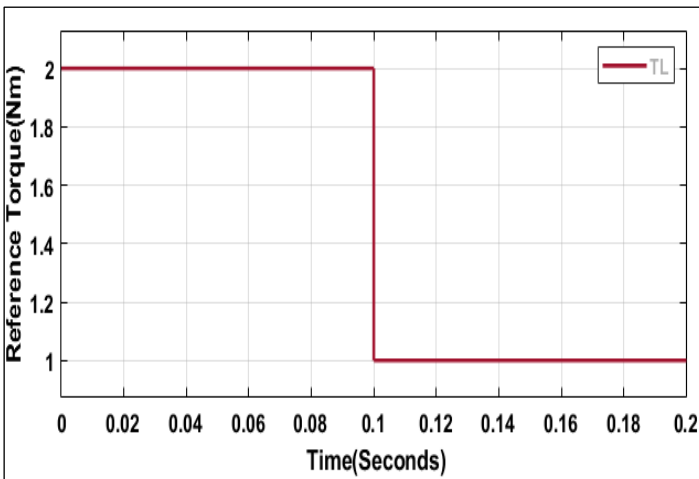
Figure 13: Load toque applied to the 3-ph IM model.
Source: Authors, (2024).
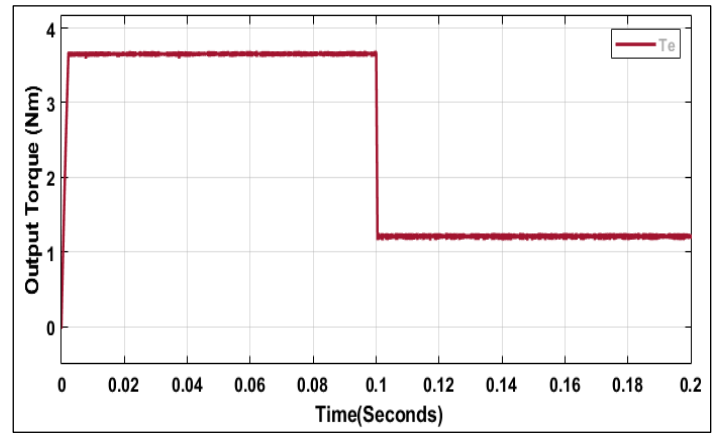
Figure 14: Torque output of FCS-MPC Method.
Source: Authors, (2024).
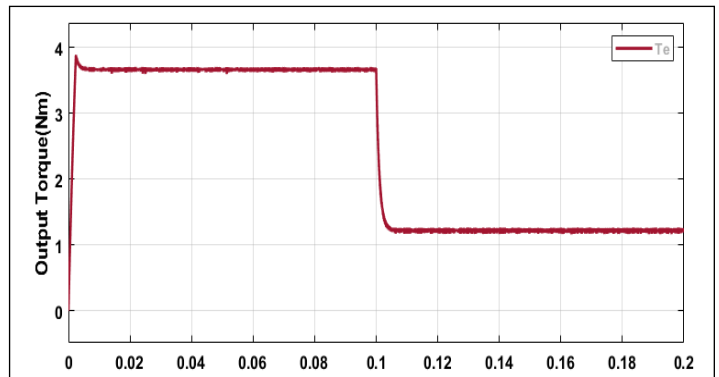
Figure 15: Torque output of IFCS-MPC Method.
Source: Authors, (2024).

IV.3 SPEED RESPONSES

As from the earlier analysis we can see that Electromagnetic Torque output, quadrature axis current, rotor flux and angular speed are dependent parameters. Behavioral change of one of the mentioned parameters will deviate the characteristics of others which directly affect the motor performance. Hence By controlling the current we can regulate torque and as a result angular speed of motor also be controlled in coordination with other dependent parameters. This concept can be defined by Equation (13) & (14) mathematically. Angular speed response of induction motor by corresponding step change in load torque and q-axis current for both the proposed predictive controllers are presented below. Figure 16 and Figure 17 respectively demonstrate the angular speed characteristics achieved by FCS & I-FCS control approach.
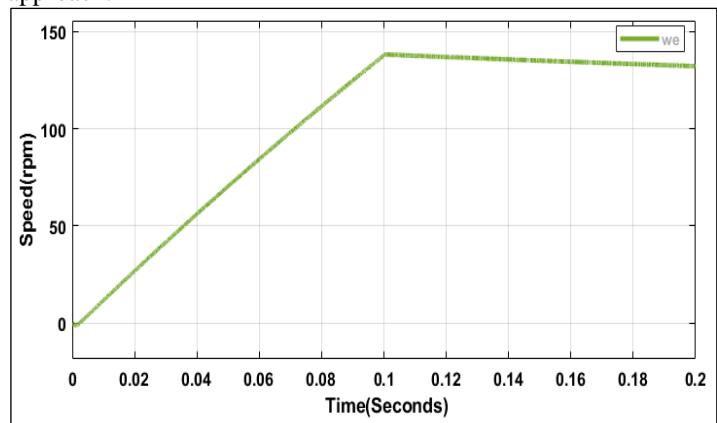
Figure 16: Angular Speed of FCS-MPC Method.
Source: Authors, (2024).
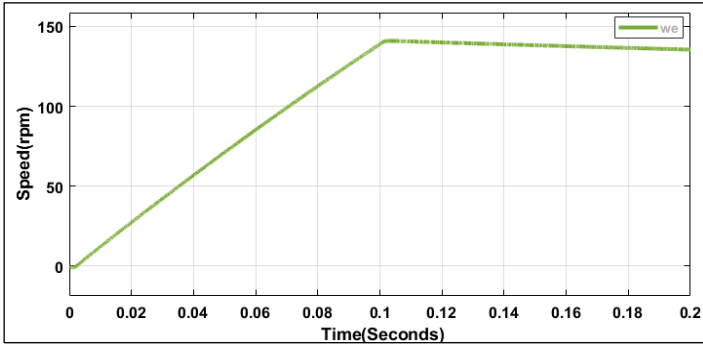
Figure 17: Angular Speed of I-FCS-MPC Method.
Source: Authors, (2024).

The model outputs of currents, torque and angular speed of designed induction motor drive have been captured for the optimum performance evaluation. Current dynamic is studied by a reference step signal of quadrature axis current. Accordingly electromagnetic torque output of the machine also follows the applied step load torque as output torque is a function of q-axis current and rotor flux defined in Equation. (11). As the rotor position angle updates after every time instant, corresponding angular speed also changes. The step responses of current, torque and speed obtained by FCS & IFCS control strategies have been demonstrated here. From the output responses, currents and torque ripples can be visualized.

It can be stated that ripple quantities for both current & torque output are lesser in IFCS-MPC as compared to FCS-MPC.

Similarly slightly more fluctuation is observed in speed response in case of FCS while comparing to integral FCS technique. Based on the model outputs of implemented MPC strategies a performance comparison has been done in terms of peak overshoot, undershoot, settling time, slew rates, rise time & fall time of q-axis current. Overall diagnosis is performed by considering the IM parameters mentioned in Table. 1.

IV.3 COMPARISON OF FCS-MPC AND IFCS-MPC

Simulation of both FCS-MPC and I-FCS-MPC models are implemented with a sampling time of 10 microseconds. Two main factors those determine the characteristics results of the predictive controllers are sampling time and integral gain constants k_d & k_q. Integral gain is applicable only in IFCS-MPC method. For higher value of integral gains, the currents trajectories will overshoot with a good performance in steady state. If we keep the integral gain low, dynamic overshoot can be compensated. Here the value of integral gains are taken as 0.1[3]. Sampling time has not much effect on dynamic performance. Its effect is mostly on steady state ripples. With a higher sampling time the ripple presents are more and hence it is needed to reduce the sampling time. But the computational burden and switching loss of the inverter are restricting the sampling time to fall below certain value. Therefore, a compromise is being made between the ripple allowable and computational time as well as switching loss. Table. 4 shows the quadrature axis characteristics of the proposed controllers based on listed parameters.

Table 4: Quadrature axis Characteristics fo FCS & IFCS

	Measured Parameters	FCS-MPC	IFCS-MPC
Rise Edge	Rise Time (µs)	1261	1273
	Slew Rate (A/ms)	1.268	1.258
	Preshoot (%)	47.727	52.419
	Overshoot (%)	0.699	8.871
	Undershoot (%)	2.764	2.036
	Settling Time(ms)	119.837	19.901
Fall Edge	Fall Time (µs)	351.639	1940
	Slew Rate (A/ms)	-4.548	-0.826
	Preshoot (%)	2.786	0.889
	Overshoot (%)	2.04	3.944
	Undershoot (%)	1.214	2.247
	Settling Time(ms)	493.881	19.865

Source: Authors, (2024).

As the IFCS-MPC carries an integral action to compensate for the currents errors as defined in the objective function, Table. 5 illustrates the measured direct and quadrature axis current errors obtained from each of the proposed predictive scheme.

Table 5: Absolute Current Errors measured from the Imposed Predictive Technique

Imposed Predictive Scheme	Absolute Current Error (Amp)		Total Current Error (Amp)
	$\lvert I_{dRef} - I_{dMeas}\rvert$	$\lvert I_{qRef} - I_{qMeas}\rvert$	
FCS-MPC	00.04037	00.007104	0.047474
IFCS-MPC	00.03069	00.004473	0.035163
Imposed Predictive Scheme	Squared Current Error(Amp)		Total Current Error (Amp)
	$\lvert I_{dRef} - I_{dMeas}\rvert$	$\lvert I_{qRef} - I_{qMeas}\rvert$	
FCS-MPC	00.00163	55.046e-5	0.00168046
IFCS-MPC	00.0009419	22.001e-5	0.00096191

Source: Authors, (2024).

V. CONCLUSIONS

Induction motor drive has wide range of applications such as in traction, process, production & mining industries. One of the important aspects of these applications is dynamics of electromagnetic torque developed and the voltage fed by the inverter. There are different methods for speed control and torque control like conventional PI, PID & hysteresis controllers. But in case of FCS-MPC method, performance can be improved for non-linear loads effectively due to the predictive nature. Still to improve transient performances, different research papers were proposed. Here a small strive has been done for further improvement in steady state performance of control structures. The torque and the current in q-axis of 3-ph IM are proportional to each other. So, throughout the control approach both the reference current in q-axis and the reference load torque are applied as step function to observe the dynamic behaviour of 3-ph IM. The performance of MPC coordinated schemes applied to IM drive is evaluated. Operating principle of proposed predictive controllers differ by their mode of control actions. Applied FCS & I-FCS strategies have specified control approach based on defined objective functions. Peak Overshoot, undershoot, preshoot, settling time & slew rates of quadrature current of IM subjected to step change are analyzed and thus the dynamic control characteristics of implemented control techniques have been diagnosed. FCS & I-FCS have almost similar control strategy but IFCS has the inherent features of reducing steady state errors and improving slew rates. Also I-FCS possesses better current & torque responses with minimum ripples and superior trajectories w.r.t step i/p signal. There is not much difference in speed responses of both FCS & I-FCS MPC except the later has slightly less ripples as compared to FCS-MPC.

All these performed predictive aspects provide a genuine control algorithm for flexible and reliable implementations. The adaptive nature of MPC methods has tremendous skills of being a superior controller in modern control dilemma. Furthermore, many initiatives such as harmonics & speed controls and switching power loss reduction of inverters by MPC based schemes can be designed. Also in extension predictive control approach can be milestone research for Electric vehicles, FACTS devices and in various power system control measures.

VI. AUTHOR'S CONTRIBUTION

Conceptualization: Shaswat Chirantan and Bibhuti Bhusan Pati
Methodology: Shaswat Chirantan and Bibhuti Bhusan Pati
Investigation: Shaswat Chirantan and Bibhuti Bhusan Pati
Discussion of results: Shaswat Chirantan and Bibhuti Bhusan Pati
Writing – Original Draft: Shaswat Chirantan and Bibhuti Bhusan Pati
Writing – Review and Editing: Shaswat Chirantan and Bibhuti Bhusan Pati
Resources: Shaswat Chirantan and Bibhuti Bhusan Pati
Supervision: Shaswat Chirantan and Bibhuti Bhusan Pati
Approval of the final text: Shaswat Chirantan and Bibhuti Bhusan Pati

VIII. REFERENCES

[1] Rodriguez, J. and Cortes, P.: "Predictive Control of Power Converters and Electrical Drives", John Wiley & Sons Ltd, United Kingdom, (2012)

[2] Wang L, Gan L. "Integral FCS predictive current control of induction motor drive. IFAC Proceedings Volumes". 2014 Jan 1;47(3):pp. 11956-11961.

[3] Wang L, Chai S, Yoo D, Gan L, Ng K. "PID and predictive control of electrical drives and power converters using MATLAB/Simulink". JohnWiley & Sons; 2015 Mar 2. pp. 171-205.

[4] Odhano S, Bojoi R, Formentini A, Zanchetta P, Tenconi A. "Direct flux and current vector control for induction motor drives using model predictive control theory". IET Electric Power Applications. 2017 Sep 4;11(8): pp. 1483-1491.

[5] Ahmed A.A., Koh, B.K., Kim, J.S. and Lee, Y.I., (2017). "Finite control set-model predictive speed control for induction motors with optimal duration". Proc. IFAC Papers On Line, Vol. 50(1), pp.7801-7806.

[6] Zhu B, Rajashekara K, Kubo H. "Comparison between current-based and flux/torque-based model predictive control methods for open-end winding induction motor drives". IET Electric Power Applications. 2017 Sep 4;11(8):pp. 1397-1406.

[7] Wang F, Zhang Z, Mei X, Rodriguez J, Kennel R. "Advanced control strategies of induction machine: Field oriented control, direct torque control and model predictive control". Energies. 2018 Jan;11(1):1-13.

[8] Norambuena M, Rodriguez J, Zhang Z,Wang F, Garcia C, Kennel R. "A very simple strategy for high-quality performance of AC machines using model predictive control". IEEE Transactions on Power Electronics. 2018 Mar 9;34(1):pp. 794-800.

[9] Rubino S, Bojoi R, Odhano SA, Zanchetta P. "Model predictive direct flux vector control of multi-three-phase induction motor drives". IEEE Transactions on Industry Applications. 2018 Apr 23;54(5):pp 4394-4404.

[10] Ramirez RO, Espinoza JR, Baier CR, Rivera M, Villarroel F, Guzman JI, Melin PE. "Finite-state model predictive control with integral action applied to a single phase Z-source inverter". IEEE Journal of Emerging and Selected Topics in Power Electronics. 2018 Sep 18;7(1):pp. 228-239.

[11] Karamanakos P, Geyer T. "Guidelines for the design of finite control set model predictive controllers". IEEE Transactions on Power Electronics. 2019 Nov 19;35(7):pp. 7434-7450.

[12] Wróbel, Karol Tomasz, Krzysztof Szabat, and Piotr Serkies. "Long-horizon model predictive control of induction motor drive." Archives of Electrical Engineering (2019): 579-593.

[13] Stando D, Kazmierkowski MP. Constant switching frequency predictive control scheme for three-level inverter-fed sensorless induction motor drive. Bulletin of the Polish Academy of Sciences. Technical Sciences. 2020;68(5).

[14] Wang, Junxiao, and Fengxiang Wang. "Robust sensor less FCS-PCC control for inverter-based induction machine systems with high-order disturbance compensation". Journal of Power Electronics (2020): pp. 1222-1231.

[15] Ortombina L, Karamanakos P, Zigliotto M. "Robustness Analysis of Long-Horizon Direct Model Predictive Control: Induction Motor Drives". IEEE 21st Workshop on Control and Modeling for Power Electronics (COMPEL) 2020 Nov 9 (pp. 1-8).

[16] Zhang, Yanqing, Zhonggang Yin, Wei Li, Jing Liu, and Yanping Zhang. "Adaptive sliding-mode-based speed control in finite control set model predictive torque control for induction motors." IEEE Transactions on Power Electronics 36, no. 7 (2020): 8076-8087.

[17] Kiani B, Mozafari B, Soleymani S, Mohammadnezhad Shourkaei H. Predictive torque control of induction motor drive with reduction of torque and flux ripple. Bulletin of the Polish Academy of Sciences. Technical Sciences. 2021;69(4).

[18] Ali, Anmar Kh, and Riyadh G. Omar. "Finite control set model predictive direct current control strategy with constraints applying to drive three-phase induction motor". International Journal of Electrical & Computer Engineering (2088-8708) (2021) vol.11(4) pp 1-9.

[19] Ayala, Magno, Jesus Doval-Gandoy, Osvaldo Gonzalez, Jorge Rodas, Raul Gregor, and Marco Rivera. "Experimental stability study of modulated model predictive current controllers applied to six-phase induction motor drives." IEEE Transactions on Power Electronics 36, no. 11 (2021): 13275-13284.

[20] Bhowate, Apekshit, Mohan V. Aware, and Sohit Sharma. "Predictive Torque Control of Five-Phase Induction Motor Drive Using Successive Cost Functions for CMV Elimination." IEEE Transactions on Power Electronics 36, no. 12 (2021): 14133-14141.

[21] Shawier, Abdullah, Abdelrahman Habib, Mohamed Mamdouh, Ayman Samy Abdel-Khalik, and Khaled H. Ahmed. "Assessment of predictive current control of six-phase induction motor with different winding configurations." IEEE Access 9 (2021): 81125-81138.

[22] Fereidooni, Arash, S. Alireza Davari, Cristian Garcia, and Jose Rodriguez. "Simplified Predictive Stator Current Phase Angle Control of Induction Motor With a Reference Manipulation Technique." IEEE Access 9 (2021): 54173-54183.

[23] Bassi, Hussain, Muhyaddin Jamal Hosin Rawa, M. Abbas Abbasi, Abdul Rashid Husain, Nik Rumzi Nik Idris, and Waqas Anjum. "Predictive flux control for induction motor drives with modified disturbance observer for improved transient response." U.S. Patent 11,031,891, issued June 8, 2021.

[24] Zhang, Yongchang, Xing Wang, Haitao Yang, Boyue Zhang, and Jose Rodriguez. "Robust predictive current control of induction motors based on linear extended state observer." Chinese Journal of Electrical Engineering 7, no. 1 (2021): 94-105.

[25] Mousavi, Mahdi S., S. Alireza Davari, Vahab Nekoukar, Cristian Garcia, and Jose Rodriguez. "Integral Sliding Mode Observer-Based Ultra-Local Model for Finite-Set Model Predictive Current Control of Induction Motor." IEEE Journal of Emerging and Selected Topics in Power Electronics (2021).

[26] Kiani, Babak. "A computationally low burden MPTC of induction machine without prediction loop and weighting factor." Bulletin of the Polish Academy of Sciences: Technical Sciences (2022): e142050-e142050

[27] Rodriguez, Jose, Cristian Garcia, Andres Mora, Freddy Flores-Bahamonde, Pablo Acuna, Mateja Novak, Yongchang Zhang et al. "Latest Advances of Model Predictive Control in Electrical Drives—Part I: Basic Concepts and Advanced Strategies." IEEE Transactions on Power Electronics 37, no. 4 (2021): 3927-3942.

[28] Rodriguez, Jose, Cristian Garcia, Andres Mora, S. Alireza Davari, Jorge Rodas, Diego Fernando Valencia, Mahmoud Elmorshedy et al. "Latest advances of model predictive control in electrical drives—Part II: Applications and benchmarking with classical control methods." IEEE Transactions on Power Electronics 37, no. 5 (2021): 5047-5061.

[29] Mousavi, Mahdi S., S. Alireza Davari, Vahab Nekoukar, Cristian Garcia, and Jose Rodriguez. "Finite-Set Model Predictive Current Control of Induction Motors by Direct Use of Total Disturbance." IEEE Access 9 (2021): 107779-107790.

[30] Mamdouh, Mohamed, Ayman Samy Abdel-Khalik, and Mohamed A. Abido. "Predictive current control of asymmetrical six-phase induction motor without weighting factors." Alexandria Engineering Journal 61, no. 5 (2022): 3793-3803.

[31] Habib, Abdelrahman, Abdullah Shawier, M. Mamdouh, Ayman Samy Abdel-Khalik, Mostafa S. Hamad, and Shehab Ahmed. "Predictive current control-based pseudo six-phase induction motor drive." Alexandria Engineering Journal 61, no. 5 (2022): 3937-3948

[32] R. Houili, M. Y. Hammoudi, A. Betka and A. Titaouine, "Stochastic optimization algorithms for parameter identification of three phase induction motors with experimental verification," 2023 International Conference on Advances in Electronics, Control and Communication Systems (ICAECCS), BLIDA, Algeria, 2023, pp. 1-6.

[33] El Ouanjli, Najib, Said Mahfoud, Ameena Saad Al-Sumaiti, Soukaina El Daoudi, Aziz Derouich, Mohammed El Mahfoud, and Mahmoud A. Mossa. "Improved twelve sectors DTC strategy of induction motor drive using Backstepping speed controller and P-MRAS stator resistance identification-design and validation." Alexandria Engineering Journal 80 (2023): 358-371.

[34] Z. Liu, Y. Han, G. Feng and N. C. Kar, "Efficient Nonlinear Multi-Parameter Decoupled Estimation of PMSM Drives Based on Multi-State Voltage and Torque Measurements," in *IEEE Transactions on Energy Conversion*, vol. 38, no. 1, pp. 321-331, March 2023, doi: 10.1109/TEC.2022.3187130.

[35] J. Cui, T. Tao and W. Zhao, "Optimized Control Set Model Predictive Control for Dual Three-Phase PMSM With Minimum Error Duty Cycle Regulation," in *IEEE Transactions on Power Electronics*, vol. 39, no. 1, pp. 1319-1332, Jan. 2024, doi: 10.1109/TPEL.2023.3324209

[36] Chirantan, Shaswat, and Bibhuti Bhusan Pati. "Torque and dq axis current dynamics of an inverter fed induction motor drive that leverages computational intelligent techniques." *AIMS Electronics and Electrical Engineering* 8, no. 1 (2024): 28-52.
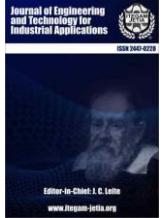
RESEARCH ARTICLE   **OPEN ACCESS**

FLOOD PREDICTION AND MANAGEMENT

Aryan Bisht*[1], Asish Nath[2] and Pratibha Dimri[3]

[1,2] Uttaranchal University, Dehradun, Uttarakhand, India
[3] Assistant Professor, Uttaranchal University, Dehradun, Uttarakhand, India.

[1] http://orcid.org/0009-0007-4839-2014, [2] http://orcid.org/0009-0005-6958-8679, [3] http://orcid.org/0009-0004-4568-3762

Email: *[1]aryanbisht380@gmail.com, [2]asish11nath@gmail.com, [3]pratibhadimri96@gmail.com

ARTICLE INFO

ABSTRACT

Floods are one of the most devastating forces of nature, that destroy thousands of lives every year. Not only does the economy of a country suffer because of such a disaster, but the loss of agriculture and people is physically and mentally exhausting for a country. Especially, in a country like India where floods are frequent, and the prevention department lacks, it becomes crucial to early detect these floods, and inform the local authorities to safeguard the lives of thousands of people.

Through this paper, we aim to work on a comprehensive flood prediction system that utilizes machine learning algorithms to enhance the efficiency and accuracy of a flood prediction and management system. In this study, we have used the dataset with 142193 entries and to work with such large data we have used multiple algorithms. These machine learning algorithms have made it easy to analyze or to work with large datasets. We used multiple algorithms that have worked well with this dataset but some of them have performed better than others. Out of all algorithms, XGBoost has performed best. Along with XGBoost algorithms like CatBoost and Random Forest have also performed well as they all have accuracies of more than 90%.

Our target is accurate and early prediction of floods in an area, and then to inform the required local authorities about the forecast. So, that necessary action can be taken, and the flood-prone area can be evacuated in an organized manner.

I. INTRODUCTION

Floods are recurring and devastating natural disasters taking countless lives every year all over the world. Millions of lives are lost to this disaster, and the unpredictability with which it happens makes it worse, and very hard to tackle.

Multiple factors take part in causing a flood, which often involves an excess of water in areas that are normally dry or have less amount of water. Some common factors that are heavily responsible for flooding are:

1. Overflowing of rivers: One of the most prominent cause of a flood is the overflowing of water bodies. When a river body contains more water upstream than usual, it can flow downstream to the areas at a lower level, which is referred to as floodplains. When a huge amount of water discharges suddenly into adjacent lands it leads to flooding. The people living along the river bodies are at a high risk of flood from the overflowing of rivers, hence in a greater risk of damage. Such people need to be informed about an upcoming flood on priority and be evacuated from the scene as soon as possible.

2. Heavy Rainfall: Another big reason for a natural disaster like a flood can be heavy rainfall. Heavy rainfall can not only contribute to the overflowing of rivers, but when there is a significant amount of rainfall, it can also overpower the capabilities of a drainage system and the capabilities of a soil's absorption, which can then ultimately lead to flooding. And now with the changing climate, the intensity, frequency, and duration of rainfall is increasing. The North Indian floods of 2023 are an accurate example of heavy rainfall causing floods.

3. Deforestation: Apart from natural causes, humans contribute to floods greatly. With the reckless and unbiased cutting of trees, deforestation is a major man-made cause of flooding. As trees hold on to the soil through their roots, it prevents soil erosion and blocks the massive flow of rain, in turn preventing flooding of the area. But when a large number of trees are cut down, there are no roots to hold the soil and soak in the extra water, which then flows freely, flooding the entire deforested area.

Especially in a country like India. Where the terrains vary to a great extent, and the climate conditions change dramatically. In such a geological complexity, the prediction and prevention of natural disasters, such as floods becomes crucial. If we were to refer to the survey conducted by the National Disaster Management Authority, then according to them, an average of 1,600 lives are lost, and 75 lakh hectares of land are affected every year due to floods. Not only this, there is also the economic damage caused to crops, houses, and public utilities, amounting to Rs.1805 crores annually. With the frequency of major floods being more than once in five years, the need for effective flood detection and management systems is more critical than ever.

To tackle this exact problem, and to predict the occurrence of floods, so that appropriate measurements can be taken and countless lives can be saved, through this paper we're aiming to delve into various ML models to understand the best method to predict a flood before it happens and to develop a Flood Detection and Management system that can accurately predict a flood before it destroys countless lives, and inform the relevant authorities to take preventive measures for it, especially from an Indian perspective.

II. THEORETICAL REFERENCE

In this Literature review, we have discussed the previous research work that has been conducted on the topic of flood detection and management systems and the justification of this research. Researchers have used qualitative and quantitative data for the prediction of floods in various papers. The qualitative approach consists of identifying the vulnerable areas where flood generally occurs during monsoon on the other hand quantitative approach consists of Machine Learning algorithms that are used for the prediction of floods before they can cause destruction.

Many scholars [1-3]. have worked with different algorithms to predict the flood using different datasets. Kerala in India has faced many floods over the years due to irregular monsoons, also in the northern part where flood management is not very precise many casualties occurs [2] so we are conducting research on the rainfall pattern.

According to Adnan et al. [4], flood prediction has grabbed the attention of many scholars and as a result, Mosavi et al. [5] have combined Machine Learning technology with traditional methods so the accuracy of the prediction could be increased. This research's main purpose is to compare multiple algorithms and also use hybrid Machine Learning algorithms to find out which one is best suitable for predicting floods [2]. According to Chen et al. [6], a particular area is divided using latitudes and longitudes, and rainfall data along with the drainage of that particular area is taken into consideration because not only the rainfall but the drainage system is also responsible for the flood in a particular area.

According to Maspo et al. [7] currently used machine learning algorithms are not accurate enough. Therefore, we aim to find the best algorithm that could be used for flood prediction. Sankaranarayanan et al. [8], review the public and government plans for the rescue operations, and provide a proper system for

flood victims and is very much possible if they get an early warning about the disaster but there is no accurate method for flood prediction in advance. Previously data was manually entered which made the process time-consuming so the warning was impossible with that. A new operational approach has been given by Parag et al. [9], therefore taking it as a reference we also want to conduct the study to find a new and accurate approach to predict the flood. We are generating as well as using data on a daily basis which promotes the trend of data-driven studies, as Furquim et al. [10] have reviewed the use of data to forecast the floods in order to decrease the damage caused during the floods. The neural network was considered the most accurate regarding the forecasting of floods. Adnan et al.'s [11] have suggested different plans to increase the quality of current warning systems. In order to determine the major flooding location in the Teesta River basin, Talukdar et al. [12] used multiple machine-learning modeling strategies. The Machine Learning algorithm like random forest was used by adnan et al. [4] in turn a range of Machine Learning algorithms are used to analyze the previously collected data and to get an accurate prediction with the help of our models. Gauhar et al. [13] also used the K-NN technique for forecasting a flood and for feature selection coefficients of association is used. We also work with the Bayesian forecasting methods which are used for flood prediction. Haque et al. [14] in his study finds out that 180 models were produced when he used 5 different Machine Learning algorithms during his study. Every algorithm had different accuracy depending on their mode of working and dataset compatibility.

Hossain et al. [15] points out the creation a system for predicting rainfall for a long period of time in western Australia with the help of multiple artificial-based methodologies. As per the research of Aswad et al. [16] flood prediction is very challenging and in-depth study/research is required in this field for predicting the flood also he used a TpoT-based model for predicting the time for flooding in any river. Ighile et al. [17]. This marks the flood-prone areas near Nigeria using past flood records in the time period of 1985 to 2020. His study focuses on making a perfect flood prediction model with the help of Machine Learning algorithms, as Kunvergi et al.

According to [18] research. The boosted regression tree (BTR), generalized additive model (GAM), and multivariate adaptive regression splines (MARS), were the most accurate model according to his study. Sarasa-Cabezuelo's study [19] points out the qualitative investigation for using artificial methods in order to predict rainfall. Also, he come to the conclusion that neural networks are the best approach for predicting rainfall. Liyew and Melese [20] worked with different algorithms for analyzing floods and according to their study, artificial neural network (ANN) was proved to be the best algorithm for this purpose.

III. MATERIALS AND METHODS

We aim to determine the difference in accuracy and efficiency between traditional methods and new-age technology in order to predict flood outbursts in India. We have used a very popular dataset that is about the rainfall in Kerala to predict the flood. After the data collection, we applied techniques like feature engineering, feature encoding, and data normalization to extract useful information from the dataset. Then we split data into 2 parts, 1 for training and another for testing in a 75:25 ratio, then we apply 7 different algorithms to compare the accuracy between them and find the best algorithm that can be used to in order\ to predict floods accurately and give an emergency warning in advance. The

algorithms used in our study are Logistic Regression, Decision Tree, Neural Network, Random Forest, Light GBM, CatBoost, and XGBoost. In the end the model best to predict the flood is identified based on the f1-score of the algorithms used.

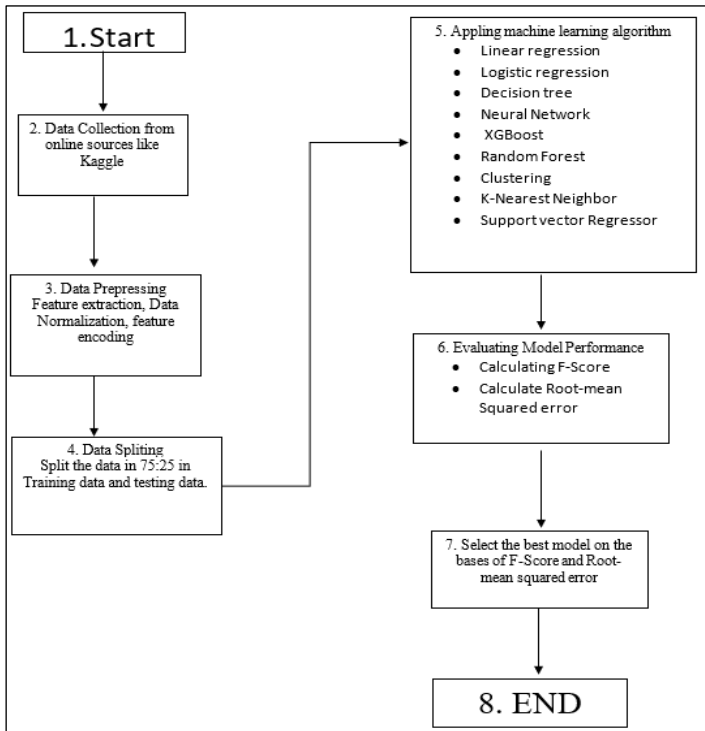Figure 1 is dedicated to showing the methodology details.

Figure 1: Pipeline to demonstrate the methodology of the Project.
Source: Authors, (2024).

Figure 2 is about the workflow of the study. We aim to use computer intelligence to get the maximum result on our training data.
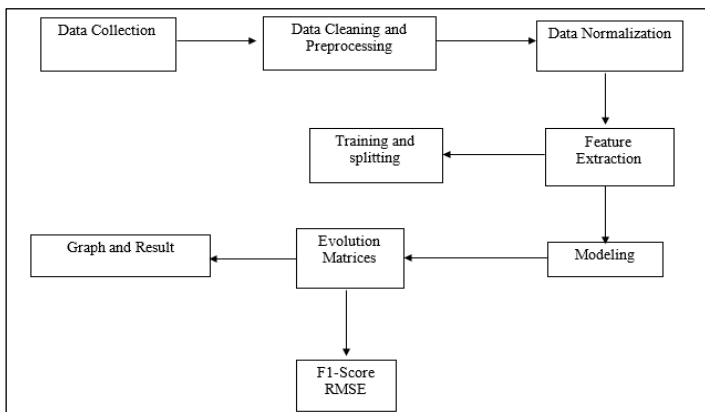
Figure 2: Block Diagram to demonstrate the workflow of the Project.
Source: Authors, (2024).

A. Dataset Description

The data we used is obtained from the Kaggle dataset which is based on the rainfall and floods caused due to rainfall. This dataset includes information about the amount of rainfall that happened in the past and did it resulted in floods or not, also it has the maximum and minimum temperature, humidity, amount of clouds, and many other factors resulting in rainfall.

Figure 3 consists of the head of our dataset used.

Figure 3: Dataset Used in our Project.
Source: Authors, (2024).

Figures 4 & 5 represent the monthly and yearly rainfall happened in India. As we all know months like July August and September are more prone to floods so with the help of Figure 5, we can observe clearly. Also, Figure 4 helps us to identify the areas that are prone to floods. So, in order to predict floods, we want basic information like annual rainfall and monthly rainfall.
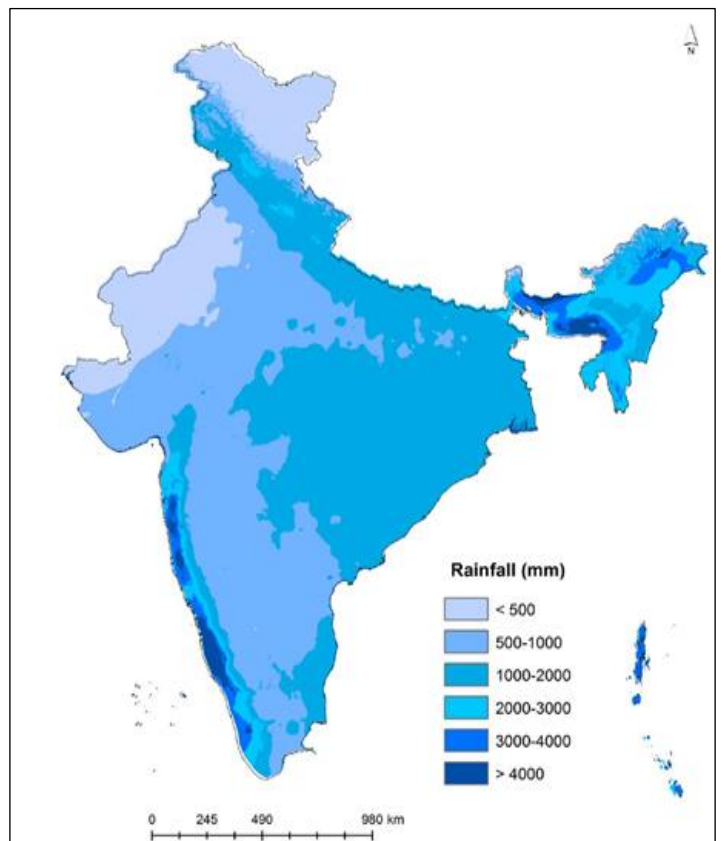
Figure 4: Yearly Rainfall in India.
Source: Authors, (2024).
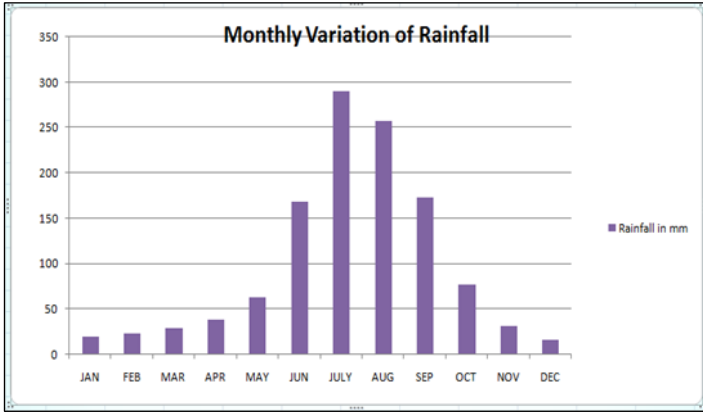
Figure 5: Monthly Rainfall in India.
Source: Authors, (2024).
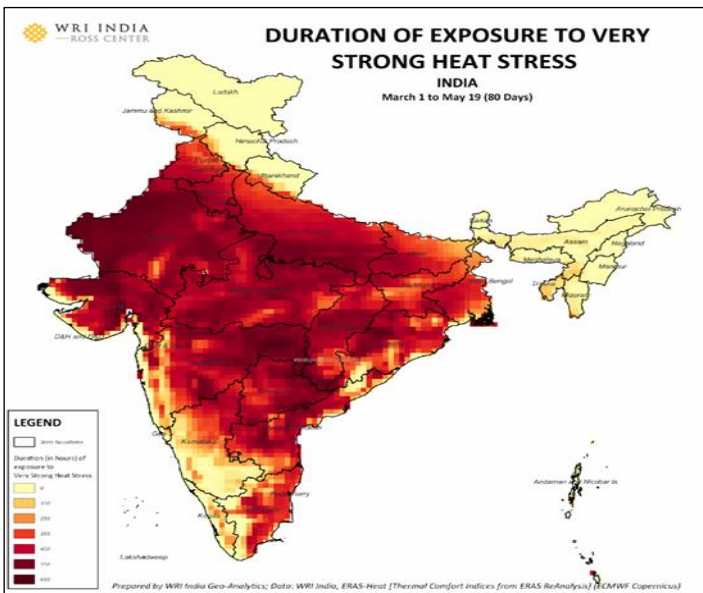
Figure 5: Yearly Temperature of India.
Source: Authors, (2024).
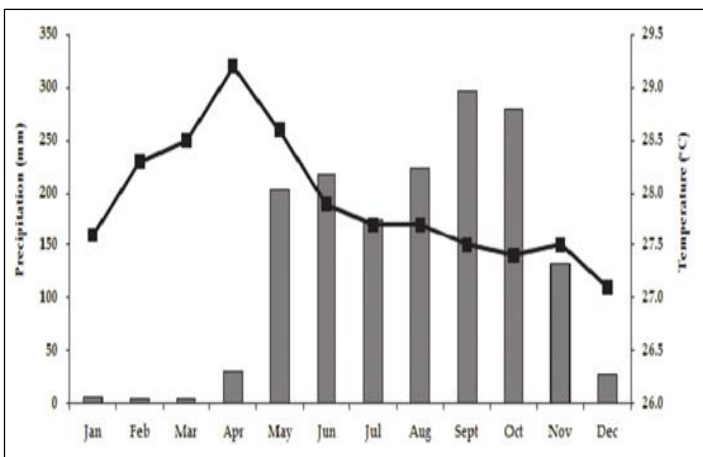
Figure 6: Monthly Temperature of India.
Source: Authors, (2024).

Figure 6 & 7 represent the maximum and minimum temperature in India. As we can observe the hottest area in India and months which have the highest temperature.

Table 1: Features used in training of the machine learning model.

S.No.	Attribute	Description	Type	Measurements
1	City Name	This consist of the name of the city.	String	Categorical
2	Year	This consist of the year of which the data is.	Integer	Numerical
3	Monthly Rainfall	This consist of amount of rainfall monthly in a particular year.	Float	Millimetre
4	Annual Rainfall	This consist of total rainfall of any particular year.	Float	Millimetre
5	Floods	This consist of the if the flood has occurred in that year or not.	String	Yes/No

Source: Authors, (2024).

This work uses multiple concepts of the machine learning and deep learning. With the help of multiple algorithms, we can find a better way to predict the floods that may occur in future in advance. With the help of concepts of data prepressing we can find the rainfall that has occurred significantly in the months of June, July, August and September. This will allow us to target the specific month where rainfall has mostly occurred this will help our model to predict more accurately. Figure 8 is the bar plot of the rainfall in India.
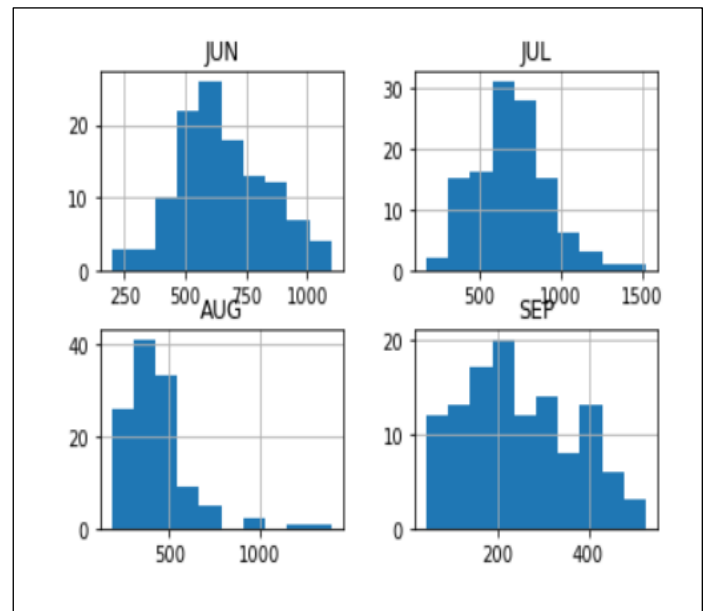
Figure 7; Histogram Depiction of the amount of rainfall occurred in particular year.
Source: Authors, (2024).

B. Data Normalization

Whenever there is any redundant data in dataset therefore to decrease that in any particular dataset, we use the techniques like data normalization so that we may get a good data. The equation used in data normalization is

$$x_{norm} = \frac{x - \min(x)}{\max(x) - \min(x)} \qquad (1)$$

X is the original value in the dataset, min(x) is the minimum value in the dataset, max(x) is the maximum value in the dataset and x normalized is the value of the x within the range of [0, 1]. In the machine learning we use a function called min-max-scaler present in sklearn library which convert the all the values in the range of [0, 1].

C. Machine learning Models

There are 2 types of algorithms in machine learning, 1. Supervised learning 2. Unsupervised learning. In our study we have used most effective algorithm i.e., Supervised learning for the training of our models. In our dataset we have some independent as well as dependent data variables so in this type of dataset use of supervised algorithms works best. Our aim is to predict the accurate answer for the data that we may feed it to the model in future.so we have chosen the best algorithms that we have analysed while reading past research paper during our research time period.

We have used multiple algorithms to analyze the data and get the best algorithm to predict the flood. Some of them are mentioned below:

1. Logistic Regression:

This type of algorithm is used to predict the output in the form of (0,1) i.e., 1 if the event will happen and 0 if the event l not happens. With our data it has performed average in case of accuracy as it only can attain the accuracy of 78.96%.
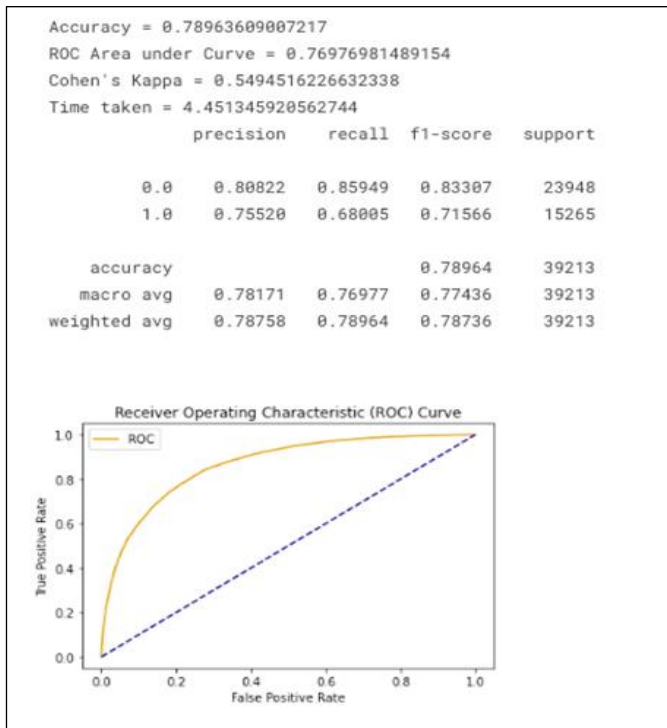
Figure 8: Experimental result of the Logistic Regression.
Source: Authors, (2024).

2. Decision Tree:

This algorithm is a powerful algorithm that is used for classification as well as regression. With 86% accuracy, this has also performed well on our data.
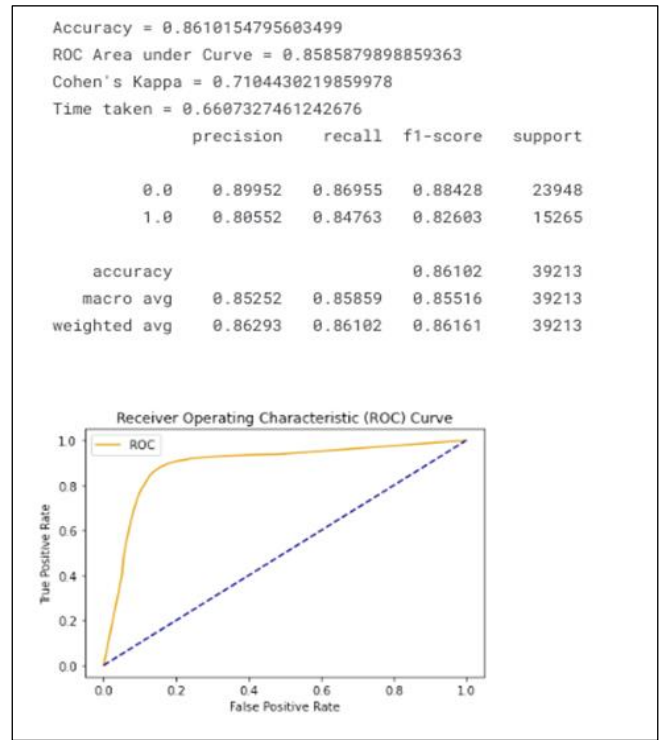
Figure 9: Experimental result of the Decision Tree.
Source: Authors, (2024).

3. Neural Network:

It is a popular algorithm that is mostly used for prediction in machine learning. It forms multiple hidden layers so that the model may process the input and may then predict any result. With 88.6% this algorithm has given good results.
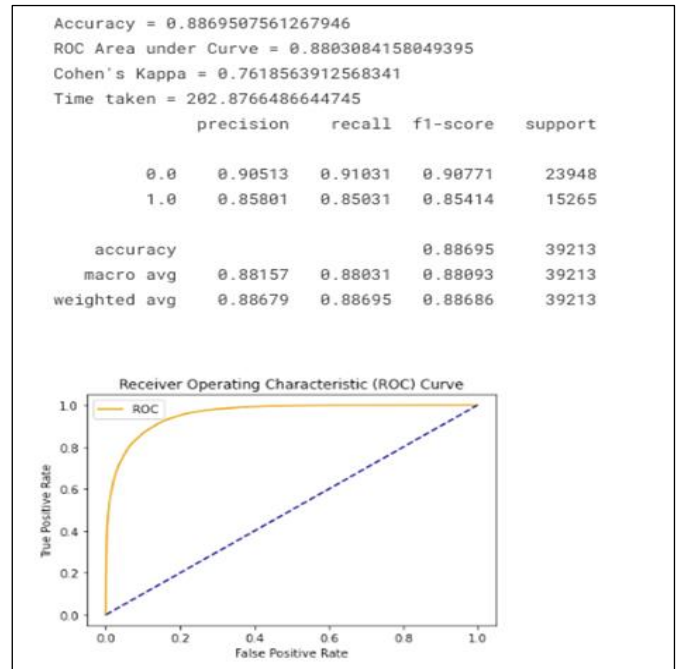
Figure 10: Experimental result of the Neural Network.
Source: Authors, (2024).

4. Random Forest:

This algorithm uses multiple concepts of decision tree to improve accuracy and prevent overfitting. This algorithm has also

had an accuracy of 92.8%, which makes it preferable to use with this type of data.

```
Accuracy = 0.9280595720806876
ROC Area under Curve = 0.9265770863620824
Cohen's Kappa = 0.8493714659078331
Time taken = 42.918816566467285
                precision    recall  f1-score   support

        0.0      0.94812   0.93327   0.94064     23948
        1.0      0.89783   0.91988   0.90872     15265

   accuracy                          0.92806     39213
  macro avg      0.92297   0.92658   0.92468     39213
weighted avg     0.92854   0.92806   0.92821     39213
```
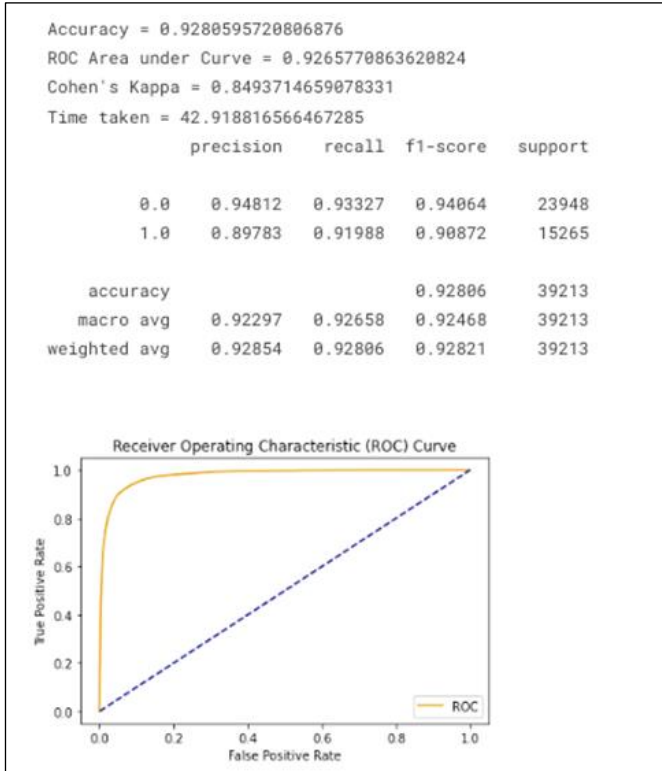

Figure 11; Experimental result of the Random Forest.
Source: Authors, (2024).

5. Light GBM (Light Gradient Boost Machine):
This is also a decision tree-based algorithm to increase the efficiency as well as the memory usage of the algorithm. It has an accuracy of 86.93%.

```
Accuracy = 0.8693800525335985
ROC Area under Curve = 0.8615408010072704
Cohen's Kappa = 0.7246823921549166
Time taken = 4.071417808532715
                precision    recall  f1-score   support

        0.0      0.89003   0.89694   0.89347     23948
        1.0      0.83633   0.82614   0.83120     15265

   accuracy                          0.86938     39213
  macro avg      0.86318   0.86154   0.86234     39213
weighted avg     0.86913   0.86938   0.86923     39213
```
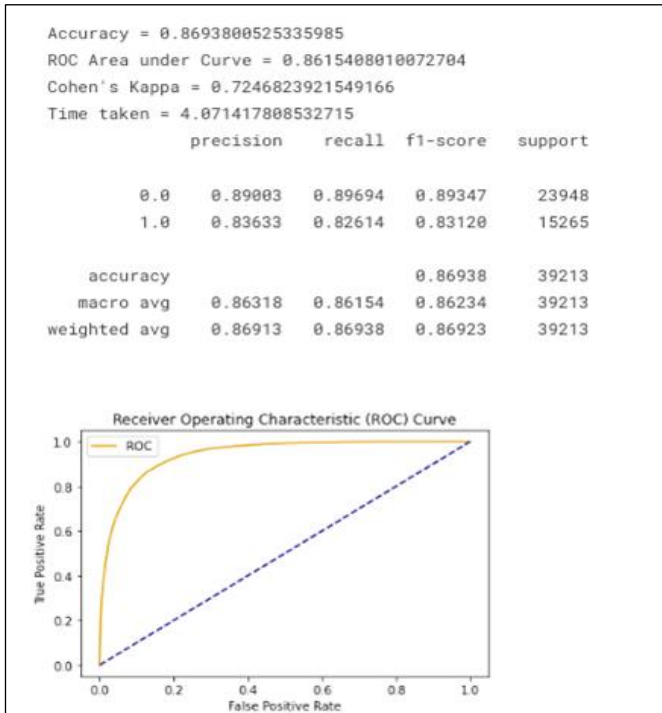

Figure 12: Experimental result of the Light GBM.
Source: Authors, (2024).

6. CatBoost:
Also called "Categorical Boost" which perform good in classification and regression tasks. With 94.1% accuracy it has performed good with our data.

```
Accuracy = 0.9418560171371739
ROC Area under Curve = 0.9449267946584342
Cohen's Kappa = 0.8791826232502136
Time taken = 170.48779153823853
                precision    recall  f1-score   support

        0.0      0.97256   0.93106   0.95136     23948
        1.0      0.89863   0.95879   0.92774     15265

   accuracy                          0.94186     39213
  macro avg      0.93560   0.94493   0.93955     39213
weighted avg     0.94378   0.94186   0.94216     39213
```


Figure 13: Experimental result of the CatBoost.
Source: Authors, (2024).

7. XGBoost:
This gradient boost algorithm is used for efficient and scalable training of our machine learning model. With 95.63% it has performed best during our research time.

```
Accuracy = 0.9563665111060108
ROC Area under Curve = 0.9565810552736519
Cohen's Kappa = 0.908683590430594
Time taken = 135.09377717971802
                precision    recall  f1-score   support

        0.0      0.97246   0.95561   0.96396     23948
        1.0      0.93221   0.95755   0.94471     15265

   accuracy                          0.95637     39213
  macro avg      0.95234   0.95658   0.95434     39213
weighted avg     0.95679   0.95637   0.95647     39213
```
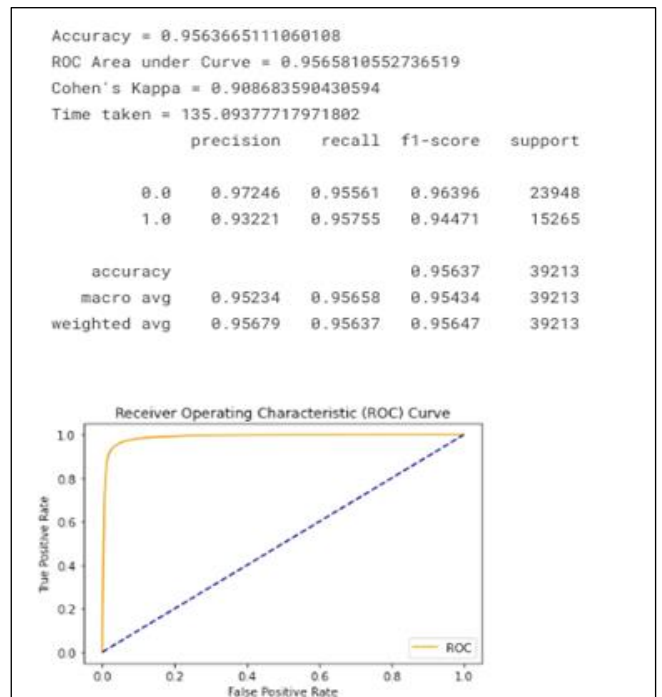

Figure 14: Experimental result of the XGBoost.
Source: Authors, (2024).

We can see that XGBoost, CatBoost and Random Forest have performed better than other algorithms as they have produced results with more accuracy.
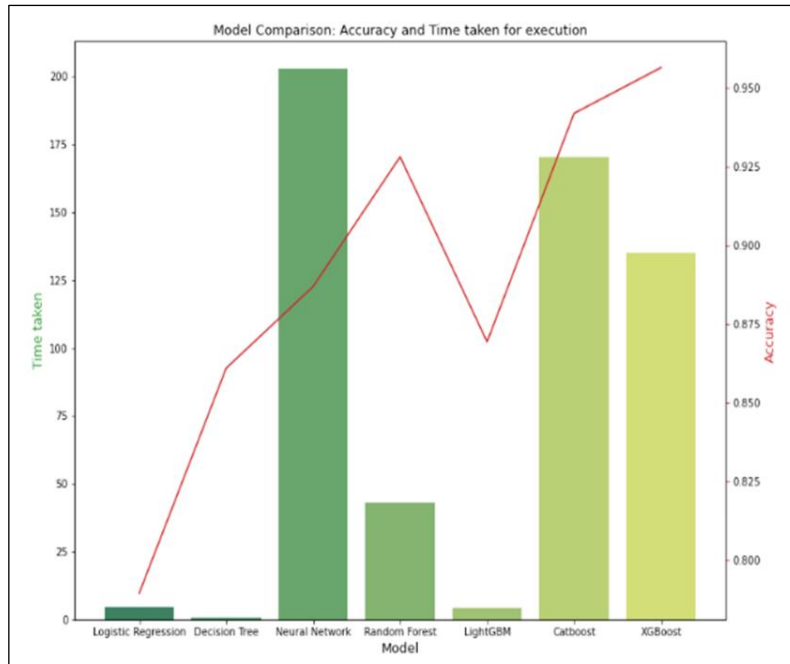
Figure 15: This figure is the comparison of Accuracy and Time taken of the algorithms used.
Source: Authors, (2024).

IV. RESULTS AND DISCUSSIONS

Figure 8-15 tells us about the accuracy of the different algorithms that are used in our study. Graphs that are placed in 8-15 along with the accuracy show the graph that mapped using False Positive and True positive values, it compares the data distribution among the predicted value and actual values.

The rainfall is recorded manually or with the help of remote sensing in India. The data that we used was from multiple sources, it was collected by the Metrological Department of India and other reliable sources.

The Aim was to find the best algorithm for flood prediction and with the help of graphs and f1-score we can determine that XGBoost and CatBoost models have performed best among our chosen algorithms and have produced good results in order to predict flood to figure out the best algorithm we have used features like accuracy score, ROC_AUC, Cohen's Kappa and total time taken for execution. Figure 16 shows the decision region for all the different models. Using this we can observe that CatBoost has a distinct regional boundary compared to all other models. However, XGBoost and Random Forest models also have a very lesser number of misclassified data points as compared to other models.
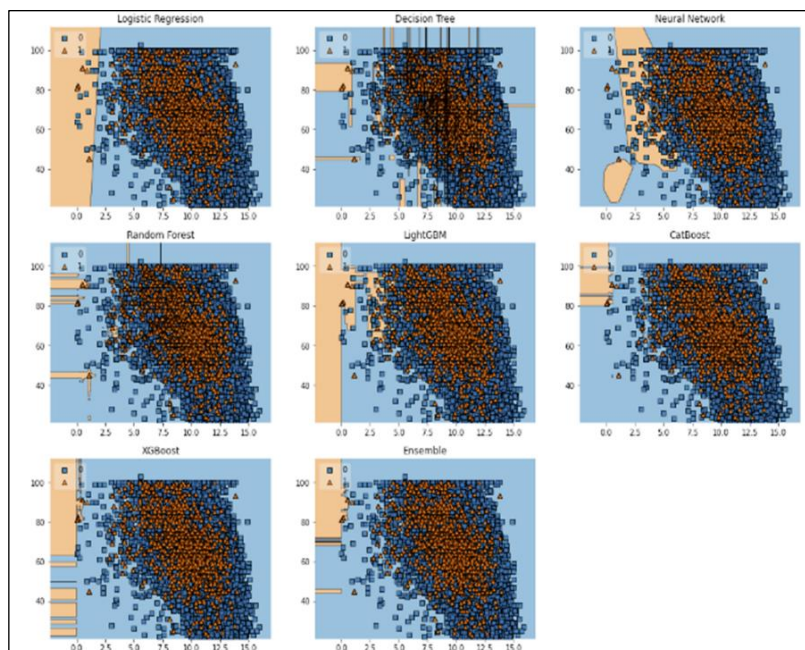
Figure 17: Rainfall Prediction with Machine Learning.
Source: Authors, (2024).

Table 2: Shows the result obtained by various statistical methods.

S.No.	Machine Learning model	Accuracy	ROC area under curve	Cohen's kappa	Time Taken
1	Logistic Regression	0.7896	0.7697	0.5494	4.4513
2	Decision Tree	0.8610	0.8585	0.7104	0.6607
3	Neural Network	0.8869	0.8803	0.7618	202.8766
4	Random Forest	0.9280	0.9265	0.8493	42.9188
5	Light GBM	0.8693	0.8615	0.7246	4.0714
6	CatBoost	0.9418	0.9494	0.8791	170.4877
7	XGBoost	0.9563	0.9565	0.9086	135.0937

Source: Authors, (2024).

V. CONCLUSIONS

In this study, we have used the dataset with 142193 entries and to work with such large data we have used multiple algorithms. These machine learning algorithms have made it easy to analyze the or to work with the large dataset furthermore the work that if done manually would have taken many days, but these algorithms save human efforts and time also, they are more accurate in many cases. This led us to use machine learning in our study.

In our study, we have used multiple algorithms that have worked well with this dataset but some of them have performed better than others. Out of all algorithms, XGBoost has performed best. Along with XGBoost algorithms like CatBoost and Random Forest have also performed well as they all have accuracies of more than 90%. Therefore, in the future, we may work with algorithms that use the same concepts that are used by the XGBoost algorithms

With this we can conclude that XGBoost has performed best according to our study, also algorithms using concepts of gradient boost perform well with this type of dataset and may be the best algorithm that may predict the floods in advance and with the help of that the government may take the prior actions in order to protect the people staying near the flood-prone area. With the help of our study and machine learning algorithms in the future we aim to build a proper structure that may help the citizens of India, also till now all the studies have been conducted related to Rainfall Induced floods but, in the future, we will also work on Glacier Induced floods.

VI. AUTHOR'S CONTRIBUTION

Conceptualization: Aryan Bisht, Asish Nath.
Methodology: Aryan Bisht.
Investigation: Aryan Bisht, Asish Nath and Pratibha Dimri
Discussion of results: Aryan Bisht, Asish Nath and Pratibha Dimri
Writing – Original Draft: Aryan Bisht, Asish Nath.
Writing – Review and Editing: Asish Nath.
Resources: Aryan Bisht, Asish Nath and Pratibha Dimri
Supervision: Asst. Prof. Pratibha Dimri.
Approval of the final text: Asst. Prof. Pratibha Dimri.

VII. ACKNOWLEDGMENTS

VIII. REFERENCES

[1] Mosavi, A., Ozturk, P., Chau, K.: Flood Prediction Using Machine Learning Models: Literature Review. Water, **10**, pp. 1-41 (2018).

[2] Felix, A., Sasipraba, T.: Flood Detection Using Gradient Boost Machine Learning Approach. In: International Conference on Computational Intelligence and Knowledge Economy, pp. 779-783 (2019).

[3] Ying, B., Sayed, A.: Diffusion gradient boosting for networked learning. In: IEEE International Conference on Acoustics, Speech and Signal Processing, pp. 2512-2516 (2017).

[4] Adnan, R.; Zain, Z.M.; Ruslan, F.A. 5 hours flood prediction modeling using improved NNARX structure: Case study Kuala Lumpur. In Proceedings of the 2014 IEEE 4th International Conference on System Engineering and Technology (ICSET), Bandung, Indonesia, 24–25 November 2014; IEEE: New York, NY, USA, 2014.

[5] Mosavi, A.; Ozturk, P.; Chau, K.-W. Flood prediction using machine learning models: Literature review. Water 2018, 10, 1536. [CrossRef].

[6] Chen, C.; Jiang, J.; Liao, Z.; Zhou, Y.; Wang, H.; Pei, Q. A short-term flood prediction based on spatial deep learning network: A case study for Xi County, China. J. Hydrol. 2022, 607, 127535. [CrossRef].

[7] Maspo, N.-A.; Bin Harun, A.N.; Goto, M.; Cheros, F.; Haron, N.A.; Nawi, M.N.M. Evaluation of Machine Learning approach in flood prediction scenarios and its input parameters: A systematic review. In IOP Conference Series: Earth and Environmental Science; IOP Publishing: Bristol, UK, 2020.

[8] Puttinaovarat, S.; Horkaew, P. Flood forecasting system based on integrated big and crowdsource data by using machine learning techniques. IEEE Access 2020, 8, 5885–5905. [CrossRef].

[9] Ghorpade, P.; Gadge, A.; Lende, A.; Chordiya, H.; Gosavi, G.; Mishra, A.; Hooli, B.; Ingle, Y.S.; Shaikh, N. Flood forecasting using machine learning: A review. In Proceedings of the 2021 8th International Conference on Smart Computing and Communications (ICSCC), Kerala, India, 1–3 July 2021; IEEE: New York, NY, USA, 2021.

[10] Furquim, G.; Pessin, G.; Faiçal, B.S.; Mendiondo, E.M.; Ueyama, J. Improving the accuracy of a flood forecasting model by means of machine learning and chaos

theory: A case study involving a real wireless sensor network deployment in brazil. *Neural Comput. Appl.* **2016**, *27*, 1129–1141. [CrossRef].

[11] Adnan, M.S.G.; Siam, Z.S.; Kabir, I.; Kabir, Z.; Ahmed, M.R.; Hassan, Q.K.; Rahman, R.M.; Dewan, A. A novel framework for addressing uncertainties in machine learning-based geospatial approaches for flood prediction. *J. Environ. Manag.* **2023**, *326*, 116813. [CrossRef] [PubMed].

[12] Talukdar, S.; Ghose, B.; Shahfahad; Salam, R.; Mahato, S.; Pham, Q.B.; Linh, N.T.T.; Costache, R.; Avand, M. Flood susceptibility modeling in Teesta River basin, Bangladesh using novel ensembles of bagging algorithms. Stoch. Environ. Res. Risk Assess. 2020,34, 2277–2300. [CrossRef].

[13] Gauhar, N.; Das, S.; Moury, K.S. Prediction of flood in Bangladesh using K-nearest neighbors' algorithm. In Proceedings of then. 2021 2nd International Conference on Robotics, Electrical and Signal Processing Techniques (ICREST), Dhaka, Bangladesh, 5–7 January 2021; IEEE: New York, NY, USA, 2021.

[14] Hamidul Haque, M.; Sadia, M.; Mustaq, M. Development of Flood Forecasting System for Someshwari-Kangsa Sub-watershed of Bangladesh-India Using Different Machine Learning Techniques. EGU General Assembly Conference Abstracts; EGU: Virtual, 2021. Available online: https://ui.adsabs.harvard.edu/abs/2021EGUGA..2315294H/abstract (accessed on 20 October 2023)

[15] Hossain, I.; Rasel, H.M.; Alam Imteaz, M.; Mekanik, F. Long-term seasonal rainfall forecasting using linear and non-linear modelling approaches: A case study for Western Australia. Meteorol. Atmos. Phys. 2020, 132, 131–141. [CrossRef]

[16] Aswad, F.M.; Kareem, A.N.; Khudhur, A.M.; Khalaf, B.A.; Mostafa, S.A. Tree-based machine learning algorithms in the Internet of Things environment for multivariate flood status prediction. J. Intell. Syst. 2021, 31, 1–14. [CrossRef]

[17] Ighile, E.H.; Shirakawa, H.; Tanikawa, H. Application of GIS and machine learning to predict flood areas in Nigeria. Sustainability 2022, 14, 5039. [CrossRef]

[18] Kunverji, K.; Shah, K.; Shah, N. A flood prediction system developed using various machine learning algorithms. In Proceedings of the 4th International Conference on Advances in Science & Technology (ICAST2021), Mumbai, India, 7 May 2021.

[19.]Sarasa-Cabezuelo, A. Prediction of rainfall in Australia using machine learning. Information 2022, 13, 163. [CrossRef]

[20] Liyew, C.M.; Melese, H.A. Machine learning techniques to predict daily rainfall amount. J. Big Data 2021, 8, 153. [CrossRef]
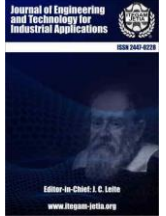
RESEARCH ARTICLE   **OPEN ACCESS**

DEVELOPMENT OF AN AI-ENABLED VIDEO CAPTURING DEVICE FOR BULLET TRAJECTORY ANALYSIS AND BALLISTIC RESEARCH

Shashanka Handique[1], Sweta Saha[2], *R Suresh[3], Lipi B Mahanta[4,]

[1,2] Dept. of Electronics & Telecom. Engg., Assam Engineering College, Guwahati, India.
[3] Ballistics, Central Forensic Science Laboratory, Kamrup, India.
[4] Mathematical and Computational Sciences Division, Institute of Advanced Study in Science and Technology, Guwahati, India.

[1] http://orcid.org/0000-0001-6888-3493, [2] http://orcid.org/0009-0005-1632-5699, [3] http://orcid.org/0009-0009-3773-532X, [4] http://orcid.org/0000-0002-7733-5461,

Email: shashankahandique@gmail.com, sahasweta1@gmail.com, r.suresh-as@gov.in, lbmahanta@iasst.gov.in*

ARTICLE INFO

ABSTRACT

A ballistic experts' discipline is the ability to compare the characteristic marks found on the surface of different fired bullets to determine whether they were fired from the same gun. These tool marks become a "ballistic fingerprint" that examiners can use to identify specific characteristics of the firearm that discharged the bullet. One such tool mark is the striation marks left on the bullet, identical to scratch marks. Manually done, a comparison microscope is used in this process, where the testing bullet is rotated until a well-defined land or groove comes into view. The sample bullet is then rotated in search of a matching region. But in this process opinions are given through only the manual experimental process and not through an automated system. The proposed solution was to develop a cost-effective automated system that captures the video of the bullet in one go. Also, the focus was to develop a lighting arrangement independent of the environment, so that the device can be efficiently used in any environment.

I. INTRODUCTION

The increasing rate of crime is a matter of concern for the country. According to a statistic by National Crime Records Bureau, a total of 51,56,172 crime incidence have been reported in 2019, and out of 44,823 cases of murder by firearms 44,513 are cases of unlicensed firearms [1].

The illegal manufacturing and smuggling of firearms have become a topic of concern for the country breaching any citizen's security. To encounter this challenge, the country's criminal investigation department plays a major role to gather evidence against a criminal using forensic science.

Forensic ballistics, a branch of forensic science, is about the examination and identification of firearm evidence from a crime scene. In our country India there are seven Central Forensic Science Laboratories (CFSL) and 30 State Forensic Laboratories that were established as a scientific department to provide scientific support and services to the investigation of crime [2].

The experts of CFSL examine the exhibits forwarded by the Investigating Agencies and render an expert opinion and substantiate their opinions in the Court of Law through court testimony and evidence.

Bullets are intentionally designed to be wider than the barrel of the firearm. When a bullet is fired, it travels through the barrel of the firearm. As the bullet passes through the barrel, the barrel compresses, thereby leaving tool marks on the bullet. These tool marks become a "ballistic fingerprint" that examiners can use to identify specific characteristics of the firearm that discharged the bullet.

These striation marks on the bullet are the target of examination because of their specific identity as depicted in **Figure 1**.

Figure 1: Striation mark captured in confocal microscope in CFSL Laboratory, Kamrup, Assam.
Source: Authors, (2024).

A ballistic expert's discipline is their ability to compare the striations found on the surface of different bullets, and to determine whether these striations indicate the different bullets were fired by the same gun. Making such determination is not an easy task as it depends on the quality of striations marks. Generally, it takes a few days for the examination, but complications arise due to segregation or overlapping of multiple marks which makes the process tedious, which further delays the service.

In forensic science laboratories, microscopes are used to study the striation marks of a bullet. An expert must be equipped with a microscope to check and compare two different bullets. The modern technology of microscopes allows us to capture pictures easily from the microscope. But there is no automated process of taking pictures of the whole bullet. At present, to do that, precision hand movements are required so that there is neither any overlapping part nor any part left out. A typical AI-based system would follow the steps as depicted below (Figure 2). But it is not possible to capture complete images of the striations of the bullet, as depicted in Figure 3, and hence only parts are taken and either analysed independently or after stitching them [3] [4] [5]. If the striations can be captured in totality, and in the desired magnification (for clear view of the marks) then the analysis of the features would be much improved and easier.
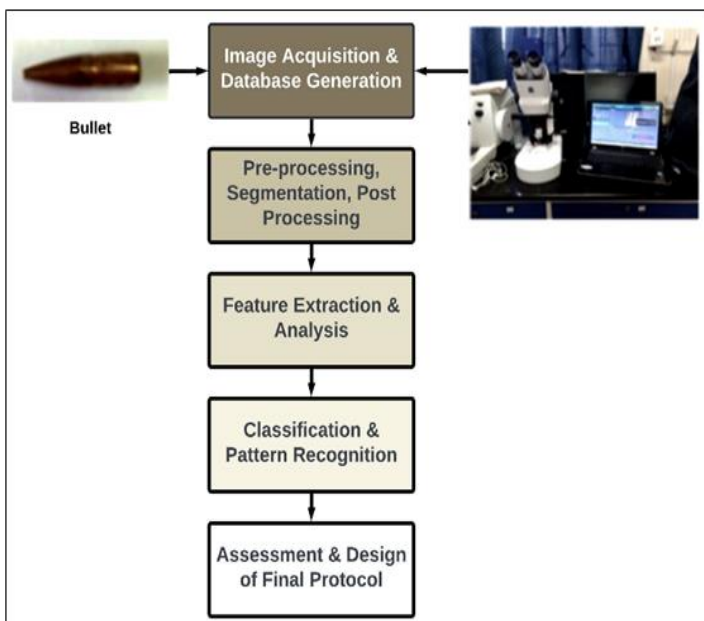
Figure 2: Usual methodology of AI-based image analysis of a bullet.
Source: Authors, (2024).

With this motivation, the idea of the device proposed in this work by us is to capture the video of a bullet in a very easy and comfortable way and eliminate the difficulties that are present in the above-mentioned item. So that all the details of any bullet can be recorded precisely in just one click without any overlapping part. The recorded footage can be successively studied, transported/distributed with the corresponding authority very conveniently. A person, who doesn't have a microscope is now able to study the bullet from the video sent to him. One can develop a computer application to study the bullet by importing the video to it. So, this method can be used as a standard procedure in near future for ballistic science studies.
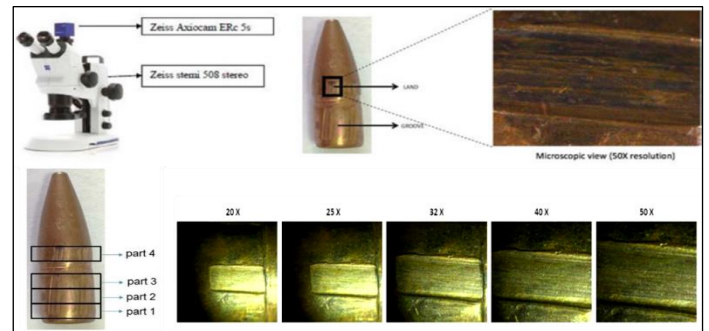
Figure 3: Depicting how images are catured in parts and different magnification views of striations marks.
Source: Authors, (2024).

II. RELATED WORKS

The prior art reveals that an imaging system, known as Fireball [6], was developed for the Police Services which can store, analyze, retrieve, and match high-resolution digital images of cartridge cases. But the system was not equipped for fired bullets. In India, there is no such device available until now which aims to solve the particular problem we intend to. However, in Thailand, there has been a system [7] developed which carries out a similar process. They have implemented a system where a 9 mm bullet is placed into a mechanism. It is rotated using a motor with the help of a micro-controller and the details of the bullet are captured using an iPhone camera. The drawbacks of the system are as follows:

i.   The system is designed to take only 9 mm bullets. One can't use any other sizes of bullets.
ii. There is no synchronization/communication between the rotation and recording. One has to manually start the rotation and start the recording, which is not an ideal condition. If there is any kind of delay, the results will be improper
iii. There is no mechanism to prevent the recording after a certain revolution so that no overlapping part occurs. One has to process the video in a machine learning model to get rid of the overlapping part.
iv. The recording system is not universal. It depends on a particular app platform.

III. PROPOSED SOLUTION

The object of the proposed device is to develop a cost-effective and efficient system that can capture/record the unique/feature details of a bullet. The main contributions of the work presented in this paper are enumerated as follows.

i.   Since different bullets have different diameters, so there is a requirement of a base where any bullet can be placed. Hence, an adhesive mechanism base has been prepared where a bullet of any diameter can be placed.

ii. Using a digital Vernier calliper will help to measure the diameter of the bullet which is to be used in the system. This diameter is used to calculate the required rotational speed so that all bullets have one steady translational speed.

iii. Usage of motor feedback mechanism. From the motor's feedback of rotation, the micro-controller can send signals to the recording device to start/stop recording. Hence the recording process has been automated.

iv. Lighting system independent of the environment light, which will make sure that the bullets are lit exactly at the required intensity with minimal reflection and ambient light can't disturb the system.

IV. STATEMENT OF THE PROPOSED DEVICE

A prototype has been built that can be used to capture all the details of a bullet in a single video. This video can then be used for several purposes. It will be easier to distribute to different experts and trainees for carrying out related forensic analysis using a computer and a common video application. It will eliminate the need for carrying an actual bullet to a laboratory with a sophisticated microscope, which is being conventionally done now. Further, the classification and identification of the bullet can also be done using machine learning and deep learning algorithm implementations from the acquired video. The use of artificial intelligence (AI) will reduce the analysis time and also increase accuracy. The USP of the prototype are:

- The bullets can be compared by studying the video footage.
- Doesn't need a costly microscope just to declare the class.
- Anyone can use the system. It is as easy as plug and play.

V. DESCRIPTION OF THE PROPOSED DEVICE

He portable device can be equipped with any type of camera, providing it has an external trigger, with any existing microscopic lens system. The bullet is placed on a 360-degree rotating base. The camera is connected to the system and placed properly in front of the microscopic lens system. As the rotating starts it starts the recording automatically and it stops before overlapping parts occur in a full rotation. Besides, there is a calliper attached to the system so that the diameter of the bullet can be measured in the beginning and the rotational speed can be determined from it to maintain a steady translational motion throughout different bullets of different diameters, this would help in reducing the blurriness and rolling shutter effect that arises in a moving object in a video by minimizing the speed of rotation

The working is described with a Block Diagram (Figure 4) and in details below:
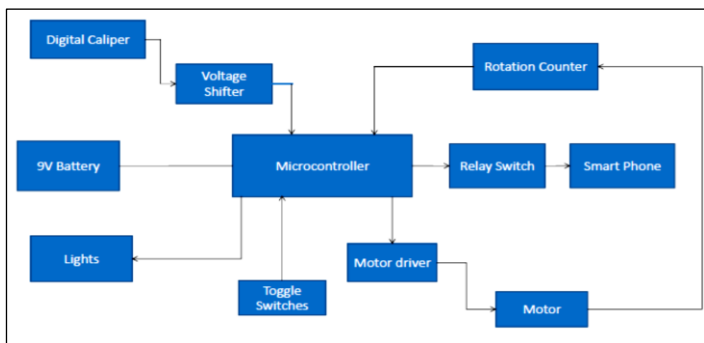
Figure 4: Block Diagram of proposed device.
Source: Authors, (2024).

V.1 DETAILED DESCRIPTION

One digital calliper has been implemented in the system to measure the diameter of the bullet. This measurement directly affects the rotational speed. The calliper has a resolution of .01" and 0.01mm. At first, the camera is connected and placed properly in the system. After the bullet diameter is measured using the calliper attached to the system it is placed on a base and it is checked whether the lens is focused or not. The lighting is set up by observing how the bullet is reflecting/reacting to the lights and how well the detailed marks are visible. After that, the speed level is set from three predetermined sets of speeds. The final rotational speed is determined by the speed level which is set by the user and the calculated speed due to the diameter of the bullet.
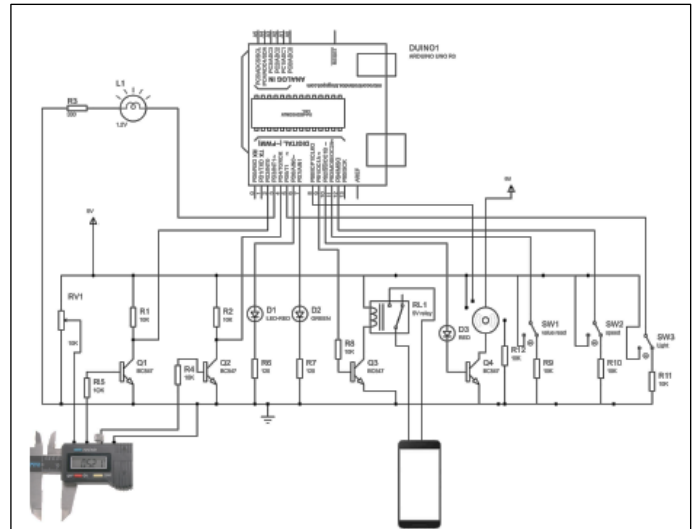
Figure 5: Flowchart of working.
Source: Authors, (2024).
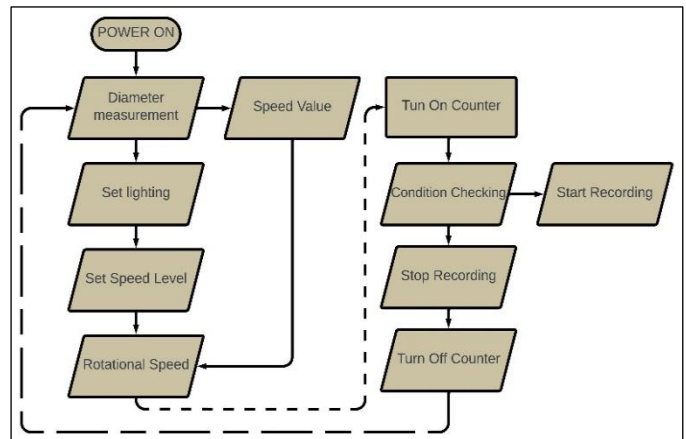
Figure 6: Circuit Diagram.
Source: Authors, (2024).

A rotational counter is attached to the rotor of the motor which is turned on after the lighting and speed are set appropriately. As for now, there are 12 divisions (which can be increased also), 30 degrees (can be decreased) each, in the counter. The value of the counter increments after crossing each division. It counts from 0 to 11. After 11 it is again set to 0 by the program. When the counter counts 1, the microcontroller triggers a relay, which toggles the recording in the smartphone via an earphone jack. When the counter Counts 11, again the

relay is triggered which stops the recording. The video is obtained that way. It is known that the focal plans are flat and the lens introduces chromatic aberrations at the edges. Here it is assumed that 60 degrees are properly covered by the camera without any chromatic aberration, focal error, as the bullet surface is not flat. If we use some advanced optical system, then this measurement can be changed. The flowchart of working is depicted the Figure 5.

VI. CIRCUIT EXPLANATION

Figure 6 depicts the proposed circuit diagram. The micro-controller board has been powered using a 9V DC battery. The micro-controller board has been powered using a 9V DC battery.

The board gives an output of 5V from its internal voltage regulator. The digital calliper operates on 1.5V, which is not enough for the Arduino board (ATmega328P) to distinguish high (1) and low (0) states, as the threshold voltage to distinguish between high and low is 2.8V for Arduino. Therefore, to power the calliper a 10K ohm potentiometer is attached to the 5V supply to provide 1.5V and also two BC547 transistor amplifiers has been used to amplify 1.5V signals to 5V signals which are being sent by the calliper from data and clock port to the Arduino board. 10K ohm resistors have been used on the base and the collector of the transistors, otherwise, the transistors may get damaged or some fault in amplification may arise.

Figure 7: A 3D representation of the prototype.
Source: Authors, (2024).

The counter is a simple design that increments the value when it reads a logic 1. A HIGH voltage is applied to the counter divisions and a low voltage is applied to the reader pin. When the reader touches the divisions, it sends HIGH logic to the board and the board increments the counter value. The LOW voltage is kept applied the rest of the time to the reader pin so that it turns back to the LOW state immediately after touching the divisions. A resistance of 10K ohm is connected so that no short circuit takes place. Green LED is an indication of the counter. Whenever the value increments, it lights up for a few milliseconds. A current-limiting resistor (100 ohms) is connected in series to protect the LED from getting burned by excessive current.

The relay works on 5V voltage. It doesn't work below that voltage. The output pins of the Arduino board provide 4.8Vwhich is not enough for the relay to work properly. Again, one transistor with appropriate resistors has been used to amplify the output pin signal to 5V. The collector of the transistor is connected to one pin of the relay. Another pin of the relay is connected to a 5V supply. In this case, the transistor is acting as a switch. When the base is HIGH, the relay circuit closes and the relay is switched on. When the base is LOW, the transistor goes to cut off state, the relay circuit becomes open and hence the relay is turned off.

The relay has a total of 5 pins. Two pins are used to control the relay. Rest three are used to switch the external circuit. The pins are- NC (normally connected), NO (normally open) and common. When the relay is not active, the common and NC remains in short. When the relay is active, the common and NO are connected in short. The triggering pin of the earphone jack is connected to common and NO. So, when the relay is active, the common and NO are shorted, so the triggering pin sends that signal to the smartphone (or any other device which supports external triggering) and the phone starts recording. Red LED is an indicator that stays ON while the recording is taking place. The motor speed control is done by the Arduino board itself. As a motor driver, another transistor (BC547) is used, which takes the signal from the microcontroller and amplifies it to motor operable 9V.

There are three digital switches, their functions are to act as speed controller, brightness controller, read calliper measurement. The lights are connected in parallel connections, i.e. the ring light, sidelights get the same voltage from the micro-controller. The brightness is adjusted by a digital switch. If we want, we may control it differently by introducing some regulators. Figure 7 showcases a 3D representation of the prototype.

VII. RESULTS AND ANALYSIS

The prototype was built with simple components to confirm the working of the device. It was found to work in smooth condition and the following were ensured:

a) Fired bullets of small arms calibre such as 0.22 in., 5.56 mm, 6.35 mm, 7.62 mm, 7.65 mm, 8 mm, 9 mm, 0.303 in., 0.32 in., 0.380 in., etc. generally used in handguns (pistols/revolvers), carbine, rifles can be mounted with the device.

b) Can measure the diameter of a mounted bullet with 0.01 mm resolution.

c) One fired bullet (of calibre as stated in 9. a) can be mounted.

d) Characteristic marks such as rifling marks and/or barrel marks and/or striated /scratch marks imprinted on the bullet can be visualized.

e) Characteristic marks present on the fired bullet can be captured using a suitable digital recording device.

f) A mounted bullet can be rotated and video capturing can be performed to a full rotation of the bullet or part of the bullet to acquire the characteristic marks present on a fired bullet.

Comparison of the proposed device with devices or processes of prior studies can be summarized in Table I.

Table 1: Comparison With Prior Art.

	Prior Art Process	Improvement of the Process
Efficiency	• Holds only one type of bullet • Fixed diameter, fixed speed • Rotation is not precise, no control over overlapping parts • A specific mobile application is developed	• Developing a system that can hold any bullet of any diameter • Bullets of different diameters can maintain a fixed translational speed • Precise and programmable rotation with no overlapping part • Doesn't need a different mobile application to run.
Cost	• Use of stepper motor which is costlier than DC motor and draws high current • 3D printed mechanism to hold a bullet • Usage of a commercially available motor driver	• Use of DC motor which is cheaper than a stepper motor and draws very little current compared to a stepper motor • A simple adhesive mechanism that is much cheaper • A self-developed, simplest motor driver which is 80% cheaper
Ease	• The developed app supports iOS for recording purposes; hence the system is not compatible with all recording devices.	• Doesn't depend on any app/OS as long as the recording device responds to an external trigger switch, which smartphones and cameras have already. • Works on the existing camera application
Environment Protection	Doesn't arise	Does not arise

Source: Authors, (2024).

VIII. CONCLUSIONS

We can draw the following conclusions from our study:

a) There is no such device available in any of the Central or State Forensic Science Laboratory (FSL) in India. Such a device is highly felt necessary to conduct necessary scientific examination on the samples to be tested in the ballistics division of Central or State FSLs. Hence, the thus developed device can help forensic scientists to perform necessary scientific examination and testing of fired bullets. Therefore, the demand for such a device could be very high for the Central or State FSLs in India and neighbouring countries or other interest countries.

b) Ballistic research organizations in civil and military establishments, Central or State Police Organizations, Academic institutes /Universities/ Colleges where Ballistic science is taught as one of the scientific subjects to impart knowledge including laboratory experimentations can be potential users of such device.

c) Law enforcement agencies, police training centres, judicial academies, central detective training institutes, crime investigating establishments can also be potential users.

IX. AUTHOR'S CONTRIBUTION

Conceptualization: Shashanka Handique, Sweta Saha, R Suresh, Lipi B Mahanta,
Methodology: Shashanka Handique, Sweta Saha.
Investigation: Shashanka Handique, Sweta Saha.
Discussion of results: Shashanka Handique, Sweta Saha, R Suresh3, Lipi B Mahanta.
Writing – Original Draft: Shashanka Handique, R Suresh.
Writing – Review and Editing: Shashanka Handique, Sweta Saha, R Suresh, Lipi B Mahanta.
Resources: R Suresh.
Supervision: R Suresh, Lipi B Mahanta.
Approval of the final text: Shashanka Handique, R Suresh.

X. REFERENCES

[1] Crime in India, National Crime Records Bureau. MoHA," 2019. [Online]. Available: https://ncrb.gov.in/sites/default/files/CII 2019 Volume 1.pdf.

[2] Ministry of Home Affairs, Directorate of Forensic Science Services, Government of India," 2021. http://www.dfs.nic.in/.

[3] P. Changmai, K. Bora, R. Suresh, N. Deb, and L. B. Mahanta, "On the Study of Automated Identification of Firearms Through Associated Striations," Dec. 2019, doi: 10.12783/ballistics2019/33156.

[4] B. Barua, G.Chyrmang, K. Bora, R. Suresh, L.B. Mahanta, "2D Image Stitching to Generate a Film

of Fired Bullets", Springer Nature Singapore Pte Ltd. 2021. https://doi.org/10.1007/978-981-33-4084-8_31

[5] Dutta, S., Saikia, S., Barman, A., Roy, R., Bora, K., Mahanta, L. and Suresh, R., 2021, " Study on enhanced deep learning approaches for value-added identification and segmentation of striation marks in bullets for precise firearm classification", Applied Soft Computing, 112, p.107789.

[6] C. L. Smith, "Fireball: a forensic ballistics imaging system," in Proceedings IEEE 31st Annual 1997 International Carnahan Conference on Security Technology, pp. 64–70, doi: 10.1109/CCST.1997.626240.

[7] P. Pisantanaroj et al., "Automated Firearm Classification From Bullet Markings Using Deep Learning," IEEE Access, vol. 8, pp. 78236–78251, 2020, doi: 10.1109/ACCESS.2020.2989673.

RESEARCH ARTICLE   **OPEN ACCESS**
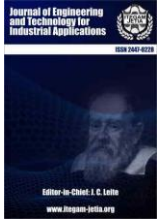
DESIGN AND ANALYSIS OF NOVEL TOPOLOGY FOR PV-FED EV CHARGING SYSTEM

*Bondu Pavan Kumar Reddy[1], Vyza Usha Reddy[2].

[1,2]Sri Venkateswara University College of Engineering, Sri Venkateswara University, Tirupati, INDIA

[1]http://orcid.org/0000-0001-8845-571X, [2]http://orcid.org/0009-0004-7070-8925,

Email: [1]pavanreddyphd@gmail.com*, [2]vyzaushareddy@yahoo.co.in.

ARTICLE INFO

ABSTRACT

This paper presents a novel design for a photovoltaic (PV) powered electric vehicle (EV) charging system. The core of the system is a modified single ended primary inductance converter, chosen for its high efficiency, reduced switch voltage stress, and ample operating range for maximum power point tracking (MPPT). This study details the redesigned SEPIC converter architecture, including with and without the MPPT algorithm. Additionally, it presents an optimized parameter selection, design methodology, and simulation technique for analysing the converter's performance in EV charging applications.

Two MPPT approaches, Perturb and Observe (P&O) and Incremental Conductance (IC), are investigated and compared based on their impact on the converter's switching time under standard solar PV panel testing conditions. To comprehensively evaluate the system's performance, a MATLAB/Simulink model is developed, simulating the charging of a 48V, 200Ah battery using a 2kW solar PV input through the modified SEPIC converter and variations in the battery state of charge (SoC), battery voltage, and charging current are monitored. The simulation results demonstrate that under identical simulated conditions (10 seconds), the battery SoC increases from 50% to 50.034% without MPPT and to 50.042% with MPPT, highlighting the effectiveness of the MPPT algorithms in maximizing harvested solar energy.

I. INTRODUCTION

The increasing adoption of electric vehicles necessitates the development of efficient and readily available charging infrastructure. This paper presents a novel approach to EV charging by utilizing a PV-powered system with a modified SEPIC converter. Compared to traditional boost converters, the modified SEPIC offers several advantages, including nearly double the static gain, wider operating range for MPPT controller and reduced switch voltage stress thereby enhancing the converter's reliability and lifespan [1].

The adoption of renewable energy alternatives has increased dramatically due to the rising costs and depletion of non-renewable energy sources. Among these, photovoltaic (PV) energy has drawn quite a bit fascination as a potential remedy for the problems posed by increased energy demand and global warming. Fuel independence, environmental friendliness, durability, and cheap maintenance are just a few advantages of PV energy.

There are many processes involved in integrating PV systems into the grid, one of which is raising the output voltage to meet grid requirements. Boost converters or high-frequency step-up transformers are used in conventional methods. Even though DC-DC converters are frequently used to boost PV system voltage, traditional topologies frequently have poor static gain, which lowers output voltage [2].

As an instance, the maximum input voltage rise that a SEPIC converter with a duty cycle of 0.82 can achieve is a factor

of 5. This would need a tenfold increase in input voltage to fulfil grid requirements, making the usage of a step-up transformer redundant.

Modified SEPIC converter architecture is suggested in this study to overcome these drawbacks. With the addition of a diode and a capacitor, the converter may increase the input voltage by up to ten times. Because of this improved capabilities, a step-up transformer is no longer necessary, simplifying the system design and perhaps increasing efficiency.

By investigating modified SEPIC converter architecture that delivers higher output voltage and better efficiency, this research seeks to further PV system integration [2].

II. MODELLING AND DESIGNING

II.1 SOLAR PV SPECIFICATIONS

The design and development of a MATLAB/Simulink model for a solar photovoltaic (PV) system intended to recharge an electric vehicle's (EV) battery is described in the present article. The system is configured to deliver 48V and 200Ah to the battery using Modified SEPIC converter. A constant irradiation of 1000W/m2 and a temperature of 25°C are assumed in the simulation. The PV system incorporates Maximum Power Point Tracking (MPPT) functionality to maximize power output. There are eight parallel modules in the simulated system, and each module has sixty solar cells. The specific design parameters of the PV modules are detailed in Table 1 [3].

Table 1: Solar PV Module Specifications at STC.

Parameter	Specification
Voltage at MPP (V_{MPP})	30.9 V
Current at MPP (I_{MPP})	8.1 A
Power at MPP (P_{MPP})	250.29 W
Open Circuit Voltage (V_{OC})	36.6 V
Short Circuit Current (I_{SC})	8.75 A

Source: Authors, (2024).

II.2 DESIGN OF MODIFIED SEPIC CONVERTER

The power circuitry of the traditional SEPIC converter is presented in Figure 1. A key feature of the SEPIC converter is its ability to both boost (step-up) and buck (step-down) the input voltage, making it suitable for applications with a wide range of input voltages. However the switch voltage is equal the sum of the input and output voltage [4],[5].
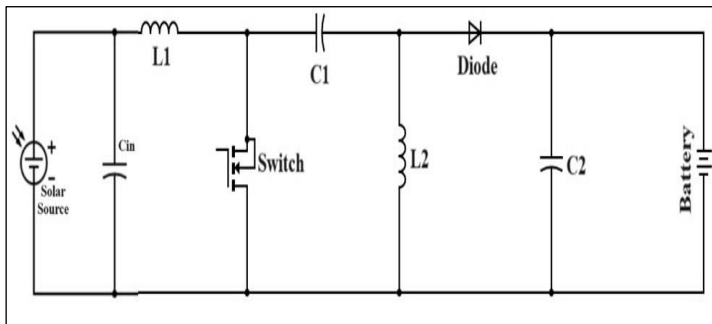
Figure 1. Schematic of Traditional SEPIC Converter.
Source: Authors, (2024).

This topology is modified by incorporating additional components and rearranging the existing components. The schematic of modified SEPIC topology is represented in Figure 2 below [6-10].
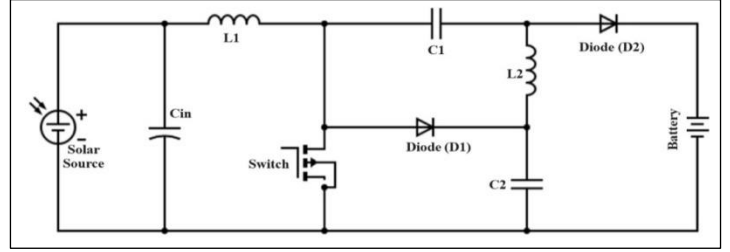
Figure 2: Schematic of Modified SEPIC Converter.
Source: Authors, (2024).

In continuous conduction mode, the duty cycle of the modified SEPIC converter can be determined by

$$Duty\ Cycle\ (D) = \frac{V_{Out} - V_{In}}{V_{Out} + V_{In}} \tag{1}$$

The input current is given by:

$$Input\ Current\ (I_{in}) = \frac{Input\ Power}{V_{In}} \tag{2}$$

The first step in designing a PWM switching regulator is figuring out how much inductor ripple current (ΔI_l) to permit. The inductor ripple current of this topology can be calculated using expression below

$$Inductor\ Ripple\ Current\ (\Delta I_l) = 0.1 * I_{in} \tag{3}$$

The value of inductances can be calculated using the formula

$$L_1 = L_2 = \frac{V_{In} \times D}{\Delta I_l \times F_s} \tag{4}$$

Considering the maximum allowable output ripple to be 2%. The values of capacitances can be determined using the formula

$$C_1 = C_2 = \frac{I_O}{\Delta V_C \times F_s} \tag{5}$$

The change in voltage across the capacitors is determined by

$$\Delta V_C = 0.02\ X\ \frac{V_{out}}{(1 - D)} \tag{6}$$

For switching frequency of 20 kHz and analogous input power and load, the various parameters of SEPIC and Modified SEPIC converters are calculated and the values are tabulated below as Table 2 [11].

Table 2: Parameters of SEPIC & Modified SEPIC Topologies.

S.No	Parameter	SEPIC	Modified SEPIC
1	Max. Duty Cycle	64 %	25.6 %
2	Min. Duty Cycle	60.83 %	21.7 %
3	Inductor (L_1)	362 mH	7 mH
4	Inductor (L_2)	362 mH	7 mH
5	Capacitor (C_1)	2.6 mf	1.7 mf
6	Capacitor (C_2)	3.9 μf	1.7 mf

Source: [11].

III. SIMULATIONS AND RESULTS

This study investigates the charging performance of a 48V, 200Ah electric vehicle (EV) battery using a 2kW solar photovoltaic (PV) source with a modified SEPIC converter. The simulation is conducted within the MATLAB/Simulink environment. Key parameters such as voltage, current, and power from the PV panel are monitored alongside the battery's state of charge (SoC), charging current, and voltage. Test conditions are maintained consistent across all scenarios. Figures 3 to 11 present the MATLAB/Simulink models, PV characteristics (voltage, current, and power), battery SoC, charging current, and voltage for the modified SEPIC converter under three configurations: without Maximum Power Point Tracking (MPPT), with Perturb and Observe (P&O) MPPT, and with Incremental Conductance MPPT.
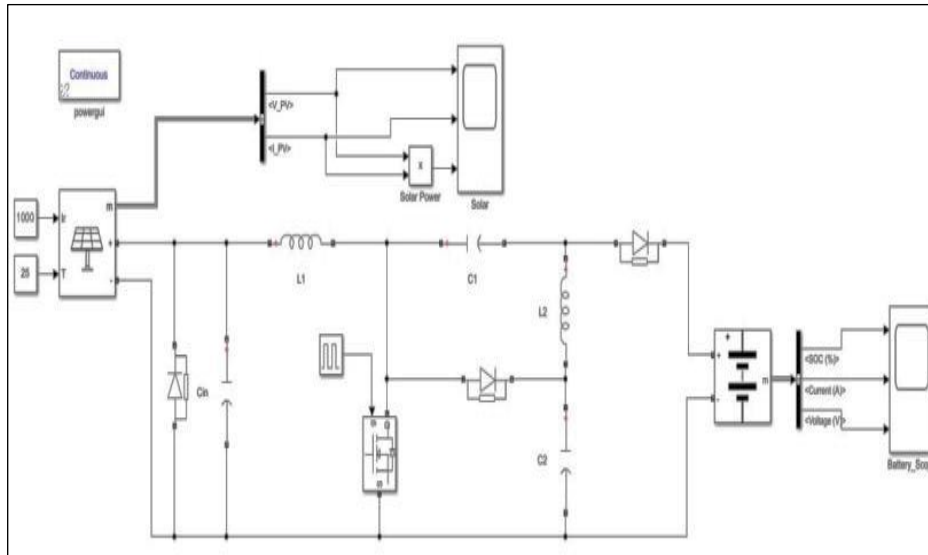
Figure 3: MATLAB/Simulink Model of modified SEPIC converter without MPPT.
Source: Authors, (2024).
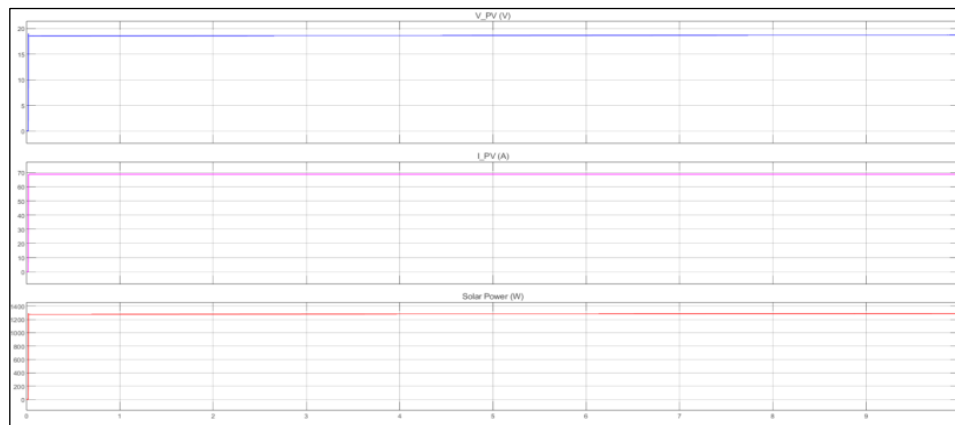
Figure 4 : PV characteristics results for modified SEPIC converter with out MPPT.
Source: Authors, (2024).
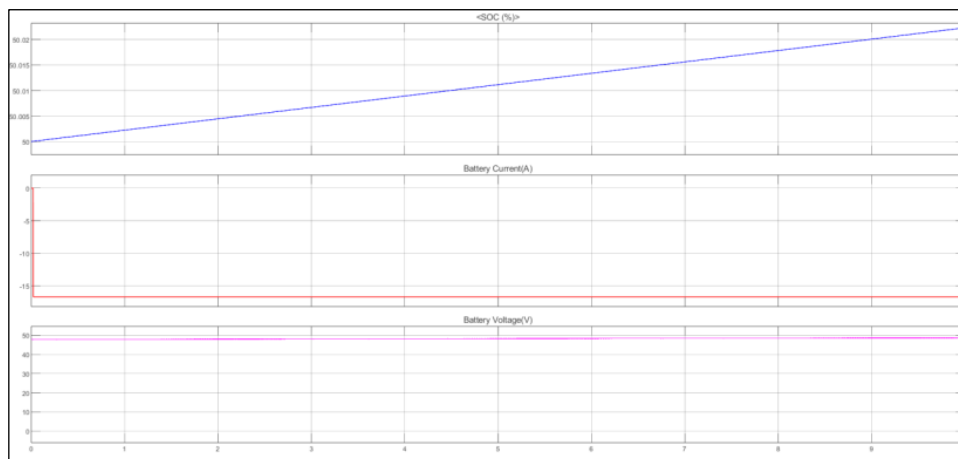
Figure 5: Battery charging results for Modified SEPIC converter with out MPPT.
Source: Authors, (2024).
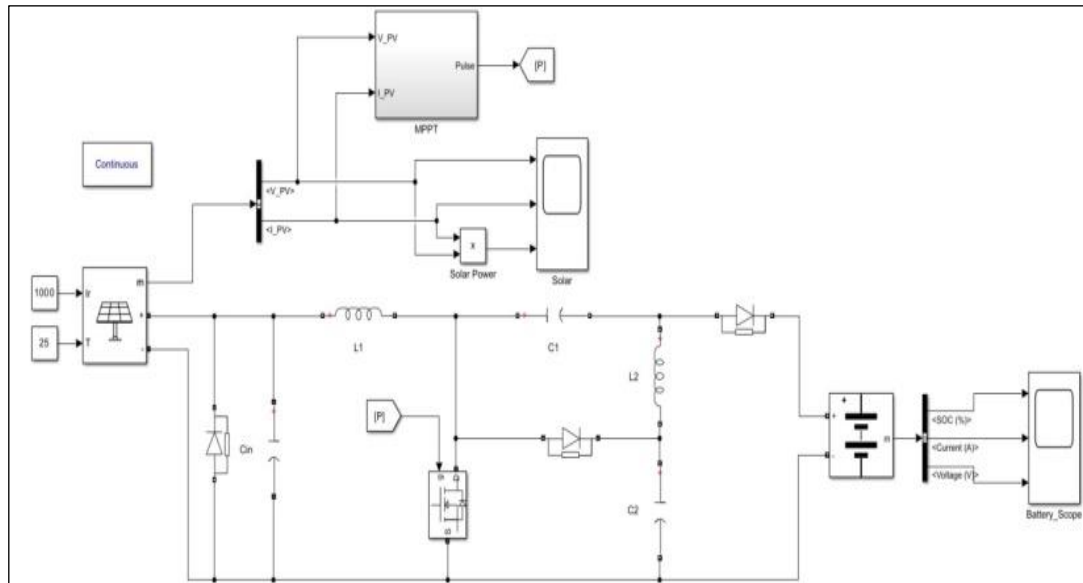
Figure 6 : MATLAB/Simulink Model of modified SEPIC converter with P&O MPPT.
Source: Authors, (2024).
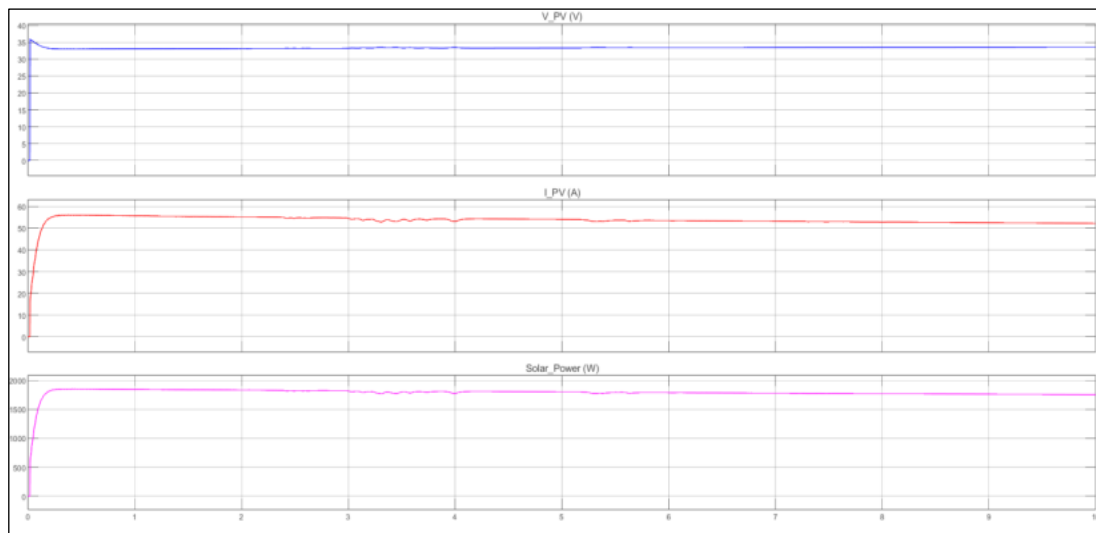
Figure 7: PV characteristics results for modified SEPIC converter with P&O MPPT.
Source: Authors, (2024).
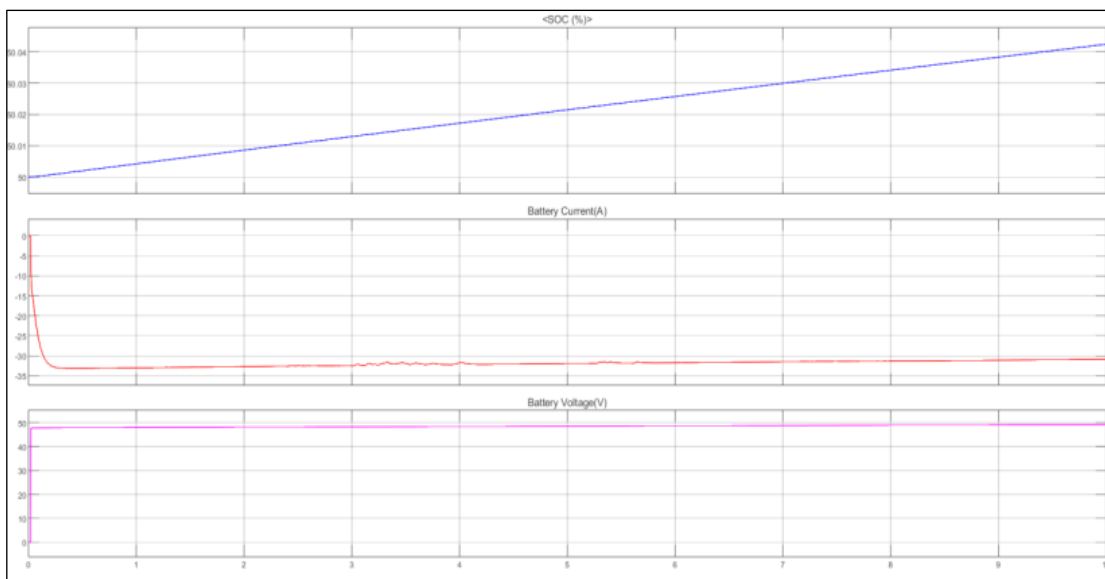
Figure 8: Battery charging results for Modified SEPIC converter with P&O MPPT.
Source: Authors, (2024).
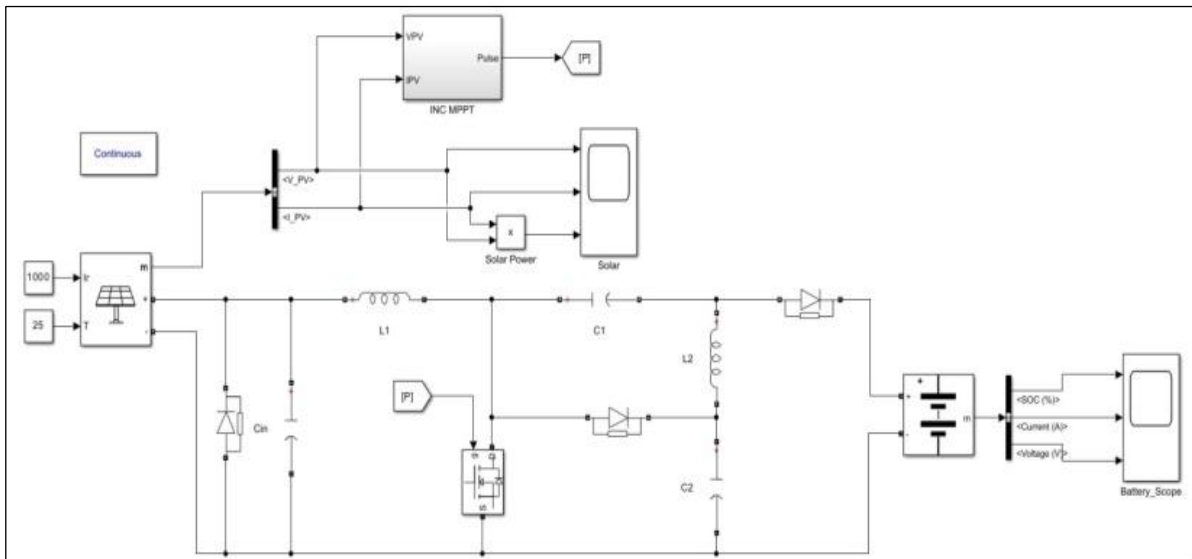
Fig. 9 : MATLAB/Simulink Model of modified SEPIC converter with INC MPPT.
Source: Authors, (2024).
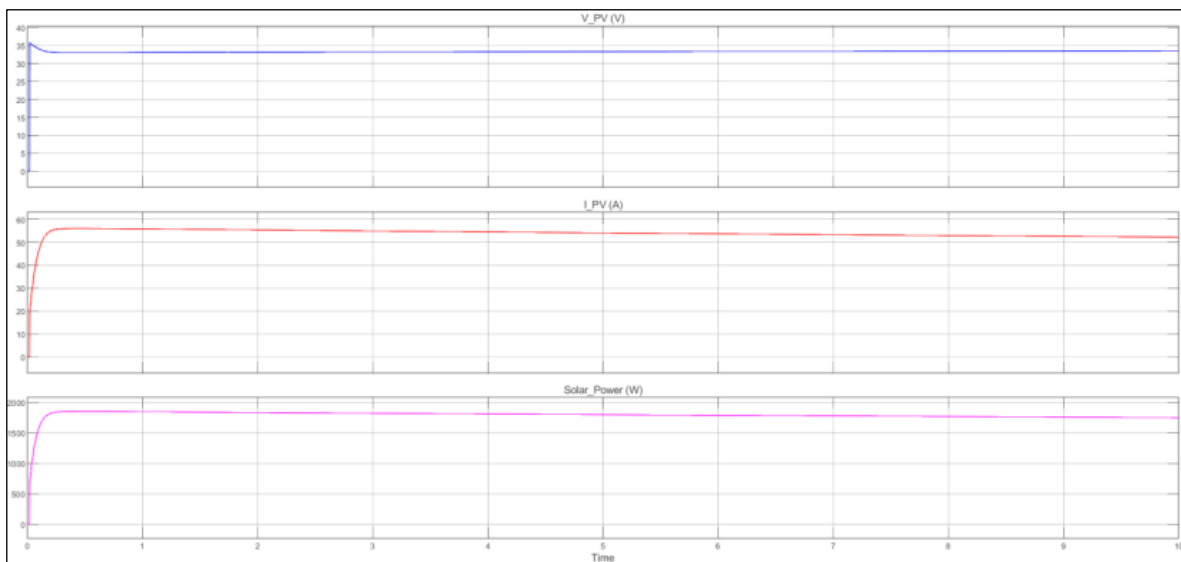
Figure 10: PV characteristics results for modified SEPIC converter with INC MPPT.
Source: Authors, (2024).
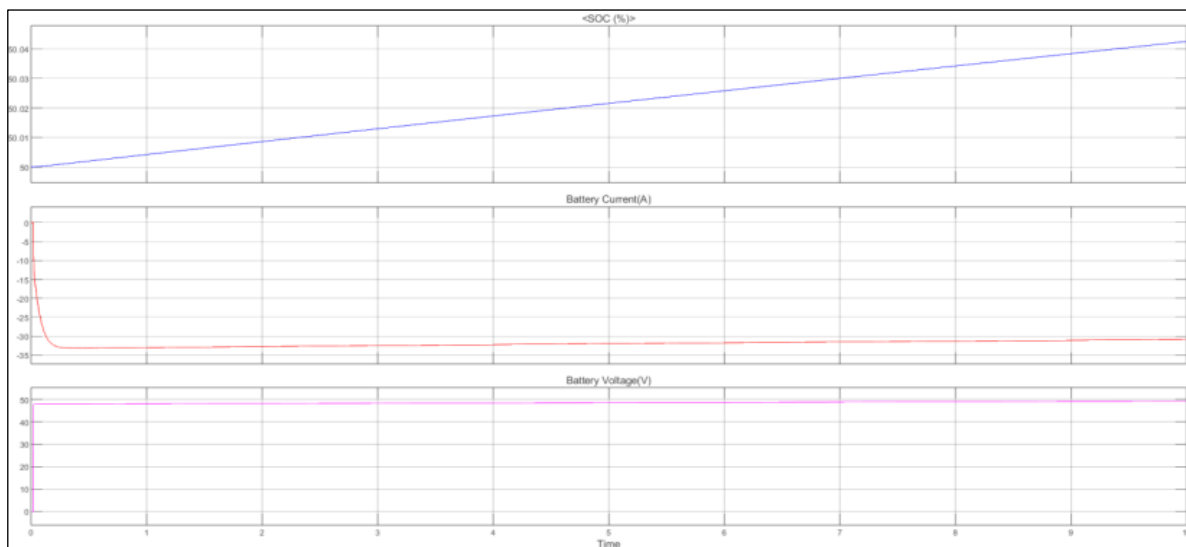
Fig. 11: Battery charging results for Modified SEPIC converter with INC MPPT.
Source: Authors, (2024).

Under identical test conditions, the performances of EV charging system powered by solar PV employing SEPIC and Modified SEPIC converters with and without MPPT methodologies are represented in the table 3. It's important to note that negative battery current values indicate the battery is in charging mode [11].

Table 3: Simulation results with SoC of 50% and simulation time of 10sec.

para meter	SEPIC Converter			Modified SEPIC Converter		
	With out MPPT	With P&O MPPT	With INC MPPT	With out MPPT	With P&O MPPT	With INC MPPT
SoC (%)	50.02	50.03	50.035	50.034	50.042	50.042
V_b (V)	48.52	48.93	49.01	48.9	49.2	49.3
I_b (A)	-14.84	-23.2	-25.1	-24.17	-30.92	-30.94
V_{pv} (V)	35.59	34.47	34.05	34.76	33.52	33.5
I_{pv} (A)	23.16	41.37	46.6	37.57	52.2	52.25
P_{pv} (W)	824.2	1426	1587	1306	1751	1752

Source: Authors, (2024).

IV. CONCLUSIONS

This paper presented a novel PV-fed EV charging system utilizing a modified SEPIC converter. The proposed system offers several advantages, including high efficiency, reduced switch voltage stress, and the ability to integrate MPPT algorithms for maximizing power extraction from the PV panels. The simulation results demonstrated the effectiveness of the implemented MPPT techniques in enhancing the system's performance compared to the scenario without MPPT. This study paves the way for further research and development of efficient and sustainable EV charging solutions utilizing renewable energy sources. The simulation results demonstrate that the modified SEPIC converter delivers significantly higher current compared to the traditional SEPIC converter, leading to a faster increase in the battery's state of charge. For instance, charging a battery without Maximum Power Point Tracking (MPPT) takes approximately 6.94 hours with a SEPIC converter, while the modified SEPIC converter achieves the same in only 4.09 hours. The advantage persists even with MPPT techniques. Regardless of the MPPT method employed (Perturb and Observe or Incremental Conductance), the modified SEPIC converter consistently achieves faster charging times (3.3 hours) compared to the SEPIC converter (4.63 hours and 3.97 hours, respectively). These findings clearly indicate that the modified SEPIC converter offers a more effective solution for charging electric vehicle batteries using solar power.

V. AUTHOR'S CONTRIBUTION

Conceptualization: Bondu Pavan Kumar Reddy and Vyza Usha Reddy.
Methodology: Bondu Pavan Kumar Reddy and Vyza Usha Reddy.
Investigation: Bondu Pavan Kumar Reddy and Vyza Usha Reddy.
Discussion of results: Bondu Pavan Kumar Reddy and Vyza Usha Reddy.
Writing – Original Draft: Bondu Pavan Kumar Reddy.
Writing – Review and Editing: Bondu Pavan Kumar Reddy.
Resources: Vyza Usha Reddy.
Supervision: Vyza Usha Reddy.
Approval of the final text: Bondu Pavan Kumar Reddy and Vyza Usha Reddy.

VI. ACKNOWLEDGMENTS

VII. REFERENCES

[1].Ali M. Eltamaly, Almoataz Y. Abdelaziz, "Modern Maximum Power Point Tracking Techniques for Photovoltaic Energy Systems", Springer international publishing, October 2019, ISBNs: 978-3-03-005577-6, https://doi.org/10.1007/978-3-030-05578-3

[2].H. Suryoatmojo, I. Dilianto, Suwito, R. Mardiyanto, E. Setijadi and D. C. Riawan, "Design and analysis of high gain modified SEPIC converter for photovoltaic applications," 2018 IEEE International Conference on Innovative Research and Development (ICIRD), Bangkok, Thailand, 2018, pp. 1-6, https://doi.org/10.1109/ICIRD.2018.8376319

[3].Data sheet, Hanselng Technologies Ltd., Available online: https://hanselng.com (Accessed on 25 January 2023).

[4].J.Falin, "Designing DC/DC Converters Based on SEPIC Topology", Available online: https://www.ti.com/lit/an/slyt309/slyt309.pdf (accessed on 9 February 2023).

[5].E. Babaei and M. E. Seyed Mahmoodieh, "Calculation of Output Voltage Ripple and Design Considerations of SEPIC Converter," in IEEE Transactions on Industrial Electronics, vol. 61, no. 3, pp. 1213-1222, March 2014, https://doi.org/10.1109/TIE.2013.2262748

[6].R. Gules, W. M. dos Santos, R. C. Annunziato, E. F. R. Romaneli and C. Q. Andrea, "A modified SEPIC converter with high static gain for renewable applications," XI Brazilian Power Electronics Conference, Natal, Brazil, 2011, pp. 162-167, https://doi.org/10.1109/COBEP.2011.6085178

[7].A. K. Mishra and B. Singh, "Modified SEPIC Converter Utilizing an Improved P&O Algorithm for Design of Low Cost and Efficient Solar Energized Water Pump," 2018 IEEE Industry Applications Society Annual Meeting (IAS), Portland, OR, USA, 2018, pp. 1-8, https://doi.org/10.1109/IAS.2018.8544680

[8].P. K. Maroti, R. Al-Ammari, A. Iqbal, L. Ben-Brahim, S. Padmanaban and H. Abu-Rub, "A Novel High Gain Configurations of Modified SEPIC Converter for Renewable Energy Applications," 2019 IEEE 28th International Symposium on Industrial Electronics (ISIE), Vancouver, BC, Canada, 2019, pp. 2503-2508, https://doi.org/10.1109/ISIE.2019.8781163

[9].P. Parthasarathy, G. J. R. Dayananth, R. Murugan and B. Umeshwaran, "Design of 24 Watts SEPIC DC-DC Converter for Renewable Source Applications," 2022 4th International Conference on Inventive Research in Computing Applications (ICIRCA), Coimbatore, India, 2022, pp. 146-149, https://doi.org/10.1109/ICIRCA54612.2022.9985635

[10]. C. Muranda, E. Ozsoy, S. Padmanaban, M. S. Bhaskar, V. Fedák and V. K. Ramachandaramurthy, "Modified SEPIC DC-to-DC boost converter with high output-gain configuration for renewable applications," 2017 IEEE Conference on Energy Conversion (CENCON), Kuala Lumpur, Malaysia, 2017, pp. 317-322, https://doi.org/10.1109/CENCON.2017.8262505

[11]. Bondu Pavan Kumar Reddy, V.Usha Reddy, "PV-Based Performance Evaluation of ZETA and SEPIC Topologies for EV Applications," Journal of Electrical Systems, vol.20, no. 5s, pp. 438-446, 2024, https://doi.org/10.52783/jes.2068
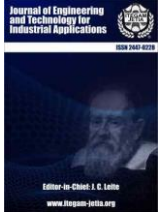
RPG BASED EDUCATIONAL GAME ON BASIC ARITHMETIC USING THE MDLC METHOD

*Dedi Saputra[1], Haryani[2], Eva Meilinda[3] and Juniato Sidauruk[4]

[1,2,3] Departement of Information System, University of Bina Sarana Informatika, Indonesia.
[4] Department of English, University of Bina Sarana Informatika, Indonesia.

[1] http://orcid.org/0000-0002-7888-7049, [2] http://orcid.org/0000-0002-4103-3058, [3] http://orcid.org/0009-0002-9336-0947,
[4] http://orcid.org/0000-0001-5872-3533

Email: [1] dedi.dst@bsi.ac.id, [2] haryani.hyi@bsi.ac.id, [3] eva.emd@bsi.ac.id, [4] juniato.jnd@bsi.ac.id

ARTICLE INFO

ABSTRACT

This study aims to build an educational game on basic arithmetic operations (addition, subtraction, multiplication and division) for elementary school students. This educational game application was created using the Multimedia Development Life Cycle (MDLC) development method developed by Luther-Sutopo, with 6 development phases including concept, design, material collection, assembly, testing and distribution. The use of RPG Maker MV to make an educational game called Hero of Mathematics is more interactive and interesting. The results of the material and multimedia test related to the feasibility of the game got a score of 4,025 and 4.4 which are included in the strong interpretation. Meanwhile, in the attractiveness test, the game got a score of 3.8 which is included in the very interesting criteria. Thus, this Pahlawan Matematika (Mathematics Hero) educational game can be said to be feasible to be used as a medium for learning mathematics, especially basic arithmetic operations material for 1st grade elementary school students.

I. INTRODUCTION

Games are now very easily accessible to the public via mobile devices, smartphones, PCs and internet cafes. Different types of games like RPG (Role Playing Game), FPS (First Person Shooter), MMO (Massively Multiplayer Online), RTS (Real Time Strategy) and others. Today's game industry is not only entertainment-oriented, but also can be used as a medium for children to learn, so that children become more interested in a subject. RPG is a game in which players take on the role of imaginary characters and work together on adventures to create a story together [1],[2]. Players choose their character's based on the character's characteristics, and the success of their actions depends on a predetermined system of game rules. Game-based learning is an educational approach that integrates multiple academic themes into a single learning activity, can facilitate learning by contextualizing new information within existing knowledge and personal experience, and can encourage active participation and responsibility [3]. Educational role play is a way to master problems by developing students' imagination and appreciation [4],[5].

Educational games are a type of games that support the learning process in a more fun and creative way, and serve to provide material or user knowledge with interactive support [6]. The use of game elements in the educational field is having positive consequences on the learning process, and motivation in students [7]. Educational games are games meant to teach certain themes, broaden concepts, boost development, comprehend a historical or cultural event, or aid in learning while playing [8],[9]. Educational games are games with educational features that may be utilized as alternative medium to transmit subject matter in an engaging manner. An educational game, often known as an edugame, is a game that is used to aid in the learning process, training, and knowledge enrichment [10]. Most countries have a high need for instructional games before children even enter school. Early childhood learning games are the most popular mobile educational games in most nations. A game learning media is a game that employs media in its operation and has rules and difficulties that must be completed or the mission to be completed or the objective to be attained [11],[12].

II. THEORETICAL REFERENCE

II.1 GAME-BASED LEARNING

Game-based learning is a learning phase in which games are used as an alternative to attaining learning goals [13]. Game-based learning is learning emphasizes achieving a goal in determining the type of game, providing clear directions for learning objectives, providing other learning stimuli and improving the abilities of users that are used in everyday life. Game-based learning is an innovative method that offers benefits to improve the training process and facilitate motivation to learn. Game-based learning increases logical-mathematical ability to think [14]. Effective game-based learning can improve students' attitudes towards mathematics and produce better learning outcomes. Game-based learning is an effective learning strategy to strengthen understanding and improve learning performance through challenges and in-game content. Therefore, further innovation in game-based learning needs to be ensured. One is with comic book games [15].

Games are privileged environments of motivation and commitment. It is only natural that some researchers have devoted some of their efforts to studying ways to import their main features into tools to support learning (serious games), improving not only student knowledge but also the development of fundamental mathematical skills such as problem solving, mathematical reasoning, and mathematical communication [16]. One of the factors causing low mathematics achievement is currently due to the lack of varied learning media fun for students. As a result, the availability of learning media that allow children to discover fundamental mathematics while having fun in the form of a digital game is required [17]. In every mathematics learning, students can have a confident sense of attachment to complicated mathematical assignments chosen by the teacher, while the teacher should assist students in creating, refining, and exploring conjectures in such a way that they can persuade themselves of the conjecture's veracity [18]. Students prefer to play dynamic games compared to listen to teacher explanations through web meeting applications or just doing tasks that tend to be monotonous and boring. These facts make the teaching staff look for alternative learning components, one of which is by developing learning media that can increase students' learning motivation. Education games are one type of media that may be created to enhance online learning activities [19],[20].

One of the reasons pupils are unable to answer mathematical problems correctly is a lack of understanding of mathematical ideas. The difficulty of understanding mathematical concepts is due to the lack of student interest in learning about mathematics. Students that are uninterested in learning will be inattentive when engaged in learning, which will hinder student success [21]. The low learning achievement of students in mathematics, occurs in most of the material being taught. One of them is material on number. The low achievement of students' mathematics learning, especially on the number material, is a very important problem to be overcome. This is due to the urgency of the material as one of the prerequisite materials for other subjects in mathematics. Although this material is a prerequisite material for other materials, in general, some students are less interested in the lessons delivered by the teacher. This condition indicates that learning mathematics in class is less attractive. Problems related to students' poor understanding of mathematical concepts can be overcome by creating learning media that piques students' interest in learning and improves their understanding of mathematical

concepts. Students can learn independently about learning materials at school using the multimedia learning method without having to wait to ask a teacher when they are having difficulties. The use of multimedia in learning can provide a stimulus to students to be more enthusiastic and focus their attention on the teaching materials being taught [22]. As a result, the creation of learning media is required to motivate kids to learn [23].

II.2 MATHEMATICS LEARNING

Most individuals find mathematics tough to learn since it is the most difficult and a plague in learning. Mathematics is not only for science but also a very important tool for people that we use to solve the problems in our daily lives [24]. It is critical to understand the four basic operations in a balanced manner if this is to aid studying mathematics. The basic mathematical operations required to study mathematics are addition, subtraction, multiplication, and division. E.A Bilgin's research "A Mobile Educational Game Design for Eliminating Math Anxiety of Middle School Students" indicates that one of the reasons students struggle with the topic of four operations known as arithmetic operations is that they misunderstand the principles of addition, subtraction, multiplication, and division or learn these rules incorrectly [25].

According to another research, the aggregate of these improved indices shows that objectives were reached while making mathematics an engaging, motivating, and entertaining topic, making VLE a valuable tool to supplement traditional teaching ways [26].

Another study, In-Game Activities to Promote Game-Based Math Learning Engagement discovered that refugee allocation and material trading actions boosted student content engagement while in-game development tools and learning assistance increased cognitive engagement. This study also discovered that students' learning engagement was related to their mathematical thinking growth in the setting of GBL [27].

A previous study by Arifah et al. recommended the development of the "Bilomatics" game, which is an educational game including Numbers information for grade 1 elementary school kids and may be utilized as a medium in learning activities. The R&D approach was employed in this investigation, together with the Waterfall development paradigm [28]. The limitation of this research is that it has not illustrated the material in the form of an adventure game, which is currently favored by many children, so it needs to be developed with other methods.

According to another study, this Android-Based Mathematical Educational Game With Children's Arithmetic Concepts intends to create a game application that may educate children or students to learn to count quickly and entertainingly so that children do not become tired of boring learning techniques. Designed in a mobile format, it is intended to be portable. Because of the appealing design of this game, players may learn to count or do mathematics more enjoyably [29],[30]. The limitation of this research is that the material presented is not varied, the new material is limited to addition and subtraction operations.

Based on prior research, the author attempts to create an educational gaming application for children in the first grade by employing more dynamic and intriguing approaches and models. Making the application with RPG Maker MV utilizes the notion of a role-playing game, such that the educational game contains components of enjoyable learning and active learning with problem-solving-based content [31]. Users will be invited to adventure and solve various mathematical problems related to

basic mathematical operations in order to continue the stages of the game.

The MDLC method is used to develop an educational game called Heroes of Mathematics, from concept to distribution, so that the advantages and disadvantages of the educational game application can be identified to achieve its goal as an alternative learning media to improve children's understanding of learning and liking mathematics.

III. MATERIALS AND METHODS

In this study, the application is utilized as an alternative learning media to generate multimedia teaching materials at the primary school level utilizing the MDLC (Multimedia Development Life Cycle) paradigm. MDLC is a technique that includes the following steps: idea, design, material collecting, assembly, testing, and distribution [32],[33]. According to Luther [34],[35] there are 6 stages in MDLC: Concept, Design, Material Collection, Manufacturing, Testing and Distribution [36],[37].

Figure 1: Multimedia Development Life Cycle (MDLC) Method.
Source: Luther's Model, (1994).

1. Concept

The concept of this application as a medium for learning basic mathematical operations in the form of addition, subtraction, multiplication and division for children. This application is named "Pahlawan Matematika" which is packaged in a game that is interactive, fun, and easy to use. This application is also accompanied by examples of exercises that challenge and test the child's ability to apply arithmetic operations.

2. Design

The design of this application consists of a story board design and an interface design.
a. Story Board, to visualize the idea of the application to be built, so that it can describe the storyline of the application, the author makes it in the form of a story board consisting of Main Menu, Intro, Bolang's House, Narration1, Pak RT's House, Narration 2, Dungeon.

3. Material Collection

Material collection is carried out as needed. Such as clipart, photos, graphics, sound and others. This stage can be done by dividing the operation into several levels (parallel) and developed together (assembly).

4. Assembly

At this assembly stage, all multimedia objects and materials are created and developed based on the design stage. By completing each section then all of them are combined into a single unit.

5. Testing

After the assembly phase is complete, testing will be carried out by running the application. This stage is also known as the testing stage. Where will be checked in the application, to find out whether there is an error or not. These checks will be carried out by the creators.

6. Distribution

This stage is done to save the application into an adequate storage media. Such as floppy disks, CD-ROOMs, tapes and others. If the storage media is insufficient to accommodate the application, a compilation stage will be performed on it.

IV. RESULTS AND DISCUSSIONS

System Requirements Analysis is used to ease system analysts to determine the whole that will be used for making the system. System requirements in this study consist of functional requirements and non-functional requirements.
    a.   Functional Needs

Functional is a type of requirement that contains any processes that will be carried out by the system. Functional requirements also contain what information must exist and be generated by the system.

The following are the functional requirements of the game to be made:

1. The game displays a *splash screen*.
2. In the menu display there are options consisting of:
   a. *New Game*, to start a *new game* or start the game from the beginning.
   b. *Continue*, to continue the game that has been saved (save).
   c. *Options*, as a sound or sound settings.

3. While playing (in game) there are also several options, consisting of:
   a. *Item*, to see what items the player has.
   b. *Skill*, to see the knowledge and magic of the character being played.
   c. *Equip*, to see the weapon or armor used by the player's character.
   d. *Status*, to see the status of the character played by the player.
   e. *Options*, serves as a sound or sound settings.
   f. *Save*, to save the game session.

   Game End, to return to the main menu

  b. Non-Functional Needs

Analysis of non-functional requirements is an analysis that contains what properties are used to support the creation of the system. In making this game requires a series of equipment to support the smoothness of the creation and testing of the game " Pahlawan Matematika (Mathematics Heroes)" including the following:

1. Software
    The software needed in making the learning application game " Mathematics Heroes " is as follows:
    a. Microsoft Windows 7 (64bit)
    b. RPG Maker MV
    c. Other programs that support the completion of this game application.

2. Hardware
    a. Computer

    Hardware specification needed to create game application "Pahlawan Matematika" is as follows:
    1. *Processor: Intel(R) Celeron(R) CPU N2920 @1.86GHz 1.86GHz*
    2. *Memory*: 4GB
    3. *HDD*: 500GB
    4. *VGA: Intel(R) HD Graphics*

    b. *Windows Device*

    The specifications of the Windows device used to run this game are as follows:
    1. Laptop: *OS Windows.*
    2. *OS: OS Windows* 32/64 bit (*XP, VISTA, 7, 8,* and *Windows* 10)
    3. *Browser*: *Mozilla Firefox 54.0.1*

    c. Interface
    In building an educational game application that suits the needs and conditions for children, of course an analysis of the interface model that will be applied is needed. The interface design in Pahlawan Matematika educational game consists of:

*   Splash Screen Display

    This display appears a few seconds before entering the main menu.
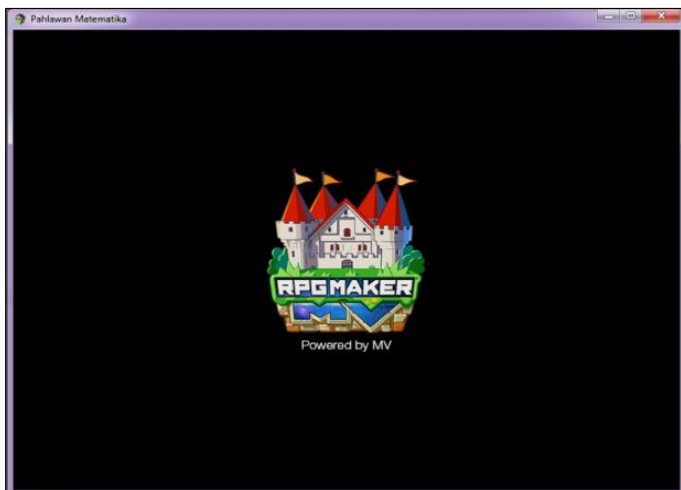
Figure 2: Splash Screen Display.
Source: Authors, (2024).

*   Main Menu Display
    This display contains the title of the application, the New Game button to start a new game, the Continue button to continue the saved game session, and the Options button for sound settings.

Figure 3: Main Menu Display.
Source: Authors, (2024).

*   Menu (*ingame*) Display
    This display contains character information, items, skills, equip, save, end game, status, options.

Figure 4: Menu (ingame) Display.
Source: Authors, (2024).

*   Item Display
    This view contains items owned by the character/player.
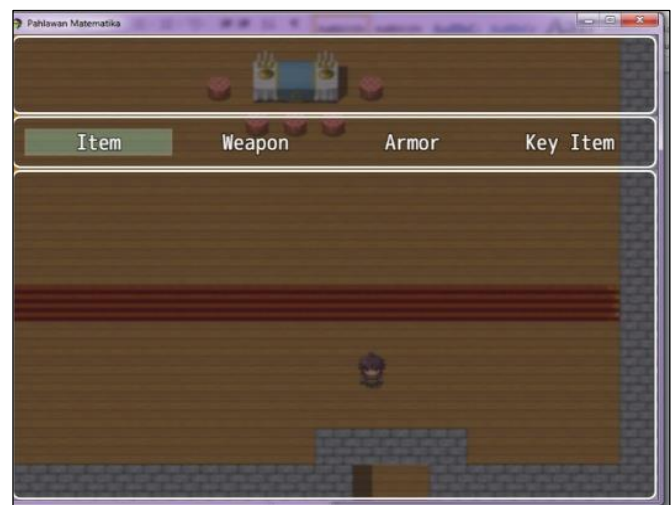
Figure 5: Item Display.
Source: Authors, (2024).

- Skill Display
  This skill display contains skills or moves that characters can use during battle.

Figure 6: Skill Display.
Source: Authors, (2024).

- Equip Display
  This display shows the status of weapons and clothes that can be used by the character/player

Figure 7: Equip Display.
Source: Authors, (2024).

- Status Display
  This view contains information about the character and the clothes or weapons used

Figure 8: Status Display.
Source: Authors, (2024)

- Save Display
  This view contains saved game sessions

Figure 9: Save Display.
Source: Authors, (2024)

- Options Display
  This display is useful for game sound settings, etc.

Figure 10: Options Display.
Source: Authors, (2024)

- Bolang's House Display
  In this display, the player cannot control the character, the character will wake up followed by a narration.

Figure 11: Bolang's House Display.
Source: Authors, (2024).

- Dungeon Display
This display is where the character must defeat 4 bosses to complete this game.
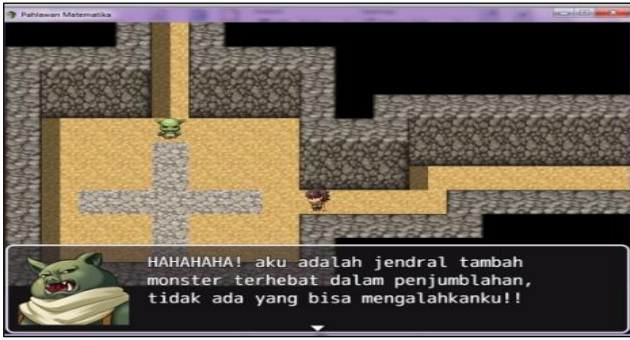
Figure 12: Dungeon Display.
Source: Authors, (2024).

- 12. Battle Display
This display shows the battle between the character and the enemy.

Figure 13: Battle A Display.
Source: Authors, (2024).

Figure 14: Battle B Display.
Source: Authors, (2024).

Testing the Unit

1. Blackbox Testing
Testing of the program made using blackbox testing which focuses on the process of input and output of the program.

Table 1. Event Blackbox testing

Event	Condition	Reaction	Testing Result
Intro	When starting "New Game" (autorun) Players will be given an intro of narration	Show intro of narration	In accordance
Bolang's House	After the intro (autorun)	Show narration, Game take over character and leave home	In accordance
Narration 1	When players leave the restaurant, they will be given narration 1	Show narration 1	In accordance
Practice	When in front of Mr. RT press the "Enter" button	Pak RT Show narration, and give exercises	In accordance
Narration 2	After practicing with Mr. RT this narrative will come out	Show narration 2	In accordance
Boss 1	Walk towards boss1 and touch him (Player Touch)	Battle with boss1	In accordance
Boss 2	Walk towards boss2 and touch him (Player Touch)	Battle with boss2	In accordance
Boss 3	Walk towards boss3 and touch him (Player Touch)	Battle with boss3	In accordance
Boss 4	Walk towards boss4 and touch him (Player Touch)	Battle with boss4	In accordance

Source: Authors, (2024).

Export Project

a. RPG Maker MV page
On the RPG Maker MV Page select Deployment.
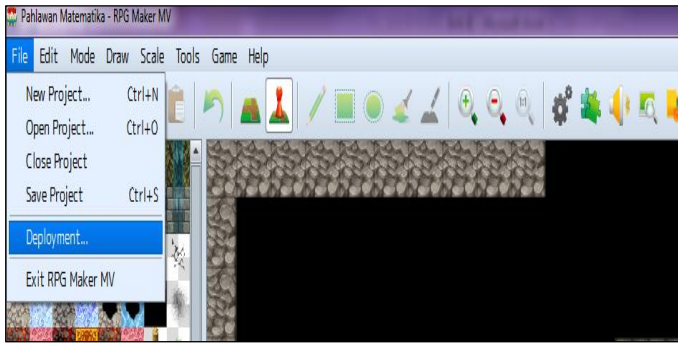
Figure 15: File Page RPG Maker MV Display.
Source: Author, (2024).

After selecting the deployment, select the platform you want to use and then specify the location of the game.
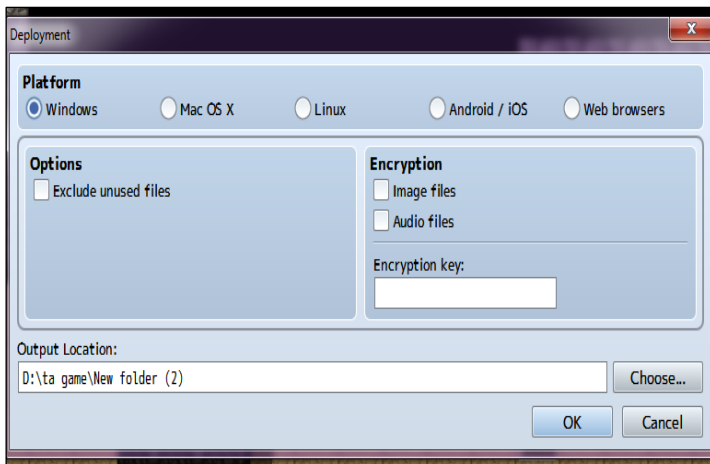
Figure 16: Deployment Display.
Source: Authors, (2024).

After that click "OK" and the game will be exported.
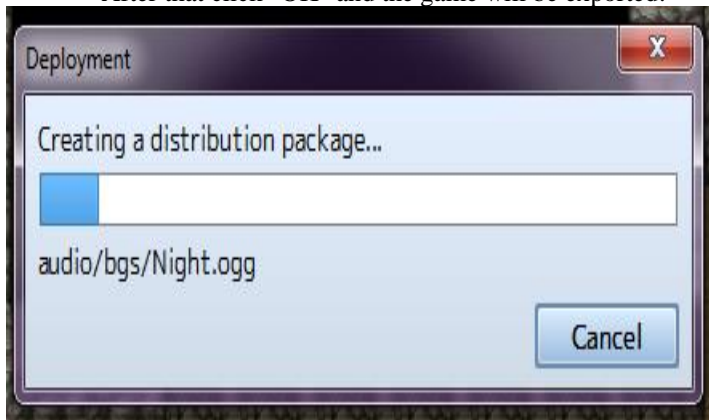
Figure 17: Process Export Display.
Source: Authors, (2024).

b. Export Results Page
After doing all the steps above, the game files and launcher can be found in the selected/defined folder
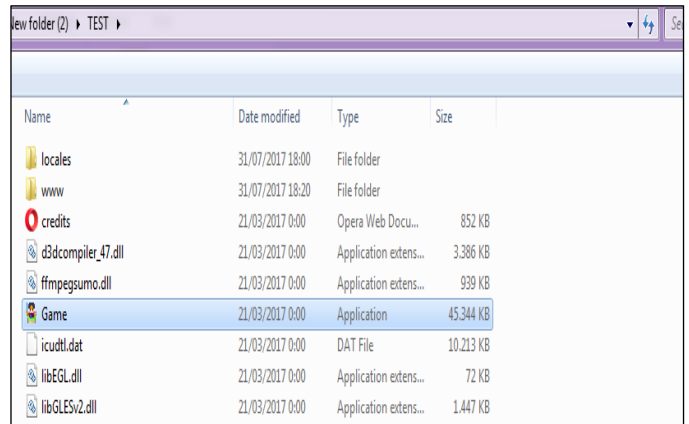
Figure 18: Folder of Export Result Display.
Source: Authors, (2024).

Testing the User Acceptance Test

This test is done by distributing questionnaires to 10 respondents as users of the application that has been made. The scoring for the results of the questionnaire is described in the table.

Table 2. Answer Options and Scoring UAT Testing

Code	Answer	Score
A	Very Easy/Good/Appropriate/Clear	5
B	Easy/Good/Appropriate/Clear	4
C	Neutral	3
D	Fairly Difficult/Good/Appropriate/Clear	2
E	Very Difficult/Bad/Inappropriate/Unclear	1

Source: Authors, (2024).

The details of the questions asked in the UAT test in this study can be seen in the following table:

Table 3. Testing questionnaire format

Code	Question	A	B	C	D	E
P1	Is the appearance of this game interesting?	?	?	?	?	?
P2	Are menu features easy to understand?	?	?	?	?	?
P3	Are the game instructions easy to understand?	?	?	?	?	?
P4	Can game materials help in understanding basic arithmetic operations?	?	?	?	?	?
P5	Does the evaluation (quiz menu) help in measuring understanding of the material?	?	?	?	?	?
P6	Does the card guessing game on this media provide its own challenges for the user?	?	?	?	?	?
P7	Is the card guessing game level good enough to sharpen user's brain?	?	?	?	?	?
P8	Does the puzzle game in this media provide its own challenges for user?	?	?	?	?	?
P9	Is the puzzle game level good enough to sharpen user's brain?	?	?	?	?	?
P10	Can this learning media be used as a learning aid?	?	?	?	?	?
P11	Is this learning media good enough?	?	?	?	?	?

Source: Authors, (2024).

User Acceptance Testing Calculation Results

UAT testing in this study was conducted by distributing question questionnaires to users/respondents. The number of respondents was taken as many as 10 respondents with a total of 11 questions.

Table 4. Questionnaire Answer Data for ICT Educational Games

Code	Answer					Percentage (%)				
	A	B	C	D	E	A	B	C	D	E
P1	7	3	0	0	0	70	30	0	0	0
P2	3	5	0	2	0	30	50	0	20	0
P3	3	6	0	1	0	30	60	0	10	0
P4	3	6	0	0	1	30	60	0	0	10
P5	2	8	0	0	0	20	80	0	0	0
P6	4	5	0	1	0	40	50	0	10	0
P7	7	2	0	1	0	70	20	0	10	0
P8	2	8	0	0	0	20	80	0	0	0
P9	7	2	0	1	0	70	20	0	10	0
P10	8	2	0	0	0	80	20	0	0	0
P11	6	4	0	0	0	60	40	0	0	0

Source: Authors, (2024).

The data obtained is processed by multiplying each answer point with a predetermined score in accordance with the answer value score table. From the calculation results by multiplying each answer with a predetermined score, the following results are obtained:

Table 5. Questionnaire Data after processing

Code	Value (Amount * Grade)					Total	Total / User	%	Final Score
	A *5	B *4	C *3	D *2	E *1				
P1	35	12	0	0	0	47	4,7	94	9,4
P2	15	20	0	4	0	39	3,9	78	7,8
P3	15	24	0	2	0	41	4,1	82	8,2
P4	15	24	0	0	1	40	4	80	8
P5	10	32	0	0	0	42	4,2	84	8,4
P6	20	20	0	2	0	42	4,2	84	8,4
P7	35	8	0	2	0	45	4,5	90	9
P8	10	32	0	0	0	42	4,2	84	8,4
P9	35	8	0	2	0	45	4,5	90	9
P10	40	8	0	0	0	48	4,8	96	9,6
P11	30	16	0	0	0	46	4,6	92	9,2

Source: Authors, (2024).

Discussion

The final score (average) of the User Acceptance Testing test is the number of % divided by 10. The range of values used are:

- Value % >= 90% then the value A is included in the Very Good category
- 80 <= % <= 89.99 then the value B is included in the Good category
- 70 <= % <= 79.99 then the value C is categorized as Good Enough
- 60 <= % <= 69.99 then the value of D is included in the Less category

- 50 <= % <= 59.99 then the value of E is included in the Very Poor category.

From the results of the User Acceptance Testing that was carried out seen from the average results, with an average value of 9, it can be concluded that this Information & Communication Technology Educational Game is Interesting, easy to understand, easy to operate, supports policies, helps / makes it easy, this application is good, good documentation, advanced application technology, error free and needs to be implemented.

V. CONCLUSIONS

More gaming research is required since teaching and curriculum creation should be evidence-based, particularly studies on the efficacy of how effectively programming games may be utilized to improve comprehension of scientific models in mathematics. There are clear impediments to the creation and innovation of instructional games. Small, scattered, and unambitious development programs are one of the issues. To have a large impact, the goods, whether they be instructional techniques games, or programming platforms, should be scalable. Common issues include a lack of investment in learning technology: even if there are good learning games, teacher competency and the availability of appropriate equipment may limit the use of computer games in schools.

VI. AUTHOR'S CONTRIBUTION

Conceptualization: Dedi Saputra.
Methodology: Dedi Saputra, Haryani.
Investigation: Dedi Saputra, Eva Meilinda.
Discussion of results: Dedi Saputra, Haryani, Eva Meilinda.
Writing – Original Draft: Dedi Saputra, Juniato Sidauruk.
Writing – Review and Editing: Dedi Saputra, Juniato Sidauruk.
Resources: Dedi Saputra.
Supervision: Haryani, Eva Meilinda.
Approval of the final text: Dedi Saputra, Haryani, Eva Meilinda, Juniato Sidauruk.

VIII. REFERENCES

[1] A. Syamsudin, R. Mufti, M. I. Habibi, I. K. Wijaya, and N. Sofiastuti, 'Pengembangan game edukasi berbasis web pada materi bangun ruang dengan construct 2', *Journal Focus Action of Research Mathematic (Factor M)*, vol. 4, no. 1, 2021, doi: https://doi.org/10.30762/factor_m.v4i1.3355.

[2] D. Kao, 'The effects of juiciness in an action RPG', *Entertain Comput*, vol. 34, 2020, doi: 10.1016/j.entcom.2020.100359.

[3] S. Koenigstein, 'A game-based education approach for sustainable ocean development', *ICES Journal of Marine Science*, vol. 77, no. 5, pp. 1629–1638, 2020, doi: 10.1093/icesjms/fsaa035.

[4] H. Haryanto, U. Rosyidah, and A. Kardianawati, 'Immersive Activities in Educational Role-Playing Game Based on Appreciative Learning and Artificial Intelligence', in *2019 Fourth International Conference on Informatics and Computing (ICIC)*, IEEE, 2019, pp. 1–6.
[5] J. Silva and I. Silveira, 'A Systematic Review on Open Educational Games for Programming Learning and Teaching', *International Journal of Emerging Technologies in Learning (iJET)*, vol. 15, no. 9, pp. 156–172, 2020.

[6] D. Saputra and A. Rafiqin, 'Pembuatan Aplikasi Game Kuis "Pontianak Punye" Berbasis Android', *Pembuatan Aplikasi Game Kuis "Pontianak Punye" Berbasis Android*, vol. V, no. 2, pp. 71–85, 2017, [Online]. Available: http://ejournal.bsi.ac.id/ejurnal/index.php/khatulistiwa/article/download/2882/1866

[7] A. H. Debón *et al.*, 'Game-based learning with role-playing elements using RPG Maker MZ', *Modelling in Science Education and Learning*, vol. 16, no. 1, pp. 55–65, 2023.

[8] A. Sukstrienwong, 'Animo math: The role-playing game in mathematical learning for children', *Tem Journal*, vol. 7, no. 1, pp. 147–154, 2018.

[9] E. Korkmaz, 'Analysis of Digital Games Related to Mathematics Education with Deconstructing.', *World Journal of Education*, vol. 11, no. 2, pp. 46–55, 2021.

[10] A. H. Sutopo, *Developing Educational Game*. Topazart, 2020.

[11] H. Agustianingrum and Y. Setiawan, 'Pengembangan Game Math-Venture terhadap Pemecahan Masalah Matematika Di Sekolah Dasar', *Jurnal Basicedu*, vol. 5, no. 4, pp. 2348–2357, 2021.

[12] J. Hamari, D. J. Shernoff, E. Rowe, B. Coller, J. Asbell-Clarke, and T. Edwards, 'Challenging games help students learn: An empirical study on engagement, flow and immersion in game-based learning', *Comput Human Behav*, vol. 54, pp. 170–179, 2016.

[13] W. Sulistio and A. Qohar, 'Development of Instructional Media "Game Math Comic Story" Based Android on Number', *Journal of Education Research and Evaluation*, vol. 4, no. 2, pp. 109–113, 2020, doi: http://dx.doi.org/10.23887/jere.v4i2.22370.

[14] M. D. M. Prez, A. G. Duque, and L. F. Garca, 'Game-based learning: Increasing the logical-mathematical, naturalistic, and linguistic learning levels of primary school students', *Journal of New Approaches in Educational Research (NAER Journal)*, vol. 7, no. 1, pp. 31–39, 2018, doi: 10.7821/naer.2018.1.248.

[15] W. Widyasari, H. Sutopo, and M. Agustian, 'QR code-based learning development: Accessing math game for children learning enhancement', 2019, doi: https://doi.org/10.3991/ijim.v13i11.10976.

[16] M. R. Almeida, P. Barros, A. Breda, H. Resende, and E. Rocha, 'The educational math board game 3DM6', *geography*, vol. 3, p. 7, 2019.

[17] M. H. Garry, Y. Yamasari, S. M. S. Nugroho, and M. H. Purnomo, 'Design and Implementation Serious Game "Tic Tac Toe Math"', in *2019 International Conference on Computer Engineering, Network, and Intelligent Multimedia (CENIM)*, IEEE, 2019, pp. 1–6. doi: 10.1109/CENIM48368.2019.8973336.

[18] N. Delima, Y. S. Kusumah, and S. Fatimah, 'Students' Mathematical Thinking and Comprehensive Mathematics Instruction (CMI) Model', *Formatif: Jurnal Ilmiah Pendidikan MIPA*, vol. 11, no. 2, 2021, doi: 10.30998/formatif.v11i2.7807.

[19] R. Adawiyah and L. N. Safrida, 'Pengembangan dan Sosialisasi Game Edukasi Matematika Berbasis Android "GESIT" sebagai Alternatif Media Pembelajaran pada Masa Pandemi COVID-19', *JPKMI (Jurnal Pengabdian Kepada Masyarakat Indonesia)*, vol. 2, no. 2, pp. 83–92, 2021, doi: https://doi.org/10.36596/jpkmi.v2i2.134.

[20] S.-Y. Wang, S.-C. Chang, G.-J. Hwang, and P.-Y. Chen, 'A microworld-based role-playing game development approach to engaging students in interactive, enjoyable, and effective mathematics learning', *Interactive Learning Environments*, vol. 26, no. 3, pp. 411–423, 2018.

[21] L. Costa and L. Santos, 'Environmental Education In Higher Education', *ITEGAM-JETIA*, vol. 3, no. 10, Mar. 2018, [Online]. Available: https://itegam-jetia.org/journal/index.php/jetia/article/view/235

[22] S. Purwanti, R. Astuti, J. Jaja, and R. Rakhmayudhi, 'Application of the Multimedia Development Life Cycle (MDLC) Methodology to Build a Multimedia-Based Learning System', *Budapest International Research and Critics Institute (BIRCI-Journal): Humanities and Social Sciences*, vol. 5, no. 1, pp. 2498–2506, 2022.

[23] L. Ariyanto, N. D. Rahmawati, and A. Haris, 'Pengembangan mobile learning game berbasis pendekatan kontekstual terhadap pemahaman konsep matematis siswa', *JIPMat*, vol. 5, no. 1, 2020, doi: https://doi.org/10.26877/jipmat.v5i1.5478.

[24] Z. Taleb, A. Ahmadi, and M. Musavi, 'The Effect of M-learning on Mathematics Learning', *Procedia Soc Behav Sci*, vol. 171, pp. 83–89, 2015, doi: https://doi.org/10.1016/j.sbspro.2015.01.092.

[25] E. A. Bilgin, 'A Mobile Educational Game Design for Eliminating Math Anxiety of Middle School Students', *Education Quarterly Reviews*, vol. 4, 2021, doi: 10.31014/aior.1993.04.02.251.

[26] J. Maitem, R. J. Cabauatan, L. Rabago, and B. Tanguilig III, 'Math world: A game-based 3d virtual learning environment (3d vle) for second graders', *arXiv preprint arXiv:1203.1964*, 2012, doi: 10.5121/ijma.2012.4101.

[27] J. Moon and F. Ke, 'In-game actions to promote game-based math learning engagement', *Journal of Educational Computing Research*, vol. 58, no. 4, pp. 863–885, 2020, doi: https://doi.org/10.1177/0735633119878611.

[28] R. E. N. Arifah, S. Sukirman, and S. Sujalwo, 'Pengembangan Game Edukasi Bilomatika untuk Meningkatkan Hasil Belajar Siswa pada Mata Pelajaran Matematika Kelas 1 SD', *Jurnal Teknologi Informasi dan Ilmu Komputer*, vol. 6, no. 6, pp. 617–624, 2019, doi: http://dx.doi.org/10.25126/jtiik.2019661310.

[29] W. J. Shudiq, N. Fila, and P. D. C. Khotimah, 'Pengembangan pembelajaran game edukasi aritmatika dasar untuk anak Madrasah Ibtida'iah Nurul Mun'im PP. Nurul Jadid', *COREAI: Jurnal Kecerdasan Buatan, Komputasi dan Teknologi Informasi*, vol. 2, no. 1, pp. 47–51, 2021, doi: DOI : http://doi.org/.

[30] D. Saputra, W. S. Dharmawan, M. Wahyudi, W. Irmayani, J. Sidauruk, and Martias, 'Performance Comparison and Optimized Algorithm Classification', *J Phys Conf Ser*, vol. 1641, pp. 12087–12093, 2020, doi: 10.1088/1742-6596/1641/1/012087.

[31] J. H. K. Smets and E. D. Spek, 'That Sound's Juicy! Exploring Juicy Audio Effects in Video Games', in *International Conference on Entertainment Computing*, Springer, 2021, pp. 319–335.

[32] F. N. Kumala, 'MDLC model for developing multimedia e-learning on energy concept for primary school students', *Journal of Physics: Conference Series*, vol. 1869, no. 1. 2021. doi: 10.1088/1742-6596/1869/1/012068.

[33] U. M. Wahyuni, J. Rahmadoni, A. D. Kartika, and H. Hanim, 'The Combination of R&D and MDLC Models in WEB-Based Interactive Learning Media', *SISTEMASI*, vol. 11, no. 3, pp. 713–723, 2022.

[34] A. C. Luther, *Authoring interactive multimedia*. Academic Press Professional, Inc., 1994.

[35] H. Sutopo and W. Pamungkas, 'Developing mathematics mobile game to enhance learning for children', in *2017 IEEE International Conference on Computational Science and Engineering (CSE) and IEEE International Conference on Embedded and Ubiquitous Computing (EUC)*, IEEE, 2017, pp. 191–197. doi: 10.1109/CSE-EUC.2017.41.

[36] Y. Sumaryana and M. Hikmatyar, 'Aplikasi pembelajaran siswa sekolah dasar menggunakan metode multimedia development life cycle (MDLC)', *TeIKa*, vol. 10, no. 2, pp. 117–124, 2020, doi: https://doi.org/10.36342/teika.v10i2.2381.

[37] H. Putri, I. Shadiq, and G. G. Putri, 'Interactive Learning Media for Cellular Communication Systems using the Multimedia Development Life Cycle Model', *Jurnal Online Informatika*, vol. 6, no. 1, pp. 1–10, 2021, doi: https://doi.org/10.15575/join.v6i1.544.
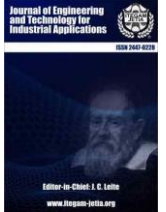
RESEARCH ARTICLE   **OPEN ACCESS**

GEOPHYSICAL INVESTIGATION OF GROUNDWATER CONTAMINATION IN URBAN AREAS: A CASE STUDY OF ACTIVE DUMPSITES IN OYO TOWN, NIGERIA

Kamaldeen Olasunkanmi Suleman[1], Testimony Dayo Owolabi [2], *Olufemi Louis Ogunmola[3], Lukman Ayobami Sunmonu[4] and Bola Abdulhamid Afolabi[5]

[1] Department of Physics, Nigeria Maritime University Okerenkoko, Warri, Delta State, Nigeria.
[2,3,4] Department of Pure and Applied Physics, Ladoke Akintola University of Technology, Ogbomoso, Oyo State, Nigeria.
[5] Department of Physics, Kwara State College of Education, Ilorin, Kwara State, Nigeria.

[1] http://orcid.org/0000-0002-9103-1974 ⓘ, [2] http://orcid.org/0007-0006-4770-4435, ⓘ, [3] http://orcid.org/0000-0003-4113-602X ⓘ
4http://orcid.org/0000-0002-4305-8363 ⓘ, 5http://orcid.org/0009-0002-9670-8697 ⓘ

Email:1 kamaldeen.suleman@nmu.edu.ng, 2owolabi@gmail.com, *3olufemilouis@gmail.com, 4lasunmonu@lautech.edu.ng, 5ba.afolabi@kwcoeilorin.edu.ng

ARTICLE INFO	ABSTRACT
	Environmental safety is a pressing global concern, particularly in Africa, where poor sanitation and contaminated water sources contribute to rising health issues. Active dumpsites are recognized as a source of groundwater pollution, yet their specific impact on water quality remains insufficiently documented. Therefore, this study aimed to evaluate potential groundwater contamination resulting from active dumpsites in the Ilaka area of Oyo town, Nigeria. Electrical Resistivity Tomography was established on two traverses at the study area with a total length of 150 m and 5 m electrode spacing. Eight Vertical Electrical Sounding points were sounded at the established profiles. The geoelectric sections revealed three distinct layers: the topsoil, the weathered layer, and the fresh basement. In Traverse One, the recorded layer resistivity ranges from 29 to 938 Ωm, while in Traverse Two, it ranges from 30 to 1243 Ωm. The corresponding layer thickness varies from 0.8 to 21 m in Traverse One and from 2.5 to 24 m in Traverse Two, indicating a shallow overburden thickness. The 2D image of ERT revealed extremely low resistivity values in all the traverses across the dumpsites which suggests the presence of clay formation underlying the topsoil which may have been trapped in the contaminant plumes. Groundwater from the study area was found to be free from contaminants.

I. INTRODUCTION

Groundwater is a body of water that is deeply-seated in soil from rain or other precipitation and migrates to fill openings in the bed of rocks and soil. It is adequately accumulated in and moves downward through pores in the geologic formation of the soil and rocks called aquifers [1]. Groundwater is a renewable resource, that completely renews itself over time. Although the rate of renewal varies greatly under some environmental conditions, aquifer recharges by rain and snow melt that seep down into the pores

beneath the land's surface [2]. An aquifer is an underground layer of water-bearing permeable rock, rock fractures or unconsolidated materials. Aquifers are generally made up of gravel, sand, sandstone or fractured rock. They allow the movement of water through their materials that have large connected spaces which make them penetrable. Aquifer's pore spaces and how well the pore spaces are connected determine the rate of flow of groundwater in the soil and rock. The exploration for clean groundwater is very significant, due to its countless advantages over surface water. However, the questions of exploration and production such as how

much groundwater is available, and what is its quality? Need to be answered [3]. Groundwater can be explored using different methods. The four major groundwater exploration methods are the areal method, surface method, subsurface method and esoteric methods. Each of the above-listed groundwater exploration methods has different sub-methods under them. Geophysical methods play important roles in locating suitable and productive groundwater reservoirs. Electrical resistivity has been routinely used for subsurface investigation and exploration of groundwater [4]. Electrical resistivity can also be used for the assessment of the hydraulic conductivity of the aquifer, transmissivity of the aquifer, specific yield level of the aquifer and contamination of groundwater [5]. Electrical resistivity methods can be used to obtain details about a location in terms of depth and resistivity of subsurface formation more accurately, rapidly and economically [6],[7].

Groundwater usually moves slowly through pore spaces in rock, and this is filtered of many contaminants and some bacteria and viruses and this makes groundwater suitable as a drinking water resource. Despite this, it never implies that groundwater does not get contaminated; there are various cases worldwide where groundwater resources have been ruined by saltwater intrusion which is peculiar to coastal areas, as well as biological contaminants such as agricultural and industrial discharge, indiscriminate waste and sewage disposal among others. Groundwater contamination may be due to human activities. For example, when wastes generated by residents within a municipality are indiscriminately dumped in an open landfill, after some years, any uncontrolled dumpsites within the municipality undergo biological, chemical, geological and hydrogeological changes which often result in weathering processes and therefore, become point source of contamination of the aquiferous unit close to them and thereby resulting in groundwater contamination [8]. Contaminated groundwater is purely unsafe for consumption and greatly affects human health, even the environmental quality and socio-economic development negatively. The effects of exposure to contaminated groundwater by the populace include chronic and sub-chronic toxicity and carcinogenic effects depending on the type and nature of the contaminant present. Studies have shown that high levels of nitrate, trace metals and persistent organic pollutants cause major health risks to the human population [9], [10].

Pollution by heavy metals in the last decades has been of great concern because of their health hazards to man and other organisms when accumulated within a biological and food production system. For instance, Irrigation with groundwater contaminated by heavy metals and wastewater containing persistent contaminants can result in the accumulation of toxic elements in cereals and vegetables, causing health risks to humans [11],[13]. On the part of socio-economic, some billions of US dollars that can be utilized by worldwide associations and non-legislative offices for enhancing the prosperity of nearby neighbourhoods is fundamentally occupied for water-borne disease eradication. Numerous of these cases are available today in various Nigerian and international publications, the major concern remains how the problems could be fully addressed. It is on this note that this research was chosen to re-address the problem of groundwater contamination within the Ilaka community of Oyo Metropolis using the geophysical approach.

II. THEORETICAL REFERENCE

As interest in groundwater potential and the impact of contaminants from active dumpsites on groundwater continues to rise, several scholars have conducted extensive research to elucidate its multifaceted nature and impact. For [14] assessed the groundwater contamination around Ajakanga active dumpsite in Ibadan, South-western Nigeria using integrated electrical resistivity and hydro-chemical methods. A total number of ten traverses were established within and outside the dumpsite using Wenner array configuration with constant electrode spacing ranging from 5 to 25 m. The geochemical assessment of groundwater samples was also carried out in accordance with American Public Health Association (APHA) (2005) standards. It was concluded that low resistive zone with resistivity values < 20 Ωm was observed as an indication of leachate plume and 15.9 m as the maximum depth of investigation. It was also observed from the result of the physiochemical analysis that some of the hand-dug wells lie within the WHO (2007)/Nigerian standard for drinking water quality (NSDWQ) (2007) specification limit for drinking purposes except for those close to the dump site. For [15] conducted a geophysical investigation utilizing the Vertical Electrical Sounding (VES) method in the residential area of Aaba in Akure, employing a Schlumberger array. The choice of the study area stemmed from the prevalent water scarcity experienced by inhabitants, attributed to low yields from surrounding wells. The geoelectrical approach was selected due to its efficacy in elucidating subsurface geological characteristics. The study was structured to facilitate spatial mapping of geoelectrical parameters, with sixteen (16) VES points strategically acquired across four (4) traverses to ensure comprehensive coverage. Specifically, VES 2, VES 10, and VES 12 were executed in proximity to existing wells approximately 9 meters deep. Notably, this investigation represents the inaugural effort to evaluate the groundwater potential within the study locale. Despite initiatives such as the "water for life by 2015" campaign spearheaded by the United Nations, the persisting water scarcity in the area persisted through 2017.

Also carried out geophysical and hydro chemical investigation of Jembewon dumpsite located in basement complex area of Ibadan, South-western Nigeria using integrated electrical resistivity method with a view to assess the impact of effluent from the ancient dumpsite on the soil and groundwater system [16]. Dipole-dipole and vertical electrical sounding (VES) was carried out while the hydro chemical investigation of the area involves the physical, chemical and microbial analysis of water sample within the active dumpsite. It was concluded that the area was made up of maximum of four layer which are; the topsoil, the weathered layer, the partly weathered/fractured basement and fresh basement with the partly weathered/fractured basement constitutes the major aquifer unit. It was also suggested that the weathered layer and the overlying layers which were characterized by low resistivity value < 30 Ωm have been impacted by effluent from both the active and reclaimed dumpsites. However, the research suggested that the aquifer in the study area is safe from contaminant due to the fact that the suspected leachates are held within the weathered layer by the presence of suspected geological barriers.

Adopted the use of Vertical Electrical Sounding (VES) and 2-D resistivity imaging (employing Schlumberger and Wenner array configurations) to investigate and map the extent of leachate's migration and its possible impacts on groundwater within Abata Asunkere dumpsite, Ilorin, Kwara State [17]. The 2-D resistivity imaging and VES data were processed using Res2D and IPI2Win software respectively. The outcome of this study was able to indicate that some regions around the dumpsite are susceptible to leachate's contamination, which has tendencies to permeate the unconfined aquifers in the study area if not properly monitored and controlled.

II.1 SITE DESCRIPTION AND GEOLOGY

Oyo town is located in Oyo State, and lies within Latitude 7°47`02``N to 7°62`01``N and Longitude of 3°53`27``E to 4°00`00``E (Figure 1). The study area can be found within the humid and sub-humid tropical climate of southwestern Nigeria. It is well accessible as there are well-developed road networks in the town. The area is relatively rugged; characterized by an undulating surface topography. The elevation ranged from 270 m to 290 m (Figure 1). The vegetation cover is sparse in the developed section of the town but exist as a forest in the undeveloped area.

The study area experiences two seasons which are the rainy season which runs from March to October and the dry season which runs from early November to February. Oyo town is found within the basement complex area of southwestern Nigeria, containing distinguishable Gnesis-migmatite complex [18].
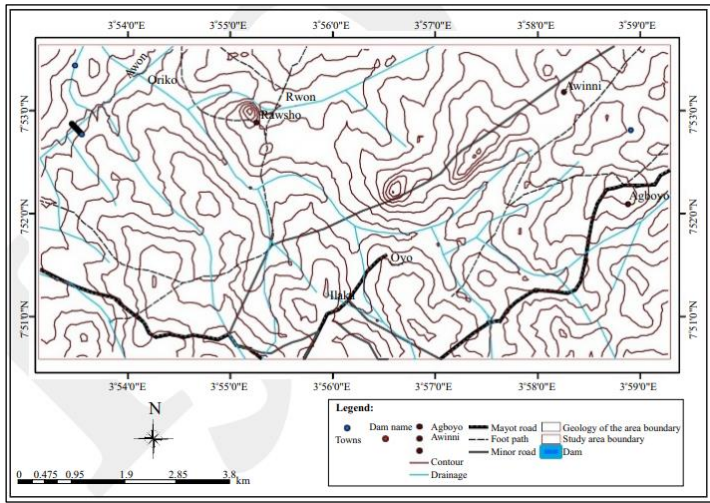
Figure 1: Topographic Map of the Study Area.
Source: [19].

III. MATERIALS AND METHODS

An integrated electrical resistivity method was employed for this survey. The following data were acquired from each of the approaches.

III.1 ELECTRICAL RESISTIVITY TOMOGRAPHY DATA ACQUISITION

Electrical Resistivity Tomography was carried out at Ilaka dumpsite using a dipole-dipole configuration. Two traverses were occupied at each location with a total length of 130 m at electrode spacing of 5 m as indicated in Figure 2.
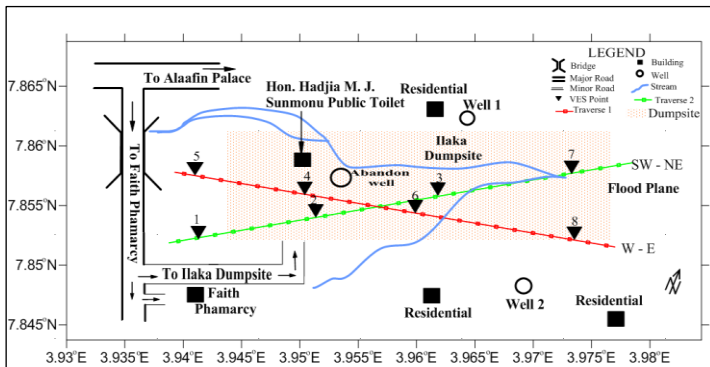
Figure 2: Base Map of Ilaka Dumpsite.
Source: Authors, (2024).

The two current electrodes occupy the first two stations (that is Positions number one and two) while the potential electrodes occupy the third and fourth positions. The data was taken by the instrument (R-50 resistivity meter) at the mid-point between the current and potential dipole. Then the potential electrodes move to position number four and five respectively. This process continues as current electrodes remain in positions one and two and the potential electrodes move out one electrode spacing for each reading. The space between the second current and first potential increases by expansion factor n varies from 1 to 5 which represents the maximum depth of the probe. After attaining the expansion factor of n = 5, the current electrodes then move out a step from position one and two to position two and three respectively while the potential electrode comes back to position four and five. This cycle continues throughout the electrode array and the data were acquired.

III.2 VERTICAL ELECTRICAL SOUNDING (VES) DATA ACQUISITION

The vertical electrical sounding (VES) approach was carried out on the field at the established traverses in each location using the Schlumberger array. A total of three VES points at least was established on each traverse in all the locations as shown in Figure 2 using an R-50 DC resistivity meter. The current electrodes were moved between AB/2 of 1 to 65m while the potential electrodes varied from 0.5 to 5m that is, MN/2 of 0.25 to 2.5m. The apparent resistivity values in each VES data were computed using Equation 1.

$$\rho_{Sa} = R \frac{\pi(L^2 - l^2)}{2l} \tag{1}$$

Where;

$$\frac{\pi(L^2 - l^2)}{2l}$$

Is the geometry factor K
$$L = \frac{AB}{2}, \text{ and } l = \frac{MN}{2} \tag{2}$$

III.3 DATA PRESENTATION AND INTERPRETATION

In all, a total number of eight (8) VES points were established as a control to the results of Dipole-Dipole. The apparent resistivity values obtained from the data were then plotted against half of the current electrode spacing (AB/2) on a bi-log graph and the smooth curve was produced using a free hand sketch to give a typical Schlumberger curve for each location.

The conventional manual curve matching was used to obtain the preliminary layer parameter while a computer iteration of the preliminary layer parameter was also done using WinResist software. The iterated geo-electric parameters obtained from WinResist were later used to generate the geo-electric sections beneath each traverse using surfer 12.

IV. RESULTS AND DISCUSSION

IV.1 ELECTRICAL RESISTIVITY RESULTS

The results of the eight (8) VES points within the study area revealed varieties of H-type curves as shown in Figure 3a – 3h. It was also observed that the VES curves obtained from the study area indicate three layering models in terms of layer thickness and layer resistivity as shown in Table 1.
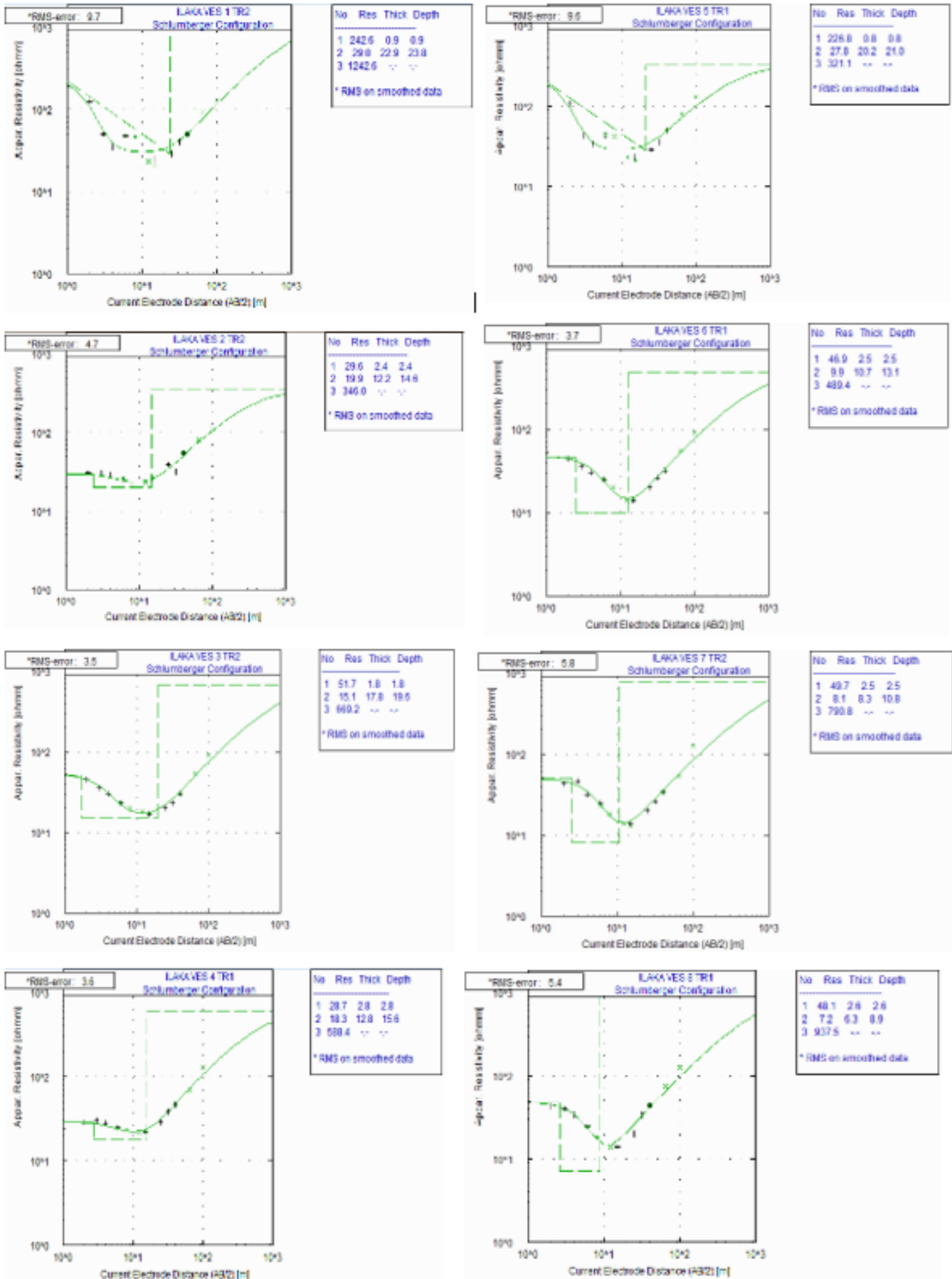
Figure 3a – 3h: Results from computerized sounding curve interpretation, the estimated geo-electric parameters and depth estimate.
a) VES 1 (b) VES 2 (c) VES 3 (d) VES 4 (e) VES 5 (f) VES 6 (g) VES 7 (h) VES 8.
Source: Authors, (2024).

Table 1: Summary of Results of the Processes VES Data within Ilaka Dumpsite.

VES Station	Number of Layers	Curve Type	Layer Resistivity (Ωm)			Layer Thickness (m)		Depth to Bedrock (m)
			ρ_1	ρ_2	ρ_3	h_1	h_2	
1	3	H	243	29	1242	0.9	22.9	23.8
2	3	H	30	20	346	2.4	12.2	14.6
3	3	H	52	15	669	1.8	17.8	19.6
4	3	H	29	18	588	2.8	12.8	15.6
5	3	H	227	28	321	0.8	20.2	21.0
6	3	H	47	10	489	2.5	10.7	13.1
7	3	H	50	8	791	2.5	8.3	10.8
8	3	H	48	7	938	2.6	6.3	8.9

Source: Authors, (2024)

IV.2 GEO-ELECTRIC SECTION PARAMETERS AT ILAKA DUMPSITE

The geo-electric equivalence of the geologic sections of Traverse 1 and Traverse 2 across the dumpsite are depicted in Figures 4 and 5, respectively. In Traverse 1, comprising VES 4, VES 5, VES 6, and VES 8, with VES 5 serving as the control VES at a distance of approximately 60 m from the dumpsite, three distinct geologic sequences are delineated. These include the topsoil, clay layer, and the basement. The topsoil exhibits varying thicknesses from 0.8 m to 2.8 m and its corresponding resistivity values are between 29 Ωm to 227 Ωm indicating a sand lithology. The underlying clay layer displays low resistivity values between 7 Ωm to 28 Ωm and thicknesses from 6.3 m to 20.2 m, indicative of clay lithology. The basement layer, encountered at depths of 8.9 m to about 21 m, is characterized by resistivity values ranging from 321 Ωm to 938 Ωm, presumed to be infinite. In Traverse 2, connecting VES 1, VES 2, VES 3, and VES 7, with VES 1 as the control VES, similar geologic sequences are identified. The topsoil, ranging from the ground top to a depth of about 2.5 m, exhibits resistivity values of 30 Ωm to 245 Ωm, indicating a sand lithology. The underlying clay layer, with thicknesses varying from 8.3 m to 22.9 m and resistivity values between 8 Ωm and 29 Ωm, suggests the presence of clay lithology. The basement layer, encountered at depths of 10.8 m to about 24 m, displays resistivity values ranging from 346 Ωm to 1243 Ωm.
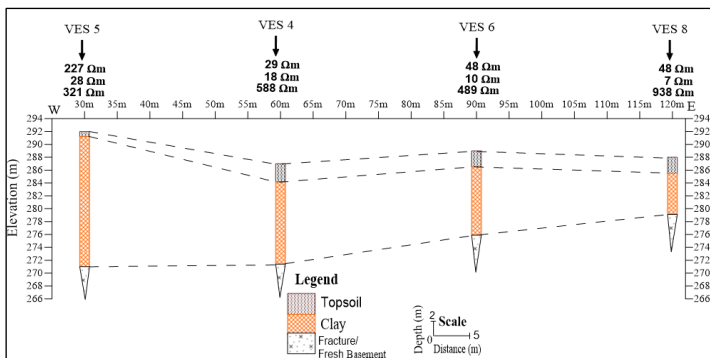
Figure 4: E–W Geo-Electric Section along Traverse One (TR1) of Ilaka Dumpsite.
Source: Authors, (2024).
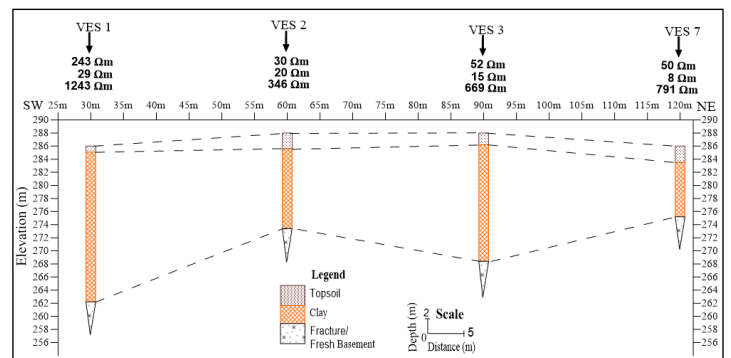
Figure 5: SW–NE Geo-Electric Section along Traverse Two (TR2) of Ilaka Dumpsite.
Source: Authors, (2024).

IV.3 ELECTRICAL RESISTIVITY TOMOGRAPHY AT ILAKA DUMPSITE

The result of 2D resistivity imaging obtained from the dipole-dipole electrode configuration of each traverse established across Ilaka dumpsite in the W – E and SW – NE directions were presented in Figures 7 and 8 respectively. Figure 6 shows a 2D image beneath the first traverse along the W – E orientation. From the result obtained, low resistivity values typically of clay lithology were observed underlying the dump site. Between the origin to about 35 m of the profile, it was characterized mainly by low resistivity values ranging from 2 Ωm to about 23 Ωm at both the near-surface, and middle layers. Between 40 m to about 90 m on the profile, a gradual variation in the resistivity values was observed at the near surface and the middle layer of these regions, there was an increase in resistivity ranging from 12 Ωm to 41 Ωm. Between 90 m to about 130 m, the overburden thickness was observed to be generally shallow, while the near-surface was characterized by layer resistivity of between 3 Ωm to about 12 Ωm. However, highly conductive zones delineated in most of the subsurface could be attributed to the hydration of the clay from the surrounding stream across the dump site.

Along the Traverse two (TR2), the 2D image beneath this traverse was established along SW – NE orientation according to Figure 7 between the origin and 45 m, the near-surface was characterized by low resistivity values ranging from 29 Ωm to 55 Ωm. This is indicative of the near-surface being sandy. The middle layer of this section has a layer resistivity value of about 8 Ωm to

about 14 Ωm indicative of clay as a dominant material within the depth of about 5 m to 14.5 m and beyond this depth is the fresh basement at 15 m to 25 m. Between 45 m to about 75 m, the section is characterized by low resistivity values ranging from 12 Ωm to 68 Ωm at the near-surface. This layer is predominantly clay with a little presence of sand occurring from about 0.3 m to about 3.8 m.

The rest of the section is characterized by thick overburden between 30 m and 34 m, but with low resistivity varying between 1 Ωm and to a maximum of 16 Ωm. This section is predominantly clay/sandy clay. Between 75 m to about 130 m of the profile, the near-surface has characteristics of clayey material with a layer resistivity of between 2 Ωm to about 12 Ωm and a thin middle layer with a variation in layer resistivity between 7 Ωm and 17 Ωm having a characteristic of clay. The overburden is generally shallow at this section and ranges between 8.0 m and 18.5 m. The rest of the section has resistivity values ranging between 100 Ωm and about 180 Ωm. The observation of highly conductive zones delineated in most parts of the subsurface could be attributed to hydration and dispersed leachate plumes within the clay formation.
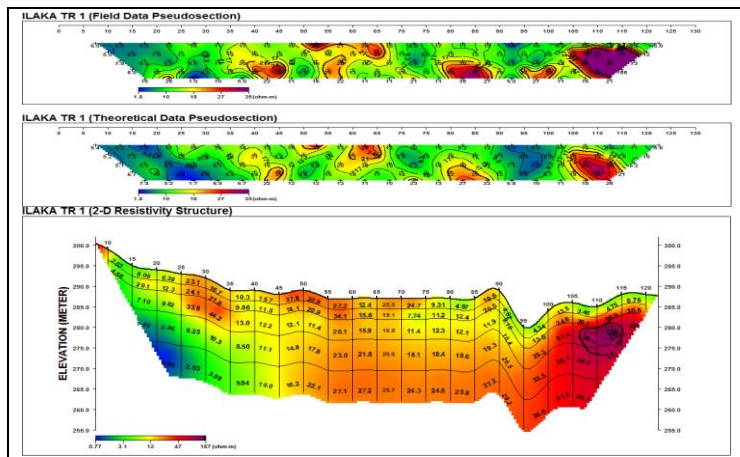
Figure 6: 2D Resistivity Image along W–E of Ilaka Traverse One (TR1) Dumpsite.
Source: Authors, (2024).
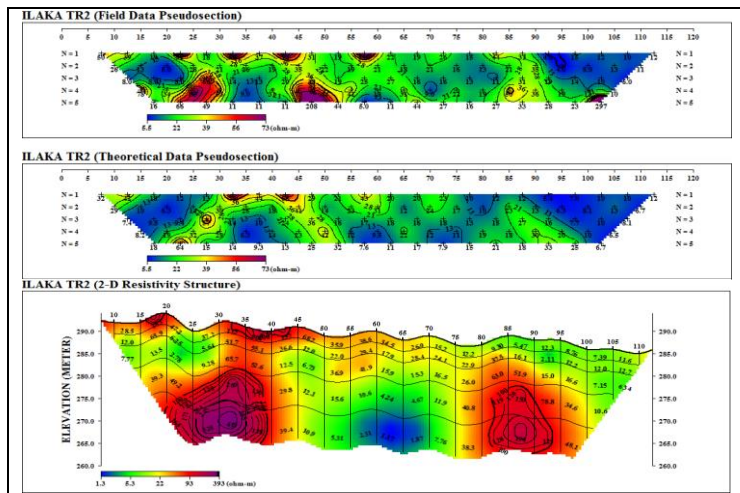
Figure 7: 2D Resistivity Image along SW–NE of Ilaka Traverse Two (TR2) Dumpsite.
Source: Authors, (2024).

IV.4 CORRELATION OF VES SECTION AND ERT IMAGE OF ILAKA DUMPSITE

The correlation of the VES section of Ilaka Traverse one with its corresponding Electrical Resistivity Tomography (ERT)

image as shown in Figure 8, reveals that the majority of the profile is characterized by clay formation. This clay formation is likely influenced by leachate plumes and hydration by the stream traversing the dump site. The impermeable nature of clay inhibits further percolation of leachates into the aquifer unit, trapping them within the environment. Similarly, the comparison of the VES section of Ilaka dumpsite Traverse two with its ERT image, as shown in Figure 9, indicates that the profile is predominantly composed of clay formation, particularly in the second layer beneath the topsoil. This clay layer, influenced by dumpsite leachate, exhibits relatively low electrical resistivity values. Consequently, it can be inferred that clay's impermeable nature has trapped leachate plumes, preventing their further percolation into the aquifer unit.
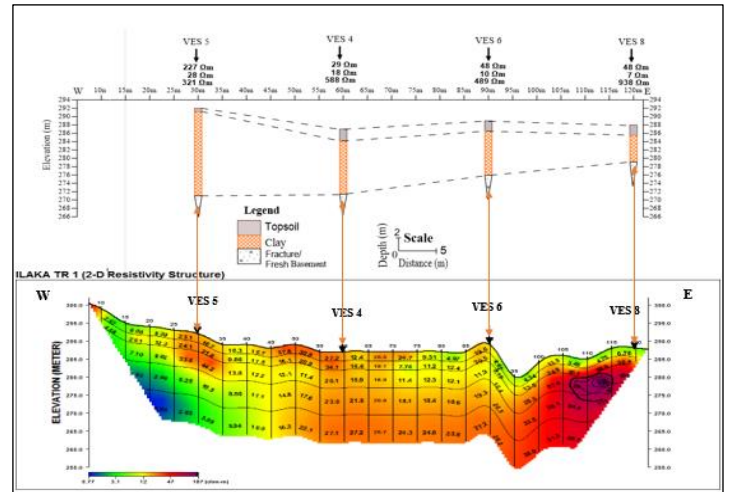
Figure 8: Correlation of VES Section with ERT Image for Traverse One.
Source: Authors, (2024).
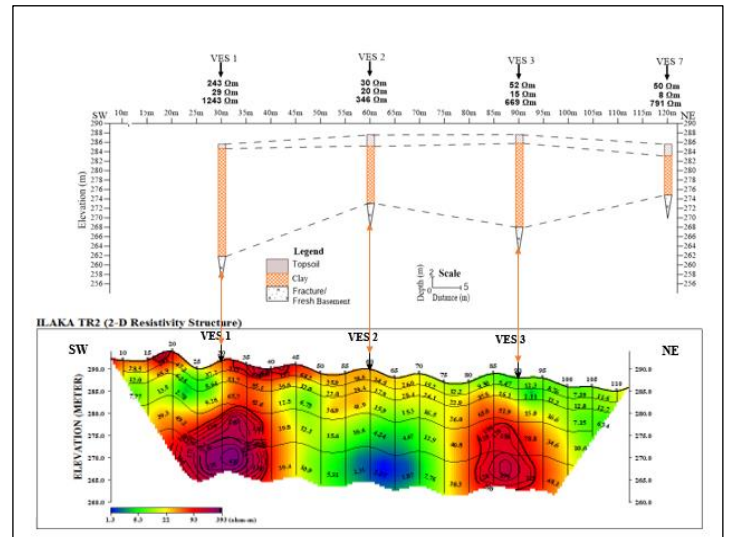
Figure 9: Correlation of VES Section with ERT Image for Traverse Two.
Source: Authors, (2024).

V. CONCLUSIONS

A geophysical survey was carried out within Oyo town to investigate the effect of some dumpsites on groundwater in Ilaka area of Oyo metropolis. The survey utilized an integrated approach which included geophysical methods involving 2D electrical

resistivity imaging and vertical resistivity sounding (VES) within the study area. The geo-electric sections of the study area delineated three main subsurface geo-electric layers which include; the topsoil, the weathered layer and the last layer within the investigated depth which may be considered as the fresh basement. The topsoil is made up of clay/sandy clay with layer thickness ranging from 0.8 m to 2.8 m and layer resistivity values ranging from 29 Ωm to 245 Ωm, the weathered layer has layer thickness ranging from 6.3 m to 22.9 m and corresponding layer resistivity values ranging from 7 Ωm to 29 Ωm, while the last layer is characterized with layer resistivity values ranging from 321 Ωm to 1243 Ωm. The ERT image obtained from the processed data from the dipole-dipole revealed that the topsoil is composed of the contaminant plume from the dump site. However, this leachate was observed to have been prevented from infiltrating into the subsurface due to the predominant presence of clay underlying the dump site. Generally, some parts of the study locations were observed to be characterized by thin overburden thickness with the weathered layer constituting the major aquifer zone in the study area.

Therefore, from the results obtained from the geophysical analysis, it is evident that dissolved solid and contaminant plumes have in no way undermined the suitability and potability of groundwater in the study areas rather the streams have a greater influence on the well water obtained from the study area. It can be concluded that most of the surroundings within the study area are metres away from the dumpsites, in all the locations visited, may be suitable for groundwater development within the investigated depth.

VI. AUTHOR'S CONTRIBUTION

Conceptualization: Kamaldeen Olasunkanmi Suleman and Sunmonu Lukman Ayobami
Methodology: Ogunmola Olufemi Louis and Owolabi Dayo Testimony
Investigation: Ogunmola Olufemi Louis and Owolabi Dayo Testimony
Discussion of results: Kamaldeen Olasunkanmi Suleman and Ogunmola Olufemi Louis
Writing – Original Draft: Kamaldeen Olasunkanmi Suleman and Ogunmola Olufemi Louis
Writing – Review and Editing: Kamaldeen Olasunkanmi Suleman and Ogunmola Olufemi Louis
Supervision: Sunmonu Lukman Ayobami and Suleman Kamladeen Olasunkanmi
Approval of the final text: Kamaldeen Olasunkanmi Suleman, Testimony Dayo Owolabi, Olufemi Louis Ogunmola, Lukman Ayobami Sunmonu and Bola Abdulhamid Afolabi.
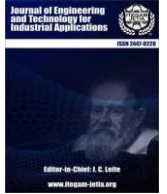
VII. ACKNOWLEDGMENTS

VIII. REFERENCES

[1] T. A. Adagunodo, M. K. Akinloye, L. A. Sunmonu, A. P. Aizebeokhai, K. D. Opeyemi and F. O. Abodunrin, "Groundwater Exploration in Aaba Residential Area of Akure, Nigeria," vol. 6, no. June, pp. 1–12, 2018, doi: 10.3389/feart.2018.00066.

[2] L. E. Condon, S. Kollet, M. F. P. Bierkens, G. E. Fogg, R. M. Maxwell, M. C. Hill, H. H. Fransen, A. Verhoef, A. F. Van Loon, M. Sulis, and C. Abesser, "Global Groundwater Modeling and Monitoring: Opportunities and Challenges," Water Resour. Res., vol. 57, no. 12, pp. 1–27, 2021, doi: 10.1029/2020WR029500.

[3] H. M. Nazifi, and L. Gulen, "The Use of Electromagnetic and Vertical Electrical Sounding Methods in Groundwater Exploration," Bull. Miner. Res. Explor., vol. 158, pp. 327–344, 2019, doi: https://dx.doi.org/10.19111/bulletinofmre.451557.

[4] B. N. Satpathy, and D. N. Kanungo, "Groundwater Exploration in Hard-Rock Terrain—A Case History," Geophysical Prospecting, vol. 24, no. 4, 1976, doi: 10.1111/j.1365-2478. 1976.tb01569.x.

[5] K. Choudhury, D. K. Saha, and P. Chakraborty, "Geophysical study for saline water intrusion in a coastal alluvial terrain," J. Appl. Geophys., vol. 46, no. 3, 2001, doi: 10.1016/S0926-9851(01)00038-6.

[6] K. O. Suleman, O. L. Ogunmola, R. O. Adesina, T. O. Adeoye, and L. A. Sunmonu, "Groundwater Exploration for Water Well Sites in Abata Asunkere," Malaysian Journal of Geosciences (MJG) vol. 01, no. 1, pp. 27–30, 2023, doi: 10.26480/mjg.01.2023.27.30.

[7] O. O. Osinowo, M. A. Agbaje, and S. O. Ariyo, "Integrated Geophysical Investigation Techniques for Mapping Cassava Effluent Leachate Contamination Plume, At A Dumpsite in Ilero, Southwestern Nigeria," Sci. African, vol. 8, 2020, doi: 10.1016/j.sciaf. 2020.e00374.

[8] N. Abdullahi, I. Osazuwa, and P. Sule, "Application of Integrated Geophysical Technique in The Investigation of Groundwater Contamination: A Case Study Of Municipal Solid Waste Leachate. Ozean J," Appl. Scie, vol. 4, no. 1, 2011.

[9] O. O. Okunowo, O. Y. Adeogun, K. S. Ishola, and S. Alli, "Delineation of Leachate at A Dumpsite Using Geo-Electrical Resistivity Method: A Case Study of Abule Egba, Lagos, Nigeria," SN Appl. Sci., vol. 2, no. 12, 2020, doi: 10.1007/s42452-020-03573-6.

[10] J. Wu, Y. Zhang, and H. Zhou, "Groundwater Chemistry and Groundwater Quality Index Incorporating Health Risk Weighting in Dingbian County, Ordos Basin of Northwest China," Chemie der Erde, vol. 80, no. 4, p. 125607, 2020, doi: 10.1016/j.chemer.2020.125607.

[11] M. A. Jenifer and M. K. Jha, "Comprehensive Risk Assessment of Groundwater Contamination in A Weathered Hard-Rock Aquifer System of India," J. Clean. Prod., vol. 201, 2018, doi: 10.1016/j.jclepro.2018.08.005.

[12] S. M. Njuguna, V. A. Makokha, X. Yan, R. W. Gituru, Q. Wang, and J. Wang, "Health Risk Assessment by Consumption of Vegetables Irrigated with Reclaimed Waste Water: A Case Study in Thika (Kenya)," J. Environ. Manage., vol. 231, 2019, doi: 10.1016/j.jenvman.2018.10.088.

[13] Y. Yuan, M. Xiang, C. Liu, and B. K. G. Theng, "Chronic Impact of an Accidental Wastewater Spill from A Smelter, China: A Study of Health Risk of Heavy Metal(loid)s Via Vegetable Intake," Ecotoxicol. Environ. Saf., vol. 182, 2019, doi: 10.1016/j.ecoenv.2019.109401.

[14] A. S. Ganiyu, S. B. Badmus, A. M. Oladunjoye, P. A. Aizebeokhai, and T. O. Olurin, "Delineation of Leachate Plume Migration Using Electrical Resistivity Imaging on Lapite Dumpsite in Ibadan, Southwestern Nigeria," Geosciences, vol. 2015, no. 2, 2015.

[15] T. A. Adagunodo, M. K. Akinloye, L. A. Sunmonu, A. P. Aizebeokhai, K. D. Oyeyemi, and F. O. Abodunrin, "Groundwater Exploration in Aaba Residential Area of Akure, Nigeria," Front. Earth Sci., vol. 6, 2018, doi: 10.3389/feart.2018.00066.

[16] A. Olla, A. Akinlalu, M. Olayanju, O. Adelusi, and A. Adiat, "Geophysical and Hydrochemical Investigation of a Municipal Dumpsite in Ibadan, Southwest Nigeria," J. Environ. Earth Sci., vol. 5, no. 14, 2015, [Online]. Available: www.iiste.org.

[17] K. O. Suleman, T. A. Adagunodo, O. L. Ogunmola, T. O. Adeoye, L. A. Sunmonu, G. A. Alagbe, R. O. Agboola, M. R. Usikalu, P. O. Isibor, S. A. Akinwumi, O. C. Olawole, and I. O. Babarimisa "Investigation of Subsurface Contaminants Leachate Within Ansaru-Islam Secondary School, Ilorin, Nigeria," IOP Conf. Ser. Earth Environ. Sci., vol. 1197, no. 1, 2023, doi: 10.1088/1755-1315/1197/1/012011.

[18] Oyawoye M.O., "The Basement Complex of Nigeria," Dessauvagie and A. J. Whiteman (Eds) African Geology. pp. 67–99, 1972.

[19] N. K. Olasunkanmi, L. A. Sunmonu, D. T. Owolabi, M. Bawallah, and A. Oyelami, "Investigation of Dam Integrity from Electrical Resistivity Methods: A Case of Erelu Dam, Southwestern Nigeria," Indones. J. Geosci., vol. 8, no. 2, pp. 265–274, 2021, doi: 10.17014/IJOG.8.2.265-274.

Journal of Engineering and Technology for Industrial Applications

RESEARCH ARTICLE   **OPEN ACCESS**

UNVEILING THE NEXUS BETWEEN FUEL CONSUMPTION, VEHICLE REGISTRATION, POPULATION AND GDP OF NEPAL

*Niraj Bohara[1], and Hemant Tiwari[2]

[1]Lecturer/ Executive Member, Department of Civil Engineering, United Technical College/Safe and Sustainable Travel Nepal, Bharatpur -11, Chitwan, Nepal.
[2]General Secretary, Society of Transportation Engineers of Nepal, Kathmandu, Nepal

[1] http://orcid.org/0009-0002-0948-4956, [2] http://orcid.org/0000-0003-4409-1787,

Email: *nbohara@unitedtechnicalcollege.edu.np1, hemu.ioe.edu.np2

ARTICLE INFO	ABSTRACT
	Vehicle numbers soar with the increase in travel demand, thus increasing petroleum consumption, one of the extensive non-renewable resources. The increased demand for travel is also linked to Gross Domestic Product (GDP). However, due to the rise in fuel standards and higher fuel efficiency vehicles, the fuel consumption per vehicle is following the decreasing patterns. Thus, this study is about the relationship between petroleum consumption, vehicle registration and GDP of Nepal using regression analysis. Data for analysis were between 1994 and 2022 for registered vehicles, petroleum consumption and GDP whereas population data were collected from 1930 to 2021. The linear regression model came to be statistically significant between variables, (a) vehicles registered and petroleum consumption (diesel and petrol sales); (b) operating vehicles and petroleum consumption; and (c) operating light vehicles and petrol consumption. Similarly, significant exponential regression models were observed between (a) GDP and operating vehicles; and (b) GDP and petroleum consumption. Additionally, the study presented a logistic population growth model and vehicle growth model as significant models to put forth predicted population and vehicles in 2030 and 2040. These models were used to estimate the possible petroleum consumption in 2030 and 2040. Alongside, a situation, where high electric vehicle penetration might be observed, was also taken to predict the possible petroleum consumption. Rising petroleum consumption can be curbed to a certain limit with proper policy interventions and research and development in electric vehicles.

I. INTRODUCTION

The burning of fuels generates locomotive power for internal combustion engines. In the present world, diesel, petrol (gasoline), and natural gases are being used widely for light vehicles and heavy vehicles movement. Light fuels are generally used for lighter vehicles generating higher fuel efficiency movements whereas heavy fuels such as diesel are being used for heavy duty operations. There have been studies on the use of biofuels and additives to increase efficiency and control pollution, however, the use of these non-renewable sources hasn't stopped petroleum product sales from soaring.

Internal combustion engines, though have improved their efficiency in terms of km per litre consumption and even in terms of emission, as per the study by Yeu and Liu. They forecasted that internal combustion engine technology in future continually would dominate other vehicles. This in turn would increase demand for more petroleum consumptions. The study also stated that increased efficiency is the main reason behind the popularity of IC engine technology [1].

The study "The Role of Regulations, Gasoline Taxes and Autonomous Technical Change" cited that EU and US standards for vehicles have increased the fuel efficiency standards between 2015 and 2020. EU raised the standard limit of mileage from 17.85

km/lit in 2015 to 24.21 km/lit in 2020 AD while in the US, as per the Mandatory fuel efficiency standards, the fuel efficiency was increased from 15 km/lit to 20 km/lit in 2020 for light trucks and cars operating with gasoline (petrol). This also shows the demand for higher fuel-efficient vehicles. As per the same study, the improvement in fuel efficiency is also induced because of increased standards [2].

In addition, standards are introduced to control the emissions and to sustain the engine efficiency. Standard in Europe started in the 70's and was mostly focused on the reduction of lead, benzene, sulfur, polyaromatic hydrocarbons, manganese, and volatile organic components. The main reasons these components were regarded as pollutants were because of their incomplete combusting nature, and volatility, which were specifically harmful to humans [3].

To predict the condition of Nepal regarding emission and energy consumption Bajracharya in 2013 produced a relation between vehicle population and different variables such as population, and the Gross Domestic Product. The relationship observed had an excellent correlation for Minibus and population, motorcycle (2-wheeler), and urban population whereas those associated with GDP had only a strong correlation. The relation was best fit by a logarithmic function. The study also suggested the diminishing vehicle km travelled with the increased age of vehicles [4].

A study by Bajracharya and Bhattarai in 2016, studied the vehicle and energy consumption in Kathmandu Valley and predicted different scenarios in 2030. The study incorporated the estimation of the vehicle fleet using the equation $N_{i,y} = 0.5 * D_{i,y} + \sum_{x=1990}^{y-1} D_{i,y} * \phi_i(y-x)$. The study was conducted with the base year data of 1990 as x and for y year where ϕ represents the survival probability of that particular group of vehicles. The other data estimated in the study were annual mileage and emissions. The study predicted that the vehicle population will reach 1 million in the year 2030 where the highest proportions would be covered by light vehicles whereas the petrol demand is to soar to 257,000 kL in 2030 while the model predicted that diesel consumption is going to boom to 135,000 kL in Kathmandu Valley alone [5].

II. VEHICLE REGISTRATION, PETROLEUM CONSUMPTION AND GDP STATUS

In reference to the Department of Transport Management [6] and the economic survey data of 2023 [7]The registered vehicles, after reducing the number of e-rickshaws (electric vehicles) when plotted against the year (1990 -2022), depict a vehicle trend with three different growth rates. It ranges from a low to a high rate of growth. A low growth rate was seen between 1990 and 2007, a mild growth rate was seen between 2007 and 2016, whereas a steep growth rate (high) was seen after 2016. The vehicle growth is continuous and follows a smooth curve with year as shown in the Fig. 1. The total vehicle registration observed in the year 1994 was 139,858 which later rose uninterruptedly to 5,032,666 registered vehicles in 2022.
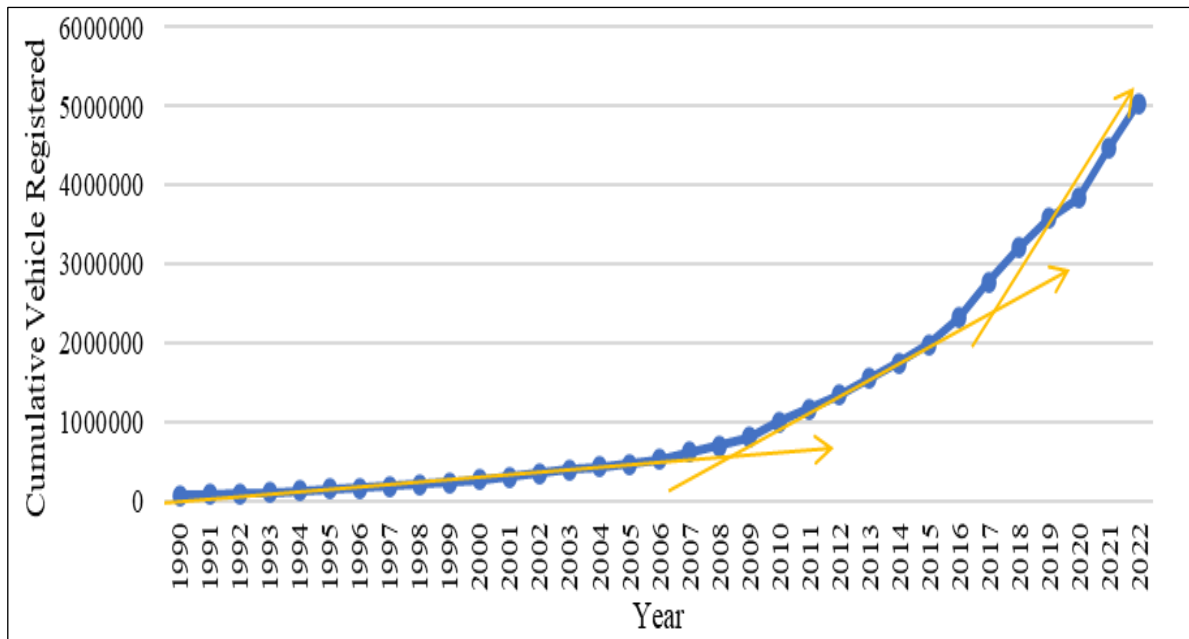
Figure 1: Growth trend of cumulative vehicles registered in Nepal (1990 – 2022).
Source: [7].

According to the database of Nepal Oil Corporation, the only fuel importer of Nepal, fuel consumption has been ever-increasing. Diesel sales and petrol sales in kL are taken as the fuel consumption for the study. There are two distinct drops in petroleum consumption as seen, in 2016 and 2020 which is due to the blockade in 2015 and COVID-19 in 2020. Thus. collected data were arranged chronologically from 1994 to 2022. The trend in fuel consumption suggests that from 1994 till 2008, the growth rate was low, from 2008 till 2016, the growth rate was medium whereas the growth rate after 2016 seems to have risen steeply as shown in

Figure. 1, which follows a similar trend as registered vehicles. This displays, there exists a close relationship between fuel sales and the vehicle number. The total petroleum consumption (diesel + petrol) seems to be 226,750 kL in 1994 which rose to 2,460,408 kL in 2022. Similarly, the petrol consumption in 1994 was 31,061 kL which was 732,837 kL in 2022. While for diesel, the consumption of 195,689 kL in 1994 is seemed to increase to 1,727,571 kL in 2022 [8].
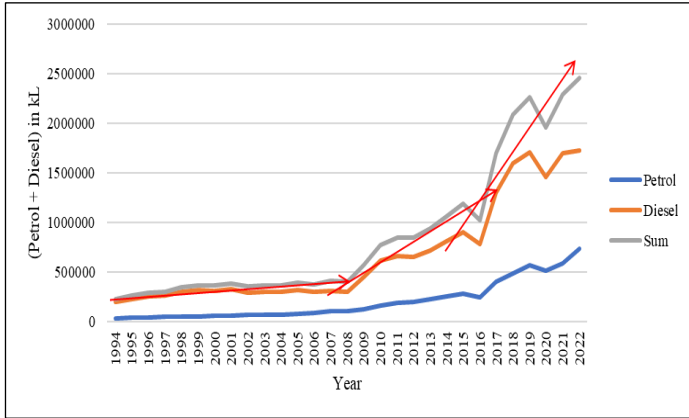
Figure. 1: Growth trend of petroleum consumption in Nepal (1994 – 2022).
Source: [8].

For Gross Domestic Product, the World Bank Global Outlook (indicator) has been taken GDP (constant 2015 US$). The trend is similar to that of vehicle growth and petroleum product sales but not on a similar scale. The three trends/growth rates are seen between 1991 and 2004, 2004 to 2015 and 2015 to 2022 in Figure 2. The GDP is observed to be 8,779 million US$, 10,271 million US$ and 33,084 million US$ in 1991, 1994 and 2022 which demonstrates the progressive trend of GDP (constant 2015 US$) [9]. So, this study is focused on finding out the relationship between vehicle numbers, petroleum product sales (petroleum consumption) and gross domestic product of the country.
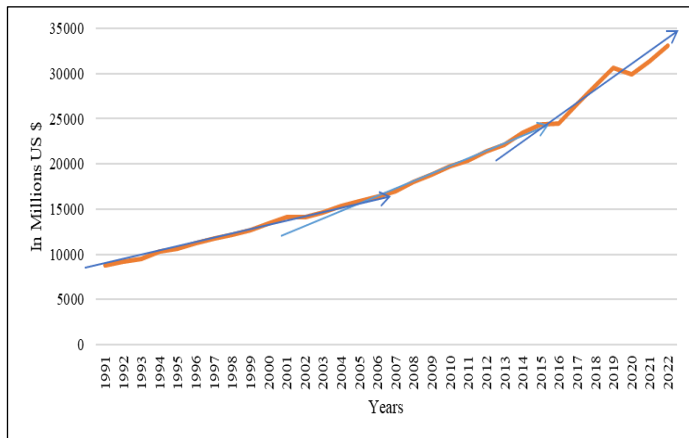
Figure 2: Growth trend of GDP (constant 2015 US$) of Nepal (1991 – 2022).
Source: [9].

III. LIMITATIONS OF THE STUDY

The study is only limited to the relationship between vehicles, fuel consumption, population and GDP based on the available data from government sources and the World Bank. Electric vehicles (cars and motorcycles) have been introduced to the Nepali market since mid-2010, but it only started rising in early 2020. Thus, the proper data set for electric vehicles except for e-rickshaws hasn't been available in the records. So, petroleum-consuming vehicles were computed by only reducing the e-rickshaws number. Likewise, all the registered vehicles for various reasons, do not get to ply on roads. Because of the unavailability of provisions for de-registration of these vehicles, the exact number of vehicles plying on the road could not be extracted. Thus, for computing the operating vehicles, an approach with the consideration of phased-out vehicles has been made in this study. Phased-out vehicles were considered The cabinet in January 2015 and February 2017 decided to ban vehicles older than 20 years operating on roads in Nepal [10]. The construction industry is another component responsible for fuel consumption and increased fuel sales, but the unavailability of this specific data led to ignoring this aspect during the study.

IV. METHOD OF STUDY

For the study, the majority of the data were collected from secondary sources, i.e. published databases from respective government organizations summarized in Table 1. The annual petroleum consumption was considered to be equal to the annual sales. With all the data collected, the analysis period was taken between 1994 and 2022. To establish the relationship between various variables, various regression models were used, and the significance of such relationships was accessed by Coefficient of Determination (R^2) and P-values. The regression analysis were performed using MS Excel.
Linear Regression models were developed for the following set of variables.
  a. Vehicle number and Petroleum Consumption
  b. Operating vehicles and petroleum consumption
  c. Light vehicles and petroleum consumption
Exponential Regression models
  a. GDP and Operating vehicles
  b. GDP and Petroleum Consumption
Logistic models
  a. Population and t – years
  b. Vehicle/1000 population and t-years

Table 1: Basic document specifications.

Year	Cum. Vehicles ('00,000)	Petroleum Consumption ('00,000 kL)	Population (in millions)	GDP in Million $ (Constant 2015)
94	1.40	2.27	19.78	8,779.12
95	1.59	2.62	20.23	9,139.62
96	1.80	2.92	20.69	9,491.48
97	2.03	3.03	21.16	10,271.31
98	2.24	3.48	21.64	10,627.56
99	2.48	3.66	22.13	11,193.83
00	2.76	3.66	22.64	11,758.96
01	3.17	3.85	23.15	12,113.66
02	3.64	3.50	23.47	12,648.18
03	4.02	3.67	23.78	13,432.37
04	4.42	3.67	24.11	14,077.11

05	4.82	3.91	24.43	14,094.02
06	5.37	3.75	24.77	14,650.03
07	6.26	4.09	25.10	15,336.04
08	7.11	4.04	25.44	15,869.60
09	8.13	5.71	25.79	16,403.56
10	9.39	7.75	26.14	16,963.17
11	10.89	8.43	26.49	17,998.71
12	12.42	8.48	26.75	18,814.61
13	14.36	9.38	27.01	19,720.80
14	16.16	10.63	27.27	20,395.61
15	18.36	11.85	27.53	21,348.11
16	21.48	10.21	27.80	22,100.66
17	25.78	16.99	28.07	23,429.24
18	29.85	20.82	28.34	24,360.80
19	33.34	22.65	28.61	24,466.31
20	35.59	19.61	28.89	26,662.72
21	41.45	22.86	29.16	28,695.05
22	46.68	24.60	29.54	30,605.30

Source: Authors, (2024)

The study also computed the fuel consumption per vehicle in a year and the trend of the consumption set throughout the study period.

To add up, a scenario analysis was performed to predict petroleum consumption in the years 2030 and 2040 AD. For this, logistic models for population prediction of Nepal and vehicle prediction were prepared and used.

IV.1 LOGISTIC MODEL

This model is used for those growing variables which reach a constant saturation limit at a certain point. D. Das et al in 2009 [11] used this equation to model the vehicle per population whereas a similar equation was also used to model the population in Uganda and Nepal [12],[13]. In this model, the rate of increment of the variable is slow at first whereas becomes rapid when it reaches near saturation.

The logistic model is represented as

$$Y_t = \frac{S}{1+ce^{-\alpha t}} \qquad (1)$$

Where,

S represents the saturation

α is the Malthusian Factor, represents the shape of the curve and growth factor

whereas c represents the constant, which represents the start of the curve

t represents the time where t = 0, 1…. Years for consecutive years

The work also involves the estimation of the saturation for population and vehicle population. A methodology adopted by Wali, Kagoyire and Icyingeneye in 2012 [13] of modelling Uganda's Population and work by Adhikari and Raya in 2018 [12] where the population of Nepal was modelled is used to estimate the saturation limit.

Where,

In the exponential growth law,

$$\frac{dY_t}{dt} = \alpha y_t \qquad (2)$$

Whose solution would be as:

$$Y_t = Y_o e^{\alpha t} \qquad (3)$$

This represents that the growth rate keeps increasing with time without the consideration of the saturation period. To correct this nature, to understand the growth rate, the correction is applied with coefficients α and β which represent the position of the variable near the saturation such that:

$$\frac{dY_t}{dt} = \alpha Y_t \frac{(\alpha - \beta Y_t)}{\alpha} \qquad (4)$$

If the variable reaches near saturation represented by $Y_t = S = \frac{\alpha}{\beta}$, then the growth rate reaches zero at this stage which signifies the saturation state. The solution to this equation is as:

$$Y_t = \frac{\frac{\alpha}{\beta}}{1+\left(\frac{\frac{\alpha}{\beta}}{Y_o}-1\right)e^{-\alpha t}} \qquad (5)$$

If t_k is the time of inflection and S is the saturation, when $\left(\frac{\frac{\alpha}{\beta}}{Y_o}-1\right) = e^{\alpha t}$ and $Y_t = \frac{S}{2} = \frac{\alpha}{2\beta}$, the point of inflection occurs when the rate of growth is maximum.

The equation (Eq. 5) is redefined as:

$$Y_t = \frac{S}{1+e^{-\alpha(t-t_k)}} \qquad (6)$$

Least square error is computed to estimate saturation where:

$$e = \sum (Y_i - y_i)^2 \qquad (7)$$

For this,

$$y_i = \text{predicted value at } i^{th} \text{year} = S*h_i \qquad (8)$$

Where,

$$H_i = \frac{1}{1+e^{-\alpha(t_i-t_k)}} \qquad (9)$$

Thus,

$$e=\sum(Y_i-S*h_i)^2$$

For minimum e, differentiating with respect to S,

$$\frac{de}{dS}=0=-2\sum(y_i*h_i)+2S\sum(h_i^2)$$

And, thus, saturation can be estimated as:

$$S=\frac{\sum h_i * Y_i}{\sum(h_i * h_i)} \qquad (10)$$

The value of error is minimized with t_k and α value iterated multiple times with the help of the MS Excel Solver tool.

$$e = \sum(Y_i*Y_i)-\frac{(\sum(Y_i*h_i))^2}{\sum(h_i*h_i)} \qquad (11)$$

To, measure the goodness of fit, R^2 is computed for the developed model as

$$R^2=1-\frac{\sum(Y_i-y_i)^2}{\sum(Y_i-\overline{Y_i})^2} \qquad (12)$$

Where, $\overline{Y_i}$ is the mean of the variable

This method of saturation estimation and model fitting is performed only with population data collected from the census years between 1930 and 2021. In Nepal, census is taken every 10 years. [14]. Thus, intermediate data are interpolated considering exponential growth between two points of the census ($P = \beta e^{\alpha t}$). Adhikari also did this practice [12].
However, the vehicle fleet saturation is estimated through literature. From the literature, it is found that saturation vehicle fleet varies with per capita GDP of that country. A study performed by Huo et al, 2007, studied the saturation point of highway vehicle registration for 18 countries. The higher the per capita income, the greater the saturation vehicle fleet. The study suggested that the saturation point for different countries looks different. Vehicles per thousand people in Asian countries were predicted smaller even with similar GDP per capita when compared to European and North American Countries. The study depicted that for densely populated countries, the value of saturation doesn't reach very high. A high degree of saturation can be assumed up to 850 vehicles per 1000 people whereas for China it can be assumed to be 600 vehicles for a high growth scenario [15]. A similar result was also observed in the work of Dargay et al, 2007 where different vehicle models with their coefficients and saturation were explained [16]. Another study performed by Bottiny, an economist, in 1966, emphasized the importance of understanding saturation in vehicle ownership which is eventual. However, the successful prediction, as per the study, is difficult. 2 passenger cars per household, or 1 and 7/10th persons per passenger cars, registered vehicle per 2 and 2/10th of residents, and ownership of one car for every 2.5 persons were some of the saturation points estimated through literature reviews in that study [17]. In a work of Singh in 2019, where a projection of vehicles was made for 2050, two different saturation points were taken for modelling. One was a conservative approach and the other was an aggressive growth approach for two-wheelers and cars as 250 and 350 two-wheelers per 1000 persons and 150 and 250 cars per 1000 persons [18].
For this study, to estimate the future vehicle fleet in similar growth conditions, a logistic model is being used. As suggested by the works of literature, sighting to difficulty in proper estimation, two growth models have been generated with 400 vehicles per 1000 persons and 550 vehicles per 1000 persons have been taken and the least square method, with Excel regression tool, has been used to model the vehicle fleet per 1000 persons. To explain the significance of the model, the coefficient of determination R^2 and p-value are used.

V RESULTS AND DISCUSSION

V.1 VEHICLE FUEL CONSUMPTION PER YEAR

As per the study, the fuel consumption per vehicle even with the increase in the number of vehicles is decreasing which can be seen in Figure 3.
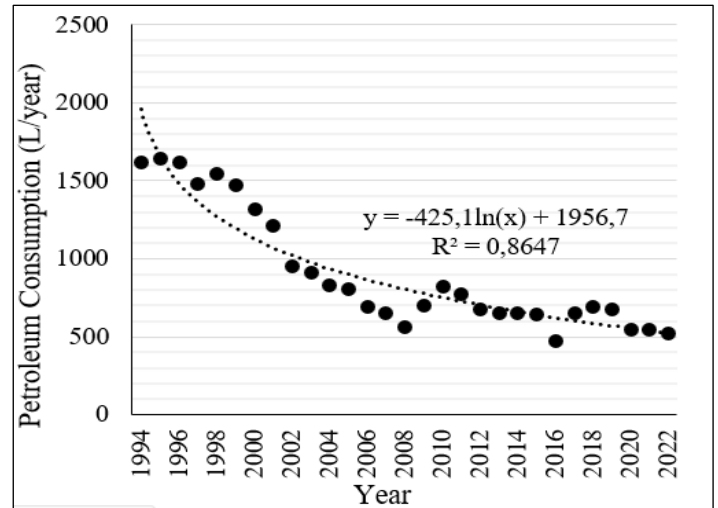
Figure 3: Trend of Diminishing per Vehicle Annual Petroleum Consumption (litre).
Source: Authors, (2024).

The figure shows the diminishing annual petroleum consumption per vehicle. This shows the increment of higher fuel-efficient vehicles in the context of Nepal. A similar trend of fuel consumption per year is even seen in the United States as per the Bureau of Transportation Statistics [19]. While observing the data of 1998 and 2020 of fuel consumption per vehicle in a year, the fuel consumption reduced from 2729.097 litres to 2183.617 litres which means a reduction of 19.987% within this period in the United States. With Nepal currently importing Euro 6 standard fuel from India and sooner applying the same to the vehicles, a greater decrease in fuel consumption is to be expected. This is further supported by the policy of the current global leaders and the Nepalese government to promote electric vehicles. The trend of the reduced petroleum consumption in litre/year/vehicle can be seen in the figure which seems to follow the logarithmic curve with an R^2 value of 0.864.

V.2 PETROLEUM CONSUMPTION AND THE REGISTERED VEHICLES

With the regression analysis between the vehicle population (registered) and the petroleum sales (Diesel and petrol), an excellent correlation was observed with R^2 of 0.969 and with the P value of $5.22 *10^{-6}$ for the intercept and $6.32*10^{-6}$ for the vehicle number. The P values suggest the significant characteristics of the variables in the regression equation. Thus, a usable regression equation based on the analysis is given:

"Petroleum Consumption (in '00,000 kL)
= 0.491* Cum. Vehicle ('00,000) + 1.88," (13)

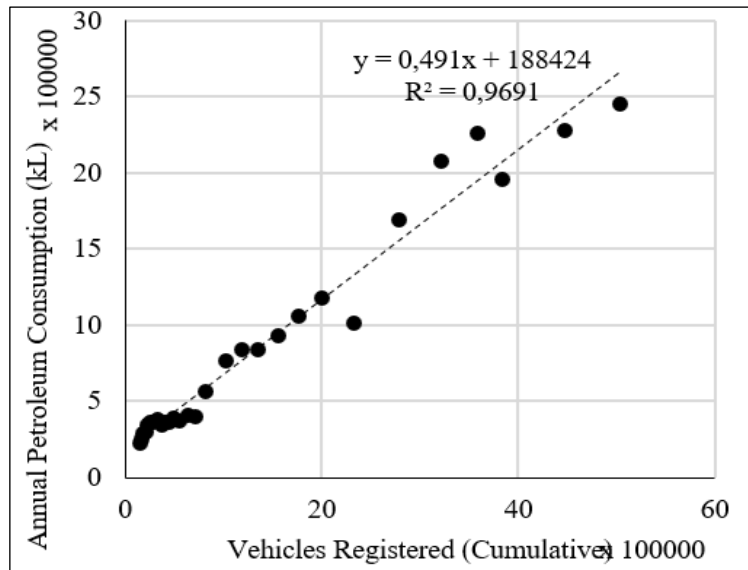Thus, the relationship suggests that there is a positive and significant relationship between the annual petroleum consumption and the cumulative number of registered vehicles. This trend is set to go further with time since the demand for the vehicles is still on rise. A scatter plot is shown in Figure 4.

Figure 4: Scatter plot between Annual Petroleum Consumption and Vehicles Registered
Source: Authors, (2024)

Figure 5 above shows that the rise in petroleum consumption and the rise in vehicle numbers in Nepal are inevitable irrespective of the time. Another thing evident from the graph is the higher growth in the later period compared to the initial period of the study. This can be due to the fact that the country entered into a period of stability after a long era of insurgency.

V.3 PETROLEUM CONSUMPTION AND OPERATING VEHICLES

Vehicles due to various reasons are taken out of the road and do not consume petroleum products. Thus, the study presents .

the correlation between the number of vehicles after deducting the phased-out vehicles (20-year-old vehicles) and petroleum consumption. The regression analysis observed a similar result with the R^2 of 0.968 and P values of $1.78*10^{-5}$ for intercept and $8.5*10^{-22}$ for variable operating vehicles. Thus, a significant regression equation, of linear type, formed as:

$$\text{Fuel consumption (in '00,000 kL)} = 0.532 * \text{Cum. Veh. ('00,000)} + 1.765 \quad (14)$$

The scatter plot between these variables is shown in Figure 5.
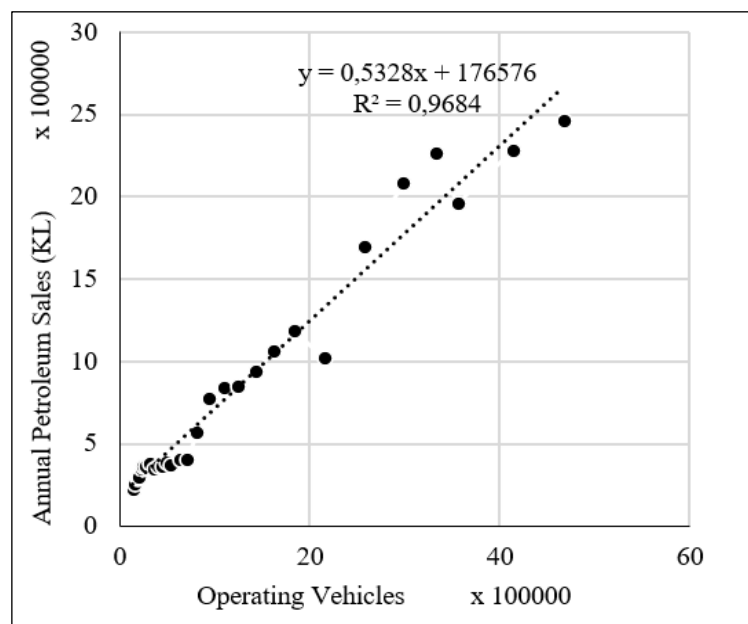
Figure 5: Scatter plot between Annual Petroleum Consumption (kL) and Operating Vehicles.
Source: Authors, (2024).

V.4 PETROL CONSUMPTION AND LIGHT VEHICLES

With the advent of light vehicles, lighter fuels (petrol) with high efficiency resulting in lower consumption of fuel have been in use. Because of the lower cost of these vehicles and preference for personal use, the proportions of light vehicles have increased significantly in these years. An 87% proportion is covered by these vehicles which can be seen in the Figure 6.
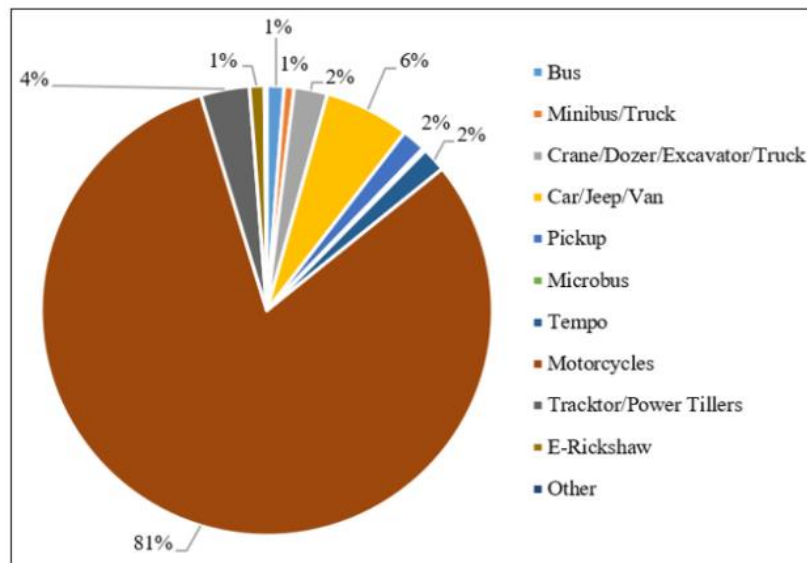
Figure 6: Distribution of Different Category of Vehicles in Nepal.
Source: [7].

Upon, model fitting, linear regression, there existed a significant relationship between petrol sales (kL) and the light vehicle numbers with an R^2 value of 0.983 and P values 0.019 between intercept and variable petrol consumption and $1.1*10^{-25}$ between the variable and number of light vehicles. The usable linear regression equation is as:

Petrol consumption ('00,000 kL per annum)
$$=0.157*\text{Light vehicles ('00,000)} +1.642 \quad (15)$$

The scatter plot between annual petrol sales and operating light vehicles is shown in the Figure 7.
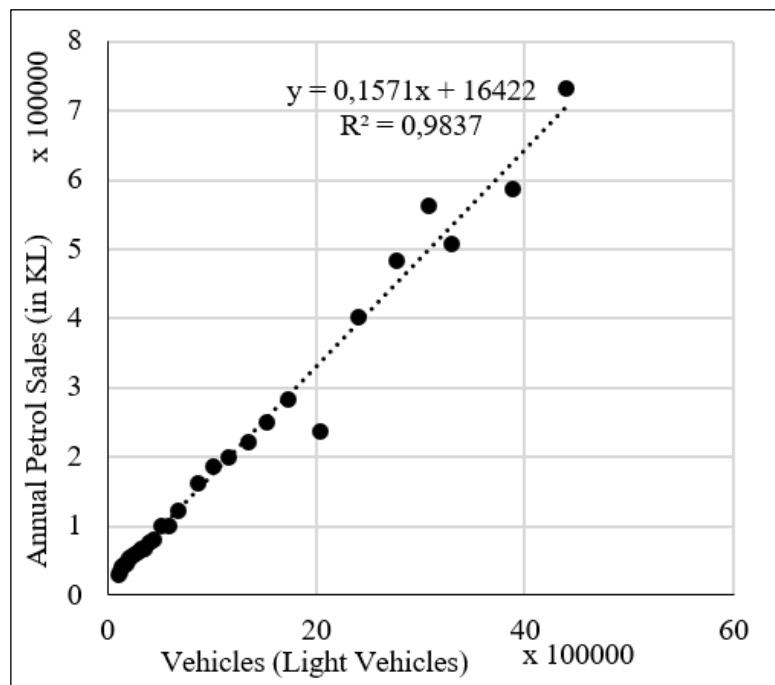
Figure 7: Scatter Plot between Annual Petrol Consumption and Operating Light Vehicles.
Source: Authors, (2024).

From the equation, it can be seen that the coefficient is lower for petrol consumption than that for the equation between vehicles and total petroleum consumption, i.e., 0.157 compared to that of 0.532. This can be supported by the nature of these vehicles i.e., being light and easy to propel. This is also observed in the total annual petrol consumption whose average sales are comparatively lower than the total annual diesel sales.

V.5 RELATIONSHIP WITH GROSS DEVELOPMENT PRODUCT

The need for travel rises with the increased income of an individual. Thus, there is the existence of a relationship between the number of vehicles and the GDP (constant 2015 US$) of the country and consequently with petroleum consumption. The regression equation formed between operating vehicles and the GDP is as:

Cum Vehicles ('00,000) = $0.381*e^{0.000153*GDP \text{ (in millions)}}$ (16)
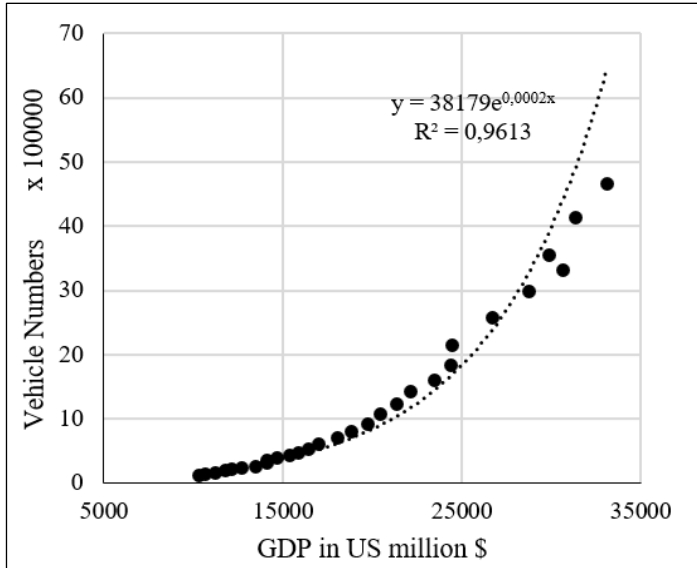
Figure 8 a): A Scatter Plot Between Operating Vehicles and GDP (in million $).
Source: Authors, (2024).

With the p-value near zero and the coefficient of determination (R^2) 0.961, the relationship between the vehicle and the GDP proves to be significant in the context.
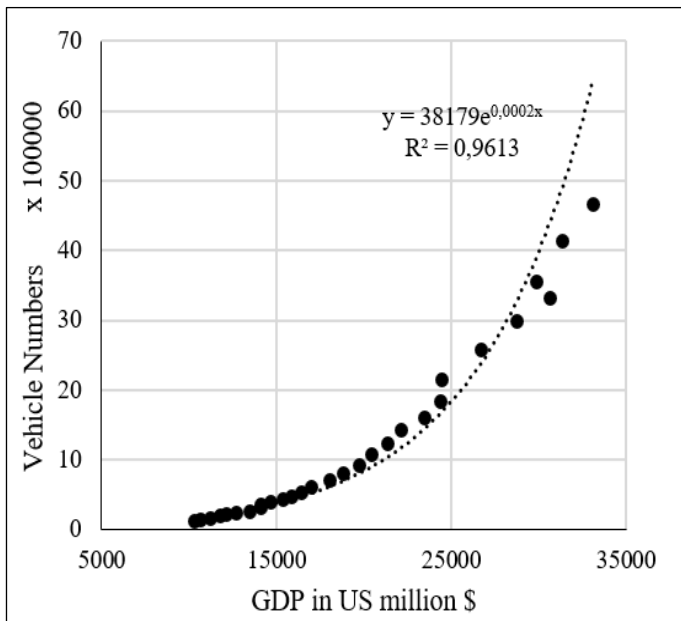
Figure 8 b): illustrates the scatter plot between these two variables along with the exponential trendline.
Source: Authors, (2024).

Taking exponential expression for regression again between petroleum consumption and gross domestic product in million US $ led to the following equation with the significant relationship with near to zero P value and R^2 of 0.971:

Petroleum Consumption (kL) = $0.793*e^{0.00011*GDP \text{ (in millions)}}$ (16)
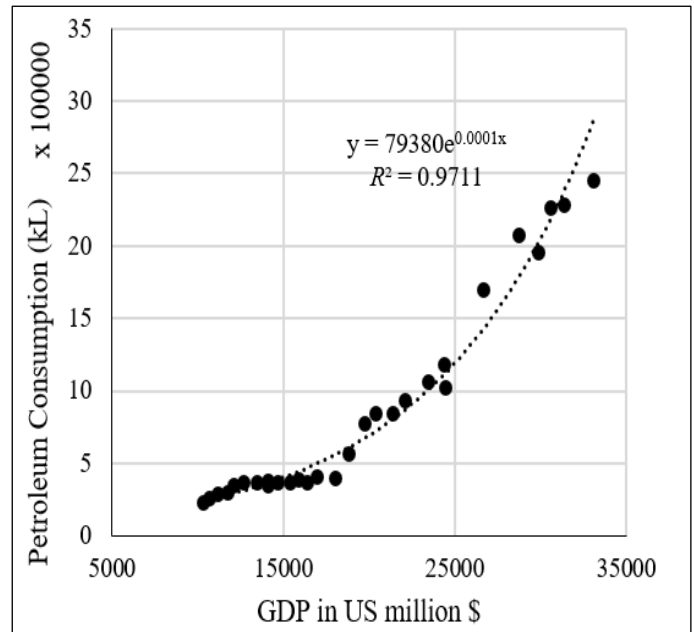
Figure 9: A Scatter Plot Between Petroleum Consumption (kL) and GDP (million $).
Source: Authors, (2024)

VI FORECAST MODEL

VI.1 POPULATION FORECAST MODEL

As the growth rate hovers around 3%, the iteration started $\alpha = 0.03$ and $t_k = 2100$. Special care was taken to take this point such that the saturation population is believable After minimizing the error function with α and t_k, the saturation population computed was 58,783,356 with $\alpha = 0.027$ and $t_k = 2019$, year of inflection with the highest growth rate of population. Here,

$$\beta = \frac{S}{\alpha} = 4.71*10^{-10}$$

Thus, the population model prepared is as:

$$P_t = \frac{58,783,356}{1+11.761e^{-0.027t}}$$ (17)

Where,
P_t represents the population at t years
t years is $(Year - 1930)$

Upon computation of the coefficient of determination, an excellent fit has been observed. An R^2 of 0.995. Figure 10 shows the model fitting in actual data.
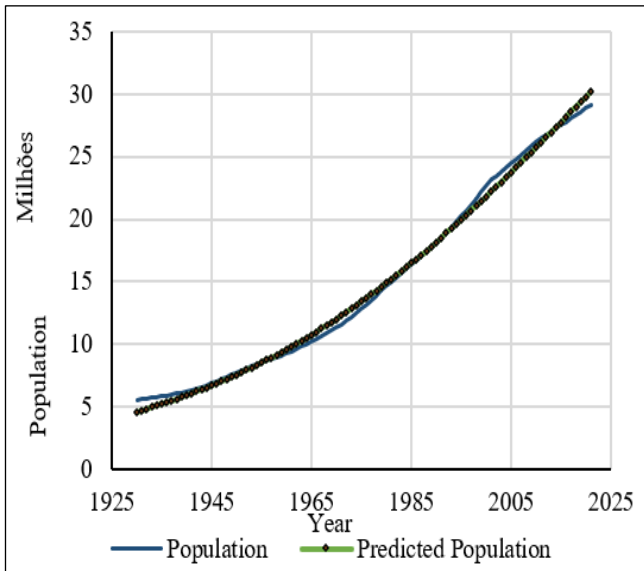
Figure 10: The resemblance between population model and the population through a scatter plot.
Source: Authors, (2024).

VI.2 CUMULATIVE VEHICLES PER 1000 POPULATIONS FORECAST MODEL

Two growth models have been computed with two saturation values using the least square method with Excel. Excellent goodness of fit for both the models have been observed for both the models.

For a Saturation of 400 cumulative vehicles per 1000 persons, where an assumption of 2.5 persons per vehicle is made, the medium growth model developed is as:

$$\text{Cum. Vehicles per 1000 persons} = \frac{400}{1+67.524e^{-0.127*t}} \qquad (18)$$

With R^2 of 0.986, where the inflection year is 2027, and with p-values for both the coefficients negligible, shows the significant relationship of the equation.
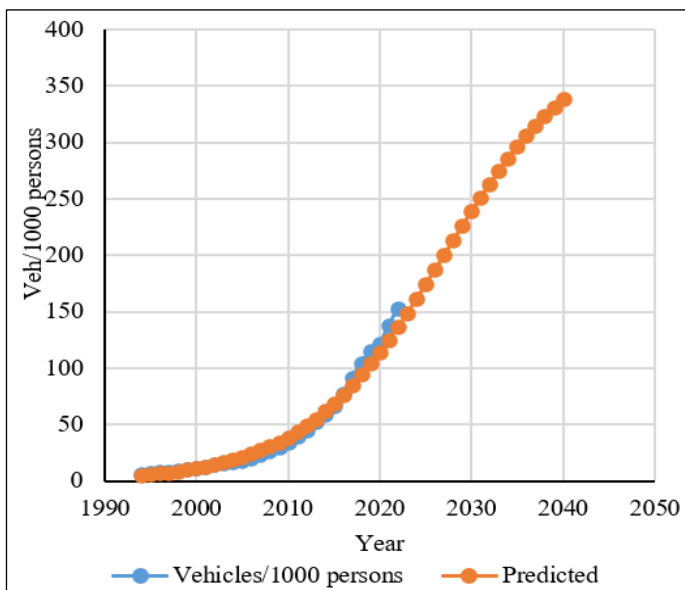
Figure 11: A plot of vehicle population model and vehicle population per 1000 persons in different years for medium growth.
Source: Authors, (2024).

While for saturation of 550 cum. Vehicles per 1000 persons for high growth:

$$\text{Cum. Vehicles per 1000 persons} = \frac{550}{1+90.78e^{-0.122*t}} \qquad (19)$$

An R^2 of 0.9906 and p-values that tend to zero have been observed for this equation as well. This can also be observed in Figure 12.
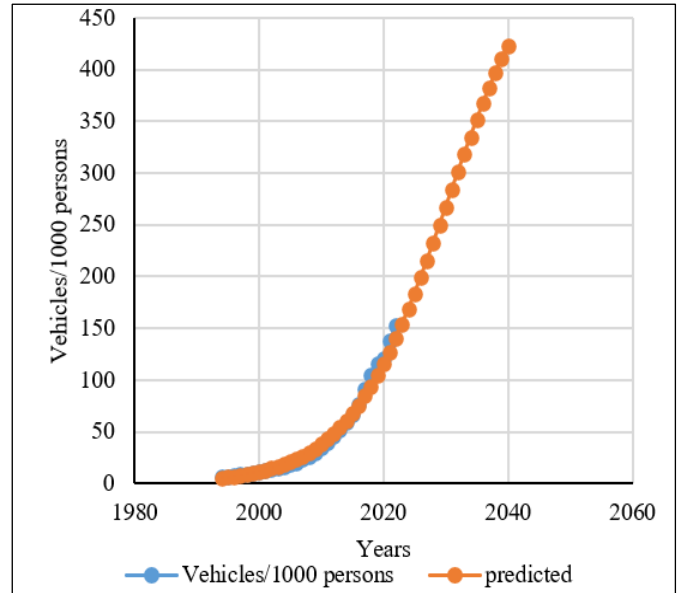
Figure 12: A plot of vehicle population model for high growth.
Source: Authors, (2024).

VI.3 PREDICTED SCENARIO

With the population model and vehicle population model, the predicted corresponding population and the vehicle fleet in year 2030 and 2040 is shown in Table 2

This prediction is based on the developed models of the study. The prediction shows that, while comparing to the situation of 2022, the vehicle fleet will almost double in 2030 while considering high growth and will almost three-fold in 2040. The vehicle fleet size seems to reach 76.65 ('00,000) as per the medium growth model in 2030 whereas seems to reach 119.80 lakhs in 2040. Similarly, for high growth, 46.68 ('00,000) vehicles would grow to 85.18 ('00,000) and 148.94 ('00,000) vehicles in 2030 and 2040 respectively. Apparently, a similar growth pattern is observed in fuel consumption in 2030 and 2040 which has been depicted in Table 3. A 24.61 ('00,000) kL fuel consumption in 2022 grows to 42.54 ('00,000) kL in 2030 and almost trebles to 65.5 ('00,000) kL in 2040 in the medium growth model. In high growth model of vehicle growth, fuel consumption rises 2 folds and 4 folds to 47.08 ('00,000) kL and 81 ('00,000) kL in 2030 and 2040 year respectively.

VI.4 ELECTRIC VEHICLE PENETRATION

In the action plan for electric mobility for Nepal, targets have been set to gain 20% electric vehicle share and reduction of fossil fuel consumption by 50% as long-term target [20]. A scenario analysis performed by Andre et al in 2020 in France provided a scenario with more preferences for electric vehicles through policy, incentives and infrastructure, predicted that electric vehicles would penetrate 10.9%, 2.3%, 15% and 42% share of light duty vehicles, trucks, buses and two-wheelers in 2025 [21].

Lutsey, 2015 work suggested in future of the zero-emission vehicles, electric vehicles, and fuel cell electric, with policy support, research and development, and regulation that the share of these vehicles may reach up to 20% to more than 50% whereas also predicted that the share may also reach a value of only 5 to 10% in the time frame 2025-30 if not supported with policy and development [22].

Thus, in this study, a conservative approach with a 20% light vehicle share is assumed to be occupied by electric vehicles in 2030 and 2040 to predict the probable fuel consumption. 87% of the total vehicle share is covered by light vehicles in the context of Nepal which leads to our computation. In 2030 and 2040, a reduction of 17.4% in the total vehicle fleet is taken to estimate the fuel consumption and tabulated in Table 3. The comparative graphic representation has also been shown in Figure 13. The prediction suggests that there would be a reduction of around 7 ('00,000) kL and 11 ('00,000) kL consecutively, 7 ('00,000) kL and 14 ('00,000) kL with the consideration of replacement by electric vehicles for medium growth scenario and high growth scenario in 2030 and 2040 respectively.
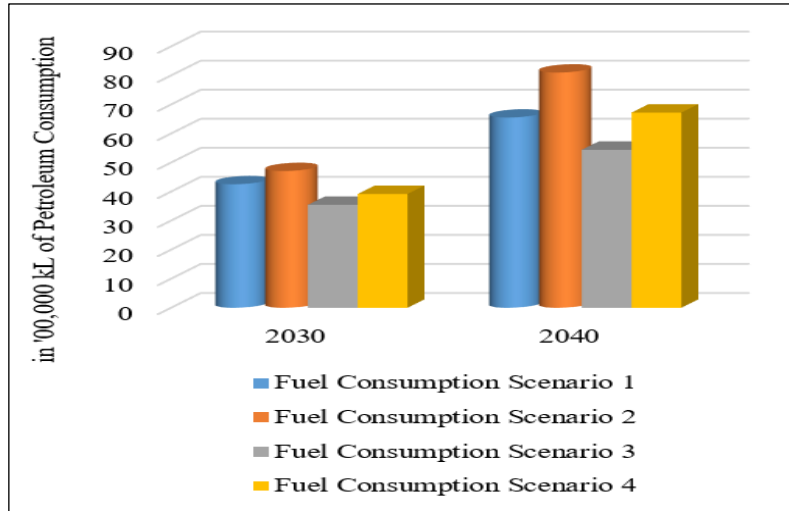
Figure 13: Comparative chart between Fuel Consumption in 4 different scenarios in year 2030 and 2040.
Source: Authors, (2024).

VII. CONCLUSION

The study explored a correlation between GDP, petroleum consumption, and vehicle population. The study showed that the significant linear regression model between petroleum consumption and the vehicle population, petroleum consumption and the operating vehicles population, and petrol consumption and the operating light vehicles are all statistically significant with a high coefficient of determination. Additionally, the relationship between GDP and petroleum consumption; and GDP and operating vehicles is also statistically significant in exponential regression form. The growth trend was observed in all the contexts, but in different scales, with three phases between 1994 to 2005, 2005 to 2016, and 2016 to 2022. Subsequently, logistic models to predict vehicle population and population with high coefficient of determinations and significant relations have been developed to predict the 2030 and 2040 vehicle fleet and population. Two scenarios for vehicle growth have been used to predict fuel consumption in those years. To address the current electrification in the transportation sector, adjustments have been made to the prediction which will yield lesser fuel consumption in the near future. However, this trend has to be supported by action plans, research and incentives. Two growth scenarios, medium and high growth of vehicle fleets, don't make a high difference in the year 2030 while a huge difference is marked in 2040 in fuel consumption.

Table 1: Predicted Values of Year 2030 and 2040 and comparison with year 2022.

Attributes	Existing	Prediction		Remarks
	Year 2022	Year 2030	Year 2040	
Population	29,544,413	32,403,852	35,745,611	Logistic Model
Vehicle/1000 persons	158.01	236.55	335.15	Medium Growth
		262.87	416.68	High Growth
Vehicle Fleet in '00,000'	46.68	76.65	119.80	Medium Growth
		85.18	148.94	High Growth
Fuel Consumption in '00,000 kL'	24.61	42.54	65.5	Medium Growth (Scenario 1)
		47.08	81.00	High Growth (Scenario 2)

Source: Authors, (2024).

Table 2: Prediction of Petroleum Consumption with Considerable Electric Vehicle Share.

Attributes	Existing	Prediction		Remarks
	Year 2022	Year 2030	Year 2040	
Fuel Consumption in "00,000 kL"	24.61	35.45	54.41	Medium Growth (Scenario 3)
		39.19	67.21	High Growth (Scenario 4)

Source: Authors, (2024).

The study also found that there was an increase in fuel efficiency over time, which could be attributed to induced fuel standards and high-efficiency petrol-powered lighter vehicles. Finally, the study concludes with different regression equations that are statistically significant between variable vehicles, GDP, and petroleum consumption with the given sets of data between 1994 and 2022.

VIII. AUTHOR'S CONTRIBUTION

Conceptualization: Niraj Bohara and Hemant Tiwari.
Methodology: Niraj Bohara and Hemant Tiwari.
Investigation: Niraj Bohara and Hemant Tiwari.
Discussion of results: Niraj Bohara and Hemant Tiwari.
Writing – Original Draft: Niraj Bohara
Writing – Review and Editing: Niraj Bohara and Hemant Tiwari.
Resources: Niraj Bohara and Hemant Tiwari.
Supervision: Niraj Bohara and Hemant Tiwari.
Approval of the final text: Niraj Bohara and Hemant Tiwari.

IX. ACKNOWLEDGMENTS

X. REFERENCES

[1] Z. Yue and H. Liu, "Advanced Research on Internal Combustion Engines and Engine Fuels," *Energies*, vol. 16, no. 5940, 2023, doi: https://doi.org/10.3390/en16165940.

[2] I. Tikoudis, R. M. Mebiame, and W. Oueslati, "Projecting the Fuel Efficiency of Conventional Vehicles: The Role of Regulations, Gasoline Taxes and Autonomous Technical Change," OECD Publishing, 2022. doi: https://doi.org/10.1787/13b94818-en.

[3] TNO, "Petrol Fuel Quality and its Effects on the Vehicle Technology and the Environment," TNO, Netherland, 2020.

[4] I. Bajracharya and T. R. Bajracharya, "Scenario Analysis of Road Transport Energy Consumption Emission in Nepal," in *Proceedings of IOE Graduate Conference*, 2013, pp. 11–21.

[5] I. Bajracharya and N. Bhattrai, "Road Transportation Energy Demand and Environmental Emission: A Case Study of Kathmandu Valley," *Hydro Nepal J. Water Energy Environ.*, vol. 18, pp. 30–40, 2016, doi: 10.3126/hn.v18i0.14641.

[6] Ministry of Physical Infrastructure and Transport, "Vehicle Registered Till Fiscal Year 2075/76," MoPIT, 2018.

[7] Ministry of Finance, "Economic Survey 2022/23," Kathmandu, 2023.

[8] Nepal Oil Corporation, "Sales of Petroleum Products in kL," 2023. https://noc.org.np/import (accessed Aug. 10, 2023).

[9] The World Bank, "World Bank Open Data," *World Bank national accounts data, and OECD National Accounts*, 2023. World Bank national accounts data, and OECD National Accounts (accessed Aug. 10, 2023).

[10] A. Ojha, "Countrywide Ban on Vehicle Older than 20 Yrs From March 15," *The Kathmandu Post*, Feb. 06, 2018. [Online]. Available: https://kathmandupost.com/national/2018/02/06/countrywide-ban-on-vehicles-older-than-20-yrs-from-mar-15#:~:text="The documents of the vehicles,the Transport Management Regulation Act.

[11] D. Das, A. Sharfuddin, and S. Datta, "Personal Vehicles in Delhi: Petrol Demand and Carbon Emission," *Int. J. Sustain. Transp.*, vol. 3, no. 2, pp. 122–137, 2009, doi: 10.1080/15568310802165907.

[12] K. Adhikari and H. B. Raya, "Population Projection of Nepal: A Logistic Approach," *J. Nepal Math. Soc.*, vol. 1, no. 2, pp. 1–8, 2018, doi: 10.3126/jnms.v4i2.41482.

[13] A. Wali, E. Kagoyire, and P. Icyingeneye, "Mathematical Modeling of Uganda Population Growth," *Appl. Math. Sci.*, vol. 6, no. 84, pp. 4155–4168, 2012.

[14] Nepal Statistics Office, "National Population and Housing Census 2021," Thapathali, Kathmandu, 2021.

[15] H. Huo, M. Wang, L. Johnson, and D. He, "Projection of Chinese Motor Vehicle Growth, Oil Demand, and CO2 Emissions Through 2050," *J. Transp. Res. Board*, no. 2038, pp. 69–77, 2007, doi: 10.3141/2038-09.

[16] J. Dargay, D. Gately, and M. Sommer, "Vehicle Ownership and Income Growth, Worldwide: 1960-2030," *Energy J.*, vol. 28, no. 4, pp. 143–170, 2007, doi: 10.5547/ISSN0195-6574-EJ-Vol28-No4-7.

[17] W. H. Bottiny, "Trends in Automobile Ownership and Indicators of Saturation," *Highw. Res. Rec.*, vol. 106, pp. 1–21, 1966.

[18] N. Singh, T. Mishra, and R. Banerjee, "Projection of Private Vehicle Stock in India up to 2050," in *Transportation Research Procedia*, 2020, vol. 48, no. 2019, pp. 3380–3389. doi: 10.1016/j.trpro.2020.08.116.

[19] U.S. Department of Transportation, "Motor Vehicle Fuel Consumption and Travel | Bureau of Transportation Statistics," 2021. https://www.bts.gov/content/motor-vehicle-fuel-consumption-and-travel

[20] Global Green Growth Institute, "National Action Plan for Electric Mobility: Accelerating Implementation of Nepal's Nationally Determined Contribution," 2018. [Online]. Available: https://gggi.org/site/assets/uploads/2018/07/GGGI-Nepal_Action-Plan-for-Electric-Mobility.pdf

[21] M. Andre, K. Sartelet, S. Moukhtar, J. M. Andre, and M. Redaelli, "Diesel, Petrol or Electric Vehicles: What Choices to Improve Urban Air Quality in the Ile-de-France Region? A Simulation Platform and Case Study," *Atmos. Environ.*, vol. 241, no. 2, p. 117752, 2020, doi: 10.1016/j.atmosenv.2020.117752.

[22] N. Lutsey, "Transition to a Global Zero-Emission Vehicle Fleet: A Collaborative Agenda for Governments," 2015.
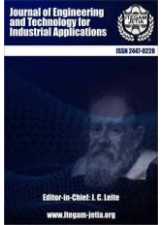
SIMULATION AND ANALYSIS OF LIGHTNING STRIKES IN ELECTRICAL SYSTEMS BY MATLAB/SIMULINK AND ATP/EMTP

Mohamed. Elbar[1], Aissa Souli[2], Abdelkader Beladel[3] and Mohamed Khaleel[4]

[1,3] Applied automation and industrial diagnostic Laboratory (LAADI), Faculty of Science and Technology, University of Djelfa, Algeria.
[2] Electrical Engineering Department. Nuclear Research Center of Birine. Djelfa, Algeria
[4] Dept of Electrical-Electronics Eng. Faculty of Engineering. Karabuk University. Karabuk., Turkey.

[1] http://orcid.org/0000-0002-2636-9469, [2] http://orcid.org/ 0009-0001-5463-8267, [3]http://orcid.org/0000-0002-3857-0063,
[4]http://orcid.org/0000-0002-3468-3220

Email: [1]m.elbar@univ-djelfa.dz, [2]a.souli@crnb.dz, [3]a.beladel@univ-djelfa.dz, [4]lykhaleel@yahoo.co.uk.

ARTICLE INFO	ABSTRACT
	Lightning is a major disruptive phenomenon in the operation of all electrical installations. Lightning has always been a cause of disruption in the use of electricity. However, it is important to note the fairly recent and growing requirement for the quality of electrical systems (reliability, availability, continuity of service, etc.) as well as the constant concern to minimize the costs of using and producing electricity. This leads us to see that lightning becomes a hard point in improving all these factors. In this article, we present the ATP software that we will use in the simulation. After that, we discussed the description of lightning strikes and how to protect facilities from them. The next important step, which represents the novelty of this work, was to create a lightning strike model using the MATLAB/SIMULINK program, based on the mathematical equation of a lightning strike. After that, by using the model created, we simulated a lightning strike that attacked two different nodes of an electrical network, generators, and nine nodes, using the two-simulation software's ATP/EMTP and MATLAB/SIMULINK to study the effect of the lightning strike on the voltages and currents of our network system. At the end of the work, we compared the results obtained by the two-simulation software, ATP/EMTP and MATLAB/SIMULINK, and we discussed and explained the results obtained by the two software.

I. INTRODUCTION

Lightning-induced overvoltage in electrical power net-works is one of the main causes of problems with the quality of power supplied to consumers and with electromagnetic compatibility [1],[2]. In recent years, due to the growing demand for better quality electrical power and the widespread use of sensitive electronic devices connected to distribution lines, protection against lightning-induced disturbances has become of paramount importance.

Therefore, the accurate assessment of lightning-induced over-voltages has become essential for the effective protection of electrical and electronic systems [2]. Thus, the idea of having tools that simplify the study, the analysis, and the simulation has been perceived for a long time, and computer software specialized in the study of the transitory regimes of electrical systems appeared to be used by electricity companies and by research centres specializing in the field of electrical networks [3],[4].

A simulator can therefore be developed to simulate not a single particular physical phenomenon but to study a vast quantity of phenomena that can be very different from each other [5],[6].

Lightning is a lightning bolt that falls to the ground. It is a frequent phenomenon that behaves like a perfect genera-tor of electric current. To protect yourself in 95% of cases, the current that should be taken into account is 100 kA with a very short rise time. In addition to the conduction phenomenon, the ionized

channel of lightning behaves like a long wire that radiates an electromagnetic field. This field induces voltages in large ground loops, which are counted in kilovolts. These surges can destroy interface components. Lightning is therefore not a phenomenon to be feared only during a "hit on goal"; the effect induced by the field matters.

In this work, a lightning strike model will be created un-der the MATLAB/SIMULINK environment for use in simulation tests with an IEEE 9 node power grid.

In this article, we simulate a lightning strike that attacks two different nodes in an electrical network with three generators and nine nodes. The lightning strike was created with the MATLAB/SIMULINK software, and the lightning strike exists in the ATP library with the ATP software to have their impact on the voltages and currents of this network [7].

II. PRESENTATION OF SOFTWARE'S

II.1 ALTERNATIVE TRANSIENT PROGRAM (ATP)

ATP is a universal program system for digital simulation of transient phenomena [8],[9] of electromagnetic as well as electromechanical nature. With this digital program, com-plex networks and control systems of arbitrary structure can be simulated.

ATP has extensive modelling capabilities and additional important features besides the computation of transients. It has been continuously developed through international contributions over the past 20 years [10],[11].

The ATP program can model almost anything that exists in the network. However, users can still create the various elements themselves thanks to additional modules and pro-grams such as for example, TACS (Transient Analysis of Control Systems) or MODELS (simulation language), which allow the modelling of control systems or non-linear characteristics [12].

III. LIGHTNING STRIKE THEORY

III.1 DEFINITIONS

Lightning is a manifestation of electricity of atmospheric origin, comprising an electric discharge accompanied by a bright light (lightning) and a violent detonation (thunder). Lightning is a set of luminous manifestations caused by discharges of atmospheric origin [13],[14].

Fundamental thunderstorms are, for the meteorologist, linked to cumulonimbus clouds. The stormy mechanism consists of a succession of very rapid lifts, causing the formation of cumulonimbus clouds and determining two series of parallel but distinct effects; Electrical phenomena include lightning, which does not always exist, and electromagnetic disturbances, which always exist. Mechanical and rainfall phenomena include gusts of wind and showers.

III.2 CLASSIFICATION OF LIGHTNING STRIKES

The asperities of the ground or structures create a "point effect", which greatly amplifies the local electric field. This increase in the electric field results in a "Corona" effect - local ionization of the air. An ionized air channel linking the cloud to the ground allows the flow of the lightning strike. There are four characteristic types of lightning strikes: negative, positive, descending and ascending. In France, 90% of lightning strikes are descending negative. The amplitude of the current can be very strong, varying from 2000 to 200000 amperes [15].

III.3 PRIMARY PROTECTIONS

Their purpose is to protect installations against direct lightning strikes. These protections make it possible to capture and route the lightning current to the ground. The principle is based on a protection zone determined by a structure higher than the others. It is the same for any peak effect caused by a pole a building, or a very tall metallic structure.

- There are three main types of primary protection [16],[17].
- The lightning rod, which is the oldest and best-known protection.
- Stretched wires.
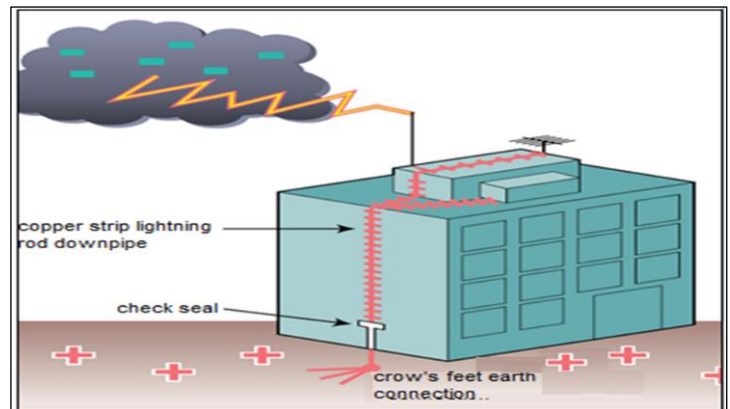- The mesh cage, or Faraday cage

Figure 1: Principle of the rod lightning rod.
Source: Authors, (2024).

III.3.1 THE TAUT THREADS

These are cables stretched above the work to be protect-ed. They are used for special works include rocket launch pads, military applications and above all ground wires above high voltage lines [18].
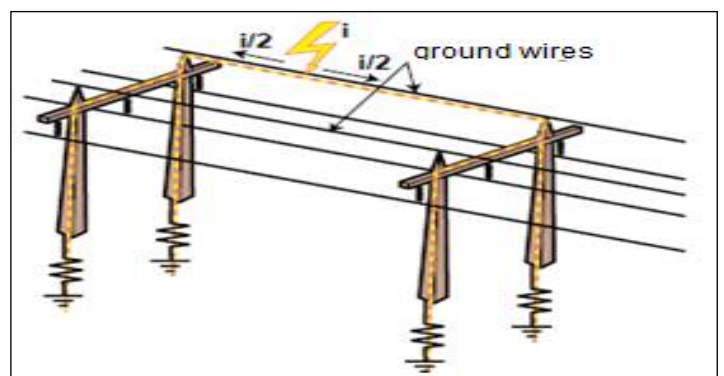

Figure 2: Ground Wires.
Source: Authors, (2024).

III.3.2 The Mesh Cage (Faraday Cage)

This principle is used for very sensitive buildings housing computer equipment or the manufacture of integrated circuits. It consists of multiplying the descent strips outside the building in a symmetrical manner. Horizontal links are added if the building is tall; for example, every two floors (Figure 3). The down conductors

are earthed by the crow's feet. The result is to obtain meshes of 15 x 15 m or 10 x 10m.

The effect results in a better bedded equipotential of the building and the division of the lightning currents, thus strongly reducing the electromagnetic fields and inductions [19],[20].
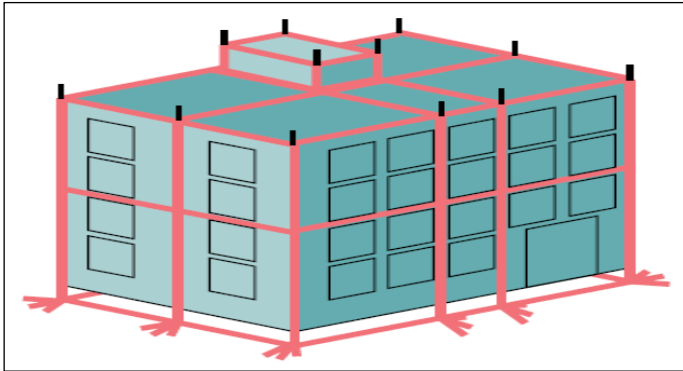

Figure 3: Principle of a mesh cage (Faraday cage).
Source: Authors, (2024).

III.4 SECONDARY PROTECTIONS

The protection of electrical loads against overvoltages of atmospheric origin most commonly used is protection by lightning arresters [21],[22]. The arrester is generally placed between a conductor and the ground, and sometimes between active conductors. The two cases are represented in Figure 4. Under normal tension, the surge arrester behaves practically like an infinite resistance, and the current that crosses it is null or negligible (leakage current). On the other hand, on the appearance of an overvoltage, as soon as the voltage at the terminals of the surge arrester exceeds a certain limit, the surge arrester becomes conductive, letting a current flow, which limits the voltage at its terminals and thus protects the installation and receivers. For each use case, the arrester is chosen mainly according to the following parameters:

- The overvoltage permitted by the devices to be protected.
- The intensity of the current that the surge arrester will have to withstand for the duration of the overvoltage.
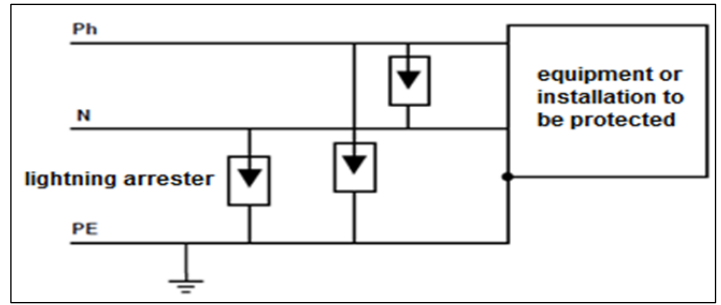
Figure 4: Use of Lightning Arresters.
Source: Authors, (2024).

IV. LIGHTNING MODEL

The lightning strike is represented by the following mathematical equation [23],[24].

$$f(t) = Amplitude(e^{At} - e^{Bt}) \qquad (1)$$

So that each of the amplitude, A and B, are represented in the following Table 1.

Table 1: Lightning Parameters.

Lightning Parameters	
Constant	Value
A	-9500
B	-600000
Amplitude	34000
Tstart	0.00
Tstop	0.0006

Source: Authors, (2024).

If we click on the lightning strikes block, illustrated in Figure 5, we obtain the following figure:
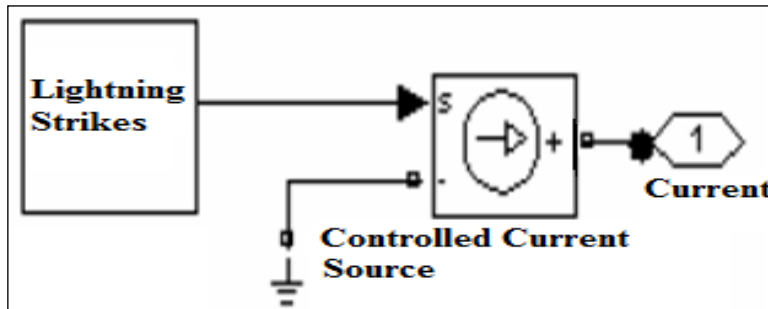
Figure 5: Model of a Lightning Strike (Current Wave) Masked in SIMULINK.
Source: Authors, (2024).
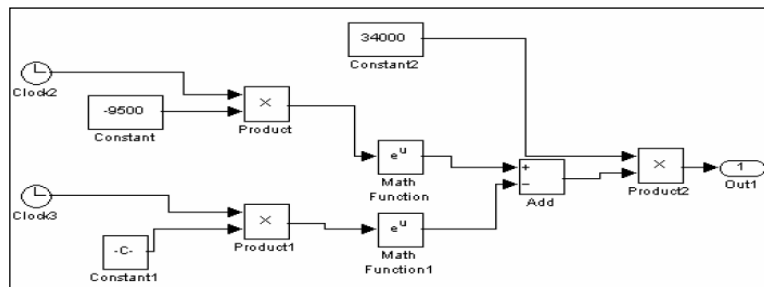
Figure 6: Lightning Model in SIMULINK.
Source: Authors, (2024).
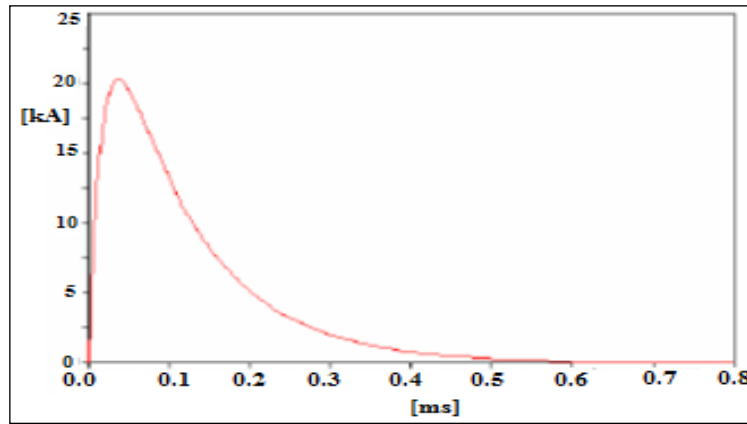
Figure 7: Lightning Strike Wave Current 20KA 0.6ms.
Source: Authors, (2024).

V. TEST NETWORK

A 9-bus 3-machine system [25], includes three generators and three large equivalent loads connected in a meshed transmission network through transmission Lines, as shown in Figure 8.

VI. APPLICATIONS EXAMPLES

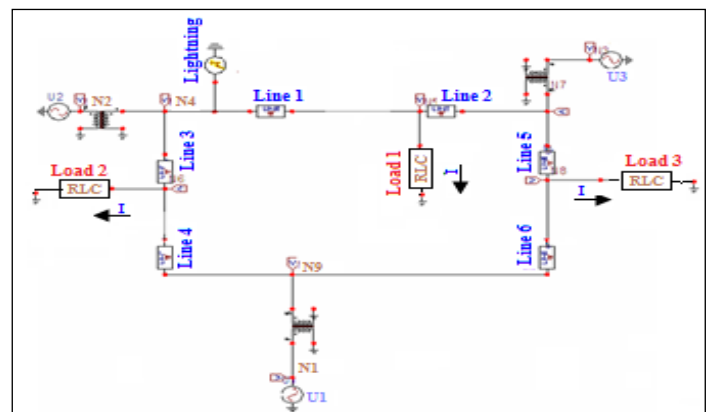### VI.1 EXAMPLE 1: SIMULATION OF LIGHTNING STRIKE AT NODE 4
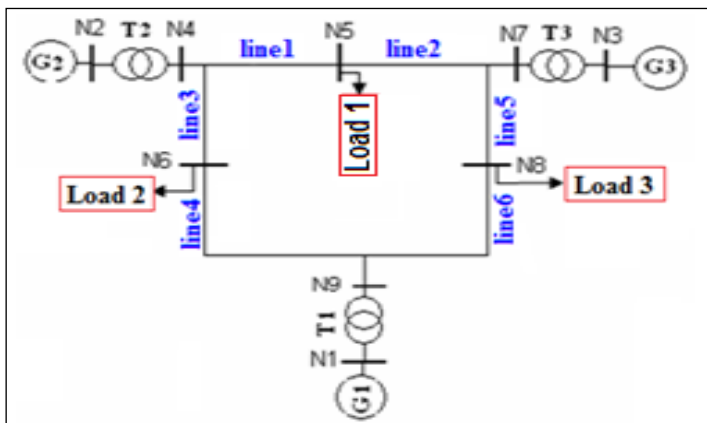
VI.1.1 With Atp

Figure 8: Synoptic Diagram of the WSCC Network (3G, 9N).
Source: Authors, (2024).

Figure 9: Simulation of lightning strike at node 4 with ATP.
Source: Authors, (2024).

VI.1.2 With Matlab/Simulink
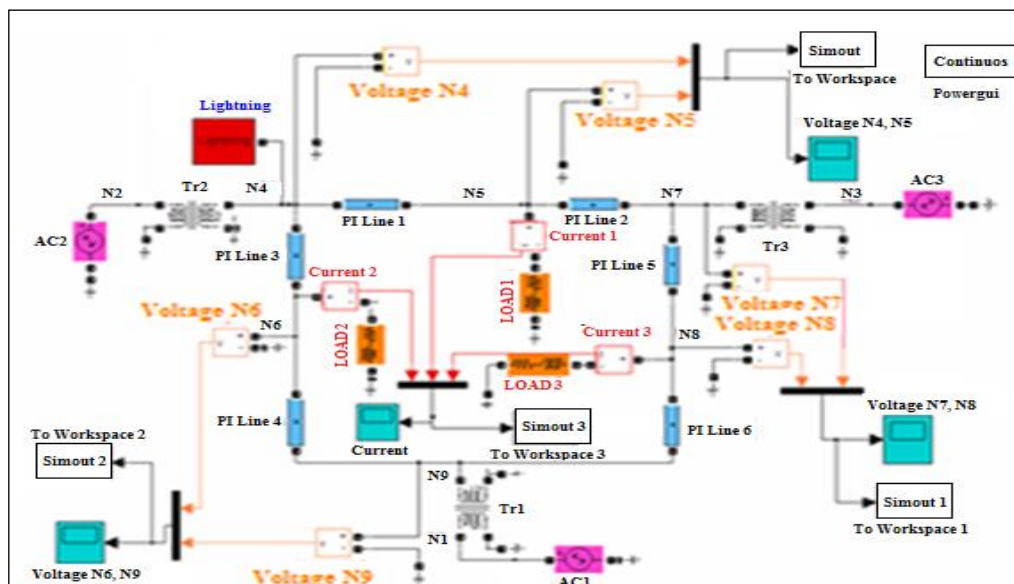
Figure 10: Simulation of lightning strike at node 4 with SIMULINK.
Source: Authors, (2024).

VI.2 EXAMPLE 2: Simulation of Lightning Strike at Node 5

VI.2.1 With Atp
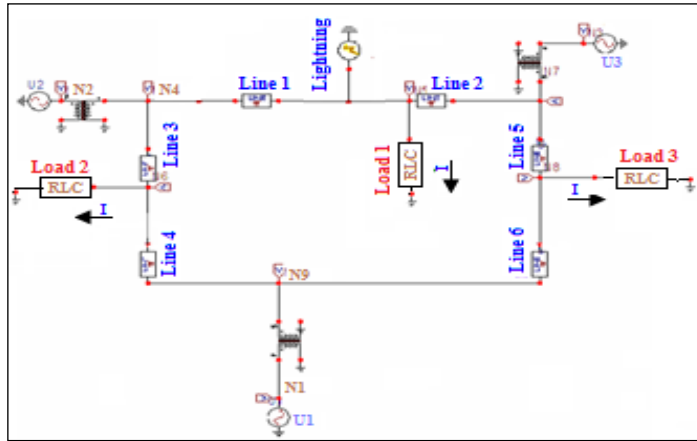
Figure 11: Simulation of lightning strike at node 5 with ATP.
Source: Authors, (2024).

VI.2.2 With Matlab/Simulink
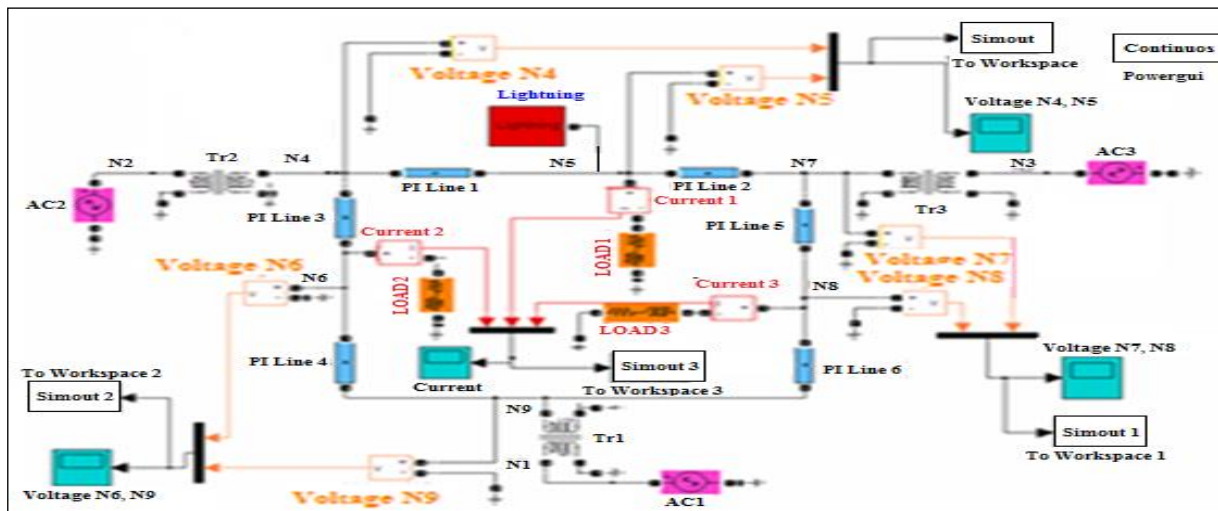
Figure 11: Simulation of lightning strike at node 5 with SIMULINK.
Source: Authors, (2024).

VII. SIMULATION RESULTS

VII.1. EXAMPLE 1

VII.1.1. With Atp
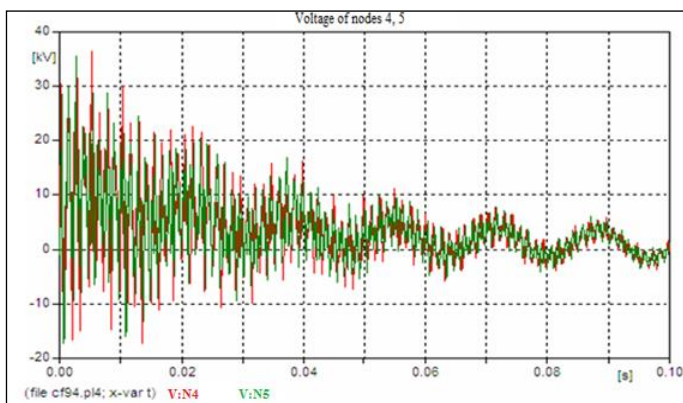
Figure 13.a: Voltage of node 4,5
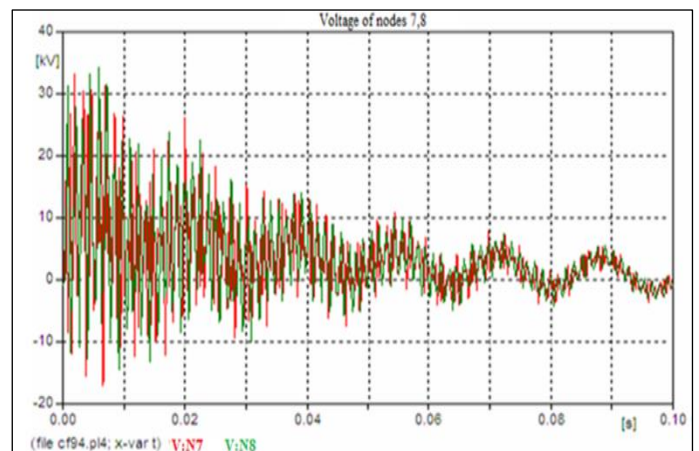
Figure 13.b: Voltage of node 7,8
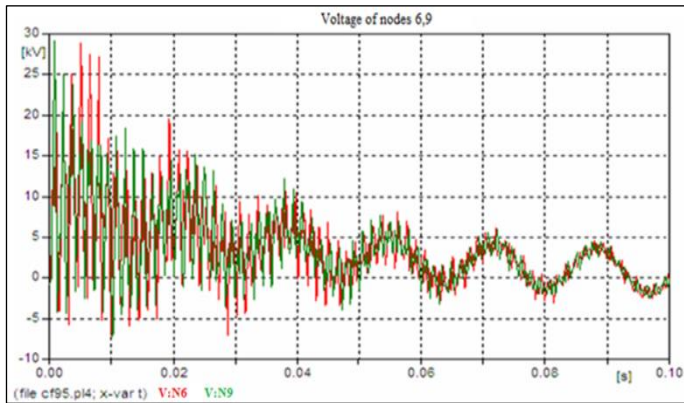
Figure 13.c: Voltage of node 6,9
Figure 13: (a, b, c) Voltage Curve of Example 1
Source: Authors, (2024).

Figure 14: Current Curve of Example 1
Source: Authors, (2024).
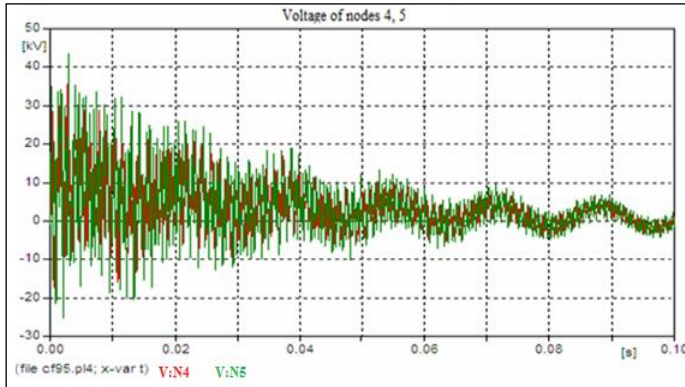
VII.1.2. With Matlab
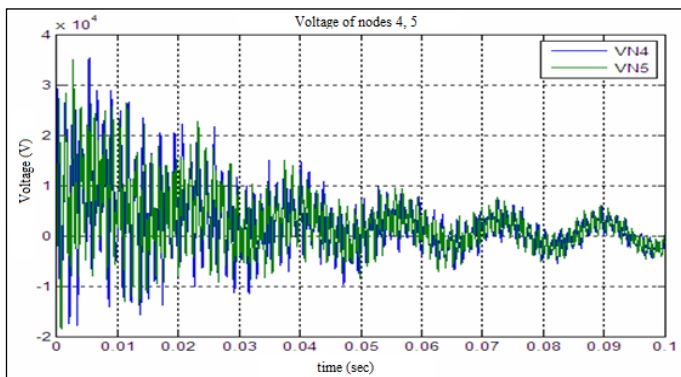
Figure 15.a: Voltage of node 4,5
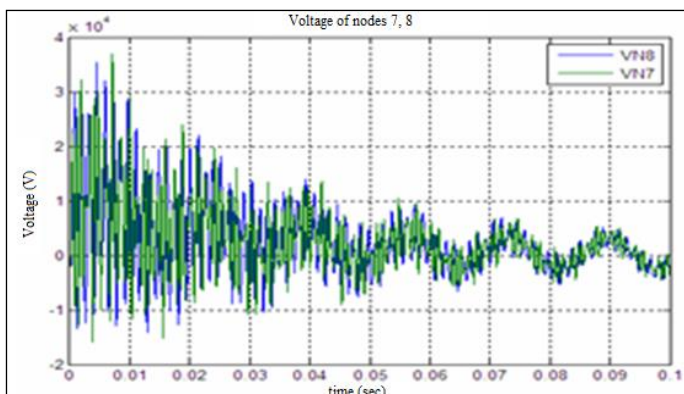
Figure 15.b: Voltage of node 7,8

Figure 15.c: Voltage of node 6,9
Figure 15: (a, b, c) Voltage Curve of Example 1
Source: Authors, (2024).

Figure 16: Current Curve of Example 1
Source: Authors, (2024).

VII.1.3. Interpretation

For example, 1, a lightning strike hits node 4 of the 9N-3G network. The voltages of nodes 4 and 5, VN4, VN5 then reach peaks between -20kV and 40kV, before decreasing at the end of the cycle to around 3.5kV. The voltages VN7, VN8 of nodes 7 and 8 respectively reach -20kV and 40kV at the start of the fault then oscillate to reach 3.5kV at the end of the cycle. At nodes 6 and 9 have voltages VN6, VN9, for their part, reach peaks of - 5kV and 25kV to stabilize around 2 kV at the end of the cycle.

We noticed that the voltage peaks did not reach very large values compared to the previous example because the reactance's of the lines in this example have slightly smaller values.

The currents of loads 1 and 3 show peaks that reach 20A, then decrease and stabilize towards the end of the second cycle around their initial values.

The current of load 2 has a peak that reaches 25A, then decreases and stabilizes towards the end of the second cycle around its initial value. We notice that the load current increases in this example by 5 and 6 times the nominal value due to the lightning strike, and it takes a time of 0.16sec (10 periods) to return to its normal value.

We note in this example that the results obtained under ATP software are quite similar to the results obtained under MATLAB/SIMULINK.

VII.2. Example 2

VII.2.1. With Atp
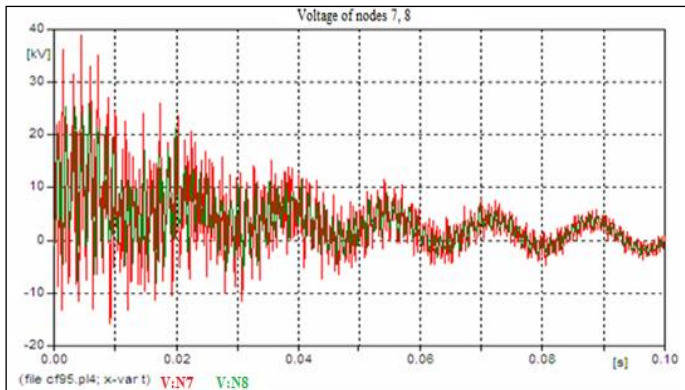

Figure 17.a: Voltage of node 4,5
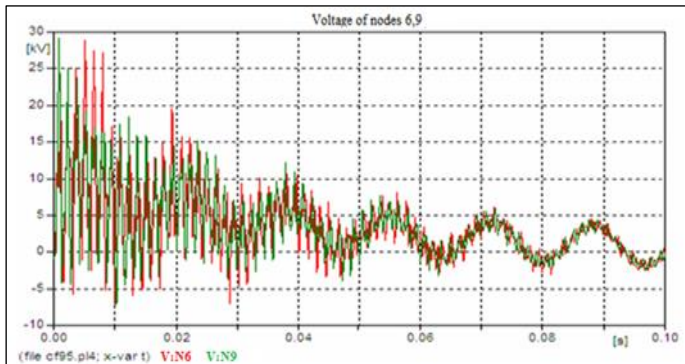

Figure 17.b: Voltage of node 7,8

Figure 17.c: Voltage of node 6,9
Figure 17: (a, b, c) Voltage Curve of Example 2
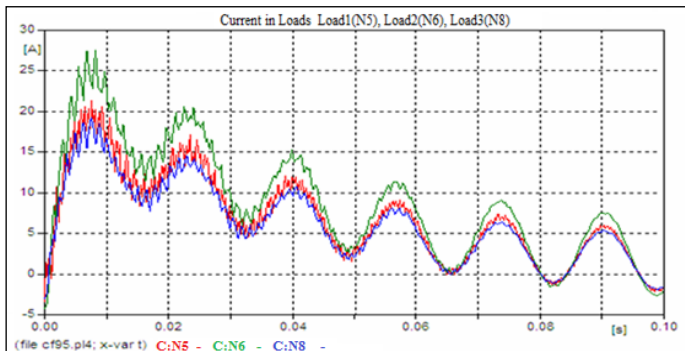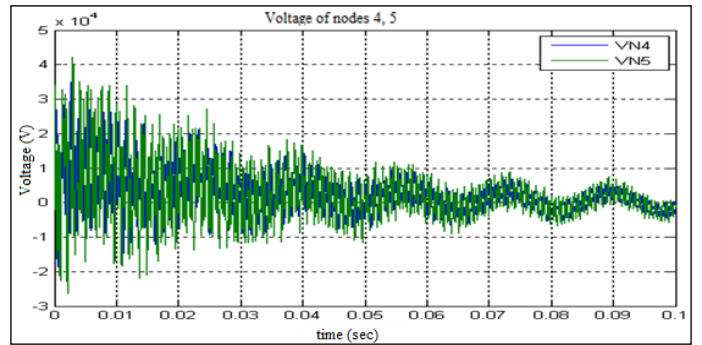Source: Authors, (2024).

Figure 18: Current Curve of Example 2
Source: Authors, (2024).

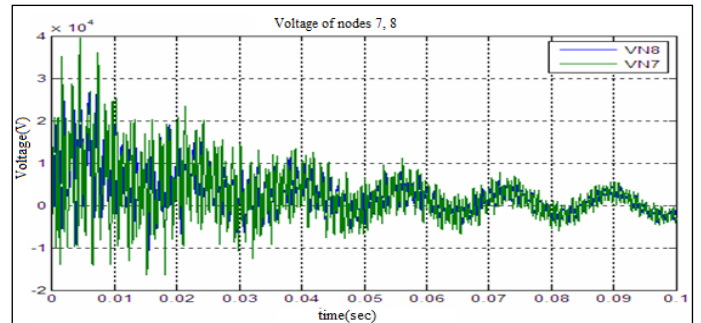### VII.2.2. With Matlab

Figure 19.a: Voltage of node 4,5
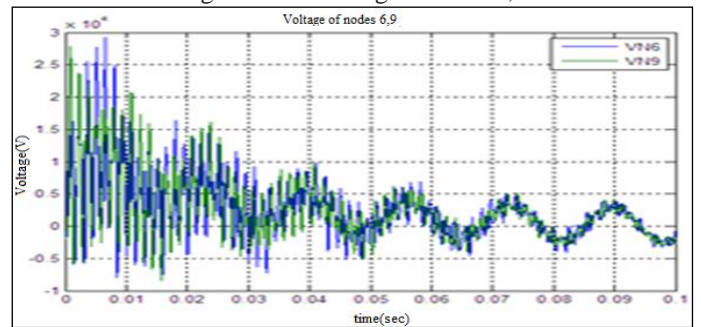

Figure 19.b: Voltage of node 7,8

Figure 19.c: Voltage of node 6,9
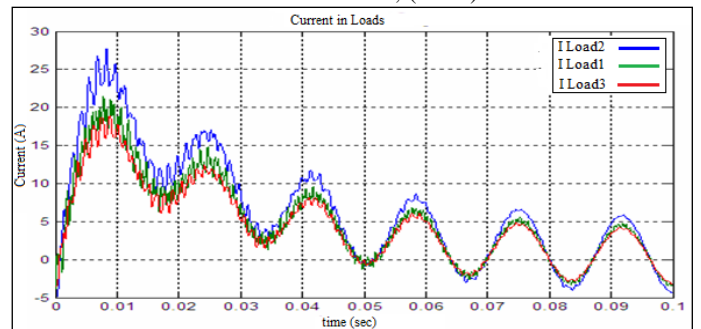Figure 19: (a, b, c) Voltage Curve of Example 2
Source: Authors, (2024).

Figure 20: Current Curve of Example 2
Source: Authors, (2024).

VII.2.3. Interpretation

For example, 2, a lightning strike hits node 5 of the 9N-3G network. The voltages of nodes 4 and 5, VN4, VN5then reach peaks between -30kV and 50kV, before decreasing at the end of the cycle to around 4kV. The voltages VN7, VN8 of nodes 7 and 8 respectively reach -20kV and 40kV at the start of the fault, then oscillate to reach 3.5kV at the end of the cycle. At nodes 6 and 9

have voltages VN6, VN9, for their part, reach peaks of -10kV and 30kV to stabilize around 2.5kV at the end of the cycle.

We notice that the voltage peaks did not reach very large values compared to the previous example because the reactance of the lines in this example have slightly smaller values.

The currents of load 1 and load 3 show peaks that reach 20A, then decrease and stabilize towards the end of the second cycle around their initial values. The current of load 2 has a peak that reaches 25A, then decreases and stabilizes towards the end of the second cycle around its initial value.

We notice that the load current increases in this example by 5 and 6 times the nominal value due to the lightning strike, and it takes a time of 0.16sec (10 periods) to return to its normal value. We note in this example that the results obtained under ATP software are quite similar to the results obtained under MATLAB/SIMULINK.

VIII. INTERPRETATION

This work focused on the use of MATLAB/ SIMULINK and ATP software for the simulation of lightning strikes in electrical networks, the impact of lightning strikes on the behaviour of an electrical network, and on the other hand, a comparison between the results obtained from the two simulation Programs, MATLAB/SIMULINK and ATP.

In this work, a lightning strike model will be created in the MATLAB/SIMULINK environment for use in simulation tests with an IEEE 9-bus power grid.

Our work consisted in simulating lightning faults at different points of the IEEE 9bus network by using ATP/EMTP and MATLAB/SIMULINK simulation software to study and analyse the results and curves obtained by each simulation program so that they could be interpreted and compared.

I note that whatever the point of the lightning strike in the electrical network, the voltages and currents are severely affected and reach significant values, up to ten times the real value of the voltage or the intensity of the electric cur-rent.

We can say that the lightning strike is a very severe short-circuit; therefore, it is necessary to protect the electrical networks as much as possible from these lightning strikes.

The results obtained by the MATLAB/SIMULINK program were thus tested on the same examples and gave complete satisfaction for the simulations carried out by the ATP software, which confirms the relevance of the work.

IX. AUTHOR'S CONTRIBUTION

Conceptualization: Mohamed. Elbar, Aissa Souli, Abdelkader Beladel and Mohamed Khaleel.
Methodology: Mohamed. Elbar, Aissa Souli, Abdelkader Beladel and Mohamed Khaleel.
Investigation: Mohamed. Elbar, Aissa Souli, Abdelkader Beladel and Mohamed Khaleel.
Discussion of results: Mohamed. Elbar, Aissa Souli, Abdelkader Beladel and Mohamed Khaleel.
Writing – Original Draft: Mohamed. Elbar, Aissa Souli, Abdelkader Beladel and Mohamed Khaleel.
Writing – Review and Editing: Mohamed. Elbar, Aissa Souli, Abdelkader Beladel and Mohamed Khaleel.
Resources: Mohamed. Elbar, Aissa souli.
Supervision: Mohamed. Elbar, Aissa Souli, Abdelkader Beladel and Mohamed Khaleel.
Approval of the final Mohamed. Elbar, Aissa Souli, Abdelkader Beladel and Mohamed Khaleel.

X. REFERENCES

[1] M. ELBAR, A. SOULI, A. BELADEL, B. Ali, and A. Benhaimoura, "Impact study of flexible alternating current trans-mission system on power flow and power loss in power systems using MATLAB and PSAT", SEES, vol. 4, no. 1, pp. 348–369, Dec. 2023. https://doi.org/10.54021/seesv4n1-021.

[2] B. Korich, D. Bakria, D. Gozim, R. D. Mohammedi, M. Elbar, and A. Teta, "Shifting of Nonlinear Phenomenon in the Boost converter Using Aquila Optimizer", J. Eng. Exact Sci., vol. 9, no. 3, pp. 15744–01e, May 2023. https://doi.org/10.18540/jcecvl9iss3pp15744-01e.

[3] Mohamed, ELBAR; Ahmed Zohair, DJEDDI; Hafaifa, Ahmed; Naas, CHARRAK; Iratni, Abdelhamid; and colak, ilhami (2023) "Evaluation of Reliability Indices for Gas Turbines Based on the Johnson SB Distribution: Towards Practical De-velopment," Emirates Journal for Engineering Research: Vol. 28: Iss. 2, Article 5. https://scholarworks.uaeu.ac.ae/ejer/vol28/iss2/5.

[4] ELBAR M., MERZOUK I., BEALDEL A., REZAOUI M.M., IRATNI A., HAFAIFA A., "Power Quality Enhancement in Four-Wire Systems Under Different Distributed Energy Re-source Penetration", in Electrotehnica, Electronica, Automati-ca (EEA), 2021, vol. 69, no. 4, pp. 50-58, ISSN 1582-5175. https://doi.org/10.46904/eea.21.69.4.1108006.

[5] Solouk A, Shakiba-Herfeh M, Kannan K, Solmaz H, Dice P, Bidarvatan M, et al. Fuel Economy Benefits of Integrating a Multi-Mode Low Temperature Combustion (LTC) Engine in a Series Extended Range Electric Powertrain. In: SAE Technical Papers. 2016. http://dx.doi.org/10.29228/

[6] Chikhi K. (2007). Contribution à l'analyse de la qualité de l'énergie électrique dans le cas de la stabilité de la tension. Thèse Docteur d'Etat préparée au Département d'Electrotechnique Université de Batna.

[7] Prabha Kundur and All. (2004). Definition and Classification of Power System. IEEE Transactions on Power Systems, Vol. 19, no. 2, pp. 1387–1401.

[8] M. Bourennane, N. Terki, M. Hamiane, and A. Kouzou, "An Enhanced Visual Object Tracking Approach based on Combined Features of Neural Networks, Wavelet Transforms, and Histogram of Oriented Gradients," Eng. Technol. Appl. Sci. Res., vol. 12, no. 3 SE-, pp. 8745–8754, Jun. 2022, doi: https://doi.org/10.48084/etasr.5026.

[9] Bell K., Tleis A. (2010). Test system requirements for model-ling future power systems. IEEE PES general meeting, pp. 1-8, 10.1109/PES.2010.5589807.

[10] A. Ametani, T. Kawamura. (2005). A method of a lightning surge analysis recommended in Japan using EMTP. IEEE Transactions on Power Delivery, vol. 20, no. 2, pp. 867-875.

[11] T A Tuan. (2006) Modélisation de la Propagation des Si-gnaux HF dans le Réseau d'Energie Electrique. Thèse de Doc-torat Es Sciences, Ecole Centrale de Lyon.

[12] ''ATP-EMTP Beginner's Guide '', BGuide02, ATP-EMTP Version 2, Copyright Deniz Celikag 1999-2002, Germany, Novembre 2002, disponible à www.eeug.org.

[13] A. Bensalem, B. Toual, M. Elbar, M. Khaleel, and Z. Belboul, "A framework to quantify battery degradation in residential microgrid operate with maximum self-consumption based en-ergy management system", SEES, vol. 5, no. 1, pp. 354–370, Feb. 2024. https://doi.org/10.54021/seesv5n1-021

[14] A. Kechida, D. Gozim, B. Toual, R. D. Mohammedi, and M. Elbar, "Management stand-alone hybrid renewable energy system based on wind and solar with battery storage", SEES, vol. 5, no. 1, pp. 97–113, Jan. 2024. https://doi.org/10.54021/seesv5n1-006.

[15] R. D. Mohammedi, D. Gozim, A. A. Laouid, and M. Elbar, "Optimal placement of phasor measurement units using topol-ogy transformation method based on Grey Wolf optimization approach", SEES, vol. 5, no. 1, pp. 131–150, Jan. 2024. https://doi.org/10.54021/seesv5n1-008.

[16] M. Khaleel and M. Elbar, "Exploring the Rapid Growth of Solar Photovoltaics in the European Union", Int. J. Electr. Eng. and sustain., vol. 2, no. 1, pp. 61–68, Feb. 2024. https://ijees.org/index.php/ijees/article/view/78.

[17] M. Khaleel, Z. Yusupov, M. Elmnifi, T. Elmenfy, Z. Rajab, and M. Elbar, "Assessing the Financial Impact and Mitigation Methods for Voltage Sag in Power

Grid", Int. J. Electr. Eng. and sustain., vol. 1, no. 3, pp. 10–26, Jul. 2023. https://ijees.org/index.php/ijees/article/view/40.

[18] Harold S. Brewer (2004). Reduction of Lightning Caused Interruptions on Electric Power Systems. Ohio Brass.

[19] A. Kushwaha, A. Iqbal, and M. A. Mallick, "Modified boost converter for renewable energy powered battery charger", ija-stech, vol. 8, no. 1, pp. 30–36, 2024, doi: 10.30939/ijastech.1379486.

[20] R. Ö. Temiz, M. Onan, H. Cebi, S. Aslanlar, and Ş. Talaş, "Effect of Electrode Type and Weld Current on Service Life of Resistance Spot Weld Electrode", ijastech, vol. 8, no. 1, pp. 52–64, 2024, doi: 10.30939/ijastech.1315759.

[21] Y. Ç. Kuyu, "Trajectory Tracking Control Using Evolution-ary Approaches for Autonomous Driving", ijastech, vol. 8, no. 1, pp. 110–117, 2024, doi: 10.30939/ijastech..1354082.

[22] A. Souli and A. Hellal, "Design of a computer code to evalu-ate the influence of the harmonics in the Transient Stability studies of electrical networks," 2014 IEEE 11th International Multi-Conference on Systems, Signals & Devices (SSD14), Barcelona, Spain, 2014, pp. 1-6, doi: 10.1109/SSD.2014.6808804.

[23] Hyungchul Kim, Sae-Hyuk Kwon, " The Study of FACTS Impacts for Probabilistic Transient Stability", Journal of Elec-trical Engineering Technology, Vol 1, No 2, pp 129-136, 2006.

[24] T Kondo et al: "Power System Transient Stability enhance-ment by STATCOM with nonlinear control system", IEEE Conf pp 1908-1912, 2002.

[25] Surya Yerramilli, " Load Flow Study and Transient Stability Study of a Multi-Machine System Using STATCOM ", B Tech A I T A M, Jawaharlal Nehru Technological University, India, 2006

PERFORMANCE EVALUATION OF NOVEL EV CHARGING TOPOLOGY FOR STANDALONE PV SYSTEMS WITH CHARGE CONTROLLER

*Bondu Pavan Kumar Reddy[1], Vyza Usha Reddy[2].

[1,2]Sri Venkateswara University College of Engineering, Sri Venkateswara University, Tirupati, INDIA

[1]http://orcid.org/0000-0001-8845-571X, [2]http://orcid.org/0009-0004-7070-8925,

Email: [1]pavankumar.eee216@gmail.com*, [2]vyzaushareddy@yahoo.co.in.

ARTICLE INFO	ABSTRACT
	This study explores the novel battery charging topology for standalone solar photovoltaic (PV) systems incorporating charge controller. The research leverages MATLAB/Simulink for modeling and simulation. In standalone PV systems, directly connecting batteries to PV modules can lead to detrimental overcharging or over-discharging, ultimately reducing battery lifespan. To mitigate this challenge, charge controllers are implemented. These intelligent devices regulate the output voltage and current from the solar panels, ensuring safe and efficient battery operation by preventing both overcharging and over-discharging. The analysis focuses on a PV-powered Single Ended Primary Inductor Converter topology alongside a modified version. These topologies integrate Perturb and Observe (P&O) and Incremental Conductance MPPT algorithms for optimal power extraction. The battery charge controller employs a three-stage strategy i.e., constant current, constant voltage absorption, and float charging to effectively manage the battery charging process. Performance evaluation considers MPPT tracking efficiency (achieving up to 98% under standard test conditions), battery charging effectiveness, and overall charge controller efficiency. The study aims to validate these results by benchmarking against a commercially available MPPT controller. The research concludes that the modified SEPIC topology with the implemented charge controller demonstrates superior suitability for EV charging applications compared to the standard SEPIC topology.

I. INTRODUCTION

In our reliance on rechargeable batteries, from smartphones to electric vehicles, a crucial but often overlooked component safeguards their health and longevity: the charge controller. This silent guardian manages the flow of electricity, preventing damage and maximizing battery life [1].

For both solar and wind energy systems, the charge controller acts as the intermediary between the power source and the battery bank. Unlike a simple on/off switch, batteries require a sophisticated charging approach. They have a specific capacity (measured in Amp-hours) and voltage tolerance. Exceeding these limits can have detrimental effects, including shortened lifespan, heat generation, and even production of harmful gases with potential electrolyte loss. Understanding how charge controllers work unlocks the secrets to optimal battery performance and extends the life of this valuable power source [2].

The block diagram of the proposed battery charging topology for standalone solar photovoltaic (PV) systems incorporating charge controller is as shown in Figure 1. Where VPV , IPV , VBatt, IBatt, SoC denotes solar PV voltage, solar PV current, battery voltage, battery current and battery state of charge respectively while dPPV, dVPV & dD denotes change in solar power, change in solar voltage and change in duty cycle respectively.
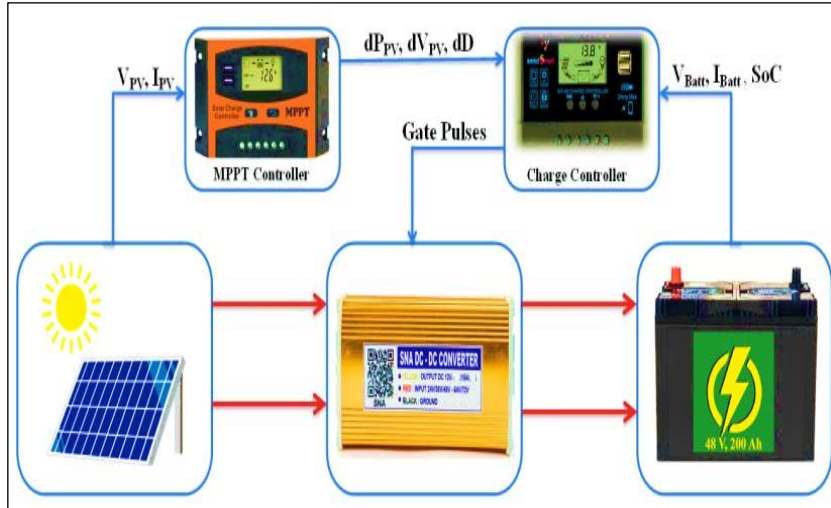
Figure 1: Block diagram of PV powered EV charging system with charge controller.
Source: Authors, (2024).

Choosing the ideal charge controller for your system depends on understanding the different types and their functionalities. Each controller caters to specific needs and applications. Here's a breakdown of some common charge controllers

a. PWM (Pulse Width Modulation):

These controllers offer a basic approach, regulating the average current delivered to the battery by rapidly turning the charging current on and off. While cost-effective and suitable for small setups, PWM controllers can result in some energy loss compared to more advanced options. These types of controllers are ideal for low-power applications like small cabins, powering lights, or trickle charging batteries in RVs [2].

b. MPPT (Maximum Power Point Tracking):

MPPT controllers represent a significant leap in efficiency. They continuously analyse the voltage and current output from the solar panels (the charging source) and adjust their input to operate at the point of maximum power generation. This translates to significantly more power extracted from the solar panels, especially under fluctuating sunlight conditions. These types of controllers are perfectly suitable for larger standalone solar systems where maximizing power output is crucial, such as powering homes or telecom towers in remote locations [2].

c. Solar-Specific Charge Controllers:

These controllers are tailored for solar power systems. They account for the unique output characteristics of solar panels and may include additional features. Examples include night-time disconnect to prevent battery drain during darkness and compatibility with various battery voltages. These are ideal for any solar PV system, particularly those with complex needs or diverse battery banks [3].

d. Multi-Stage Charge Controllers:

These advanced controllers implement a multi-stage charging process designed for specific battery chemistries. This process often involves stages like bulk charging, absorption charging, and float charging, each optimized to efficiently charge the battery and maximize its lifespan. These types of controllers are critical for systems using advanced battery technologies like lithium-ion, where precise charging profiles are essential for safety and longevity. They are also beneficial for lead-acid battery systems where maximizing lifespan is a priority [4].

II. METHODOLOGY

The solar photovoltaic (PV) system model with Maximum Power Point Tracking (MPPT) battery charge controller incorporates a PV array, a DC-DC converter, a battery, and an MPPT control block. This charge controller block generates a Pulse Width Modulation (PWM) control signal that regulates the switching device within the DC-DC converter [4].
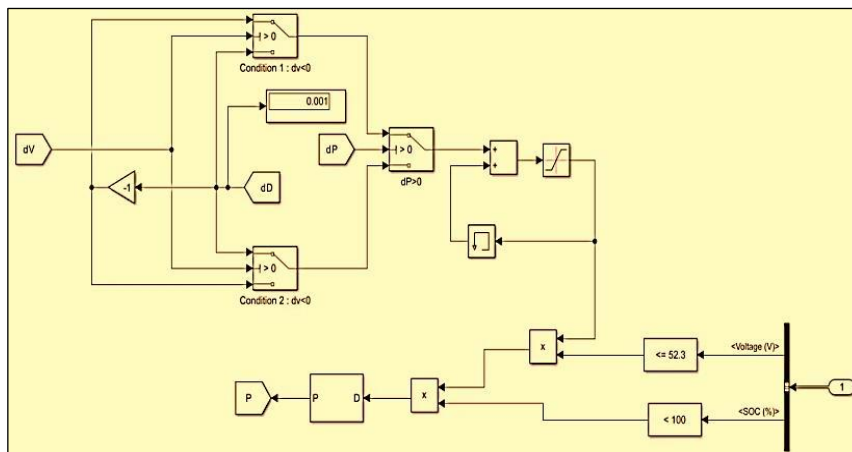

Figure 2: MATLAB/Simulink model of proposed charge controller.
Source: Authors, (2024).

The control signal considers both MPPT input and battery data, as illustrated in Figure 1. The model is designed to charge a 48V, 200Ah battery using a 2kW PV array source. It's been simulated within the Simulink environment for performance evaluation. The following sections will delve deeper into the circuit model and the MPPT control block. An illustration of the MATLAB/Simulink model for the charge controller is provided in Figure 2.

A.Battery Charge Controller:

The charge controller implements a three-stage charging strategy to optimize battery health and performance. This strategy consists of Bulk Charging, Absorption charging & float charging. The flowchart depicting the charge controller's decision-making process is presented in Figure 3 [4-5].
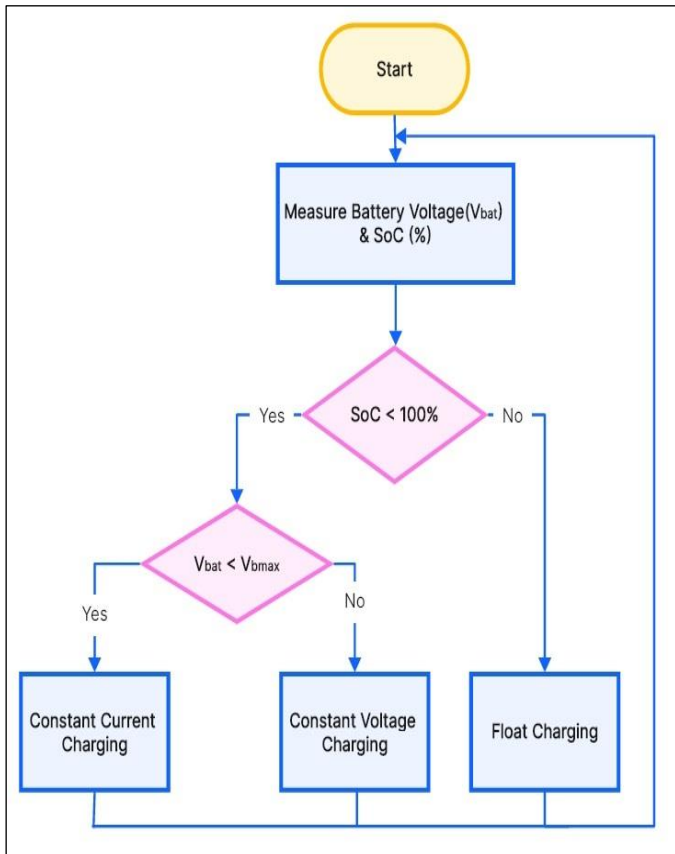

Figure 3: Flowchart depicting charge controller's decision-making process.
Source: Authors, (2024).

During this initial stage, the controller delivers a constant current to the battery, typically set at the maximum power point tracking (MPPT) value. This stage aims to bring the battery voltage up to a predetermined level. Once the battery voltage reaches the designated set point (e.g., 52.3 V in this case), the controller transitions to constant voltage charging. Here, the voltage remains fixed while the current gradually declines as the battery approaches full capacity. This stage ensures a complete charge without overfilling. When the battery reaches full charge (100% State of Charge), the controller enters the float charging

stage. In this maintenance mode, a low voltage is applied to keep the battery topped up without the risk of overcharging, preventing gassing and overheating.

The controller continuously monitors the battery's SoC and voltage. Based on these values, it transitions between the charging stages. If the SoC is below 100% and the voltage is less than the set voltage (e.g., 52.3V), the controller initiates constant current charging. If the SoC is below 100% but the voltage exceeds the set point, the controller switches to absorption charging. Once the SoC reaches 100%, the controller enters the float stage to maintain a topped-up battery.

In order to assess the performance of charge controller, a standalone PV system alongside SEPIC & modified SEPIC topologies with charge controller are designed in MATLAB/Simulink environment. The outcomes of the calculations for each parameter of SEPIC and Modified SEPIC converters are summarized as Table 1 below, with input power of 2kW to charge a 48 V, 200 Ah battery at a switching frequency of 20 kHz [6-7].

Table 1: Parameters of SEPIC & Modified SEPIC Topologies.

S. No	Parameter	SEPIC Topology	Modified SEPIC Topology
1	Max. Duty Cycle (D_{Max})	64%	25.6 %
2	Min. Duty Cycle (D_{Min})	60.83%	21.7 %
3	Inductor (L_1)	225 µH	7 mH
4	Inductor (L_2)	350 µH	7 mH
5	Capacitor (C_1)	410 µf	1.7 mf
6	Capacitor (C_2)	264 µf	1.7 mf

Source: Authors, (2024).

III. SIMULATIONS AND RESULTS

This study compares the performance of SEPIC and modified SEPIC converters in a standalone solar photovoltaic (PV) system charging a 48V, 200Ah battery for an electric vehicle (EV). A charge controller is incorporated into the system for optimal battery management. The simulations are conducted within the MATLAB/Simulink environment. Both converter configurations are evaluated under identical test conditions. Key parameters monitored throughout the simulations include voltage, current, and power output from the PV panel. Additionally, the battery's state of charge (SoC), charging current, and voltage are tracked. Figures 4 to 15 present the MATLAB/Simulink models, along with detailed results for each converter type. These results include PV characteristics (voltage, current, and power), battery SoC, charging current, and voltage. The simulations further explore the effectiveness of both Perturb and Observe (P&O) and Incremental Conductance MPPT algorithms.
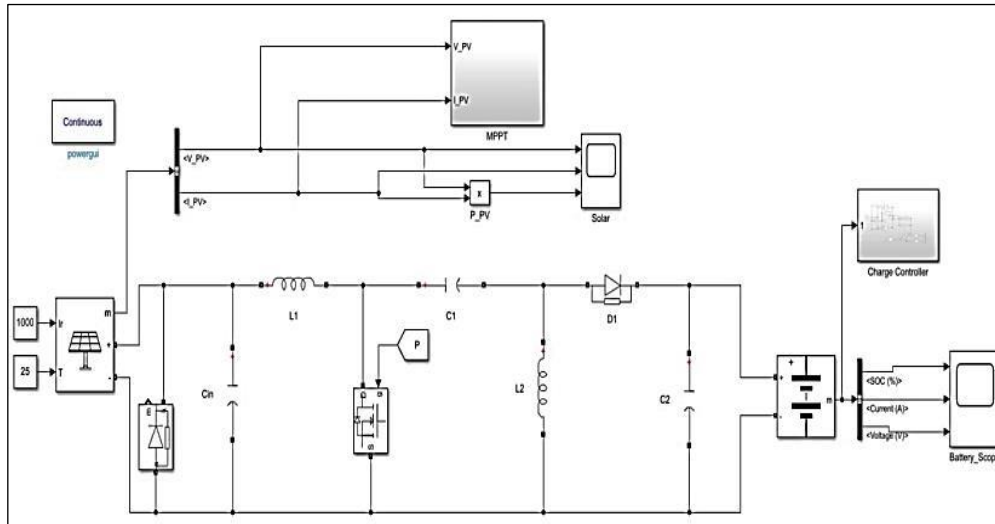
Figure 4: Simulink Model of SEPIC converter with Charge controller & PO MPPT.
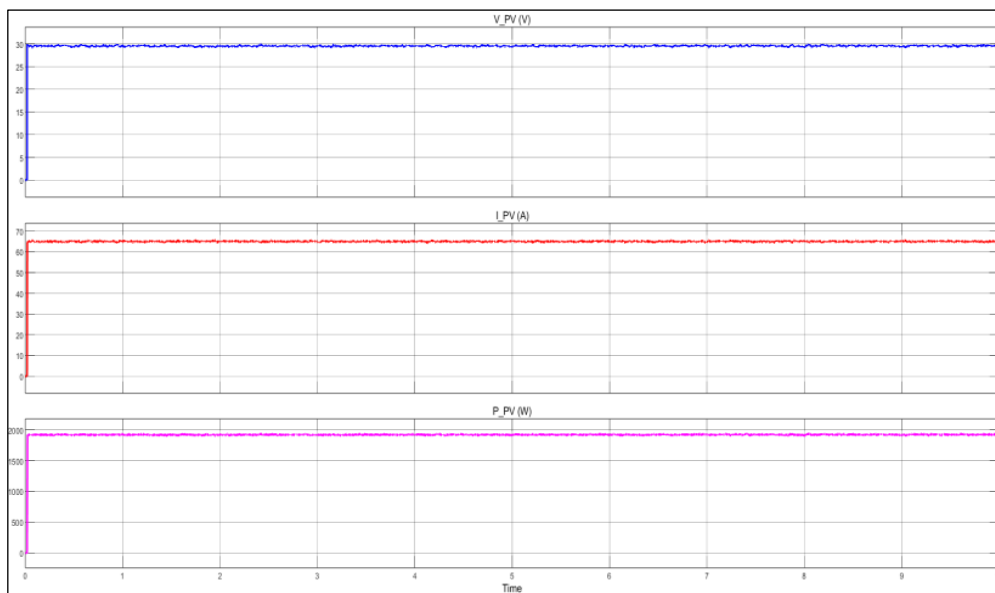Source: Authors, (2024).

Figure 5: PV characteristics results for SEPIC converter with Charge controller & PO MPPT.
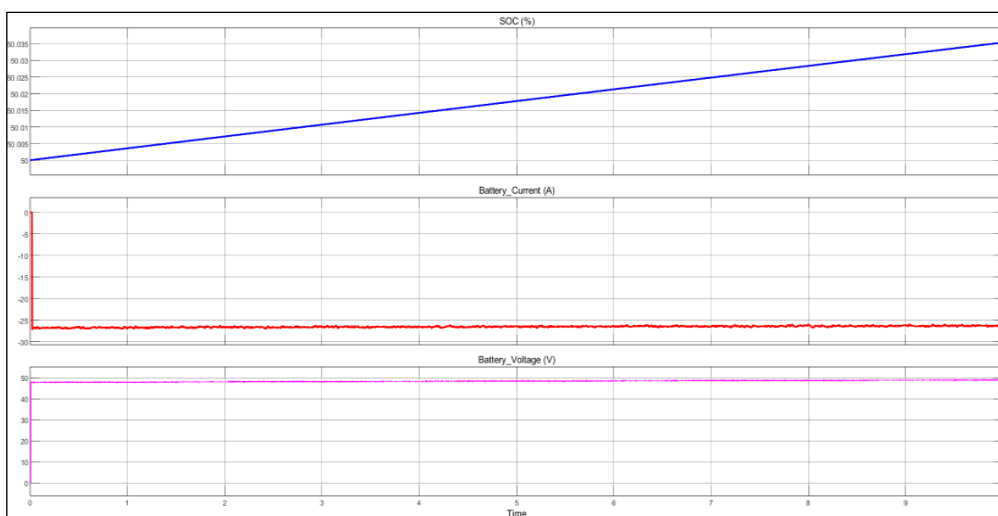Source: Authors, (2024).

Figure 6: Battery charging results for SEPIC converter with Charge controller & PO MPPT.
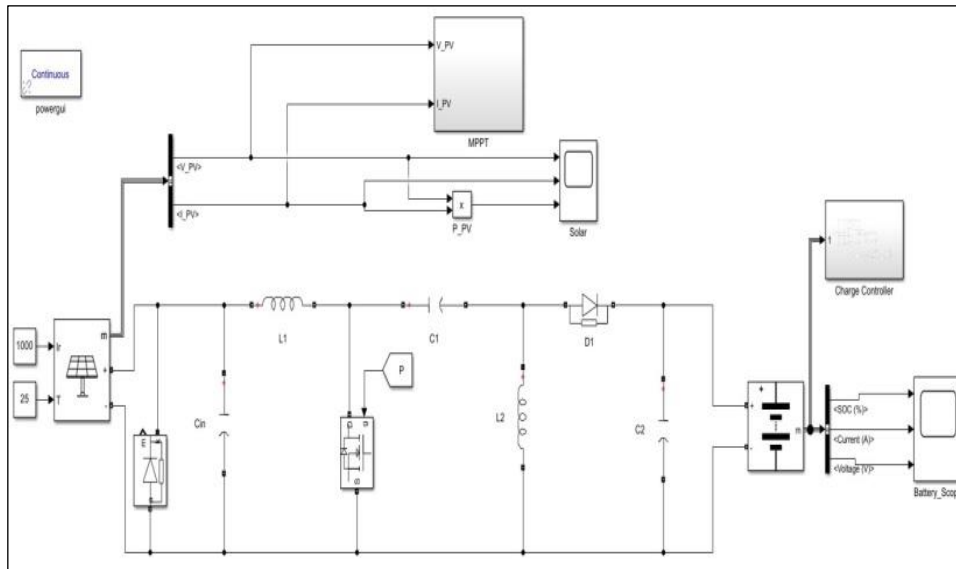Source: Authors, (2024).

Figure 7: Simulink Model of SEPIC converter with Charge controller & INC MPPT.
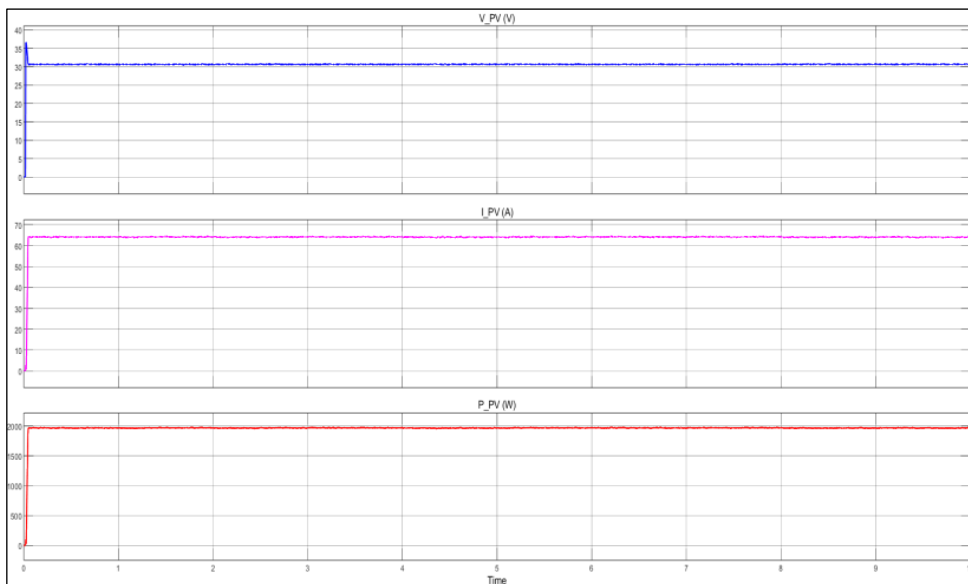Source: Authors, (2024).

Figure 8: PV characteristics results for SEPIC converter with Charge controller & INC MPPT.
Source: Authors, (2024).

Figure 9: Battery charging results for SEPIC converter with Charge controller & INC MPPT.
Source: Authors, (2024).

Figure 10: Simulink Model of Modified SEPIC converter with Charge controller & PO MPPT.
Source: Authors, (2024).

Figure 11: PV characteristics results for Modified SEPIC converter with Charge controller & PO MPPT.
Source: Authors, (2024).

Figure 12: Battery charging results for Modified SEPIC converter with Charge controller & PO MPPT.
Source: Authors, (2024).

Figure 13: Simulink Model of Modified SEPIC converter with Charge controller & INC MPPT.
Source: Authors, (2024).

Figure 14: PV characteristics results for Modified SEPIC converter with Charge controller & INC MPPT.
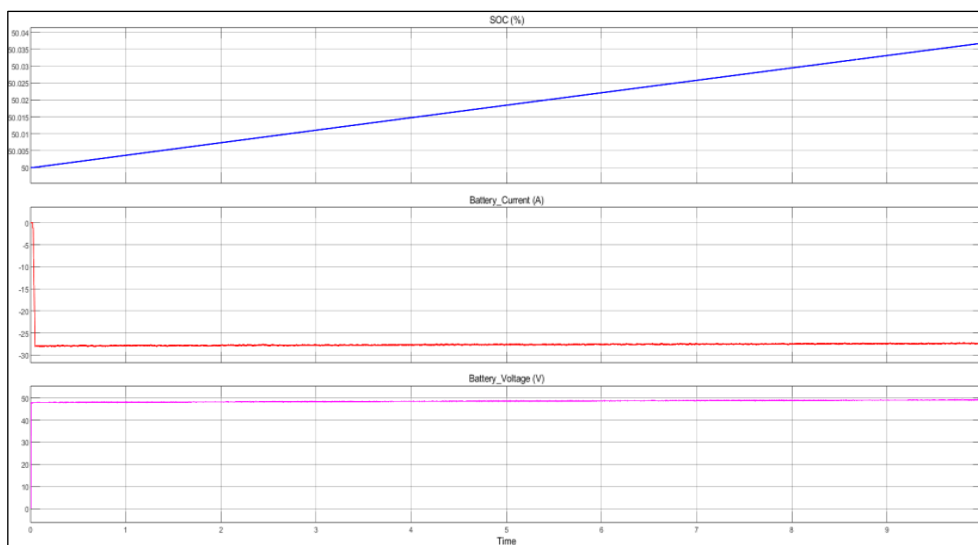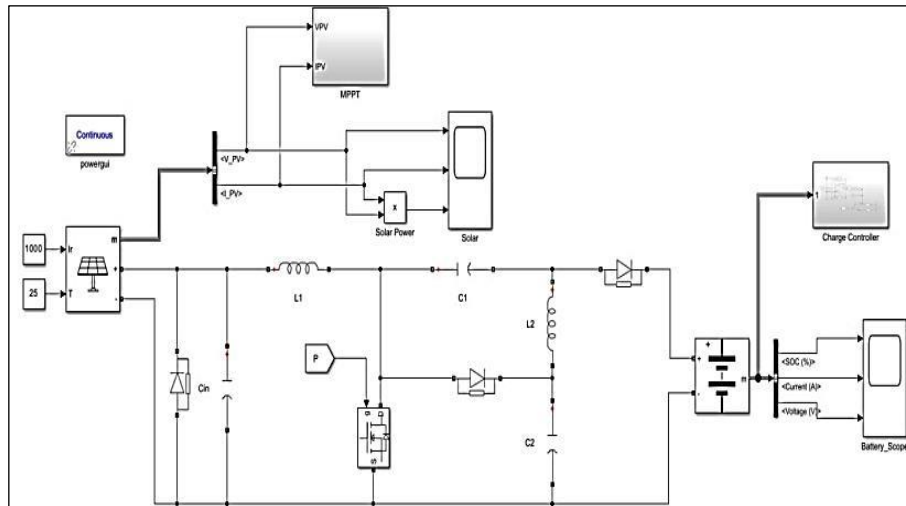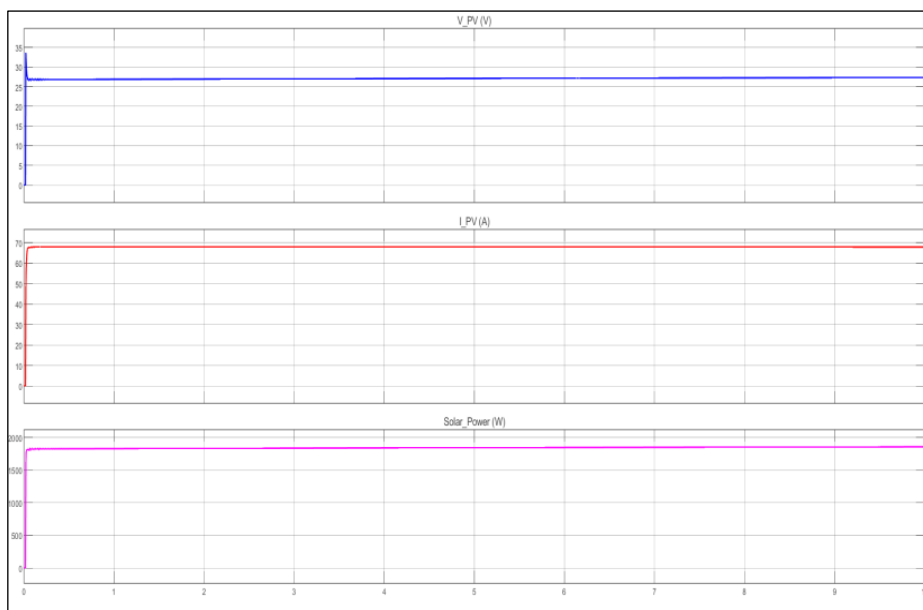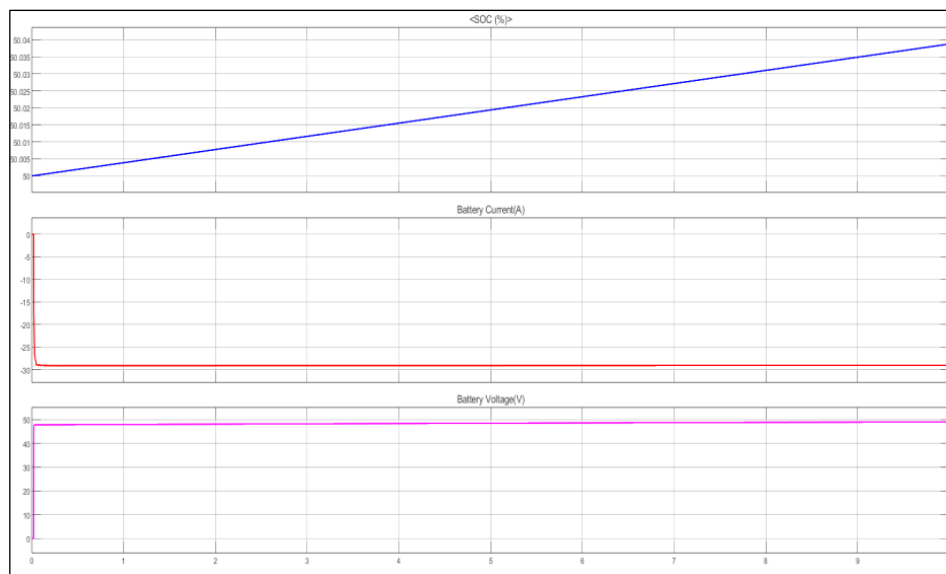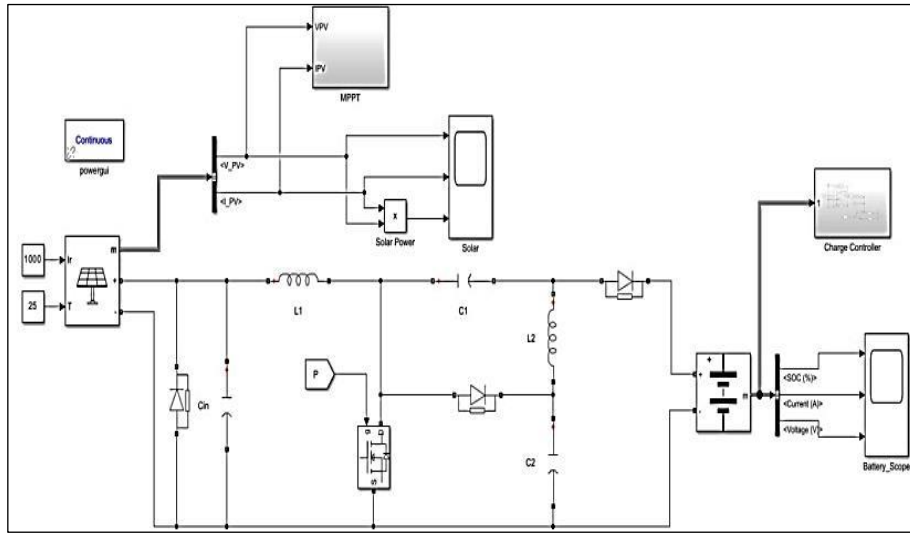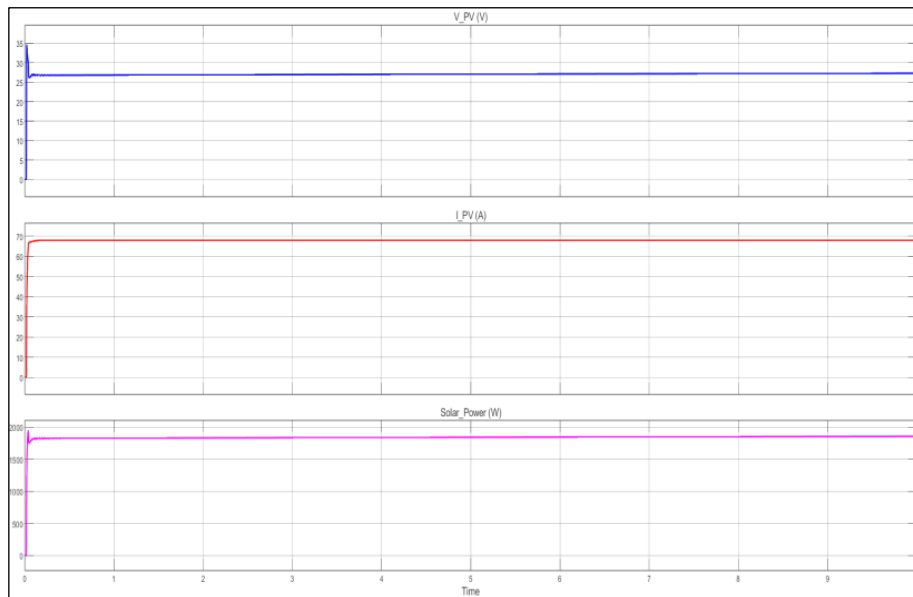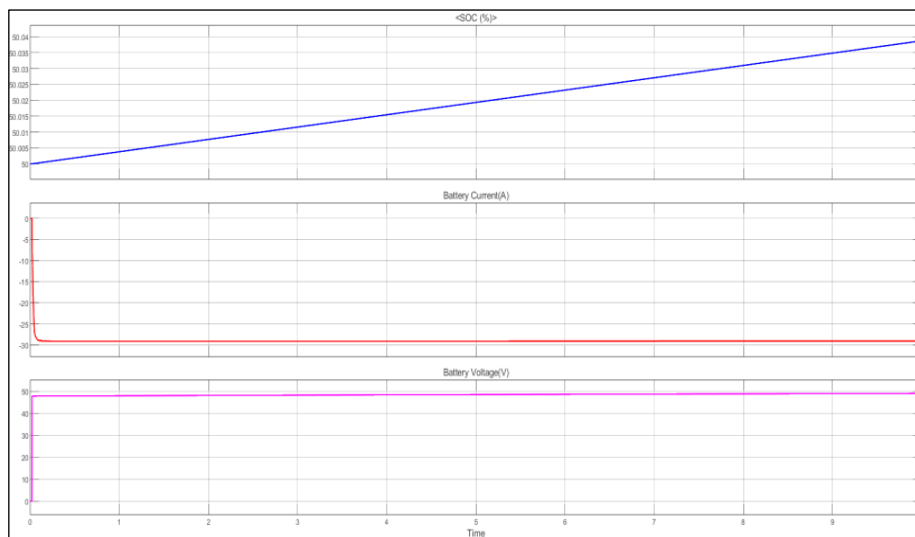Source: Authors, (2024).

Figure 15: Battery charging results for Modified SEPIC converter with Charge controller & INC MPPT.
Source: Authors, (2024).

Table 2 presents a comparative analysis of the EV charging system's performance under identical test conditions. The analysis considers both SEPIC and modified SEPIC converters, with charge controller and implementation of Maximum Power Point Tracking (MPPT) methodologies. It's important to remember that negative battery current values signify the battery is actively charging.

Table 2: Simulation results with SoC of 50% and simulation time of 10sec.

parameter	SEPIC Converter		Modified SEPIC Converter	
	With P&O MPPT	With INC MPPT	With P&O MPPT	With INC MPPT
SoC (%)	50.035	50.037	50.039	50.039
V_b (V)	49.10	49.13	49.04	49.04
I_b (A)	-26.25	-27.36	-29.09	-29.09
V_{pv} (V)	29.46	30.61	27.31	27.31
I_{pv} (A)	65.09	64.15	67.92	67.92
P_{pv} (W)	1918	1964	1855	1855

Source: Authors, (2024).

IV. CONCLUSIONS

This study explores the detailed circuit modelling of a Solar PV MPPT battery charge controller built within MATLAB/Simulink environment. The explanation covers the MPPT tracking algorithm, the design of both the traditional SEPIC converter and a modified version, along with the three-stage charge controller. The model is comprehensive and allows for complete replication. This MPPT battery charge controller effectively manages the charging process for a 48V, 200Ah battery. It achieves this by tracking the maximum power output from a 2 kW PV array and utilizes a three-stage charging strategy to regulate the battery's state of charge.

The simulation results revealed that while both converter topologies achieved similar charging times, the modified SEPIC converter offered a significant improvement in efficiency. Specifically, the modified SEPIC converter achieved an overall efficiency of 77%, compared to 67.8% for the traditional SEPIC converter. This improvement in efficiency translates to faster charging times for a given power input, or less energy wasted during the charging process.

V. AUTHOR'S CONTRIBUTION

Conceptualization: Pavan Kumar Reddy Bondu, Vyza Usha Reddy, Dr.
Methodology: Pavan Kumar Reddy Bondu, Vyza Usha Reddy, Dr.
Investigation: Pavan Kumar Reddy Bondu, Vyza Usha Reddy, Dr.
Discussion of results: Pavan Kumar Reddy Bondu, Vyza Usha Reddy, Dr.
Writing – Original Draft: Pavan Kumar Reddy Bondu, Vyza Usha Reddy, Dr.
Writing – Review and Editing: Pavan Kumar Reddy Bondu, Vyza Usha Reddy.
Resources: Pavan Kumar Reddy Bondu, Vyza Usha Reddy.
Supervision: Pavan Kumar Reddy Bondu, Vyza Usha Reddy.

**Approval of the final text:** Pavan Kumar Reddy Bondu, Vyza Usha Reddy.

VII. REFERENCES

[1] P. K. Atri, P. S. Modi and N. S. Gujar, "Design and Development of Solar Charge Controller by Implementing two different MPPT Algorithm," 2021 International Conference on Advances in Electrical, Computing, Communication and Sustainable Technologies (ICAECT), Bhilai, India, 2021, pp. 1-5, doi: https://doi.org/10.1109/ICAECT49130.2021.9392426

[1] M. Deepika, P. Karthikeyan, A.V. Keerthana, M. Lakshmanan, P. Gowtham, C. Kumar and S. Jaisiva "MPPT-Based Charge Controller for Battery Fast Charging," 2023 9th International Conference on Advanced Computing and Communication Systems (ICACCS), Coimbatore, India, 2023, pp. 449-453, doi: https://doi.org/10.1109/ICACCS57279.2023.10112852

[3] P. K. Abraham, D. Mary, M. V. Jayan and N. Paulson, "Design, Implementation, and Experimental Verification of a Solar PV Charge Controller for a Low-Speed E-Scooter Home Charging Station," 2023 9th International Conference on Smart Computing and Communications (ICSCC), Kochi, Kerala, India, 2023, pp. 754-759, doi: https://doi.org/10.1109/ICSCC59169.2023.10334970

[4] Rodney H.G. Tan, Chee Kang Er and Sunil G. Solanki, "Modeling of Photovoltaic MPPT Lead Acid Battery Charge Controller for Standalone System Applications". E3S Web of Conferences. 182. 03005(2020). doi: https://doi.org/10.1051/e3sconf/202018203005

[5] B. Pooja, S. Rajanna, N. L. Varaprasad, M. Ramesh, G. R. Sowmya and S. R. Rakshitha, "Design of a Battery Charge Controller Through MPPT Based Solar Photovoltaic System," 2022 Fourth International Conference on Emerging Research in Electronics, Computer Science and Technology (ICERECT), Mandya, India, 2022, pp. 1-6, doi: https://doi.org/10.1109/ICERECT56837.2022.10060581

[6] A. K. Mishra and B. Singh, "Modified SEPIC Converter Utilizing an Improved P&O Algorithm for Design of Low Cost and Efficient Solar Energized Water Pump," 2018 IEEE Industry Applications Society Annual Meeting (IAS), Portland, OR, USA, 2018, pp. 1-8, https://doi.org/10.1109/IAS.2018.8544680

[7] Bondu Pavan Kumar Reddy, V.Usha Reddy, "PV-Based Performance Evaluation of ZETA and SEPIC Topologies for EV Applications," Journal of Electrical Systems, vol.20, no. 5, pp. 438-446, 2024, https://doi.org/10.52783/jes.2068
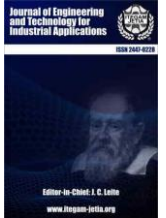
RESEARCH ARTICLE   OPEN ACCESS

DIGITAL TWIN OF A PHOTOVOLTAIC SYSTEM

Luis Gabriel Fong Mollineda[1] and José Rafael Abreu García[2]

[1,2] Central University "Marta Abreu" of Las Villas – Santa Clara, Cuba.

[1] http://orcid.org/0009-0003-7581-3276   , [2] http://orcid.org/0000-0002-8344-8796

Email: [1]lfomg@uclv.cu,[2] abreu@uclv.edu.cu

ARTICLE INFO

ABSTRACT

The creation of a Digital Twin, for the simulation of the photovoltaic park installed at the UCLV, which establishes a bidirectional data exchange in real time with the aim of providing a precise virtual copy, in order to monitor it and analyze its reaction to certain stimuli. or circumstances to improve its performance and extend its useful life. A virtual model is built using two tools: Simulink, and the PV_LIB Toolbox in Matlab. The implementation is carried out on a Raspberry Pi model B+. The connection between Matlab and the Raspberry Pi is achieved using appropriate support packages, allowing the Digital Twin to run constantly. The input data comes from the UCLV photovoltaic park, obtained through the ThingSpeak platform, while the outputs include current, voltage and power. The main focus of this work is to achieve the connection between Matlab and the Raspberry Pi, find a virtual model that fits the real plant, its implementation in code and validate the power generation of the Digital Twin in relation to the Physical Twin through root mean square error (RMSE).

I. INTRODUCTION

Various works have been carried out at the UCLV that are based on the modeling of photovoltaic systems and their control, however, the models obtained do not involve all the factors that influence their behavior and do not allow the exchange of information with the system. A step forward in working with complex systems, such as photovoltaics, is the use of a Digital Twin.

The use of a digital twin allows to simulate the behavior of the photovoltaic system in different conditions and scenarios, this makes it possible to optimize the system design and maximize its performance. It can also help identify and correct problems in the design or operation of the system before its implementation, reducing the costs associated with repairs and maintenance. Energy efficiency increases identifying the weak points of the system. It can be used to monitor the photovoltaic system in real time and detect possible failures or early anticipate problems, reducing inactivity time and facilitating its maintenance [1]. Obtaining clean and safe energy for the environment reduces the need to use polluting energy sources, thus reducing the emission of greenhouse gases and contributing to the fight against climate change [2].

Digital twin technology is relatively new, but its origin dates back to the second half of the last century, in the aeronautical industry, with the idea of creating a real-time virtual representation of physical systems. Over time, it has expanded to other industries such as energy, automotive, and manufacturing, among others. Today, digital twins are a valuable tool for the simulation and monitoring of complex physical systems in different fields [3].

Regarding the photovoltaic industry, the use of digital twins is a field in constant evolution. In recent years, there has been an increase in research and development of digital twins focused on solar energy, with the aim of improving the performance and efficiency of photovoltaic systems [4].

To establish a Digital Twin of a photovoltaic system, a digital representation of the system is needed that includes: information about the components, geometry, climate and other factors that affect the performance of the system, this being the physical model; The mathematical equations that describe the behavior of the components of the photovoltaic system: solar

panels, inverter and others, constitute the mathematical model. Implementation of software that uses physical and mathematical models to simulate the behavior of the photovoltaic system in different conditions and scenarios, having the data analysis tool to identify patterns, trends and anomalies in real-time monitoring data on the climate, solar radiation, temperature and other affecting factors. The user interface allows you to interact with the Digital Twin, view the data and results of the simulation [5].

This article proposes to create a Digital Twin of the UCLV photovoltaic park. To achieve this, it is necessary to characterize the installed photovoltaic park, determine the fundamental parameters necessary to form a Digital Twin, analyze the characteristics of the main software to be used in digital twins and select the most suitable for the application

II. STATE OF THE ART OF DIGITAL TWINS IN PHOTOVOLTAIC SYSTEMS.

II.1 DIGITAL TWIN.

A Digital Twin is a digital representation of a physical object or system, which establishes a bidirectional data exchange in real time. The objective of a Digital Twin is to provide an accurate and detailed virtual copy of a physical element, in order to monitor it and analyze its reaction to certain stimuli or circumstances [6],[7].

It must be clear that the Digital Twin is not a new idea since its concept originated during the penultimate decade of the last century, dating back to the APOLO program of the National Aeronautics and Space Administration (NASA). In this program, two identical space vehicles were built in order to simulate the behavior of their ships, equipment and the physical integrity of the crew members. During the mission to space, the terrestrial acted as a twin and was used to reflect flight conditions using available flight data [6].

The Digital Twin has constantly evolved over the years and is expected to continue evolving in the next decade. Currently, it has become an essential component for the digital transformation of the industry. This technology is used in 34% of companies globally, and with improvements of more than 25% in system performance. Its implementation has shown a 15% increase in key sales and operational metrics with an average of 16% in

sustainability, driving implementation by 36% over the next five years; This is revealed by the report "Digital Twins: Adding Intelligence to the Real World" from the Capgemini Research Institute (Spain) in 2022 [8].

Implementation can be complex, given the wide range of functionalities it must support. It is built so that it can receive information from sensors to measure real-time parameters of physical elements, interacting with virtual space through the industrial internet of things [9].

II.2 DIGITAL TWINS IN THE PHOTOVOLTAIC INDUSTRY.

In the photovoltaic industry, digital twins are used to represent photovoltaic systems, from individual solar panels to entire solar parks. They allow photovoltaic system engineers and operators to simulate different operating scenarios and evaluate their impact on system performance. For example, different weather conditions, variations in the inclination and orientation of the solar panels, and changes in the electrical load of the system can be simulated. In addition, they can help predict and prevent possible failures or problems in the photovoltaic system [10].

In recent years, research has been conducted on the use of digital twins to improve the efficiency and performance of photovoltaic systems, especially in terms of power production prediction, fault detection and predictive maintenance.

Figure 1 presents the architecture of a Digital Twin in the photovoltaic industry, in which several blocks that work together to create a virtual replica of the system can be identified [11]:

• Digital shadow: digital footprint left by the Digital Twin and is made up of a database and interfaces, the latter being responsible for interacting with the database and implementing machine learning methods; since it is necessary for data prediction and to restore the system's behavioral model.

• Digital model: is responsible for the operation of the entire system by implementing the interface of interactions with the other components of the digital model, such as a mathematical model and a system for collecting operational information.

• Control system: introduces a control action on a real object, whose prototype is a Digital Twin.

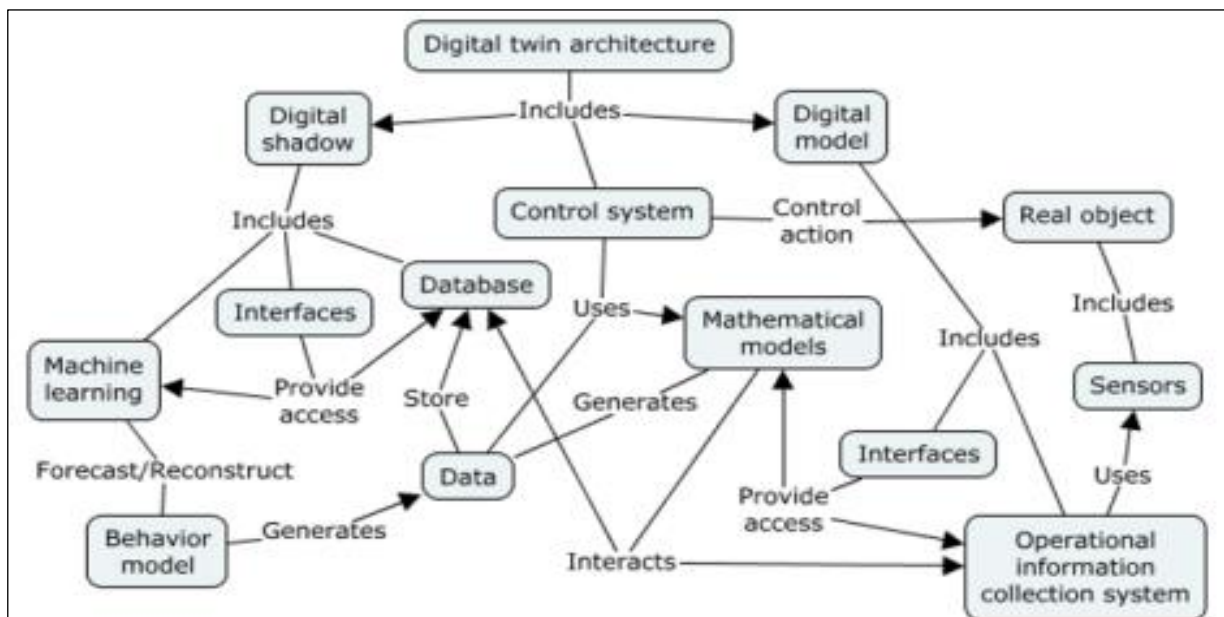
Figure 1: Digital twin architecture.

Source: Authors, (2024).

III. FUNDAMENTAL ASPECTS OF PHOTOVOLTAIC FIELDS EXEMPLIFYING THE ONE INSTALLED AT UCLV.

III.1 CELL, PANEL AND PHOTOVOLTAIC SYSTEM.

The solar cell is the central component of photovoltaic solar panels, playing a fundamental role in converting solar radiation into electrical energy through the photovoltaic effect. In its composition, a semiconductor material is mainly used, silicon being the most commonly used. Depending on the desired level of efficiency, monocrystalline or polycrystalline silicon can be used. Monocrystalline silicon is considered one of the most efficient materials for manufacturing solar cells, due to its ability to achieve high efficiency in converting sunlight into electricity [12],[13].

In 1905, Einstein proposed the model of the photoelectric effect, where he assumed that the light energy was not distributed uniformly throughout the expanding wave front, but in separate packets. The energy of light, in the form of a beam that has a certain frequency, is presented in discrete packets called photons. Each photon carries with it an amount of energy represented by the formula $E = h*f \geq Eg$ (Forbidden Energy Band), where h is Planck's constant (h = $6.626 \cdot 10\text{-}34$ J·s) and f is the frequency of the light beam. In this way, for the effect to occur, the energy of the photon must be greater than the energy of the electron for it to be expelled from the material [14].

There are two fundamental parameters that define the electrical properties of a photovoltaic solar cell: the open circuit voltage and the short circuit current. The open circuit voltage (Voc) refers to the difference in electrical potential that occurs at the terminals of the cell when there is no load connected, which means that the current is zero. On the other hand, the short circuit current (Isc) is the maximum value reached by the current at a given instant when the cell is directly connected without resistance, that is, when the voltage is equal to zero. These parameters are of vital importance to understand the behavior and efficiency of a solar cell [15].
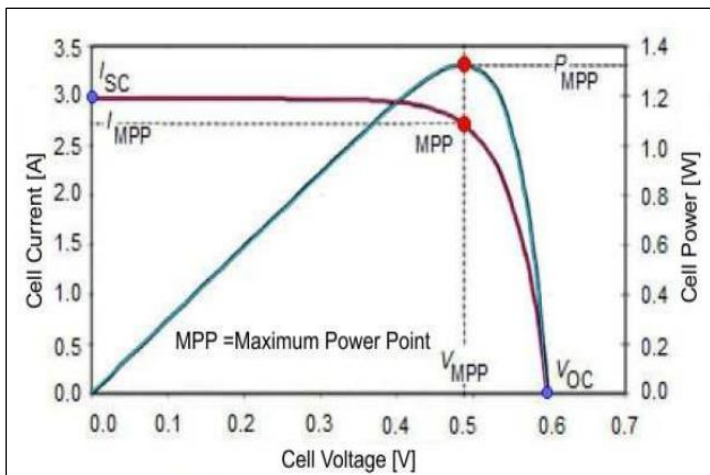
Figure 2: Characteristic curves of a photovoltaic solar cell.
Source: Authors, (2024).

The representation of a solar cell is made through a model that uses a simplified circuit composed of a classic p-n junction diode, and electronic components such as sources and resistive elements that emulate the losses represented in a real environment.
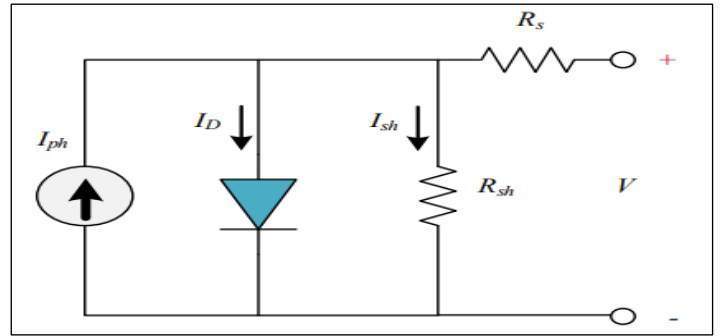
Figure 3: Equivalent circuit of a solar panel.
Source: Authors, (2024).

The simple diode model proposed by Gow 1999 demonstrates the relationship between current and voltage delivered by a photovoltaic module. By applying Kirchhoff's law to the circuit in Figure 3, the current generated (Icel) by the solar panel can be deduced:

$$Icel = Iph - Id - Ish \qquad (1)$$

$$cel = Iph - Io[e^{\frac{q(V+Icel*Rs)}{KTcA}} - 1] - \frac{V + Icel * R}{Rsh} \qquad (2)$$

Where Iph is the photogenerated current, Io is the reverse saturation current of the diode, q is the electron charge (1.6 x 10-19 C), V solar cell voltage, K is the Boltzmann constant (1, 38 x 10-23 J/K), Tc cell operating temperature and A ideality factor. The currents exhibit an almost linear relationship with respect to radiation (Iph) and temperature (Tc).

The current generated by a solar cell is affected by the intensity of solar radiation and the temperature of the cell at the time of measurement. These two factors influence the amount of photogenerated current, as stated in equation 3.

$$Iph = \frac{R}{Rref}[Ilref + UIsc(Tc - Tcref)] \qquad (3)$$

Considering the following parameters: R represents the solar radiation measured at the current moment, Rref is the solar radiation under standard conditions of 1000 W/m2, Ilref is the photogenerated current under reference conditions, which is taken as the short circuit current (Isc =Ilref), UIsc is the temperature coefficient of the short circuit current, and Tcref is the working temperature of the cell under standard conditions (298°K). Furthermore, the reverse saturation current of the diode also depends on temperature, and this is described by equation 4:

$$Io = Ioref \left(\frac{Tc}{Tcref}\right)^3 * e^{\left[\frac{qEg\left(\frac{1}{Tref} - \frac{1}{Tc}\right)}{KA}\right]} \qquad (4)$$

In relation to this, Ioref represents the reverse saturation current under reference conditions, while Eg corresponds to the energy of the semiconductor in its bandgap. The current Ioref is defined according to equation 5.

$$Ioref = \frac{Isc}{e^{\left(\frac{Voc}{Ns*K*Tc*A}\right)} - 1} \qquad (5)$$

Typically, solar cells have an output of around 2W at 5V [16], which requires them to be grouped in series or parallel configurations to achieve the desired power. To do this, the coefficients Np, which denotes the number of modules in parallel, and Ns, which represents the number of cells in series, are added to the current-voltage characteristic equation of a photovoltaic cell described in 2. Equation 6 describes the current-voltage relationship of a solar panel.

$$\text{Ipanel} = \text{Np} * \text{Iph} - \text{Np} * \text{Io} \left[e^{q\left(\frac{V}{Ns} + \frac{Icel * Rs}{Np}\right) \over K * Tc * A} - 1 \right]$$
$$- \frac{V\left(\frac{Np}{Ns}\right) + Icel * Rs}{Rsh} \tag{6}$$

Equation 6 is generally reduced to 7, since authors such as Granda-Gutiérrez [17], Huan-Liang Tsai [16], De Soto, Klein, and Beckman [18], Xuan Hieu Nguyen and Minh Puhong Nguyen [19], simplify the equation because the shunt resistance does not affect the efficiency of a solar cell, because the resistance tends to be very large or infinite, so we can assume Rsh=∞. But the series resistance does significantly affect the behavior of the cell, therefore [20], [21]:

$$\text{Ipanel} = \text{Np} * \text{Iph} - \text{Np} * \text{Io} \left[e^{q\left(\frac{V}{Ns} + \frac{Icel * Rs}{Np}\right) \over K * Tc * A} - 1 \right] \tag{7}$$

Photovoltaic modules are born from a mosaic of solar cells. A solar panel is a broader term used to describe a complete system that includes multiple interconnected photovoltaic modules, along with other components necessary for its operation, such as cables, connectors, inverters, and mounting structures. It is responsible for converting solar radiation into electrical energy, transforming it into direct current. These panels are composed of multiple configurations of solar cells connected in series and/or in parallel to achieve the desired voltage and current conditions. First, the desired voltage is established by grouping the solar cells in series. Once the voltage is determined, the branches with the solar cells in series are grouped in parallel to achieve the necessary current. Therefore, the specific power is achieved through the combination of the number of solar cells and the type of connection between them [22].

Elements of a photovoltaic panel [23]:

• Solar cells: These are the fundamental components that convert sunlight into electricity.

• Frame: It is the structure that surrounds and protects the solar cells.

• Front glass: It is a transparent layer of glass that covers the solar cells. It protects cells from mechanical damage, such as impacts, dust and moisture, while allowing sunlight to pass through.

• Encapsulating: It is a resistant and transparent material, generally a polymer sheet such as EVA (ethylene-vinyl acetate), which is placed between the solar cells and the front glass.

• Electrical connections: Photovoltaic panels have electrical connections that allow the transfer of current generated by the solar cells.

• Junction Box: This is a sealed box located on the back of the panel that houses the electrical connections and protects the cables and connections from damage and adverse environmental conditions.

There are two main categories of photovoltaic systems: stand-alone systems and grid-connected systems. The key distinction between these two systems lies in their ability to manage excess energy. In a stand-alone photovoltaic system, it is necessary to have a regulator that manages the storage of additional energy generated during sunlight hours in batteries. This allows this stored energy to be used at times when solar production is not enough. On the other hand, a system connected to the electrical grid has the advantage of taking advantage of the support of the grid to supply energy in times of generation deficiency and also to inject excess generated energy. The energy exchange is recorded through a meter that measures both the amount of energy demanded from the electrical grid when solar production is insufficient, and the amount of energy delivered to the grid when there is a surplus of energy generated [24].

III.2 SOFTWARE AND PHYSICAL DEVICE ENVIRONMENTS USED.

Software environments used

The advancement of the Digital Twin has been made using two different approaches: Simulink and PV_LIB. The reason for using both tools is that Simulink does not allow modeling the impact of temperature, while PV_LIB cannot be implemented on the hardware board. In addition to these Matlab tools, the help of other utilities has also been required such as ThingSpeak to obtain the input data from the cloud, and VNC Viewer to establish a remote connection between the computer and the Raspberry Pi.

Matlab: is a programming and numerical computing platform that has an integrated development environment and its own programming language based on matrices, the M language. Its features include data analysis, representation of data and functions using graphs, development and implementation of algorithms, creation of web and desktop applications, ability to use Matlab with other languages, cloud computing and connection between Matlab and other hardware equipment [25].

Simulink: is a visual programming environment based on block diagrams from the Matlab programming environment. This tool is used to design systems based on multi-domain models, design and simulate before hardware implementation and deploy without having to write code [26].

PV_LIB Toolbox – Provides a set of well-documented functions to simulate the performance of photovoltaic power systems. It allows calculating irradiation and solar position, decomposition of irradiance and transposition to the plane of the matrix, dirt and shading, cell temperature, obtaining power through irradiance, losses due to mismatch in resistance and due to electrical mismatch of direct current, maximum power point tracking, inverter efficiency, alternating current losses and long-term degradation [27].

ThingSpeak: is an Internet of Things (IoT) analytics platform created in 2010 by ioBridge. Its primary goal is to provide support for IoT applications by enabling real-time data collection, visualization, and analysis in the cloud. Facilitates the sending of data from devices connected to the internet. Then, you can analyze and visualize that data using the Matlab tool [28].

VNCviewer: is a free source software based on a client-server structure, in which the client computer can view the screen and control and interact with the server computer's equipment remotely. It does not take into account the operating system of the server computer with respect to the client computer, any operating system that supports VNC is needed to establish communication. This software was created in the United Kingdom, specifically at "AT&T Olivetti Research Laboratory" based on the RFB (Remote Frame Buffer) protocol [29].

Raspberry Pi

The Raspberry Pi is an inexpensive, low-power, compact-sized computing device. Its main objective is not to have an extremely powerful processor, but to be a small computer capable of operating 24 hours a day with minimal energy consumption.

This small board computer requires additional components to function correctly. It is necessary to use a microSD card to load the Raspberry Pi operating system (in this case, a 16 GB microSD card is used). The official operating system is the Raspberry Pi OS, which is a version of Debian, although it is also compatible with other operating systems such as Windows 10. Additionally, an external power supply is required for the Raspberry Pi, which must provide at least 2 amps. of current [30].

Raspberry Pi model B+

The Raspberry Pi model B+ figure 4, was released by the Raspberry Pi Foundation in July 2014 as an upgrade to the original Raspberry Pi model B. It has the following characteristics [31]:

1. Processor: Uses a 32-bit Broadcom BCM2835 processor, with an ARMv6 core running at 700 MHz.

2. Memory: it has 512 MB of RAM.

3. Connectivity: It has four USB 2.0 ports, an Ethernet port (RJ-45), an HDMI output, a composite video output, a microSD card slot, a 3.5 mm audio jack and a CSI camera connector.

4. Storage: Use a microSD card as the main storage medium.

5. GPIO: It has 40 GPIO pins that allow the connection of additional electronic components.

6. Power: Powered through a 1.8 A – 5V microUSB connector.

7. Size: It has a compact form factor, with dimensions of approximately 85 x 56 x 17 mm.

It's important to note that the Raspberry Pi Model B+ has been replaced by newer models, such as the Raspberry Pi 3 Model B+ and Raspberry Pi 4 Model B, which offer better performance and additional features.
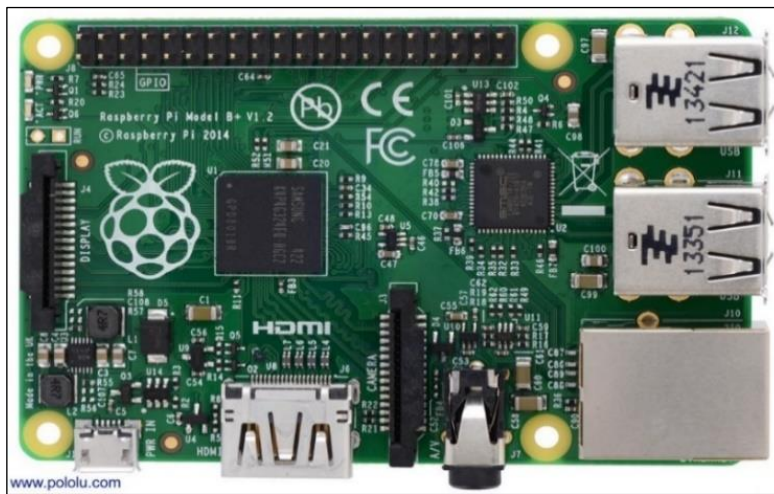

Figure 4: Raspberry Pi model B+.
Source: Authors, (2024).

III.3 ANALYSIS AND DESCRIPTION OF THE PHOTOVOLTAIC PARK CONNECTED TO THE GRID.

The park is located in the southwest area of the Faculty of Electrical Engineering of the "Marta Abreu" Central University of Las Villas, which injects energy into the network through a 315 V/34.5 kV central connection transformer.

It has 189 supporting structures, with 4x5 modules of 265 Wp, organized in 15 rows with a separation of 2.60 m, each row with 252 photovoltaic modules, the length of the rest structure is 3.97 m and the length of the tables in rows is 107 m, with an array width of 95 m, in addition, the photovoltaic modules are anchored to the metal structures with a plane of 19º with respect to the horizontal and facing pure South (azimuth 0º). It has a small automatic control room that houses the general protection and measurement cabinets, with basic facilities to support verification and maintenance tasks.

It has completed technological equipment:

• 3780 silicon (polycrystalline) photovoltaic modules, with a design of 21 modules in series and 3 branches in parallel to achieve the required voltage and current.

• Connections between modules using cables with multi-contact type connectors, guaranteeing quick installation with maximum reliability and durability of the connections.

• It has an independent power supply for plant service that ensures energy for the vitality of the inverters, the monitoring and physical protection system.

• It has a remote supervision system for communication, registration and data transmission, where two independent communication channels are used, as established by the Electrical Union regulations, in addition to external sensors to monitor additional meteorological variables.

The basic composition of the photovoltaic system, shown in figure 5, is given by the panel that generates direct current power through energy conversion. To stabilize the output voltage and reach the values required by the user, a DC-DC converter is used, which generally uses a boost converter so that the voltage generated in the cells is in the desired range, taking values up to ten times more than that generated by the photovoltaic cell.
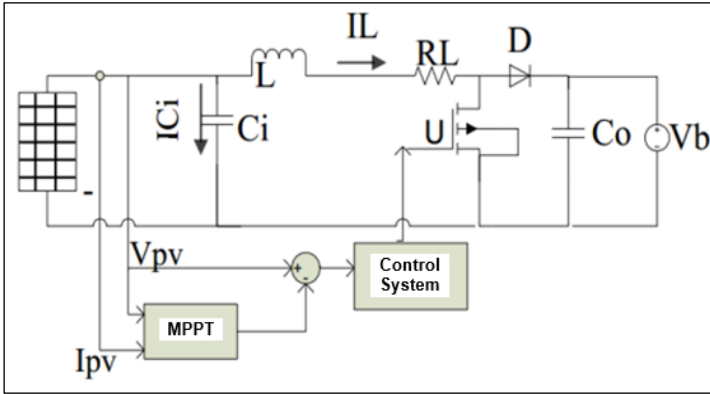
Figure 5: Composition of the photovoltaic system.
Source: Authors, (2024).

Photovoltaic systems connected directly to the electrical grid differ from those installed in isolation in that they do not have an energy accumulation bank or backup in the absence of solar radiation; These systems deliver directly to the network according to the standards and requirements of the electricity company (UNE) and their composition is broken down in figure 6.
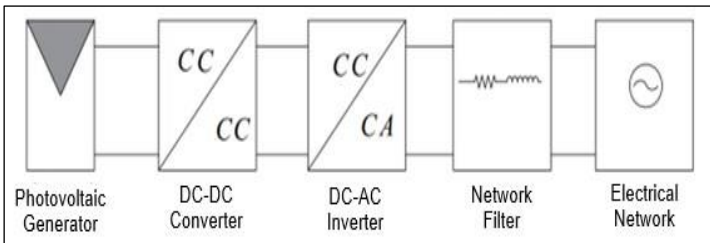

Figure 6: Photovoltaic system connected to the electrical grid.
Source: Authors, (2024).

The UCLV photovoltaic park is taken as an example:

Photovoltaic Generator: 265W Peak Hour Photovoltaic Solar Modules, Manufacturer Shanghai Aerospace Automobile Electromechanical Co.,Ltd. (HT-SAAE), model HT60 156P-265, with voltage at the maximum power point of 30.5 V, current at the maximum power point equal to 8.70 A, open circuit voltage 37.6 V, short circuit current at 9.28 A and efficiency approximately 16.3%.

Inverters: it has two Chinese-made inverters from 2015, SUNGROW SG500MX with: nominal input voltage 460-850V, nominal current 1220 A, operating temperature – 40…+65 °C and with an input at the maximum power point. The output values have a nominal power of 500 kW, maximum current of 1008 A and nominal voltage of 315V for three-phase connection and variable frequency 45-55 Hz and 55-65 Hz.

The performance of the photovoltaic solar park is monitored from a control booth where operators can supervise remotely through conventional communication systems (SCADA) [32].

III.4 MODELING OF THE PHOTOVOLTAIC PARK AT UCLV.

To simulate the behavior of a system similar to the Physical Twin of the photovoltaic park of the Universidad Central de las Villas, the mathematical software tool Simulink Matlab R2023b is used, developing a model that represents an installation connected to the grid. This model includes the following components: a photovoltaic solar panel, a DC-DC boost converter, the Perturbation and Observation (P&O) algorithm for maximum power point tracking (MPPT), the inverter which features voltage source control (VSC) and finally an output transformer to the electrical network.
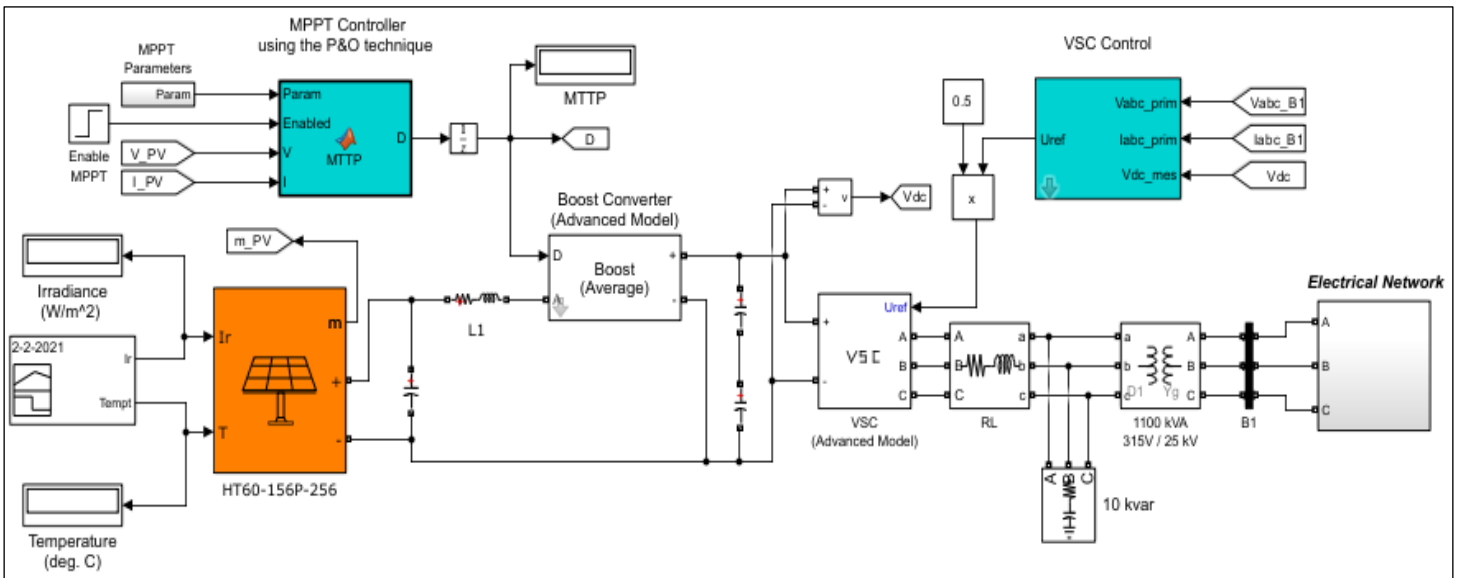

Figure 7: Digital Twin Model of the UCLV photovoltaic park.
Source: Authors, (2024).

Operation and description of the photovoltaic solar panel or PV array block.

The PV array block implements a series of photovoltaic modules. The array is made up of chains of modules connected in parallel, and each chain consists of modules connected in series. This block allows you to model preset PV modules from the National Renewable Energy Laboratory (NREL) Systems Advisor model (January 2014) under standard test conditions (STC) (irradiance=1000 W/m², temperature=25 °C), as well as the photovoltaic modules that you define. In this case, the photovoltaic module is defined as it is not pre-established, consisting of 180 modules connected in parallel, and each one consists of 21 modules connected in series.

After testing using constant temperature and irradiance inputs of 25ºC and 1000W/m^2 respectively, an error was discovered in the PV array block. This specific error only appeared when a fixed-step solver was applied and the "Break algebraic loop in internal model" option was enabled in the "Advanced" tab to generate C code from the model. The problem originated at a certain time, where the exponential used in the linearized equation of the photovoltaic panel diode reached an infinite value, resulting in the abrupt termination of the simulation.

Due to the error that occurred in the PV array block and that prevented its operation, the decision was made to replace said block

with the electrical circuit that represents the photovoltaic solar panel, as shown in figure 3. In this way, the final model shown in figure 8 was obtained. This final model has the same elements as the main model, with the only difference that a subsystem is used to model the photovoltaic panel. However, it is important to highlight that in this new model it is not possible to use temperature as an input parameter, since the selected diode does not have a port for temperature.

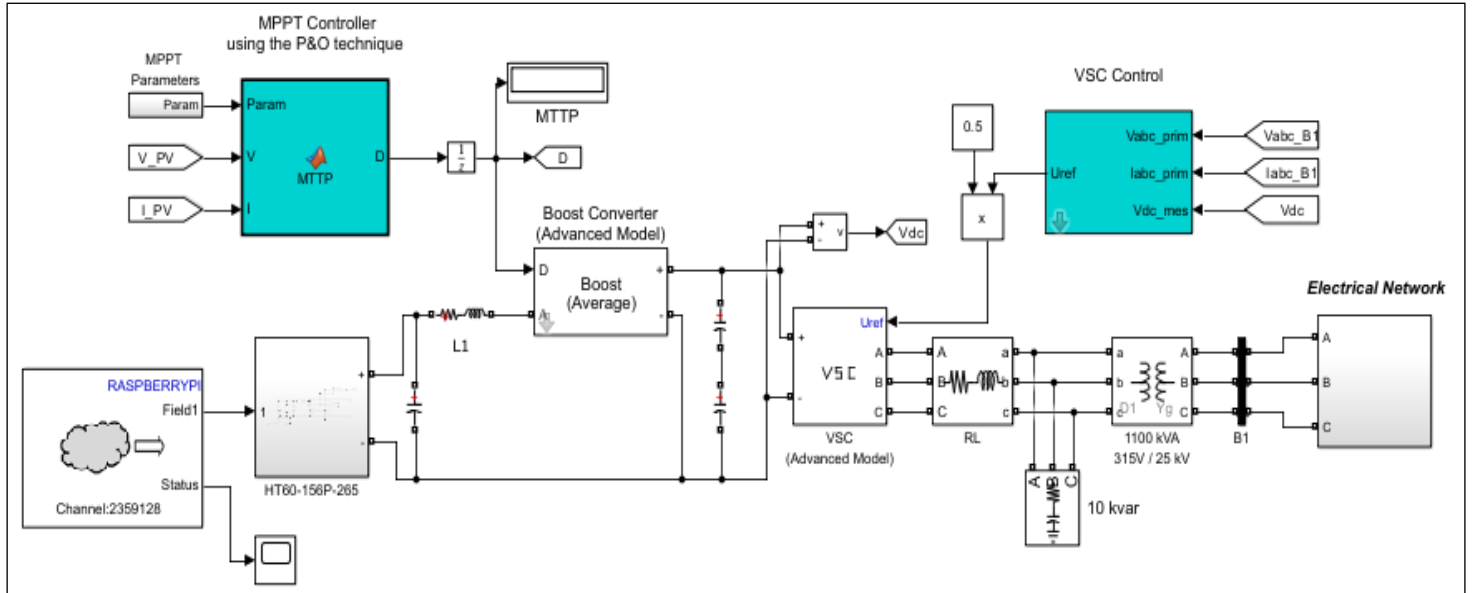Figure 8: Digital Twin Model of the UCLV photovoltaic park with the electrical circuit subsystem of the photovoltaic panel.
Source: Authors, (2024).

Inside the photovoltaic panel subsystem there is the corresponding electrical circuit, which is represented in figure 9:
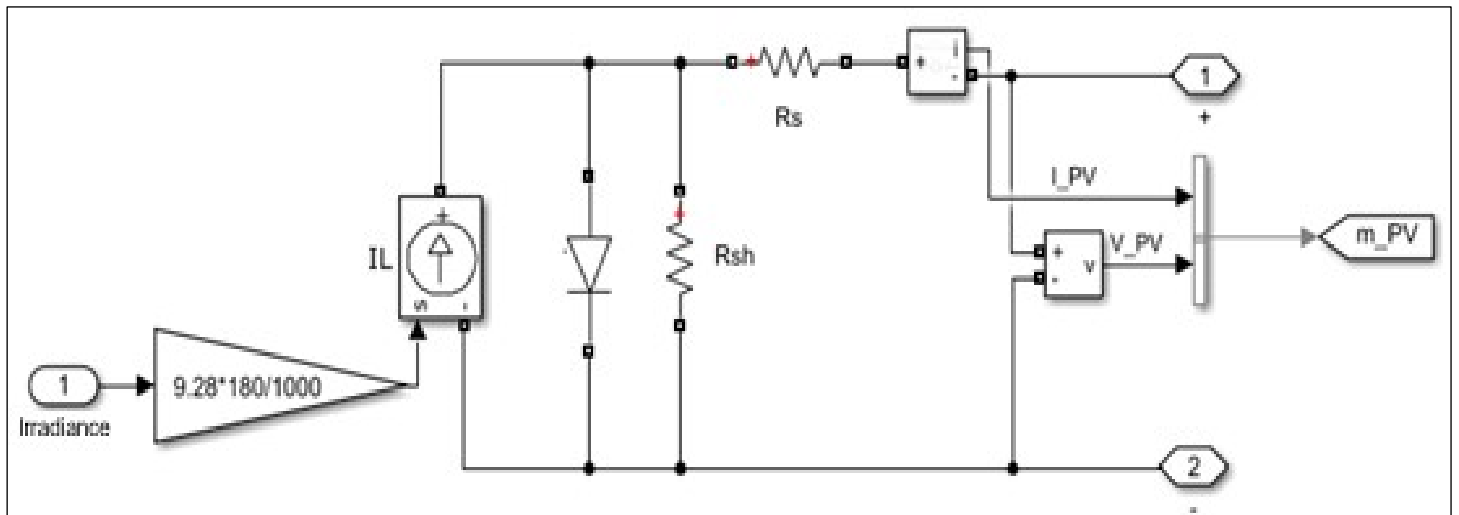

Figure 9: Electrical circuit of the photovoltaic panel.
Source: Authors, (2024).

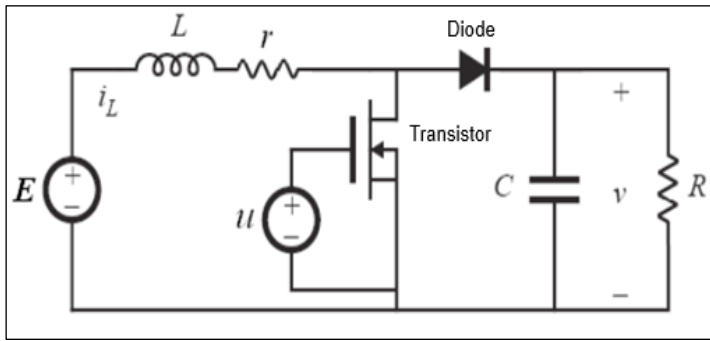Description of DC-DC Boost Converter and P&O algorithm for MPPT:

Figure 10: Boost converter with transistor and diode.
Source: Authors, (2024).

A Boost or DC-DC converter is used, being a voltage boosting circuit, which uses the characteristics of the inductor and the capacitor as energy storage elements to raise the current coming from the power supply and use it to inject it into the capacitor. Thus, producing higher voltage levels at the load than at the source [33].

The maximum power point is tracked to maintain optimal system charging based on the solar panel inputs. The implementation of the MPPT is carried out using the perturbation and observation (P&O) algorithm. This algorithm consists of observing the voltage variation as a function of power, so that the increase in voltage is compared with the increase in power. If both increments are of the same sign, it means that the operating voltage has to increase to reach the maximum power point (MPP) and if they are of different sign the operating voltage has to decrease. With this algorithm, the duty cycle of the boost converter is adjusted, achieving the desired setting.

Voltage Source Controlled (VSC) Inverter Operation:

A power inverter is an electronic power converter, its main function is to facilitate the exchange of energy between two or more subsystems and this is achieved by transforming continuous signals (DC) to alternating signals (AC). The task can be performed through a wide variety of configurations in which we find (electronic) power switches, passive components and a control system that also has the protection function. The link between the control system and the power switches is through switching signals. These switching signals act on the power switches, controlling their switching (ON and OFF). By properly switching these power switches we achieve proper transfer of power from the DC side to the AC side. A type of average model voltage source converter is used to represent power electronic switches. Unlike other power electronic devices, this model uses reference signals (Uref) that represent the average voltages generated at the ABC terminals of the bridge. This model does not represent harmonics. It can be used with longer sampling times while preserving average voltage dynamics [34].

The VSC inverter is a device that offers precise control over the generated alternating current output waveform. It provides high power quality, regulation capability, reactive power injection, fast response and design flexibility. These features make the VSC inverter a popular choice in renewable energy systems and electrical transmission applications.

Description of the mains connection transformer:

The output transformer has two main functions: voltage matching, it allows the output voltage of the converter to be adjusted to match the mains voltage, and impedance matching, it is used to match the output impedance of the converter to the impedance of the electrical network. This ensures that power transfer between the converter and grid is efficient and minimizes wave reflections. It is composed of two or more coils of wire wound around a laminated iron core. The primary coil is connected to the voltage source converter and the secondary coil is connected to the mains. The turns ratio between the coils determines the voltage transformation ratio. In addition to the voltage and impedance matching function, it also provides galvanic isolation between the converter and the mains. This means there is complete electrical separation between the two, ensuring safety and preventing the transfer of unwanted currents [35].

The transformer present in the UCLV has a power capacity of 1100 kVA, being the maximum, it can deliver to the connected load. The transformation ratio is expressed as 315 V/34.5 kV. This means that the primary (input) voltage is 315 volts (V) and the secondary (output) voltage is 34.5 kilovolts (kV). Transformers are passive devices and do not directly modify power. Its main function is to adapt voltage and current levels for the efficient transmission of electrical energy between different systems or loads.

IV. CONFORMATION OF THE DIGITAL TWIN OF THE UCLV PHOTOVOLTAIC FIELD.

IV.1 INTEGRATION, COMMUNICATION AND IMPLEMENTATION OF THE DIGITAL TWIN.

Once the Digital Twin model has been obtained and its implementation on the Raspberry Pi, it is necessary to establish bidirectional communication between the Digital Twin and the real plant. This involves finding suitable connection methods between the Raspberry Pi and the physical system. The real plant must send the data obtained from its sensors to the Digital Twin to ensure that both models have the same input parameters. Additionally, both models must be able to exchange output data for later comparison. In this sense, two viable options are presented for a secure and orderly exchange of data between both entities. One option is by using Sockets, it is defined by two IP addresses (one for the local computer and one for the remote computer), a transport protocol and two port numbers that identify the programs involved. Another option is to use the cloud as a platform for data exchange. In this case, the ThingSpeak tool can be used to establish the connection. The actual plant collects input data from IoT sensors and stores it in specific ThingSpeak fields. The Digital Twin accesses this data to use as input parameters in its model. Likewise, both the real plant and the Digital Twin send the output data to separate fields in ThingSpeak. It is chosen to save the information obtained from the model in a text file (CSV). This choice facilitates access to the data from Matlab and allows a simple comparison with the results obtained from the real plant.

The Raspberry Pi is used to implement the Digital Twin due to its ability to meet the necessary hardware requirements. To do this, two support packages are installed, one for Matlab ("MATLAB Support Package for Raspberry Pi Hardware") and another for Simulink ("Simulink Support Package for Raspberry Pi Hardware") on the Raspberry Pi. On the other hand, the development of the solar plant model is carried out in two programming environments: Simulink and PV_LIB.

In each of these environments, different methods are used to obtain the virtual model. In Simulink, it is built using a block diagram, which can be converted to C code thanks to one of the applications of these tools. On the other hand, in PV_LIB, the virtual model is developed by using the specific functions provided by this Toolbox.

The model represented in figure 8 illustrates the Digital Twin developed in Simulink. The limitation of this model is that it has not been possible to incorporate the effect of temperature in the electrical circuit of the photovoltaic panel (Figure 9). This is

because the diode used does not allow the temperature port to be displayed, so we will only work with irradiance as an input parameter. As a result, this model does not realistically represent the UCLV photovoltaic park, since temperature is a crucial factor that affects the output power of the photovoltaic panel. However, the advantage of this model is that it uses the same components as the physical model, making it an accurate representation of the solar PV plant in that regard.

To transfer the models developed in Simulink to the Raspberry Pi, there are two alternatives to generate this code. The first is to use the Simulink Embedder Coder Toolbox, through the Matlab Coder package. The C code is generated, the "main" is modified to save the variables in a text file (.txt) and the folder with the code is sent to the Raspberry Pi, being executed in the terminal and obtaining the variables from Matlab with location on the Raspberry Pi using communication established by SSH. The second alternative, which is the one used, involves generating the code directly on the Raspberry Pi, without the need to make subsequent modifications. This allows for a more direct and efficient transfer of models from Simulink to the Raspberry Pi.

The model built with PV_LIB is made up of a photovoltaic solar system, since these are the elements that this tool models. The same photovoltaic panel is used with the same characteristics as that used in the Simulink model. This allows a direct comparison of the results obtained from both models, since it is based on a consistent basis. The input values are obtained, defining the cell temperature at 25 °C. The .m file is then converted into a function that can be sent to the hardware board in Simulink, with the PV_LIB model implemented.

The main advantage of this approach is that it allows the effects of irradiance and temperature at the input of the photovoltaic panel to be easily modeled, unlike the Simulink model where it was not possible to include temperature as an input variable. However, a limitation of this method is that additional components such as converters, transformer or tracking algorithms cannot be added to obtain a complete model of a solar PV plant, since the corresponding functions are not defined. Another drawback is that it is not possible to establish a direct connection to the Raspberry Pi because Matlab code generation does not support PV_LIB functions. As a result, the behavior of this model can only be visualized in Matlab and it does not faithfully represent the complete operation of the photovoltaic park, but only the solar panel.

IV.2 RESULTS OBTAINED FROM THE DIGITAL TWIN WITH THE REAL PLANT.

A visit is made to the UCLV photovoltaic park, where the input (irradiation and temperature) and output (active power) data of the Gemelo Real (photovoltaic system) were provided. Data from the photovoltaic park system connected to the grid was obtained, in a 12-hour sample, on February 2, 2021.
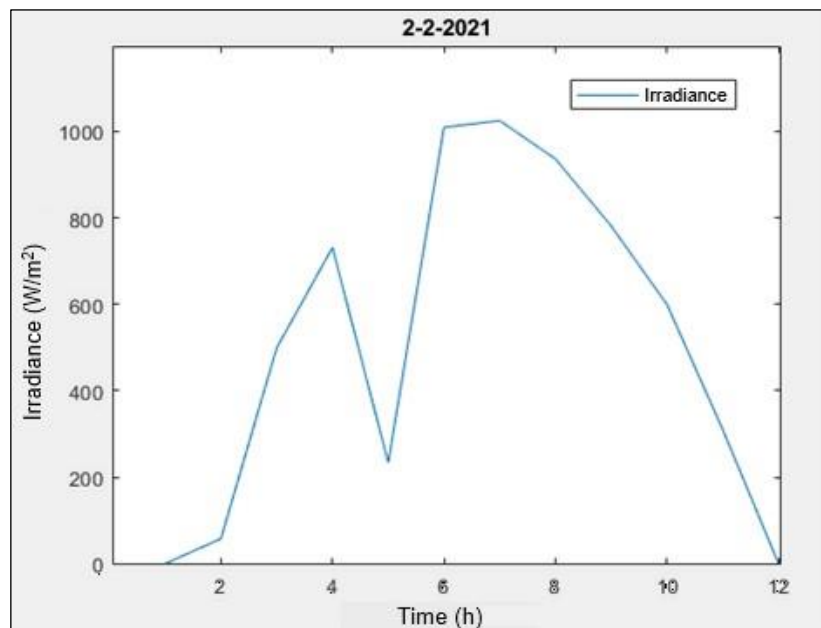

Figure 11: Irradiance input parameter.
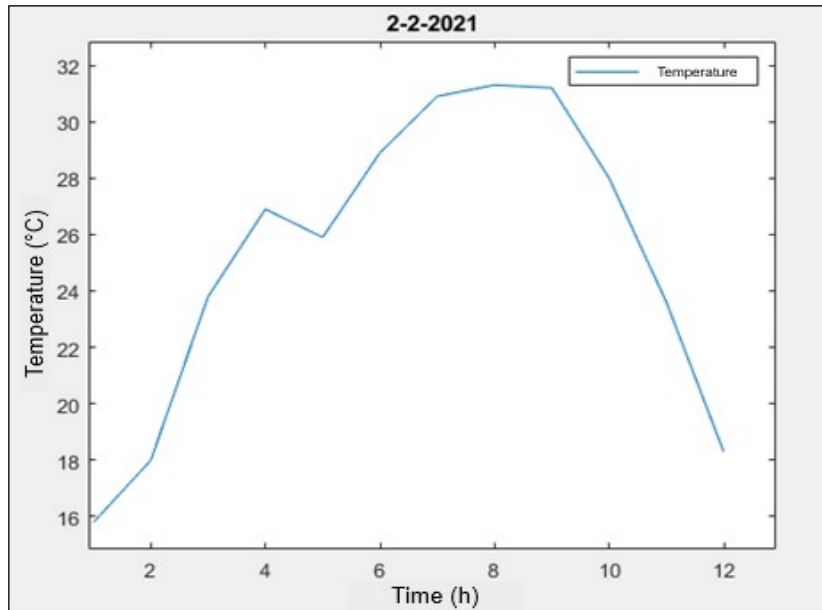Source: Authors, (2024).

Figure 12: Temperature input parameter.
Source: Authors, (2024).

Digital Twin Model of the UCLV photovoltaic park.

The model used in the faithful representation of the UCLV photovoltaic park is used in the comparison between Simulink and the Real Twin, figure 13. The purpose of this model is to validate the operation only in the Simulink development environment, because it has the PV array block, which makes its implementation on the Raspberry Pi impossible.
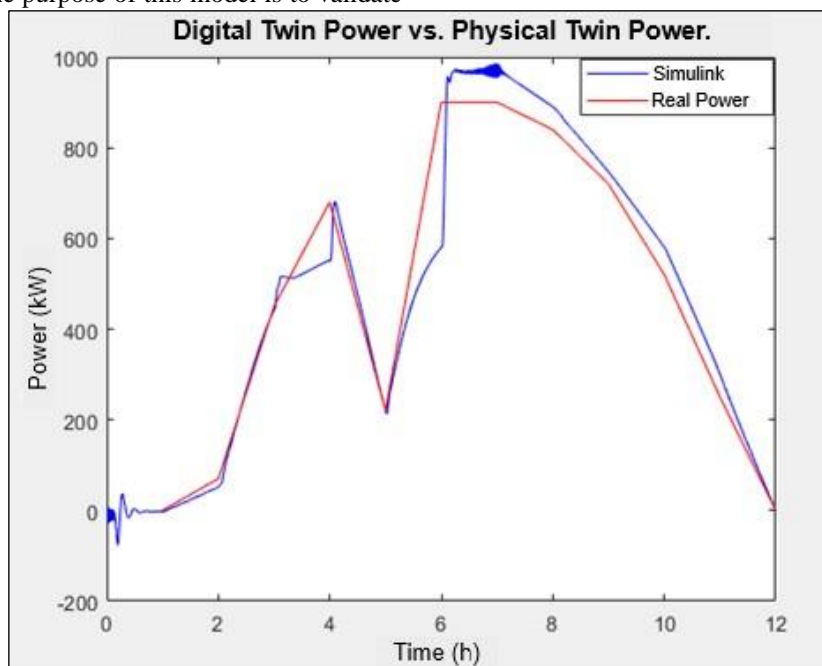
Figure 13: Comparison of powers between the outputs of the models.
Source: Authors, (2024).

Performing a statistical analysis, the square root of the root mean square error (RMSE) is calculated to evaluate the accuracy of the forecast model, which provides a quantitative measure of how close the predicted values are to the actual values, resulting in 51.04 kW (4.64 % precision error).

Model of the electrical circuit of the photovoltaic panel present at the UCLV.

In this comparative study between PV_LIB, Simulink and Raspberry Pi, the model that represents an electrical circuit of a solar panel is used (figure 9). The objective is to validate the operation of the developed circuit, and all models are configured with the same parameters and the same irradiance input. Although PV_LIB allows temperature to be entered as an additional input, the Simulink model does not include this option and only works with irradiance.

In Simulink, a load is added to the circuit by including a resistor whose value corresponds to the relationship between the voltage at the maximum power point and the current at the maximum power point. This guarantees optimal loading conditions for the model to reach the maximum power point (MPPT). Since

these values of the maximum power point correspond to an irradiance of 1000 W/m².
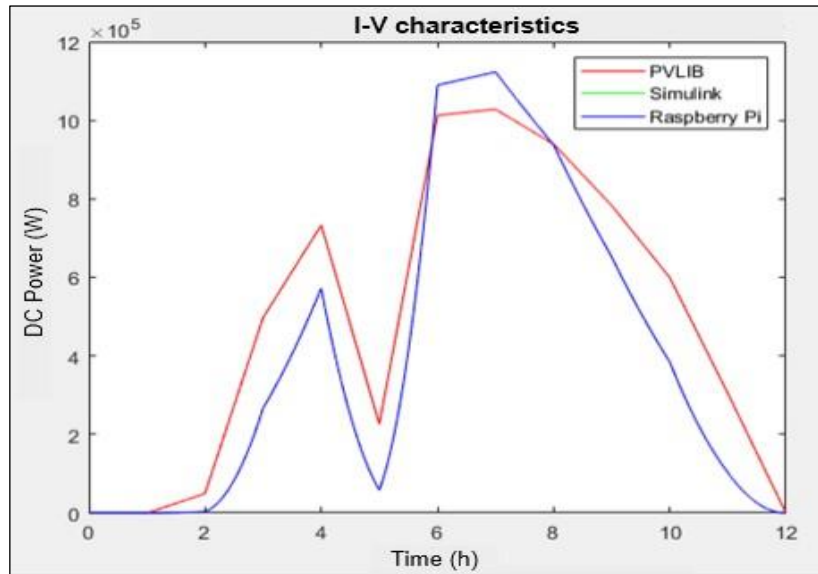
Figure 14: Pmp output signal comparison.
Source: Authors, (2024).

It can be seen that the outputs generated by Simulink and the Raspberry Pi in the graph are completely the same. This is because the sampling period of the hardware board is smaller than that of Simulink, therefore the Digital Twin is running in real time in both cases, which guarantees precise synchronization between the results obtained.

In terms of the results obtained, it is expected to reach specific values at the maximum power point, such as Vmp = 640.5 V, Imp = 1566 A and Pmp = 1.003 MW. These values exactly match the outputs of the model implemented in PV_LIB, confirming that the model developed in this tool works correctly. However, Simulink returns higher values (Vmp = 559.1 V, Imp = 1960 A, Pmp = 1.095 MW). This is because, although Simulink represents circuit losses using series and parallel resistors, there are differences in the parameters compared to the PV_LIB model. The reason for these discrepancies is that the PV_LIB model is more precise, since it takes into account all the variables and nonlinearities of the solar panel.

Regarding the data achieved by the sample values, the result is an RMSE value of 136.03 kW precision of the Simulink and Raspberry Pi model with respect to PV_LIB.

Complete model of the UCLV photovoltaic park.

In order to analyze the effects of a complete solar photovoltaic installation, a comparative study is carried out using the model presented in Figure 8. Although it is not possible to define all the components using the functions provided by PV_LIB, this model can be used for comparison. with Simulink and its implementation on the Raspberry Pi, assuming that the solar panel is operating at the maximum power point. Since this model is more complex than the one presented above, it is necessary to evaluate whether the board is capable of running the Digital Twin in real time.
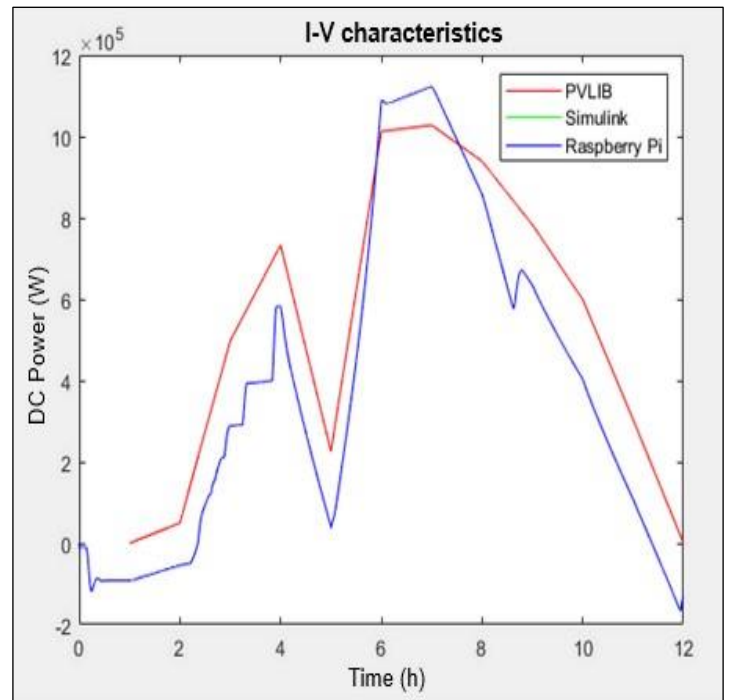
Figure 15: Comparison of Pmp output in the full model.
Source: Authors, (2024).

In relation to the data obtained in the sample, an accuracy of 146.46 kW has been obtained from the Simulink and Raspberry Pi model compared to PV_LIB.

Figure 16 shows the comparison between the power generated by the photovoltaic solar installation and the power of the Digital Twin model, the PV array block has been replaced by the photovoltaic panel circuit and the irradiance input variable has been used to simulate solar radiation conditions. This comparison allows us to evaluate how the Digital Twin behaves in terms of power generation in relation to the Physical Twin.
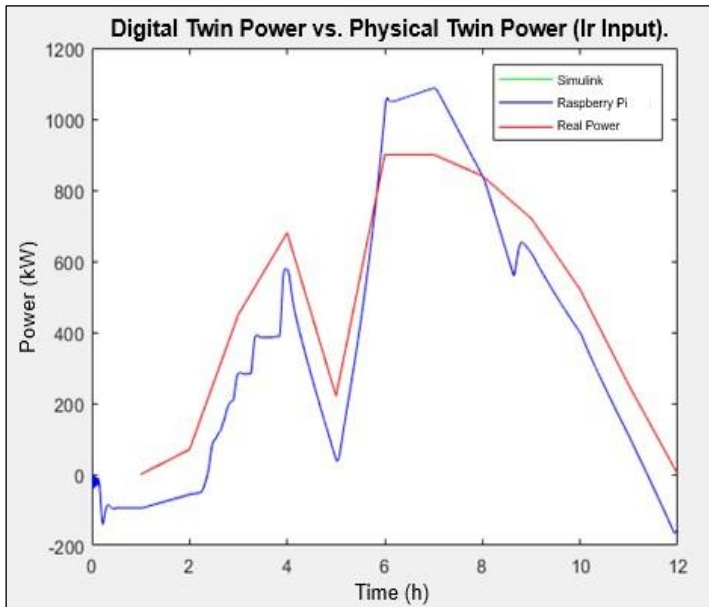
Figure 16: Comparison of output powers.
Source: Authors, (2024).

Statistical analysis reveals a root mean square error value of 134.02 kW (12.18%), which evaluates the accuracy of the forecast model by measuring the proximity of the predicted values to the actual values.

V. CONCLUSIONS

A Digital Twin of the photovoltaic park installed at the UCLV has been created, using the Matlab programming environment together with the Simulink and PV_LIB tools, executing the C code on a Raspberry Pi model B+, which has allowed the system to be implemented and controlled in time. real. During the implementation of the Digital Twin, challenges have been faced due to the novel nature of this technology and its current limitations. Obtaining significant results:

A comparison of the ideal model was carried out between the power generated in Simulink and the real power of the UCLV photovoltaic park, obtaining an RMSE of 51.04 kW, with a precision error of 4.64% in the power estimation.

The full model, in terms of power generation of the Digital Twin in relation to the Physical Twin the RMSE value is 134.02 kW, this implies a precision error discrepancy of 12.18% in the power estimation.

VI. AUTHOR'S CONTRIBUTION

Conceptualization: Luis Gabriel Fong Mollineda and José Rafael Abreu García.
Methodology: Luis Gabriel Fong Mollineda and José Rafael Abreu García.
Investigation: Luis Gabriel Fong Mollineda and José Rafael Abreu García.
Discussion of results: Luis Gabriel Fong Mollineda and José Rafael Abreu García.
Writing – Original Draft: Luis Gabriel Fong Mollineda and José Rafael Abreu García.
Writing – Review and Editing: Luis Gabriel Fong Mollineda and José Rafael Abreu García.
Resources: Luis Gabriel Fong Mollineda and José Rafael Abreu García.
**Supervision:** Luis Gabriel Fong Mollineda and José Rafael Abreu García.

Approval of the final text: Luis Gabriel Fong Mollineda and José Rafael Abreu García.

VIII. REFERENCES

[1] Z. Song *et al.*, "Digital Twins for the Future Power System: An Overview and a Future Perspective," *Sustainability 2023, Vol. 15, Page 5259*, vol. 15, no. 6, p. 5259, Mar. 2023, doi: 10.3390/SU15065259.

[2] I. Tecnológico, S. Jubones, M. Lourdes, C. Linares-Vizcarra, E. T. Montero-Zuñiga, and J. Luna-Nemecio, "Ecología, energías renovables y sustentabilidad socioformativa," *Sociedad & Tecnología*, vol. 6, no. 2, pp. 261–274, May 2023, doi: 10.51247/ST.V6I2.371.

[3] C. del Bosque Peón, "Los gemelos digitales en la industria 4.0," 2019, Accessed: Feb. 28, 2024. [Online]. Available: http://uvadoc.uva.es/handle/10324/40037

[4] K. Arafet Cruz, "Gemelo Digital en Parques Solares: enfoque mediante series temporales y aprendizaje profundo," Nov. 2020, Accessed: Feb. 28, 2024. [Online]. Available: https://repositori.uji.es/xmlui/handle/10234/193565

[5] "Gemelo digital de centrales solares fotovoltaicas: prueba de concepto Girasol | Artículos y entrevistas." Accessed: Jun. 29, 2023. [Online]. Available: https://energetica21.com/articulos-y-entrevistas-online-ver/gemelo-digital-de-centrales-solares-fotovoltaicas-prueba-de-concepto-girasol

[6] W. D. Chicaiza, J. Gómez, A. J. Sánchez, and J. M. Escaño, "El Gemelo Digital y su aplicación en la Automática," *Revista Iberoamericana de Automática e Informática industrial*, Feb. 2023, doi: 10.4995/RIAI.2024.20175.

[7] A. A. SALVADOR-NAVARRO, "Modelado de un gemelo digital para Internet de las Cosas," Oct. 2023, Accessed: Feb. 28, 2024. [Online]. Available: http://crea.ujaen.es/jspui/handle/10953.1/20475

[8] "Gemelos digitales: agregando inteligencia al mundo real - Capgemini España." Accessed: Jun. 01, 2023. [Online]. Available: https://www.capgemini.com/us-en/insights/research-library/digital-twins/#

[9] A. Bosch Serra, "Simulación de componentes de un vehículo eléctrico mediante gemelo digital," Nov. 2022, Accessed: Feb. 29, 2024. [Online]. Available: https://riunet.upv.es:443/handle/10251/190137

[10] M. V. Chiquito, M. V. Chiquito, J. C. G. Plua, M. B. Chong, and C. B. Chong, "Gemelos digitales y su evolución en la industria," *RECIMUNDO*, vol. 4, no. 4, pp. 300–308, Nov. 2020, doi: 10.26820/recimundo/4.(4).noviembre.2020.300-308.

[11] L. Massel, N. Shchukin, and A. Cybikov, "Digital twin development of a solar power plant," *E3S Web of Conferences*, vol. 289, p. 03002, Jul. 2021, doi: 10.1051/E3SCONF/202128903002.

[12] D. S. Moreno Esparza, A. J. Escárraga González, M. en A. de E.-M.-V. 63320946, and M. en A. de E.-M.-V. 1015397124, "Análisis de la Factibilidad de la Implementación de Sistemas de Energía Fotovoltaica en Residencias Rurales de Chocontá-Cundinamarca," 2024, Accessed: Feb. 28, 2024. [Online]. Available: https://repository.universidadean.edu.co/handle/10882/13208

[13] A. SALAZAR-PERALTA, P.-S. Alfredo, and U. PICHARDO, "La energía solar, una alternativa para la generación de energía renovable," *Revista de Investigación y Desarrollo*, vol. 2, no. 5, pp. 11–20, 2016.

[14] A. Beléndez, "Einstein 1905: De los «cuantos de energía» a los «cuantos de luz»," Nov. 2015, Accessed: Feb. 29, 2024. [Online]. Available: http://rua.ua.es/dspace/handle/10045/95405

[15] V. Ossa Arango, "Ensamble y caracterización de un panel solar fotovoltáico." Pereira: Universidad Tecnológica de Pereira, 2017. Accessed: Mar. 01, 2024. [Online]. Available: https://repositorio.utp.edu.co/handle/11059/7616

[16] H.-L. Tsai, T. Ci-Siang, and S. Yi-Jie, "Development of generalized photovoltaic model using MATLAB/SIMULINK," *Lecture Notes in Engineering and Computer Science*, vol. 2173, Mar. 2008.

[17] E. Granda-Gutiérrez, O. Orta, J. C. Díaz-Guillén, M. Jiménez, M. Osorio, and M. González Albarrán, "MODELADO Y SIMULACIÓN DE CELDAS Y PANELES SOLARES," Mar. 2013. doi: 10.13140/2.1.4192.8968.

[18] W. De Soto, S. A. Klein, and W. A. Beckman, "Improvement and validation of a model for photovoltaic array performance," *Solar Energy*, vol. 80, no. 1, pp. 78–88, Jan. 2006, doi: 10.1016/J.SOLENER.2005.06.010.

[19] X. H. Nguyen and M. P. Nguyen, "Mathematical modeling of photovoltaic cell/module/arrays with tags in Matlab/Simulink," *Environmental Systems Research 2015 4:1*, vol. 4, no. 1, pp. 1–13, Dec. 2015, doi: 10.1186/S40068-015-0047-9.

[20] "Item 1004/2338 | Repositorio CIMAV." Accessed: Sep. 04, 2023. [Online]. Available: https://cimav.repositorioinstitucional.mx/jspui/handle/1004/2338

[21] T. Ahmad, S. Sobhan, Md. F. Nayan, T. Ahmad, S. Sobhan, and Md. F. Nayan, "Comparative Analysis between Single Diode and Double Diode Model of PV Cell: Concentrate Different Parameters Effect on Its Efficiency," *Journal of Power and Energy Engineering*, vol. 4, no. 3, pp. 31–46, Mar. 2016, doi: 10.4236/JPEE.2016.43004.

[22] A. Krenzinger and C. W. Massen Prieb, "Clasificación y selección de módulos fotovoltaicos para una central conectada a la red," *Avances en Energías Renovables y Medio Ambiente*, vol. 9, 2005, Accessed: Feb. 28, 2024. [Online]. Available: http://sedici.unlp.edu.ar/handle/10915/82225

[23] "Partes de un panel solar, estructura y componentes." Accessed: Sep. 10, 2023. [Online]. Available: https://solar-energia.net/energia-solar-fotovoltaica/elementos/panel-fotovoltaico/estructura-de-un-panel-fotovoltaico

[24] M. A. Abella, "Sistemas fotovoltaicos," *SAPT Publicaciones Técnicas, SL*, 2005.

[25] H. Moore, V. C. Olguín, and R. M. Nuño, *MATLAB para ingenieros*, no. 620.0013 M66 2007. Pearson Educación, 2007.

[26] L. Matlab, "MATLAB & Simulink." Retrieved September, 2021.

[27] J. S. Stein, "The photovoltaic Performance Modeling Collaborative (PVPMC)," in *2012 38th IEEE Photovoltaic Specialists Conference*, 2012, pp. 3048–3052. doi: 10.1109/PVSC.2012.6318225.

[28] M. A. G. Maureira, D. Oldenhof, and L. Teernstra, "ThingSpeak–an API and Web Service for the Internet of Things," *World Wide Web*, vol. 25, pp. 1–4, 2011.

[29] T.-H. Lee, K.-H. Lee, G.-T. Ahn, and M.-J. Lee, "Sharing Display Based on VNC," in *Proceedings of the Korean Information Science Society Conference*, Korean Institute of Information Scientists and Engineers, 2008, pp. 241–244.

[30] M. Richardson and S. Wallace, *Getting started with raspberry PI*. " O'Reilly Media, Inc.," 2012.

[31] "Pololu - Raspberry Pi Model B+." Accessed: Nov. 30, 2023. [Online]. Available: https://www.pololu.com/product/2752

[32] J. Borges, J. García, and A. Martínez, "Comparación de algoritmos MPPT aplicados a sistemas fotovoltaicos," 2018.

[33] F. F. Valderrama Gutiérrez, H. Moreno C, and H. M. Vega, "Análisis, simulación y control de un convertidor de potencia DC- DC tipo boost," *Ingenium, ISSN 0124-7492, Vol. 12, Nº. 24, 2011 (Ejemplar dedicado a: INGENIUM), págs. 44-55*, vol. 12, no. 24, pp. 44–55, 2011, Accessed: Mar. 01, 2024. [Online]. Available: https://dialnet.unirioja.es/servlet/articulo?codigo=5038442&info=resumen&idioma=SPA

[34] J. C. Jorge and C. L. Eloy, "Control de un inversor fotovoltaico conectado a la red eléctrica trifásica," 2011.

[35] L. D. Caiza Betancourt, "Análisis dinámico para el diagnóstico de transformadores de potencia basada en su condición," 2024, Accessed: Mar. 01, 2024. [Online]. Available: http://dspace.ups.edu.ec/handle/123456789/26770
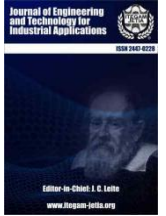
RESEARCH ARTICLE

EXPLORING THE IMPORTANCE OF TUTORING IN DISTANCE EDUCATION (DE): A CASE STUDY AT THE FICTITIOUS SOLARES UNIVERSITY

André Ricardo Nascimento das Neves*[1], Diego Macedo Almeida[2], Daiara Antonia de Oliveira Teixeira[3], Karen Cristina Barreto Trovão Rodrigues[4], Rodrigo Luiz Pereira da Silva[5], Aniklay de Oliveira Lamarão[6], Lucicleia Pantoja Pinheiro[7].

[1]Fametro University Center, Amazonas, Brazil,
[2, 3,4,5,6] Faculty of Technology SENAC Amazonas, Brazil,

[1]http://orcid.org/0000-0002-2911-5376 , [2]http://orcid.org/0000-0002-9088-8992, [3]http://orcid.org/0000-0002-7763-4488, [4]http://orcid.org/0009-0004-2730-2372, [5]http://orcid.org/0009-0007-1059-9642 ,[6]http://orcid.org/0009-0002-3086-8145,[7]http://orcid.org/0009-0004-9982-3740

Email: * aricardo.neves@gmail.com[1], diegobaiano18@gmail.com[2], teixeiradaiara@gmail.com[3], karencristinatrovao@gmail.com[4], rodrigo02luiz@gmail.com[5], ani.contratos@gmail.com[6], lucicleia.pinheiro@outlook.com[7].

ARTICLE INFO	ABSTRACT
	Distance education (DE) has undergone significant evolution in recent decades, largely propelled by advancements in information and communication technologies (ICT). Playing a vital role in DE is e-tutoring, serving as a mediator between teaching and learning, fostering autonomy and collaboration. This article aims to investigate the origins of DE tutoring, tracing its evolution and examining its current importance in educational contexts. In the 19th century, correspondence courses marked the early stages of DE, with tutors and students exchanging letters for interaction. In the early 20th century, institutions like the University of London and the Open University in the United Kingdom pioneered formalized DE programs supported by tutorial systems. The period between the 1980s and 1990s witnessed the emergence of digital DE platforms, driven by the rise of computers and the internet, enabling more immediate interaction between tutors and students.

I. INTRODUCTION

Distance Education (DE) is one of the major milestones in the evolution of education in recent decades, driven by the continuous growth of ICT – information and communication technologies. This evolution has not only facilitated access to education in various contexts, but also brought significant changes to our learning methods and teaching techniques.

These developments gave rise to the pedagogy of distance education, an indispensable element positioned between the teacher and the student: responsible for guiding educational activities while mediating teaching and promoting autonomous and collaborative learning.

This article aims to explore the historical origins and development of distance education, which plays an increasingly significant role in today's educational contexts. The evolution began in the 19th century with what became known as Correspondence Teaching, or EaD, which involved sending teaching materials and receiving students' work by mail; later introduced correspondence tutorial support. This method allowed students from different regions to have access to education, even though they were far from educational institutions.

Only at the beginning of the 20th century, with significant milestones such as the University of London and the Open University established in the United Kingdom, did formalized distance education programs with structured tutorial support emerge.

The University of London, for example, was a pioneer in offering exams to students studying at home. The UK Open

University, created in 1969, revolutionized the model by using a combination of radio, television and printed materials to reach its students. These institutions demonstrated that distance education could be organized in a more formal and effective way, increasing its credibility and acceptance.

Despite these notable precursors, each subsequent model has failed to address all of the shortcomings identified in its predecessors; Thus, the history of distance education can be seen as a continuous process of innovation that aims to find better ways to facilitate distance learning.

The digital age had a significant impact in the 1980s and 1990s, along with the rise of computers and the Internet as popular items; is mainly responsible for the birth of a new generation of digital distance education platforms.

This advanced technology ensured better real-time communication between teachers and students – thus broadening the horizons of joint learning and cooperation. The introduction of emails, discussion forums, videoconferences and learning management platforms transformed distance learning, allowing for more immediate and effective interaction.

Furthermore, the internet has facilitated access to a wide range of educational resources, promoting a richer and more diverse learning environment. Tools such as digital libraries and interactive platforms have made education more accessible and personalized.

Technological advances have also allowed the creation of more sophisticated monitoring and evaluation systems, which help to identify students' needs and offer more targeted support.

Therefore, the history of distance education is marked by constant evolution, driven by the desire to overcome the limitations of previous methods and take advantage of new technologies to improve the teaching and learning experience.

From correspondence teaching to modern digital platforms, distance learning continues to adapt and innovate to meet the educational demands of an increasingly interconnected and digitalized world.

Given the historical scenario presented, this article aims not only to analyze the evolution of tutoring in Distance Education, but also to highlight its growing importance nowadays, where the search for flexible and accessible teaching is increasingly urgent. By investigating the origins and development of tutoring in distance learning, we hope to contribute to a deeper understanding of contemporary educational dynamics and the refinement of more effective practices in distance learning.

II. METHODOLOGY

To investigate the origins and evolution of tutoring in distance learning and understand its importance today, we will adopt a methodological approach that combines historical research and contemporary analysis. Initially, we will carry out a broad bibliographical review, searching for historical sources on distance education, especially those related to tutoring. We will examine documents, books and articles that address the emergence and development of distance learning, highlighting the role of tutoring over time.

In addition, we will conduct interviews with experts in distance education and professionals who act as tutors in virtual learning environments. These interviews will allow us to learn about current distance tutoring practices, the challenges faced and the strategies adopted to promote effective and collaborative learning.

To enrich our investigation, we will analyze secondary data sources, statistical data and reports from educational institutions that offer Distance Education (EaD) programs. This analysis allows us to identify recent trends in online tutoring, including the use of digital platforms and virtual communication tools, as well as the impact of these trends on students' educational experiences.

We also use direct and indirect observation of participants and non-participants as research techniques for bibliographic and documentary consultation, interviews, and life experiences.

Furthermore, we will carry out a case study in an institution that offers distance learning courses, focusing on the implementation and effectiveness of tutoring strategies. This study will allow for a more in-depth analysis of how online tutoring is applied in practice and how it contributes to students' academic success.

By combining different research methods, we aim to gain a comprehensive understanding of distance tutoring, from its historical roots to its importance today. We hope that the results of this study will provide valuable information for teachers, educational institutions and policymakers, contributing to the continuous improvement of distance education.

III DE TUTORING: CRUCIAL ASPECTS IN THE EVOLUTION OF DISTANCE EDUCATION

The evolution of distance education (DL) is a complex phenomenon that involves a series of interconnected factors. Among these factors, technological advances play a fundamental role. From the 19th century to the present day, distance learning has benefited from the constant development of information and communication technologies (ICT), which have provided new forms of interaction between tutors and students. These technological innovations, ranging from correspondence courses to sophisticated digital distance learning platforms, have been crucial in facilitating more dynamic and collaborative learning [1].

In addition to technological advances, the popularization of distance learning is also intrinsically linked to profound transformations in the educational field. Distance tutoring, for example, appears as an essential element in this transformation process, promoting a student-centered approach that values autonomy and collaboration as fundamental pillars of the learning process [2].

The flexibility and accessibility provided by distance tutoring are crucial aspects for the democratization of education. Through online tutoring, students can access the support they need anywhere and at any time, overcoming geographic and temporal barriers that traditionally limit access to education [3].

Consider the existence of five generations, throughout the history of the distance learning modality [4], which are: study per correspondence; The streaming per radio It is television; The university open; The conference calls; computer and internet-based virtual classes.

Despite the obvious benefits, distance learning tutoring faces a series of challenges, ranging from ensuring the quality of teaching to the effectiveness of interaction between tutors and students in virtual environments.

Accessibility and technological infrastructure are fundamental, as many students still do not have adequate access to devices and stable Internet. Furthermore, maintaining student engagement and motivation without face-to-face interaction is a challenge, as is ensuring the quality of online teaching and assessments. The need for effective technical and pedagogical support for students and teachers, together with the promotion of interactivity and collaboration in a virtual environment, are also crucial.

The quality of content and teaching materials, the complexity of assessments and monitoring of learning, and ensuring inclusion and accessibility are also significant concerns.

Ensuring equity and inclusion, adapting distance learning for all students, and investing in the ongoing development of educators are essential steps to overcoming these challenges and offering effective and accessible distance education.

However, it is important to emphasize that these challenges are not just obstacles, but also opportunities for continuous innovation and improvement of tutoring practices [5]. Considering these different aspects, the importance of distance tutoring as a central element in the evolution of distance education and in the search for more inclusive, flexible and effective education becomes evident.

IV THE CASE "VIRTUAL UNIVERSITY SOLARES
IV.1 EMERGING PROBLEM: SHORTAGE OF DE TUTORS

The shortage of qualified distance learning teachers at the Virtual Solares University is a problem that directly affects the quality of education offered by the institution. Without a sufficient number of tutors able to meet the growing demand for distance learning courses, students may struggle to receive the support they need for their learning.

To illustrate the situation, recent data on distance tutoring at the Virtual University Solares are presented:

Table 1. Number of Students/Tutor.

Year	No. Students	No. Tutors	Students/Tutor
2020	5000	50	100
2021	6500	55	118
2022	8000	60	133
2023	-	-	-

Source: Authors, (2024).

Own preparation based on data collected from the University

The data in the table shows an increasing trend in the number of students enrolled at the Virtual Solares University over the years, indicating an increase significant of 5000 students in 2020 to 8000 in 2022.

At the same time, the number of tutors also increased from 50 to 60 in the same period. The average number of students per tutor increased from 100 in 2020 to 133 in 2022, suggesting an increase in the workload per tutor over the years.

With all this context, the significant growth of Distance Education (EaD) is redefining the contemporary educational scenario by offering accessible educational opportunities. This advance not only promotes socioeconomic development, increasing the qualifications of the workforce and reducing educational inequalities, but also facilitates social mobility through access to quality educational opportunities, resulting in better professional qualifications. Furthermore, it drives innovation in both educational technologies and teaching methodologies, highlighting the importance and need for investment and promotion in distance learning.

However, the challenge of the growth of Distance Education (EaD) must be accompanied by a proportional increase in the number of tutors, as the lack of balance can lead to several significant negative consequences:

- **Workload**: Existing tutors may be overwhelmed with large numbers of students, which may hamper their ability to provide *feedback* personalized and individualized support.

- **Decreased quality of interactivity**: With a limited number of tutors to serve a large student base, interaction between students and tutors may be reduced, negatively impacting the effectiveness of teaching.

- **Delays in resolving doubts**: With a shortage of tutors, students may face delays in getting answers to their academic doubts and queries, which may hamper their progress in the course.

- **Student dissatisfaction**: Lack of adequate tutor support can lead to student dissatisfaction with the educational experience offered by the university, resulting in decreased student retention and the institution's reputation.

V. DISCUSSION

The shortage of distance tutors at Virtual University Solares is not only an operational challenge, but a significant obstacle that directly affects the quality of education offered to students.

One of the main consequences of this shortage is the workload faced by existing tutors. With an insufficient number of professionals to serve a large student base, tutors can become overwhelmed, compromising their ability to provide personalized feedback and individualized support to students. This can result in a decrease in the quality of interactivity between students and tutors, which is essential for an effective learning environment.

The lack of qualified tutors can lead to delays in resolving students' doubts, which significantly impacts the quality of learning. In a dynamic and interactive learning environment, it is essential that students receive quick and efficient support for their academic questions and concerns. The shortage of tutors can make this process difficult, negatively impacting students' academic progress.

Qualified tutors play a crucial role in mediating knowledge and supporting students' skills development. They not only provide answers to queries, but also guide students on their learning journey, helping them understand complex concepts and apply knowledge in a practical way. The absence of adequate support can lead students to feel unmotivated and helpless, which can result in lower academic performance and even dropping out of school.

Furthermore, the lack of qualified tutors can directly affect the teaching methodology adopted by the institution. Pedagogical models that are based on continuous feedback and constant interaction between students and tutors become ineffective without a sufficient number of professionals prepared to offer this support.

Isso can lead to a less personalized and more standardized learning experience, where individual student needs are not met satisfactorily.

To mitigate these problems, it is essential that educational institutions invest in training and hiring qualified tutors. Continuing professional development programs for tutors can ensure they are up to date with best pedagogical practices and educational technologies. Additionally, hiring an adequate number of tutors is crucial to maintaining a healthy balance between student numbers and available support, ensuring that everyone receives the attention and support they need to thrive academically.

To resolve this issue, it is essential that Virtual University Solares adopts proactive measures, such as recruitment and retention strategies for qualified tutors, professional development

and training programs, and implementation of educational technologies that can help optimize the efficiency of tutorial support. Develop various techniques, frameworks and plugins to encourage interaction in discussion forums between student/tutor through the use of educational technology.

By comprehensively and strategically addressing the issue of the shortage of tutors in Distance Education (EaD), educational institutions not only mitigate operational challenges, but also recognize the fundamental importance of tutors for the quality of teaching. Tutors play a crucial role as facilitators of learning, providing individualized support, constructive feedback, and academic guidance to students. The active and engaged presence of tutors is essential to maintain student motivation, promote understanding of content and encourage active participation in educational activities.

Furthermore, well-trained and qualified tutors are able to adapt their teaching strategies to the specific needs of students, thus facilitating a more personalized and effective learning process. Investing in recruitment, ongoing training and adequate support for tutors not only increases the overall quality of the distance learning courses offered, but also directly contributes to a more enriching and satisfying educational experience for your students.

V. CONCLUSIONS

The expansion of distance learning has been a positive response to the search for more accessible and flexible education, driven by advances in information and communication technologies. However, in light of the Virtual University Solares case study, it becomes apparent that the shortage of qualified tutors is a significant challenge that not only affects individual institutions, but reflects broader issues facing distance education across the world.

The distance learning modality has grown considerably, offering educational opportunities to a diverse audience, especially those who face geographic or time restrictions.

This expansion is fueled by the ability of information and communication technologies to connect students and educators regardless of physical location. However, the lack of qualified tutors threatens to seriously compromise the quality of this type of teaching.

The shortage of tutors results in several negative consequences. Firstly, existing tutors end up overloaded, which can lead to a reduction in the quality of interactivity between students and tutors. This situation prolongs the resolution of students' doubts, directly affecting their learning experience. Student dissatisfaction not only harms their education, but can also affect the overall reputation and effectiveness of the educational institution.

The case of the Virtual Solares University clearly illustrates these challenges. The situation experienced by this institution is not unique; many others around the world face similar problems. The growing demand for qualified tutors, driven by the expansion of distance learning, creates intense competition for these professionals. Consequently, institutions need to find innovative ways to attract and retain talented tutors to ensure the quality of education offered.

To address these challenges, it is essential that distance learning institutions adopt a multifaceted approach. Firstly, improving working conditions and offering attractive incentives are key strategies for attracting qualified tutors. Furthermore, investing in the ongoing training of these professionals ensures that

they are always up to date with the latest educational methodologies and technologies.

Another crucial aspect is the use of advanced technologies to facilitate class management and improve interaction between students and tutors. Technological tools can help optimize tutors' time, allowing them to offer more efficient and effective support to students. Furthermore, establishing partnerships with other institutions or companies can be an effective way of sharing resources and knowledge, benefiting everyone involved.

In summary, the solution to the shortage of tutors in distance learning requires a comprehensive approach that involves improvements in working conditions, investments in ongoing training and the adoption of innovative technologies. Only through coordinated and strategic efforts will it be possible to overcome this challenge and ensure the quality and effectiveness of distance learning in the future.

To overcome this challenge, it is crucial that institutions adopt a proactive approach, implementing robust strategies to recruit, train and retain qualified tutors. Furthermore, it is essential to invest in innovative educational technologies that can optimize the efficiency of tutorial support, ensuring an enriching learning experience for students.

The research and best practices presented in this study highlight the importance of distance tutoring as a central element in the evolution of distance education. By addressing the challenges faced by Virtual University Solares and similar institutions, we hope to contribute to the continuous improvement of distance learning and to the provision of quality, accessible and inclusive education for all.

VI. AUTHOR'S CONTRIBUTION

Conceptualization: André Ricardo Nascimento das Neves, Diego Macedo Almeida, Karen Cristina Barreto Trovão Rodrigues, Rodrigo Luiz Pereira da Silva, Aniklay de Oliveira Lamarão and Lucicleia Pantoja Pinheiro.

Methodology: André Ricardo Nascimento das Neves, Diego Macedo Almeida, Karen Cristina Barreto Trovão Rodrigues, Rodrigo Luiz Pereira da Silva, Aniklay de Oliveira Lamarão and Lucicleia Pantoja Pinheiro.

Investigation: André Ricardo Nascimento das Neves, Diego Macedo Almeida, Karen Cristina Barreto Trovão Rodrigues, Rodrigo Luiz Pereira da Silva, Aniklay de Oliveira Lamarão and Lucicleia Pantoja Pinheiro.

Discussion of results: André Ricardo Nascimento das Neves, Diego Macedo Almeida, Karen Cristina Barreto Trovão Rodrigues, Rodrigo Luiz Pereira da Silva, Aniklay de Oliveira Lamarão and Lucicleia Pantoja Pinheiro.

Writing – Original Draft: André Ricardo Nascimento das Neves, Diego Macedo Almeida, Karen Cristina Barreto Trovão Rodrigues, Rodrigo Luiz Pereira da Silva, Aniklay de Oliveira Lamarão and Lucicleia Pantoja Pinheiro.

Writing – Review and Editing: André Ricardo Nascimento das Neves, Diego Macedo Almeida, Karen Cristina Barreto Trovão Rodrigues, Rodrigo Luiz Pereira da Silva, Aniklay de Oliveira Lamarão and Lucicleia Pantoja Pinheiro.

Resources: André Ricardo Nascimento das Neves, Diego Macedo Almeida, Karen Cristina Barreto Trovão Rodrigues, Rodrigo Luiz Pereira da Silva, Aniklay de Oliveira Lamarão and Lucicleia Pantoja Pinheiro.

Supervision: André Ricardo Nascimento das Neves, Diego Macedo Almeida, Karen Cristina Barreto Trovão Rodrigues,

Rodrigo Luiz Pereira da Silva, Aniklay de Oliveira Lamarão and Lucicleia Pantoja Pinheiro.

Approval of the final text: André Ricardo Nascimento das Neves, Diego Macedo Almeida, Karen Cristina Barreto Trovão Rodrigues, Rodrigo Luiz Pereira da Silva, Aniklay de Oliveira Lamarão and Lucicleia Pantoja Pinheiro.

VIII. REFERENCES

[1] Clark, A. (2019). Technological Innovations in Distance Education. *Journal of Distance Learning*, 25(3), 45-60.

[2] Johnson, R. (2018). Student-Centered Approaches in Distance Education. *Educational Technology & Society*, 21(2), 35-48.

[3] Smith, T. (2020). The Role of E-Tutoring in Distance Education. *Educational Research and Reviews*, 15(5), 123-135.

[4] Santos, M. de S. dos, & Branco, J. C. S. (2024). The Tutor in Distance Education: ANPED Literature Review from 2015 to 2021: EaD Em Foco, 14(1), and 1958. https://doi.org/10.18264/eadf.v14i1.1958.

[5] García, M. (2017). Challenges and Opportunities in Online Tutoring. *International Review of Research in Open and Distributed Learning*, 18(4), 100-118.